NASA TECHNICAL MEMORANDUM

June 1974

NASA TM X-64822

MSFC SKYLAB THERMAL AND ENVIRONMENTAL CONTROL SYSTEM MISSION EVALUATION

Skylab Program Office

NASA

George C. Marshall Space Flight Center

Marshall Space Flight Center, Alabama

MSFC - Form 3190 (Rev June 1971)

TECHNICAL REPORT STANDARD TITLE PAGE

1. REPORT NO.	2. GOVERNMENT ACCESSION NO.	3. RECIPIENT'S CATALOG NO.
NASA TM X-64822		

4. TITLE AND SUBTITLE	5. REPORT DATE
MSFC SKYLAB THERMAL AND ENVIRONMENTAL CONTROL SYSTEM MISSION EVALUATION	June 1974
	6. PERFORMING ORGANIZATION CODE
7. AUTHOR(S)	8. PERFORMING ORGANIZATION REPORT #
G. D. Hopson, J. W. Littles, W. C. Patterson	
9. PERFORMING ORGANIZATION NAME AND ADDRESS	10. WORK UNIT NO.
George C. Marshall Space Flight Center Marshall Space Flight Center, Alabama 35812	11. CONTRACT OR GRANT NO.
12. SPONSORING AGENCY NAME AND ADDRESS	13. TYPE OF REPORT & PERIOD COVERED
National Aeronautics and Space Administration Washington, D. C. 20546	Technical Memorandum
	14. SPONSORING AGENCY CODE

15. SUPPLEMENTARY NOTES

16. ABSTRACT

An evaluation of the performance of the Skylab Thermal and Environmental Control System is presented. Actual performance is compared to design and functional requirements and anomalies and discrepancies and their resolution are discussed.

The Thermal and Environmental Control Systems performed their intended role. Based on the experience gained in design, development and flight, recommendations are provided which may be beneficial to future system designs.

17. KEY WORDS	18. DISTRIBUTION STATEMENT
	Unclassified-unlimited James D. Lebetter

19. SECURITY CLASSIF. (of this report)	20. SECURITY CLASSIF. (of this page)	21. NO. OF PAGES	22. PRICE
Unclassified	Unclassified	488	NTIS

ACKNOWLEDGEMENT

This report was generated by the Skylab ECS/TCS Mission Support Group. In addition to the listed authors, the following individuals contributed significantly to the report through data analysis, text preparation and review: MDAC-W, Rob Grenier, Dave Daniels; MDAC-E, Dick Smith, Marion Peeples, Charlie Schultz, Les Calhoun; MMC, Stan Hightower, Dick Sosnay, Coyne Prenger, Jim Neuman, Gary Wilson; Brown Engineering, Co., Wylie Ward, Hugh Watkins, Ed Pierce, Larry Turner, T. L. Thompson; NASA, Charles Ray, Larry Bradford, Doug Moss, Randy Humphries.

TABLE OF CONTENTS

TABLE OF CONTENTS (Continued)

TABLE OF CONTENTS (Continued)

TABLE OF CONTENTS (Continued)

TABLE OF CONTENTS (Continued)

LIST OF ILLUSTRATIONS

LIST OF ILLUSTRATIONS (Continued)

LIST OF ILLUSTRATIONS (Continued)

LIST OF ILLUSTRATIONS (Continued)

LIST OF ILLUSTRATIONS (Continued)

LIST OF ILLUSTRATIONS (Continued)

LIST OF ILLUSTRATIONS (Continued)

LIST OF TABLES

LIST OF ABBREVIATIONS AND SYMBOLS

The following abbreviations and symbols were used in the preparation of this text.

AC	alternating current
A/C	air-conditioning
ACCU	accumulator
A/D	Actuator/Damper
AEDC	Arnold Engineering Development Center
ALT	alternate
AM	Airlock Module
AM (also A.M.)	before noon
AMS	Airlock Missile Station
ASSY	Assembly
ATM	Apollo Telescope Mount
AUX	auxiliary
AVE	average
B/F	Beam/Fairing
Btu (also BTU)	British Thermal Unit
CAL	Calories
CAP.	Capacitor
C/B	Circuit breaker
CCU	Coolant Control Unit
C&D	Control and Display
C_DA	Discharge coefficient X Area = Effective Vent Area
CFM	Cubic feet per minute

$C_{11}H_{24}$	Undecane
℄	Center line
CLO	Clothing value
CM^2	square centimeters
C/O	checkout
CO	Carbon Monoxide
CO_2	Carbon Dioxide
COMPT.	compartment
COND.	condensing
CONST.	constant
Cp	specific heat at constant pressure
CPR	Cabin Pressure Regulator
CRDU	Charger Relay Driver Unit
CRT ḦV	Cathode Ray Tube High Voltage
CSM	Command Service Module
CTCV	Chiller Thermal Control Valve
C&W	Caution and Warning
CYL	cylinder
DA	Deployment Assembly
DC	Direct Current
DCS	Digital Command System
DEG (also deg.)	degrees
DEP'L	deployed
DIA	diameter
DOY	Day of the Year

E	Error
ECS	Environmental Control System
EDT	Eastern Daylight Time
Elect.	electrical
EQP	equipment
EREP	Earth Resources Experiment Package
ESS	Experiment Support System
EVA	Extravehicular Activity
EXP	experiment
EXT	exterior
°F	degrees Fahrenheit
FAC	facility
FAS	Fixed Airlock Shroud
F/C	forward compartment
FPM	feet per minute
FRZ	freezer
ft (also FT)	feet
ft^2	square feet
FWD	forward
GCHX	Ground Cooling Heat Exchanger
GFE	Government Furnished Equipment
GMT	Greenwich Mean Time
GN_2	gaseous nitrogen
GPM	gallons per minute
GSE	Ground Support Equipment
GTCS	Ground Thermal Conditioning System

H_2	Hydrogen
H/A	Habitation Area
HAB	Habitability
HI	High
H_2O	Water
HPI	High Performance Insulation
HR	hour
HX	heat exchanger
IITRI	Illinois Institute of Technology Research Institute
in^2	square inches
in^3	cubic inches
INCL.	included
in. H_2O	inches of water
INT	interior
INV	inverter
IR	infra-red
IU	Instrument Unit
IVA	Intravehicular Activity
JOP	Joint Operation Plan
JSC	Johnson Space Center
KSC	Kennedy Space Center
lb	pounds
Lbm	pounds-mass
LBNP	Lower Body Negative Pressure Device
LCG	Liquid Cooled Garment

LH_2	liquid Hydrogen
LiOH	Lithium Hydroxide
LM	Lunar Module
LO	Low
LOX	liquid Oxygen
LSU	Life Support Umbilical
LUT	Launch Umbilical Tower
$\dot{m}$	mass flow rate
M^2	square meters
MAX (also max.)	maximum
MD	mission day
MDA	Multiple Docking Adapter
MDAC-ED	McDonnell Douglas Astronautics Corporation - Eastern Division
MIN (also min.)	minimum
MIN (also min.)	minutes
MLI	multi-layer insulation
mm	millimeters
mmHg	millimeters Mercury
MMS	McDonnell Material Specification
Mod.	Module
MSC	Manned Spacecraft Center
MSFC	Marshall Space Flight Center
mv	millivolts
MVR	maneuver

N_2	Nitrogen
No.	number
NOM	nominal
O_2	oxygen
O&C	Operations and Checkout
OSH	off scale high
OSL	off scale low
OZ	ounces
P	Pressure
PCM	Power Conditioning Module
PCO_2(also $PPCO_2$)	partial pressure of carbon dioxide
PCU	Pressure Control Unit
Pkg	package
PLV	Post Landing Ventilation (fan)
PM (also P.M.)	afternoon
PNEU	pneumatic
PNL	panel
PO_2	partial pressure of Oxygen
PO_4	phosphates
PP I	Position Plane I
PP II	Position Plane II
PP III	Position Plane III
PP IV	Position Plane IV
PPM	parts per million

PRI (also PRIM)	primary
PS	Payload Shroud
PS	Pressure Switch
PSI	pounds per square inch
PSIA	pounds per square inch, absolute
PSID	pounds per square inch, differential
PSIG	pounds per square inch, guage
PWS	Power Supply
q (also Q)	dynamic pressure
Qa	albedo constant
QIR	Earth's infra-red flux
QS	solar flux
QD	quick disconnect
RAD	radiator
RBPV	radiator bypass valve
RCRS	Regenerable CO_2 Removal System
Rec.	recorder
REF	reference
REG	regulator
REGEN	regenerative
RPRV	Radiator Pressure Relief Valve
RS	refrigeration system
RTTA	Range Tone Transfer Assembly
SAL	Scientific Airlock
SAS	Solar Array System

SCFM	Standard cubic feet per minute
SEC	Secondary
Sec	section
sec	second
SEDR	Service Engineering Department Report
SEVA	Stand-up Extravehicular Activity (from CSM)
SI	Solar Inertial
SL	Skylab
SLP	sleep
SOL	solenoid
SST	Skylab Systems Test
STA.	station
STS	Structural Transition Section
SUS	Suit Umbilical System
SWS	Saturn Workshop
SYS	system
TACS	Thruster Attitude Control System
TCS	Thermal Control System
TCU	Thermal Conditioning Unit
TCV	Thermal Control Valve
TCVB (also TCV-B)	Thermal Control Valve B
TCVC	Thermal Control Valve C
TDI	Toluene Diisocyanate
TEMP	temperature
THM	thermal

THRU	through
TM	telemetry
TRW	Thompson-Ramo-Wooldridge, Inc.
TV	television
TYP	typical
U-1	Unit-1 (Skylab Flight Unit)
V	volts
VAB	Vertical Assembly Building
VDC	Volts direct current
VHF	Very High Frequency
VLV	Valve
W	watts
WMC	Waste Management Compartment
W/O	without
WRF	Wardroom freezer
WST	waste
Z-LV (also ZLV)	Z-axis - Local Vertical
α (also α_s)	absorptivity
β	Beta angle
ΔP	delta pressure (differential pressure)
ΔPS	delta pressure switch
ϵ	emissivity
μ	microns
%	percent
^{o}	degrees

#	number
=	equal
$\leq$	less than or equal to
$\geq$	greater than or equal to
±	plus or minus
"	inches
'	feet

SECTION I. INTRODUCTION

The Skylab program provided man's first opportunity to live and work in near Earth space for extended periods. Skylab utilized expertise and hardware from the earlier Mercury, Gemini and Apollo programs. The Skylab program consisted of three separate missions designated SL-1/2, SL-3 and SL-4. SL-1 was the designation for the Saturn V inserted orbital assembly with SL-2, SL-3 and SL-4 being designations for crew delivery via Uprated Saturn I's including the stay period in the orbital assembly and the return flight.

The Skylab missions were designed to investigate the ability of man to live and work in the alien environment of "zero-g" near Earth space for prolonged periods of time. Evaluation of man's aptitudes and physiological responses in space and his postflight adaptation were prime goals. Performance of corollary and student derived experiments in a variety of scientific and technological regimes as well as performance of solar astronomy and Earth resource observations were also major objectives.

Three crewmen manned the orbital assembly during each mission. Crews consisted of a commander, a science pilot and a pilot. Listed below are the crews for each mission.

SL-2

Commander	Charles Conrad, Jr.
Science Pilot	Joseph P. Kerwin
Pilot	Paul J. Weitz

SL-3

Commander	Alan Bean
Science Pilot	Owen Garriott
Pilot	Jack R. Lousma

SL-4

Commander	Gerald P. Carr
Science Pilot	Edward G. Gibson
Pilot	William R. Pogue

Skylab consisted of four separate modules. These four modules assembled together formed the orbital assembly (see figure 1-1). The module designations were the Apollo Telescope Mount built in-house at Marshall; the Orbital Workshop built by McDonnell-Douglas Western Division;

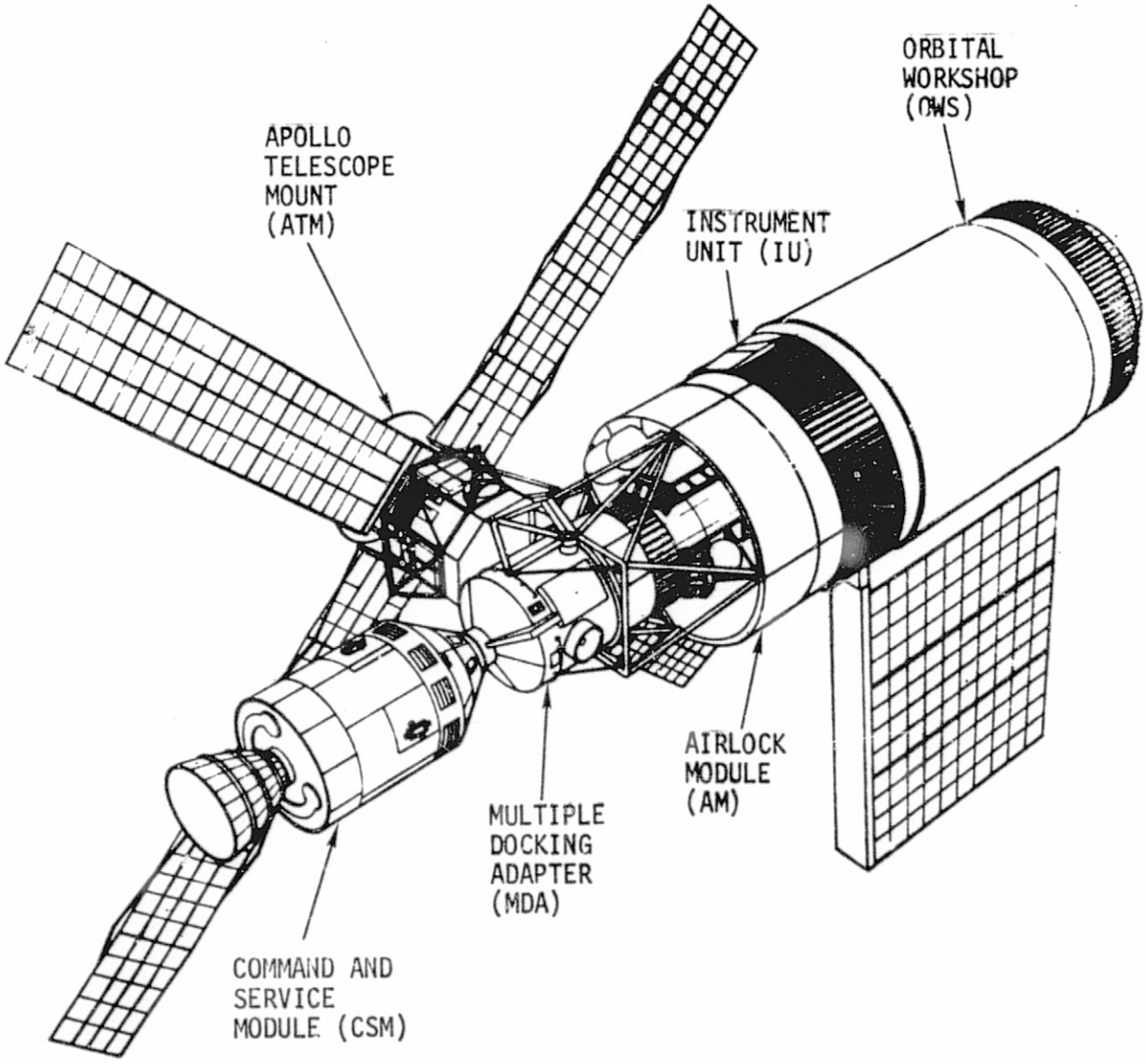

Figure 1-1. Skylab Configuration

the Multiple Docking Adapter built by the Martin-Marietta Denver Division; and the Airlock Module constructed by the McDonnell-Douglas Eastern Division. The Command Service Module was built by North American Rockwell, docked with the Multiple Docking Adapter and was a part of the habitable environment during manned missions. Although the Instrument Unit was situated in the orbital assembly, it was considered part of the alunch vehicle and became inactive as planned during the early orbital phase of SL-1. The payload shroud was built by the McDonnell-Douglas Western Division and was successfully flown and jettisoned following orbital insertion of SL-1.

The four Skylab modules, which were first mated together to form the orbital assembly at Kennedy Space Center were mounted atop the S-II/S-IC stages of the Saturn V vehicle. The vehicle formed therefrom was launched from Kennedy Complex 39A on May 14, 1973. Eleven days later on the 25th day of May, the first flight crew, SL-2, was launched from Complex 37 to rendezvous with the orbital assembly which was circling the Earth in a 234 nautical mile orbit with a period of 93 minutes. The SL-2 crew returned to Earth on the 22nd of June. After a 36 day storage period the SL-3 crew was launched on a 59 day mission. The last storage period between SL-3 and SL-4 lasted 52 days with SL-4 being launched on 16 November for a mission lasting until the 8th of February, 1974. When the last crew returned to Earth, the final day of the Skylab mission was the 9th of February, which was devoted to unmanned engineering evaluation of selected systems. At this time the orbital assembly was inerted and "parked" in a gravity gradient attitude. A mission profile is provided in figure 1-2.

Table 1.1 correlates the calendar date with the two standard temporal references used during the flight which were Day of the Year (DOY) and Mission Day (MD).

This report is concerned with the mission performance of the Skylab environmental and thermal control systems. The report was prepared by the Life Support and Environmental Branch of the Propulsion and Thermodynamics Division in Marshall Space Flight Center's Astronautics Laboratory. The document also gives a brief description of each sybsystem to familiarize the reader with the basic system configuration. Preflight anticipated and actual flight performance are discussed including significant anomalies and discrepancies as well as remedial actions. The environmental and thermal control systems of the Airlock, Multiple Docking Adapter and Orbital Workshop modules of the orbital assembly are addressed. The thermal systems in the Apollo Telescope Mount are covered in TMX 64811. Th crew EVA/IVA support systems from the airlock umbilical interface, including the astronaut suit and support equipment, were the responsibility of elements of the Johnson Spacecraft Center and as such are not detailed herein. Performance of other Skylab subsystems are reported in separate documents (see Table 1.2).

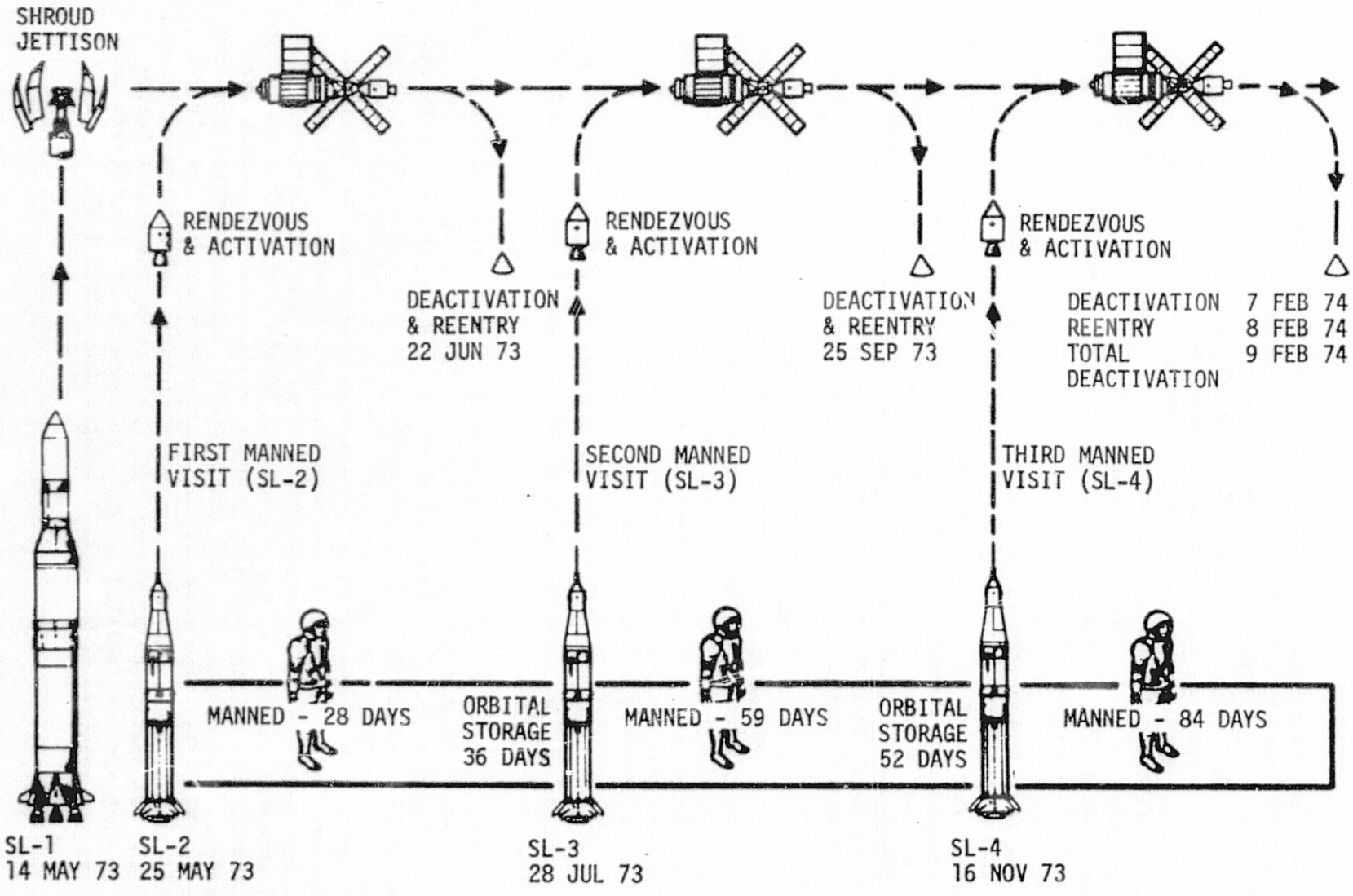

Figure 1-2. Skylab Mission Profile

DAY	DATE (1973)	DAY OF YEAR	MISSION PERIOD
1	5-14	134	(FIRST UNMANNED PERIOD)
2	5-15	135	
3	5-16	136	
4	5-17	137	
5	5-18	138	
6	5-19	139	
7	5-20	140	
8	5-21	141	
9	5-22	142	
10	5-23	143	
11	5-24	144	
12	5-25	145	1
13	5-26	146	2
14	5-27	147	3
15	5-28	148	4
16	5-29	149	5
17	5-30	150	6
18	5-31	151	7
19	6-1	152	8
20	6-2	153	9
21	6-3	154	10
22	6-4	155	11
23	6-5	156	12
24	6-6	157	13
25	6-7	158	14
26	6-8	159	15
27	6-9	160	16
28	6-10	161	17
29	6-11	162	18
30	6-12	163	19
31	6-13	164	20
32	6-14	165	21
33	6-15	166	22
34	6-16	167	23
35	6-17	168	24
36	6-18	169	25
37	6-19	170	26
38	6-20	171	27
39	6-21	172	28
40	6-22	173	29
41	6-23	174	(SECOND UNMANNED PERIOD)
42	6-24	175	
43	6-25	176	
44	6-26	177	
45	6-27	178	
46	6-28	179	
47	6-29	180	
48	6-30	181	
49	7-1	182	
50	7-2	183	
51	7-3	184	
52	7-4	185	
53	7-5	186	
54	7-6	187	
55	7-7	188	
56	7-8	189	
57	7-9	190	
58	7-10	191	
59	7-11	192	
60	7-12	193	
61	7-13	194	
62	7-14	195	
63	7-15	196	
64	7-16	197	
65	7-17	198	
66	7-18	199	
67	7-19	200	
68	7-20	201	
69	7-21	202	
70	7-22	203	
71	7-23	204	
72	7-24	205	
73	7-25	206	
74	7-26	207	
75	7-27	208	
76	7-28	209	1
77	7-29	210	2
78	7-30	211	3
79	7-31	212	4
80	8-1	213	5
81	8-2	214	6
82	8-3	215	7
83	8-4	216	8
84	8-5	217	9
85	8-6	218	10
86	8-7	219	11
87	8-8	220	12
88	8-9	221	13
89	8-10	222	14
90	8-11	223	15
91	8-12	224	16
92	8-13	225	17
93	8-14	226	18
94	8-15	227	19
95	8-16	228	20
96	8-17	229	21
97	8-18	230	22
98	8-19	231	23
99	8-20	232	24
100	8-21	233	25
101	8-22	234	26
102	8-23	235	27
103	8-24	236	28
104	8-25	237	29
105	8-26	238	30
106	8-27	239	31
107	8-28	240	32
108	8-29	241	33
109	8-30	242	34
110	8-31	243	35
111	9-1	244	36
112	9-2	245	37
113	9-3	246	38
114	9-4	247	39
115	9-5	248	40
116	9-6	249	41
117	9-7	250	42
118	9-8	251	43
119	9-9	252	44
120	9-10	253	45
121	9-11	254	46
122	9-12	255	47
123	9-13	256	48
124	9-14	257	49
125	9-15	258	50
126	9-16	259	51
127	9-17	260	52
128	9-18	261	53
129	9-19	262	54
130	9-20	263	55
131	9-21	264	56
132	9-22	265	57
133	9-23	266	58
134	9-24	267	59
135	9-25	268	60
136	9-26	269	
137	9-27	270	
138	9-28	271	
139	9-29	272	
140	9-30	273	
141	10-1	274	
142	10-2	275	
143	10-3	276	
144	10-4	277	
145	10-5	276	
146	10-6	279	
147	10-7	280	
148	10-8	281	
149	10-9	282	
150	10-10	283	
151	10-11	284	
152	10-12	285	
153	10-13	286	
154	10-14	287	
155	10-15	288	
156	10-16	289	
157	10-17	290	
158	10-18	291	
159	10-19	292	
160	10-20	293	
161	10-21	294	
162	10-22	295	
163	10-23	296	
164	10-24	297	
165	10-25	298	
166	10-26	299	
167	10-27	300	
168	10-28	301	
169	10-29	302	
170	10-30	303	
171	10-31	304	
172	11-1	305	
173	11-2	306	
174	11-3	307	
175	11-4	308	
176	11-5	309	
177	11-6	310	
178	11-7	311	
179	11-8	312	
180	11-9	313	
181	11-10	314	
182	11-11	315	
183	11-12	316	
184	11-13	317	
185	11-14	318	
186	11-15	319	
187	11-16	320	1
188	11-17	321	2
189	11-18	322	3
190	11-19	323	4
191	11-20	324	5
192	11-21	325	6
193	11-22	326	7
194	11-23	327	8
195	11-24	328	9
196	11-25	329	10
197	11-26	330	11
198	11-27	331	12
199	11-28	332	13
200	11-29	333	14
201	11-30	334	15
202	12-1	335	16
203	12-2	336	17
204	12-3	337	18
205	12-4	338	19
206	12-5	339	20
207	12-6	340	21
208	12-7	341	22
209	12-8	342	23
210	12-9	343	24
211	12-10	344	25
212	12-11	345	26
213	12-12	346	27
214	12-13	347	28
215	12-14	348	29
216	12-15	349	30
217	12-16	350	31
218	12-17	351	32
219	12-18	352	33
220	12-19	353	34
221	12-20	354	35
222	12-21	355	36
223	12-22	356	37
224	12-23	357	38
225	12-24	358	39
226	12-25	359	40
227	12-26	360	41
228	12-27	361	42
229	12-28	362	43
230	12-29	363	44
231	12-30	364	45
232	12-31	365	46
233	1-1	1	47
234	1-2	2	48
235	1-3	3	49
236	1-4	4	50
237	1-5	5	51
238	1-6	6	52
239	1-7	7	53
240	1-8	8	54
241	1-9	9	55
242	1-10	10	56
243	1-11	11	57
244	1-12	12	58
245	1-13	13	59
246	1-14	14	60
247	1-15	15	61
248	1-16	16	62
249	1-17	17	63
250	1-18	18	64
251	1-19	19	65
252	1-20	20	66
253	1-21	21	67
254	1-22	22	68
255	1-23	23	69
256	1-24	24	70
257	1-25	25	71
258	1-26	26	72
259	1-27	27	73
260	1-28	28	74
261	1-29	29	75
262	1-30	30	76
263	1-31	31	77
264	2-1	32	78
265	2-2	33	79
266	2-3	34	80
267	2-4	35	81
268	2-5	36	82
269	2-6	37	83
270	2-7	38	84
271	2-8	39	85
(FOURTH UNMANNED PERIOD)			
272	2-9	40	86
273	2-10	41	87

Table 1.1 SKYLAB MISSION DAY TIME REFERENCE

Table 1.2
Skylab System Reports

TMX-64808	MSFC Skylab Final Program Report
TMX-64809	MSFC Skylab Corollary Experiments Final Technical Report
TMX-64810	MSFC Skylab Airlock Module Final Technical Report
TMX-64811	MSFC Skylab Apollo Telescope Mount Final Technical Report
TMX-64812	MSFC Skylab Multiple Docking Adapter Final Technical Report
TMX-64813	MSFC Skylab Orbital Workshop Final Technical Report
TMX-64814	Skylab Mission Report-Saturn Workshop
TMX-64815	MSFC Skylab Apollo Telescope Mount Summary Mission Report
TMX-64817	MSFC Skylab Attitude & Pointing Control System Mission Evaluation Report
TMX-64818	MSFC Skylab Electrical Power System Mission Evaluation Report
TMX-64819	MSFC Skylab Instrumentation & Communication System Mission Evaluation Report
TMX-64820	MSFC Skylab Corollary Experiments Systems Mission Evaluation Report
TMX-64821	MSFC Skylab Apollo Telescope Mount Experiment Systems Mission Evaluation Report
TMX-64822	MSFC Skylab Thermal & Environmental Control System Mission Evaluation Report
TMX-64823	MSFC Skylab Apollo Telescope Mount Thermal Control System Mission Evaluation Report
TMX-64824	MSFC Skylab Structures & Mechanical Systems Mission Evaluation Report
TMX-64825	MSFC Skylab Crew Systems Mission Evaluation Report
TMX-64826	MSFC Skylab Contamination Control Systems Mission Evaluation Report

A number of integrated subsystems were utilized in making the Skylab a comfortable "home" in space for the astronauts. The active heating and cooling systems, the gas circulation loop and the passive thermal control coatings combined to maintain the internal thermal environment within an acceptable band. The active cooling system also provided a heat sink for numerous coldplated components. The two gas control system along with venting and pressurization components served to provide a 5 PSIA mixed oxygen/nitrogen atmosphere during manned operations as well as providing control pressure for some equipment and pressurant gas for certain operational equipment and experiments. The gas system also provided oxygen to the crewmen during EVA activities. The carbon dioxide and humidity removal systems controlled the levels of these two metabolic products, along with providing removal of contaminants from other sources, to assure a safe and comfortable atmosphere. The ATM C&D and EREP water loops provided cooling for coldplated electronic components in these prime experiment packages and a water cooling loop providing cooling to the crewmen during EVA activities. Finally, the food and certain biological wastes were maintained in an acceptable temperature regime by the refrigeration subsystem. Taken collectively these subsystems made up the Skylab environmental and thermal control systems.

The planned orbital attitude of Skylab was nominally to be solar inertial with the exception of Z-local vertical maneuvers to make resource observations. However, due to the loss of the meteoroid shield during SL-1 boost, certain maneuvers were necessary to avoid overheating the orbital assembly prior to deployment of an improvised solar shield at the beginning of the first manned mission. As an added mission bonus the comet Kohoutek passed in near proximity to Earth looping around the Sun in the time frame of SL-4. To take advantage of this scientific event special maneuvers were executed to optimize observation and study of this celestial visitor.

To circumvent the loss of the meteoroid shield, an umbrella type shield was ferried up to Skylab with the SL-2 crew. Deployment of this shield allowed living a near normal first mission. Later, during SL-3, another shield was deployed external to the original shield allowing the internal temperatures to reach preflight anticipated values. Assessment of the design and performance of these shields are detailed herein.

Overall, the thermal and environmental control systems maintained an acceptable environment for the crews and experiments. However, in addition to the shield anomaly discussed above, other anomalies occurred such as sticking of the temperature control valves in the Airlock Module cooling loop, leakage of coolant in both of the airlock coolant loops and failure of the refrigeration subsystem bypass valve. Management of these

systems and remedial actions to achieve a successful mission despite these anomalies required the close coordination and ingenuity of various design and analysis groups within the Marshall and Johnson Centers supported by elements of the prime contractors. Completion of mission objectives, a wealth of scientific information, along with favorable crew comments on the livability of Skylab attest. to the success of these coordinated efforts.

SECTION II. ATMOSPHERE CONTROL SYSTEM

A. Configuration

The configuration of the CO_2, humidity, and odor control subsystems are discussed in the following paragraphs.

1. Carbon Dioxide Control System Configuration. The partial pressure of CO_2 was controlled in the cluster during the Skylab missions by the molecular sieves located in the Airlock Module. There was also a lithium hydroxide (LiOH) system located in the CSM which was capable of controlling the partial pressure of CO_2 when the CSM was isolated from the rest of the cluster. The LiOH System also could have been used for a short time in a contingency mode to control the partial pressure of CO_2 in the cluster should the two molecular sieve systems have failed.

Figure 2-1 presents an overall schematic of the cluster Atmosphere Control System, showing the location of the molecular sieves. Figure 2-2 presents a schematic of one of the two molecular sieves, also called the Regenerable CO_2 Removal Systems (RCRS). As shown in figure 2-1, the cluster atmosphere containing O_2, N_2, water vapor and CO_2 was pulled into the Atmosphere Control System by one of the two compressors in each of the molecular sieve systems, after first passing through solids traps. Check valves were located downstream of each compressor to prevent backflow through the inactive compressor. The gas then flowed through one of the two condensing heat exchangers where the dewpoint of the gas was lowered to approximately 47°F. The condensing heat exchanger to be used was selected by an air flow diverter valve downstream of the two condensing heat exchangers.

Only one of the two molecular sieves (Mole Sieve A) was in use at one time for CO_2 removal. However, cluster atmosphere was also circulated through one condensing heat exchanger, the charcoal canister and the bypass muffs in the inactive molecular sieve, in order to provide additional water vapor and odor removal capability. In the RCRS with the active molecular sieve, preflight test data indicated that approximately 34 CFM would be pulled in by the compressor and split into three paths so that approximately 10 CFM would flow through the molecular sieve, 11 CFM would flow through the charcoal, and 13 CFM would flow through the bypass muffs. In the RCRS with the inactive molecular sieve, approximately 29.0 CFM would be pulled in by the compressor and split into two paths so that 13.0 CFM would flow through the bypass muffs.

Each molecular sieve consisted of two separate beds, each bed containing 10.35 pounds of type 13X Zeolite (used as a pre-dryer section) and 7.0 pounds of type 5A Zeolite (used for CO_2 removal).

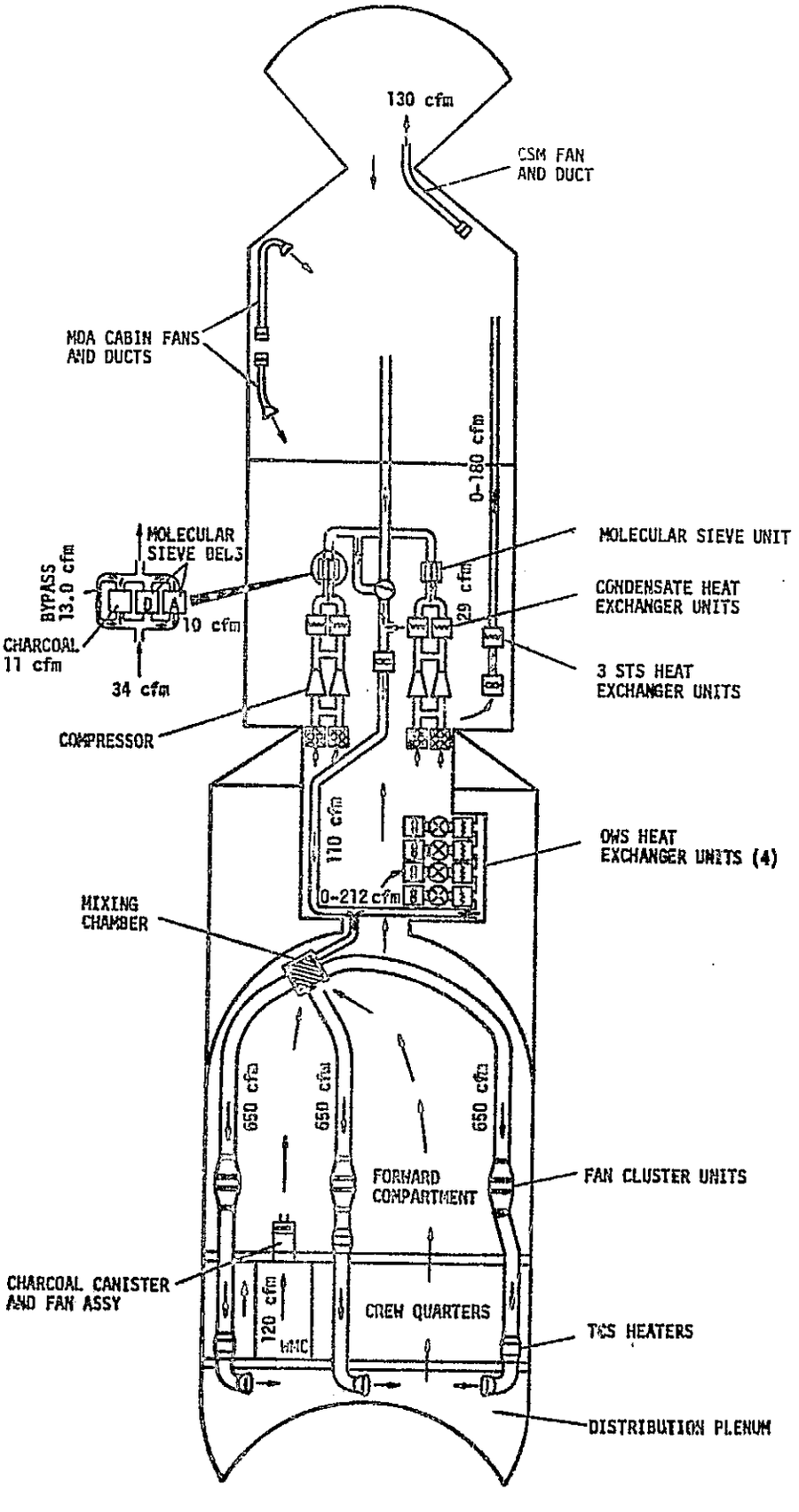

Figure 2-1. Atmosphere Control System

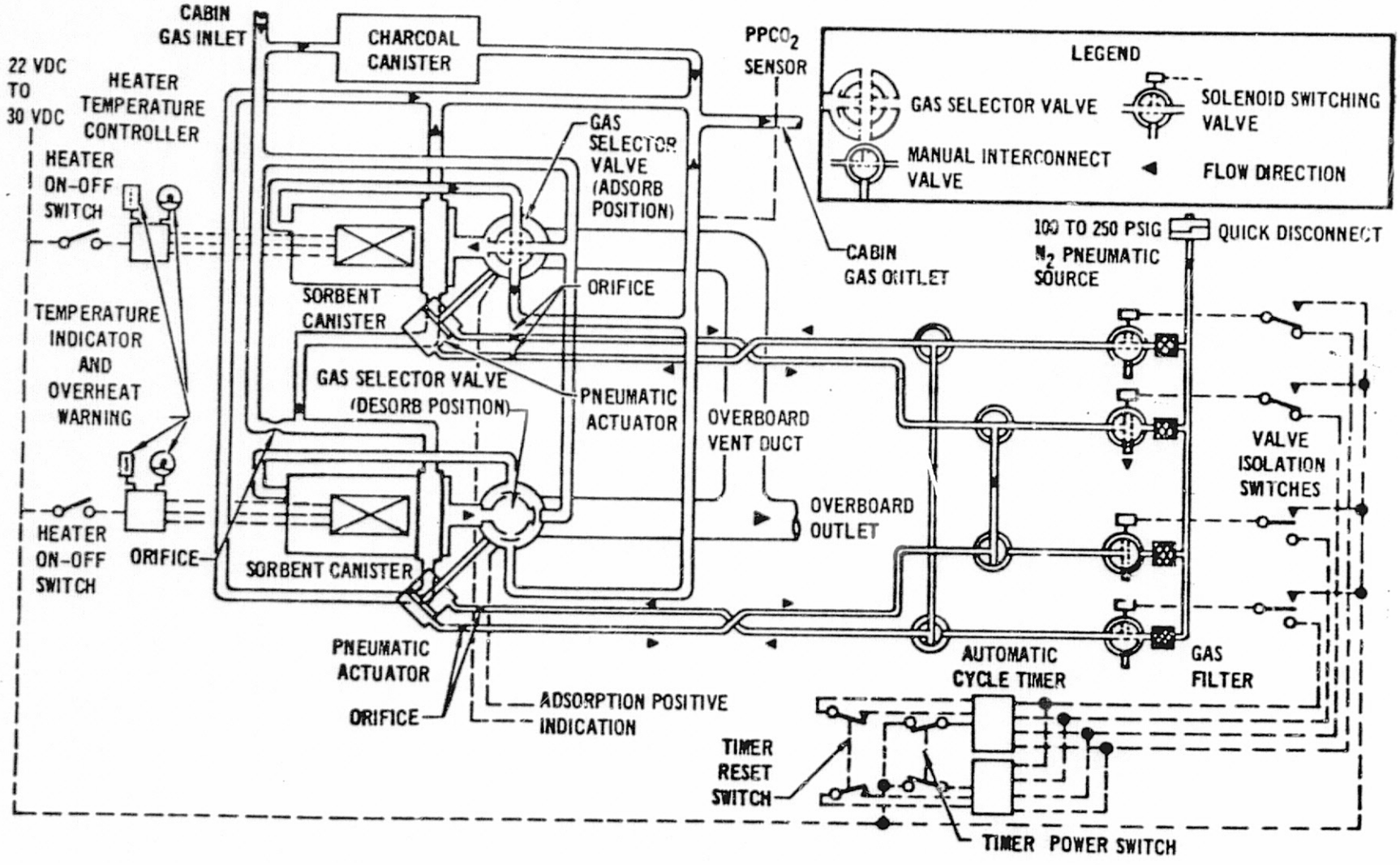

Figure 2-2. Single Molecular Sieve System

The moisture present in the 10 CFM that flowed into the molecular sieve would have almost all of the moisture in it removed by the 13X Zeolite in order to maximize the CO_2 removal efficiency of the 5A portion of the bed.

During the normal operation of a molecular sieve system, each sorbent canister operated on a 15-minute half cycle to alternately adsorb CO_2 and H_2O from 10.0 CFM (15.5 lb/hour) cabin gas flow and desorb to vacuum. The gas selector valves were cycled automatically by the pneumatic valves and the solenoid valve selector switches. The design CO_2 removal rate was 6.75 lb/day. The design inlet CO_2 partial pressure was 5.5 mm Hg or less with one molecular sieve system operating. The electrical power required for the operation of each system was 57.7 watt-hours/day at 24 VDC, exclusive of exhaust duct heaters.

Cabin CO_2 partial pressure was measured at the inlet to each molecular sieve system. Outlet CO_2 partial pressure was measured by two sensors at the outlet of the sorbent canisters of the operating molecular sieve. Onboard display and telemetry (TM) of the inlet measurements for both molecular sieve systems and one of the outlet measurements for the active molecular sieve system were provided. The outlet measurements both fed the Caution and Warning (C&W) System. Maximum specification inaccuracy of the transducers was ± 1.4 mm Hg.

The sorbent canisters could be baked out electrically when required. The active molecular sieve canisters were baked out at the beginning of each manned phase of the mission. During the manned phases of the mission, they were to be baked out when the PCO_2 level indicated bed degradation. A maximum of 1912 watt-hours at 24 VDC were required for bakeout of both sorbent canisters in each molecular sieve system. The sorbent canister housing was cooled by gas flow through the bypass muff during bakeout. Bakeout time was a minimum of five hours/canister followed by a 12-hour cool down period during which time the bed could be used.

Each molecular sieve system had redundant cycle timers and manual interconnect valves which provided isolation and permitted use of redundant solenoid switching valves. In addition, each sorbent canister had a separate bakeout heater temperature controller.

In the event that more than one sorbent canister could not have been operated, the inlet PCO_2 could have been limited to 12 mm Hg maximum with one canister operation for the design CO_2 removal rate of 6.75 lb. day and an inlet dewpoint temperature of 52°F or less.

The overboard gas loss for a molecular sieve system was shown by ground tests over an inlet dewpoint temperature range of 40°F to 52°F to be 2.0 to 2.5 lb/day. The O_2 and N_2 losses varied from 1.5 to 2.1 lb/day for O_2 and 0.44 to 0.69 lb/day for N_2.

After passing through the molecular sieve bed, the charcoal bed and the bypass muffs, the flows were recombined in the active molecular sieve system and the charcoal and bypass flows were recombined in the inactive molecular sieve system. The flows from the two systems were then combined and dumped into the molecular sieve outlet duct. A diverter valve located in the duct allowed the crew to direct the atmosphere control system outlet either to the MDA, to the OWS, or to split the flow between the two.

Monitoring capability for the CO_2 Control System is summarized in Table 2.1.

Table 2.1. CO_2 Performance Monitoring Capability

	MEASUREMENT	TM	C&W	ONBOARD DISPLAY
1.	CO_2 PARTIAL PRESSURE AT COMPRESSOR INLET	D209, D213	X	Panel 203
2.	CO_2 PARTIAL PRESSURE AT MOLECULAR SIEVE OUTLET	D210, D214	X	Panel 203
3.	MOLECULAR SIEVE BED TEMPERATURE		X	Panel 203
4.	MOLECULAR SIEVE OVERBOARD DUMPLINE TEMPERATURE	C266, C267		
5.	MOLECULAR SIEVE FLOW RATE	F210, F211	X	
6.	COMPRESSOR DELTA P	D212, D216		

2. Humidity Control System Configuration - The cluster humidity was controlled during the Skylab missions by the four condensing heat exchangers and by the two molecular sieves, all of which were located in the Airlock Module. There was also a condensing heat exchanger located in the CSM which was capable of controlling humidity when the CSM was isolated from the rest of the cluster.

Of the four condensing heat exchangers in the system, two were nominally in use, one in each molecular sieve system. The capability of the condensing heat exchangers to condense moisture was determined by the coolant inlet temperatures. Nominal specification temperature of the coolant inlet to the condensing heat exchangers was 47°F with a controlled range of ± 2°F. The performance capability of the condensing heat exchangers was great enough so that the dewpoint of the outlet gas flow was normally within one or two degrees of the coolant inlet temperature. There were two coolant loops which flowed through the condensing heat exchangers, each flowing approximately 265 lb/hour. Half of the primary and half of the secondary coolant flows went to each molecular sieve system. In each molecular sieve system, there were shut-off valves located such that the crew could direct all of the coolant flow that came to each system through one condensing heat exchanger, or allow half to each, thus putting one quarter of the total primary and one quarter of the total secondary flow through each condensing heat exchanger. The nominal operating mode was to route all of the primary and all of the secondary flow that came to each molecular sieve system through condensing heat exchanger A in each system.

Gas flow into the condensing heat exchanger in the active molecular sieve system was approximately 34.0 CFM while specification gas flow into the condensing heat exchanger in the inactive molecular sieve system was approximately 29.0 CFM.

The Condensate Removal System, figure 2-3, provided the capability of removing the condensate collected in the condensing heat exchangers and storing it in the AM condensate tank, located in the STS portion of the AM and in the OWS condensate holding tank, located in the forward dome area of the OWS. The primary method of subsequent disposal of the stored condensate was to dump the condensate through a dump probe, located in the Waste Management Compartment (WMC), into the waste tank. An alternative method of disposal was to dump the condensate from the AM condensate tank overboard through one of the two AM condensate vents. Other usages of the Condensate Removal System included the provision to remove gas from the liquid/gas separators, the capability to evacuate and deservice Life Support Umbilicals (LSUs) and Pressure Control Units (PCUs), the capability to receive CSM waste tank water, and the provision to initially wet the plates in the condensing heat exchangers. Both liquid/gas separators were built into a single unit which was connected to the water side of the condensate removal system. The separators were isolated from each other and protected against back flow by redundant check valves. Two spare liquid/gas separators units were stored in the AM. The HX plate service QD

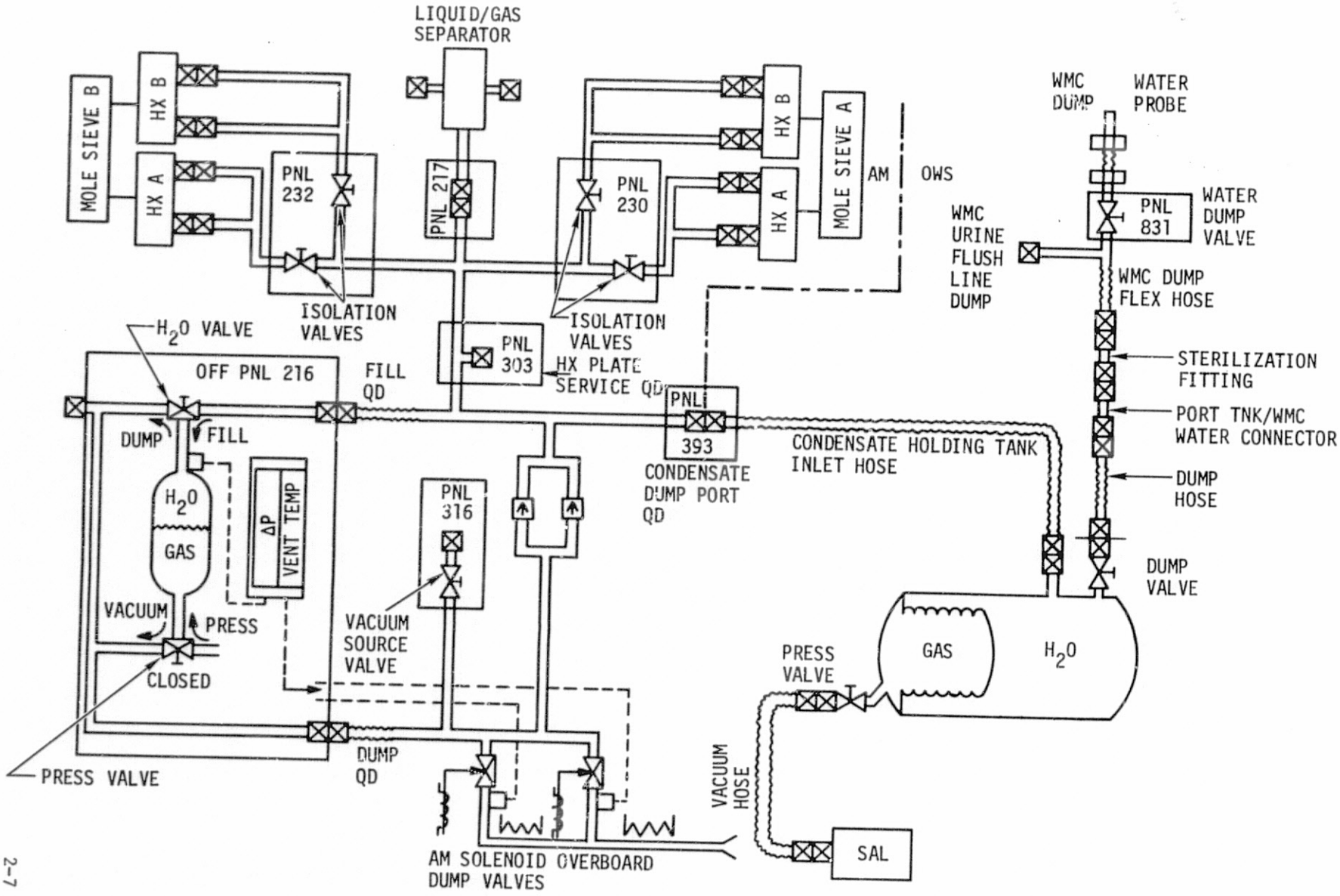

Figure 2-3. Condensate Control System

was used to provide an initial delta P for wetting the plates in the condensing heat exchangers. It was also used to transfer water from the CSM waste tank to the condensate holding tank.

Each condensing heat exchanger contained two in-flight replaceable water separator plate assemblies. An additional four water separator assemblies were carried in permanent stowage container No.202 in the AM for use as in-flight replacements. All 12 water separator assemblies were launched dry with both sides of the plates vented to cabin. These plates could be serviced in orbit by the moisture which was initially condensed in the heat exchanger (self-wetting) or by several inflight servicing techniques.

Servicing and deservicing support consisted of providing 13 pounds of condensing heat exchanger separator assembly wetting solution stored within the spare condensate module. The water solution contained 10% Roccal (biocide), and 1% Sterox NJ (wetting agent) by volume. For normal plate servicing, the tank module was strapped down adjacent to the H_2O separator service position QD in the STS and connected sequentially to each separator plate by a plate adapter. Valving on the spare module was used to force water from the tank through the plate.

To preserve fluid and the normal service capability after an in-flight condensate module replacement, a jumper hose permitted transfer of service fluid between condensate modules. When water solution was unavailable from either module, the manual pump could be used as a pressurant source to service with condensate from the installed module. In addition, the manual pump could have been used with the spare module for a fast service of a single plate in the OWS or STS. During the flight, servicing was performed normally so these alternate methods were not required.

After servicing, the pressure within the storage tanks was sufficiently low to cause moisture condensed in the heat exchangers to be forced through the exchanger water separator plates and transferred into the storage tank by compartment ambient pressure. When the condensate tank pressure increased to approximately 0.5 PSI below cabin ambient pressure, the collected condensate and gas were dumped. A caution signal on the C & W system was provided when the cabin ambient-to-condensate tank pressure differential decreased to 0.4 PSID.

Operation of the Condensate Removal System was accomplished primarily from panel 216 (figure 2-3). During normal operation, the H_2O valve was in the "FILL" position and the PRESS valve was in the "CLOSED" position. The FILL QD and the DUMP QD were connected. The OWS inlet hose (also called the OWS condensate tank inlet hose) was connected at both the OWS condensate holding tank and at panel 393 (figure 2-3_. The PRESS valve and the DUMP valve on the holding tank were both closed. Condensate from the condensing heat exchangers could fill up the water sides of the AM condensate tank and the OWS condensate holding tank. Since the holding tank was over 40 times as large as the condensate tank, over 40 times as much condensate could be stored in the holding tank. Either tank could have been operated without the other on line, except that, unless the AM condensate tank was on line and the H_2O valve was in the "FILL" position, it was not possible to monitor the delta P betweem condensate system and cabin. When the AM condensate tank was full, the condensate and gas in the system could be dumped overboard through 1 of the 2 AM solenoid dump valves, or dumped back into the holding tank. Condensate and gas in the holding tank were dumped into the waste tank by dumping through the WMC water dump prove. Figure 2-4 presents a schematic of all dump proves into the waste tank. The holding tank was connected to the WMC water dump probe by using the holding tank dump hose, the portable tank/WMC H_2O connector, the sterilization fitting, and the WMC water dump line. The water dump valve on panel 831 and the dump valve on the holding tank controlled the dumping of condensate into the waste tank. The PRESS valve on the holding tank and the condensate press fitting allowed cabin gas into the gas side to help "push" the condensate out of the holding tank and into the waste tank. After this had been accomplished the PRESS valve was connected to a QD in one of the SALs by the vacuum hose and the gas side of the holding tank was dumped to a vacuum again.

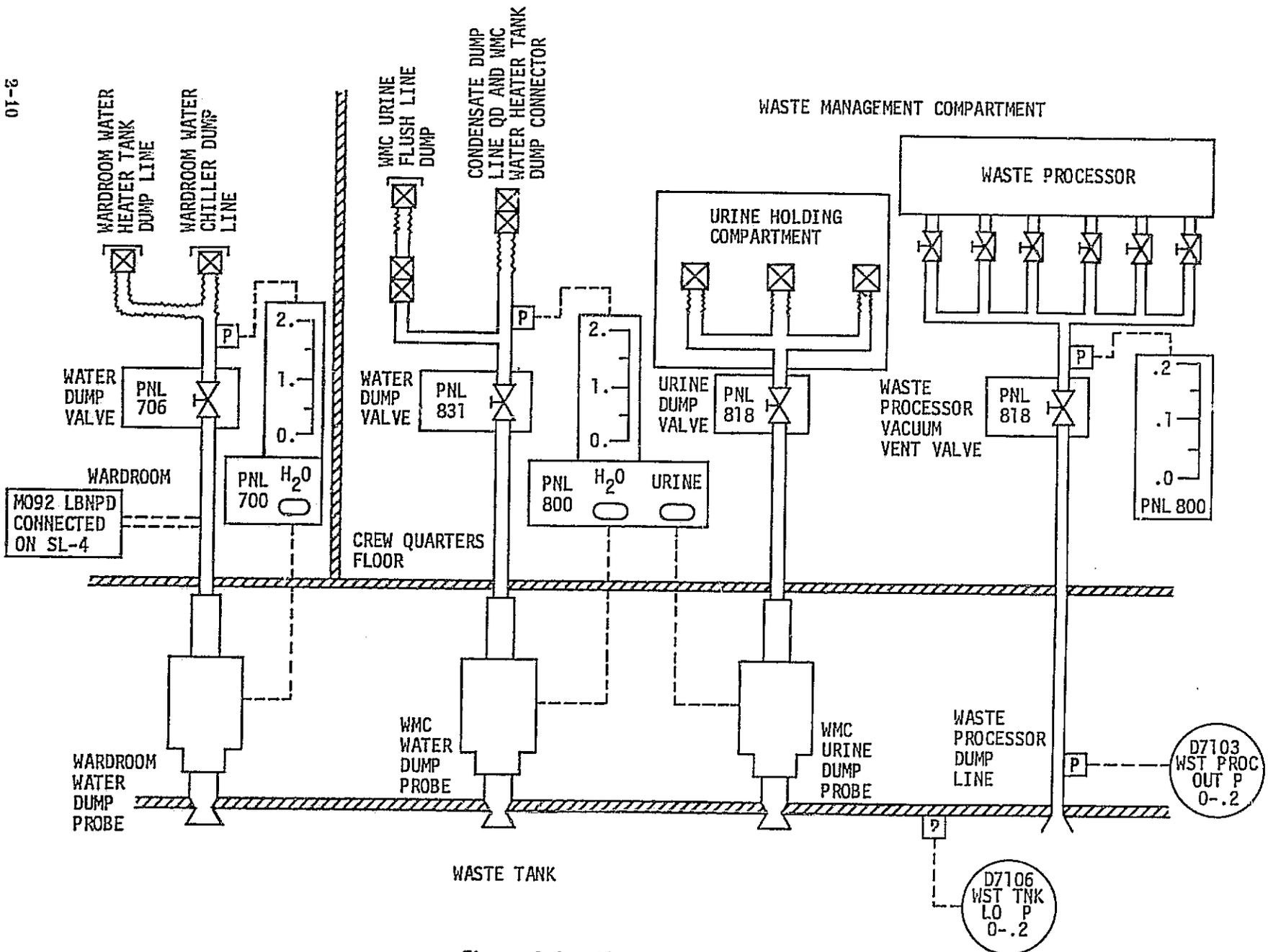

Figure 2-4. Cluster Waste Tank Dumps

Dumping of the AM condensate tank overboard was accomplished by positioning the manual condensate tank pressure valve in the "PRESS" position so that cabin pressure was applied to the gas side of the bladder, placing the manual condensate tank H_2O valve in the "DUMP" position, and opening the valve in the dump line. When the position of the condensate tank bladder indicated the water was dumped, the condensate tank H_2O valve was placed in the "FILL" position. The valve in the dump line was then closed. Prior to the AM overboard dump operation, the exit line electrical heater was used to warm the exit line as required, and one of the two solenoid valves at the exit was powered.

The Condensate Removal System employed redundant check valves in the transfer line, overboard dump line exits, solenoid valves and electrical heaters. The condensate tank module was in-flight replaceable. A spare condensate tank module was carried in the STS and transferred to the OWS during initial activation. Table 2.2 presents a summary of the monitoring capability for the dewpoint control system.

3. Odor Removal System Configuration - Odor removal in the cluster was provided during the Skylab missions by two charcoal canisters in the AM and by one charcoal canister in the OWS. The charcoal canister in the OWS was part of the Waste Management Compartment (WMC) ventilation unit, which was mounted on the forward compartment floor over the WMC. This assembly was composed of a fan, charcoal bed, filters, and sould suppressor assembly. The fan was an Apollo PLV (Post-Landing Ventilation) fan and was replaceable. The charcoal canister contained activated charcoal and was also replaceable. Removal of Particulate matter, hair, and lint from the OWS atmosphere was provided by the combination of a fine and coarse filter at the inlet to the assembly. A cut-away view, shown in figure 2-5, indicates the overall

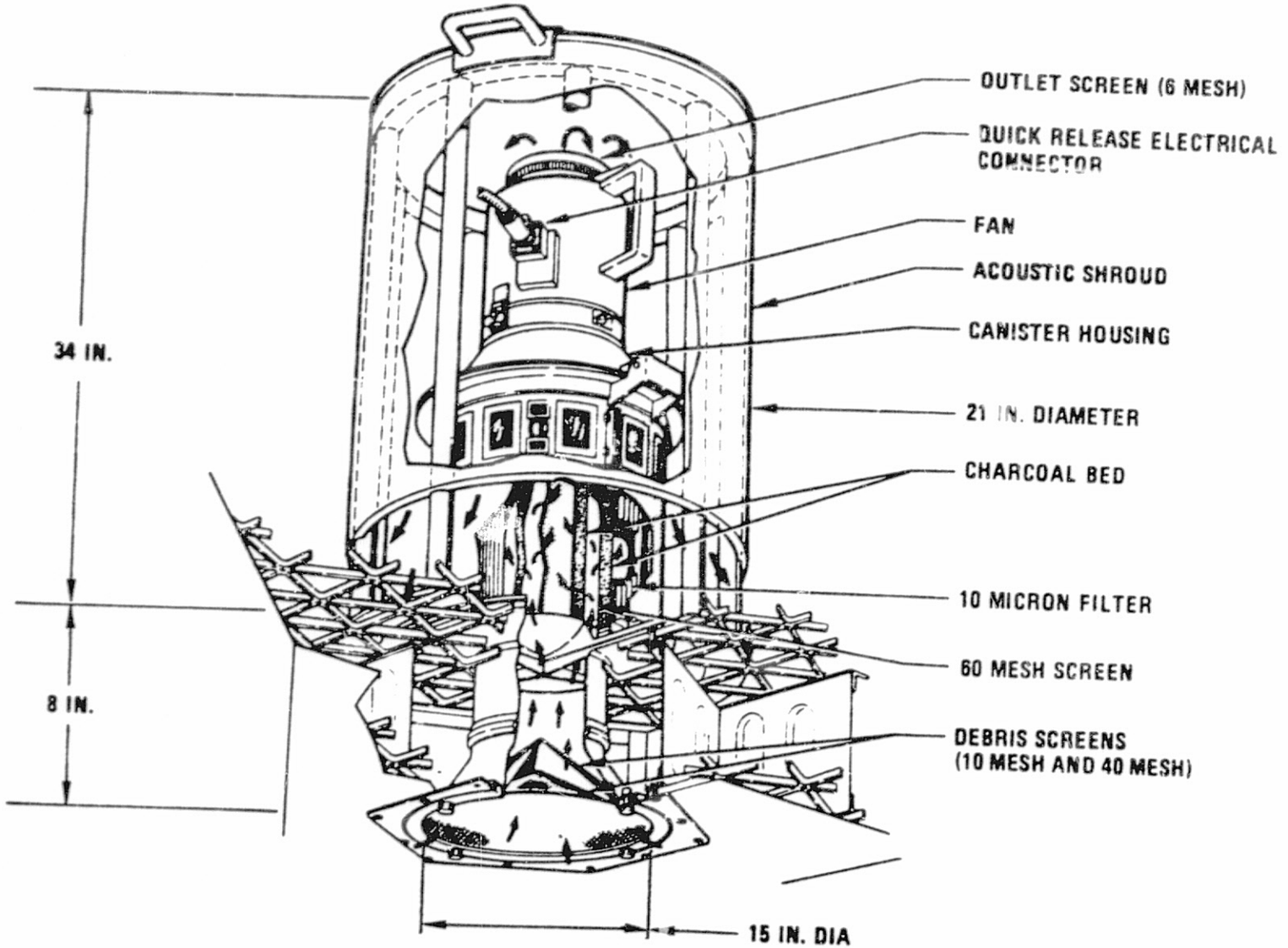

Figure 2-5. Waste Management Compartment Ventilation Unit

dimensions and the various screen mesh sizes. The fine inlet screen was upstream of the coarse inlet screen. The upstream restraining screen for the activated charcoal was 60 mesh, with the downstream restraining screen being a 10-micron filter. All of the atmosphere flowing through the WMC, except compartment leakage, was drawn in through the circular diffuser in the floor of the WMC, passed through the fan/filter assembly, and was discharged into the forward compartment.

During normal operation, the WMC fan was planned to be operated continuously whenever the WMC was occupied. The anticipated fan/WMC flow at a nominal 26 VDC was 105 CFM with fan operation and approximately 18 CFM without fan operation.

The configuration of the AM odor removal charcoal canister in the Molecular Sieve System was discussed in paragraph II. A.1.

Table 2.2. Humidity Performance Monitoring Capability

	MEASUREMENT	TM	C&W	ON BOARD DISPLAY
1.	DEWPOINT TEMPERATURE	C207, C215		Panel 203
2.	COOLANT INLET TEMPERATURE TO COND. HX.	C209, C210 C217, C218		
3.	COOLANT OUTLET TEMP. TO COND. HX.	C211, C212 C219, C220		
4.	COMPRESSOR GAS INLET TEMPERATURE	C205, C213		Panel 203
5.	CONDENSING HX. GAS OUTLET TEMPERATURE	C206, C214		Panel 203
6.	CONDENSATE TO CABIN DIFFERENTIAL PRESSURE	D208	X	Panel 216
7.	CONDENSATE VENT TEMPERATURE			Panel 216
8.	CONDENSATE HX. GAS FLOW RATE	F210, F211	X	
9.	CONDENSATE HX. COOLANT FLOW RATE	F214, F215		

4. Contamination Removal System Configuration - Material selection control was utilized to minimize material offgassing and subsequent buildup of contaminant levels. In addition atmospheric analysis of the MDA/AM at McDonnell Douglas-Eastern Division and the OWS at KSC during preflight checkouts were used to provide confidence that this material selection control was adequate in minimizing contaminant levels. No measurable contaminant levels were noted during OWS testing but a carbon monoxide level of 23 PPM was noted during MDA/AM testing. Because of dispersion of simultaneous CO readings during the MDA/AM test it was concluded that the 23 PPM level was unrealistic and a much lower level could be expected in-flight.

The charcoal canisters in the molecular sieve unit and waste management systems, condensing heat exchangers (CHX) and 13X and 5A molecular sieve material had considerable capability to scrub the cabin air of generated contaminants (figure 2-6). Analysis of Apollo charcoal canisters indicated the presence of many contaminants. Tests run at MSFC indicated that the CHX had some capability to remove contaminants while the mole-sieve material was a very effective contaminant removal device. A list of contaminants tested along with mole-sieve and CHX removal efficiency is shown on Table 2.3. This list of contaminants was compiled from those found in Apollo flights as supplied by JSC and others selected because of the likelyhood that they would be found in the Skylab atmosphere. The possibility that significant buildup of contaminants would occur was very small because of material selection control and the presence of onboard removal devices.

B. System Performance

1. Carbon Dioxide (CO_2) Control System Performance - The CO_2 control system performed very well throughout all of the Skylab missions. No hardware failures of any type were experienced on molecular sieve A and, as a result, molecular sieve B was never activated. Molecular sieve A was operated continuously throughout the 84 days of the SL-4 mission without requiring a mid-mission bakeout. The molecular sieve had been qualified based on bakeouts at 28 day intervals.

a. CO_2 levels - Preflight analysis had indicated that the molecular sieve would maintain the CO2 level at approximately 5.0 mm Hg. Although flight levels were subject to some interpretation due to molecular sieve system CO_2 sensor accuracy ($\pm$ 1.4 mm Hg), evaluation of all available data indicates they performed near predicted values. Means other than the molecular sieve sensors to monitor CO_2 levels were available onboard the Skylab. Unfortunately,

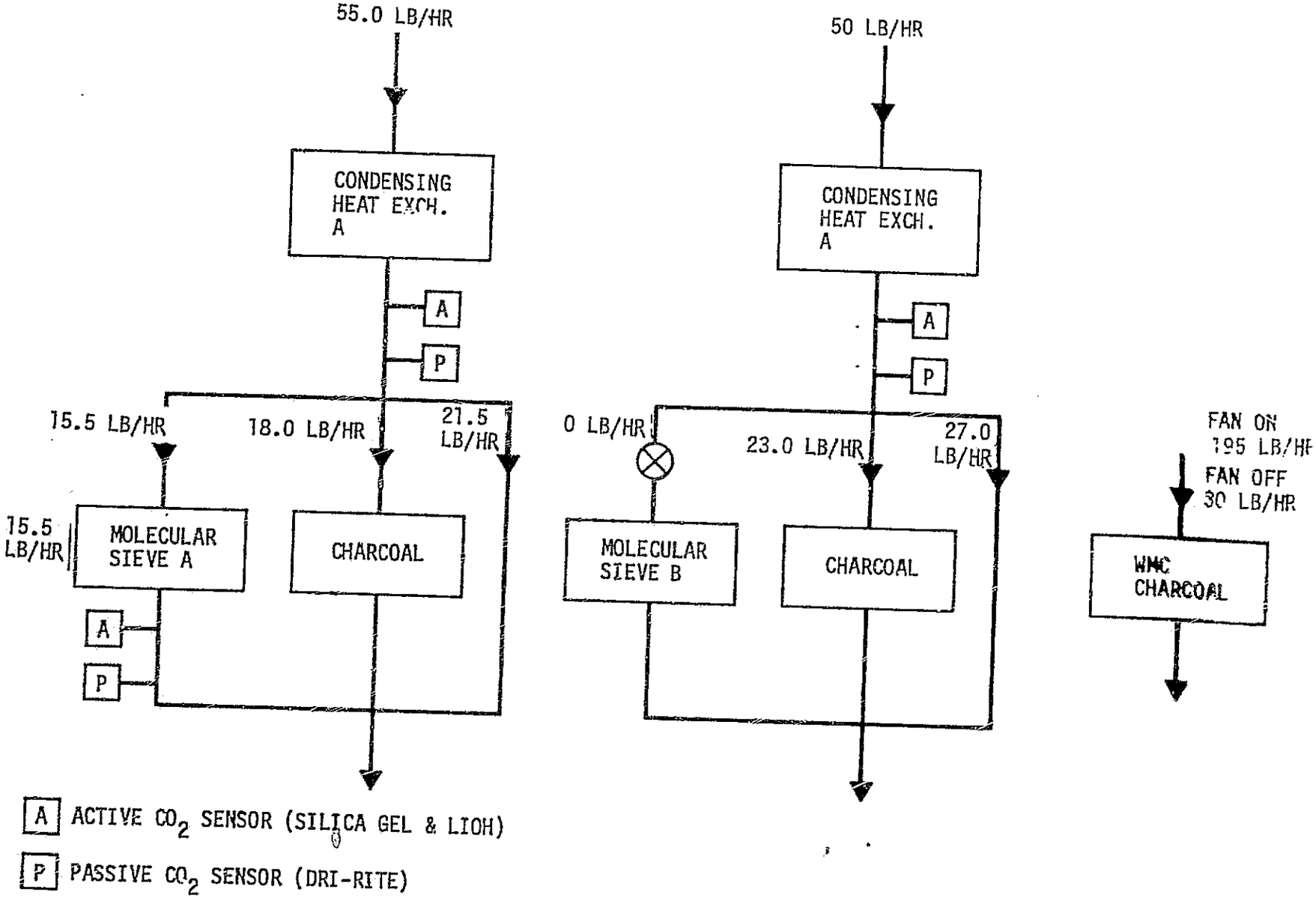

Figure 2-6. Atmosphere Contaminant Removal

Table 2.3. Molecular Sieve Contaminant Test List

CONTAMINANT	TEST INLET CONCENTRATION, PPM	REMOVAL EFFICIENCY, % CHX	MOLE-SIEVE
1. HYDROGEN	900.	(1)	0.
2. AMMONIA	60.	(1)	100.
3. METHYL CHLORIDE	20.	(1)	100.
4. FREON 12	500.	(1)	100.
5. BENZENE	5.	8.7	100.
6. FREON 113	500.	(1)	100.
7. XYLENE	50.	(1)	100.
8. TOLUENE	50.	(1)	100.
9. ACETONE	500.	(1)	100.
10. ISOPROPYL ALCOHOL	100.	(1)	100.
11. ACETALDEHYDE	50.	2.6	100.
12. METHYL ISOBUTYL KETONE	10.	33	100.
13. DICHLOROMETHANE	25.	(1)	100.
14. CARBON MONOXIDE	75.	(1)	0.
15. METHYL CHLOROFORM	90.	15.2	100.
16. METHYL ETHYL KETONE	100.	1.1	100.
17. COOLANOL 15	50.	89.	100.

(1) Not tested.

one of them - the portable CO_2/dewpoint monitor - had failed earlier due to the high temperatures in the OWS where it had been stowed, and could not be used. The other method involved using the M171 mass spectrometer in the OWS. Prior to and following each M171 performance, a sample of cabin gas was analyzed by the mass spectrometer, and the percent, by volume, of O_2, H_2O, and CO_2 in the cabin gas were read out to the ground by the crew. By knowing the cluster total pressure at the time, it was possible to calculate the partial pressures of O_2, H_2O, and CO2. (It was decided to only use the data for the cabin gas sample taken prior to M171. It was felt that any residual gases from the crews' breath remaining in the system following an M171 performance could affect the values of the sample obtained after an M171 performance.)

Soon after MDA hatch opening on SL-2, it became apparent that the readings from the molecular sieve PCO_2 sensors varied somewhat from each other and from the preflight predictions. Throughout all of the missions, the M171 mass spectrometer data were used to "calibrate" the molecular sieve inlet CO_2 sensors. Eighteen data samples during SL-2, 27 samples during SL-3 and 36 samples during SL-4 were obtained and used. Analysis of all the data resulted in the conclusion that the molecular sieve A inlet sensor (D209) remained within specification limits while the molecular sieve B inlet sensor (D213) was sometimes outside of specification limits.

Since both D209 and D213 provided lower indicated CO_2 levels than expected during SL-2, the cartridges were returned and checked. They were found to be good. In order to provide a further check on the sensors, a special set of cartridges was carried by the SL-3 crew which could be used to check the zero calibration of the CO_2 sensors. The D209 sensor was calibrated and found to be very accurate near zero (within .15 mm Hg). Although a calibration was performed on the D213 sensor, it was not successful. It was later determined that the sensor had a faulty O-ring (replaced during SL-4) which caused erratic readings throughout SL-3.

The calibration data from the M171 mass spectrometer have been used, along with the molecular sieve inlet sensor (D209) readings, to produce CO_2 profiles for the missions and the results are presented in figures 2-7, 2-8, and 2-9. The correction used on the D209 data averaged approximately 0.9 mm Hg and the correction always increased the quoted level from the level indicated by D209. As a result, the data provided are believed to represent an upper limit on the actual CO_2 levels. As indicated by the data, the CO_2 level during SL-2 was near the preflight prediction of 5.0 mm Hg. The level was slightly higher during SL-3 with the daily average generally being 5.5 mm Hg or lower. The level increased above

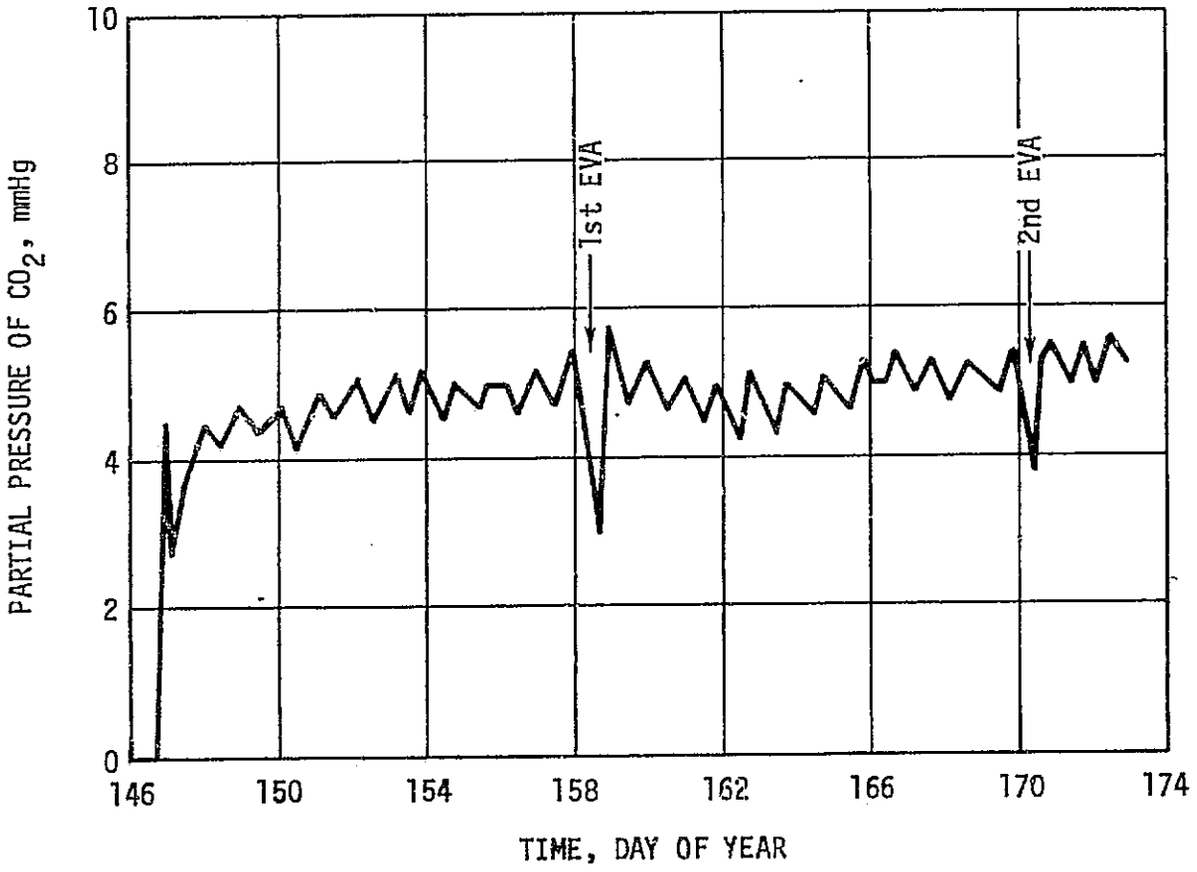

Figure 2-7. SL-2 Partial Pressure of CO_2 Profile

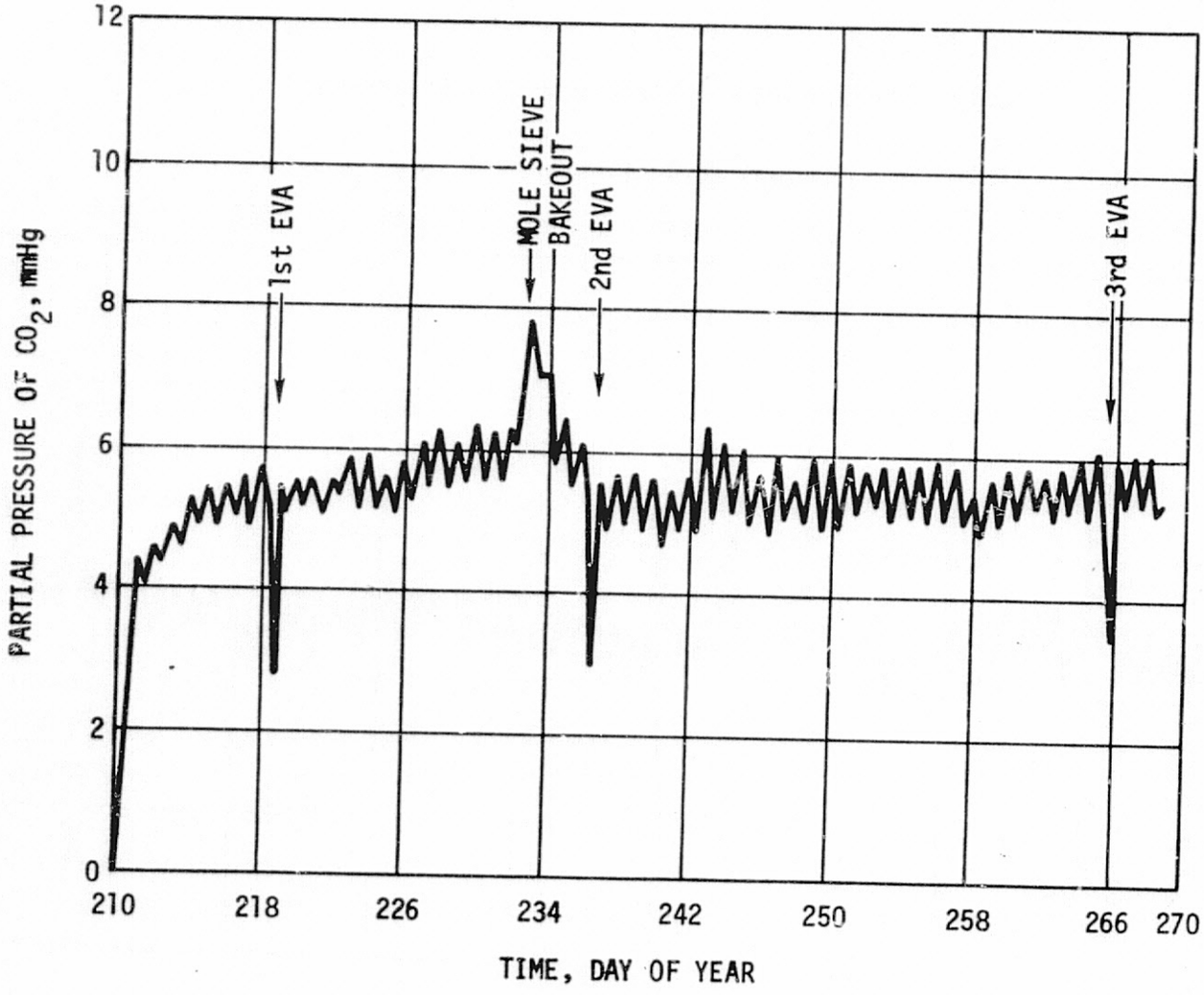

Figure 2-8. SL-3 Partial Pressure of CO_2 Profile

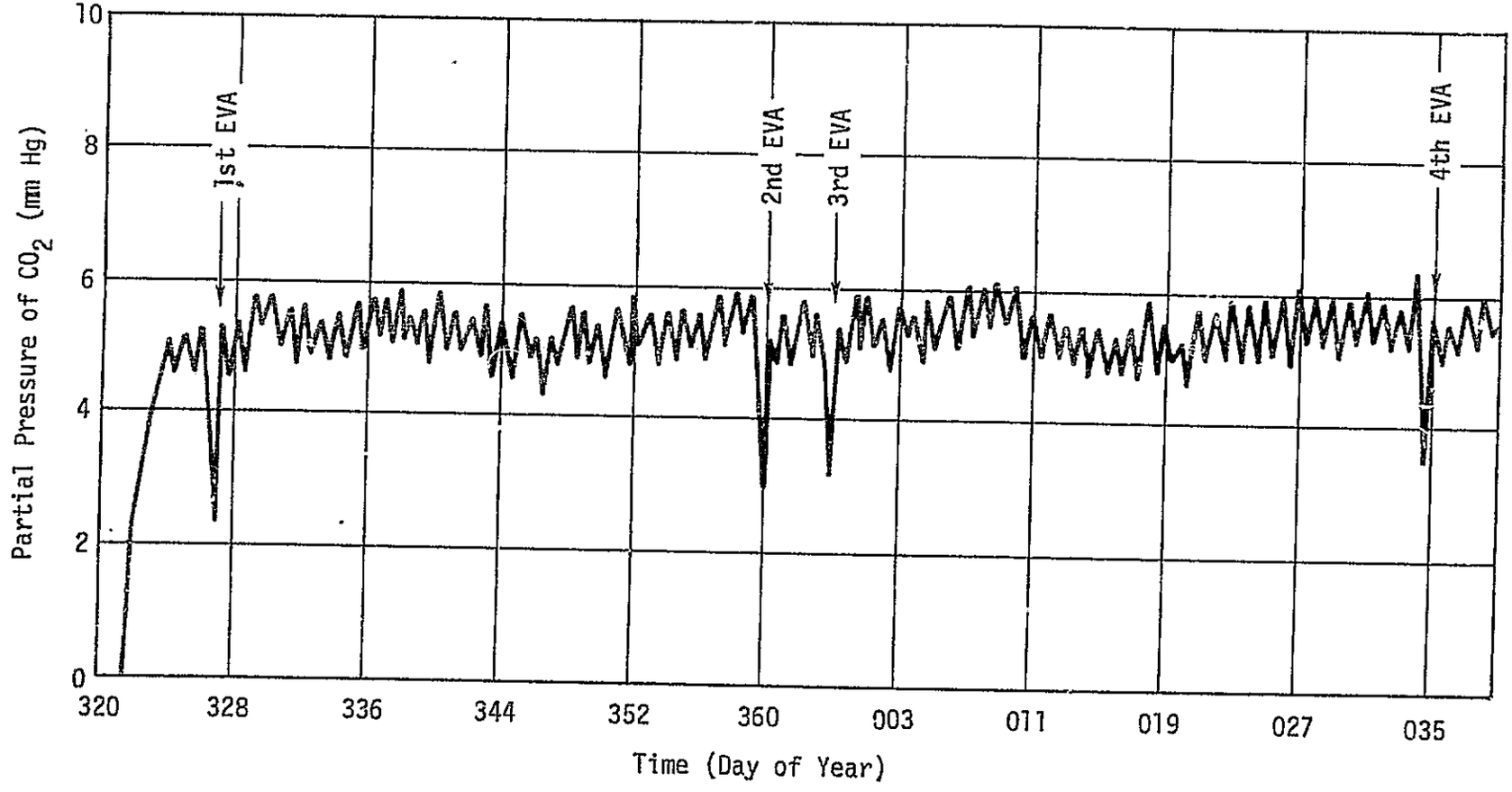

Figure 2-9. SL-4 Partial Pressure of CO_2 Profile

5.5 mm Hg after DOY 227 and a bakeout was performed on DOY 231 after which the level returned to lower values. The higher CO_2 levels during the bakeout (figure 2-8) were a result of the long bakeout times (Table 2.4) with only one bed functioning. As reported previously, the CO_2 levels were maintained at desired levels throughout SL-4 without a molecular sieve bakeout. The significantly lower CO_2 levels depicted during EVA days were a result of reduced CO_2 generation rates with only one crewman internal to the vehicle and the smaller volume of atmosphere being conditioned with the hatches closed.

b. Molecular Sieve Bakeout Summary - In additon to the mid-mission bakeout during SL-3, bakeouts were performed at the beginning of each mission. A summary is provided in Table 2.4. The long bakeout times reflected for the bakeout of bed 1 during SL-3 activation and for both beds during the SL-3 mid-mission bakeout resulted from scheduling convenience.

Table 2.4. Mole Sieve Bakeout Summary

		Bed 1	Bed 2
SL-2	Initiate Bakeout	146:18:05	147:14:45
	Terminate Bakeout	146:23:30	147:19:41
	Total Duration (Hours)	5:25	4:56
SL-3	Initiate Bakeout	210:01:30	210:11:50
	Terminate Bakeout	210:11:50	210:17:40
	Total Duration (Hours)	10:20	5:50
	Initiate Bakeout	232:01:10	233:02:04
	Terminate Bakeout	232:12:30	233:16:12
	Total Duration (Hours)	11:20	14:08
SL-4	Initiate Bakeout	321:15:43	321:21:15
	Terminate Bakeout	321:21:15	322:03:15
	Total Duration (Hours)	5:32	6:00

c. Molecular Sieve Timers - The molecular sieve A timers functioned properly throughout the mission. The primary timer was used during most of the missions and accumulated over 13,500 cycles. The secondary timer accumulated approximately 2500 cycles. The cycle time was normal for both timers and was a few seconds less than 15 minutes.

On several occasions during the missions, cycle interrupts occurred but all were found to be due to crew activities. An apparent cycling problem during SL-3 activation was found to be due to a failure of the crew to properly open the bed cycle N_2 supply valve. Molecular sieve bed "2" remained in adsorb for approximately three hours as a result of this problem. However, the bed recovered after cycling was initiated.

d. Molecular Sieve Compressor Performance - Molecular sieve compressors performed satisfactorily throughout the missions. As expected, based on preflight testing, the indicated flows from the flow sensors were erratic (a discussion is provided in Section III). However, compressor delta P was available via telemetry and the use of these data along with compressor delta P versus flow allowed the determination of compressor flow rates. The resulting flow rates are provided in Table 2.5 and compare well with expected values of 34 CFM for an operating molecular sieve and 29 CFM for a non-operating sieve.

Table 2.5. Mole Sieve Compressors ΔP and Flow Rate Summary

Mole Sieve Compressor	Mole Sieve	ΔP at 5.0 PSIA (in. H_2O)	Compressor Flow Rate (CFM)
MS A Pri	Off	7.13	28.3
MS A Pri	On	5.96	31.5
MS A Sec	Off	6.66	29.3
MS A Sec	On	5.42	33.6
MS B Pri	Off	5.82	31.9
MS B Sec	Off	6.98	28.5

During SL-3 activation the molecular sieve B secondary compressor inverter failed. The primary compressor was operated throughout the remainder of the missions. Normal operation for molecular sieve A was switched to the secondary compressor in order to provide balancing of AM electrical bus loads.

e. CO_2 Instrumentation Discrepancies - In addition to the concern relative to specification sensor accuracy (± 1.4 mm Hg), which was discussed in paragraph B.1.a of this section, several instrumentation discrepancies occurred during the missions. They are summarized briefly in the following paragraphs.

(1) Molecular Sieve B Inlet Sensor (D213) O-Ring - Data provided by the subject sensor were erratic during the SL-3 mission. The cause of the problem was determined to be associated with seating of the O-ring on the sensor endplate. The O-ring was replaced at the beginning of SL-4 and the sensor data stabilized.

(2) Tape Recorder Data Dump Effect on Molecular Sieve B Inlet Sensor (D213) - Each time the AM tape recorders were dumped via telemetry a transient increase in the indicated CO_2 level from the molecular sieve B inlet sensor was observed. The indicated level returned to normal within one to two minutes.

(3) Molecular Sieve Bed Cycling Effect on the Outlet CO_2 Sensor (D210) - A transient increase in indicated outlet CO_2 level was seen after each bed cycle. Typical outlet sensor profiles are provided in figure 2-10. It was determined that the increase was caused by a backflow of unconditioned gas (from the bypass and charcoal bed flow paths) into the sensor during the bed cycle. The indicated level returned to normal during the adsorb cycle.

2. Humidity Control System Performance

a. Cluster Dewpoint Levels - Dewpoint levels in the cluster were generally maintained within the required 46 to 60°F band during the Skylab missions. Profiles for the three missions are provided in figures 2-11, 2-12, and 2-13. Off nominal coolant inlet temperatures to the condensing heat exchangers during the periods of time when the thermal control valves (TCVB) were stuck (Section VII.) influenced the cluster dewpoint and produced transient dewpoints below 46°F. This influence is seen clearly in figure 2-11 and is also evident in figure 2-12 and 2-13. While the system was operating with the secondary coolant loop TCVB stuck and not modulating, the outlet temperature increased with beta angle. While this change was not normally great, its influence can be seen in figure 2-13 during the high beta period beginning at approximately DOY 11. Dewpoints somewhat below 46°F during EVA periods were expected due to the lower water production rates with only one crewman providing moisture and a reduced effective volume. The level quickly returned to normal following the EVA. A typical EVA dewpoint profile is provided in figure 2-14. Another factor which influenced the dewpoint for short periods of time was operation of the shower. This was most evident during SL-4 and some of the showers are designated on figure 2-13. On one occasion (DOY 19) the increased dewpoint level during a shower contributed to condensation in the aft cabin heat exchangers (see Section VII).

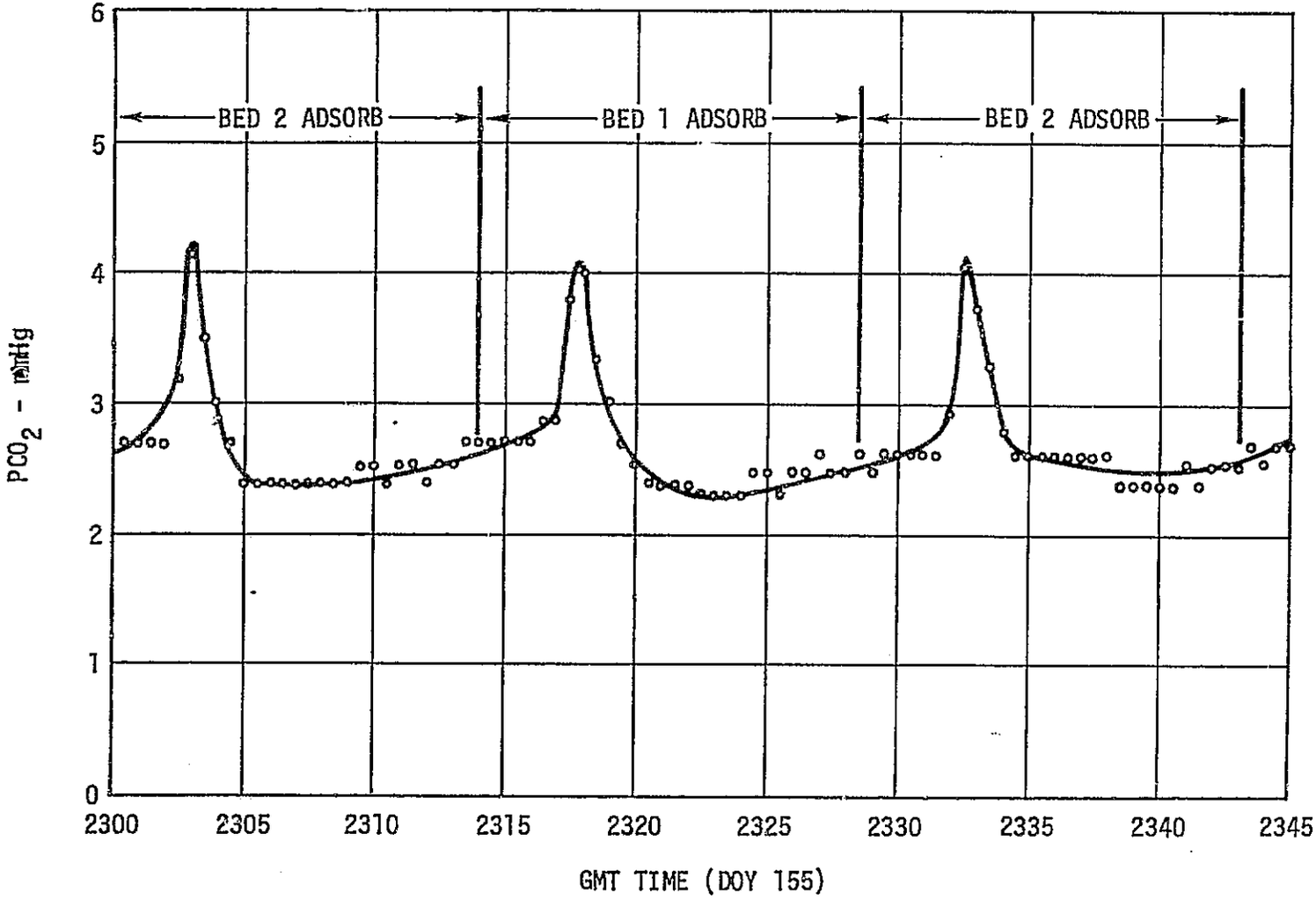

Figure 2-10. SL-2 Mole Sieve A Outlet PCO_2 (D210) During Bed Cycles

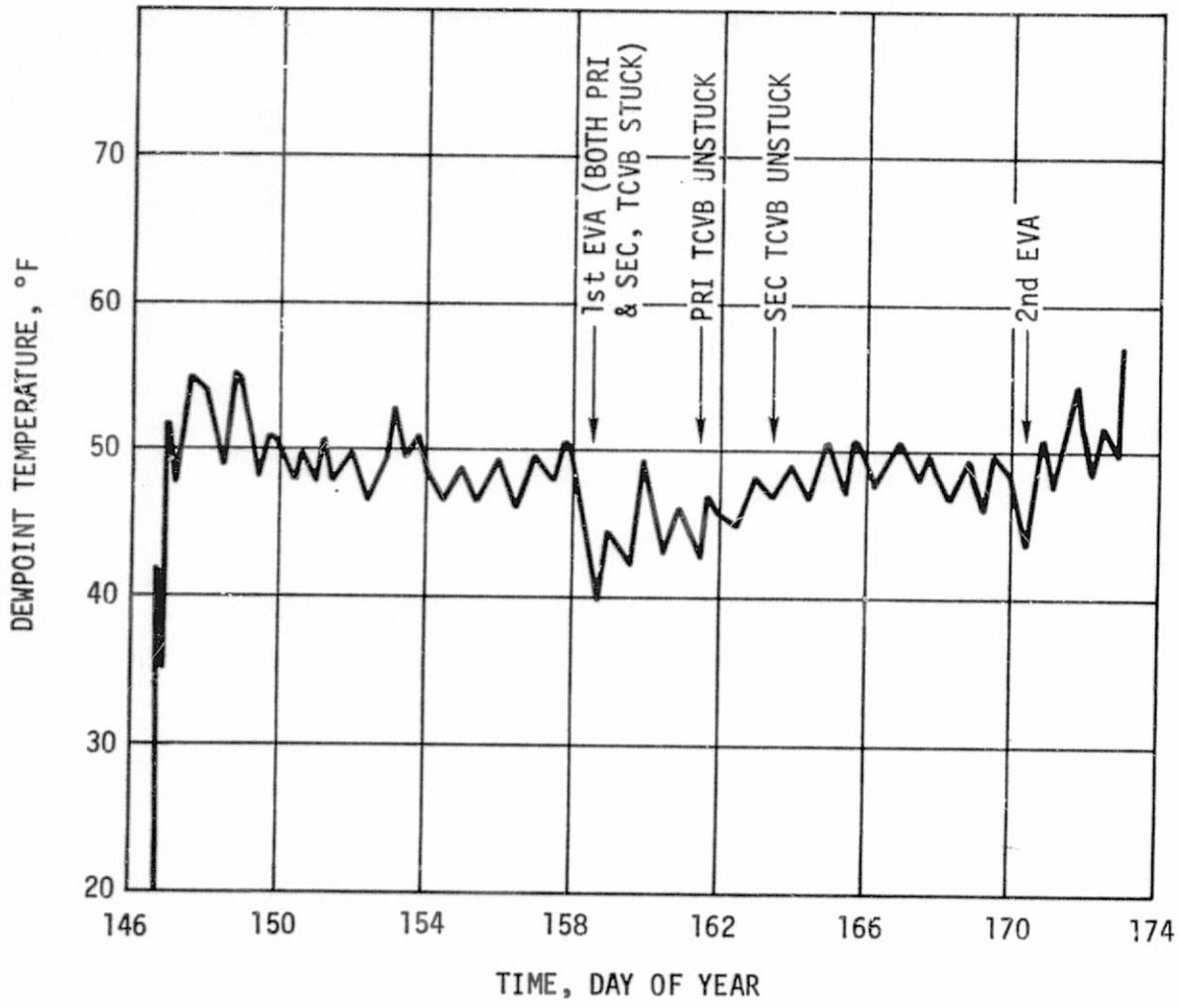

Figure 2-11. SL-2 Dewpoint Temperature Profile

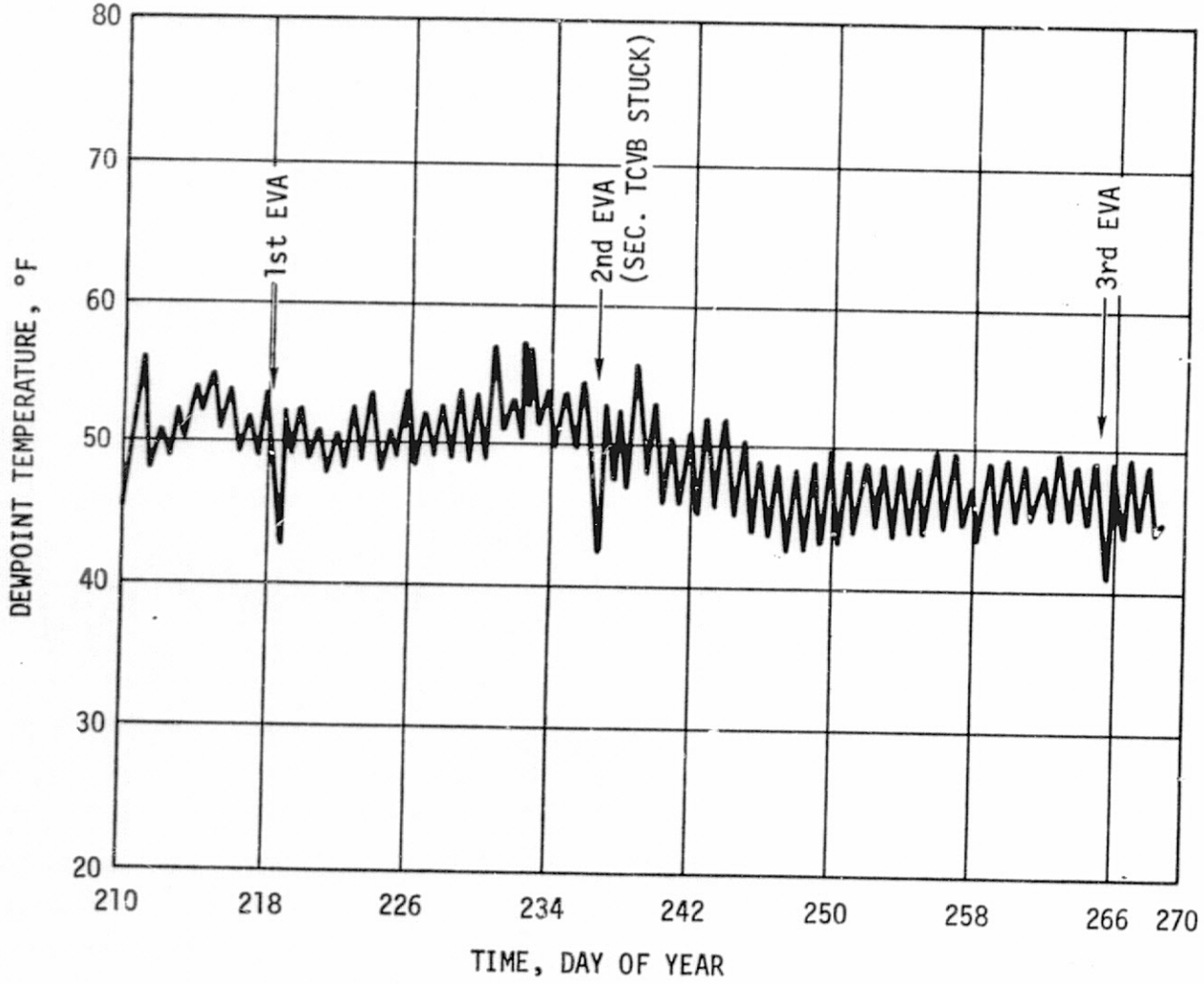

Figure 2-12. SL-3 Dewpoint Temperature Profile

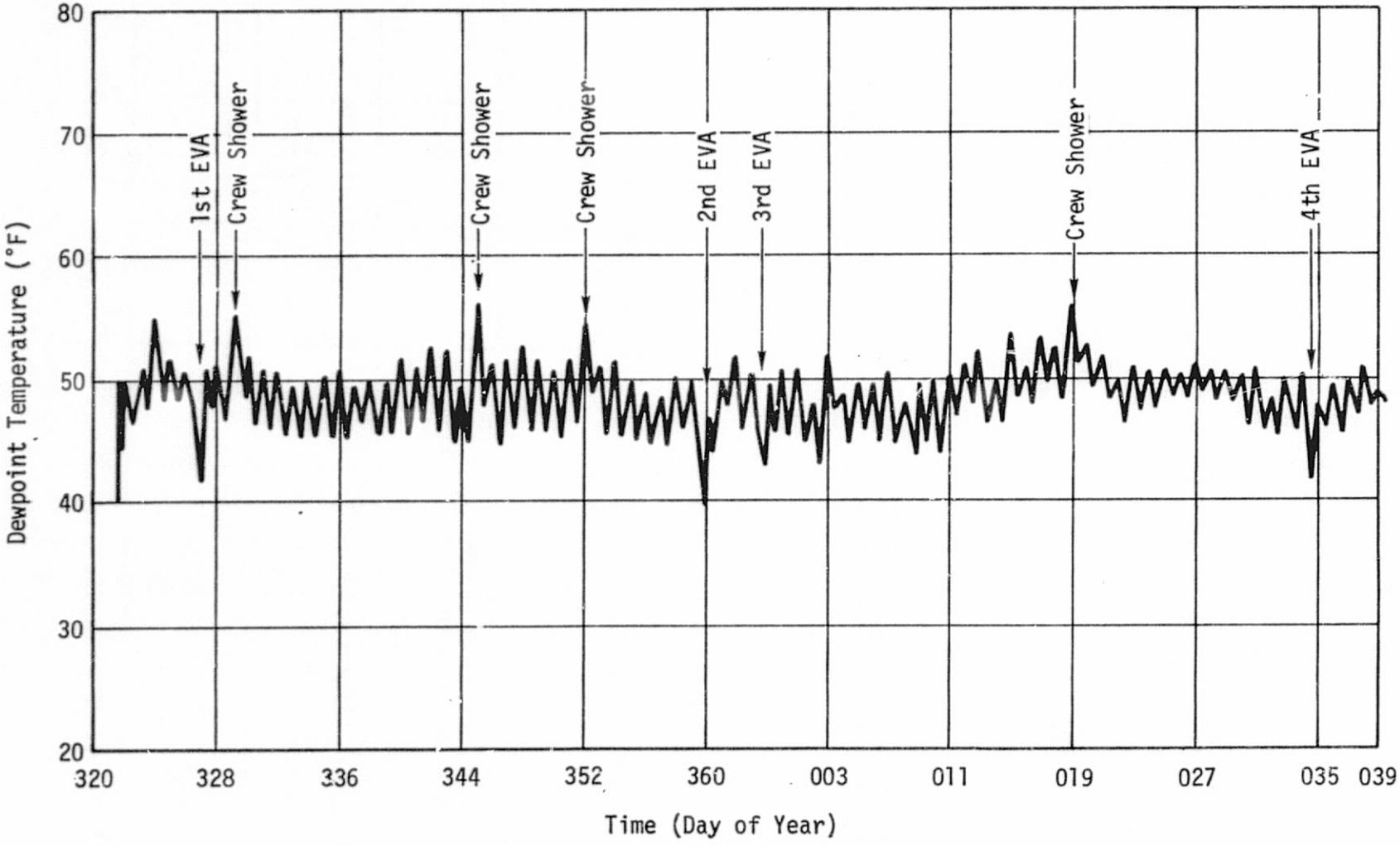

Figure 2-13. SL-4 Dewpoint Temperature Profile

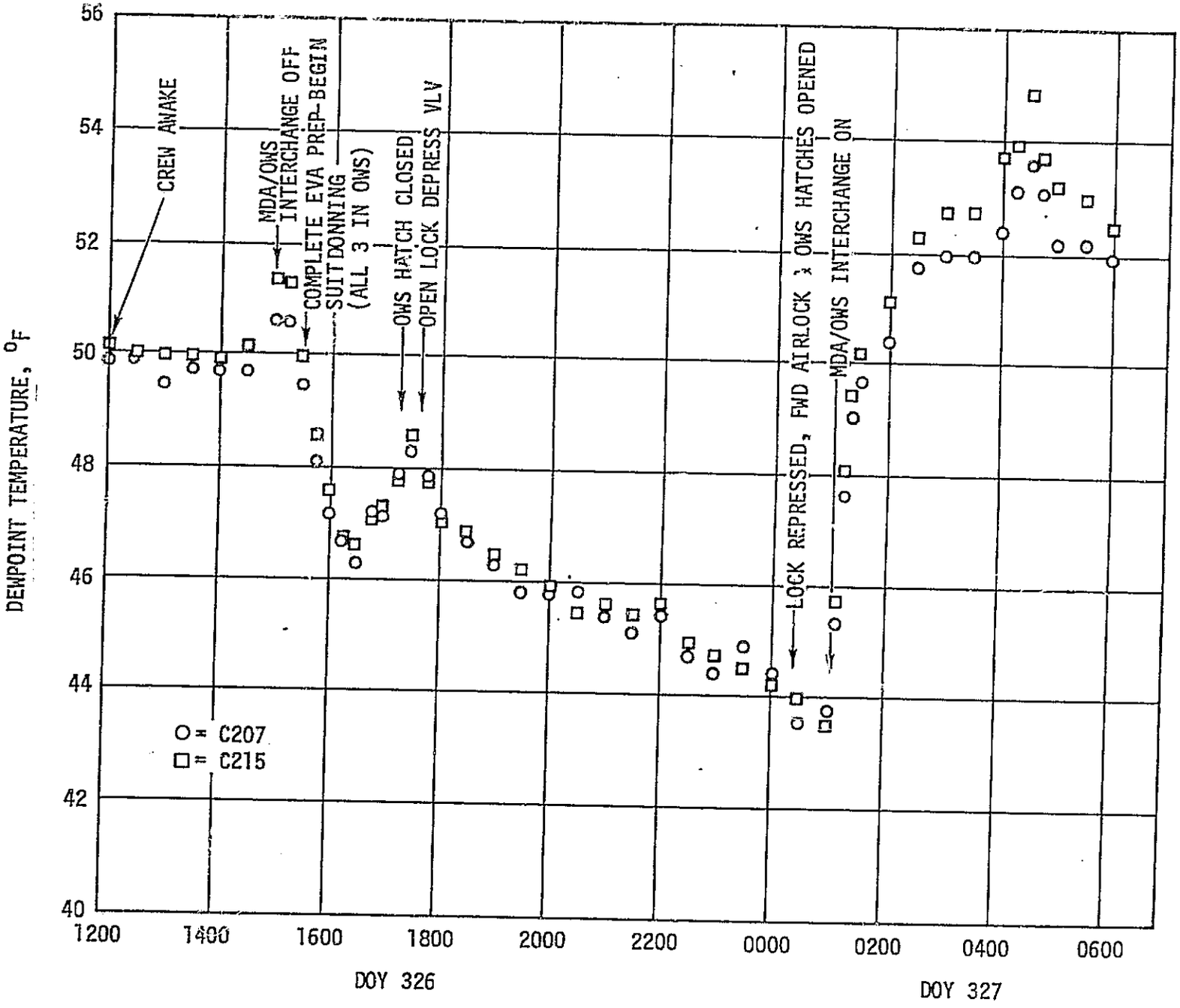

Figure 2-14. Dewpoint Profile During EVA #1 on SL-4

One concern prior to the first mission was that prelaunch purges and the unplanned purges and high temperatures during the period between SL-1 and SL-2 launch might have removed enough moisture from cluster hygroscopic materials such that moisture addition to these materials during the activation period would hold the dewpoint below the minimum level of 46°F for an excessive period of time. However, the atmospheric moisture buildup time was not excessive and the dewpoint had increased to 46°F in seven hours. This buildup was aided by high crew water production rates as they worked in the hot OWS prior to shield deployment. The effect of the cluster hygroscopic materials was seen in activation dewpoint levels during SL-3 and SL-4. The initial dewpoint levels should have been well below the initial levels shown on figures 2-12 and 2-13 due to storage depressurization and repressurization with dry gases. It is hypothesized that moisture addition to the atmosphere from the materials produced the initial levels seen.

b. Condensing Heat Exchanger Freezing - As a result of coolant inlet temperatures considerably below freezing on DOY 158 after the sticking of both the primary and secondary coolant loop thermal control valves (Section VII.), the water in the "A" heat exchangers for molecular sieves A and B froze. (The "B" condensing heat exchangers were not in operation.) No direct observation of freezing in the heat exchangers was made by the crew. However, the crew reported noise associated with the compressor gas flow and commented that they could feel no flow through the compressor, indicating a blocked flow path. After the heat exchangers thawed out, the system operated normally.

c. Molecular Sieves A and B Heat Exchanger Gas Outlet Temperature Instrumentation Discrepancy - On DOY 219 following EVA #1 on SL-3, the crew notified the ground that the Mole Sieve heat exchanger outlet temperatures were reading low. The crew later rechecked and verified that the mole sieve A gas outlet temperature reading onboard was 36°F and the mole sieve B gas outlet temperature was 25°F. This data was also available via telemetry and at the same time the ground readings were over 49°F for both MS A and MS B. The coolant inlet temperatures at that time were around 47°F and since the gas outlet temperature was known to be 1-2°F above the coolant inlet temperatures, it was concluded that the TM values on the ground were correct and the onboard meter readings were incorrect.

The readings onboard were incorrect for the remainder of SL-3. On DOY 329 of SL-4 the ECS systems housekeeping check (HK70U) was performed for the first time on SL-4 and the readings were 45°F for mole sieve A gas outlet and 47°F for mole sieve B gas outlet, which were within a few degrees of the telemetry values.

Sometime between the end of SL-3 and MD 10 of SL-4 the problem had corrected itself. No more problems with the onboard gas outlet readings were experienced.

d. Condensing Heat Exchanger Plate Wetting - Comments from all the crews on voice tapes and in debriefings indicated that wetting of the plates for the condensing heat exchangers was performed nominally. On SL-2, the crew commented that the wetting went well, but it was hard to tell when the plate became wetted. On both SL-3 and SL-4 the crews commented that the plates appeared to be already wetted prior to performance of the wetting procedure. However, the procedure was completed to insure complete wetting.

On SL-2 the plates were wetted beginning about 9 hours after opening the hatch. During this 9 hours only about an hour had been at conditions where the dewpoint was greater than the coolant inlet temperature. On SL-3, the plates were wetted about 24 hours after opening the MDA hatch. Almost all of this period was with the dewpoint greater than the coolant inlet temperature. On SL-4, not quite 8 hours elapsed from opening the MDA hatch until wetting the plates, but during all of this period the dewpoint temperature was higher than the coolant inlet temperature. The original set of condensing heat exchanger plates were used throughout all the missions.

e. Condensate Removal System - The system performed its required function of atmospheric moisture control as is evident from the dewpoint levels presented in paragraph B.2.a. in this section. Other functions such as servicing/deservicing LSU/PCUs, servicing heat exchanger separator plates and removing water from the CSM waste tank were supported in a normal manner

However, many more condensate dumps were performed than had been planned due to gas leaks into the system. The leaks are discussed in C.1. of this section. Figures 2-15, 2-16, 2-17 present the condensate system to atmospheric differential pressure profiles for the missions. During the period of SL-3 when the gas leak persisted for 32 days, the system was dumped on a daily basis in order to provide the differential pressure required for the condensate removal function to be carried out.

An incident of OWS waste tank dump probe blockage occurred during SL-3 and is reported in C.2. of this section.

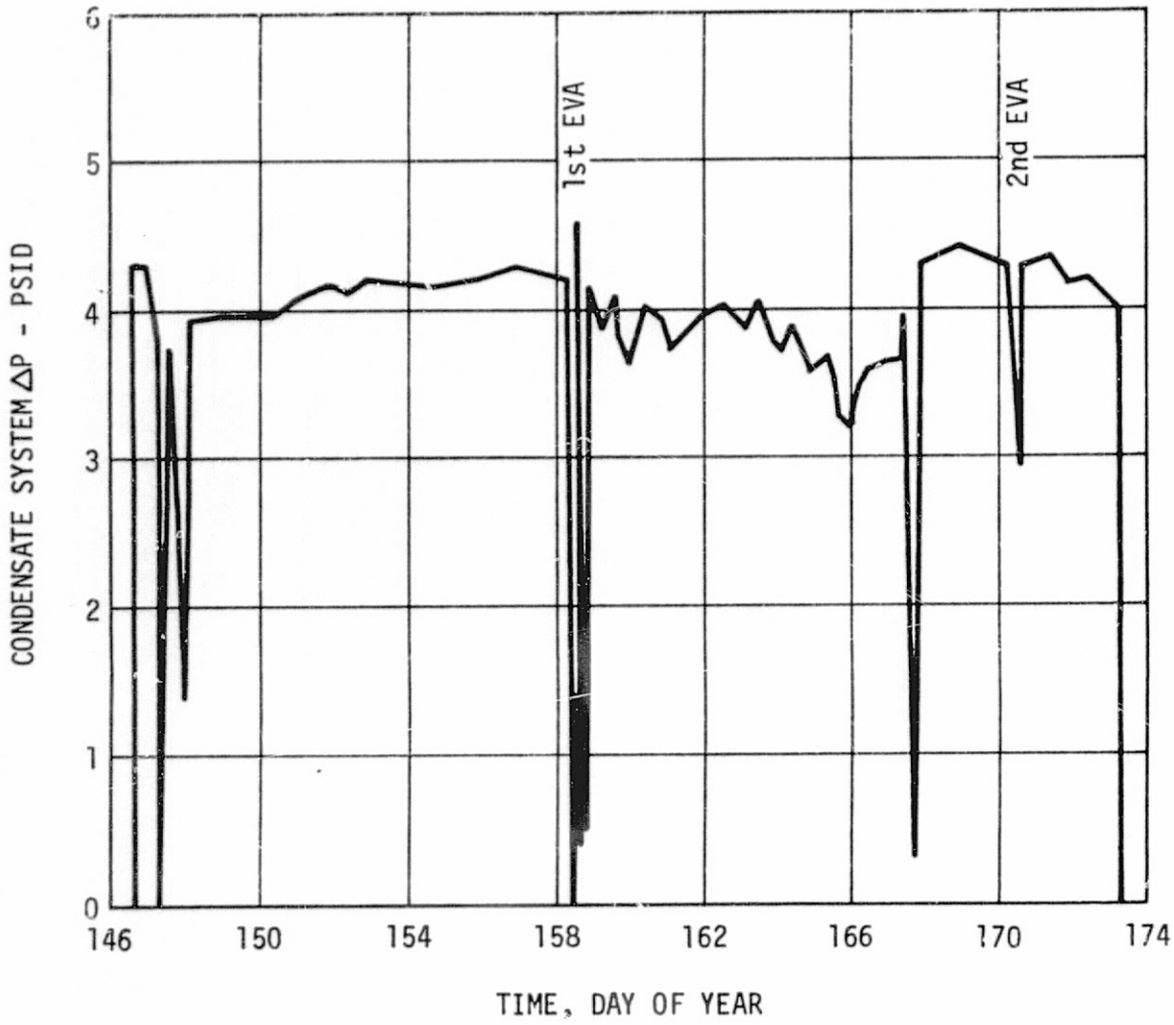

Figure 2-15. SL-2 Condensate Tank ΔP Profile

Figure 2-16. SL-3 Condensate Tank ΔP Profile

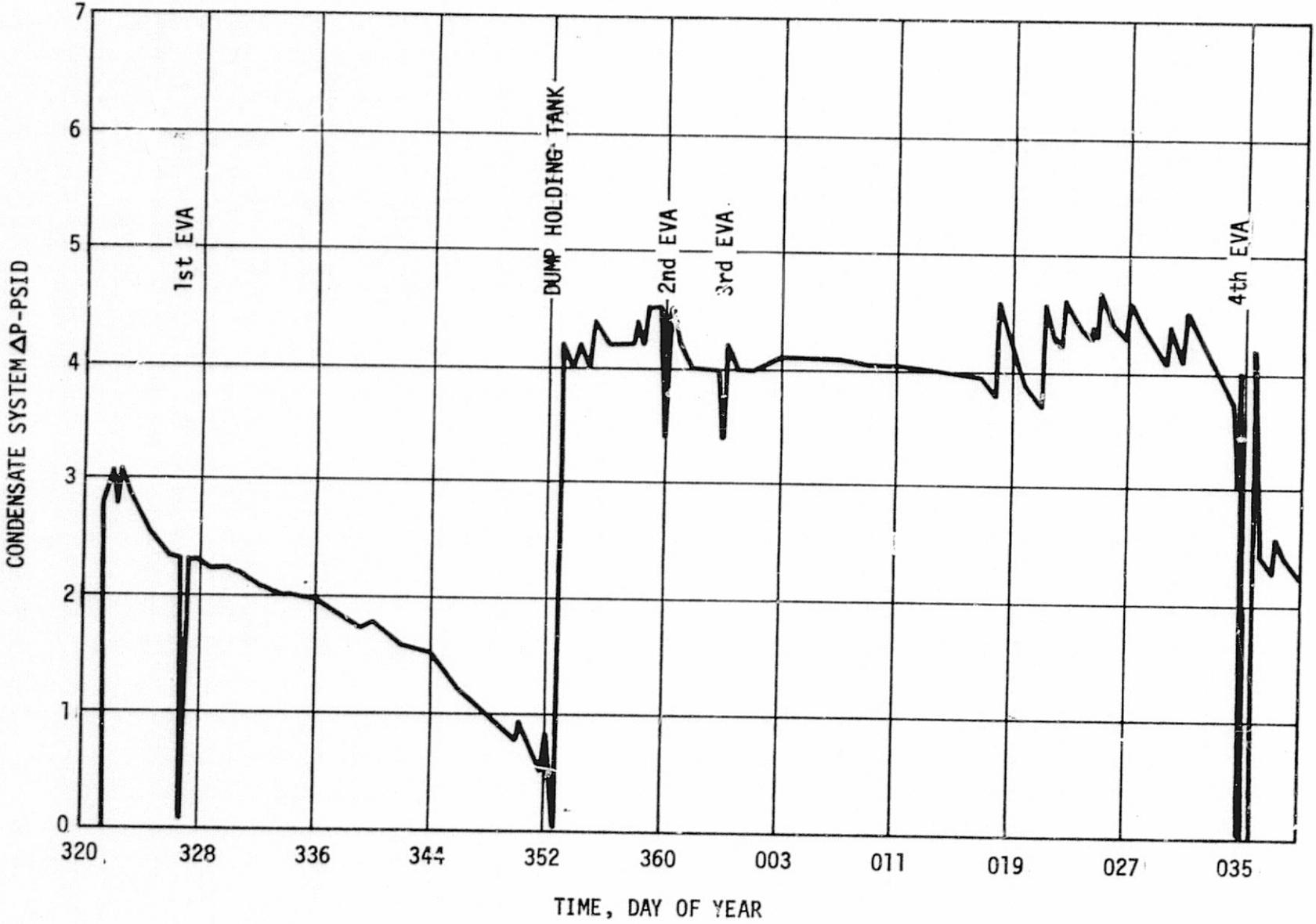

Figure 2-17. SL-4 Condensate Tank ΔP Profile

3. Odor Removal System Performance - The only means available to evaluate the performance of the odor removal system was via crew comments. Comments received during technical debriefings of all three crews indicated that the system performed very well. The following is taken from the SL 1/4 Technical Debriefing, pg. 12-24.

Odor Removal: "No problems. The odor removal system in the workshop was outstanding. Odors just did not persist. They were very quickly removed. The waste management compartment odor removal was outstanding. There way no way anyone using the waste management compartment offended or bothered anyone else in the workshop. We were amazed how well the odors were removed and how good the workshop smelled in general. I thought that we were going to have to get used to some very peculiar odors during our mission up there. When we entered the workshop, we were quite pleasantly surprised to find that there was no particular odor that bothered us. It stayed that way the entire time. I wouldn't guarantee that very much longer, because as we mentioned before, we left the workshop in the as-used condition, with little or no cleaning."

Table 2.6 summarizes the charcoal canister useage and replacements during the missions.

Table 2.6. Charcoal Canister Usage

MISSION	REPLACE MOLE SIEVE CHARCOAL CANISTERS (2)	REPLACE WMC CHARCOAL CANISTERS
SL-2	172/10:50	172/08:25
SL-3	247/17:20 267/15:30	247/16:00 267/09:00
SL-4	364/20:50	346/(time not known) 009/(time not known)
	Total Used - 10 (2 Installed + 8 spares)	Total Used - 6 (1 Installed + 5 spares)
	Total Launched - 10 (2 Installed + 8 spares)	Total Launched - 6 (1 Installed + 5 spares)

4. Contamination Removal System Performance --Loss of the meteoroid shield during boost caused high OWS temperatures with suspected off-gassing of contaminants (carbon monoxide and toluene diisocyanate) from the OWS polyurethane foam. A vent/repressurization scheme described in Section VI.B.3 was initiated to purge the cluster of the contaminants prior to SL-2 crew entry. The SL-2 crew took toluene diisocyanate (TDI) samples using Draeger tubes and CO samples with a Mine Safety Appliance device prior to entry. There was no indication of the presence of TDI and less than 25 PPM of CO. The device used to measure CO levels gave only an approximate value since it was a color changing material and one color represented 0-25 PPM. Also problems had been encountered with the material changing color in the 0-25 PPM range while stored. The SL-3 and SL-4 crew took one TDI sample each with no indication that this contaminant was present in the cluster. The last two crews, on every occasion that they sampled for CO, found that the sensing material had changed to the 0-25 PPM color during storage. Therefore the CO level was less than 25 PPM, but no estimate of the absolute value could be made.

During SL-3, Coolanol-15 leaks in the AM primary and secondary coolant loops were detected. It was impossible to determine whether these leaks were inside or outside the spacecraft so the possibility existed that amounts of Coolanol were leaking into the cabin area. A conservative analysis (leak rate of .15 lb/day of Coolanol) indicated a level of less than 10 PPM of Coolanol in the cluster atmosphere. This analysis assumed Coolanol removal by the WMC and Mole-Sieve charcoal canisters, condensing heat exchangers, and mole-sieve material. This calculated level could be in the form of Coolanol-15 as well as secondary butyl alcohol and isopropyl alcohol which result when water and Coolanol combine.

Analysis was performed on five CO_2 cartridges returned from the SL-2 and SL-3 missions. Three of the cartridges showed no evidence of either Coolanol-15 or the products of Coolanol-15 hydrolysis. Two of the sensors showed both Coolanol-15 chemical signature and traces of isopropyl alcohol and secondary butyl alcohol. It was concluded, therefore, that Coolanol was present within the Skylab. However, due to the demonstrated ability of onboard equipment to remove Coolanol from the atmosphere, it is unlikely that any significant amount of Coolanol was present in the atmosphere.

An analysis was also performed on three AM charcoal filter samples which were returned as well as one unexposed sample for control. The samples were vacuum-thermally desorbed and the desorbates were analyzed by gas chromatography-mass spectrometry. In addition, one sample from mid-mission SL-4 was selected for a wet chemical analysis to determine the presence of Ammonia, Hydrogen Sulfide, and Mercaptans.

Individual component identification was accomplished for the presence or absence of over 240 compounds.

There were more than thirty compounds which were identified in these samples. Four compounds; methyl, ethyl, and isopropyl alcohols and acetone; constituted 81-93% of the total recovery, exclusive of water. Water recovery constituted approximately 20% of the weight of charcoal desorbed. Traces of Coolanol 15 were also present. The complete results of the chemical analysis is shown in Table 2.7.

TABLE 2.7

COMPONENTS DESORBED FROM SKYLAB CHARCOALS

Unexposed Charcoal

Compound	MW	µg/g
Propane	44.09	0.077
Butane	58.12	0.061
Propylene	42.08	1.2
1-Butene	56.10	0.12
2-Pentene	70.13	0.047
Isoprene	68.11	0.017
2-Hexene	84.16	0.0012
Cyclohexane	84.16	0.24
Toluene	92.13	0.21
Methyl alcohol	32.04	0.28
Ethyl alcohol	46.07	0.068
Isopropyl alcohol	60.09	0.26
Acetone	58.08	0.28
Acetonitrile	41.05	0.049
Total Excluding Water		2.90
Water		1.5×10^4

TABLE 2.7 (Cont.)

Charcoal #S/N 101-135 Mid Mission SL-3

Compound	MW	µg/g
Freon 12	121.00	0.30
Freon 113	187.39	3.6
Propane	44.09	1.1
Butane	58.12	1.1
Hexane	86.17	0.24
n-Heptane	100.20	0.089
Propylene	42.08	8.4
Methyl acetylene	40.07	0.05
1-Butene	56.10	5.9
2-Butene (cis)	56.10	2.4
2-Pentene	70.13	0.90
Isoprene	68.11	1.0
2-Hexene	84.16	1.7
Methylcyclohexene	96.17	0.029
Cyclohexane	84.16	0.11
Benzene	78.11	0.0018
Toluene	92.13	0.096
p-Xylene	106.16	0.098
Furan	68.07	1.3
Methyl alcohol	32.04	33.
Ethyl alcohol	46.07	37.
Isopropyl alcohol	60.09	61.
Isobutyl alcohol	74.12	9.11
Acetone	58.08	40.
Ethyl acetate	88.10	5.5
Butyl acetate	116.16	0.12
Coolanol 15		< 0.3
Total Excluding Water		205.8
Water		2.07×10^5

TABLE 2.7 (Cont.)

Charcoal S/N 30-111 End of Mission SL-3

Compound	MW	µg/g
Freon 12	121.00	0.49
Freon 113	187.39	0.97
Ethane	30.07	0.049
Butane	58.12	0.25
Hexane	86.17	0.40
n-Heptane	100.20	0.067
Ethylene	28.05	0.041
Propylene	42.08	2.4
Methyl acetylene	40.07	0.03
1-Butene	56.10	2.0
2-Pentene	70.13	0.37
Isoprene	68.11	0.13
2-Hexene	84.16	0.86
Methylcyclohexene	96.17	0.035
Cyclohexane	84.16	0.075
Benzene	78.11	0.072
p-Xylene	106.16	0.15
Furan	68.07	0.075
Methyl alcohol	32.04	7.6
Ethyl alcohol	46.07	7.5
Isopropyl alcohol	60.09	17.
Isobutyl alcohol	74.12	0.074
Acetone	58.08	18.
Ethyl acetate	88.10	3.4
Butyl acetate	116.16	0.041
Coolanol 15		<0.2
Total Excluding Water		61.84
Water		2.11×10^5

TABLE 2.7 (Cont.)

Charcoal S/N 00-117 Mid-Mission SL-4

Compound	MW	µg/g
Freon 12	121.00	0.12
Freon 113	187.39	0.28
Propane	44.09	0.021
Butane	58.12	0.032
Hexane	86.17	0.11
Propylene	42.08	0.15
Methylacetylene	40.07	0.020
1-Butene	56.10	0.12
2-Butene (cis)	56.10	0.033
2-Pentene	70.13	0.61
Isoprene	68.11	.061
2-Hexene	84.16	0.013
Cyclohexane	84.16	0.030
Benzene	78.11	0.0068
Toluene	92.13	0.018
Furan	68.07	0.058
Methyl alcohol	32.04	7.8
Ethyl alcohol	46.07	2.8
Isopropyl alcohol	60.09	12.
Isobutyl alcohol	74.12	0.0065
Acetone	58.08	13.
Ethyl acetate	88.10	0.20
Acetonitrile	41.05	0.20
Unidentified C_{10} -C_{13} Hydrocarbons		0.10
Coolanol 15		< 0.04
Ammonia		12.20
Hydrogen Sulfide		1.41
Mercaptans (as ethyl mercaptan)		1.09
Total Excluding Water		38.30
Water		1.98×10^5

C. Anomalies

1. Condensate System Leaks - As reported in paragraph B.2.e., of this section gas leaks were experienced into the condensate system during the Skylab missions.

During SL-2, after the OWS condensate holding tank had been connected to the system, a delta P level of 3.2 to 4.5 PSID was maintained at all times except during those periods when the holding tank was disconnected for EVA or a holding tank dump. With the holding tank disconnected, system delta P decreased more rapidly than expected. Since system pressure was not affected while connected to the holding tank, it was concluded that gas leakage into the gas side of the AM condensate tank was responsible (figure 2-18). The spare condensate module was not installed, however, since EVA and holding tank dumps were performed infrequently and were of short duration. This leak was also observed on subsequent missions.

During SL-3 activation, the holding tank was reconnected to the system and the delta P of 4.23 PSID initially remained constant indicating a leak-free system. However, following use of the system for water separator plate servicing and transfer of CM waste water to the holding tank, delta P had decreased to 3.6 PSID and began a steady decline. Although troubleshooting was performed and the gas leakage was isolated to plumbing within the Airlock Module, the exact location of the leak could not be established. Further evaluation led to the belief that leakage was occurring in one or more quick disconnects. As a result, procedures for lubrication of quick disconnects were developed and incorporated into crew malfunction procedures. Leakage disappeared on DOY 245 following disconnection of the dump QD (figure 2-18) from the condensate module. No further evidence of leakage was observed throughout the remainder of SL-3 and system deactivation was limited to closing the condensing heat exchanger condensate isolation valves.

Condensate system activation was completely normal at the start of SL-4 with a system delta P of 2.86 PSID having been maintained during the storage period. No evidence of significant gas leakage into the system was observed until DOY 034 when the QD was disconnected from the liquid/gas separator at Panel 217 (figure 2-18) after EVA operations. Following disconnection, system delta P decreased to zero within approximately 15 minutes. After attempts to stop the leak using a universal sealant were unsuccessful, a cap launched on the SL-4 CSM was installed on the disconnected QD and no further evidence of leakage was observed.

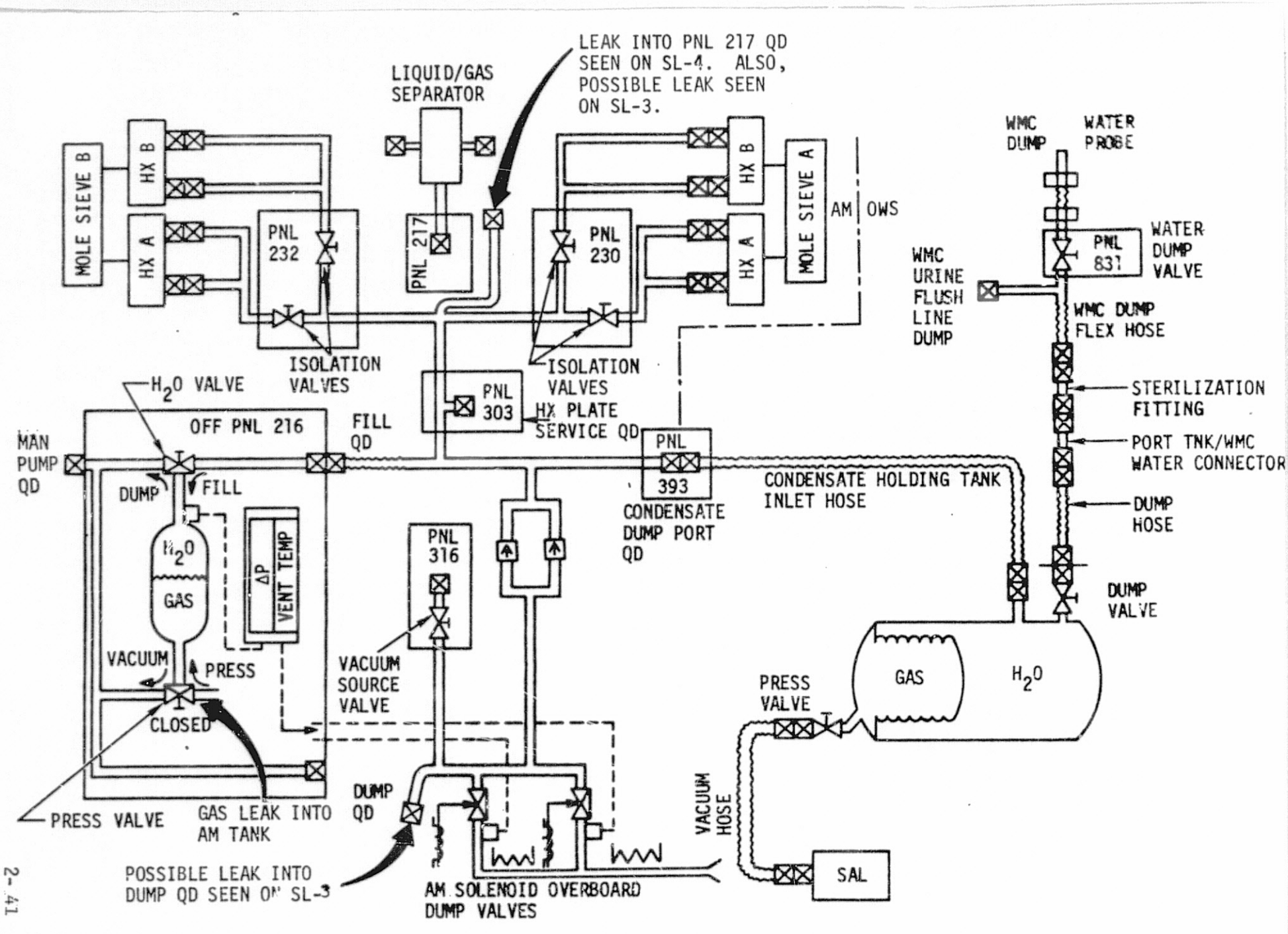

Figure 2-18. Condensate Control System Leakage Paths

2. Waste Tank Dump Probe Blockage - On DOY 242 during SL-3, the waste management system failed to completely dump the OWS condensate holding tank per procedure HK60T; maximum condensate system delta P was 3.8 PSID., whereas the normal level following a dump was 4.0 to 4.5 PSID.. At this time the dump probe was being operated on the Bus 2 heater. The following morning the crew turned on the dump probe Bus 1 heater for about 30 minutes, but the dump line remained clogged. The water dump valve was also cycled some ten times to no avail. At 242:18:38 a brief 35-PSI hot water dump utilizing the WMC water heater did clear the dump line; the dump probe Bus 2 heater was in use at this time. A condensate holding tank dump operation was then initiated, but the maximum delta P obtained was only 3.7 PSID; a crew check of the dump line using the condensate press fitting revealed that the line was again clogged. Another 35-PSI hot water dump was attempted, during which the dump probe Bus 2 heater was turned off and the Bus 1 heater was turned on. About 30 minutes after this operation the condensate press fitting showed the dump line was clogged. Because of the elapsed time between this hot water dump and the installation of the condensate press fitting, a third hot water dump was initiated at 243:00:53, still utilizing the dump probe Bus 1 heater. Immediately after this dump the condensate press fitting was installed so as to purge the dump line. This did clear the dump line, after which a slow but successful holding tank dump was performed. On DOY 243 another successful holding tank dump was performed. This dump was very slow, indicating that the probe was partially blocked. On DOY 244, the holding tank dump per procedure HK60B' (which pressurizes the gas side of the holding tank bellows) was unsuccessful. At this time the decision was made to replace the WMC water dump probe assembly. At 244:21:07 the CDR reported that the probe replacement was complete, and that the old probe had ice in the tip. The holding tank was then dumped per HK60B' without incident, indicating proper operation of the new probe assembly. On MD-42 the crew performed an electrical continuity test of the removed dump probe; all readings were normal. The crew also checked the probe for contamination by inserting and withdrawing a length of safety wire, and by blowing through the probe; no contamination was found. Exact cause of probe freezeup is not known; however, all subsequent water dumps through the new probe were successful.

SECTION III. CLUSTER VENTILATION SYSTEM

A. Configuration

The Cluster Ventilation System is shown schematically by figure 3-1. There were two molecular sieve systems to provide for atmosphere purification (CO_2 removal), odor removal, and moisture removal. Two parallel ducts with a compressor and condensing heat exchanger in each duct supplied flow to each molecular sieve system. Normally, one compressor and one condensing heat exchanger in each system were operated for humidity control. However, only one molecular sieve unit was operated. The second unit was redundant and would have been used in the event of a failure of the primary unit. Total flow through the system with the operational molecular sieve unit was approximately 34 CFM with 10 CFM through the active sieve bed, 11 CFM through a charcoal canister, and 13 CFM through the bypass. Total flow through the system with the redundant molecular sieve operation and the function of the various elements of the molecular sieve unit are discussed in Section II.

Exhaust flow from the molecular sieve systems was delivered to a distribution duct in the STS. This flow could then be diverted to the MDA or the OWS or split between the two depending upon the position of the air selector valve located in the STS duct. The position of the selector valve was manually controlled. Ambient atmosphere from the STS was drawn into the duct, mixed with the revitalized atmosphere from the molecular sieve systems and routed toward the OWS. Four fan/heat exchanger assemblies, located in the AM aft compartment, provided atmosphere cooling for the OWS. The cool gas from these heat exchangers was mixed with the molecular sieve/interchange duct flow and delivered to the OWS mixing chamber.

Three OWS ventilation ducts were routed from the mixing chamber to the distribution plenum, which was between the crew quarters and the waste tank dome. Atmospheric flow was produced by the fan clusters mounted in each duct. The crew quarters floor was equipped with adjustable diffusers which allowed the atmosphere to circulate through the crew quarters and back to the forward compartment. A portion of the flow then went to the AM through the OWS forward hatch for revitalization. The remainder

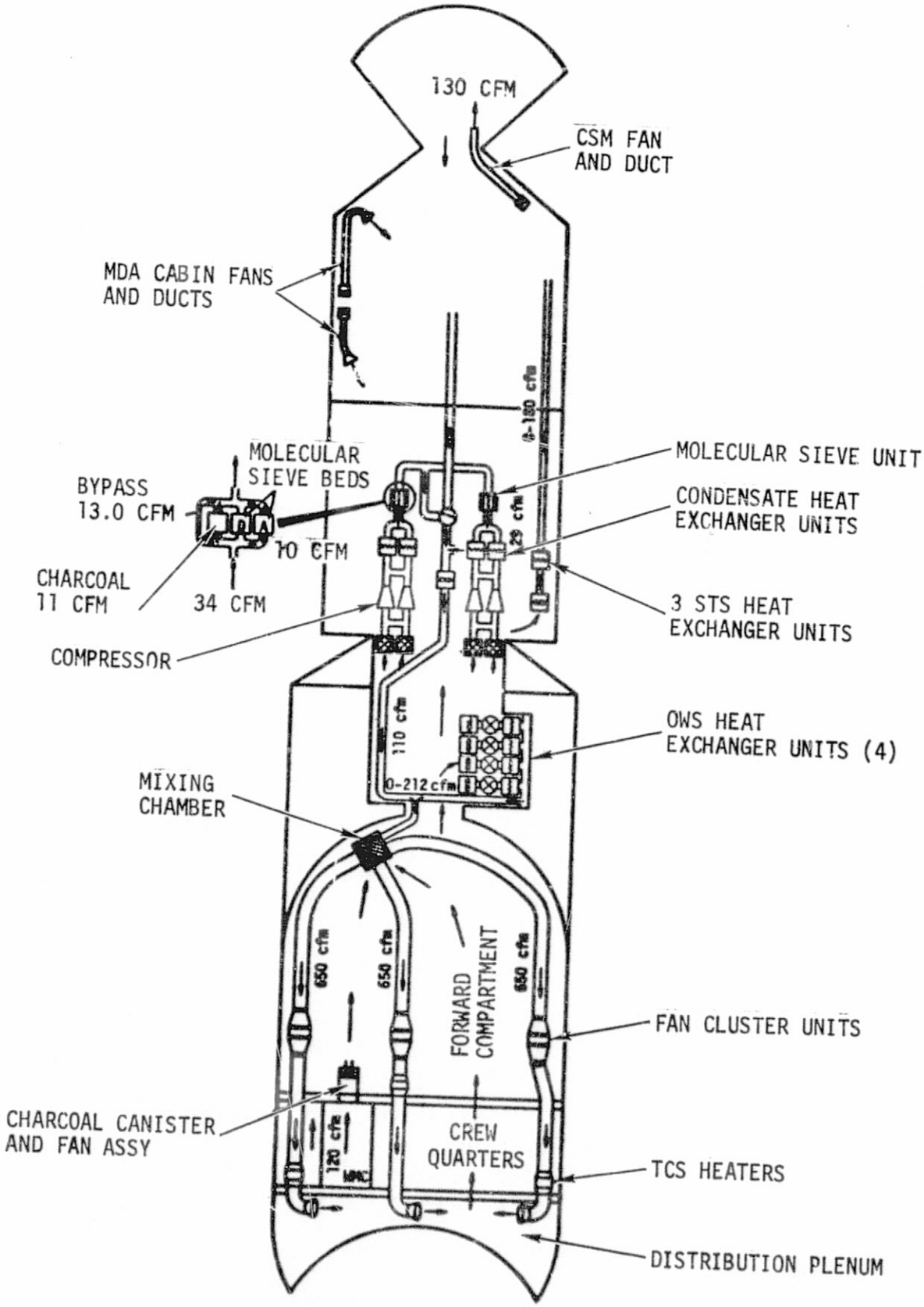

Figure 3-1. Cluster Ventilation System

was drawn into the mixing chamber and recirculated in the OWS. Figure 3-2 is a plan view of the OWS crew quarters floor showing the arrangement of the ventilation diffusers.

When the Waste Management Compartment (WMC) door was closed, the WMC became a sealed compartment. There was a charcoal canister and fan assembly located above the ceiling of the WMC to provide about 120 CFM of flow (at 28 VDC) through the compartment when the door was closed. The charcoal canister provided odor removal capability. Additional details on the cluster odor removal provisions and the WMC charcoal canister and fan assembly are given in Section II.

Three portable fans could be located anywhere on the OWS grid or on handrails, and could be connected to utility outlets for electrical power.

Three ECS fans provided atmospheric circulation (approximately 60 CFM per duct) between the STS and the MDA. Each fan was contained in a duct along with a heat exchanger for atmospheric cooling. The fans could be manually turned on or off in any combination desired. The atmospheric velocity at localized crew stations in the MDA could be varied by operating one or both MDA cabin fans and their attached diffusers. One diffuser was directed toward the vicinity of the ATM C&D console and the other toward the vicinity of the M512 experiment. Each diffuser exhaust pattern could be varied by a simple manual adjustment.

An atmosphere exchange between the MDA and the CSM of approximately 130 CFM was provided by a fan and flexible drag through duct. The duct was placed in position in the axial docking port tunnel during the cluster activation sequence. Ambient atmosphere was blown into the CSM through the duct and returned to the MDA through the docking port tunnel.

Table 3.1 summarizes the capabilities which were available for monitoring and control of the Ventilation System.

B. Performance

The ventilation system performed well and satisfied requirements. One of the prime objectives of the system was to provide a comfortable range of velocities for the crew. The crew comments provide the best means of evaluation of this requirement. The crew comments were favorable. The SL-2 crew commented that "The ventilation and atmospheric cooling were good." (Skylab 1/2 Technical

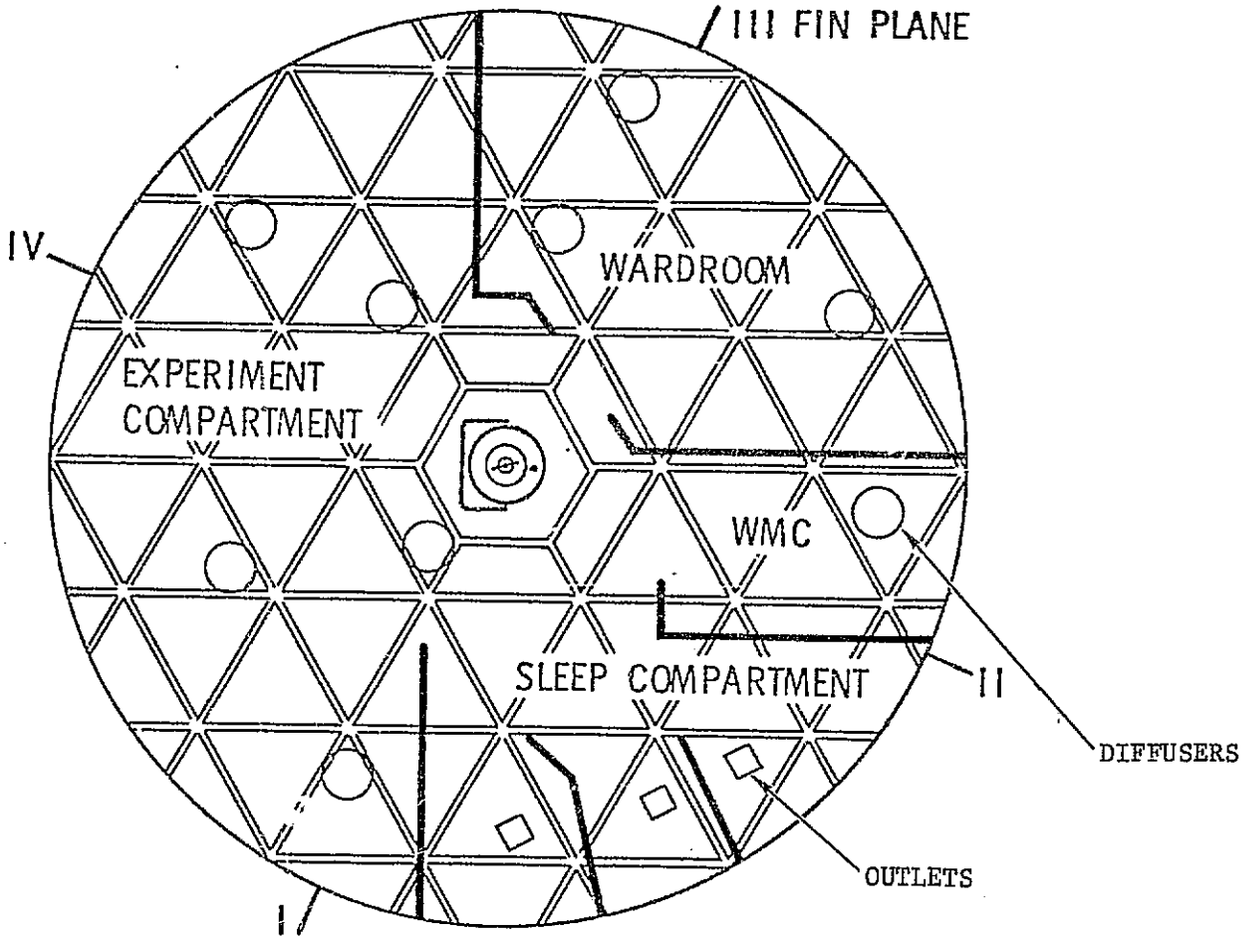

Figure 3-2 OWS Ventilation Control System Diffuser Locations

Table 3.1 Ventilation System Performance Monitoring and Control Capability

	MAJOR MEASUREMENTS	TM	C&W	ON BOARD DISPLAY	CONTROL CAPABILITY
1.	FLOW RATES, OWS DUCTS 1, 2, AND 3	X		X	MANUAL CONTROL ON/OFF
2.	OWS WASTE MANAGEMENT FAN				MANUAL CONTROL ON/OFF
3.	OWS PORTABLE FANS				MANUAL CONTROL HI/LO/OFF
4.	FLOW RATE, TOTAL OWS HEAT EXCHANGER GAS FLOW	X			AUTOMATICALLY CONTROLLED BY OWS THERMOSTAT
5.	FLOW RATE, AM/OWS INTERCHANGE DUCT FLOW	X	X		MANUAL CONTROL HI/LO/OFF
6.	STS HEAT EXCHANGER FANS				MANUAL CONTROL HI/LO/OFF
7.	CSM/MDA DUCT GAS FLOW				HI/LO/OFF
8.	MDA DIFFUSER FANS				HI/LO/OFF
9.	MOLE SIEVE A SYSTEM FLOW	X	X		MANUAL CONTROL ON/OFF
10.	MOLE SIEVE B SYSTEM FLOW	X	X		MANUAL CONTROL ON/OFF
11.	MOLE SIEVE A COMPRESSOR ΔP	X			
12.	MOLE SIEVE B COMPRESSOR ΔP	X			

Debriefing, pg. 12-4.) The SL-3 crew's comments were as follows: "Ventilation was great. Fans don't make much noise. You always got all sorts of air flowing around." (Skylab 1/3 Technical Crew Debriefing, pg. 12-13).

The SL-4 crew made the following comments on diffuser outlets. "It turned out that the atmospheric outlets, or the cooling outlets, if you will, especially the ones in the MDA, only had a control knob on them which allowed you to vary axially the size of the angle of the flow. I would like them to be swiveled and point in any direction. That way it would have been useful for cooling the rate gyros as well as cooling the crewmen at appropriate times." (Skylab 1/4 Technical Crew Debriefing, pg. 12-22).

The following paragraphs provide comments on performance of specific portions of the system. Instances of off-nominal operation and system discrepancies are discussed.

1. Off-Nominal Operation for Power Conservation - During the early portion of SL-2 (prior to the solar wing deployment) selected components in the ventilation system were left off or were turned off periodically in order to conserve power. The OWS Duct 3 fans were not activated until DOY 149 as a means of saving power. In addition, the molecular sieve B compressor and the 3 STS heat exchanger fans were turned off periodically. Turning off the compressor increased the possibility of condensation in the OWS heat exchangers by reducing their coolant inlet temperature. As a result, during periods when the compressor was off, the coolant inlet temperature and cluster dewpoint were carefully monitored to avoid condensation. Examination of data indicates that no condensation occurred as a result of turning off the compressor.

A candidate list of items for power down was developed for use during off-solar inertial maneuvers for power conservation. The list and procedure were incorporated in HK90A and HK90B in the Systems Checklist. This list included the STS heat exchanger fans, the molecular sieve B compressor and the OWS heat exchanger fans. This procedure was used several times during the three missions when pre-maneuver predictions indicated that conservation of power would be required.

2. OWS Ventilation Ducts/Flowmeters - Some problems were experienced with the OWS duct flowmeters. The OWS Duct 1 and Duct 2 fans were activated on DOY 146. (Duct 3 fans were left off in order to conserve electrical power.) The TM indicated duct flow rates were 630 CFM and 450 CFM for Duct 1 and 2, respectively as compared to the approximate 550 to 650 CFM which was expected with four fans operating per duct. On DOY 147 the telemetry (TM) flowmeter for Duct 1 failed. The failure was verified by a 500 CFM reading for the onboard flowmeter. The onboard reading for Duct 2 was 550 CFM at this time. In order to

increase circulation and make the OWS more comfortable, the fans in Duct 3 were activated on DOY 149 providing 550 to 600 CFM flow rate. All 12 duct fans were run continuously for the remainder of SL-2, except for EVA, until deactivation.

During SL-3 the flow rates taken from TM were typically 400 to 440 CFM for Duct 2 and 560 to 600 CFM for Duct 3. The only crew readout of the onboard meter for Duct 1 was 540 CFM on DOY 228. The Duct 2 TM flowmeter dropped from 440 to 340 CFM in 8 sec on DOY 228. The TM flowmeter had indicated lower than the onboard meter since the beginning of SL-2 and apparently experienced a transient failure. At this time the onboard meter indicated 500 CFM. Within 24 hours, the TM flowmeter for Duct 2 was again indicating 400 to 440 CFM.

During SL-4 the flow rates taken from TM were typically 380 to 420 CFM for Duct 2 and 520 to 570 CFM for Duct 3. The Duct 2 TM flowmeter experienced erratic or low readings several time during SL-4. On DOY 30, it failed and did not recover throughout the remainder of the mission. The onboard flowmeter for Duct 2 continued to provide nominal readings of 475 to 500 CFM throughout SL-4. A selected summary of duct flow rates for all three missions is given in Table 3.2.

Several M509 and T020 experiments were performed during SL-3 and SL-4. These maneuvering experiments require minimum gas velocities in order to minimize the effect on the experiment results. All the Duct 3 fans and two of the Duct 2 fans were off during these experiments. Typical readings were 190 CFM for Duct 2 and 100 CFM for Duct 3. The 100 CFM flow rate indicated in Duct 3 was probably a back flow since all the fans are off. With this configuration, the net flow rate through the floor diffusers was approximately 600 CFM.

3. Portable Fan Usage - During the first few days of SL-2, one portable fan was mounted in the OWS entry hatch to circulate additional hot air toward the OWS heat exchangers. The crew felt this configuration provided additional cooling for the OWS. This fan was used in the forward compartment, at times, after the interior OWS had cooled down to provide additional circulation in the compartment. The SL-3 crew used a portable fan in three locations. Prior to deployment of the Twin Pole Shield, a fan was placed in the OWS hatch to circulate more OWS air toward the OWS heat exchangers. A fan was used for convective cooling of a crewman using the ergometer. A fan was mounted in the MDA during SL-3 deactivation to provide contingency cooling of the rate gyro six pack should a heater fail on during storage.

Table 3.2 VCS Duct Flow Rate Summary

DOY: GMT	DUCT 1		DUCT 2		DUCT 3	
	TM (CFM)	DISPLAY (CFM)	TM (CFM)	DISPLAY (CFM)	TM. (CFM)	DISPLAY (CFM)
PRELAUNCH (KS0045)	OSH	OSH	671	OSH	683	650
146:2000 (ACTIVATION)	630	–	450	–	–*	–
147:0455	OSL	600	451	550	118*	75*
159	OSL	–	455	–	560	–
169	OSL	520	452	510	595	550
228:1548	OSL	–	437	–	575	–
228:1549	OSL	540	321	500	575	540
243:1938	OSL	–	166**	–	100**	–
244:0206	OSL	–	422	–	585	–
321:1617 (SL-4 ACTIVATION)	OSL	–	415	–	580	–
344:2105	OSL	–	490	–	522	–
345:1332	OSL	–	386	–	505	–
015:1756	OSL	NORMAL	207	NORMAL	560	NORMAL
016:1050	OSL	–	385	–	560	–
027:1238	OSL	–	OSL	475	566	–
027:1337	OSL	–	405	–	566	–
030:0211	OSL	NORMAL	OSL	NORMAL	552	NORMAL
039:0357 (SL-4 DEACTIVATION)	OSL	–	OSL	–	522	–

* DUCT 3 FANS OFF
** DUCT 3 FANS OFF, 2 FANS IN DUCT 2 OFF FOR M509

OSL = OFF SCALE LOW
OSH = OFF SCALE HIGH

The SL-4 crew used a portable fan during the high beta angle periods when the OWS was warm to circulate more OWS air toward the OWS heat exchangers as the SL-2 and SL-3 crews had done.

4. OWS Diffuser Adjustment - The OWS circular diffusers were adjustable so that the velocity pattern could be changed, if desired, for crew comfort. In response to questions at systems debriefings, the crews indicated that the circular diffusers were never adjusted from their launch position (wide pattern) for crew comfort. The rectangular sleep compartment outlet settings were adjusted by the crewmen to direct flow either toward them or away from them depending upon their individual preferences and thermal conditions.

5. Reduction in OWS Cooling Bay Flow Rate Due to Dust - A reduction in the OWS cooling bay flow rate was observed during the SL-2 and SL-3 missions. The decay in flow rate was attributed to blockage in the gas side of the OWS heat exchangers.

During the SL-2 mission all four of the OWS heat exchangers were operated continuously. Figure 3-3 shows the gas flow rate as a function of mission day and illustrates a general decay from approximately 230 CFM at the start of the mission to 170 CFM at the end. Correlation of heat absorbed by the cooling loop with energy removed from the gas loop verified the flow decrease to be real. Each data point is an averaged value of the sensor reading taken over several hours. This was required due to erratic flow rate indications. The scatter in data was normally 20 - 30 CFM. This behavior of the "time-of-flight" sensors was noted during ground testing and has been attributed to system turbulence. This type sensor was also used for the AM/OWS interchange duct flow rate and for the molecular sieves flow rate. These flowmeters consist of a small tube with a heater wire located at the tube entrance. This heater is pulsed and the pulse sensed downstream by a counter at the tube exit which relates the travel time to the tube length giving the flow velocity. The flow velocity had been correlated to the duct geometry and velocity profile during ground testing to give the duct flow rate.

Figure 3-4 shows the flow rate data during SL-3. Four OWS heat exchangers were operated until DOY 250 when the automatic controller turned off all heat exchangers. In an attempt to improve OWS HX flow rate, the crew was requested to inspect the heat exchangers for blockage and to use the vacuum cleaner, if required, to clean them. The face of the heat exchangers were found to be covered with dust. The crew vacuumed the heat exchangers on DOY 251 after which the combined flow of the 4 fans was 185 CFM. After checking the flow with four fans the system was returned to one heat exchanger operation. From the single-fan operation data it appears that the blockage began to reappear almost immediately.

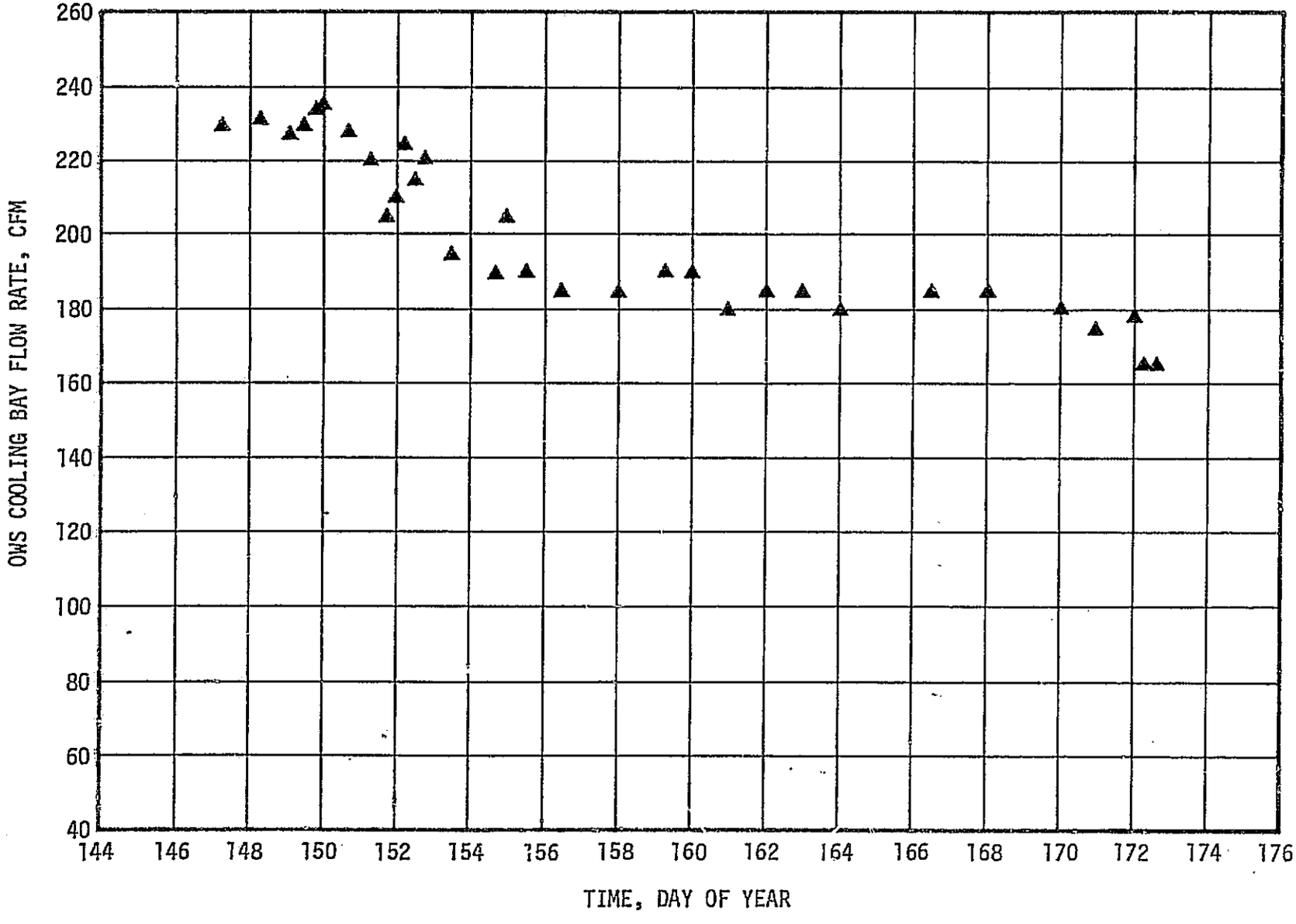

Figure 3-3 OWS Cooling Bay Flow Rate for SL-2

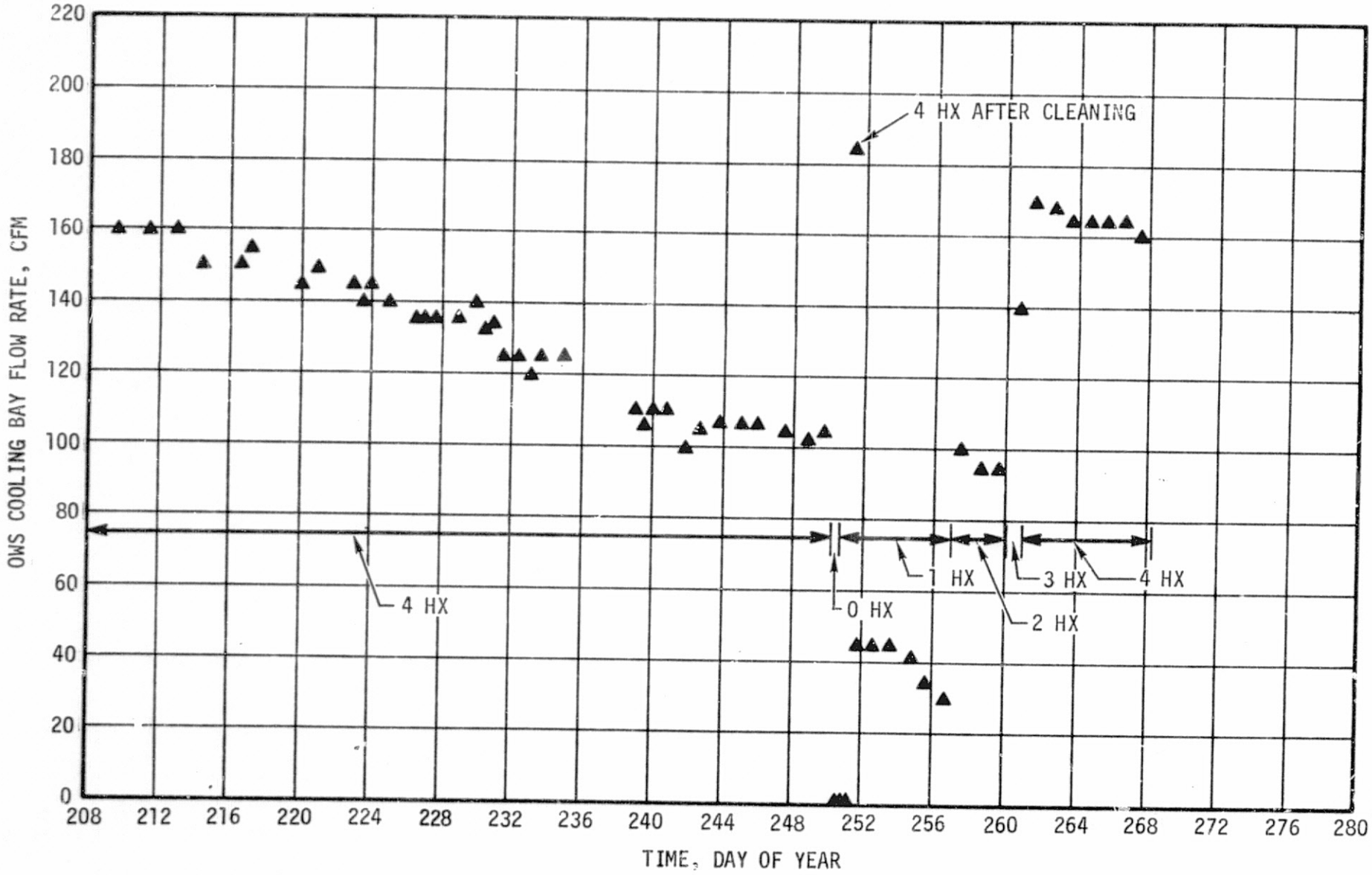

Figure 3-4 OWS Cooling Bay Flow Rate for SL-3

The automatic controller returned the system to four heat exchanger operation by DOY 261. The flowrate of the four fans had decayed to 160 CFM by the end of SL-3.

The flow rate data for SL-4 are shown in figure 3-5 and indicate an average value of 160 CFM. During SL-4 the cleaning of the OWS heat exchangers was incorporated as a housekeeping procedure and was performed every six or seven days. Typical values of the flow rate before and after cleaning were 150 CFM and 180 CFM, respectively.

6. Reduction in OWS Cooling Bay Flow Rate Due to Condensation - On DOY 18, all three crewmen took showers and the dewpoint temperature went up to approximately 57°F. This was a full sun day due to high beta angle and the Airlock Module cooling loop was being operated with two pumps in the primary and one in the secondary with a resulting OWS heat exchanger inlet temperature of 52 to 53°F. This situation resulted in condensation forming in the heat exchangers and a consequent decrease in the gas flow rate (figure 3-5). This occurrence was consistent with preflight testing which indicated that significant condensation would form if the HX coolant inlet temperature was approximately 3°F below the dewpoint temperature. The crew removed the water from the heat exchangers with the vacuum cleaner on DOY 20 and the flow rate returned to its normal value.

7. OWS Heat Exchanger Fans Replacement - Cleaning of the heat exchangers during SL-4 did not provide as much flow rate improvement as was seen after the initial cleaning during SL-3. The possibility existed that one or more of the heat exchanger fans had degraded in performance and was producing low flow rates. Since maximum performance was needed from the cooling system at full sun (high beta) conditions, a decision was made to replace the fans. All four fans were replaced on DOY 17. No increase in flow rate was seen, however, and it was concluded that no significant fan degradation had occurred. It was concluded that the dust was probably lodged within the heat exchanger which was not being removed by the vacuum cleaner.

8. AM/OWS Interchange Duct Flow Rate Reduction - The subject flow rate decreased from an initial value of approximately 120 CFM to approximately 60 CFM by the end of SL-4. The data is presented in figure 3-6 and shows the band (high and low) of values seen each day. As has previously been reported, this flow rate sensor was erratic. The cause of this low flow indication was not identified, nor was it determined whether the low flow indication was real or caused by an instrumentation problem. All screens which could influence the flow rate were cleaned with no flow rate improvement. The interchange fan was replaced temporarily on DOY 251, but the indicated flow rate did not increase. The indicated level was not low enough to cause problems.

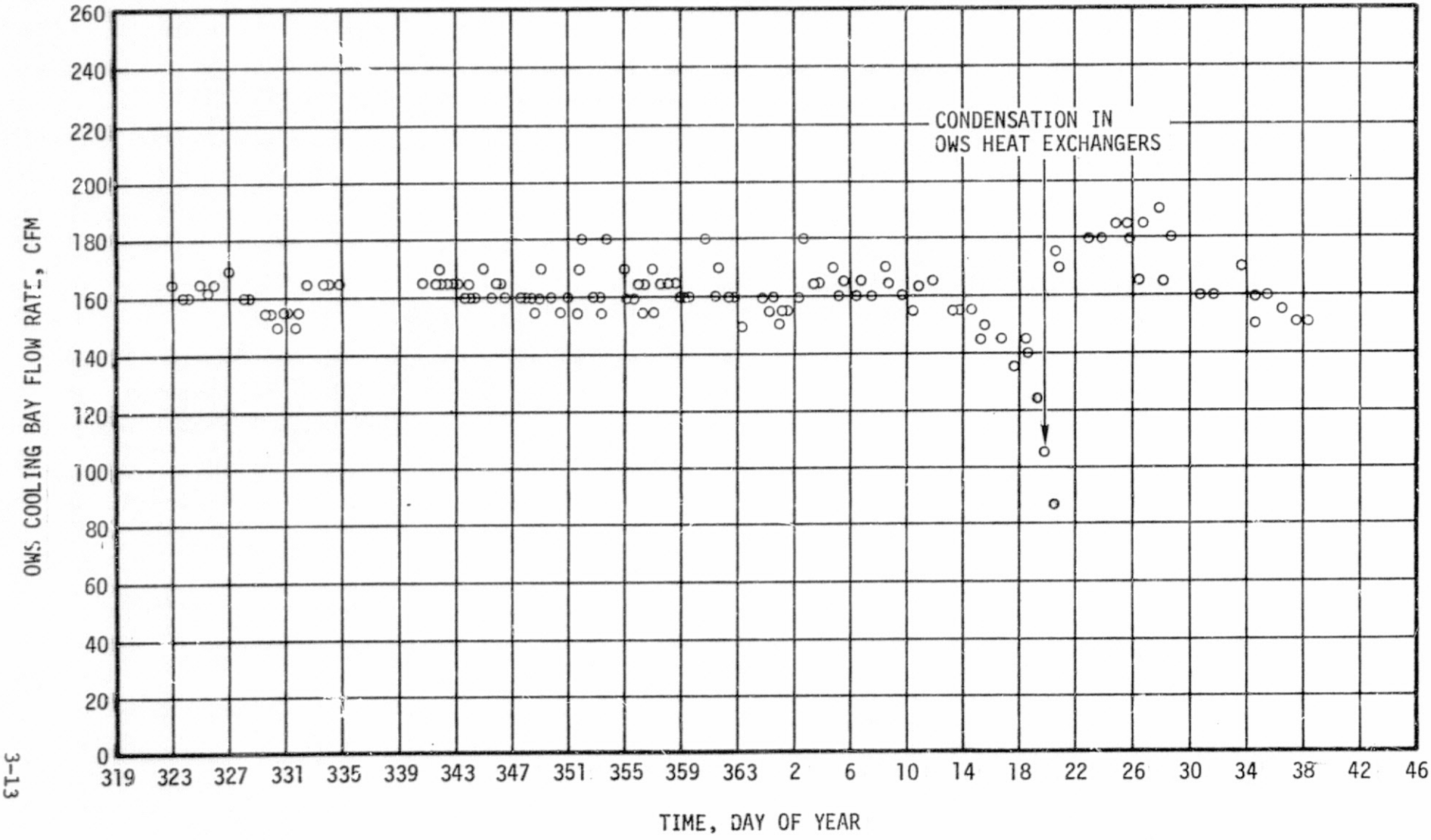

Figure 3-5 OWS Cooling Bay Flow Rate for SL-4

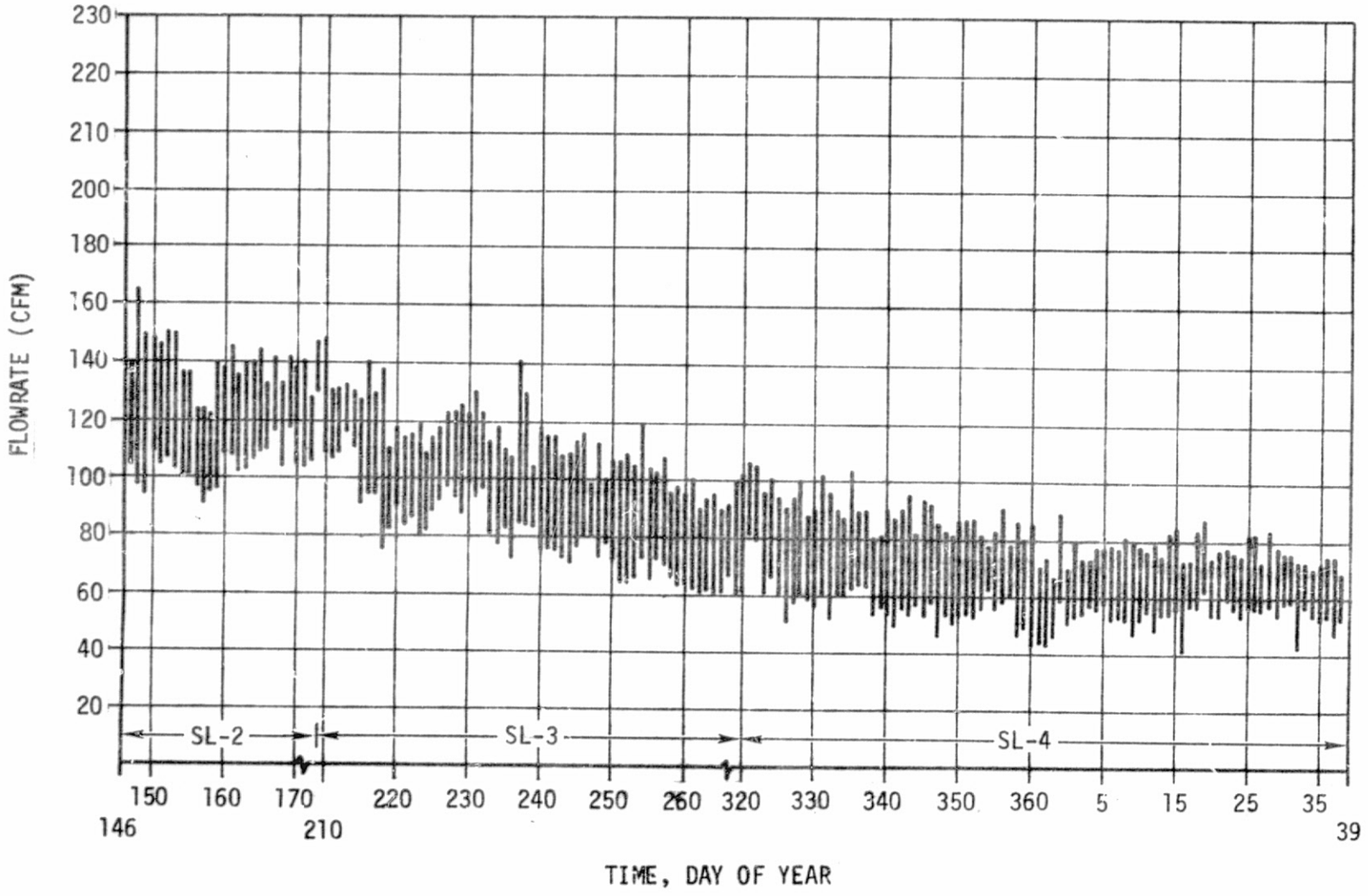

FIGURE 3-6 AM/OWS INTERCHANGE DUCT FLOWRATE

The interchange flow rate was a C&W parameter and a C&W signal was obtained a few times after the indicated flow rate decreased to values which produced data scatter within the 45 ±10 CFM C&W range.

9. Molecular Sieve B Secondary Compressor C/B Trip - During SL-3 activation on DOY 209 the mol sieve B secondary fan C/B tripped when fan activation was attempted. Troubleshooting indicated a malfunction in the electronics so that this compressor was not used in SL-3 or SL-4. To preclude operation of two compressors on one bus for the remainder of the mission, the secondary compressor in mole sieve A was selected along with the primary compressor in mole sieve B. A cable was carried by the SL-4 crew which would have allowed operation of the secondary fan in molecular sieve B from one of the molecular sieve A inverters if required. The cable was not used.

10. Molecular Sieve Flow Rates - Preflight tests revealed that the molecular sieve flow rate indications were high and, as previously discussed, the values provided were erratic. As a result, the compressor differential pressures were used with compressor flow versus delta P data to determine flowrates during the mission. Using this technique, no flow anomalies were seen during the mission. However, the flow rate indication was a C&W parameter (21 ±4 CFM) and the erratic nature of the data as well as its sensitivity to flow disturbances in the duct produced some C&W indications. In a few instances, the C&W was activated when the beds cycled and produced momentary flow disturbances in the duct. The C&W was also tripped during SL-2 when the beds were placed on line following bakeout. A review of data for this time period indicated that the flow rate sensor produced more data scatter than usual. The compressor delta P was steady and normal, however, indicating that the compressor was producing normal flow (See Section II.B.1.d). The molecular sieve C&W's were inhibited on SL-4 in order to prevent false alarms.

In addition to these false C&W alarms, abnormally high flow rate indications were noted a number of times on molecular sieve B flowmeter during repressurization/purging through the airlock fill valves. This condition resulted because the AM fill line exhausted into a duct common with the mole sieve B exhaust duct and in the immediate vicinity of the mol sieve B flowmeter. The flow disturbance created by this flow mixing typically caused maximum flow rate indications (77 CFM) for the duration of the purge.

11. OWS/AM Flex Duct Installation - During initial activation and subsequently when the OWS hatch was closed for EVA's, it was necessary to remove and/or install the gas interchange duct. The crew reported that the 2 calfax fasteners which secure the center of the duct would not mate with the attach fitting on the hatch ring. However, end support provided by the connections in the OWS and AM without center support was sufficient.

SECTION IV. OWS/MDA/AM THERMAL CONTROL SYSTEM

A. Configuration

1. Active Systems. The active Thermal Control Systems for the Skylab were composed of the Atmosphere Control System, the Coolant System and the Heater Systems as shown in figures 4-1, 4-2 and 4-3.

Heat was removed from the OWS by the four OWS heat exchangers in the AM. If needed, heat could have been added to the OWS by the twelve duct heater elements in the Ventilation Control System ducts. Automatic control of the four OWS heat exchangers and eight of the duct heater elements was provided by an onboard thermostat which was set at the desired temperature. The remaining four duct heater elements had manual control. It was planned to heat the OWS prior to initial entry by the eight radiant wall heaters and also to maintain the OWS above 40°F during the unmanned operational phase of the mission by the same heaters. However, due to the meteoroid shield failure these heaters were not needed. Other OWS heaters included those for the water tanks, the waste tank vent, the various dump heaters, and the wardroom window heater.

Eight AM tunnel and seven STS wall heaters were provided to automatically control the AM tunnel and STS wall temperatures within acceptable limits by thermostat during manned and unmanned operational portions of the mission. Each heater had nominal closing set points of 42°F, 62°F and 82°F. The design tolerance on closing was ±5°F about the nominal closing setting and the opening setting was 0.5°F to 8°F above the closing setting. The 42°F setting could only be selected by DCS command, while the 62°F setting could be selected by either manual or DCS command and the 82°F setting could only be selected manually.

The MDA and STS were cooled by the three cabin heat exchangers in the STS. Sixteen MDA wall heaters, as well as the docking port, tunnel and window heaters were thermostatically controlled to maintain the interior surface temperatures in the MDA within acceptable limits. The wall heaters had a low set point which opened and closed between 42°F and 50°F and a high set point which opened and closed between 66.5°F and 73.5°F. The open and close points could not be less than 2°F apart. Either low or high set points could be chosen by DCS command. In addition, a high temperature cutoff was provided which opened at 97 ± 3°F and closed at a minimum of 90°F. The docking port heaters had a set point between 60°F and 70°F and had a design tolerance of 2 to 6°F between open and close points. A high temperature cutoff was provided between 72°F and 82°F with a 2°F tolerance between open and close points. The tunnel heaters had a set point between 60°F and 72°F and had a design tolerance of not less than 4°F between open and close points. The high

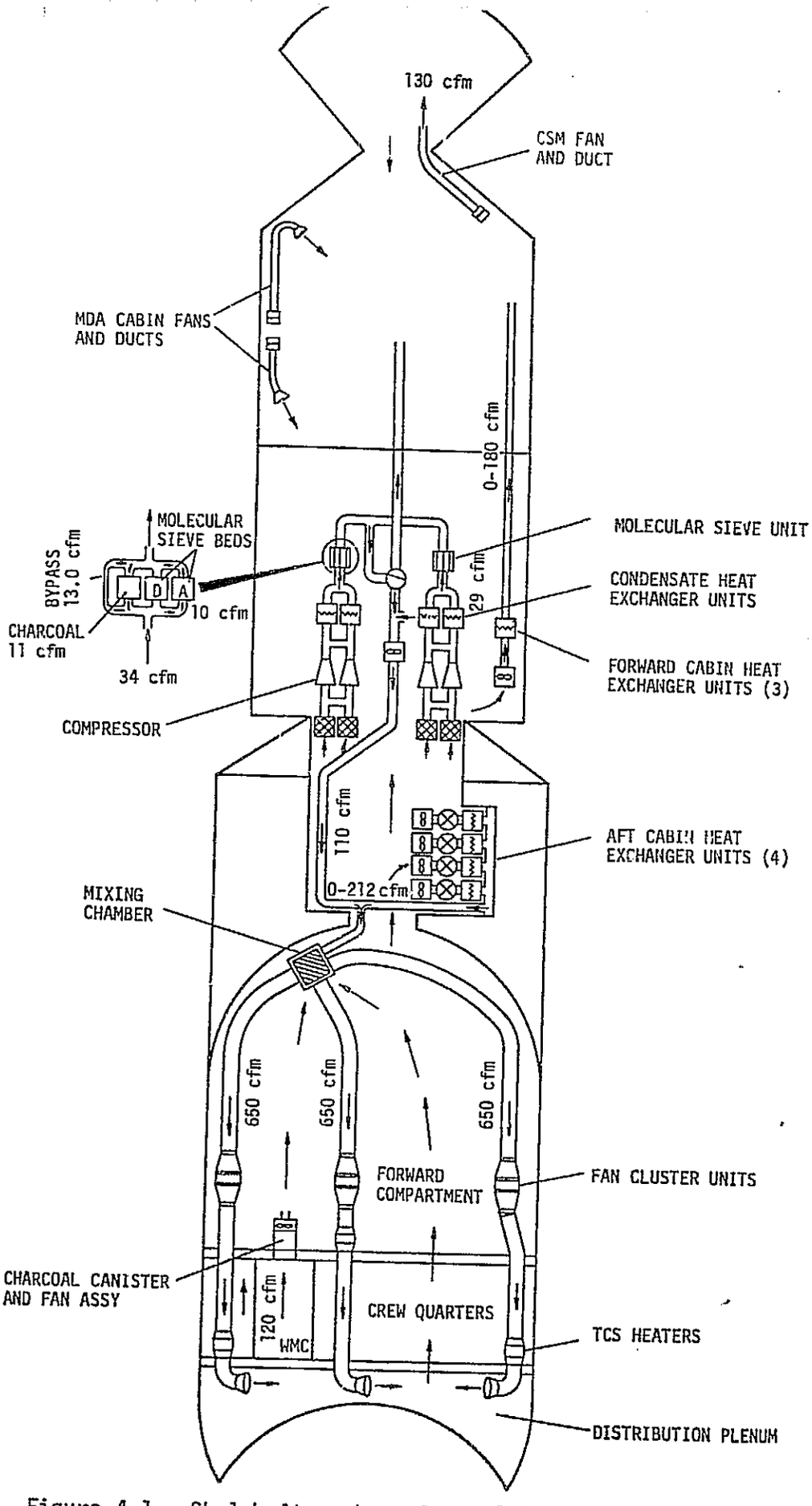

Figure 4-1. Skylab Atmosphere Control System

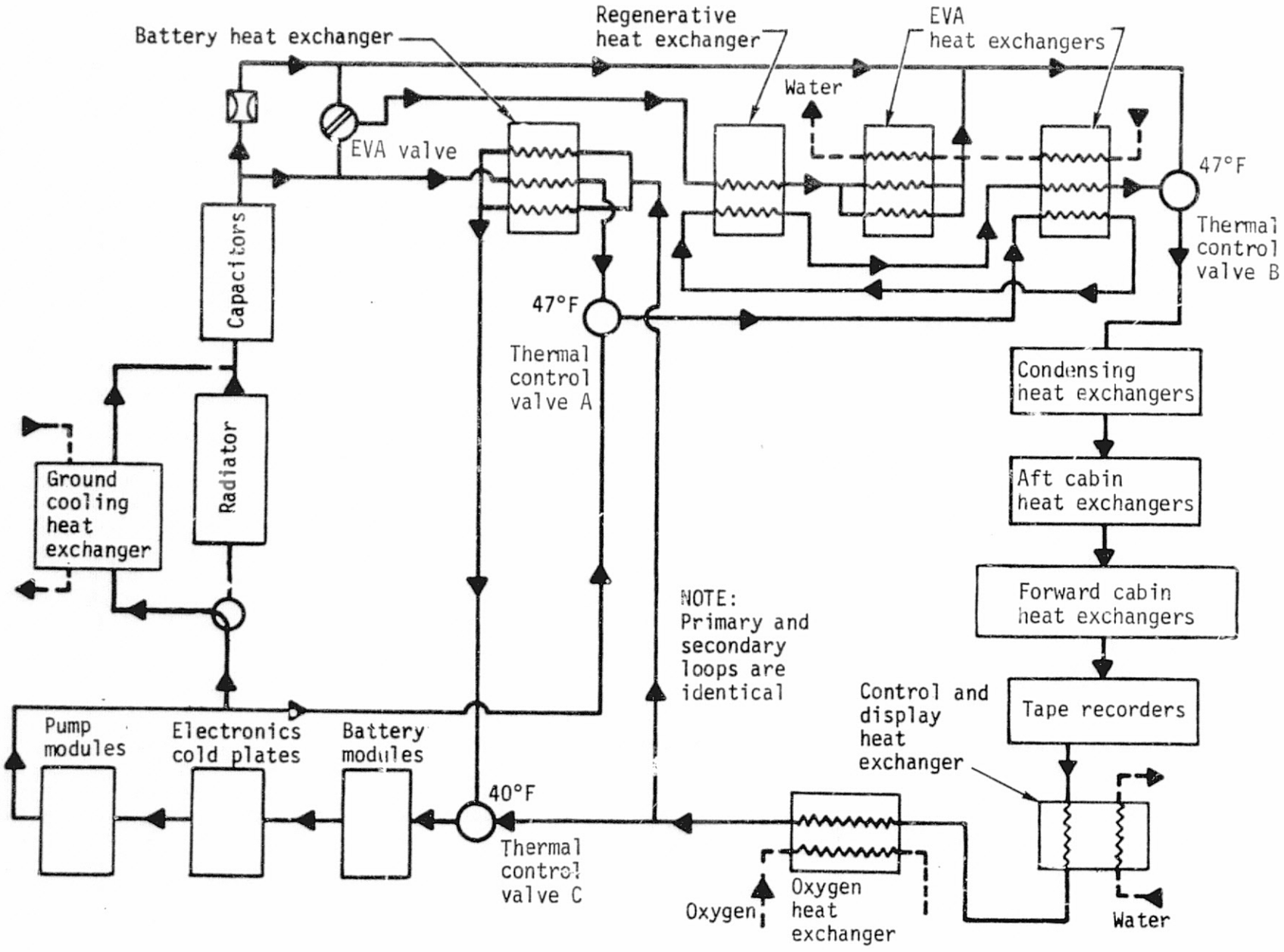

Figure 4-2. Skylab Coolant Loop System

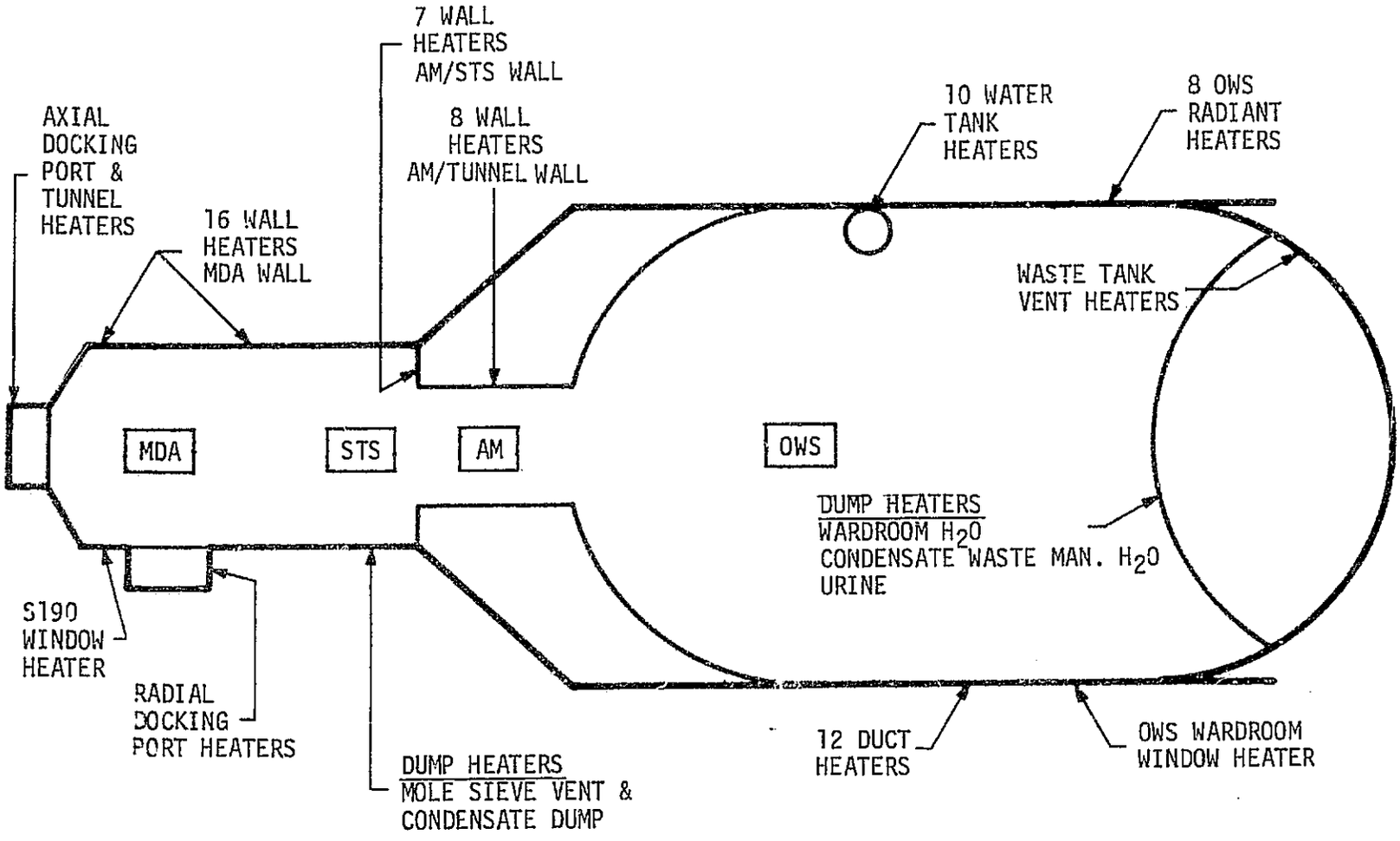

Figure 4-3. Skylab Heater Locations

temperature cutoff was provided between 92°F and 105°F with a 4°F tolerance between open and close points. The MDA heater system had redundant primary and secondary heaters which could be selected by DCS command.

An interchange fan and duct was provided between the MDA and CSM to maintain the temperature of the CSM within acceptable limits during the manned operational portion of the mission. The CSM cabin heat exchanger was not in operation during this period.

Additional sensible heat removal was provided for the SWS by the condensing heat exchangers in the STS. The outlet from these heat exchangers was directed to the OWS after activation during all manned missions but could have been directed to the MDA if desired. In addition, the OWS was cooled by the heat leak into the refrigeration system.

2. Passive Systems. The coatings and insulations which provided passive thermal control for the SWS served to optimize the heat loss or gain and to isolate the interior from the variable orbital environment. Figure 4-4 provides an overview of cluster thermal coatings and insulation.

The OWS was insulated with a polyurethane insulation lining on the inside of the pressure wall and a multi-layer insulation (MLI) blanket on the outside of the forward dome. The barrel section was further insulated by using low emissivity coatings for the outside of the pressure wall and beneath the thermal shields. The exterior coatings for the OWS are shown in figure 4-5. As shown, the surface of the meteoroid shield was primarily black except for the white paint in a cross pattern which was required to meet the comfort criteria requirement within available active cooling and heater capabilities. The meteoroid shield was lost during boost and the effect on the passive system is discussed in subsequent paragraphs. Relatively high values (approximate $\varepsilon = 0.7$) were chosen for the emissivity of the interior surfaces. This provided a greater radiant interchange between the surfaces and assured a relatively uniform temperature distribution on the inside walls.

The AM was insulated by a thermal curtain and a meteoroid curtain. The thermal curtain was a single layer of fiberglass with one side impregnated with Viton Rubber and the other side gold coated. The thermal curtain was installed with the black Viton side external except in the quadrant covering the Suit/Battery Cooling Module where it was reversed. The meteoroid curtain was similar to the thermal curtain except it was thicker and had an off-white fiberglass cloth exterior facing.

The external thermal coatings used on the surfaces of the AM, STS, and MDA employed aluminum, black, and white paints. The radiator used white paint (zinc oxide) with a low ratio of solar adsorptivity (α) to emissivity (ε) in order to provide low effective sink temperatures and resultant higher heat rejection rates. The design value used

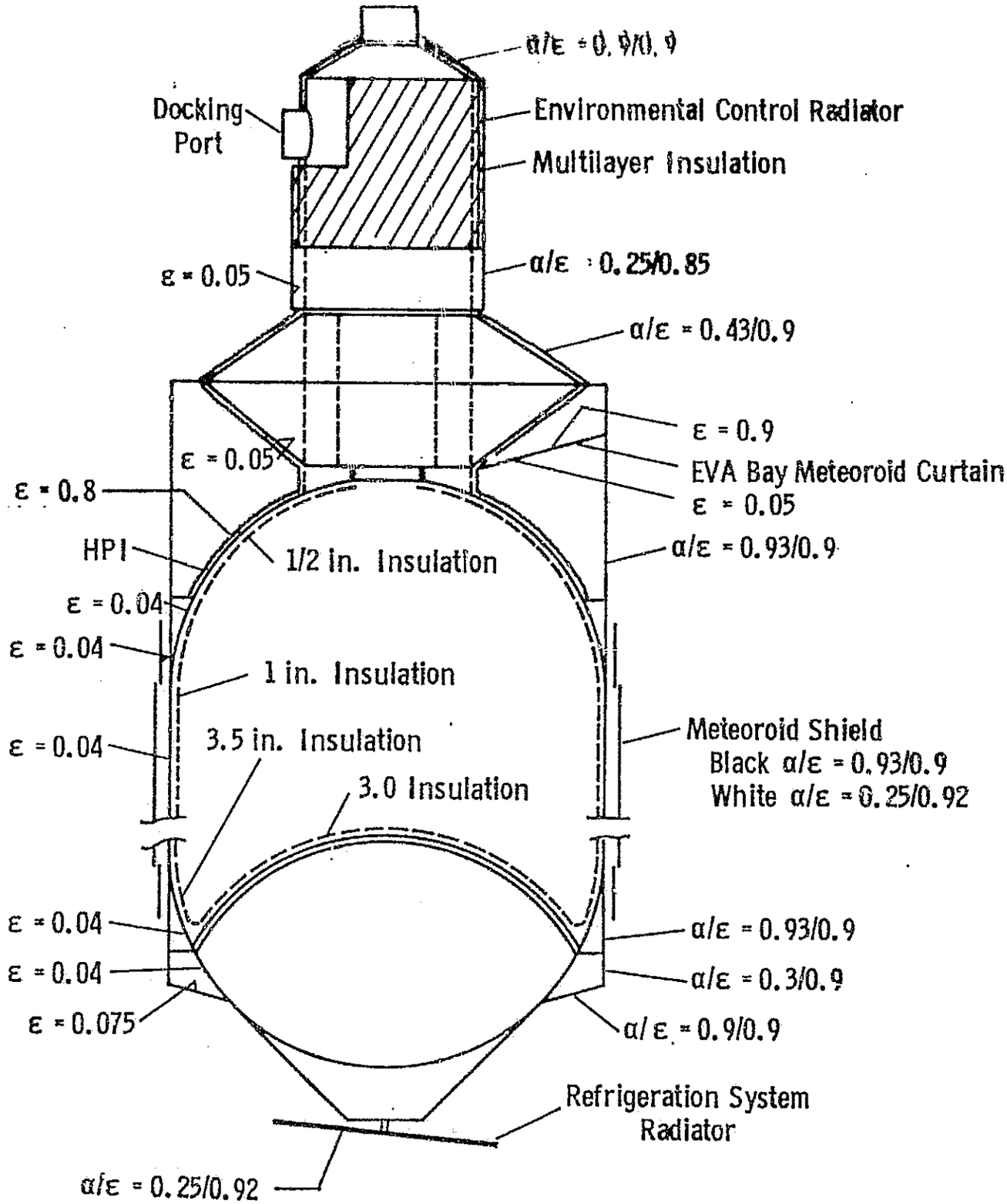

Figure 4-4. Skylab Thermal Coatings and Insulation

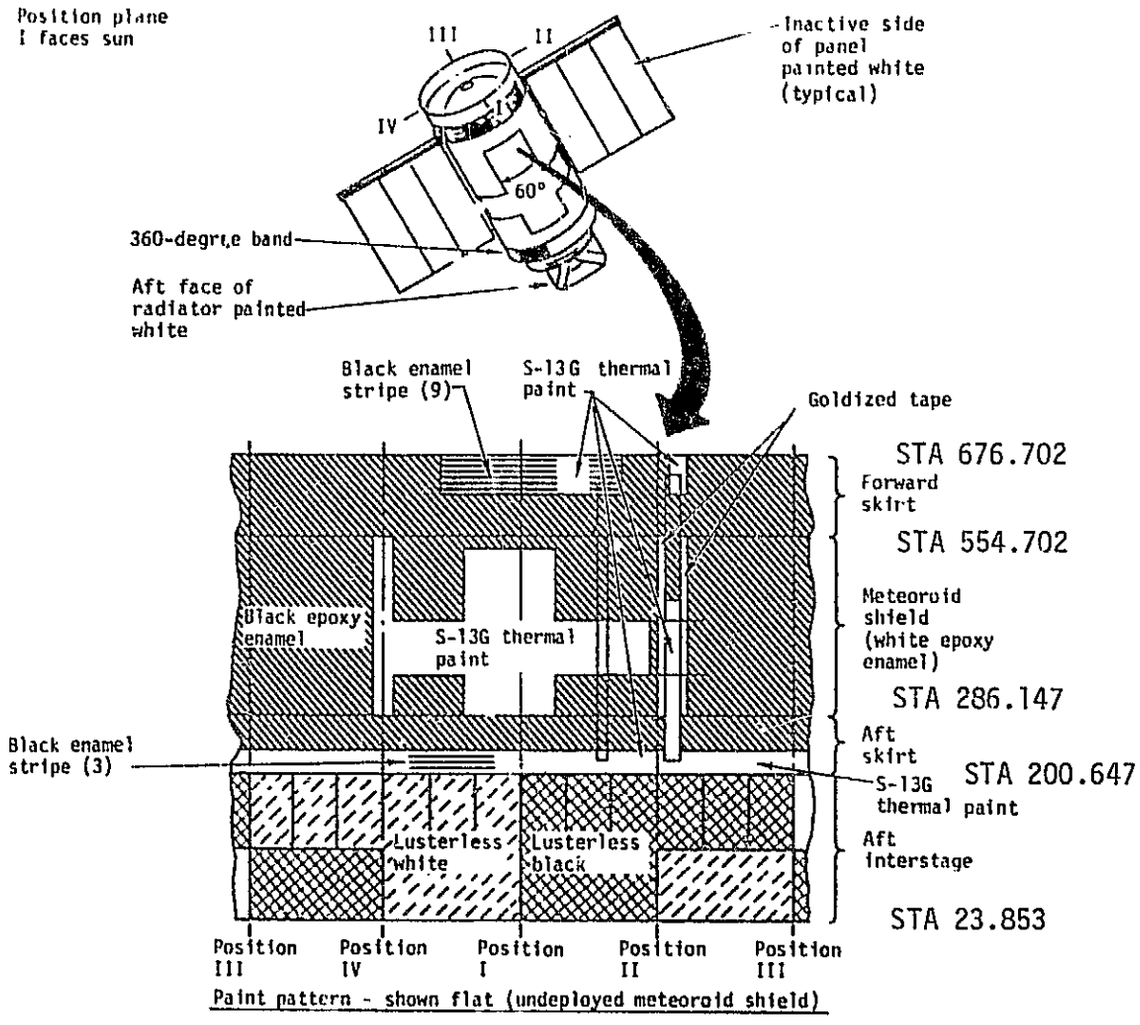

External paint pattern

Description

The external surface of the vehicle including the meteoroid shield is painted black and white.

The aft interstage is coated with white and black lusterless paint.

The forward skirt, aft skirt, main tunnel, and meteoroid shield are coated with a white (S-13G) thermal control paint and black epoxy enamel.

The cylinder is coated - both forward and aft between the gold tape and skirt attach angles with white epoxy enamel.

Gold tape is visible along each side of the main tunnel.

Figure 4-5. Orbital Workshop Paint Pattern

for the radiator surface was slightly higher than values measured for a clean surface to account for degradation during the mission caused by exposure to ultraviolet radiation, meteoroids, and contamination. Black paint was used on the IU and Fixed Airlock Shroud (FAS). An aluminum paint ($\alpha = 0.33$, $\varepsilon = 0.31$) was used on the Deployment Assembly (DA), and on squares provided around the top of the FAS to improve visibility during docking.

Bulkhead fittings were insulated from the support structure by fiberglass washers. Lines in the Suit Cooling, AM Coolant, and ATM C&D Console/EREP Cooling Systems were supported by insulated clamps. Components in these systems were insulated from the structure by fiberglass washers. Heat exchangers were covered with low density foam insulation. The thermal capacitor module was insulated with a glass fiber batt and covered with a rubberized fiberglass cloth vapor barrier with a flap type vent valve to provide launch ascent venting.

External water and coolant lines were routed together where practical and were wrapped with Microfoil insulation. Mosite insulation was used on internal water and coolant lines as required, to limit condensation and heat leak during prelaunch and orbit. The water lines in the Suit/Battery Cooling Module were not insulated. The internal portion of the condensate transfer line to the OWS was deliberately tied to the structure and was not insulated.

The MDA was insulated by a high performance insulation blanket composed of 91 layers of perforated double aluminized Mylar with Dacron net spacers, which was installed on the outside of the pressure shell. The insulation was covered by the radiator and the meteoroid shield which were attached to the pressure shell with fiberglass standoffs. Black paint was used on the outside of the MDA meteoroid shield.

In addition to the coatings and insulation systems described above, the OWS incorporated an arterial heat pipe system to control or eliminate water vapor condensation in specific locations of the OWS habitation area. The heat pipe system consisted of eight rings of heat pipes in four tank wall areas of the OWS and two sets of heat pipes on the Refrigeration System Logic Unit Containers and forward compartment freezer. The heat pipes were made of aluminum and utilized Freon-22 as the heat transfer fluid.

At approximately 63 seconds after liftoff, the meteoroid shield tore loose from the OWS tank wall. This anomaly exposed the entire circumferential tank wall surface of goldized kapton to the orbital space environment except for an area extending from beneath SAS Wing 1 to beneath the main tunnel where a small segment of meteoroid shield was still intact. Due to the high solar adsorptivity to infrared emissivity ratio ($\alpha/\varepsilon \simeq 4$ to 6) for the gold surface, the OWS quickly began to heat up. In order to stabilize the OWS temperature at a tolerable level

prior to deployment of a thermal shield, the vehicle attitude was held inertially with the ATM pitched approximately 45° toward the sun as shown in figure 4-6.

Various solar shields, which could be deployed by the SL-2 astronauts were designed and manufactured prior to SL-2 launch. The JSC parasol was chosen as the prime design. The parasol, packaged in a T027 canister, was designed to deploy through the solar scientific airlock on the OWS. The dimensions of the parasol were 22 feet by 24 feet.

The SL-2 crew deployed the parasol on DOY 147 at approximately 01:00 GMT. Crew comments and thermal instrumentation indicated that the parasol did not fully deploy. On DOY 170 at 19:00, the parasol was rotated by the crew in an attempt to provide additional coverage. Ground review of temperature data quickly indicated that the rotation actually obtained was in excess of that requested and the crew noticed increasing wall temperatures. As a result, the crew reversed the rotation and returned the parasol to its approximate original position. No further attempts were made to provide increased coverage by shield rotation. A photograph taken during SL-2 fly-around is shown in figure 4-7. Dimensions of the deployed parasol determined from the photograph are shown in figure 4-8. The parasol coverage of the gold foil was estimated to be 75 percent of the projected area.

The RCS plume caused the parasol to flap violently during the SL-3 CM fly-around prior to habitation. The crew stated that the parasol configuration was altered by the RCS plume and did not appear to be the same as the SL-2 crew described.

The MSFC Twin Pole solar shield was deployed over the existing parasol on the first SL-3 EVA to provide additional shading of the goldized kapton. The design configuration is shown in figures 4-9 and 4-10. Additional coverage of the gold foil was effected. However, the SL-3 astronauts commented that the shield material had retained the foldline creases which prevented the shield from completely shading the gold areas near Positions II and IV. Post SL-4 fly-around photos of the SWS verified the SL-3 crew observations as shown in figure 4-11. Geometric analysis of the photo indicated that approximately 89% of the projected area of the gold foil was shaded from the sun by the parasol and twin pole shields.

B. Performance

1. <u>OWS Meteoroid Shield Failure</u>. The meteoroid shield failure during the SL-1 launch necessitated a large number of thermal studies in support of the OWS and in development of a thermal protection device for the orbital workshop. As mentioned earlier, with the loss of the

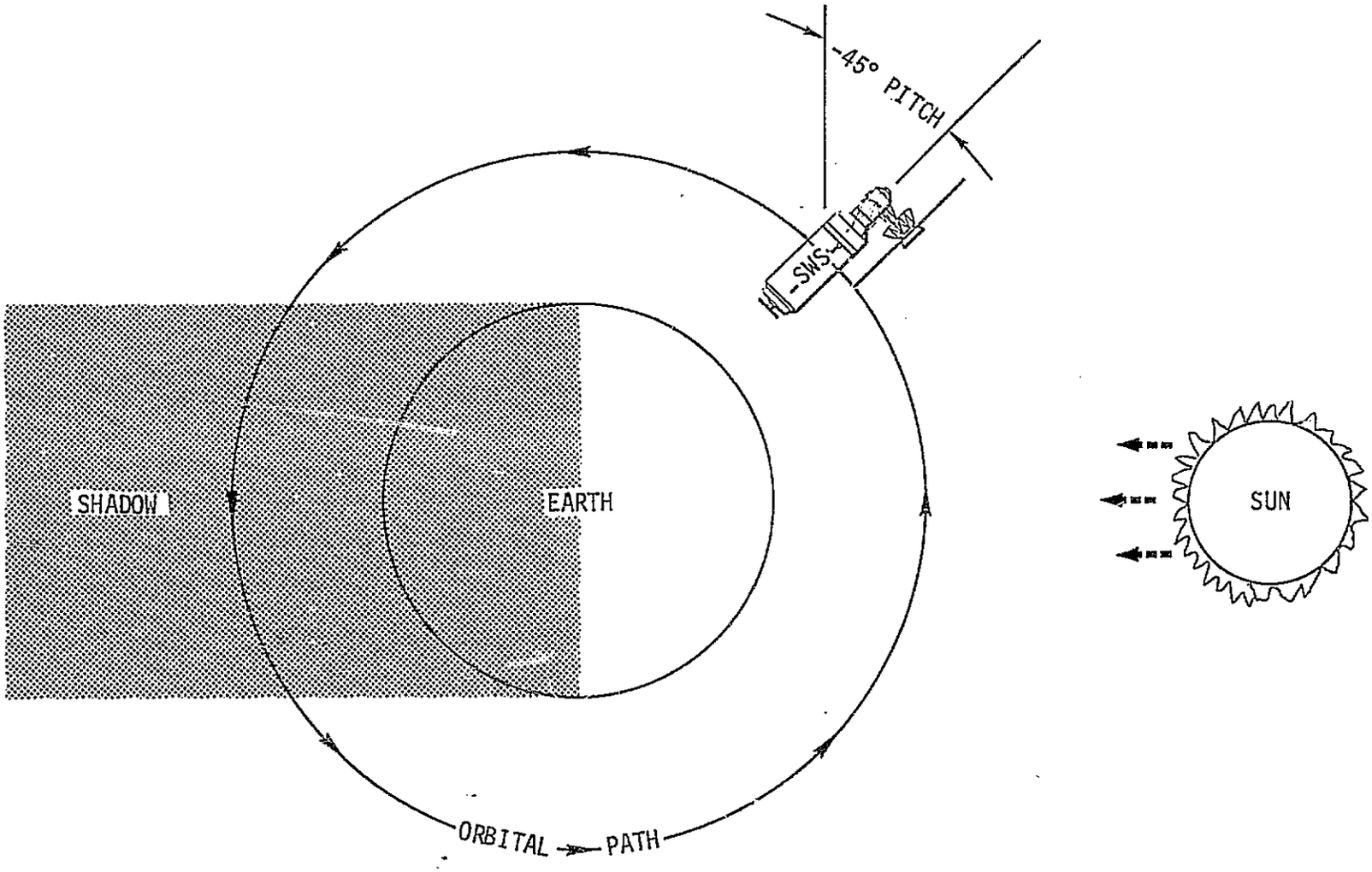

Figure 4-6. Typical SL-1 SWS Attitude

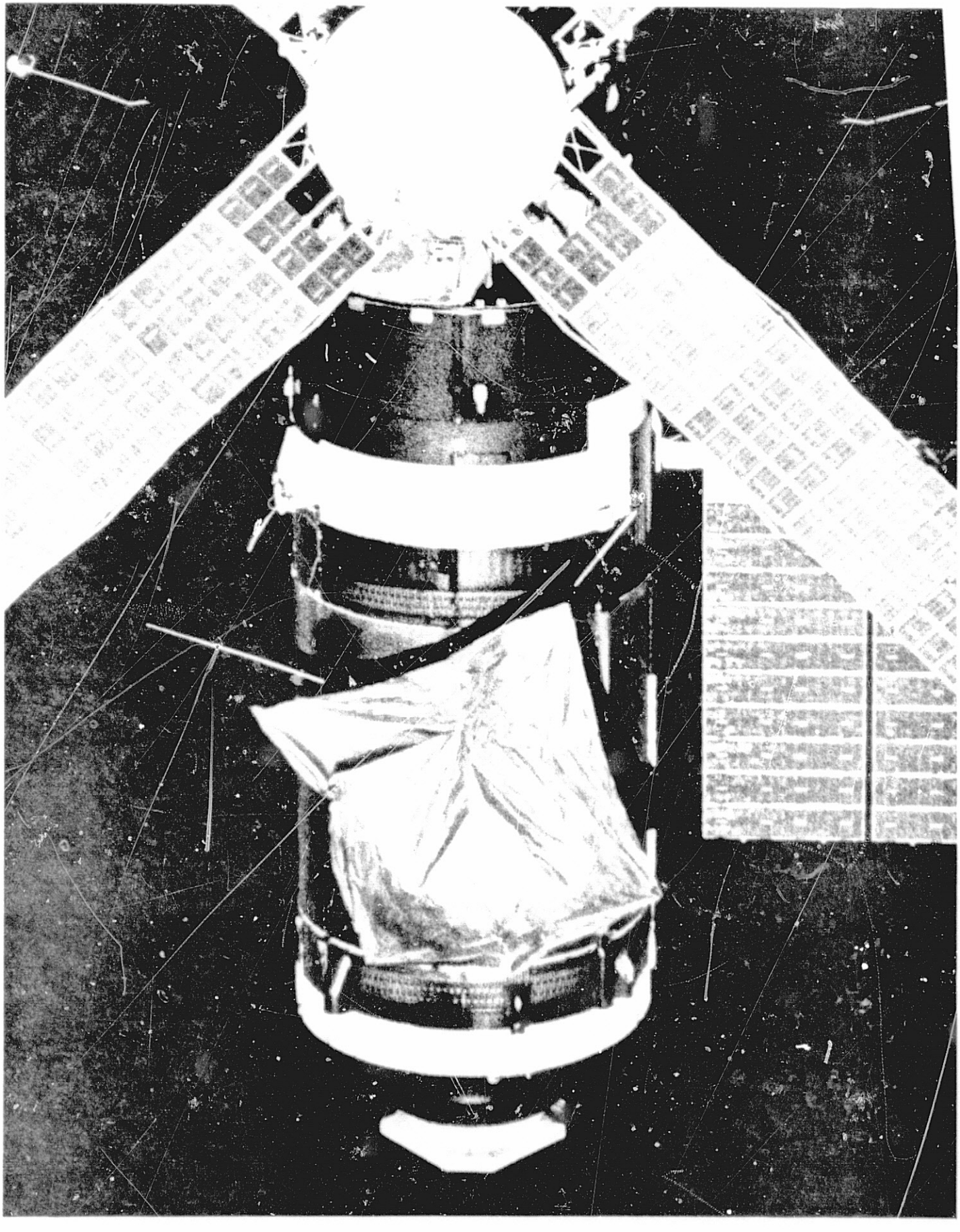

Figure 4-7. SL-2 Fly-around - Parasol Shield

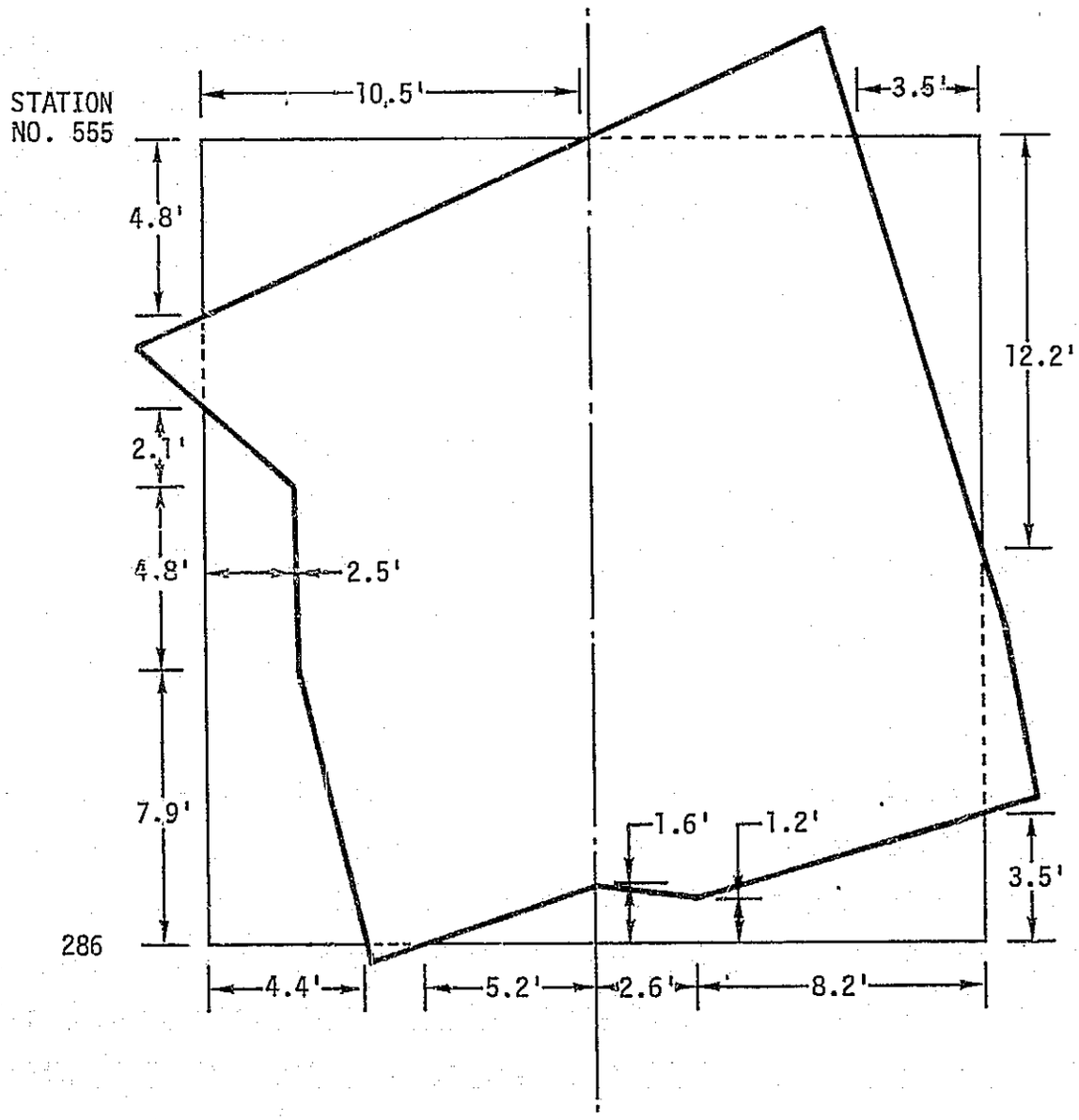

Figure 4-8. Shape of Parasol Shield Obtained from Fly-around Pictures

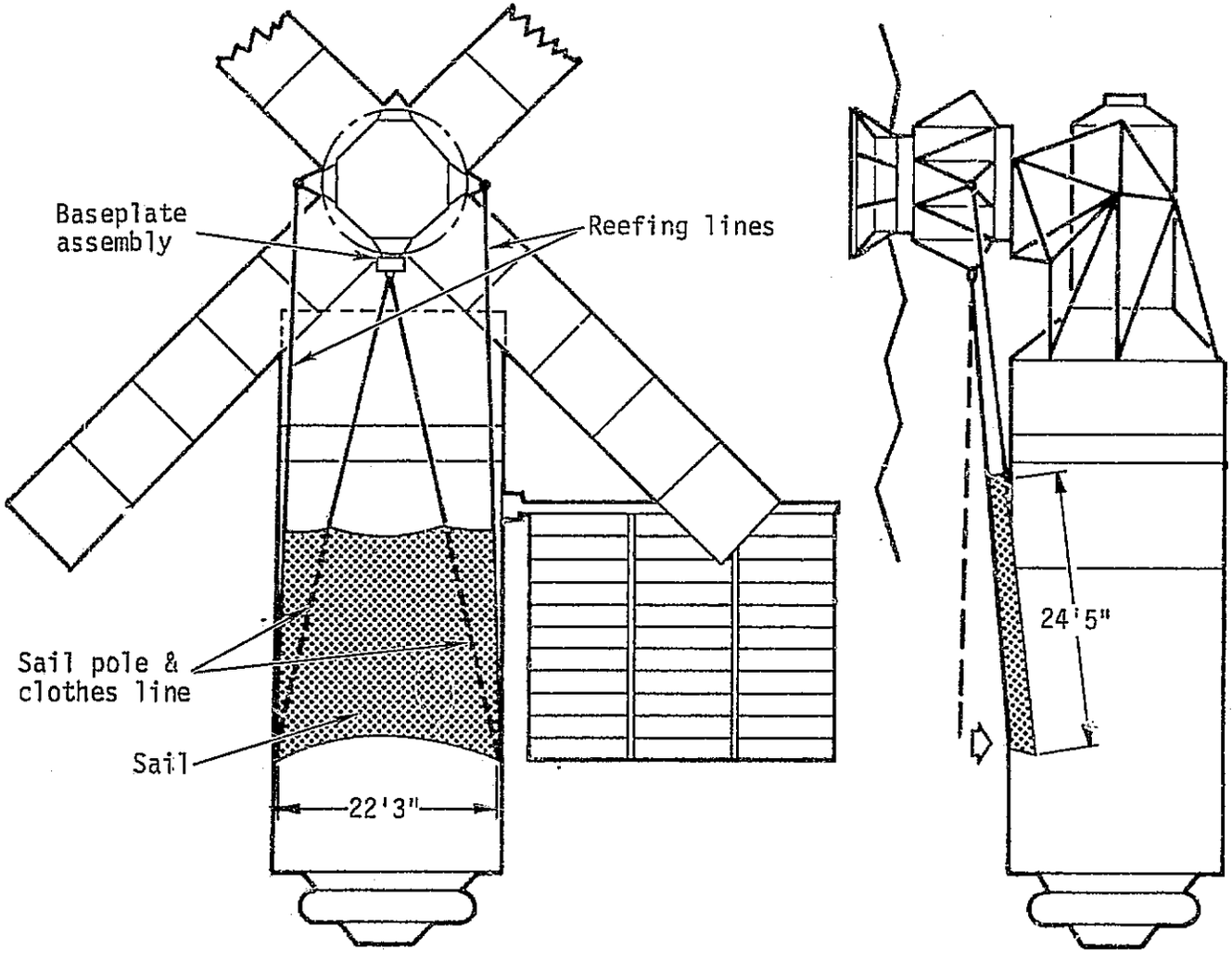

Figure 4-9. MSFC Twin-Pole Shield Configuration

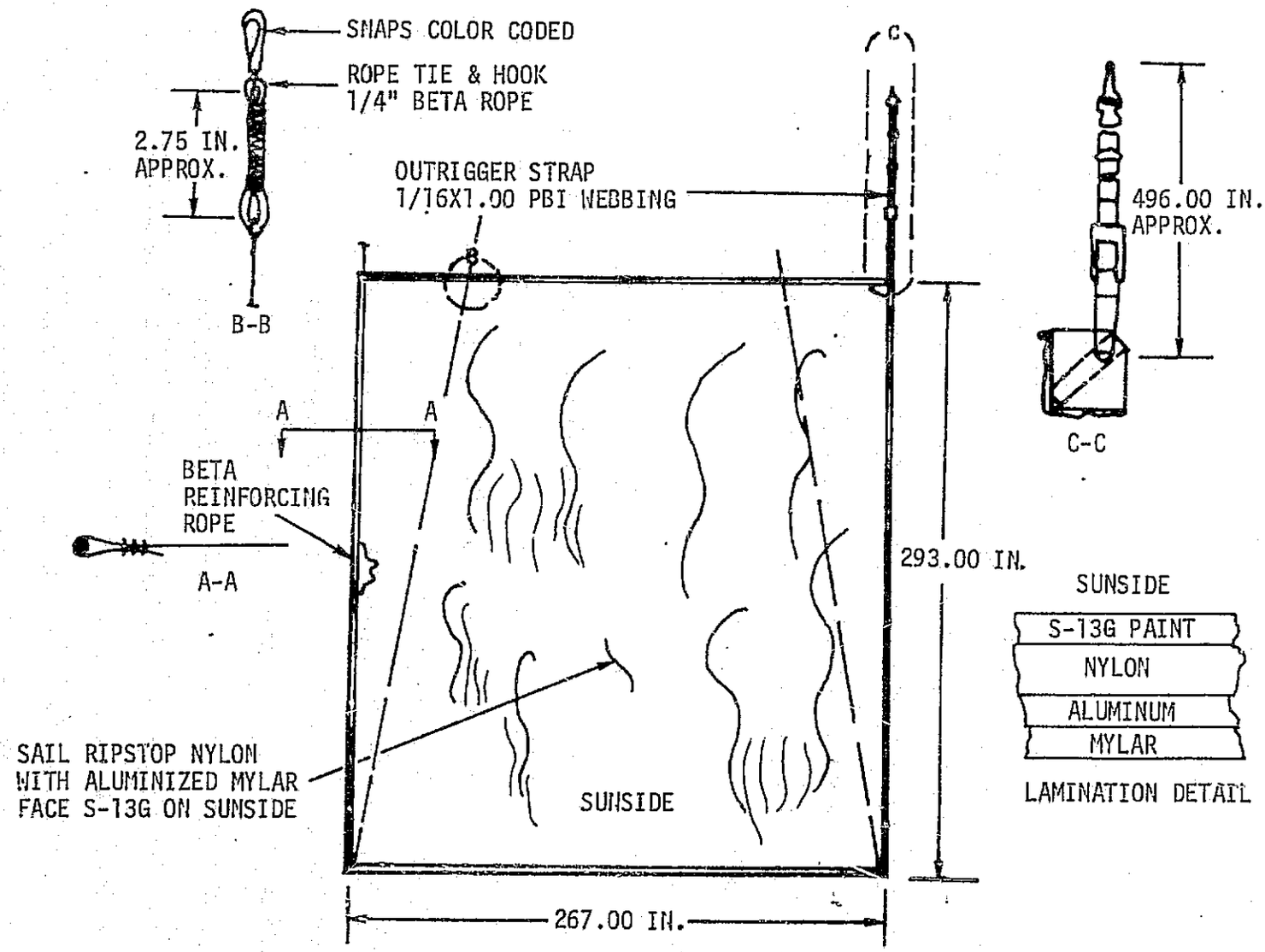

Figure 4-10. MSFC Twin-Pole Shield Details

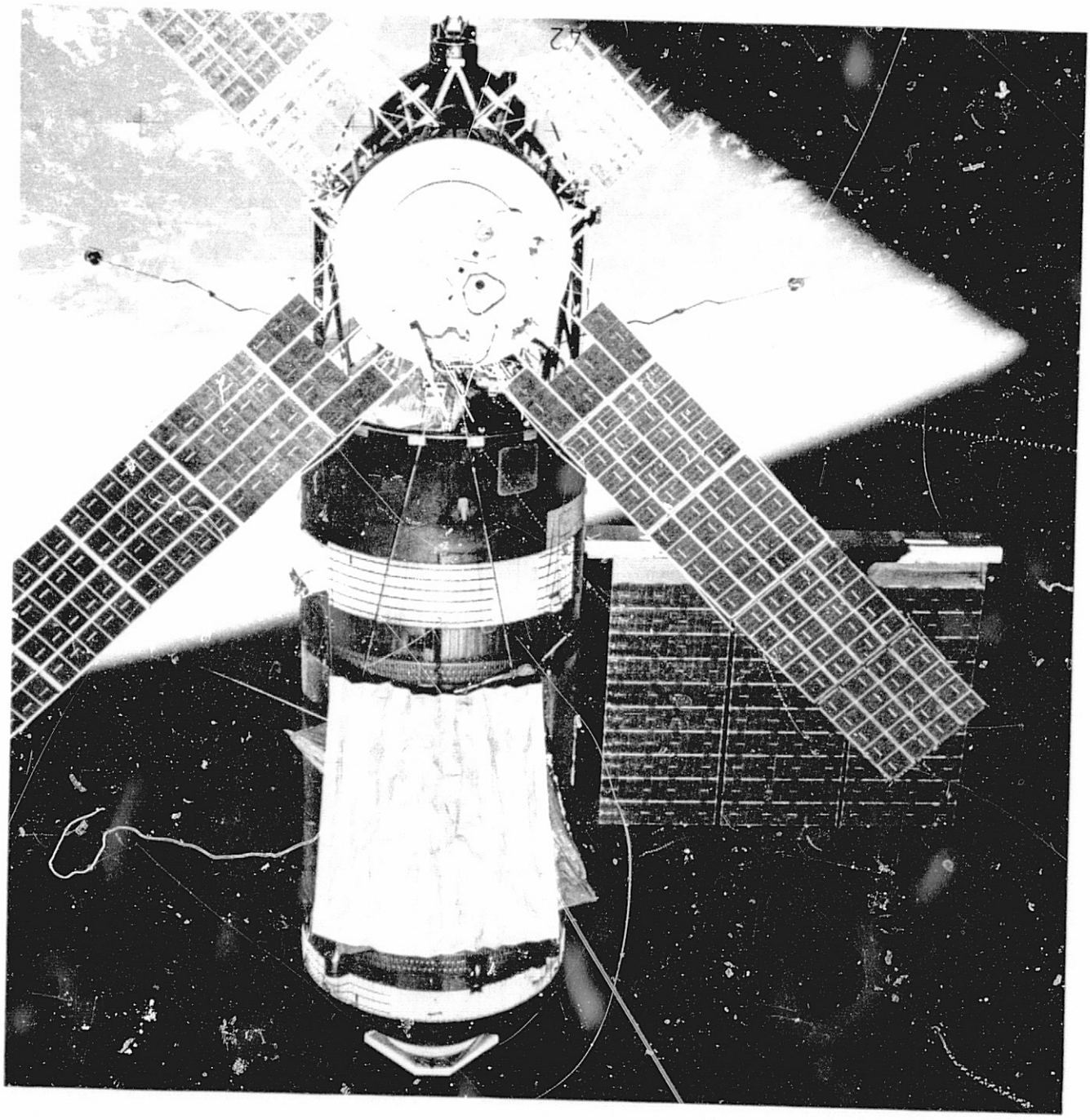

Figure 4-11. Twin-Pole Shield Deployment

meteoroid shield and the subsequent exposure of the goldized kapton-covered OWS tank wall which had an α/ε ratio of approximately 4.0 to 6.0, the solar input was increased, resulting in unacceptably high OWS structural temperatures and, consequently, high internal temperatures.

The overriding factor controlling the temperature of the OWS was the solar absorptivity (α) and the infrared emissivity (ε) of the goldized kapton on the OWS tank sidewall. The "as applied" value of α/ε was approximately .15/.03. However, the effect of boost heating, retrorocket plume contamination, high temperature exposure, and the meteoroid shield scratching of the gold was unknown.

The external skin temperature increase on Fin I from the first sunrise pass correlated with an α/ε = .275/.05. Additional analysis showed that the mean internal temperature increase correlated using α/ε = .20/.04. Since the external temperature sensors were off-scale at the end of the first sunlight pass and since the transient response of the internal temperatures was slow, only limited data was available to determine the α/ε ratio initially. Therefore, the analysis was continued using a range of α/ε values from .275/.05 to .20/.04.

Results of the initial studies indicated that the mean internal temperature would reach 160°F within 10 days after launch. This being completely unacceptable, studies were made to determine an optimum vehicle attitude to maintain acceptable temperatures and also provide sufficient incident solar energy on the ATM solar arrays. Results from the optimum attitude study indicated a vehicle pitch maneuver of approximately 45° (figure 4-6). In figures 4-12 and 4-13 flight data are compared to analytical predictions for the first 12 days of the Skylab mission.

The pitch maneuver, although successful in temporarily decreasing the rate of internal temperature increase, was not intended to be the final solution. Proposed solutions to the problem focused on placing a shield between the OWS tank wall and the sun. Since the principal attitude of the workshop was solar inertial, the shield could be fixed relative to the workshop and would provide shadowing from direct solar energy, leaving earth albedo as the only significant solar input.

Preliminary analysis showed that the OWS internal temperature was not sensitive to the optical properties or temperature of the shield principally because the low emissivity gold coating on the exterior of the OWS thermally isolated the shield from the OWS tank wall. Hence, the primary thermal requirements for the shield was complete shadowing of the solar side of the OWS tank wall.

The following sun shield configurations were analyzed using the thermal model:

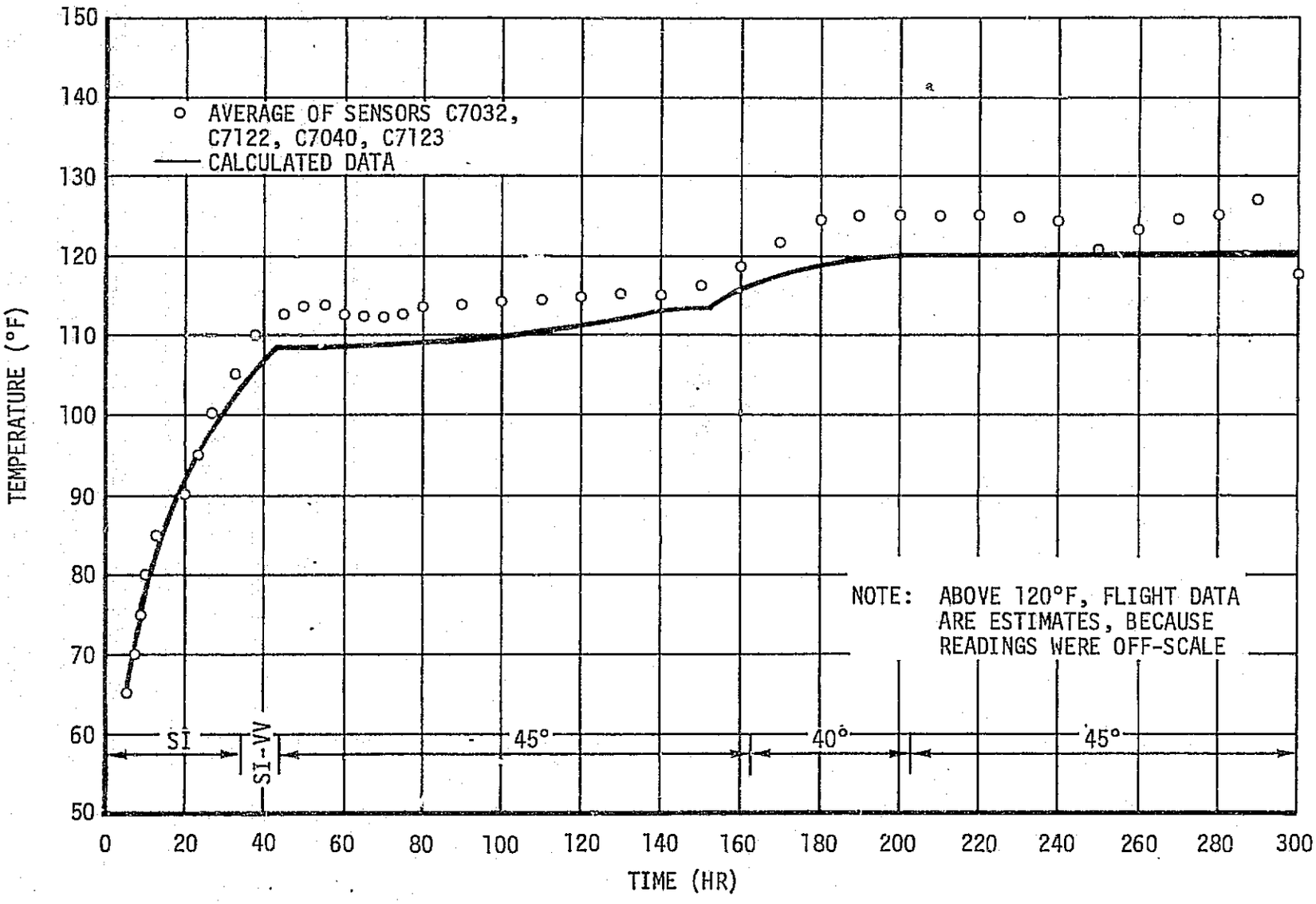

Figure 4-12. Mean Internal OWS Environment.

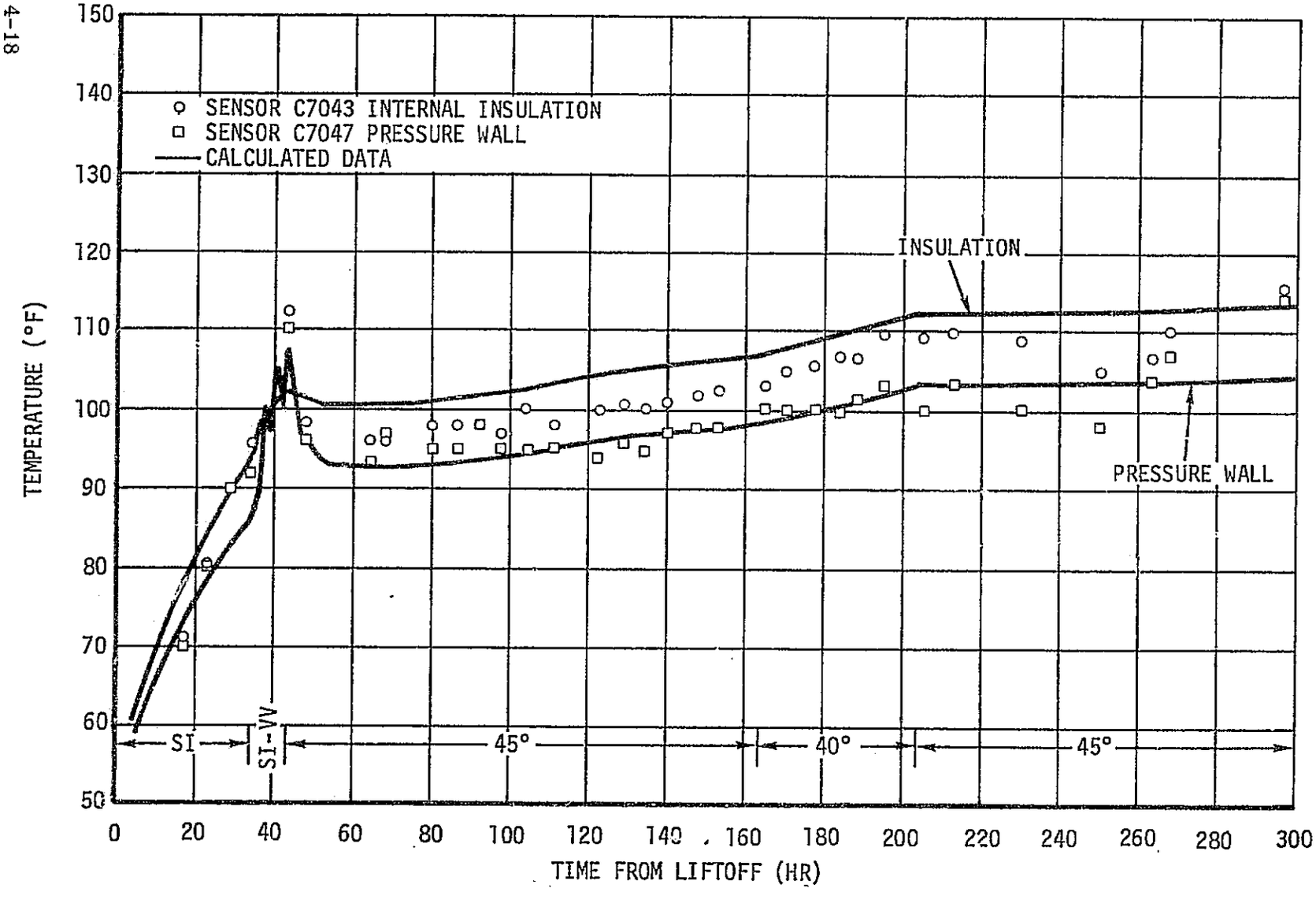

Figure 4-13. Fin III Pressure Wall and Internal Insulation

1. Sunshield wrapped 180° around and standing six inches off OWS tank wall.

2. MSFC I rectangular sunshield (20 feet by 23 feet).

3. Trapezoidal sunshield (22 foot base, 11 foot top, and 23 foot height).

4. JSC-I conical sunshield.

5. JSC II sunshield (angled from aft skirts to AM structure).

6. MSFC II sunshield (twin pole shield).

7. Douglas inflatable sunshield (20.5 feet by 22 feet).

8. Langley inflatable sunshield (22 feet by 24 feet).

9. JSC parasol sunshield (SAL deployed) (22 feet by 24 feet).

   a. 100% coverage
   b. 90 % coverage
   c. 84% coverage

10. MSFC II sunshield deployed over parasol.

Figures 4-14 through 4-23 illustrate the ten configurations. Table 4.1 contains a summary of the performance for each of the proposed shields. The percent coverage of each shield was based on projected area of the OWS gold-coated tank wall and the OWS internal temperature was based on zero internal waste heat load and no ECS heat removal. Figure 4-24 shows the relative performance of each configuration. The general trend of decreasing OWS temperature with increasing shield coverage is indicated by the solid line in figure 4-24.

The JSC parasol shield was deployed on Day 147 of 1973. With the shield deployed, internal temperatures decreased 30°F in two days as indicated by the temperature history shown in figure 4-25. After deployment, the crew observed that the shield did not completely open. Within a day after shield deployment, the analytically predicted temperature decrease began to differ from flight data (figure 4-25). Note that after four days, predicted temperatures were 15°F lower than flight data. Analyses to determine the shield size was initiated since this parameter was essential for predicting internal temperatures. Assuming all of the meteoroid shield was missing and estimating the internal loads, the results indicated that 82 percent of the projected sidewall area was shaded from the sun. Based on this percent coverage it was predicted that the mean OWS temperature would reach 86°F during the

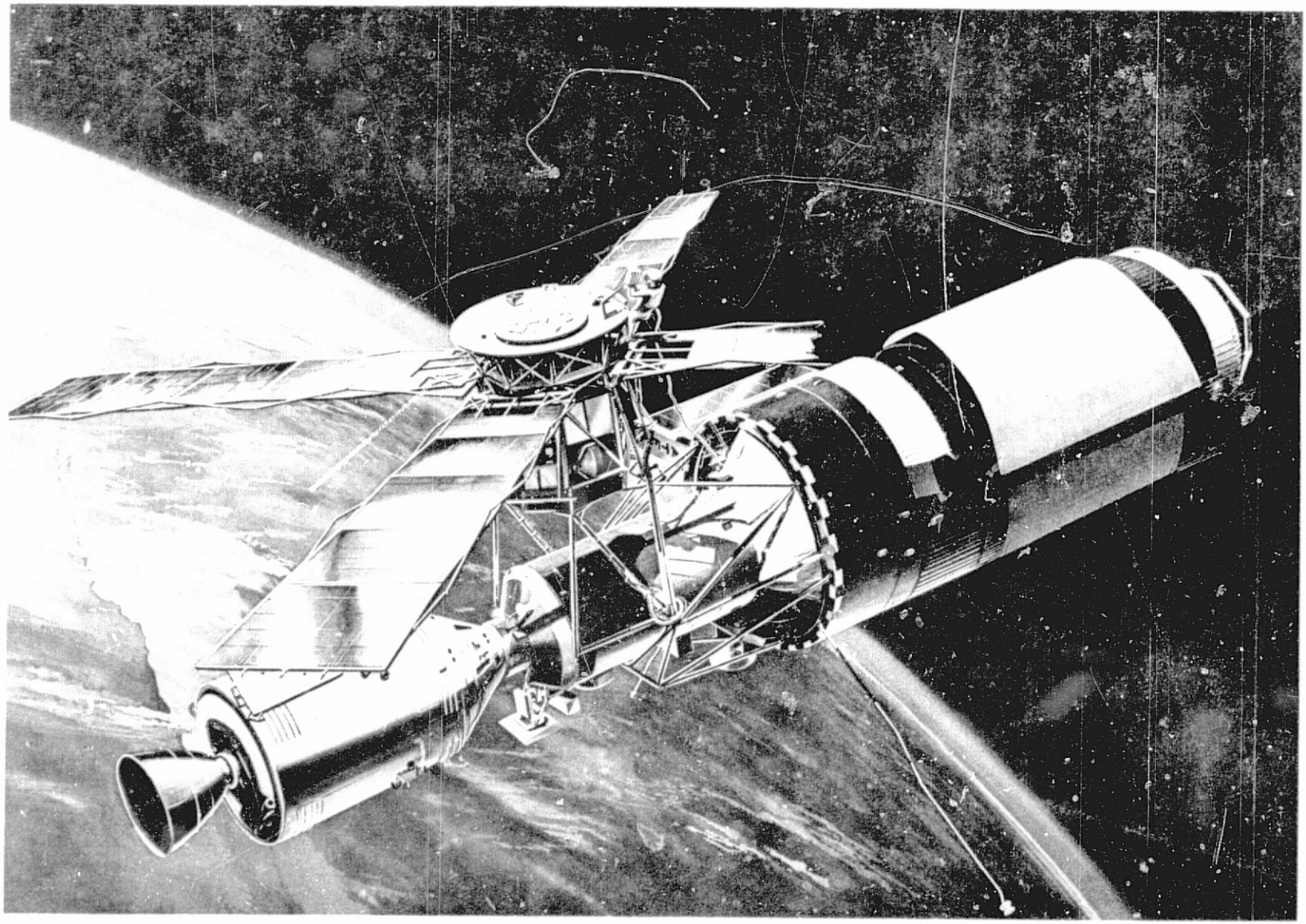

Figure 4-14. Sunshield Wrapped 180° Around and Standing 6" Off OWS Tank Wall

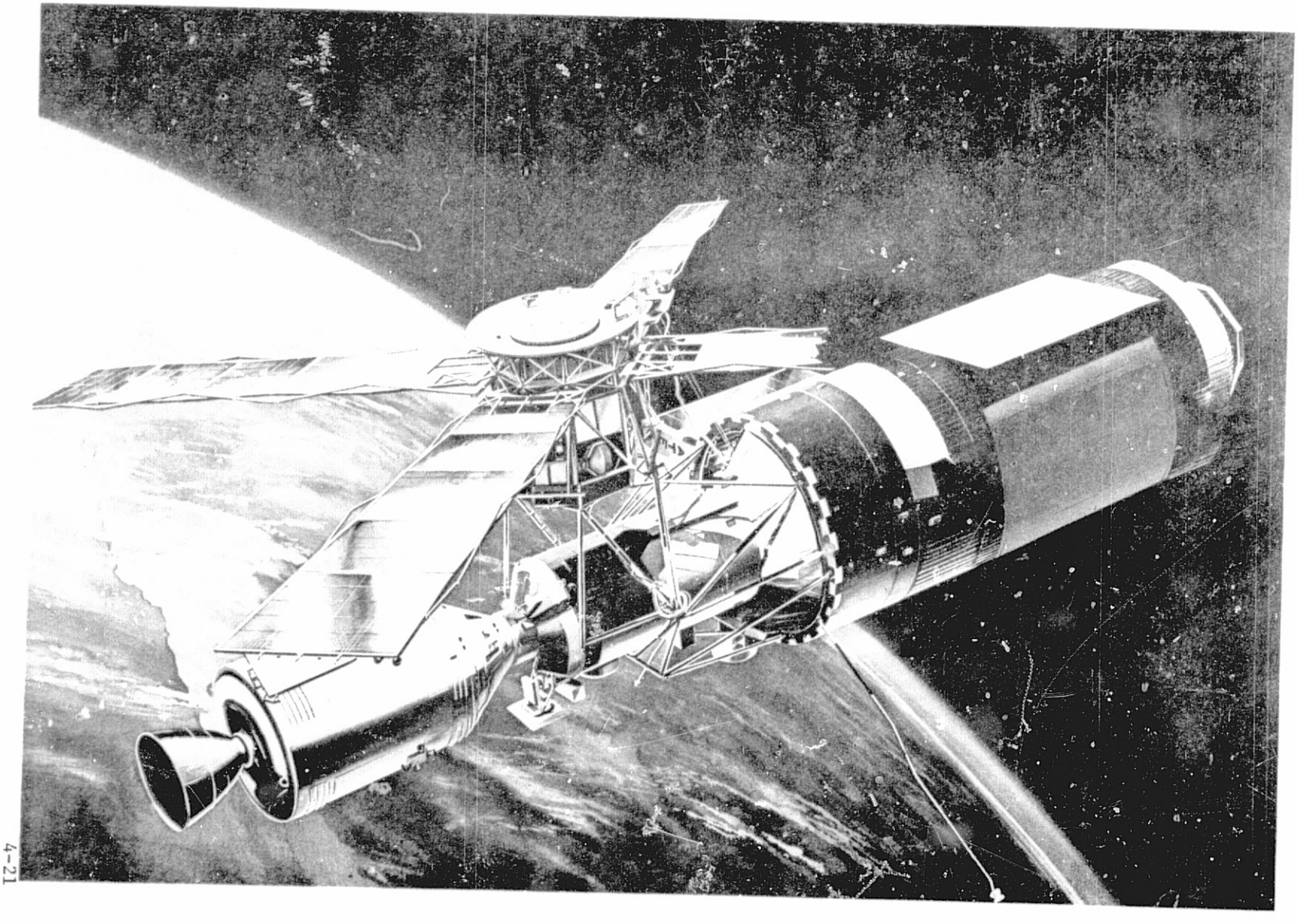

Figure 4-15. MSFC I Rectangular Sunshield

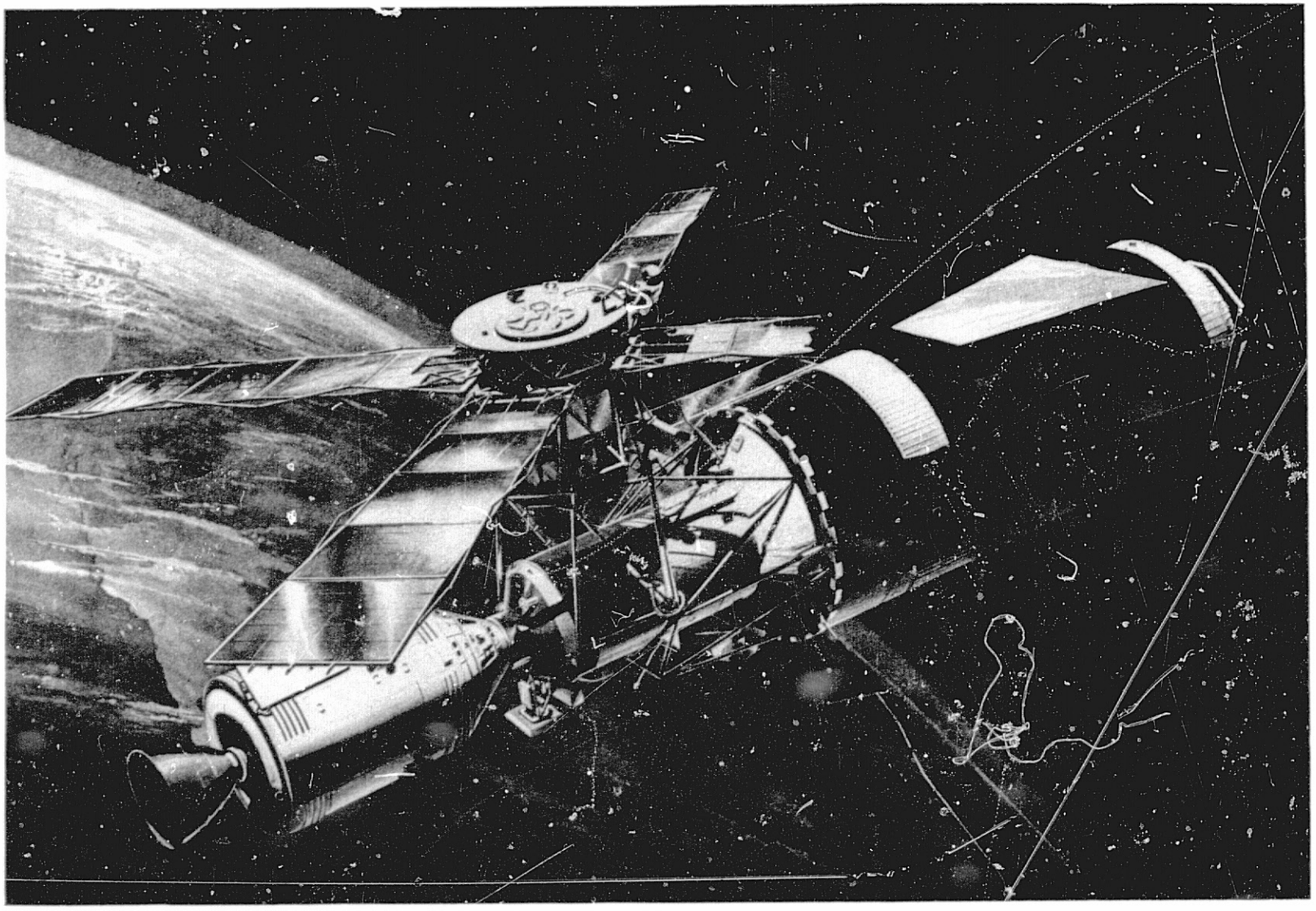

Figure 4-16. Trapezoidal Sunshield

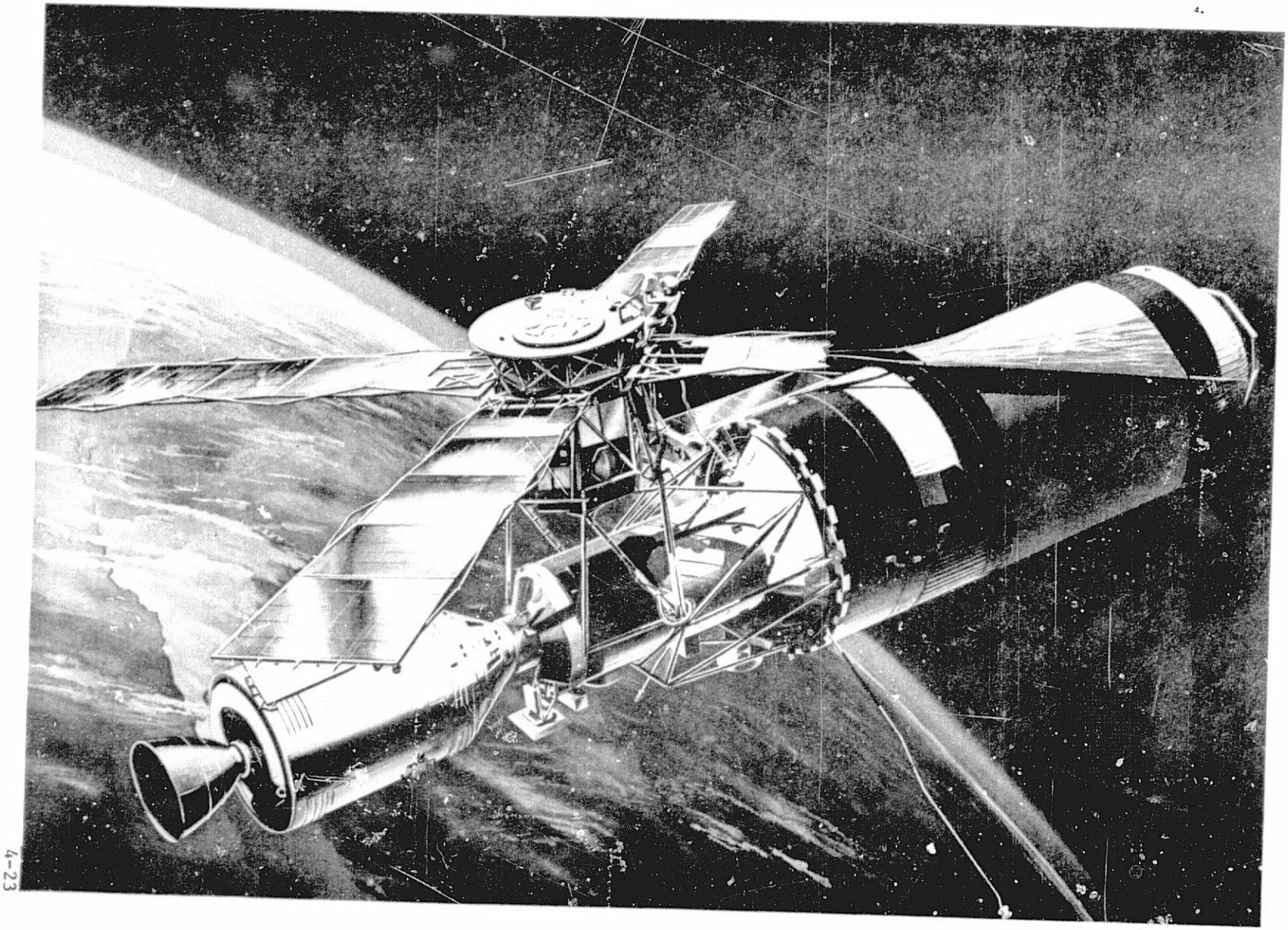

Figure 4-17. JSC I Conical SEVA Sunshield

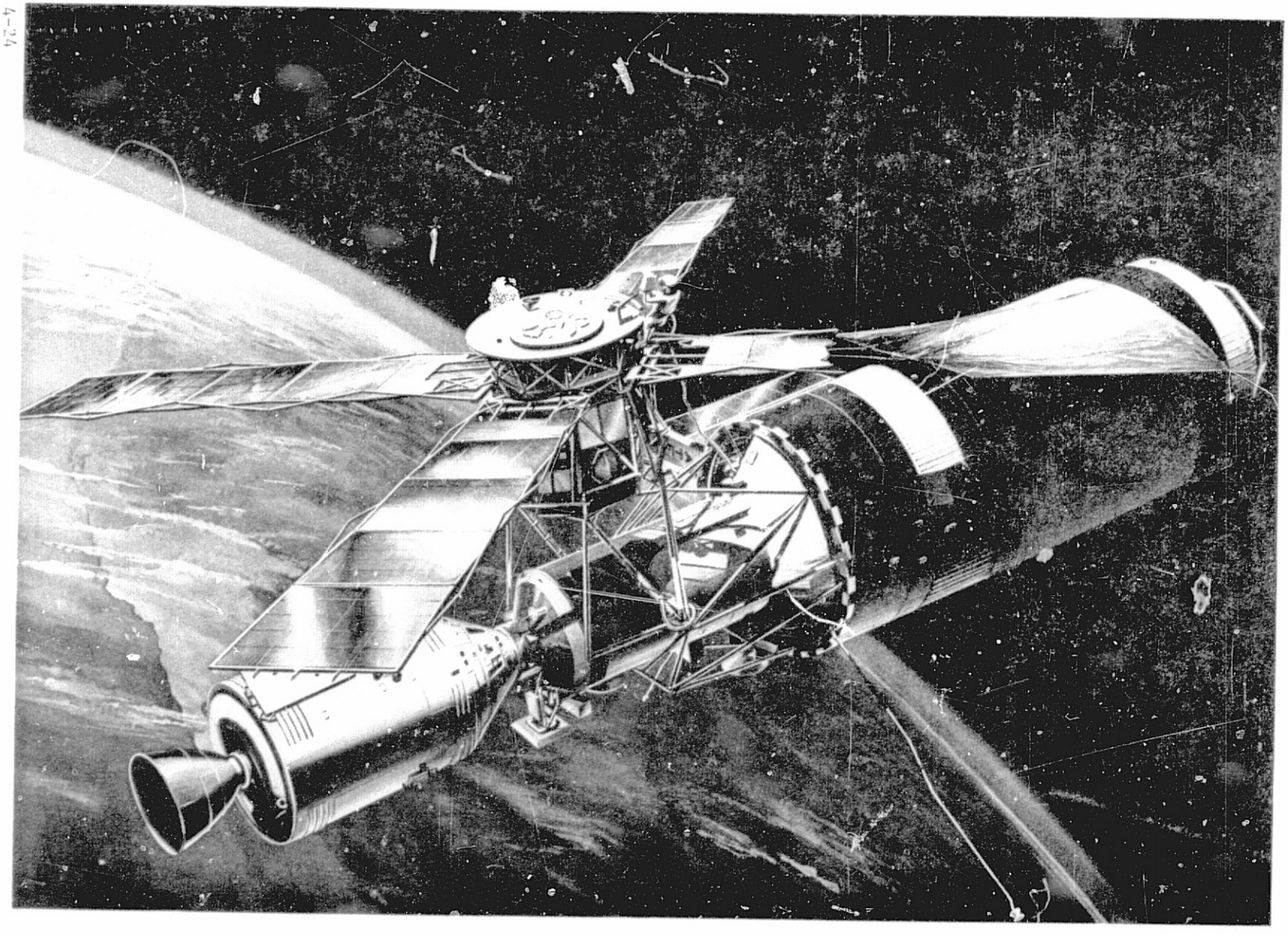

Figure 4-18. JSC I[illegible] SEVA Sunshield

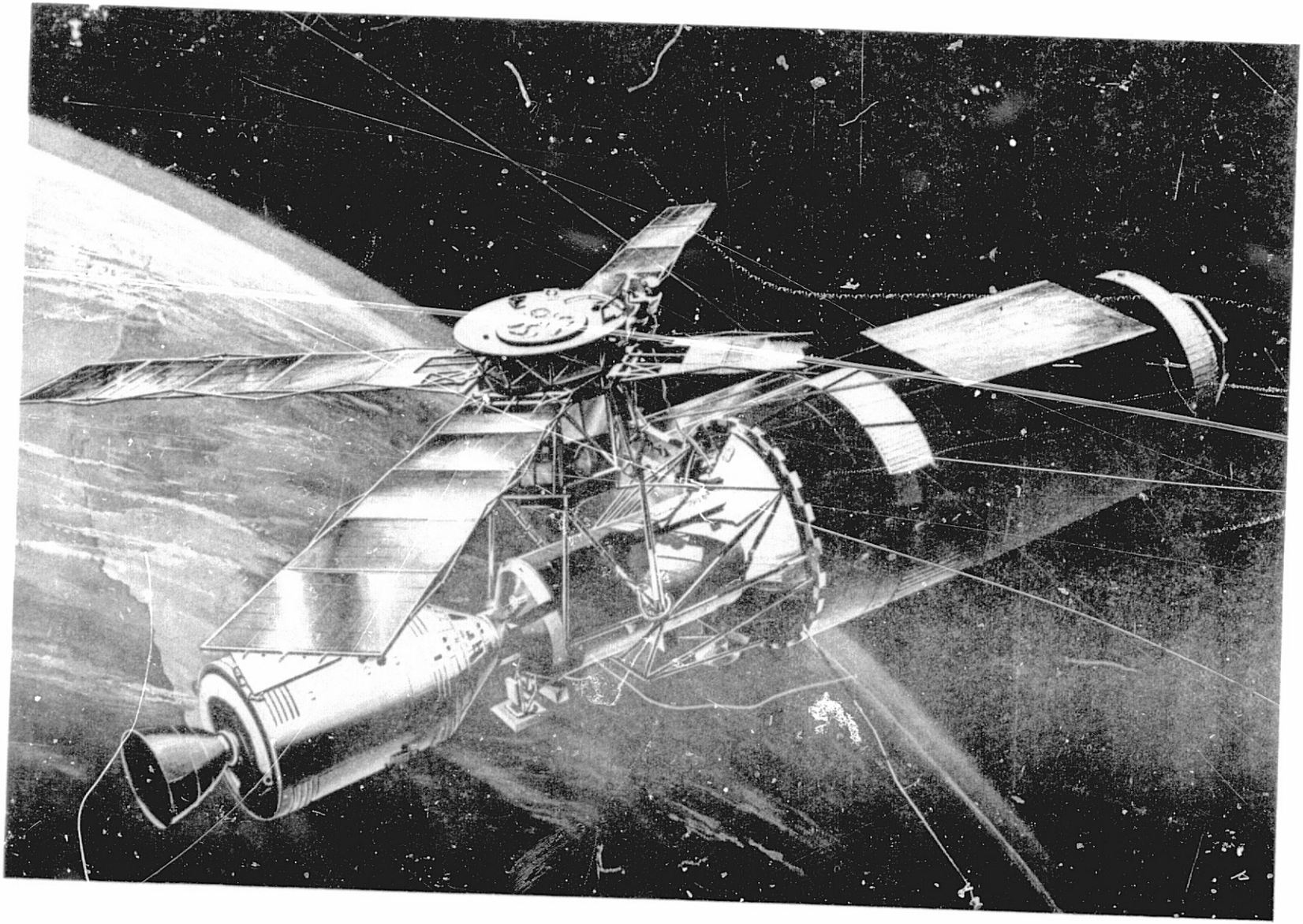

Figure 4-19. MSFC II Sunshield (Twin-Pole Shield

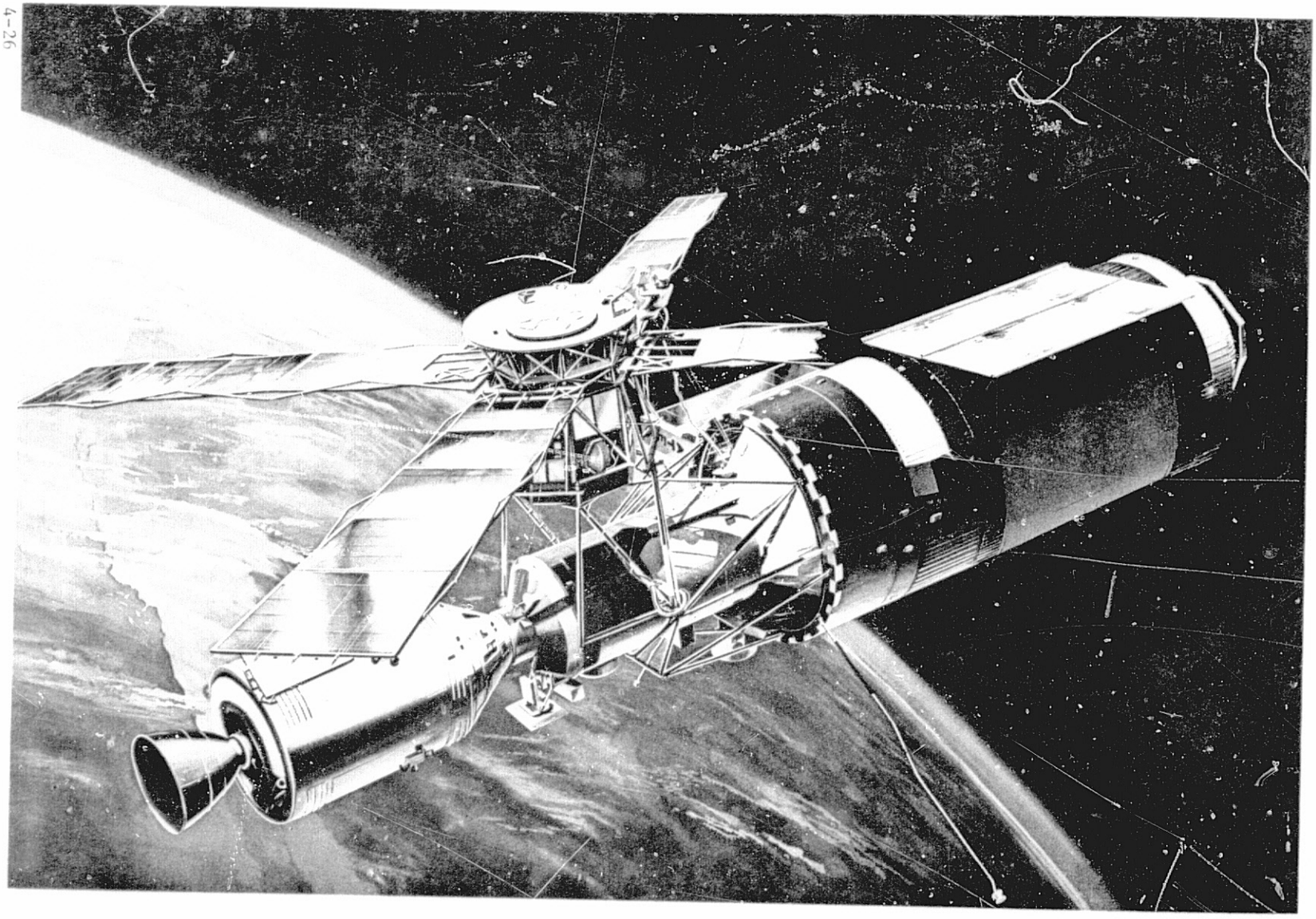

Figure 4-20. Douglas Inflatable Sunshield

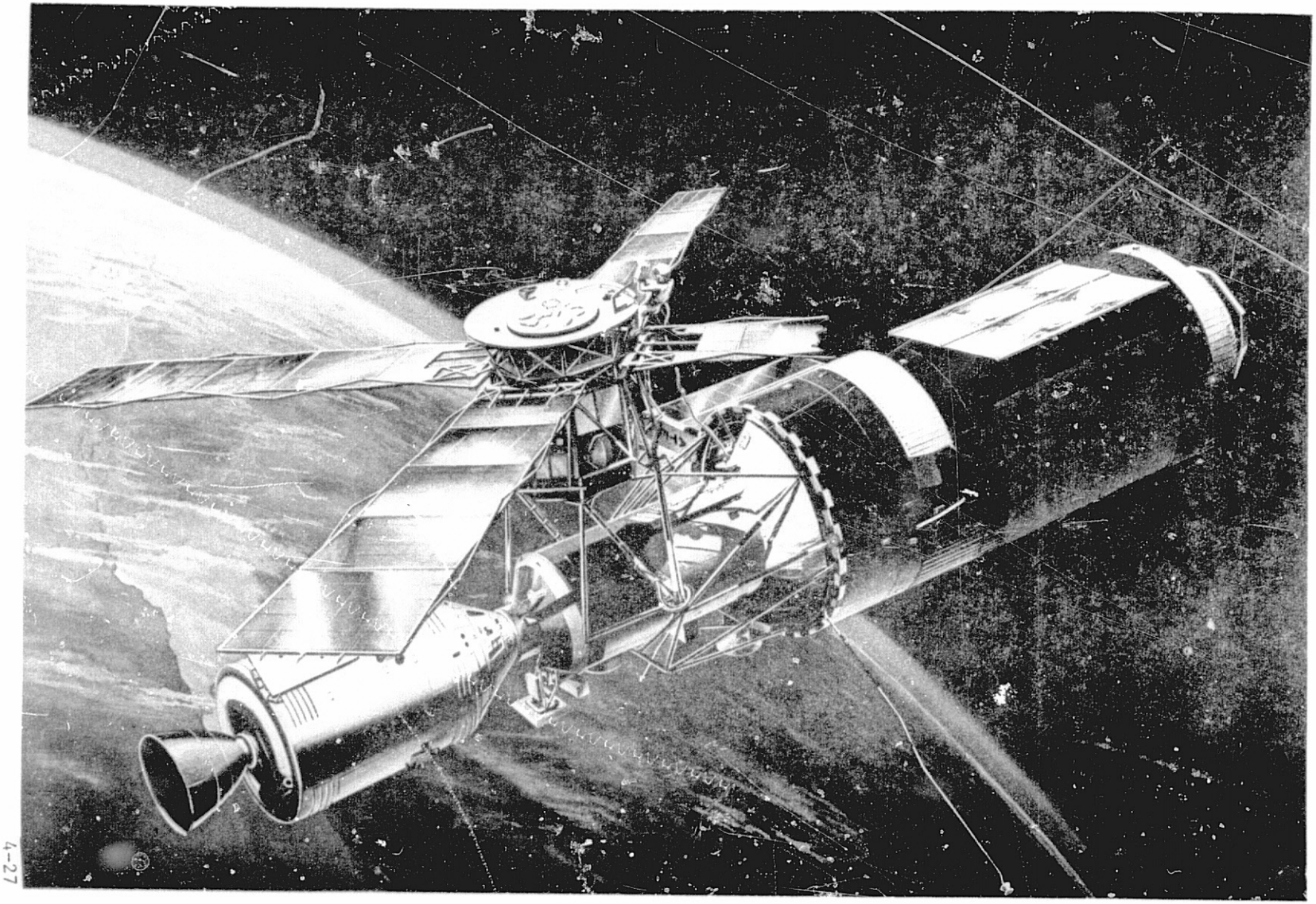

Figure 4-21. Langley Inflatable Sunshield

Figure 4-22. JSC Parasol

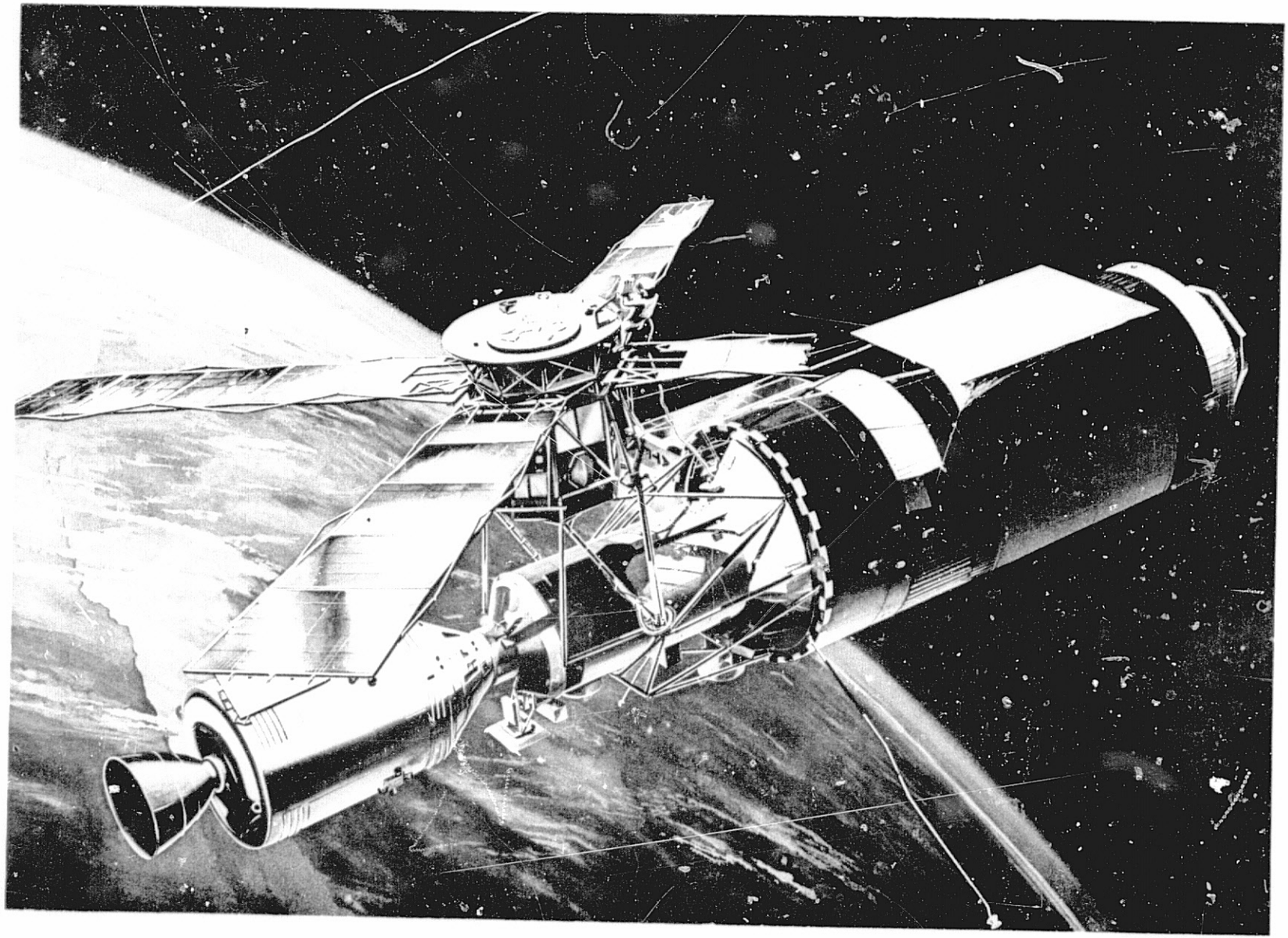

Figure 4-23. MSFC II - Parasol Combination

TABLE 4.1 SUMMARY OF SUNSHIELD STUDIES

	Configuration	% Coverage	α/ε Sunside	α/ε Backside	α/ε OWS Tank	Average Internal OWS Temperature W/No Load W/HSS No ECS
1.	Curtain Wrapped 180° Around OWS	100	.22/.88	.15/.34	.275/.05	39
2.	MSFC I Rectangular Curtain (20' x 23')	92.3	.25/.90	.30/.90	.275/.05	69
3.	Trapazoidal Curtain	76.0	.25/.90	.30/.90	.275/.05	100
4.	JSC-I Conical Curtain	85.7	.22/.88	.15/.34	.275/.05	76.5
5.	JSC-II Tent Curtain	100	.22/.88	.15/.34	.275/.05	36.5
6.	MSFC II Shield (Twin Pole)	100	.25/.90	.15/.34	.275/.05	39.5
7.	Douglas Inflatable Shield	91.8	.15/.65	.57/.04	.275/.05	44.5
8.	Langley Inflatable Shield	100	.27/.72	.18/.04	.275/.05	38.0
9.	JSC Parasol (SAL Deployed)					
	a. 100% Coverage	100	.60/.86	.12/.06	.275/.05	44.0
	b. 90% Coverage	90	.60/.86	.12/.06	.275/.05	69.0
	c. 84% Coverage	84	.60/.86	.12/.06	.275/.05	75.5
10.	MSFC Twin Pole Shield Over 75% Parasol	100	.25/.90	.15/.34	.275/.05	40

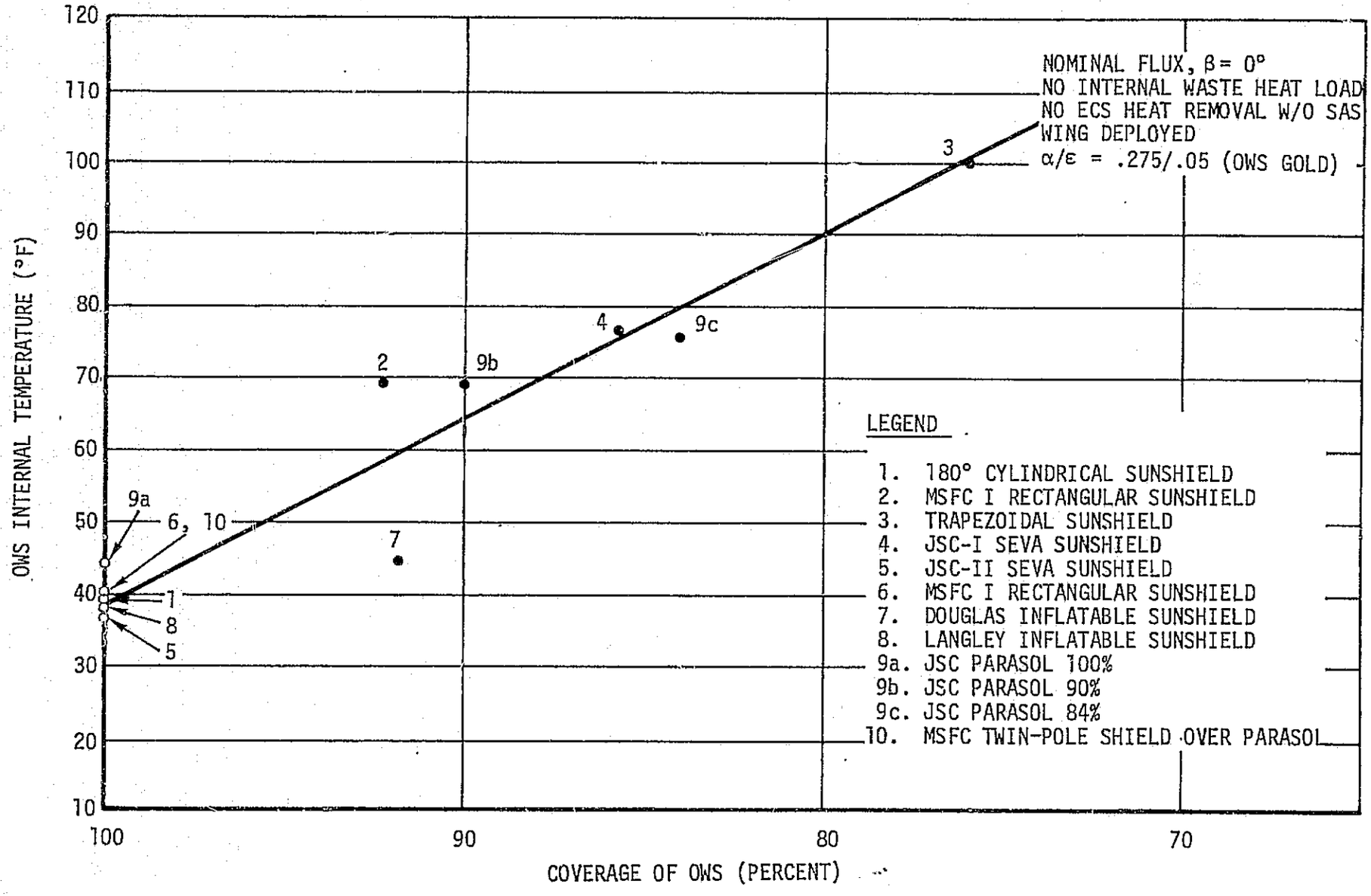

Figure 4-24. Sunshield Performance

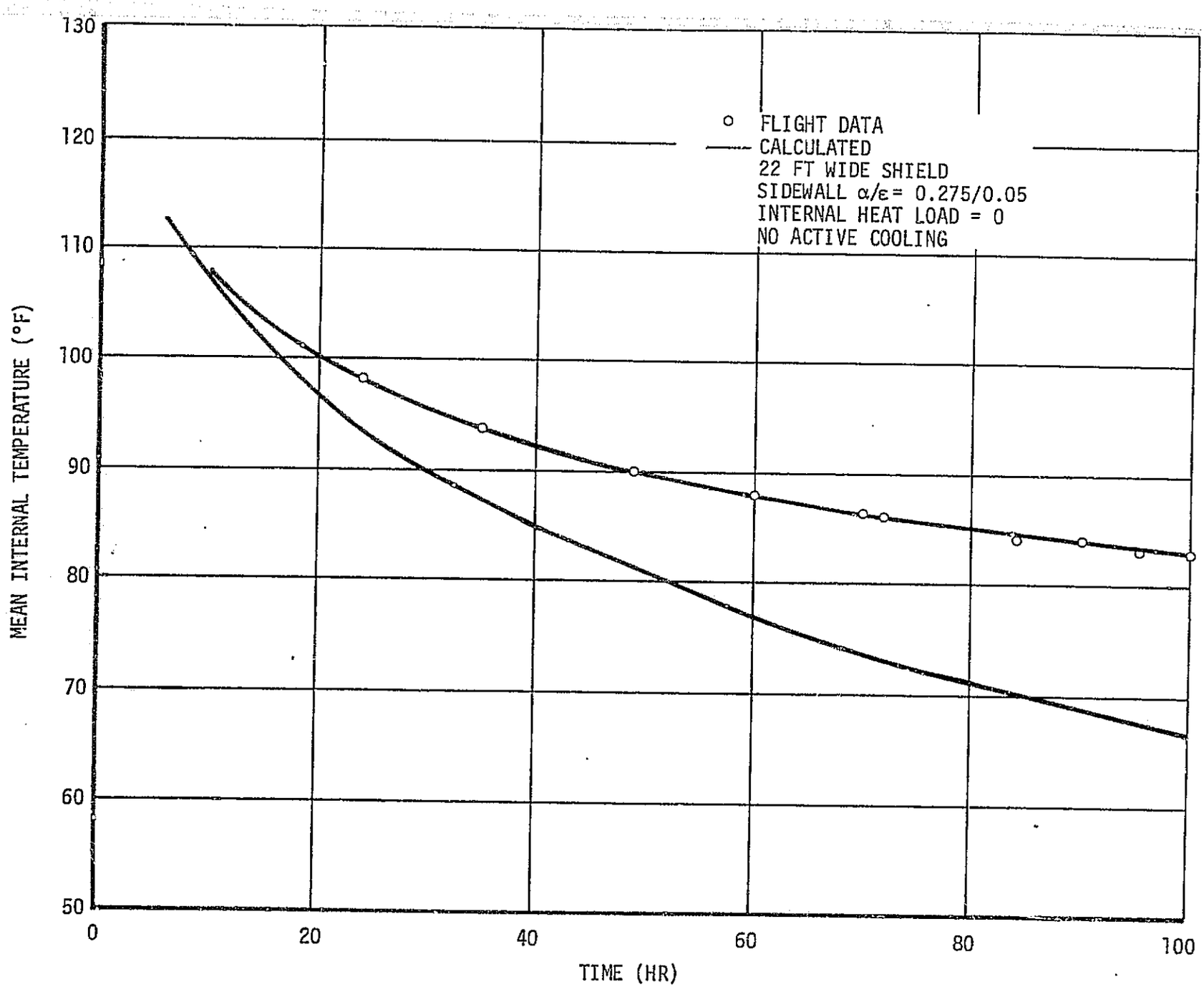

Figure 4-25. Temperature History Following Deployment of the Parasol Shield.

DOY 178 high beta period (during the SL-1/SL-2 storage period). However, the temperature reached 98°F during this time indicating a lesser coverage than estimated. The SL-2 crew fly-around photos confirmed that the coverage was only 75 percent, not 82 percent as previously estimated and a small segment of the meteoroid shield was intact. A drawing of the solar shield derived from the pictures is shown in figure 4-8.

With the parasol shield, as deployed, the solar heating overloaded the ECS, and the internal temperatures became excessive at high beta angles. In order to provide a comfortable crew environment at all Beta angles, studies were initiated to evaluate the effect of deploying a second shield (twin-pole or MSFC shield) over the parasol shield. The results of this study indicated that the OWS gas temperature band required to maintain crew comfort was 66.4 to 79.4°F, as shown in figure 4-26. The predicted maximum heater power and heat removal capability required to maintain crew comfort for 100 percent coverage and beta angles of 0°, 60.0°, and 73.5° are given in tables 4.2 and 4.3. An analysis was also performed to determine the mean internal temperature history after deployment of the twin-pole shield.

The twin-pole (MSFC) shield was deployed by the SL-3 crew at approximately 23:00 hours on day 218 of 1973. The OWS mean internal temperature decreased approximately 7°F after the MSFC shield was deployed. This can be seen in the mean OWS internal temperature history during SL-3 habitation, figure 4-35. Since the internal temperature did not decrease as much as predicted, the resulting conclusion was that the MSFC shield was not fully deployed. A subsequent investigation indicated that 85 percent of the projected area of OWS sidewall was covered. However, the SL-4 fly-around photos indicated that approximately 89 percent of the sidewall was covered. The difference between the coverage by analysis and photos was attributed to assumptions regarding the α/ε of the gold kapton and the assumed external environment. An additional discussion of the flight temperature trends and external environmental effects is contained in paragraph B.10.3 of this section.

2. <u>OWS Internal Waste Heat Loads</u>. The OWS heat loads were estimated preflight assuming specification values for the electrical component loads and assuming metabolic rates corresponding to the mission timeline of activities. Based on flight CO_2 and dewpoint levels, the metabolic heat loads estimated preflight were fairly accurate, however, the electrical heat loads in the OWS were below preflight predictions. Figures 4-27, 4-28, and 4-29 show the comparison between the actual and predicted waste heat loads. The predicted average daily waste heat load in the OWS was 2500 Btu/hour assuming constrained use of OWS lighting, i.e., turning lights off in unoccupied compartments, whereas, the actual internal waste heat load was between 1700 Btu/hour and 2300 Btu/hour after the SAS wing deployment during

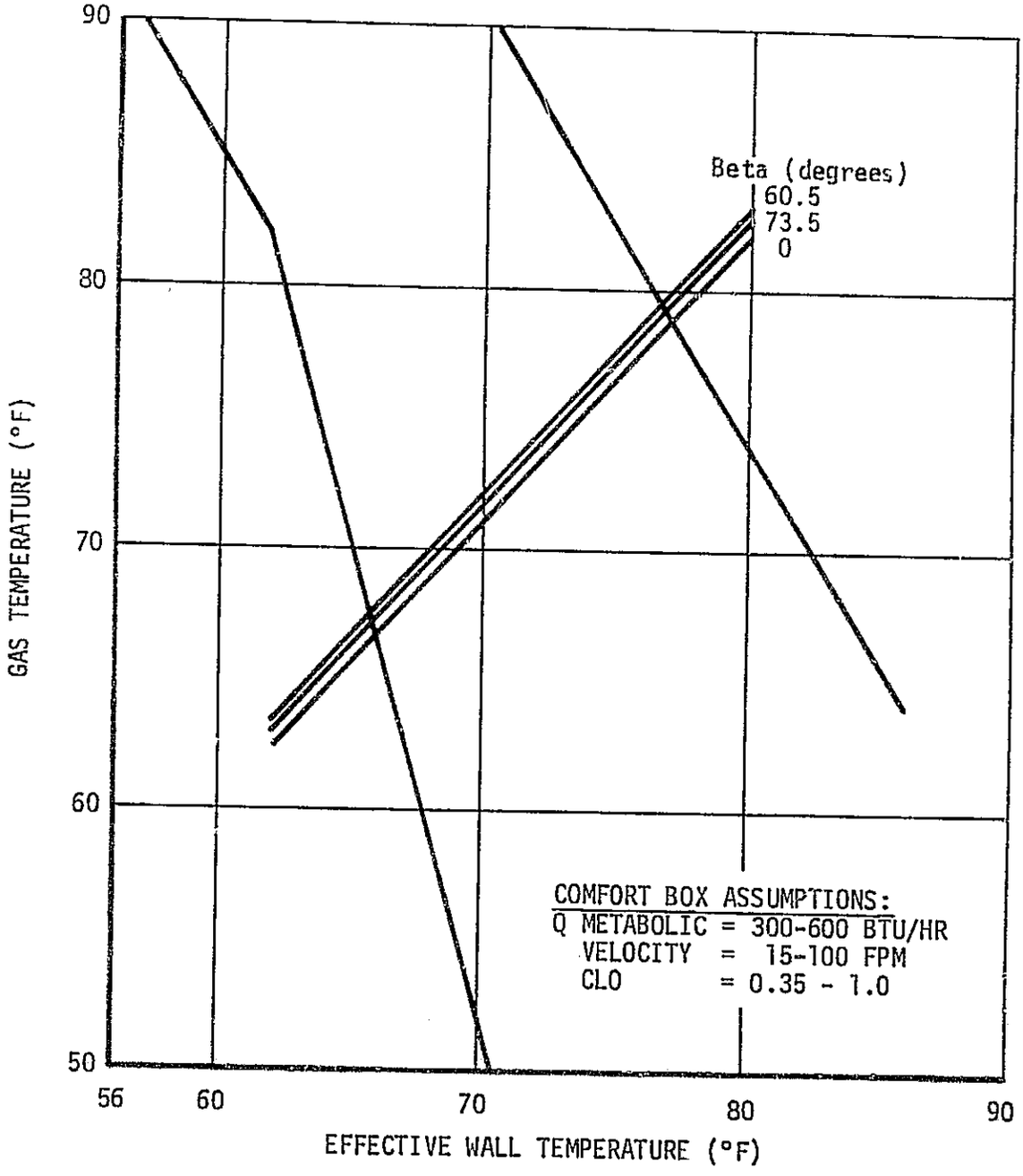

Figure 4-26. Crew Comfort Data Box, Double Shield

TABLE 4.2 MAXIMUM HEATER POWER REQUIREMENTS
(With 100% Coverage of OWS Projected Area)

Beta Angle (deg)	0	60.5	73.5
* Required Gas Temperature (°F)	66.7	67.5	67.2
**Structural Heat Loss (Btu/hour)	4010	4800	3970
Total Heat Loss (Watts)	1175	1406	1163
Minimum Waste Heat (Watts)	733	733	733
Maximum Heater Power Required (Watts)	442	673	430

TABLE 4.3 HEAT REMOVAL CAPABILITY
(With 100% Coverage of OWS Projected Area)

Beta Angle (deg)	0	60.5	73.5
*Required Gas Temperature (°F)	78.8	79.4	79.1
Structural Heat Loss (Btu/hour)	4910	5670	4840
HXS Removal (Btu/hour)	1700	1750	1725
Heat Removal Capability (Btu/hour)	6610	7420	6565

*Gas Temperature Required to Maintain Crew Comfort
**Includes 300 Btu/hr for Sublimation Effects

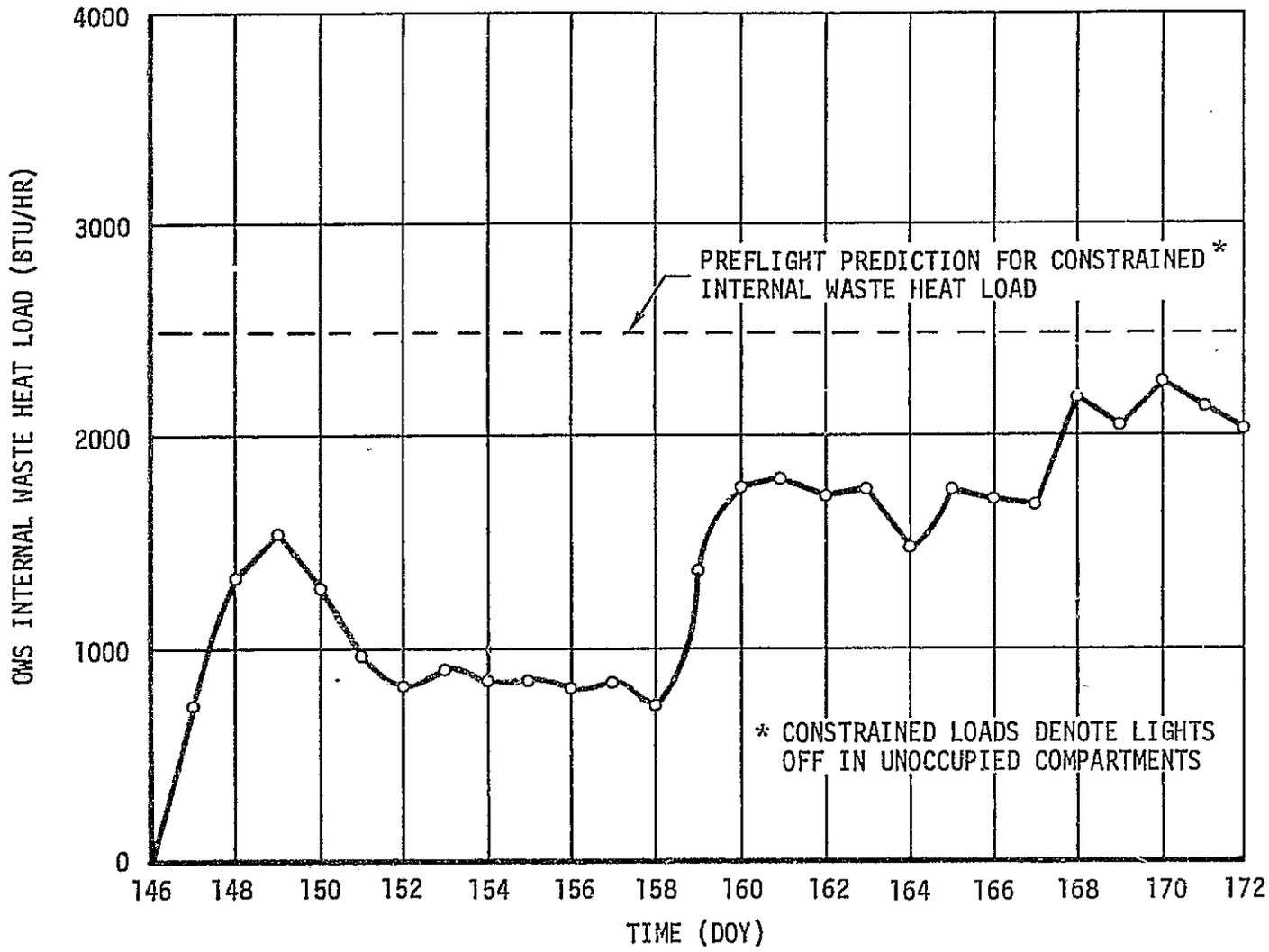

Figure 4-27. OWS Internal Waste Heat Load for SL-2 Mission

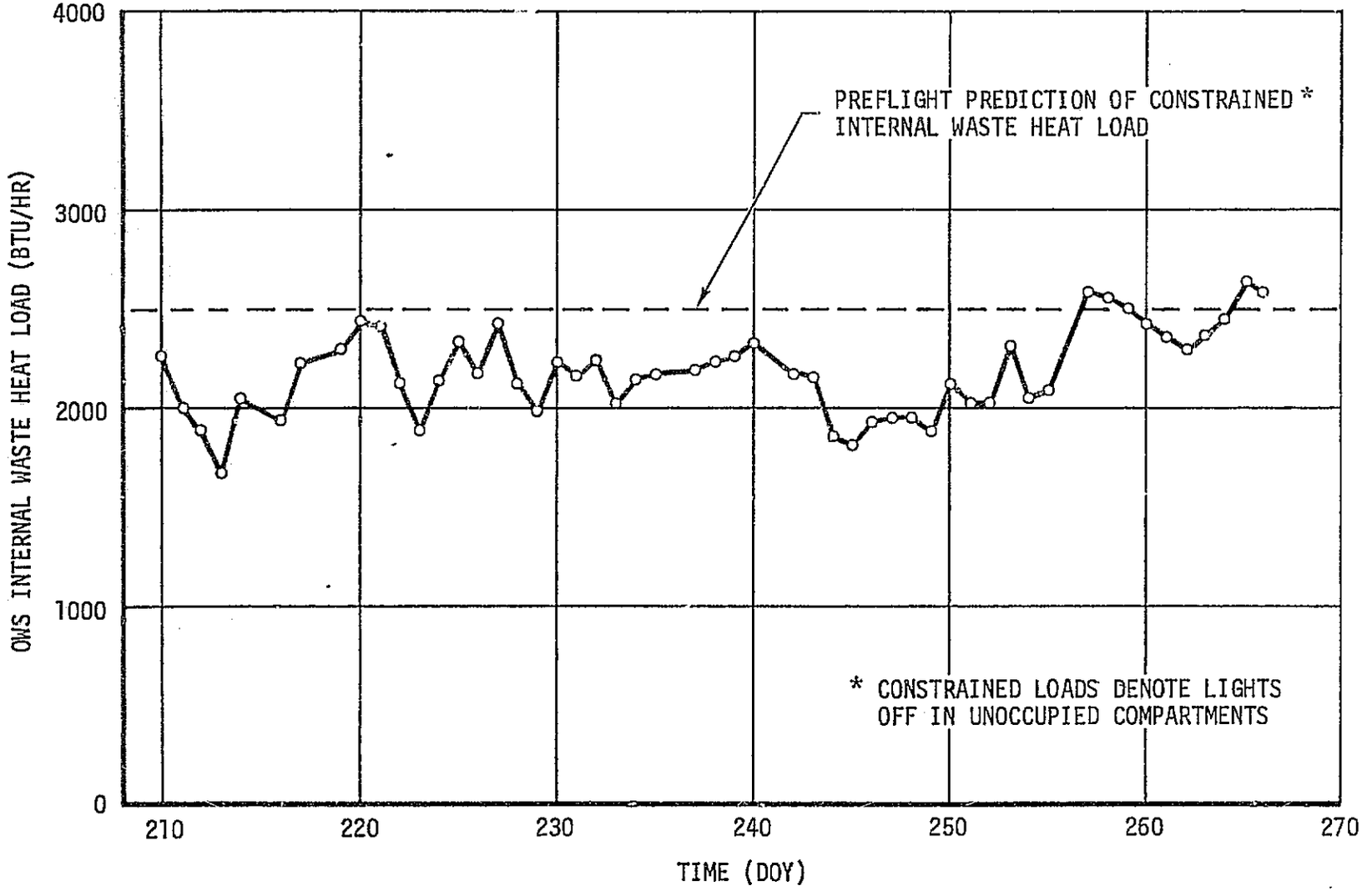

Figure 4-28. OWS Internal Waste Heat Load for SL-3 Mission

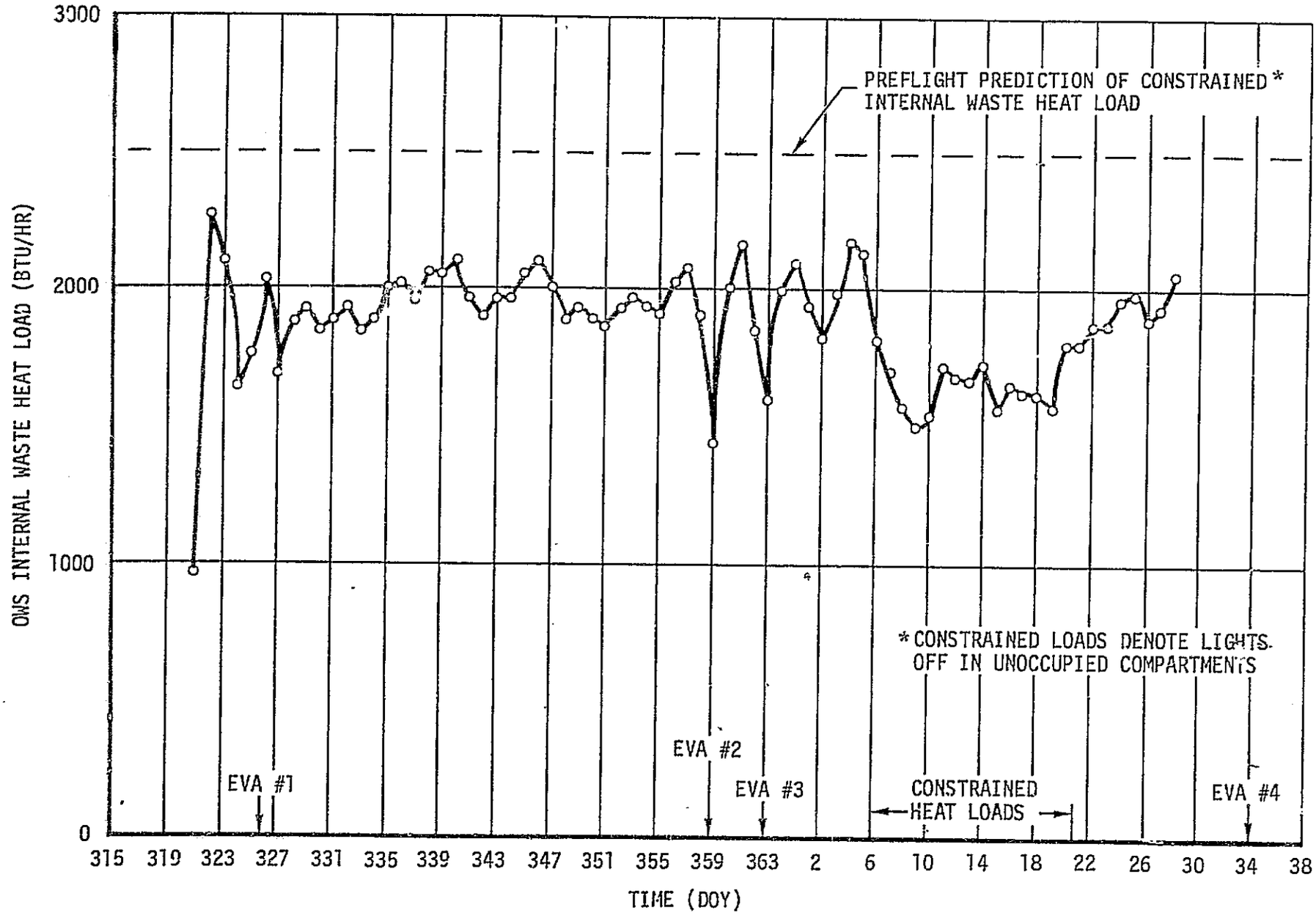

Figure 4-29. OWS Internal Waste Heat Load for SL-4 Mission

SL-2 and averaged 2200 Btu/hour and 1900 Btu/hour during SL-3 and SL-4 respectively. The flight OWS internal waste heat load was determined indirectly by comparing the apparent OWS waste heat load under steady state conditions with the OWS bus power which was available from TM data. The difference between the OWS bus power and the apparent internal waste heat load was determined to be approximately 500 Btu/hour. This difference was checked by subtracting that portion of the OWS bus load which was not dissipated as internal waste heat (approximately 1200 Btu/hour) and adding the average metabolic sensible load (approximately 700 Btu/hour). The average OWS internal heat load could thus be determined for any mission day by subtracting 500 Btu/hour from the average OWS bus power for that day.

Since the OWS internal waste heat loads were determined indirectly, uncertainties associated with the sunshield coverage and the thermal properties of the OWS exterior influenced the accuracy of the internal waste heat load calculation. Also, conservative estimates of electrical component duty cycles and internal light usage which were assumed for the preflight predictions could account for the higher preflight internal waste heat load predictions.

3. OWS Internal Temperatures. The ground thermal conditioning system controlled the average OWS internal temperature to approximately 55°F at liftoff (134:17:30 GMT). At liftoff plus 63 seconds, the meteoroid shield tore loose from the OWS exposing the goldized kapton on the cylindrical tank wall to the orbital environment. As a result, the OWS external tank wall temperatures began to climb at an abnormally high rate at orbital sunrise 67 minutes after liftoff, as shown in figure 4-30.

The OWS internal temperatures also began to rise as the heat soaked through the polyurethane insulation on the internal tank wall. At 5 hours after liftoff, the average internal temperature had risen to 65°F. Analytical predictions indicated that the OWS internal temperature would approach 160°F with the vehicle maintained in the solar inertial attitude. In order to minimize degradation to ambient food, film, tapes, and other equipment, the vehicle was commanded into various attitudes such that the solar impingement on the gold foil would be reduced. Other considerations such as electrical power availability, TACS usage, and extreme temperatures of equipment located on other areas of the SWS were taken into account in determining the optimum vehicle attitude. A history of the major attitude changes is shown in table 4.4. In general, the vehicle was maintained in a solar inertial attitude with a -40 to -50 degree pitch (MDA towards the Sun).

The internal OWS average temperature history from liftoff until parasol deployment is shown in figure 4-31. The average of the measurements located on the ceiling grid of the experiment level compartments (C7032, C7040, C7122, and C7123) was used to determine the OWS average temperature. These measurements provided an indication of

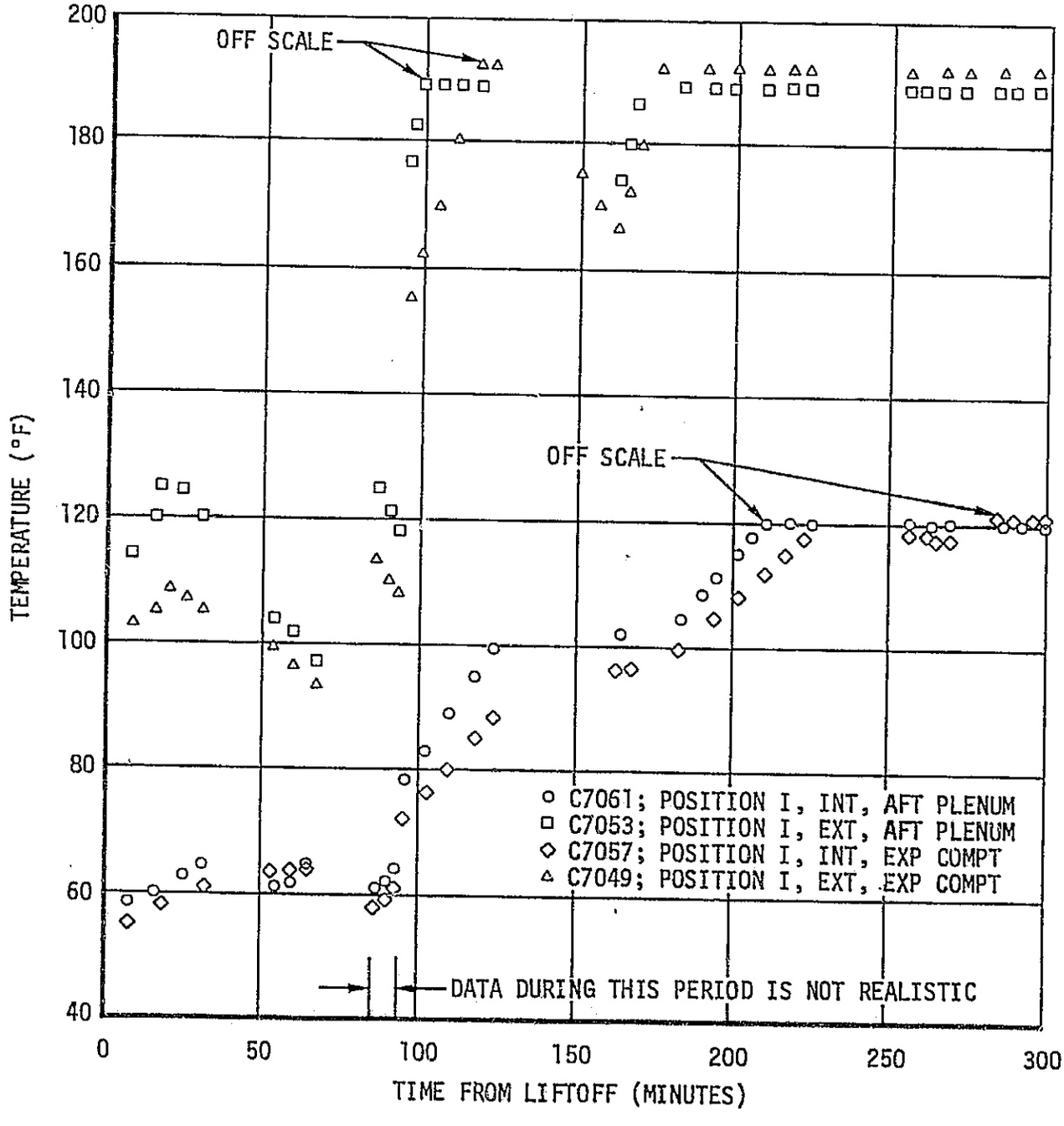

Figure 4-30. OWS Wall Temperature Response to Meteoroid Shield Loss

TABLE 4.4 ESTIMATED ATTITUDE HISTORY OF SL-1 PRIOR TO PARASOL DEPLOYMENT

TIME (GMT) DOY	HOUR:MIN:SEC	ATTITUDE	
134	17:30:00	SL-1 First Motion	
		Boost	
134	17:39:59	Gravity Gradient	
134	17:45:40	Solar Inertial	
135	06:30:00	-90 Degree pitch off SI	Rotation about y axis; MDA toward Sun, OWS away from Sun
135	08:00:00	-45 Degree pitch off SI	
135	08:45:00	Solar Inertial	
136	05:13:48	ZLV with a +10 degree pitch about Y	
136	06:51:00	Solar Inertial	
136	08:20:20	ZLV with a +10 degree pitch about Y	
136	09:53:00	Solar Inertial	
136	11:29:00	ZLV with a +15 degree pitch about Y	
136	13:04:00	-57 to -47 degree pitch (Y) off SI; X = 2 to -18°, Z - 21 to -12°	
141	11:47:55	-40 degree pitch (Y) off SI; X = 0 to -10°, Z = +15°	
142	09:27:00	Solar Inertial	
142	11:09:00	-80 degree pitch off SI about Y	
142	12:44:00	-45 degree pitch (Y) and +41 degree yaw (Z) off SI	
143	02:48:00	-48 degree pitch (Y) and +45 to 50° yaw (Z) off SI	

TABLE 4.4 ESTIMATED ATTITUDE HISTORY OF SL-1 PRIOR TO PARASOL DEPLOYMENT (CONTINUED)

TIME (GMT) DOY	HOUR:MIN:SEC	ATTITUDE
143	21:50:00	-65 degree pitch (Y) and +50° yaw (Z) off SI
144	00:30:00	-45 degree pitch (Y) and +44° yaw (Z) off SI
144	07:11:00	-50 degree pitch (Y) and +70° yaw (Z) off SI
144	20:06:00	-42 degree pitch (Y) and +70° yaw (Z) off SI
144	22:45:00	-68 degree pitch (Y) and +70° yaw (Z) off SI
145	01:21:00	-35 to -43 degree pitch (Y) and +42° yaw (Z) off SI
145	20:47:00	-43 degree pitch (Y), +42° yaw (Z) and -28° roll (X) off SI
146	01:46:00	Pitch (Y) starting at -43° and decreasing to -35° Yaw (Z) starting at +42° and decreasing to +20°
147	02:43:00	Thermal Control maneuvers ended with cluster in SI attitude

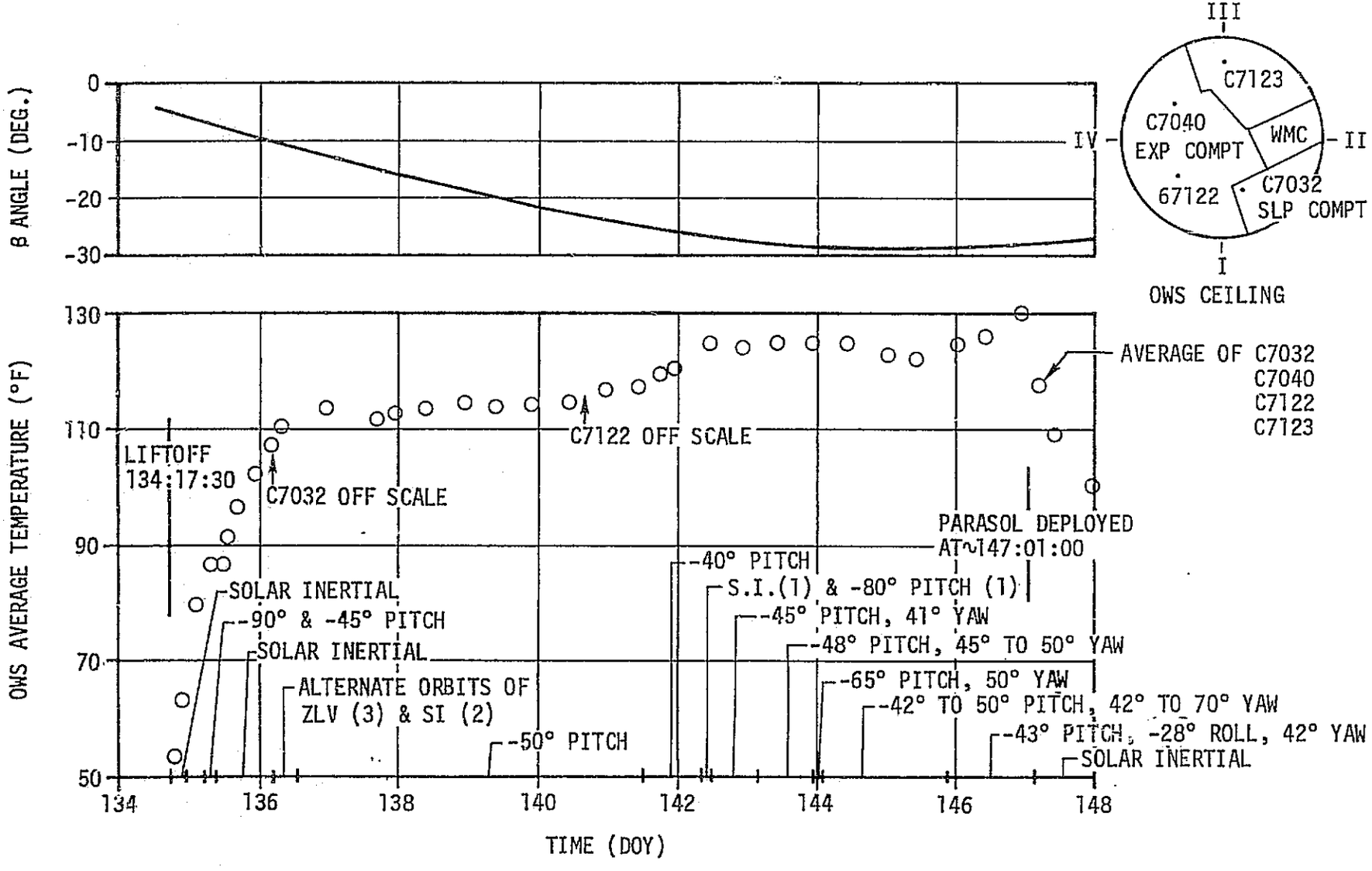

Figure 4-31. SL-1 OWS Average Temperature History

the average radiant environment of the cylindrical walls, forward dome, and experiment compartment floor because of their central location. The internal temperature rose steadily, except for a few hours following orbits of -90° and -45° pitch attitude, for approximately 2 days at which time the vehicle was commanded into an inertial attitude with a -50° pitch. This approximate attitude was maintained until DOY 141 except on DOY 136 when the attitude was alternated between ZLV and Solar Inertial orbits. Figure 4-32 shows the attitude for the ZLV condition. The OWS internal temperature was stabilized at 115°F during this period. During DOY 141 the pitch angle was changed to -40° which increased the projected area of gold foil exposed to the sun. The OWS internal temperature response was an 8°F rise to 125°F in approximately one day. The internal temperature was maintained between 122°and 125°F until the end of DOY 145. During this period the vehicle attitude was generally solar inertial with a pitch of -42°to -50° and a yaw of 41° to 70°. Prior to docking of SL-2, the vehicle was rolled -28° to provide better illumination of SAS Wing 1 near the end of DOY 145. This attitude should not have increased the solar heat flux on the gold foil, but the internal temperature rose to 130°F at the beginning of DOY 147. It is believed that the SWS attitude drifted during this period allowing a greater projected area of gold foil to be exposed to the sun than anticipated.

The OWS internal temperature sensors had a maximum calibration limit of 120°F. Sensor C7032 went off scale high on DOY 136 and C7122 on DOY 140. It was, therefore, necessary to estimate their readings by using the ΔT relationship between these sensors and the other ceiling measurements (C7040 and C7123) that existed prior to the time they went off scale high. For this reason, the OWS SL-1 average temperature history during this time should be considered an estimate.

The parasol was deployed through the solar airlock on DOY 147 at approximately 0100 GMT. OWS internal temperatures immediately dropped and approached a stabilized temperature about 8 days later on DOY 155 as shown in figure 4-33. At this time the OWS internal temperatures met the comfort box requirements as shown in figure 4-34. The four OWS heat exchanger fans were turned on immediately after parasol deployment and the maneuver to the solar inertial attitude. The heat exchangers operated continuously during SL-2 except for EVAs. Prior to SAS Wing 1 deployment, the waste heat profile was significantly lower than nominal due to severe limitations in electrical power availability.

SAS Wing 1 was deployed during EVA on DOY 158. Electrical power availability increased which resulted in higher internal waste heat dissipation. Z-LV EREP maneuvers, which exposed additional areas of gold foil to the sun as the Beta angle increased, were performed

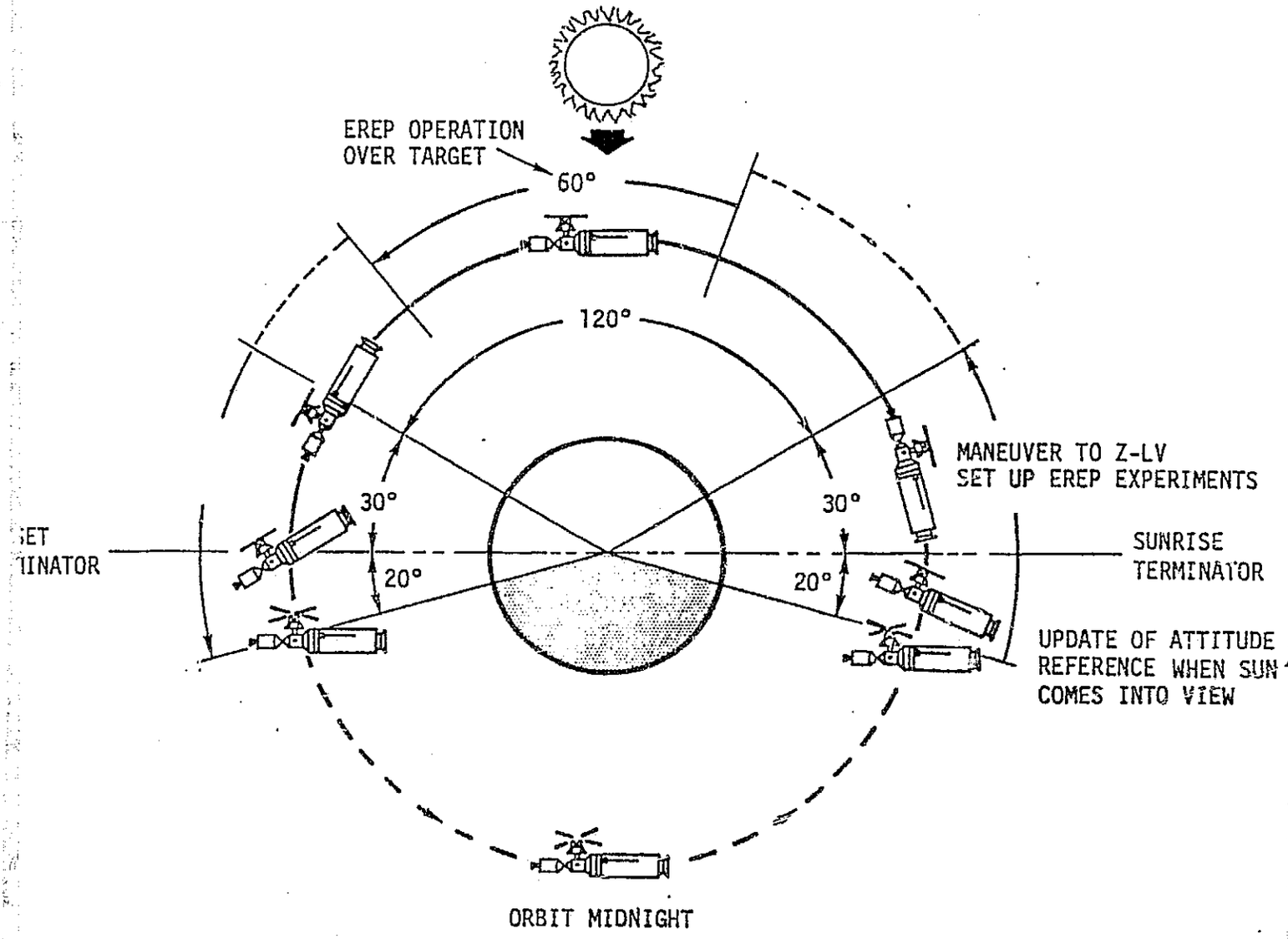

Figure 4-32. Z-Local Vertical Earth Resources Pointing Mode

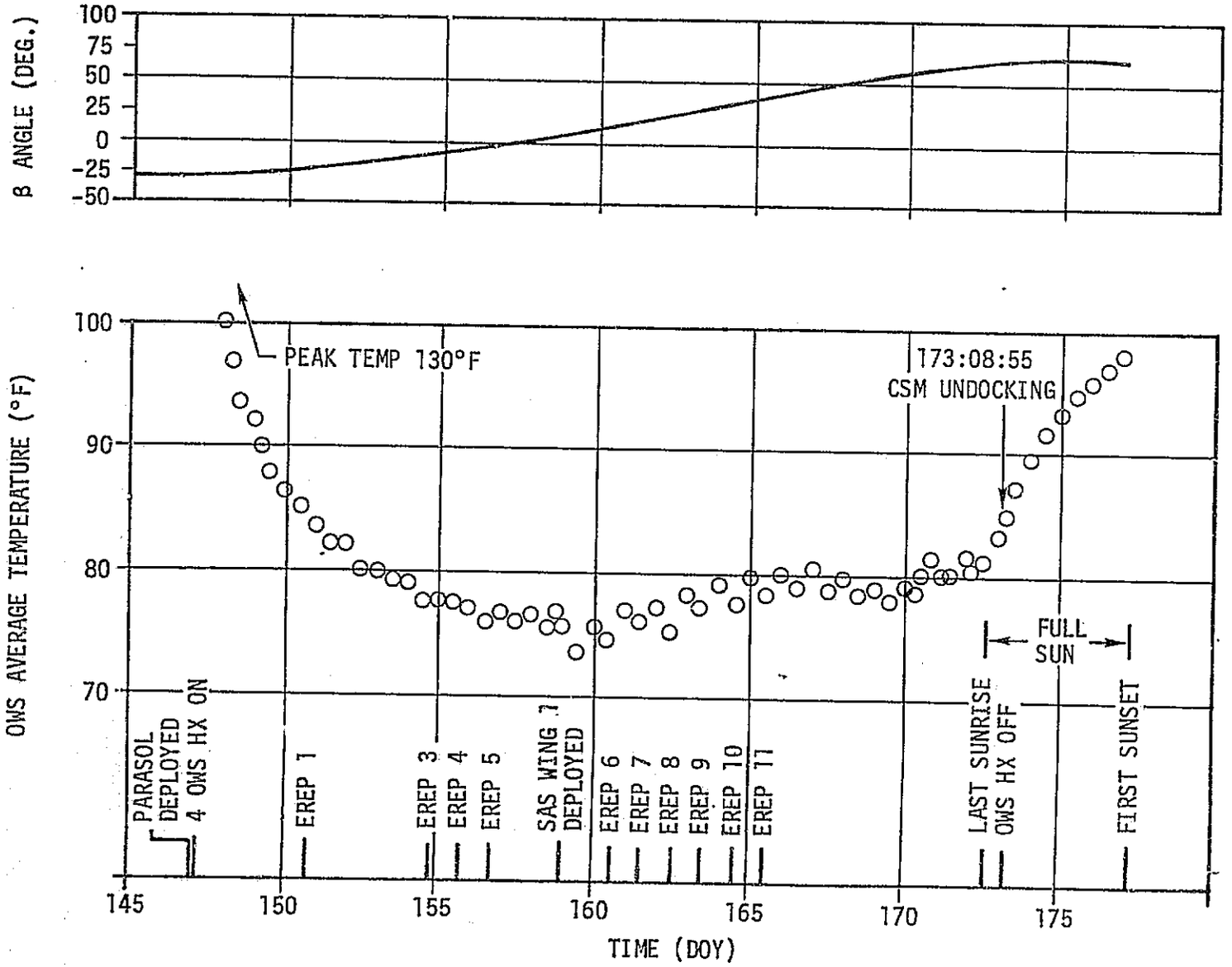

Figure 4-33. OWS Average Temperature SL-2 Manned Mission

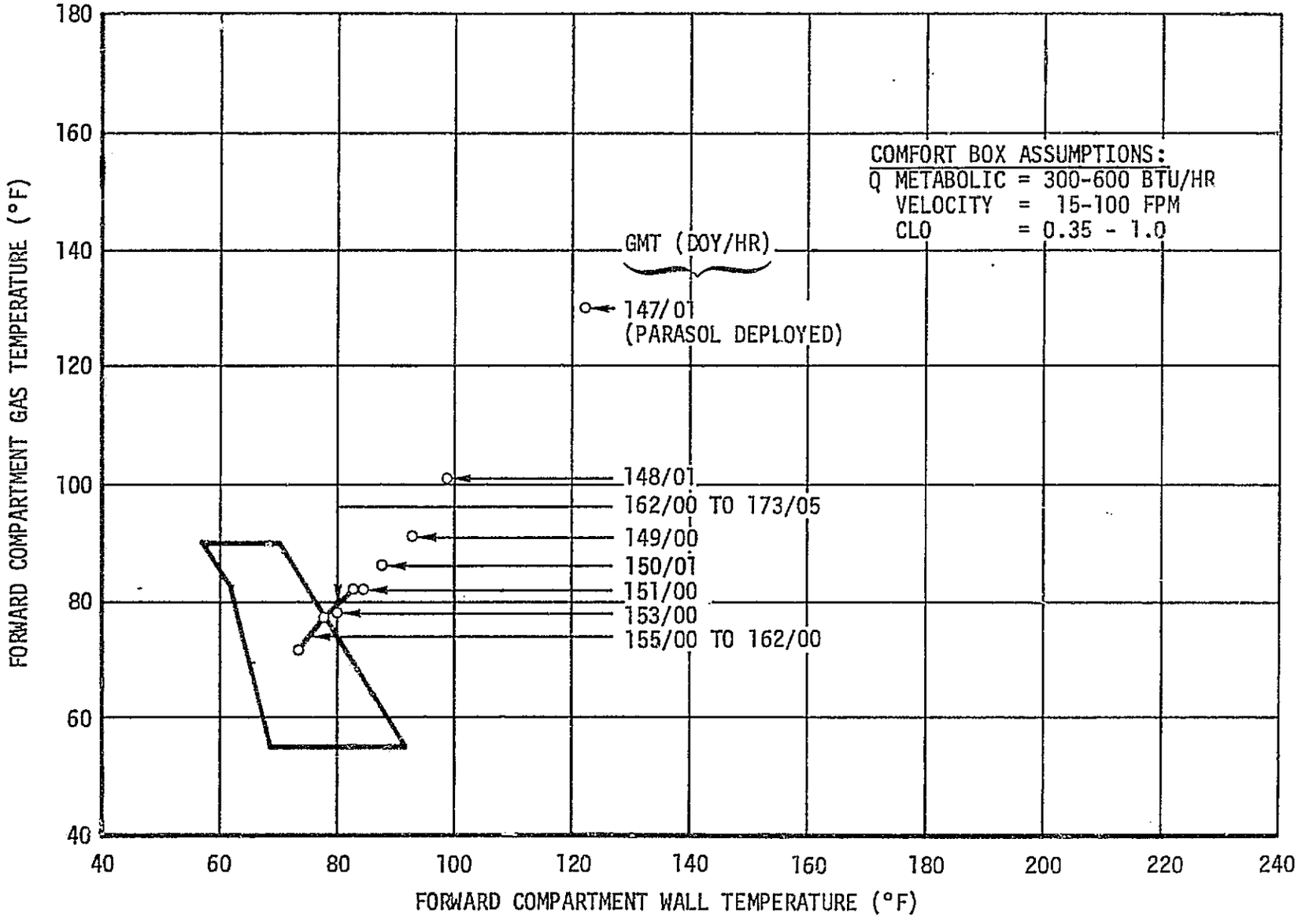

Figure 4-34. OWS Forward Compartment Temperatures During SL-2

daily from DOY 160 through 164. Analytical models indicated that the presence of the deployed SAS wing would effect a net increase in the external heat load due to reradiation and reflections. Due to the increased heat loads caused by increased power dissipation, EREP maneuvers, and the presence of the SAS wing, the OWS internal temperatures rose from DOY 159 through DOY 166. Temperatures exceeded comfort box requirements on DOY 162 as shown in Figure 4-34. Temperatures experienced a slight downward trend during DOY 167 and 168 but began to rise on DOY 169 as the β angle ($\beta > 55^{o}$) and percent time in the sun increased. The vehicle entered a four day period of full sunlight on DOY 173 about 12 hours prior to SL-2 undocking. At OWS closeout the internal temperature had risen to approximately 83°F which was 6 to 7°F hotter than the comfort requirement as shown in figure 4-34.

The average OWS internal temperature continued to rise during the storage period in the full sunlight period as shown in figure 4-35. A peak temperature of 98°F was attained on DOY 177 when the SWS began to again experience orbital night periods. The internal temperature decayed for approximately 20 days before reaching steady state at 79 to 80°F. The temperature remained near this level for the duration of the SL-2 storage period until OWS entry at the end of DOY 209.

The OWS average temperature dropped 2°F after the 4 OWS heat exchangers were activated on DOY 210 as shown in figure 4-36. However, the heat exchangers were deactivated on DOY 213 to prevent mositure condensation in them and the OWS temperature increased to approximately 81°F. The average temperature remained between 78 and 81°F until the twin pole shield was deployed at the end of DOY 219. Due to the additional shading of the gold foil, which reduced the external heat load, the OWS average temperature decreased for approximately 5 days to 72°F. Temperatures had been somewhat hotter than the comfort requirements prior to the twin pole shield deployment but subsequently were well within the comfort box as shown in figure 4-37. Typical daily fluctuations in temperature were 1 to 2°F as shown in figure 4-36 and daily variations of this magnitude were seen during all manned periods due to variations in internal heat load.

The internal temperature remained steady at about 73°F from DOY 224 to DOY 231. On DOY 231 the β angle had again increased to 55 degrees and the OWS internal temperatures also increased. The OWS temperature rose to an average of 75°F on DOY 236 and remained at that level until DOY 244. The β angle had peaked at 62°F on DOY 236. The OWS temperature began to decrease on DOY 244. The generally downward trend continued until DOY 250 when the heat exchangers were turned off by the Thermal Control System logic unit. At this time the average temperature was 72°F. The temperatures immediately began to rise from the absence of active cooling and one heat exchanger came on later in DOY 250. The heat exchanger plates were cleaned (see Section III) on DOY 251 which increased the gas flow rate and resulted in additional active cooling.

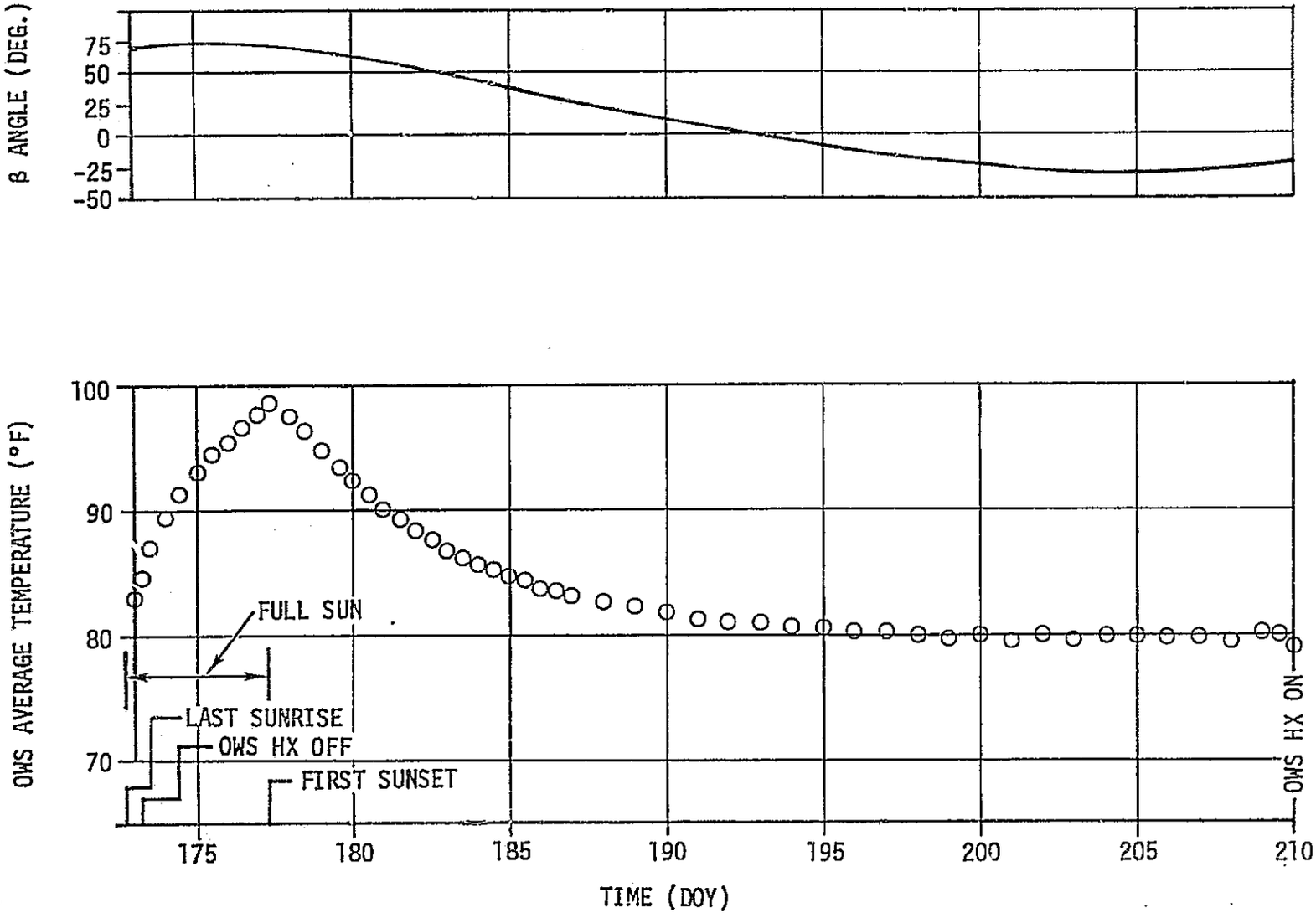

Figure 4-35. OWS Average Temperature History SL-2/SL-3 Storage Period

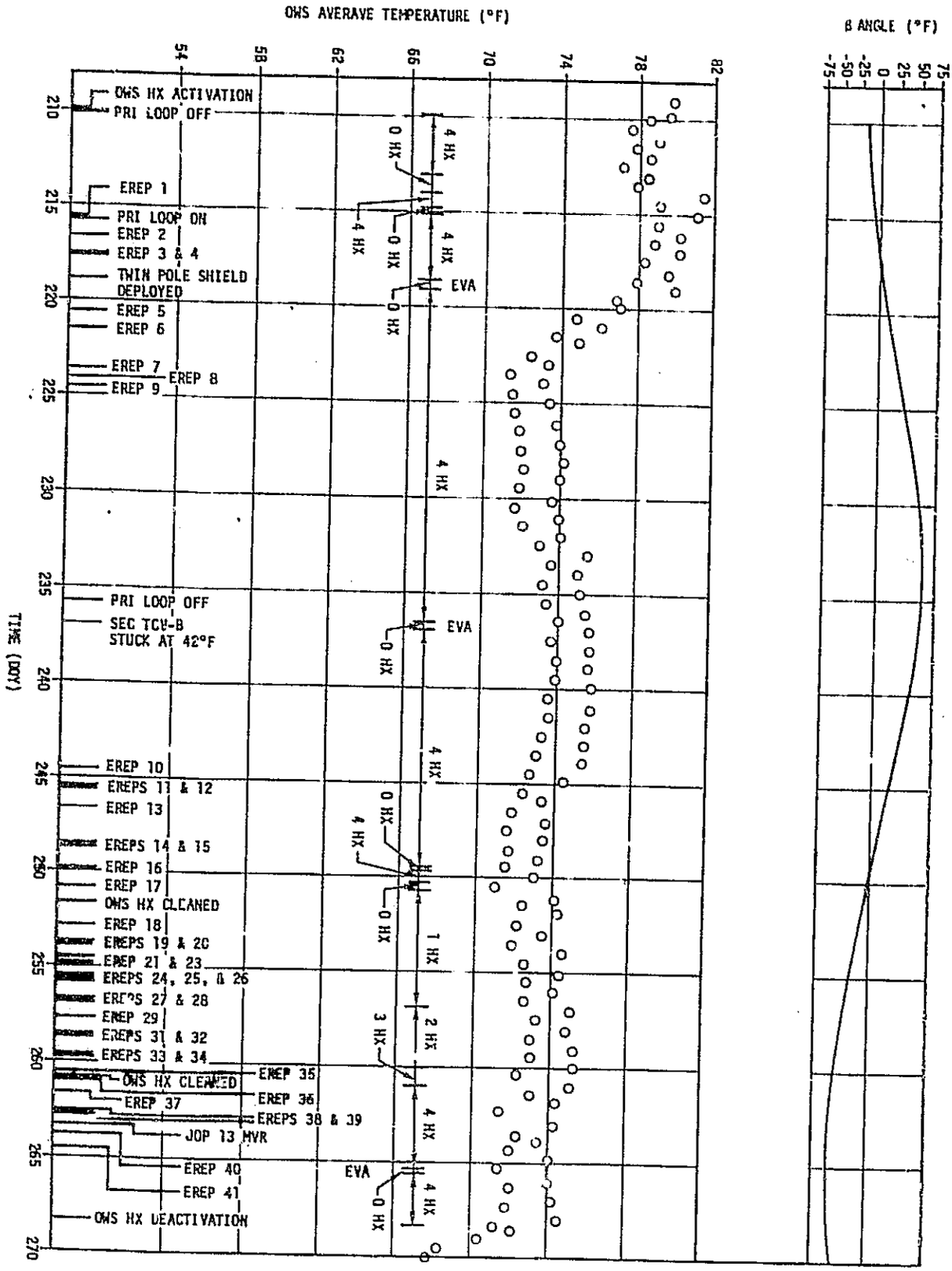

Figure 4-36. OWS Average Temperature SL-3 Manned Mission

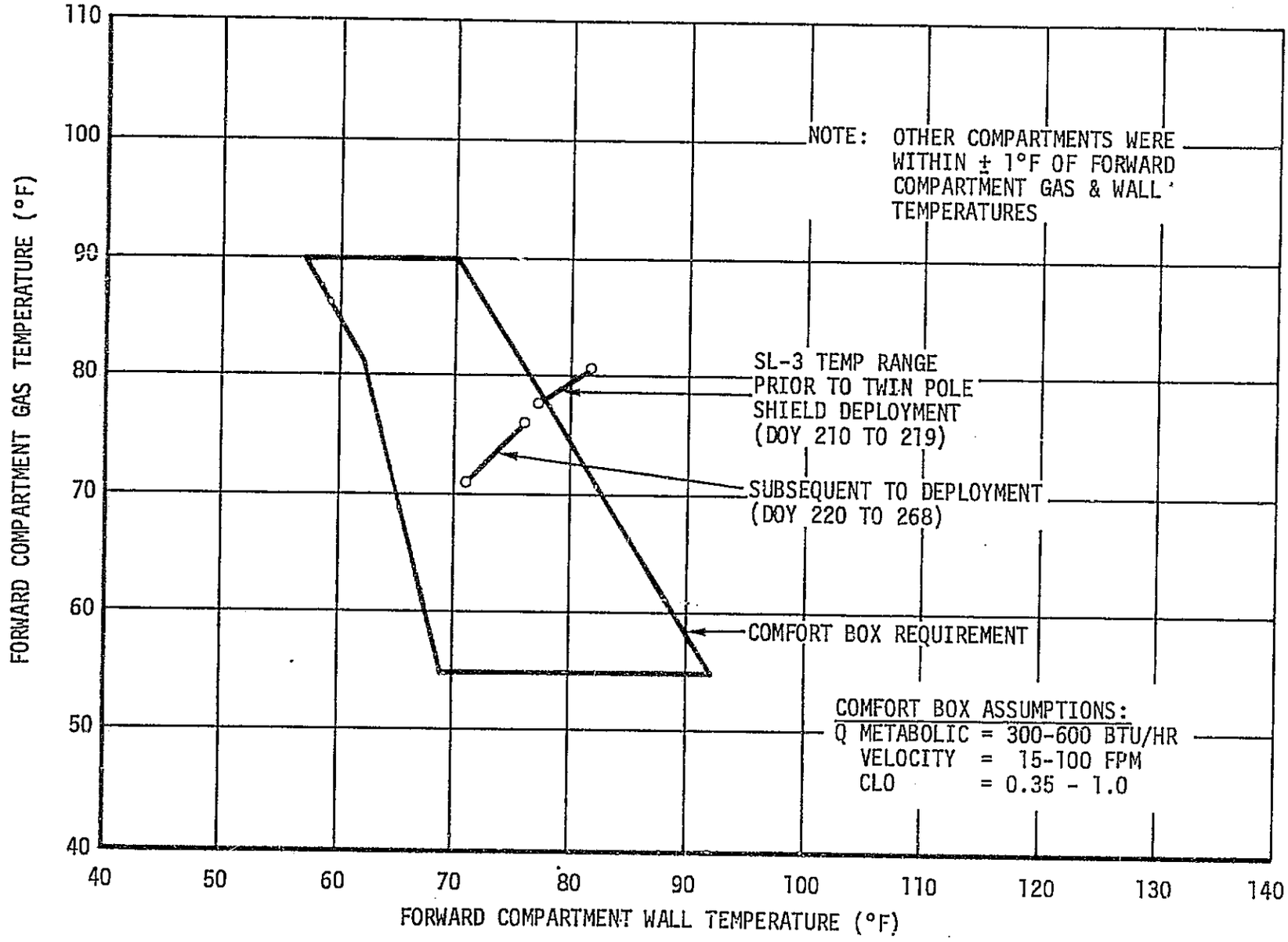

Figure 4-37. OWS Forward Compartment Temperature During SL-3

The second, third, and fourth heat exchangers came on automatically on DOYs 256, 260 and 261, respectively. From DOY 251 through SL-3 OWS closeout on DOY 268, the average temperature remained at approximately 73°F which was in the center of the comfort box as shown in figure 4-37.

During SL-3/SL-4 storage, the OWS average temperature followed the β angle curve, as shown in figure 4-38. The positive β angles caused warmer OWS temperatures than the negative β angles. During this storage phase the temperature cycled between 63° and 72°F.

Early in the SL-4 mission the OWS average temperature rose to approximately 80°F as the β angle reached -70 degrees. Orbits with 100% sunlight lasted 24 hours after which the internal temperature decreased to the middle seventies as shown in figure 4-39. The temperatures increased from DOY 335 to DOY 340 when the OWS heat exchangers were turned off and decreased when the heat exchangers were turned on during DOY 340. As the β angle became positive, the OWS internal temperatures again increased to a maximum of 81°F on DOY 352 (figure 4-39). As β decreased from 50° to -60° the OWS temperature decreased to 71°F on DOY 10. As β decreased below -60° to the full sun condition, the OWS temperature increased to a maximum of 81.6°F on DOY 18 (figure 4-39). Measures were taken to maintain the OWS temperatures below 82°F. The crew was asked to reduce the use of lighting in the OWS, and a second pump in the AM Primary Coolant Loop was activated. After the high negative β angle period, the internal OWS temperatures decreased to the 72°F to 75°F range and remained at that level for the remainder of the mission. During SL-4, the OWS internal temperature remained within the comfort box requirement except for three periods, as shown in figure 4-40. Two were caused by increased solar heating at the high β angles. The third was caused by not activating the OWS heat exchangers for five days which allowed the internal temperature to rise just prior to a period of positive β angle and high albedo.

4. MDA Internal Temperatures. Figures 4-41 through 4-45 present the MDA average internal temperatures. MDA temperatures prior to SL-2 were influenced by the vehicle attitude changes resulting from thermal management of the OWS, and by management of MDA wall heaters to conserve power. These factors resulted in MDA temperatures between 50°F and 65°F prior to SL-2. During SL-2 intermittent use of the MDA wall heaters to conserve power prior to SAS deployment on DOY 158 and to provide a cooler interchange flow with the OWS following SAS deployment contributed to continued low MDA internal temperatures. Internal temperatures were in the 46-47°F range during both the SL-2/SL-3 and SL-3/SL-4 storage periods as planned prior to the flight. During SL-3 and SL-4, the MDA wall heaters were frequently switched to the 45°F thermostat setting for power management associated with EREP and other experiment maneuvers and the resulting temperature transients are reflected in figures 4-43 and 4-45. When allowed to operate normally, the system maintained temperatures within the desired control range. Figures 4-46, 4-47 and 4-48 show MDA gas-wall temperatures relative to the comfort box for SL-2, SL-3, and SL-4.

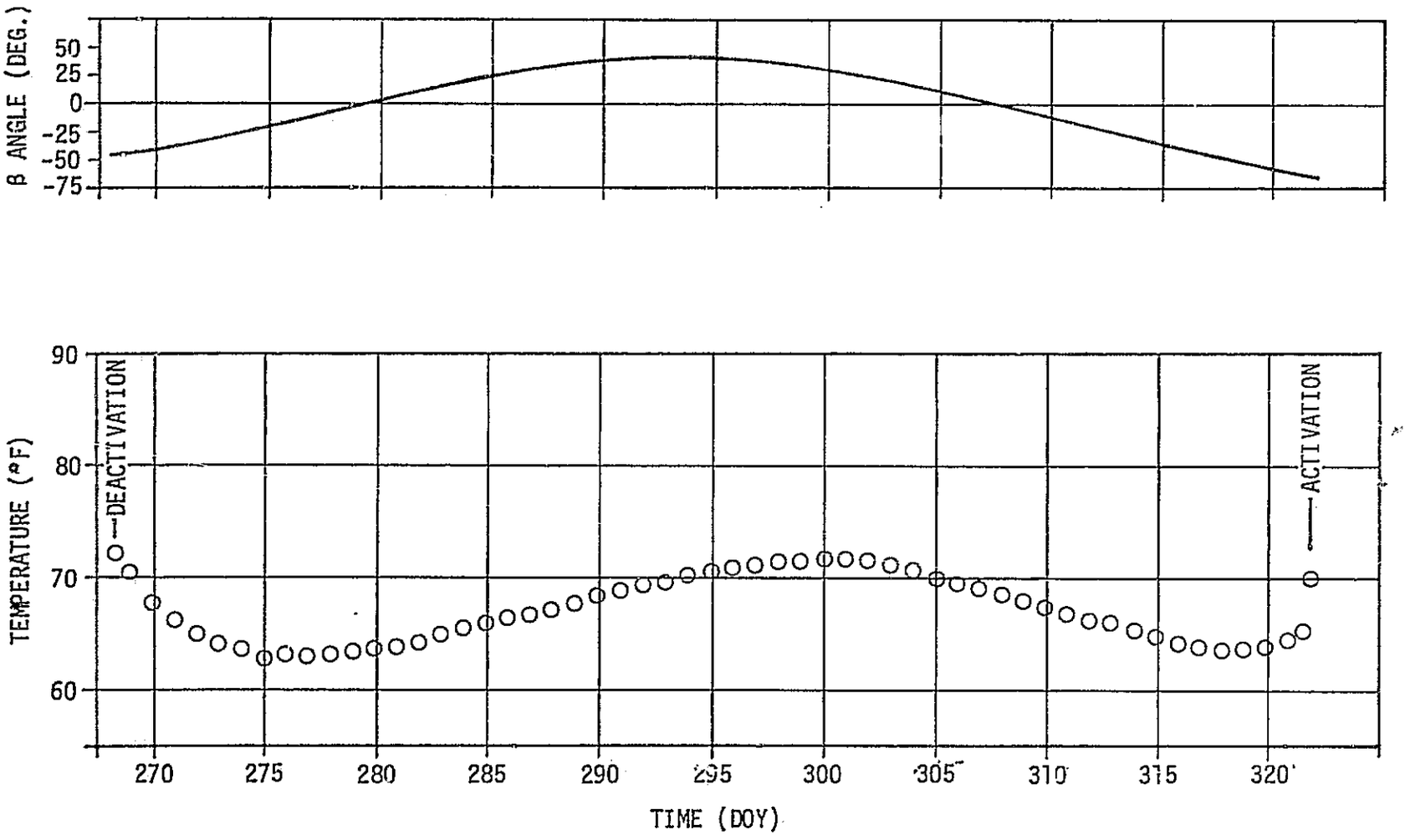

Figure 4-38. OWS Average Temperature History SL-3/SL-4 Storage Period

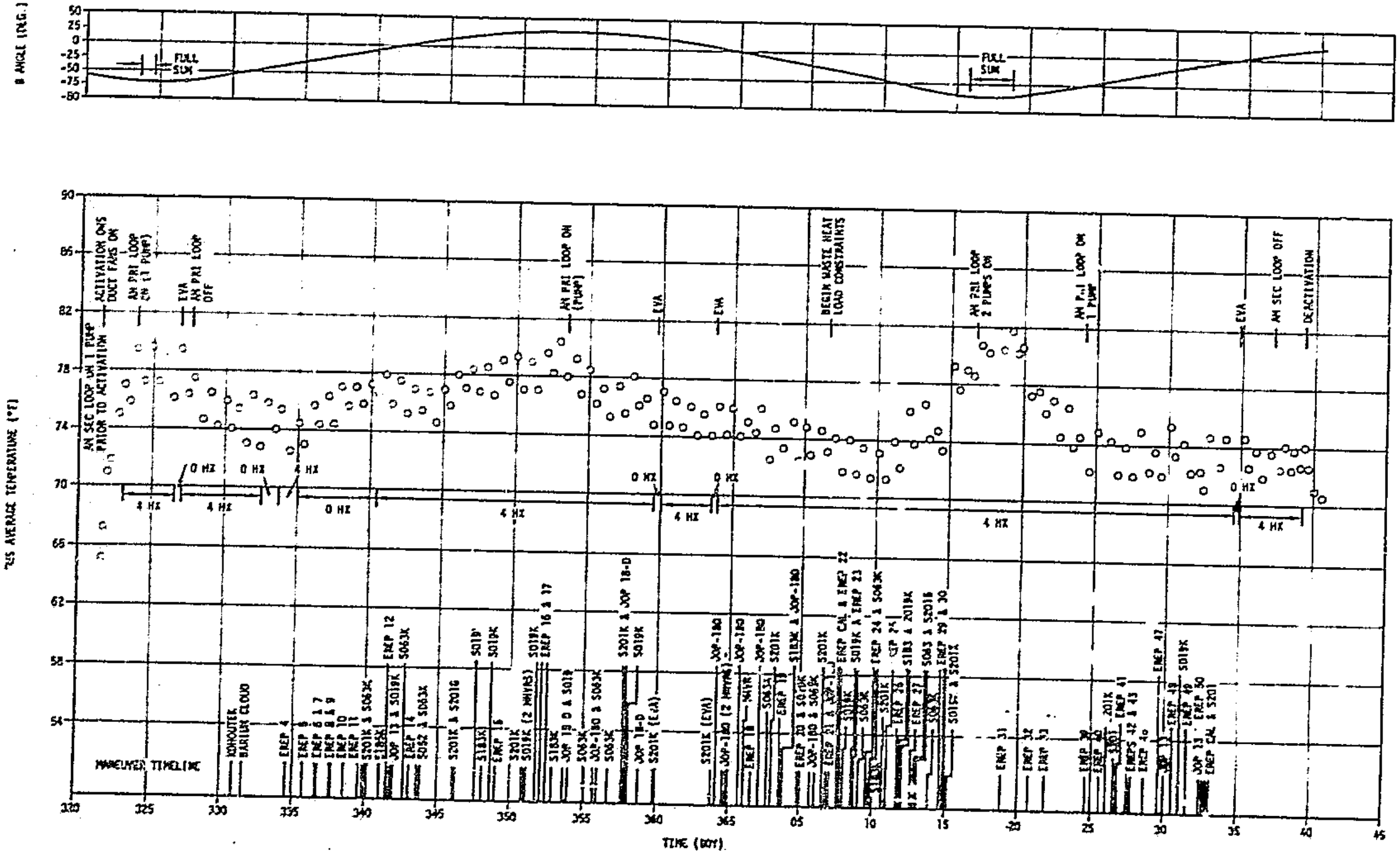

Figure 4-39. OWS Average Temperature SL-4 Manned Mission

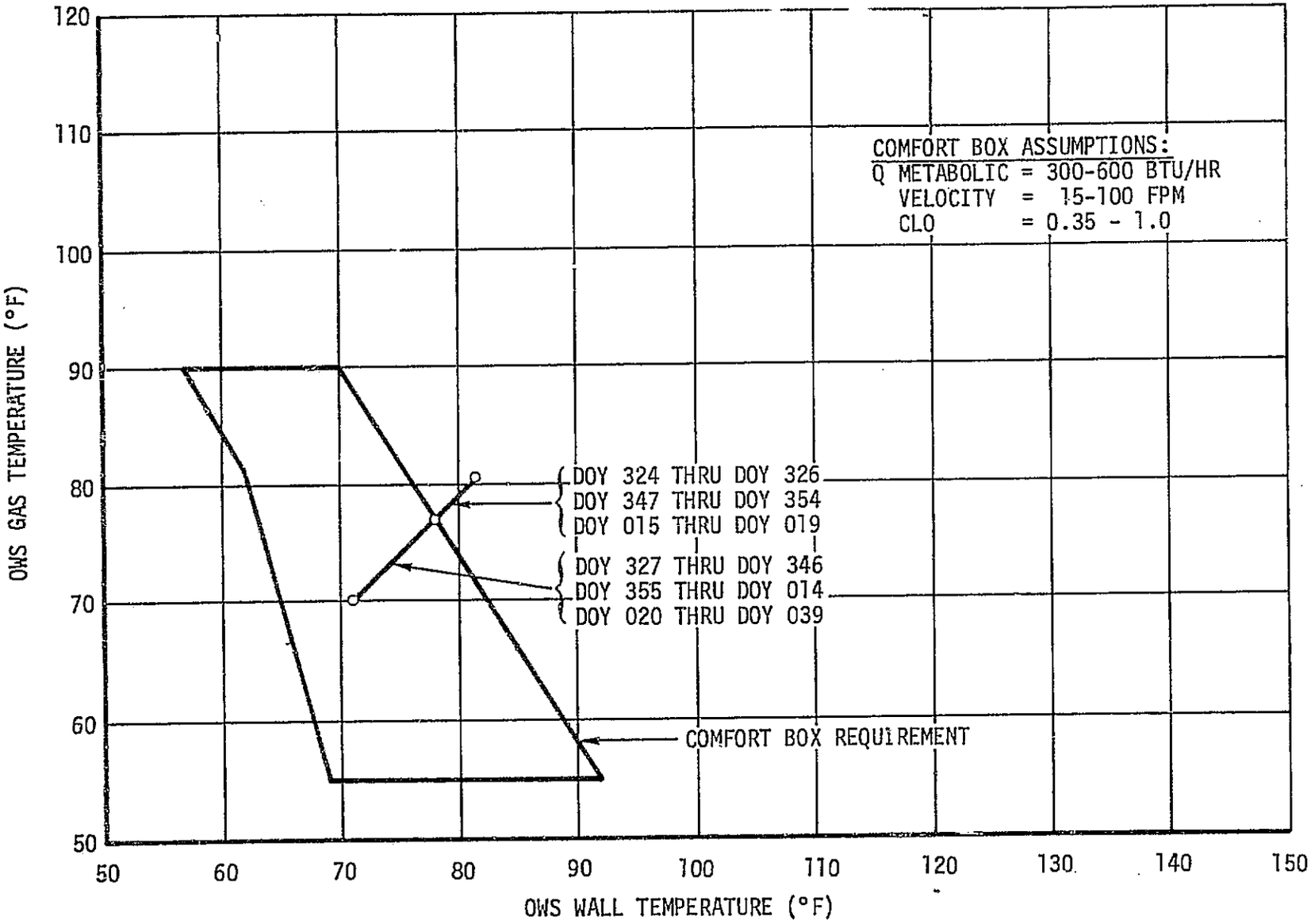

Figure 4-40. OWS Forward Compartment Temperature During SL-4

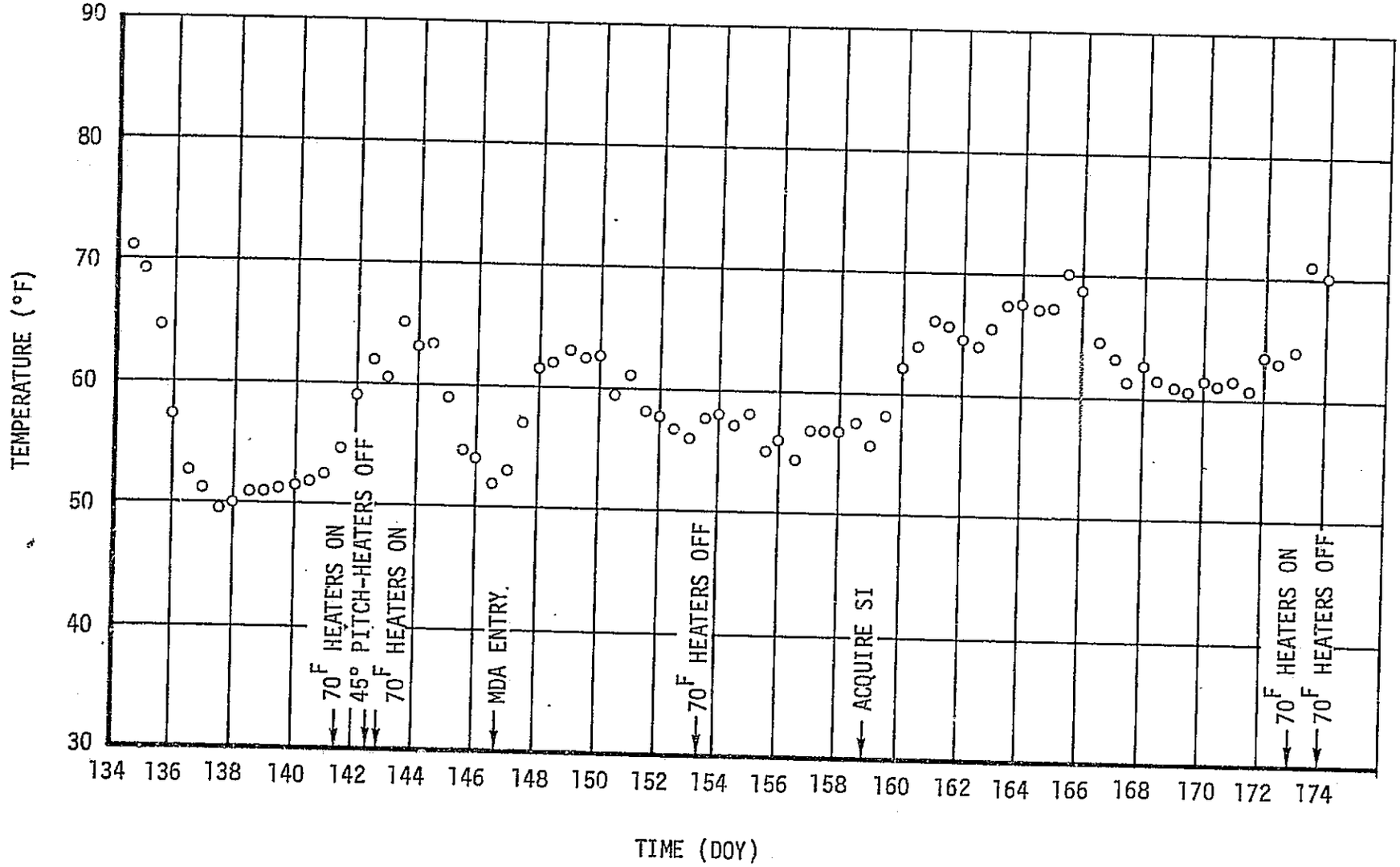

Figure 4-41. MDA Average Internal Temperature During SL-1/SL-2

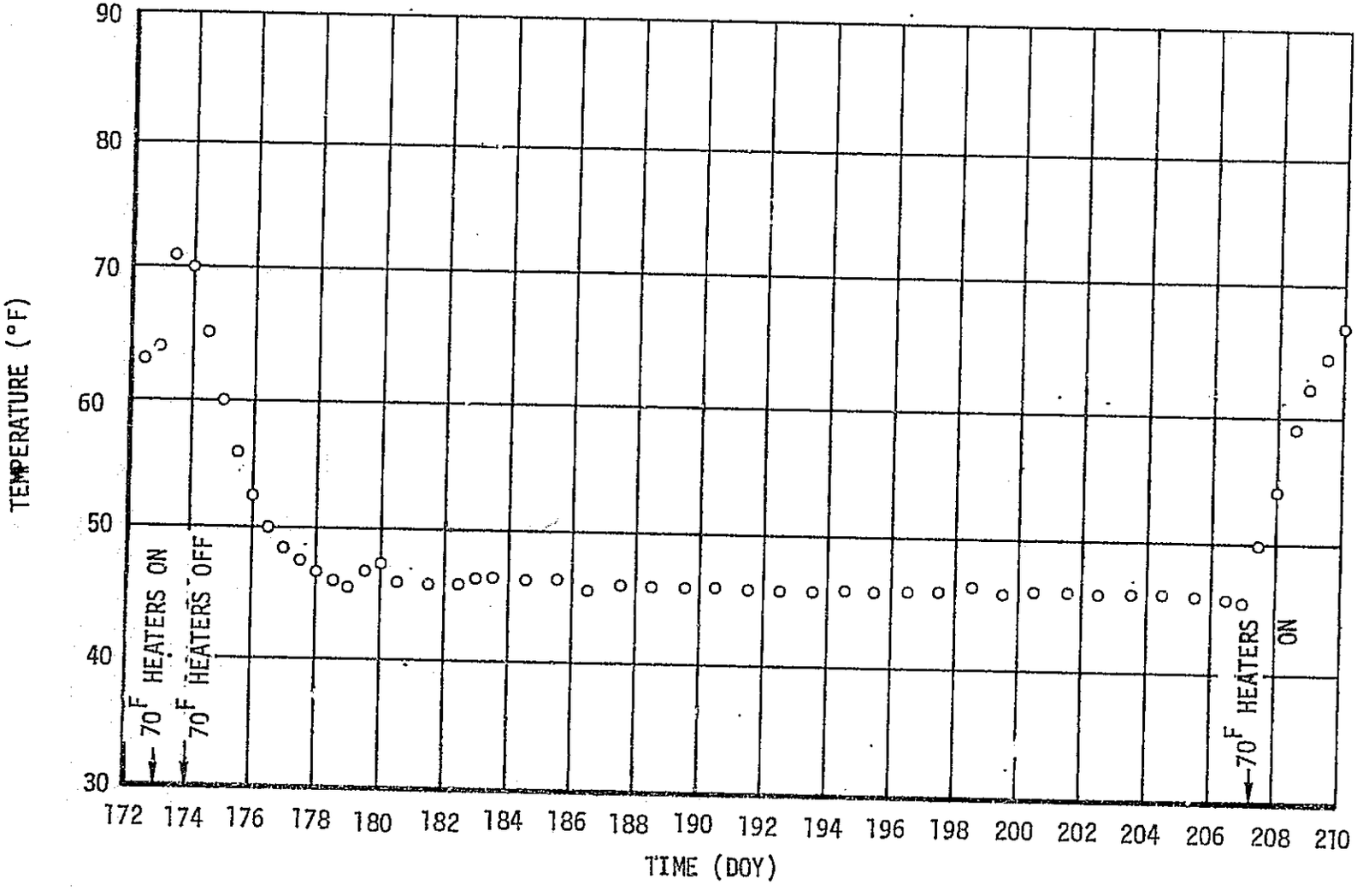

Figure 4-42. MDA Average Internal Temperature During SL-2/SL-3 Storage

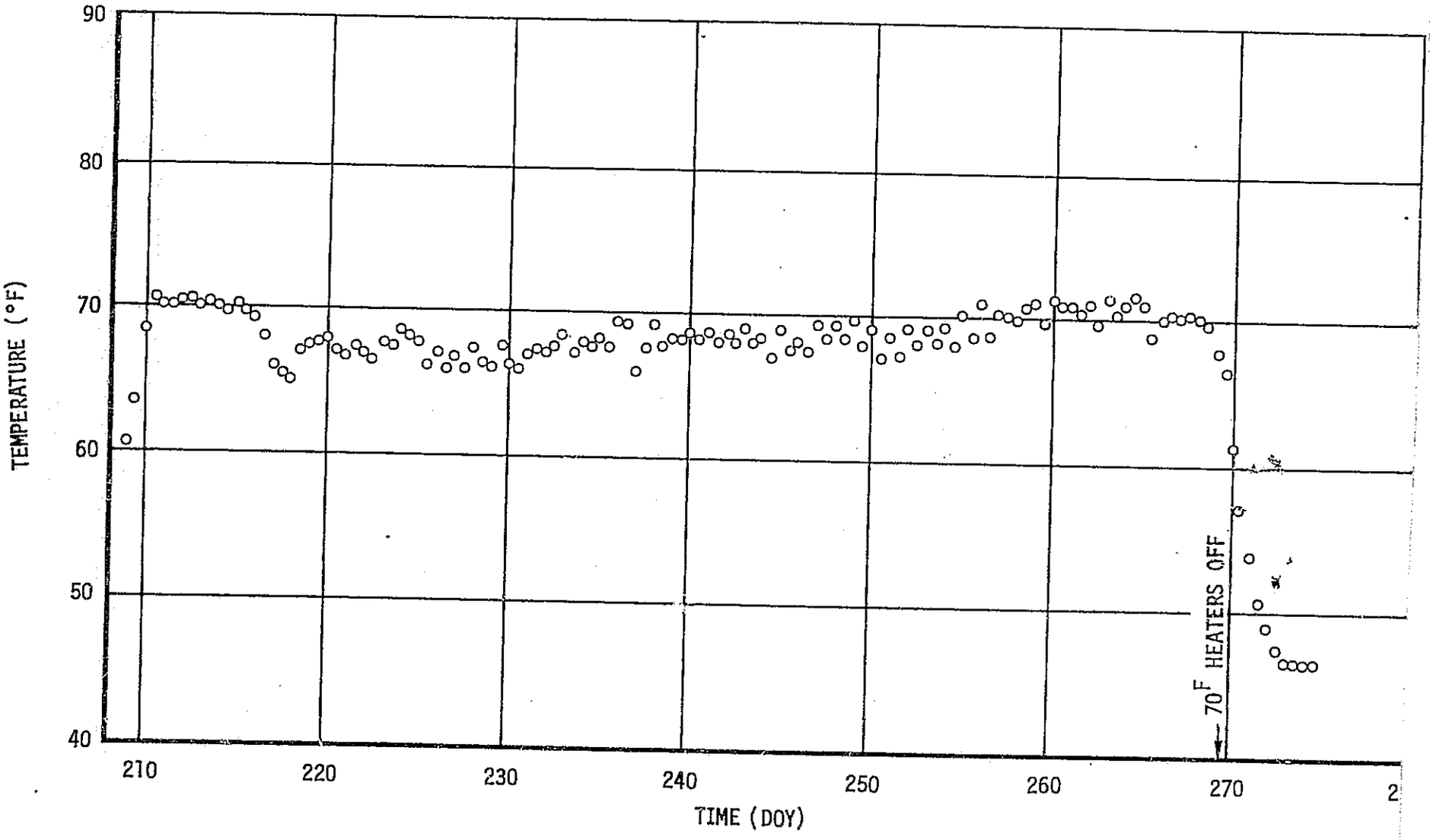

Figure 4-43. MDA Average Internal Temperature During SL-3

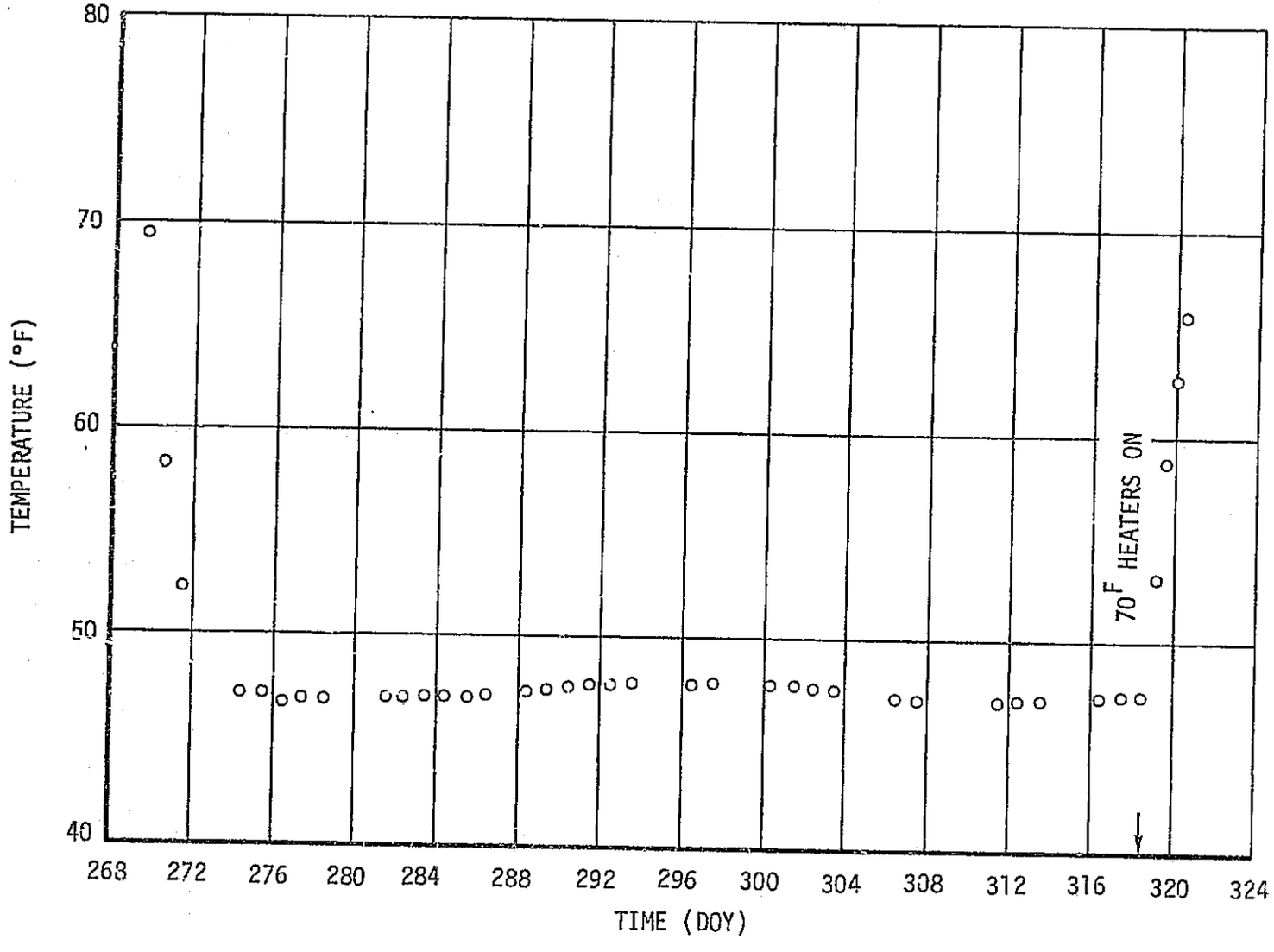

Figure 4-44. MDA Average Internal Temperature During SL-3/SL-4 Storage

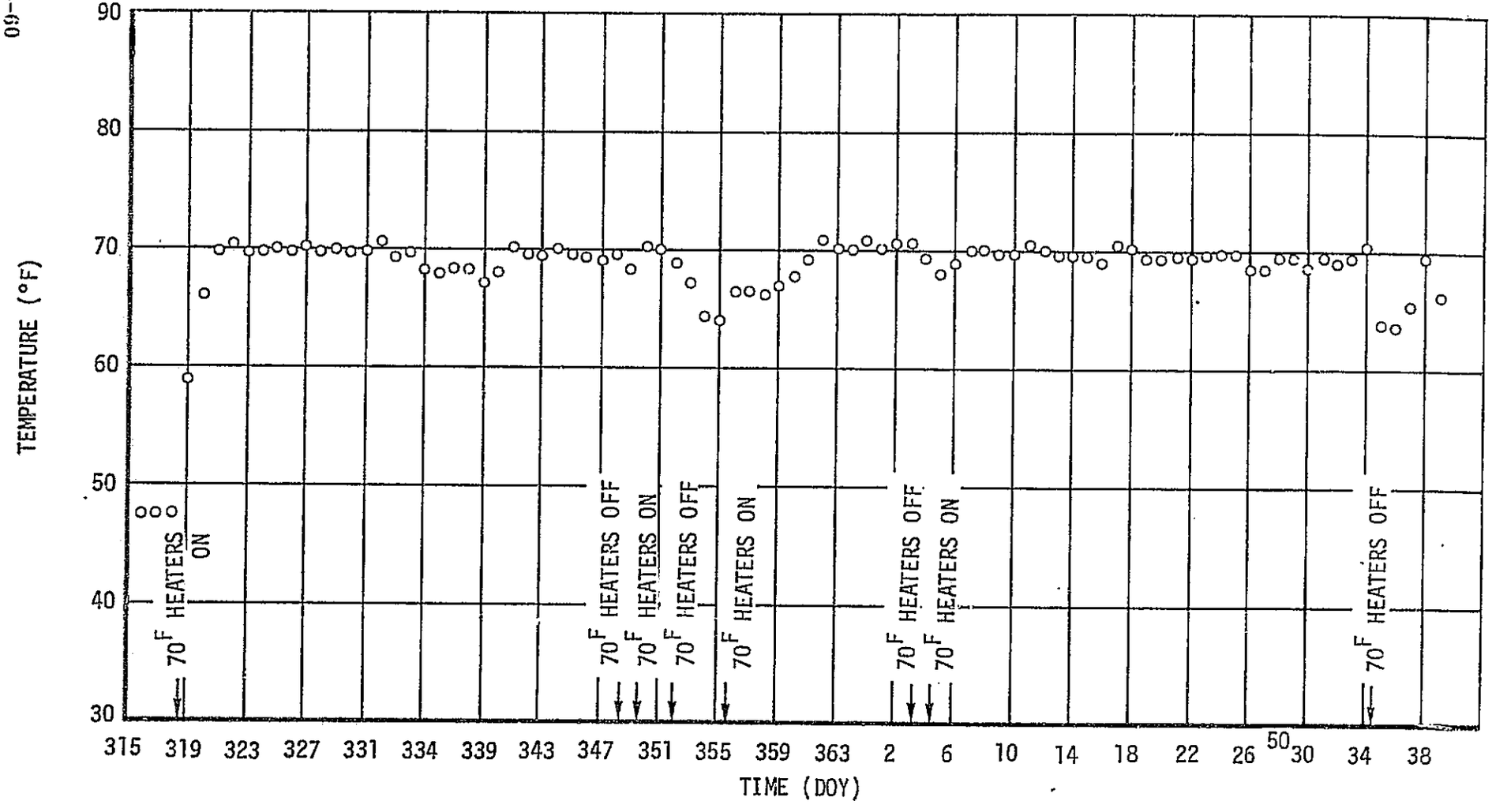

Figure 4-45. MDA Average Internal Temperature During SL-4

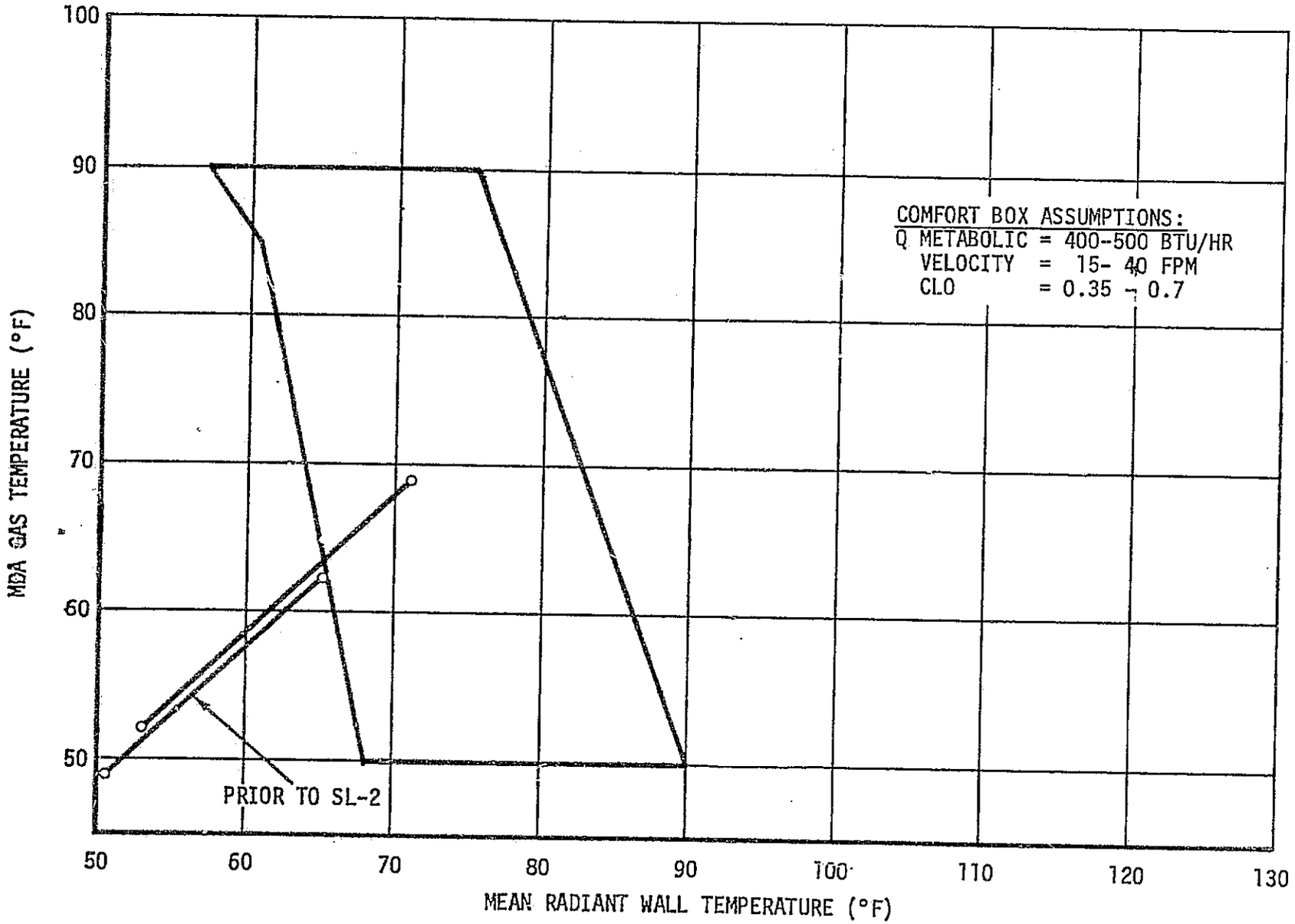

Figure 4-46. MDA Comfort Box for SL-2

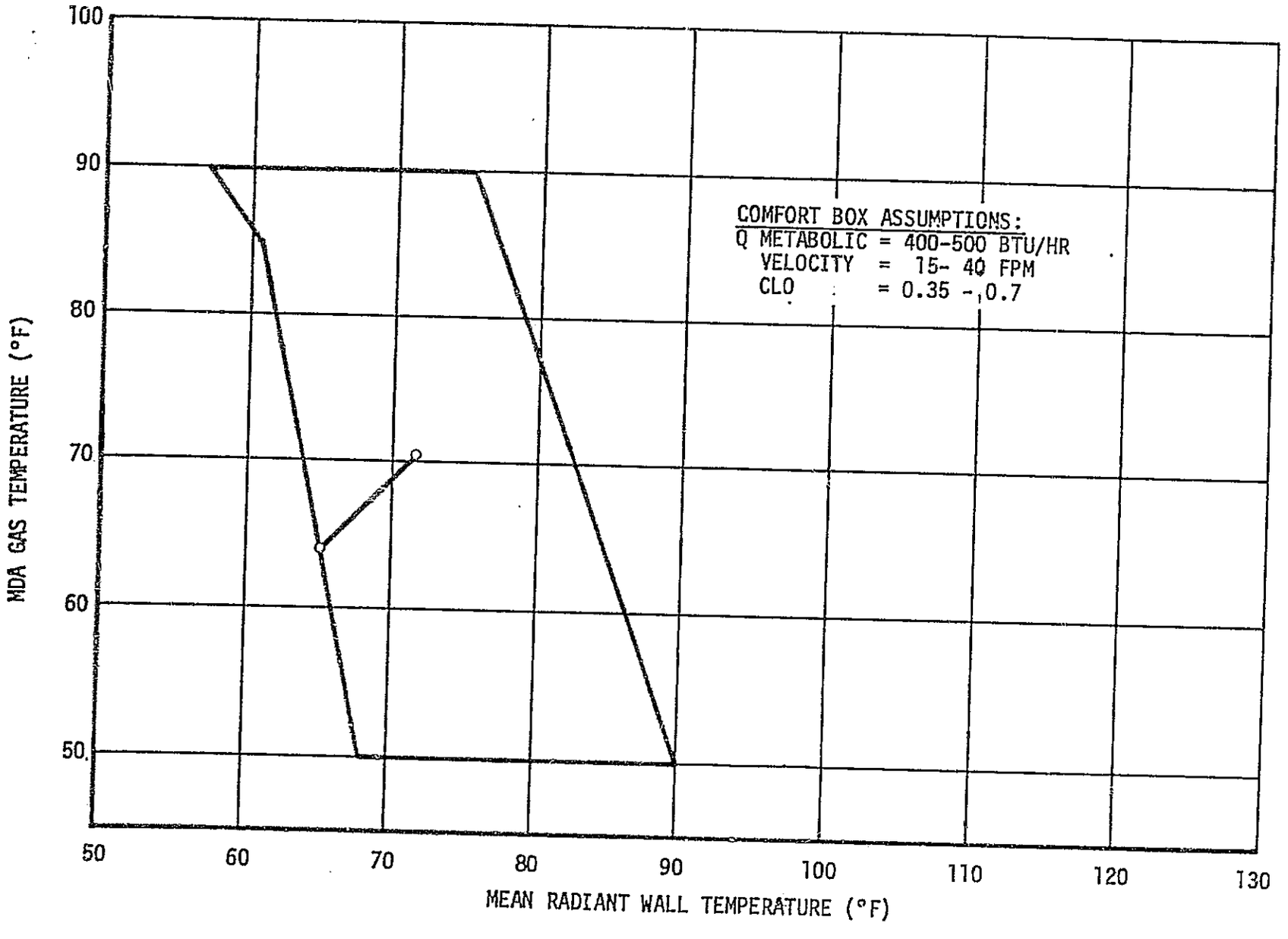

Figure 4-47. MDA Comfort Box for SL-3

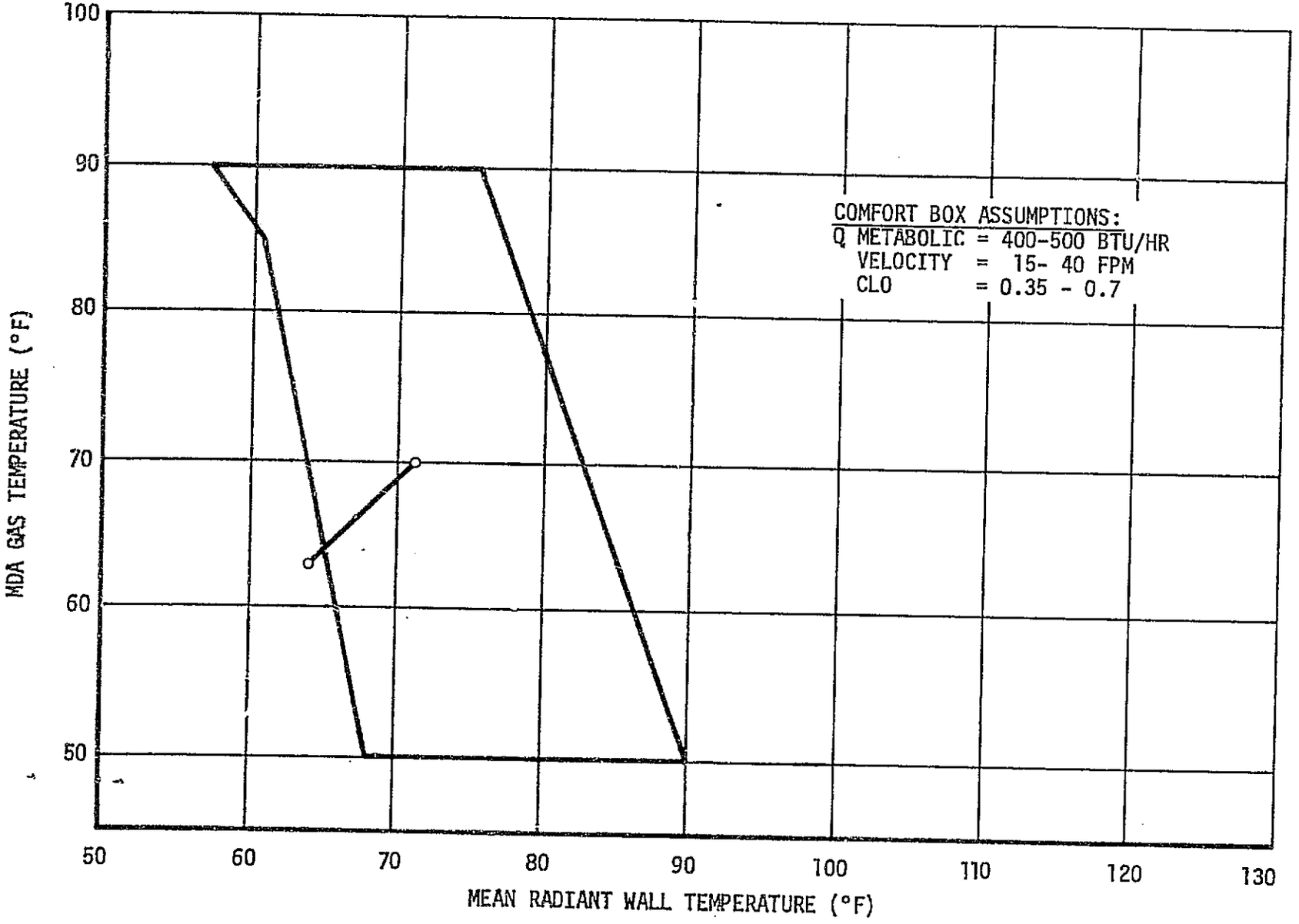

Figure 4-48. MDA Comfort Box for SL-4

5. AM Temperatures. Integrated temperature control of Airlock Module structure and non-cold-plated equipment was provided by normal operation of the active cooling system, atmospheric control system and wall heaters in conjunction with thermal coatings, curtains and insulation. Temperatures of all equipment and structure remained within acceptable limits throughout all phases of the mission.

With the unplanned vehicle attitude during the initial SL-1 unmanned phase when pitch angle was maintained at approximately 45 to 50 degrees to minimize OWS temperatures after loss of the meteoroid shield, Airlock Module temperatures were abnormally cold as shown in Table 4.5. Although indicated temperatures were still acceptable, instrumentation was rather limited and colder areas may have existed. Following deployment of the parasol on DOY 147 and return to the planned solar inertial attitude, temperatures increased to normal levels. A discussion of internal temperatures is presented in paragraph B.9 of this section.

6. OWS Food and Film Container Temperatures. The OWS thermal control system was designed to maintain the ambient food containers between 40 and 85°F. It was also required to maintain the OWS film below 80°F except for periods with |Beta| > 60° when the limit was 85°F. This design limit was revised to 100°F but since this limit was also exceeded, as shown in figure 4-49, some film was resupplied. During the period prior to SL-2 launch, the food and film containers tended to follow the average OWS temperature as the figure indicates. The food lockers located near Position II (figure 4-50) in the forward compartment were a few degrees hotter than the average temperature due to the influence of the hotter wall near Position II. The film vault, near Position IV, was a few degrees cooler due to the more moderate wall temperatures near Position IV.

The equations used to determine food and film temperatures are shown in Table 4.6 and the location of the onboard measurements used in the equations are shown in figure 4-50. It was necessary to revise the equations as sensors went off scale high or when the equations were no longer valid due to changes in Sun shield configuration or external heating due to Beta angle.

The maximum food and film container temperatures of 132 and 122°F, respectively, occurred just prior to parasol deployment on DOY 147. After parasol deployment, the containers cooled down to the low 80's and remained there until the higher Beta angles at the end of the SL-2 manned mission as shown in figure 4-51. During the full sunlight period at the beginning of the SL-2/SL-3 storage period, the food containers and film vault reached approximately 100°F before cooling down to the low 80's again.

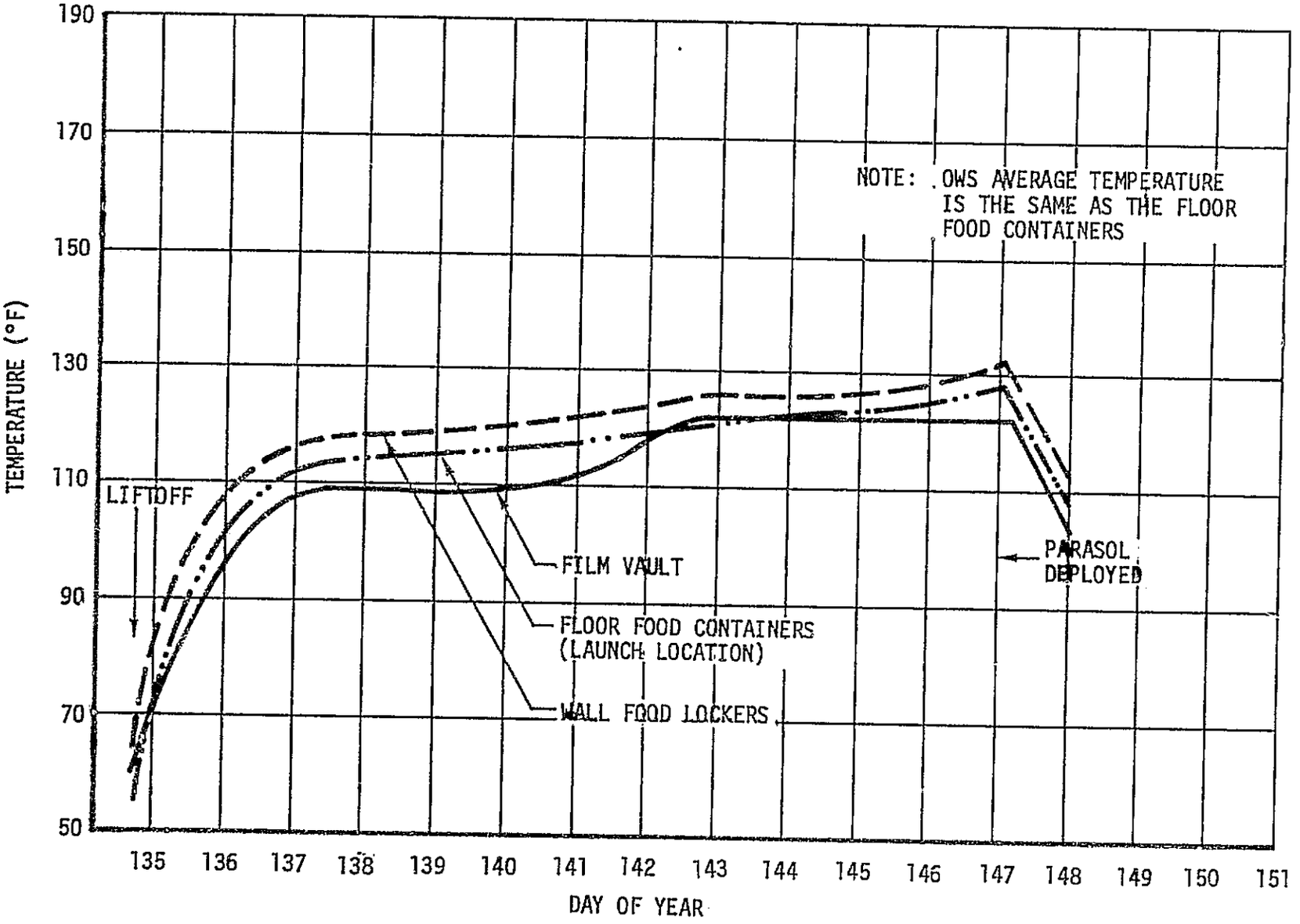

Figure 4-49. SL-1 OWS Film Vault & Food Lockers Temperature Histories

TABLE 4.5 EFFECT OF SL-1 ATTITUDE ON AM TEMPERATURES

Location	Minimum Temperature (°F) (1) SL-1 (2)	Normal (3)
FAS (-Z Axis)	-16 to -9	120 to 200
FAS (-Y Axis)	-48 to -34	15 to 40
FAS (+Z Axis)	-70 to -56	-50 to -19
FAS (+Y Axis)	-42 to -21	-21 to 0
O_2 Tank 1	-30.7	-14.4
O_2 Tank 2	-31.6	-12.6
O_2 Tank 3	-51.2	-30.8
O_2 Tank 4	-43.5	-15.2
O_2 Tank 5	5.0	82.8
O_2 Tank 6	3.4	134.6
N_2 Tank 1	32.5	88.9
N_2 Tank 2	24.0	89.2
N_2 Tank 3	17.9	47.9
N_2 Tank 4	10.0	50.7
N_2 Tank 5	1.6	25.0
N_2 Tank 6	4.0	27.4
STS Inner Skin	38.8	57.0
Lock Compt. Inner Skin	41.9	57.1
Aft Comp. Inner Skin	43.1	57.2
SUS 1 Water Line	33.7	43.0
SUS 2 Water Line	38.6	47.5

NOTES: (1) Orbital Range
(2) DOY 140-146, Beta = 22° to 28°, Pitch Angle = 45° to 50°
(3) DOY 201, Beta = 25°

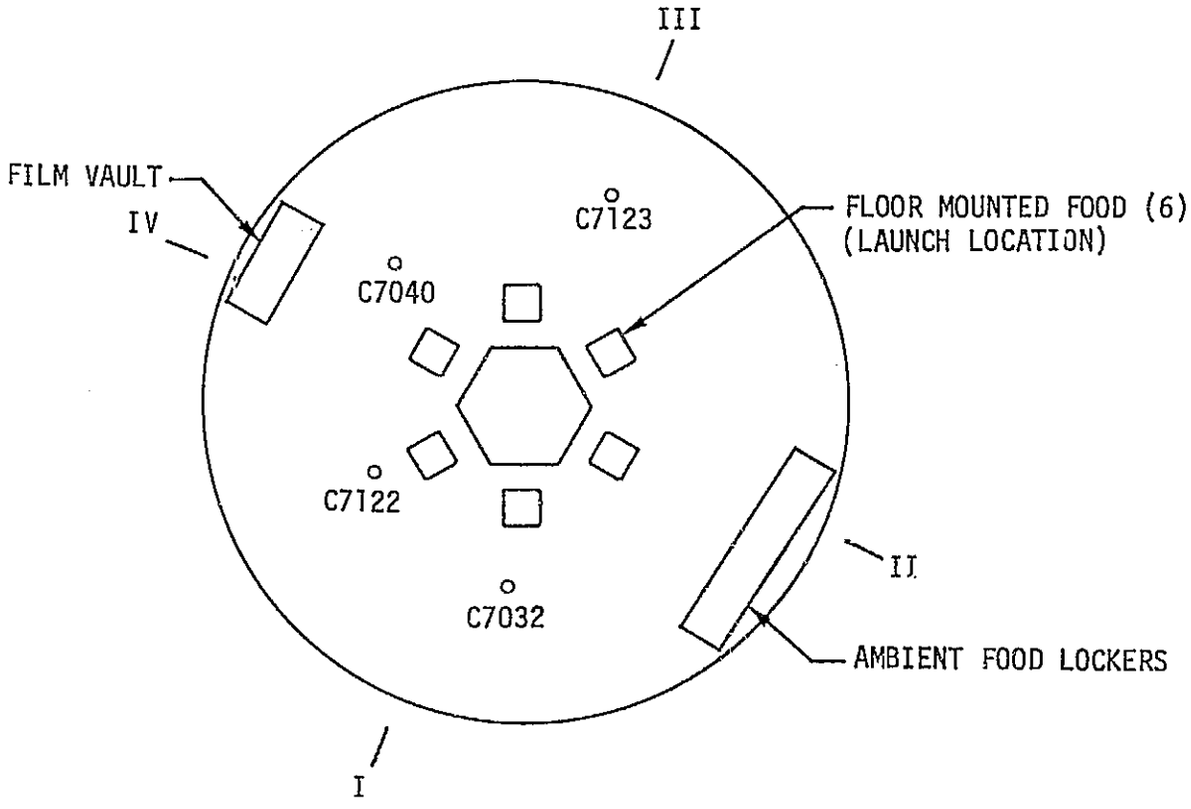

OWS FORWARD COMPARTMENT, PLAN VIEW

NOTE: C0732, C7122, C7040 & C7123 LOCATED ON CEILING GRID.
C7144 IS GAS MEASUREMENT IN EXP COMPARTMENT DIFFUSER.
OTHERS LOCATED ON INTERNAL WALL.

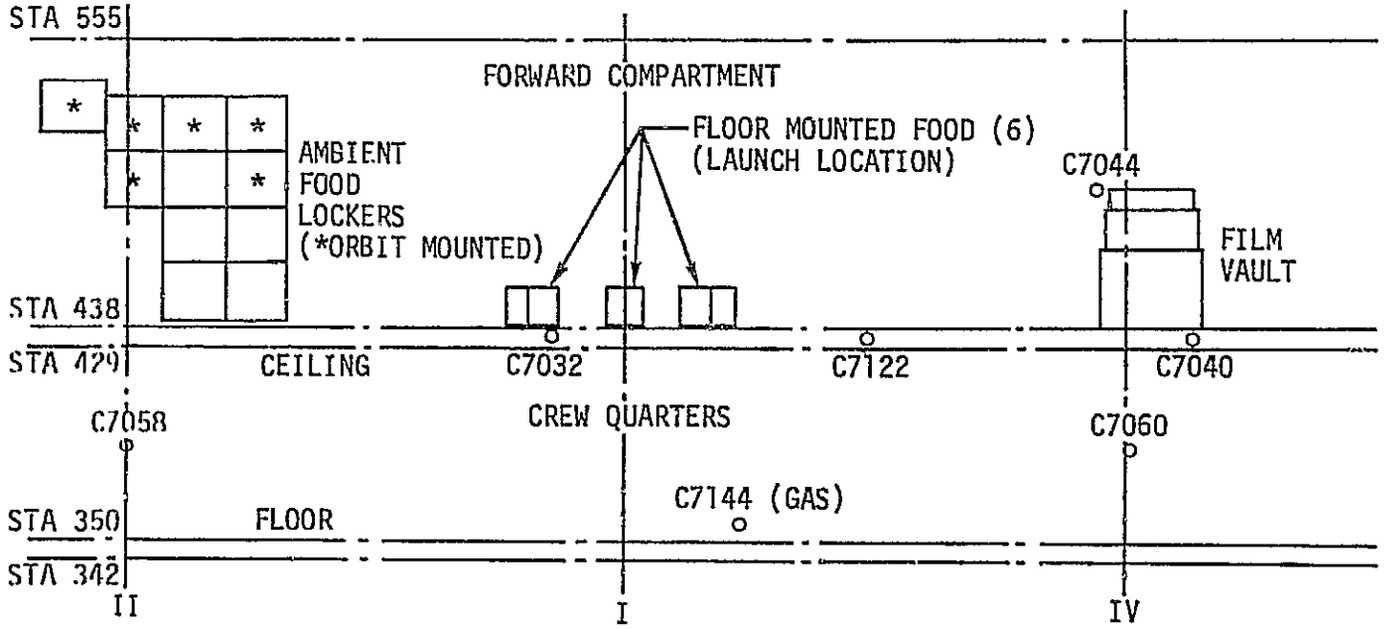

Figure 4-50. OWS Inboard Wall Profile Location of Food Lockers & Film Vault

TABLE 4.6 OWS FOOD AND FILM EQUATIONS

Time (DOY) of Equation Change	Floor Food Lockers	Wall Food Lockers	Film Vault
134	AVE*	1/2 (C7044 + C7032)	1/3 (C7044 + C7060 + C7040)
137		1/2 (C7044 + AVE*)	
142	C7123 + 14	1/2 (C7123 + C7058) +14°F	C7123 + 13°F
147	AVE*	1/2 (C7040 + C7032)	1/3 (C7044 + C7060 + C7040)
163	N/A**	AVE* + 4.4°F	AVE* + 5.0°F
169		AVE* + 3.4°F	AVE* + 4.0°F
170		AVE* + 2.4°F	
238		1/3 (AVE* + C7058 + C7144 +2°F)	
268		1/2 (AVE* + C7058)	
270			1/2 (AVE* + C7044)

*AVE = OWS Internal Average = 1/4 (C7032 + C7122 + C7040 + C7123)
**Floor Food Transferred to Wall Locker on DOY 148

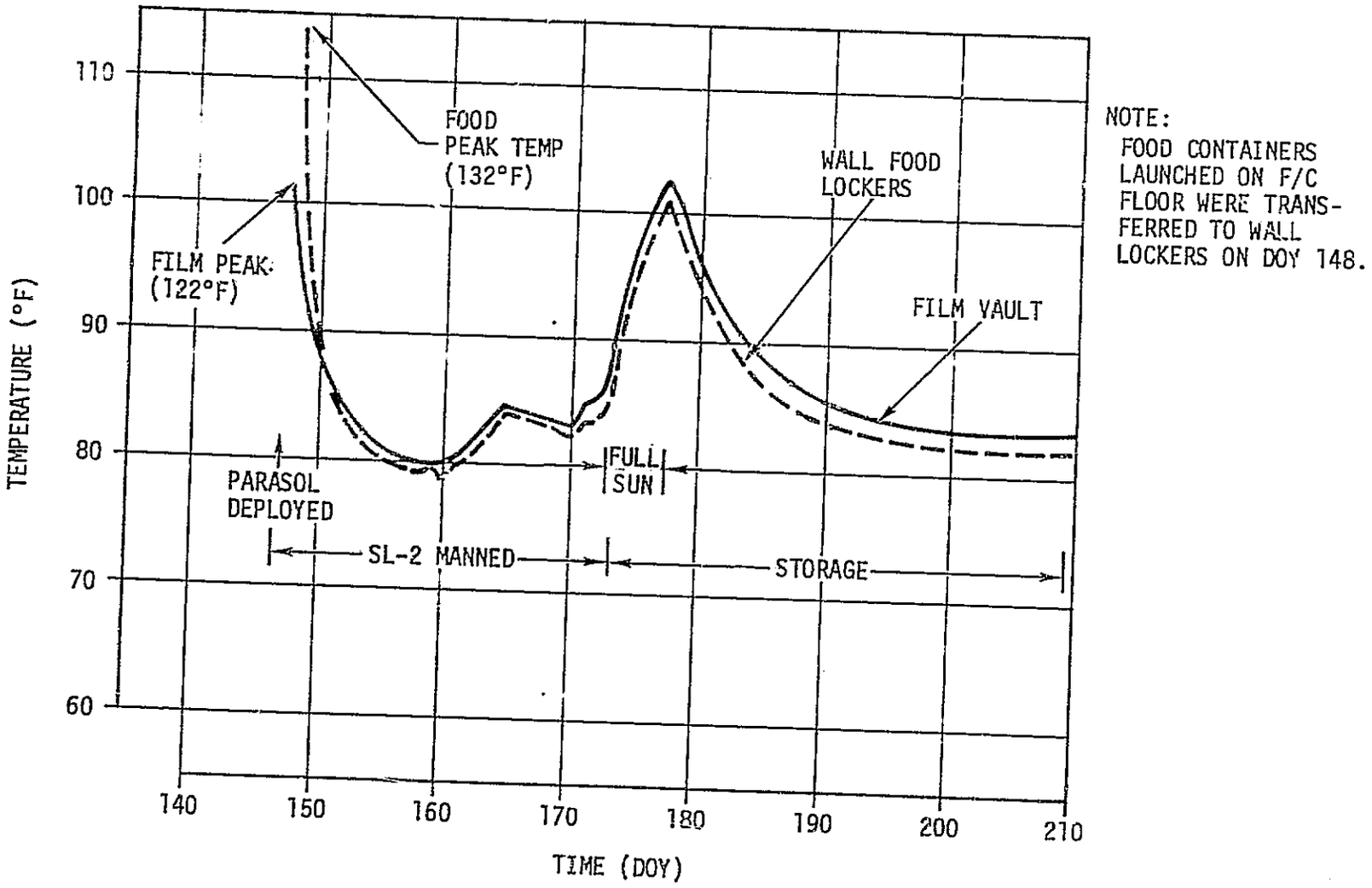

Figure 4-51. SL-2 OWS Film Vault & Food Lockers Temperature Histories

Food and film temperatures for the SL-3 mission, the SL-3/SL-4 storage period and the SL-4 mission are presented in figures 4-52 and 4-53. The deployment of the MSFC twin pole shield early in the SL-3 mission improved the environment at full sun conditions and the maximum temperature seen after that time was less than 85°F.

7. MDA Film. The MDA film vault temperature requirement (80°F maximum) was met. The film vault temperatures ranged between 48°F and 76°F during the manned periods and between 44°F and 71°F during the storage periods.

Prior to SAS deployment during SL-2, the relative humidity exceeded the desired 80 percent upper limit due to power management and resulting cold MDA temperatures. On several occasions during this period of time the relative humidity approached 100 percent. However, no condensation was reported by the crew. After SAS deployment, the relative humidity did not exceed 80 percent.

8. EREP and Special Maneuver Studies. Changes in vehicle attitude from solar inertial which exposed more of the gold surface to the Sun for any period of time had to be analyzed to determine whether the polyurethane insulation on the OWS tankwall would exceed its maximum temperature limit. Toxic off-gassing products from the insulation were the primary concern. The initial limit for habitation was 200°F. However, this limit was later revised to 250°F and later still to 275°F as additional testing data were received. Under steady-state conditions the exposed tankwall and adjacent insulation would exceed 300°F.

Since EREP data passes required Z-Local Vertical (Z-LV) attitudes which exposed the OWS tankwall to direct sunlight, transient thermal analyses were performed to determine the OWS temperature response to each proposed Z-LV maneuver. The highest temperature attained during an EREP pass was on DOY 14 when the vehicle was out of the solar inertial attitude for 123 minutes at a Beta angle of -67°. The predicted maximum external OWS temperature attained during that time was 260°F and the Fin II sensor temperature was approximately 236°F. The accuracy of the thermal predictions for OWS external temperatures was estimated to be within 10°F of the actual value. An example of EREP predictions with the corresponding sensor data is shown in figure 4-54 for DOY 20.

In addition to Z-local vertical maneuvers for gathering EREP data, numerous maneuvers away from the solar inertial attitude to other fixed attitudes which satisfied experiment pointing requirements were also made during SL-4. Most of the maneuvers were for observing the Comet Kohoutek, however, some ATM JOP 13 and one S232 Barium Cloud maneuvers were also included. In general, the fixed attitude maneuvers had roll angles that varied from 0 to 165° and pitch angles that varied from 0 to 90°. The yaw angle was usually less than 20°. The time

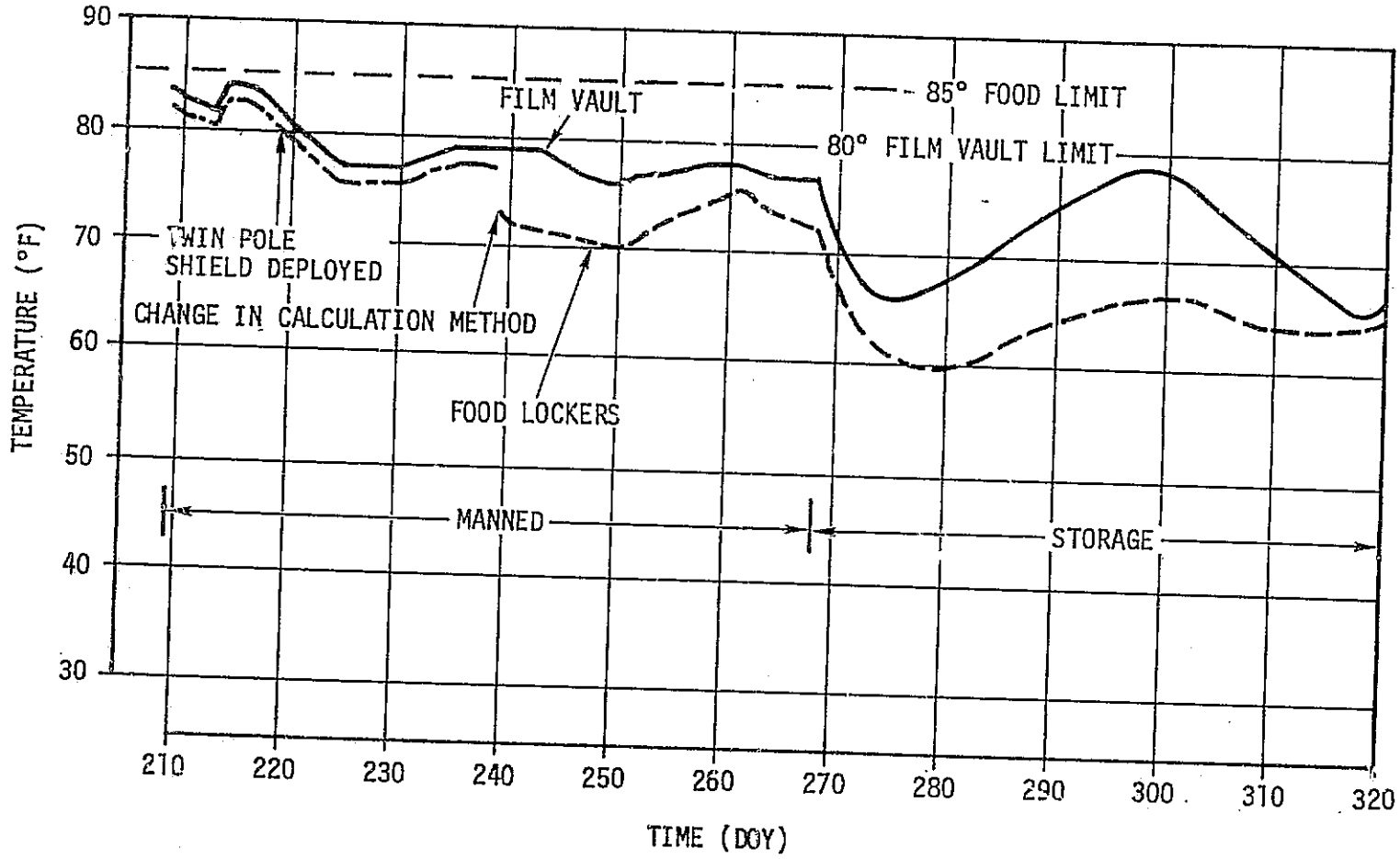

Figure 4-52. SL-3 OWS Film Vault & Food Lockers Temperature Histories

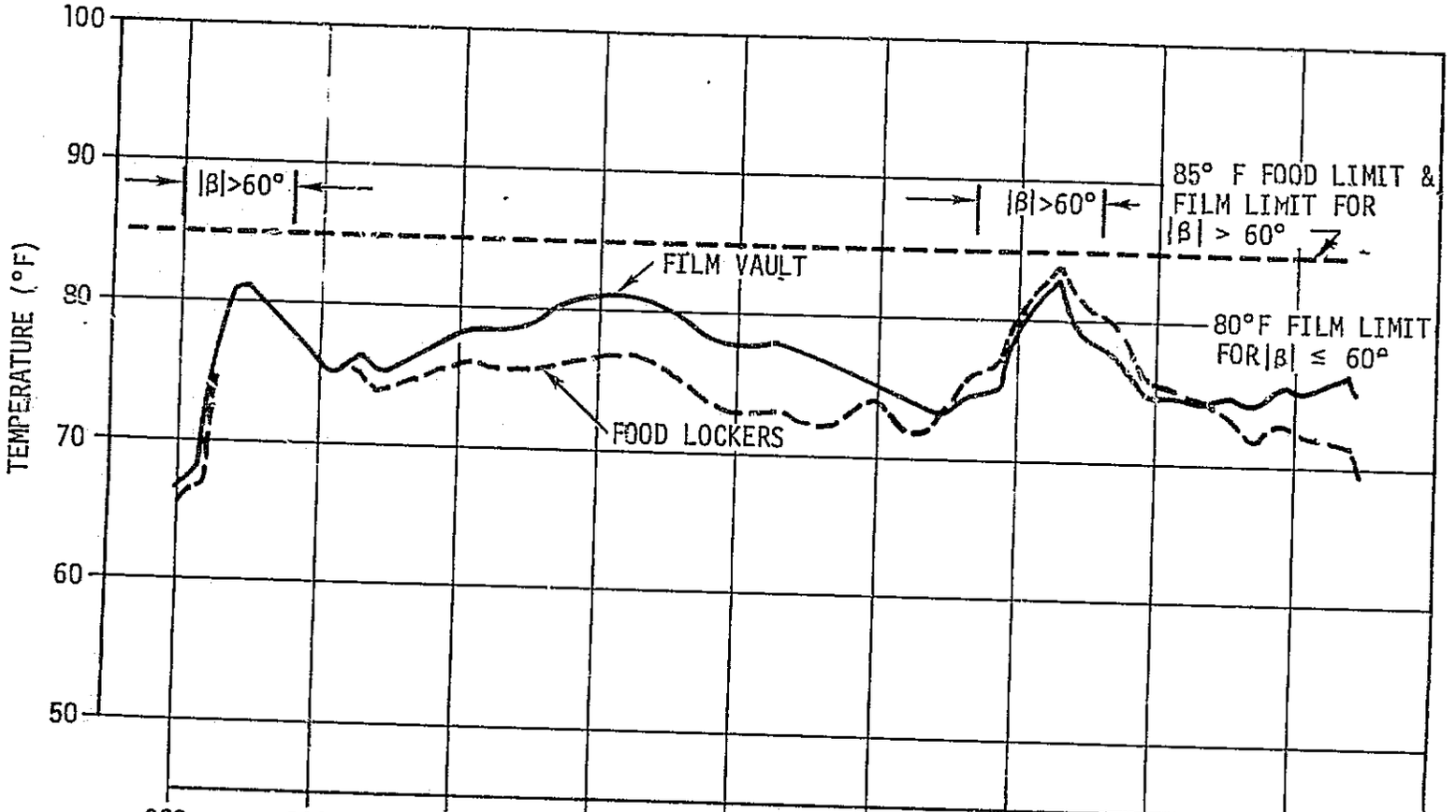

Figure 4-53. SL-4 OWS Film Vault & Food Lockers Temperature Histories

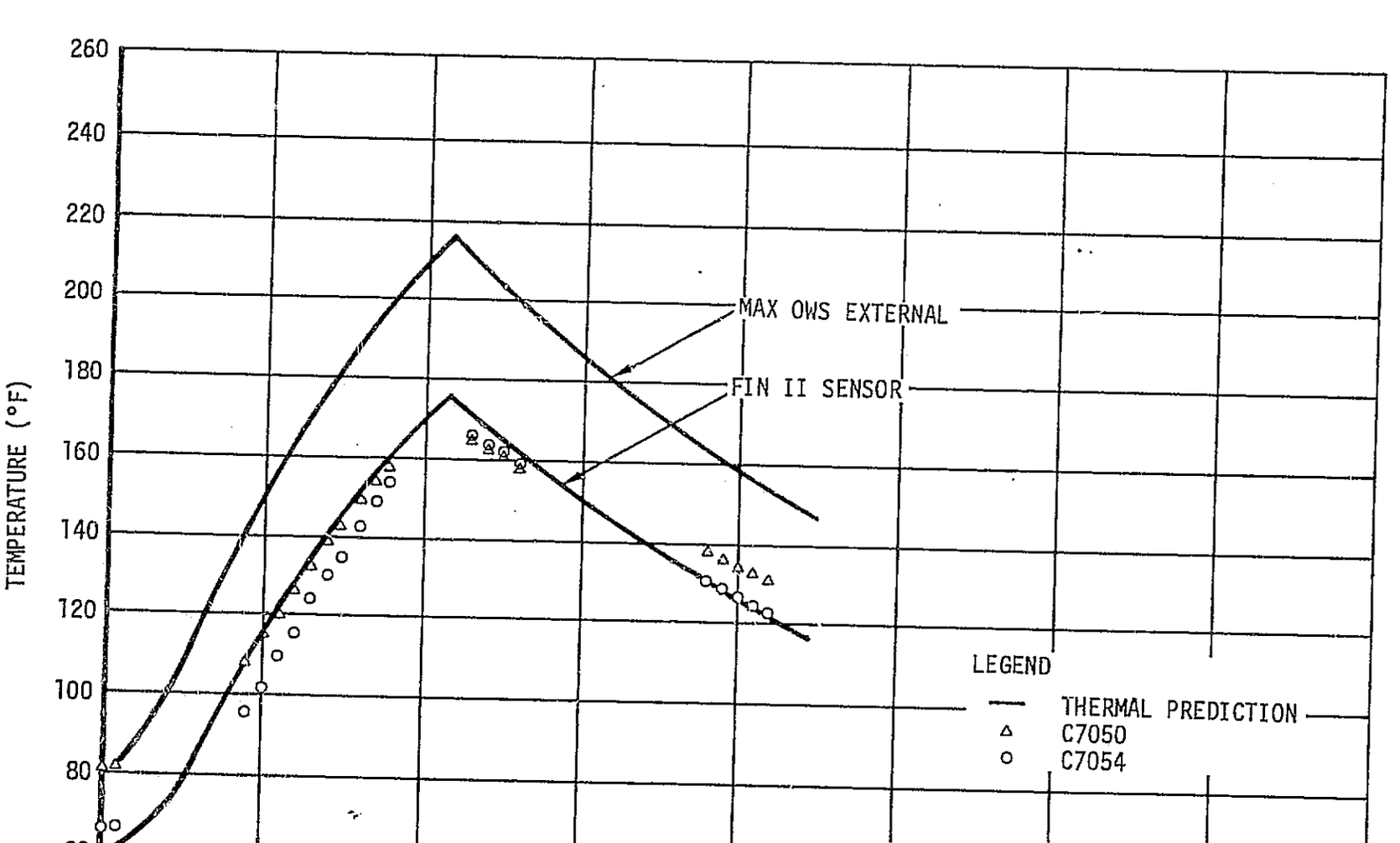

Figure 4-54. OWS Transient Response for EREP 32, DOY 20, 1849 GMT

required away from solar inertial for these maneuvers ranged from several minutes to almost 3 hours. The external temperature results from a typical experiment maneuver are shown in figure 4-55 along with the predicted response.

9. Active Systems

a. OWS Duct Heaters. The six OWS duct heaters were never required during SL-2, SL-3 and SL-4, and consequently, were never activated.

b. OWS Radiant Heaters. The OWS radiant heaters were to be commanded on at 107 minutes after liftoff according to premission plans in order to warm the OWS up to 70°F. They were commanded on at 2 hours 44 minutes GET by ground controllers. At this time the OWS internal temperature, as determined from C7032, C7044, and C7106 was 64°F. AM Bus 1 and Bus 2 current and voltage data indicated that the heaters provided 1,260 watts of power versus their design requirement of 1,000 watts, minimum. The heaters were commanded off at 134:22:44 GMT (5 hours 14 minutes GET) at which time the OWS temperature was 72°F. The 8°F increase in OWS temperature during the radiant heater operation was caused primarily by orbital heating which was an order of magnitude greater than the radiant heater power. The radiant heaters were not operated after that time.

c. OWS Window Heater. Although condensation in the form of ice, fog, and water was observed on the inner surface of the outer pane of the wardroom window during the mission, the wardroom window heater appeared to have performed its intended function of preventing condensation on the cover and inner surface. The basis for this conclusion is that the heater was turned off for one night during SL-2 (DOY 169) and the whole inner surface of the cover was foggy in the morning. The heater was turned back on and the fog disappeared. To minimize the viewing degradation due to condensation on the outer pane, the window cavity was vented through the anti-solar SAL several times during SL-3 and SL-4.

d. OWS Water Tank Heaters. OWS water tank heaters were thermostatically controlled to keep the water tanks above 56°F. Telemetry data of SL-1 OWS Bus 1 and Bus 2 current indicated that all ten water tank heaters were on soon after liftoff (10 others were disabled prior to launch by opening their circuit breakers) due to the relatively cold prelaunch thermal conditioning. The Ground Thermal Conditioning System had maintained the OWS at 55°F at liftoff. The heaters began to individually turn off after 24 minutes of flight and were all off after 6 hours of flight. Monitoring of SL-1 OWS Bus 1 and Bus 2 current indicated that the heaters cycled on and off during this period as required by the thermostat.

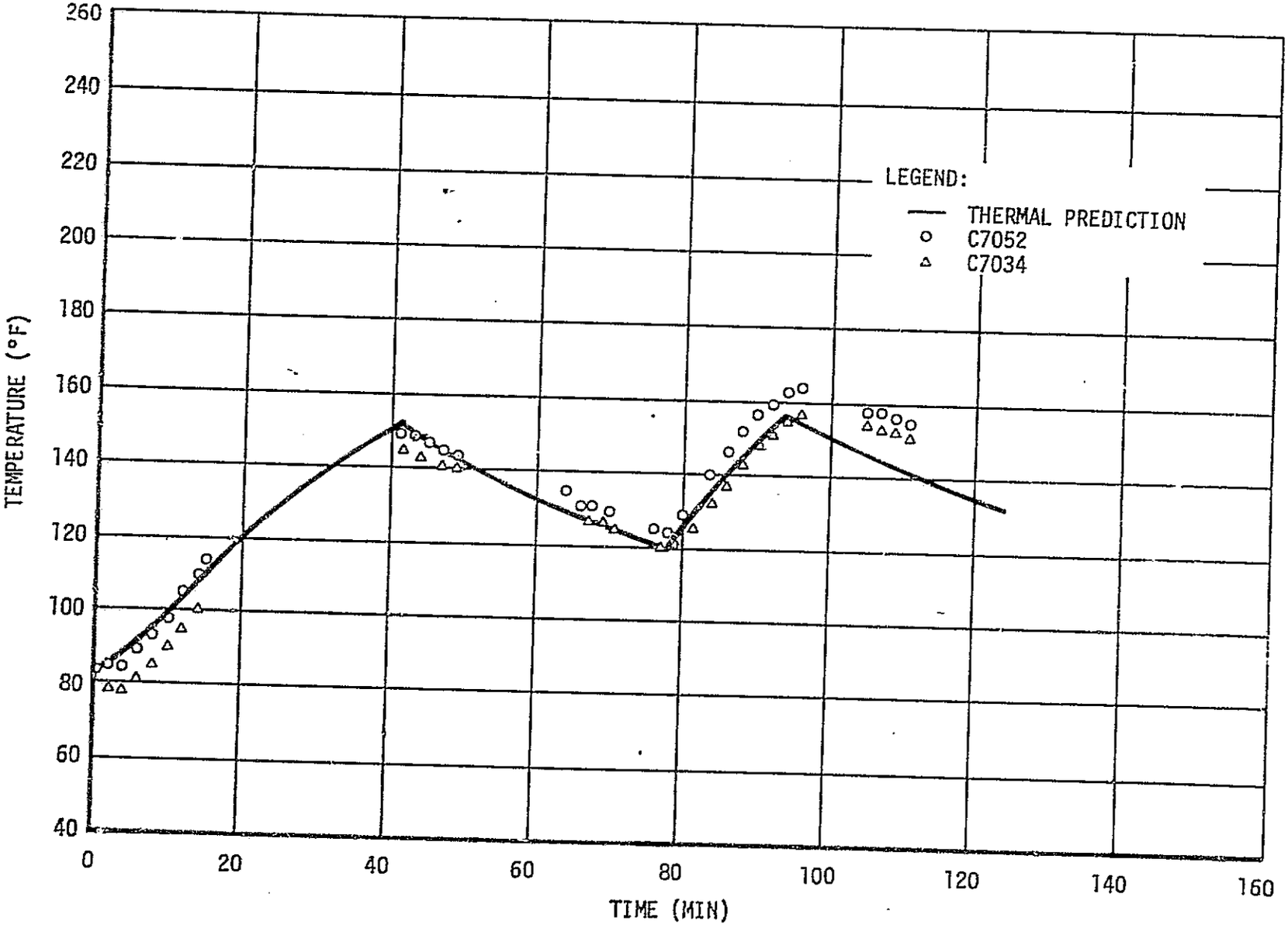

Figure 4-55. OWS Transient Response for JOP 13, DOY 32, 1225 GMT

The heaters did not operate again during the remainder of the Skylab missions. Thermal conditions in the vicinity of the water tanks during the SL-3/SL-4 storage period were low enough to require heater operation. However, the heaters had been disabled (circuit breakers opened) prior to the storage period to conserve heater power in the event that an electrical powerdown was required due to loss of coolanol from the Airlock Module cooling loop (see Section VII).

d. MDA Wall Heater System. The MDA wall heater system consisted of eight 20 watt and eight 40 watt electric wall heaters located on the internal cylindrical section of the MDA pressure wall. Four 70°F and four 45° thermostats were provided to control the internal wall temperature. Each thermostat had a primary and secondary set point providing thermostat redundancy. Seventy degree F thermostats were provided for manned operation, while 45°F thermostats were provided for orbital storage.

The MDA wall heater system was operated in an off-nominal mode from launch through the SL-2 mission. The heaters were managed by ground command as necessary to maintain MDA internal temperatures consistent with cluster power requirements prior to SAS deployment on DOY 158, and to provide additional interchange cooling to the OWS following DOY 158.

Operation during the SL-3 and SL-4 manned periods, with the wall heaters in the 70°F control mode, closely approximated nominal plans and used approximately 800 to 900 BTU/hour of heater power on the average. The only deviations were periodic shut-off of the heaters implemented during some EREP and other experiment maneuvers.

For the storage periods the MDA wall heaters were switched to the 45°F control position. During these periods the wall heater operation was characterized by heaters 1-4 being on most of the time, 5-8 cycling, 9-12 occasionally cycling, and 13-16 being off. The integrated average heater power was approximately 700 BTU/hour. The wall heaters performed as expected throughout these periods.

e. MDA Docking Port and Tunnel Heaters. Each MDA docking port had a 15 watt heater with thermostatic control between 60°F and 70°F. In addition two 80 watt strip heaters were installed in the axial port docking tunnel with thermostatic control between 60°F and 74°F. These heaters were activated most of the time except during attitude maneuvers prior to SL-2 launch, during power conservation periods before the SAS wing was deployed, and during certain EREP and other experiment maneuvers. Monitoring of TM data in the tunnel area indicated nominal performance by the heater systems. The port and tunnel heaters had an estimated average heat load of approximately 130 BTU/hour.

f. S190 Window Heater. The S190 window heater control system contained a window, electrical cable and heater controller sub-assemblies. The window heating system controlled the window temperatures such that the glass temperature gradients were minimized for photography and moisture condensation was prevented.

The S190 window heaters were operated intermittently during periods of electrical power conservation. During this period the window controller was activated approximately one hour before each EREP pass and remained active until 10 minutes after completion of the pass. The controller was activated continuously during the SL-3 and SL-4 missions.

The relatively cool MDA wall (50°F to 60°F) during SL-2 resulted in low window temperatures since the heater controller utilized the MDA wall temperature as a reference. At the same time, the MDA atmosphere dew point temperature varied between 40°F and 60°F. However, crew comments indicated that no condensation occurred on the S190 window.

g. AM Tunnel/STS Wall Heaters. AM Tunnel/STS wall heaters 42°F and 62°F thermostats were enabled throughout the mission except for short periods when electrical load reductions were required for purposes of power management. Wall temperatures between 53°F and 60°F during storage periods with the vehicle in the normal solar inertial attitude indicated that continuous heater operation was required during unmanned flight phases. STS wall and gas temperatures during manned phases of the mission are shown in figure 4-56 and 4-57, respectively. Wall temperature levels were such that only infrequent heater operation was required during these periods. Indicated temperature levels were reported by crewmen to be comfortable.

h. OWS Heat Exchangers. The OWS heat exchanger fans were operated continuously during the SL-2 mission since the OWS was biased warm due to partial deployment of the parasol sunshield. After the twin pole sunshield was deployed over the parasol early in SL-3 there were periods of time when the OWS heat exchangers were not needed to maintain crew comfort. These periods were brief and occurred at low negative Beta angles when the OWS structural heat leak was greatest.

The heat removal from the OWS by the active environmental control system was composed of heat removed by the OWS heat exchangers, the condensing heat exchangers, and by enthalpy interchange with the MDA/STS atmosphere. Figure 4-58 shows the preflight predictions for the OWS heat removal as a function of OWS gas temperature along with the flight data.

An energy balance on the OWS heat exchangers showed an imbalance between the heat rejected from the gas and coolant sides. An additional 500 BTU/hour was absorbed by the coolant loop. Since the

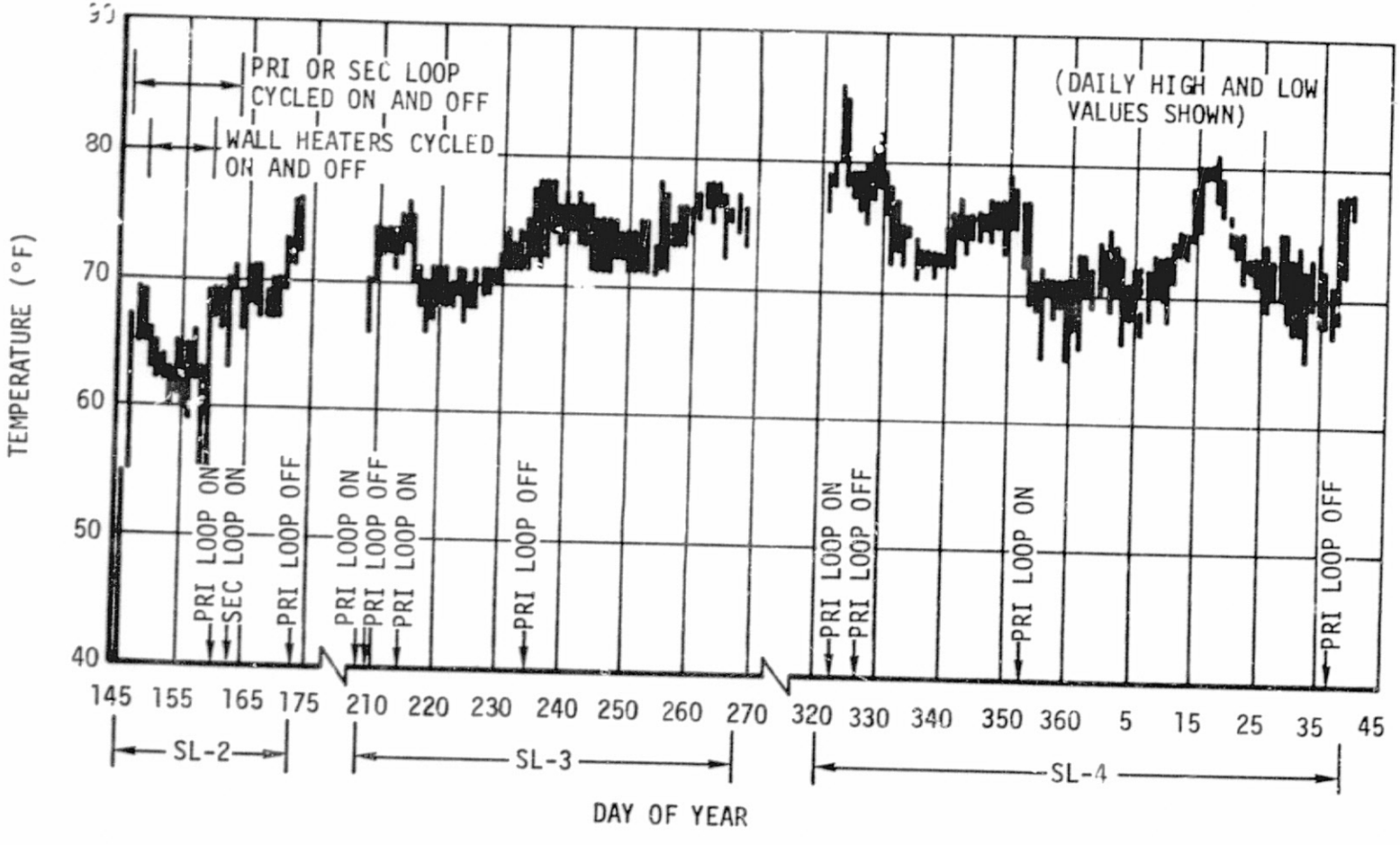

Figure 4-56. STS Wall Temperature

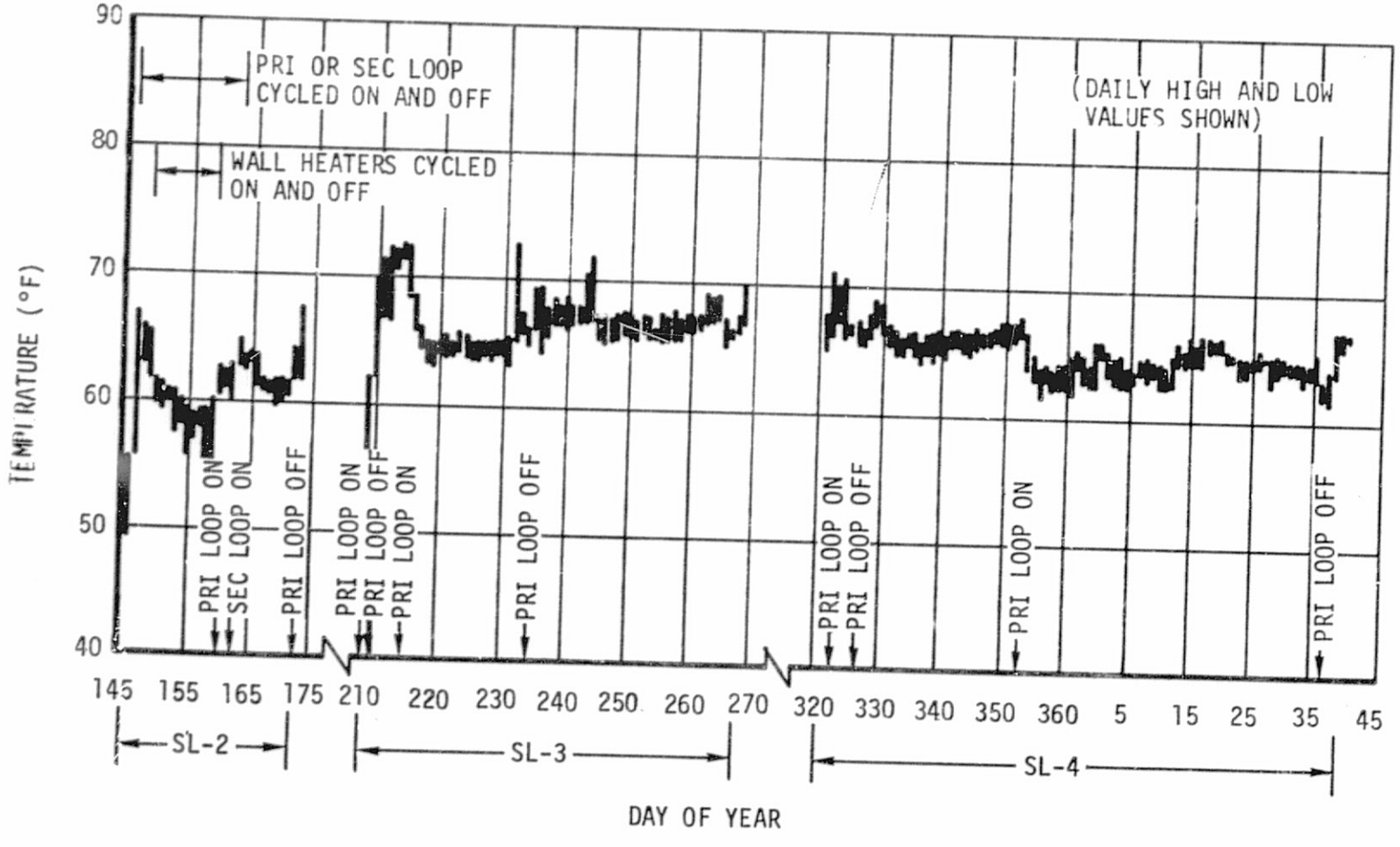

Figure 4-57. STS Gas Temperature at Mole Sieve A Compressor Inlet

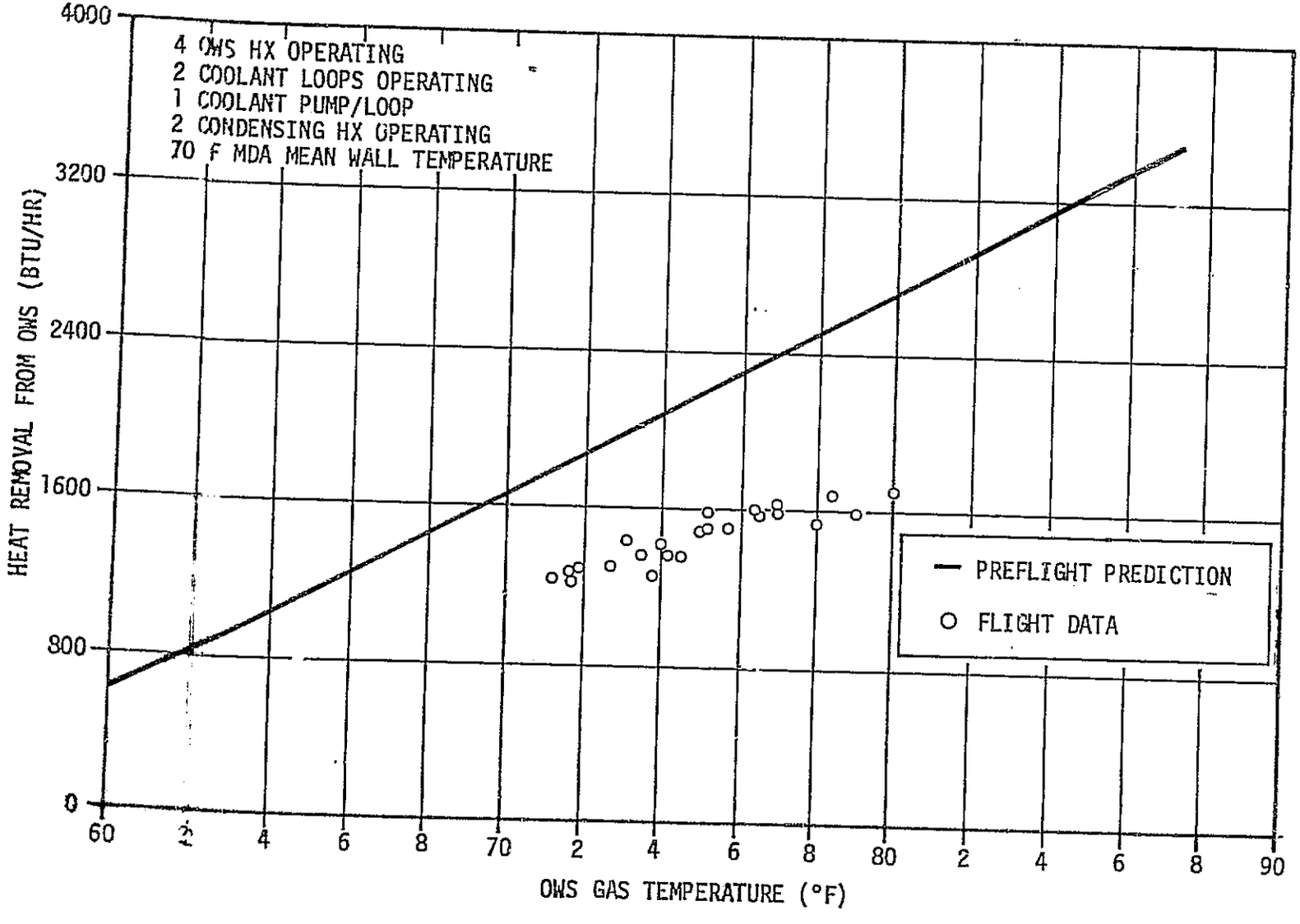

Figure 4-58. Heat Removal from the OWS

coolant inlet sensor to the OWS heat exchangers was located near the outlet of the condensing heat exchangers, heat leaks into the coolant lines between the sensor locations could have contributed to the imbalance. The performance was lower than the preflight predictions due to the low gas flow rates in the AM interchange duct and in the OWS heat exchangers. The preflight values for 4 heat exchangers were 120 CFM and 212 CFM for the interchange duct and heat exchangers, respectively, while the corresponding flight values averaged only 80 CFM and 160 CFM. A discussion of the low gas flow rate appears in Section III.

i. STS Heat Exchangers. The STS heat exchangers were controlled by the crew and were operated continuously throughout the manned missions except during periods of power management which occurred prior to SAS wing deployment and during some experiment maneuvers. Gas flow measurements were not provided for the heat exchangers. A review of the coolant loop temperature difference across the heat exchangers indicates that they performed satisfactorily. The data indicates that a gas flow rate decrease similar to that seen for the OWS heat exchangers probably occurred. However, the flow decrease was not critical in this instance since wall heater power was always required in the MDA.

j. Temperature Control Unit. The temperature control unit was designed to automatically maintain the OWS gas temperature within $\pm 4^{o}F$ of the temperature selected by the astronauts. The logic of the unit is shown in figure 4-59. The unit was activated after the OWS SAS was deployed during SL-2. The unit maintained four OWS heat exchangers on for the remainder of the SL-2 which was in accordance with the system logic.

During SL-3 the temperature control unit maintained the thermal control system in the full cooling mode (4 heat exchangers) until DOY 251. At this time the plenum gas temperature (average of C7144 and C7256) was $69.2^{o}F$ and the select temperature was $70.6^{o}F$. The unit turned off the heat exchanger fans when the temperature difference between the gas and selected value was $1.4^{o}F$. The design value was $2.^{o}F$. Subsequently, the control unit turned on the heat exchanger fans sequentially as the temperature difference between the plenum gas and selected set point increased (figure 4-60). An analysis of the data shown in figure 4-60 indicates that the unit performed its switching functions correctly within $0.6^{o}F$ of the design temperature difference.

During SL-4 the temperature control unit maintained the thermal control system in the full cooling mode until DOY 332. At that time, the crew changed the select temperature such that it was $2.3^{o}F$ hotter than the plenum gas (73.3 versus $71^{o}F$) and all heat exchangers were turned off by the control unit. On DOY 340 the crew selected a temperature of $71.1^{o}F$ when the plenum gas was $75.0^{o}F$ which caused all four heat exchanger fans to come on. During the remainder of the mission,

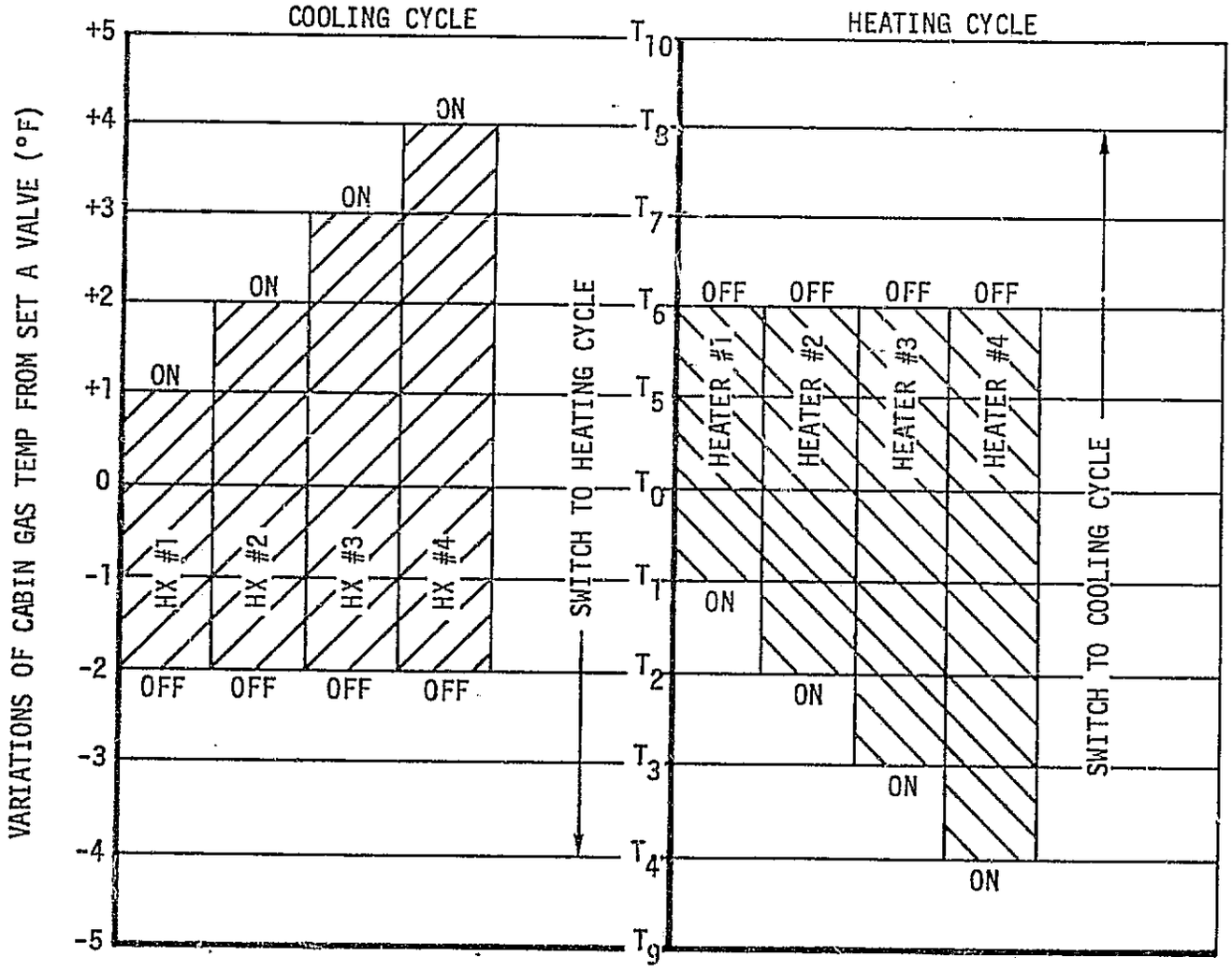

Figure 4-59. OWS Temperature Control System Logic

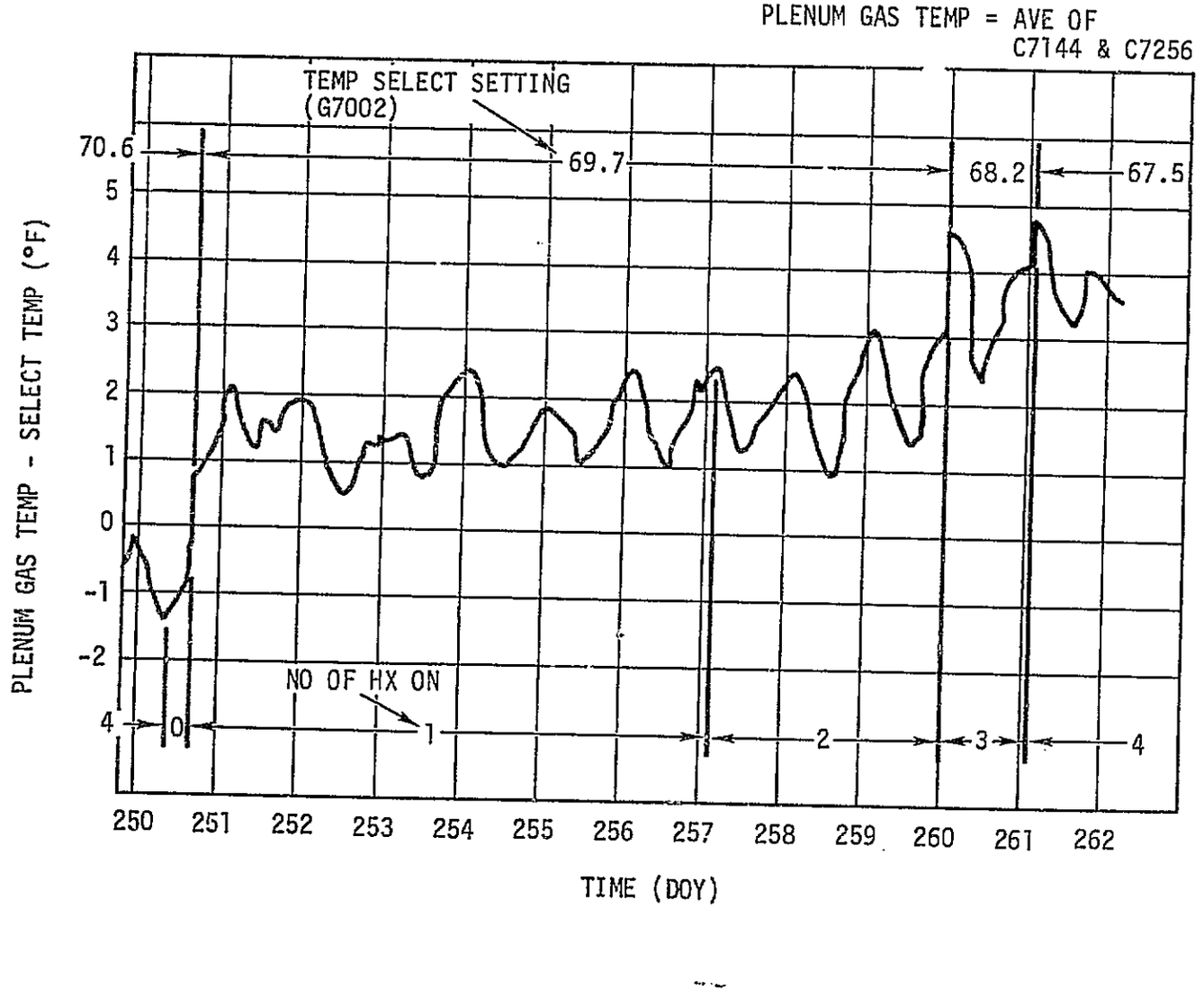

Figure 4-60. SL-3 TCS Control Unit Operational History

the control unit did not experience conditions requiring it to cycle the heat exchangers. The unit was deactivated on DOY 016 to aid in reducing the OWS internal heat dissipation.

k. Molecular Sieve Exhaust Duct Heaters. Heaters were provided to prevent freezing of water vapor during molecular sieve operation. Primary and secondary heaters (62.4w each @ 28v) were mounted on seven separate duct sections. Primary and secondary heater thermostats were set to close at 50°F and 42°F respectively. The closing design tolerance was ±5°F about the nominal. The opening range was 0.5°F to 8°F above the closing setting.

10. Passive Systems

a. Structural Heat Leaks

(1) OWS. The OWS structural heat leak for the twin pole/parasol shield configuration is shown in figure 4-61. The figure indicates that for a given temperature, the structural heat leak was greatest for Beta between -40 and -60°. The minimum heat leak occurred at Beta of ±73.5°. The heat leak was inversely proportional to the absorbed heat flux which was a function of the Beta angle.

The preflight heat leak predictions were based on a thermal model which included the meteroid shield. Since more external heat was absorbed by the goldized kapton tankwall/sunshield configuration, the structural heat leak was significantly less for the vehicle than predicted preflight.

(2) MDA/STS. The MDA/STS structural heat leak is shown in figure 4-62 as a function of internal wall temperature and AM radiator heat load. The data are presented for BETA = 0. However, the variation of heat leak with Beta angle was small for $-60 < \text{Beta} < +60$. The structural heat leak was based on the predicted internal waste heat loads for constrained conditions and the duty cycle of the MDA/STS wall heaters. The structural heat leak was greater than preflight predictions which are shown in figure 4-62 for comparison. Since much of the data necessary to compute the structural heat leak was not directly measurable (such as the CSM structural heat leak, the MDA internal waste heat load, and the wall heater duty cycle) the results in figure 4-62 are only approximate.

b. Insulation Systems

(1) OWS

(a) Common Bulkhead Insulation. The flight heat leak through the common bulkhead, and predictions are presented in Table 4.7. The predictions for the maximum heat leak during habitation were 236 BTU/hour (69.0 watts) greater than the average value from flight data at Beta = 0°, and 175 BTU/hour (51.4 watts) greater than

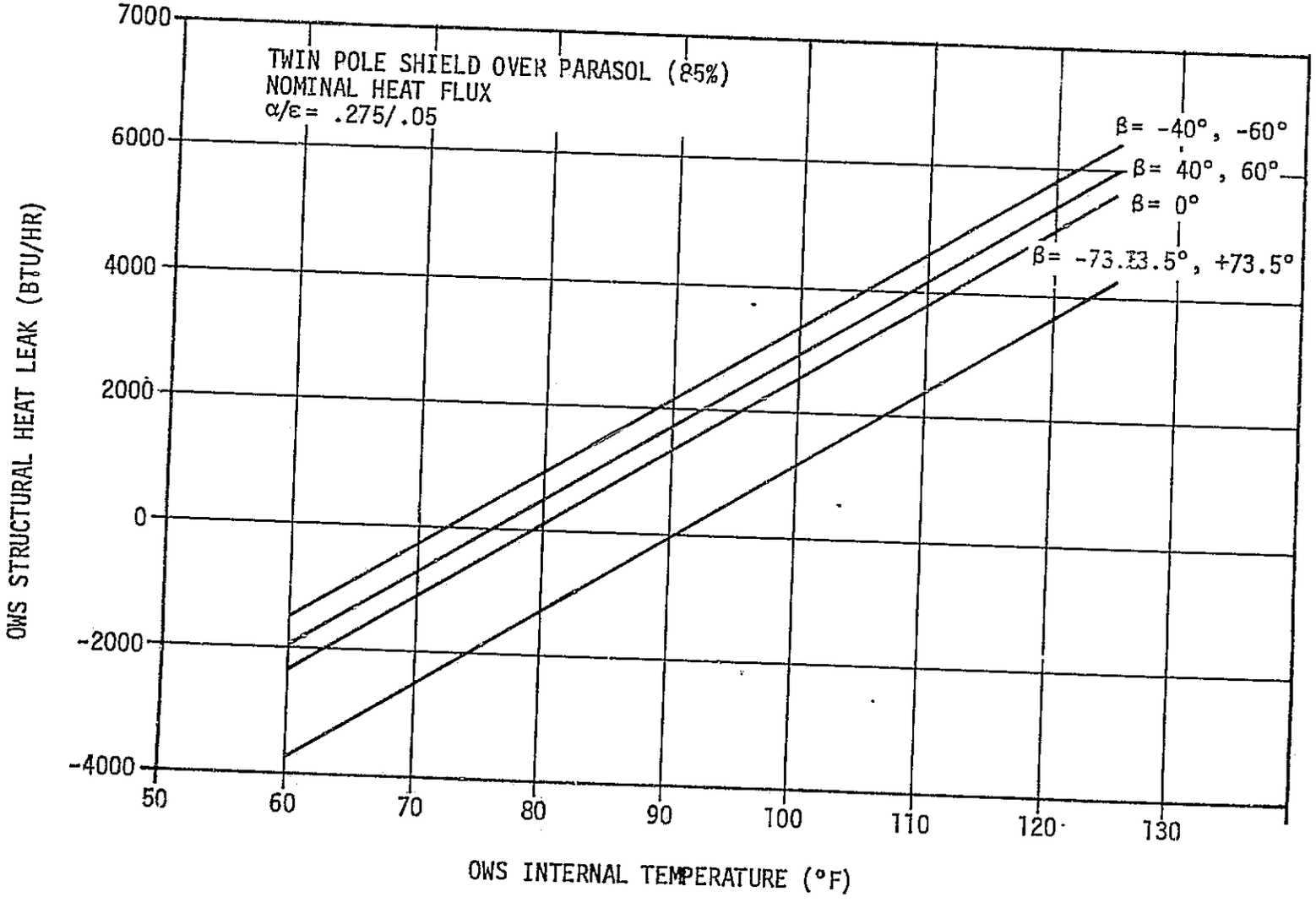

Figure 4-61. OWS Structural Heat Leak

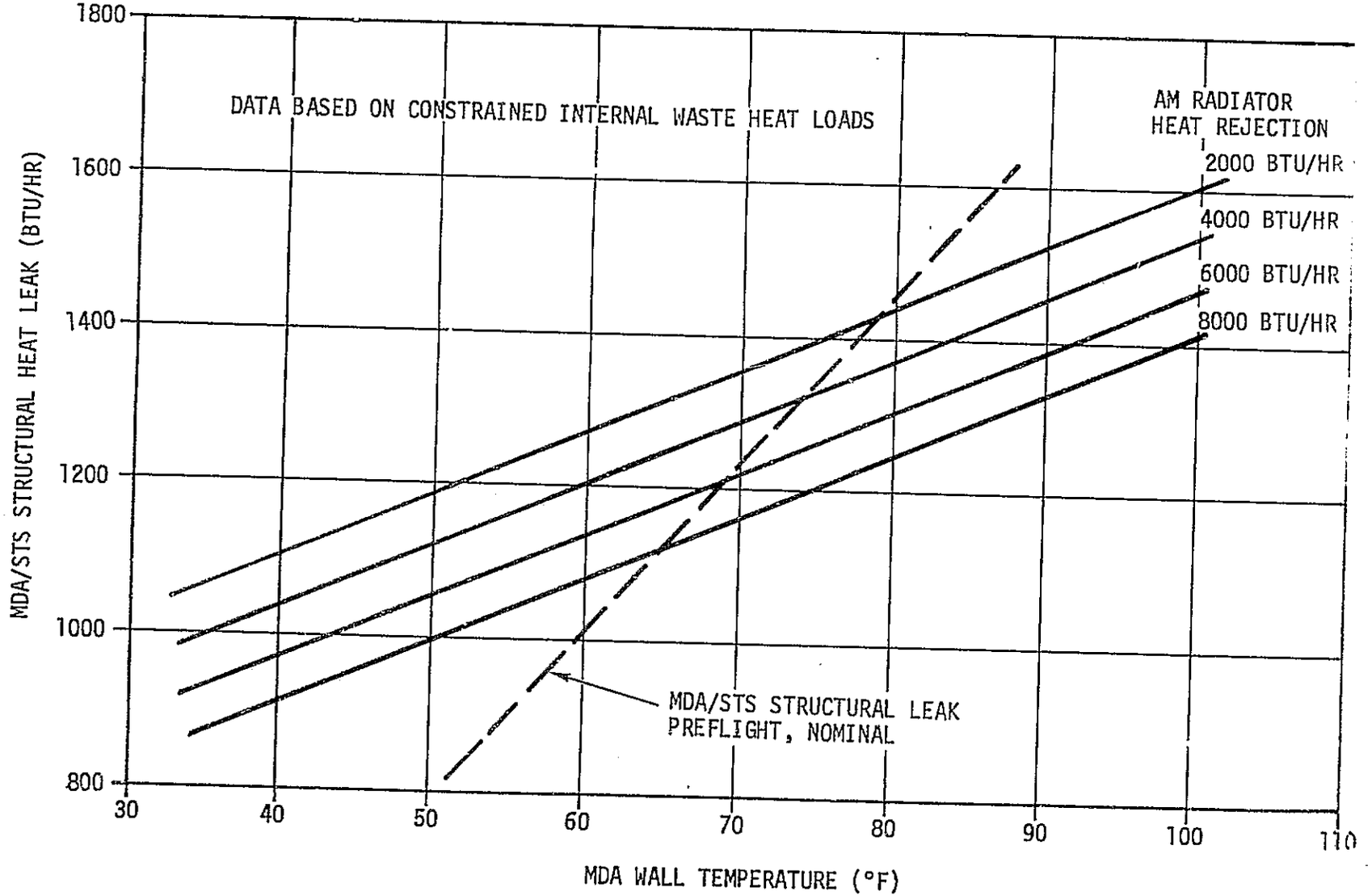

Figure 4-62. MDA/STS Structural Heat Leak for $\beta = 0°$

TABLE 4.7 COMMON BULKHEAD HEAT LEAK

Time DOY (4)	Beta Angle, deg	Source of Data	Average Temperatures Plenum Air(1) °F	Insulation OWS Face (2) °F	Average Insulation Temperature Difference (2) °F	Heat Leak (3) Btu/hour	Watts
217	0	Flight	76	75	14.5	524	154
235	62	Flight	72	72	12.0	432	126
265	-49	Flight	71	71	13.7	490	144
280 (5)	0	Flight	55	54	6.0	209	62
307 (5)	0	Flight	60	57.5	6.5	228	67
364	0	Flight	72	72	11.0	396	116
016	-71	Flight	79	78.5	8.0	292	85
*	0	Analysis	69	65	20.0	696	204
*	-73	Analysis	84	81.5	12.9	467	137

NOTES: * Analytical prediction for habitation period.
(1) Average plenum air temperature is average from sensors C7144 and C7256 (flight data only).
(2) Insulation temperatures from sensor pairs: C7181-C7179, C7095-C7097, C7182-C7180, C7091-C7092 (flight data only).
(3) Based on an insulation thickness of 3 in. and the following insulation conductivity:
0.016 Btu/hour-ft-°F at 0°F
0.019 Btu/hour-ft-°F at 100°F
(4) MSFC Sun Shade deployed after 1730 GMT on DOY 218.
(5) DOY's 280 and 307 occur during the storage period between SL-3 and SL-4.

the flight data value at near maximum negative values of Beta. The difference between the analytical and flight data heat leak values represented approximately one degree F change in the OWS average internal temperature during habitation.

The cause of the difference between the predicted and flight heat leak data appeared to be waste tank temperatures that were warmer than expected. Although the instrumentation available was not sufficient to completely verify this conclusion, there was a smaller than predicted temperature difference across the insulation. Warmer temperatures in the waste tank could have been the result of either a warmer environment for the aft skirt/thrust structure region or less sublimation of ice than expected in the waste tank.

The smaller bulkheat heat leak during storage was expected and primarily resulted from the duct fans being turned off, reducing the convection heat transfer in the plenum region at the insulation surface to essentially zero. A comparison of the data from the table shows the storage period heat leak rates on DOYs 280 and 307 to be roughly one half of the corresponding habitation period heat leak values for DOYs 217 and 364. The significance of convection heat tranfer to the common bulkhead during habitation was also shown by the difference in the average air-side insulation surface temperature between the habitation and storage periods. During the habitation period, the air-side surface of the insulation followed the plenum air temperature closely for the temperature range encountered (71 to 79°F). During storage, the plenum air temperature measurements reflected the mean radiant temperature of the floor and plenum area which was 15 to 20°F colder than during habitation.

(b) Multilayer Insulation. Conductance values for the 48-layer sections of the forward dome multilayer insulation (MLI) were determined from flight temperature measurements of the MLI exterior surface, the wall structure separating the MLI and internal foam insulation, and the interior surface of the foam insulation. There was one set each of temperature sensors on Position Planes I and III (PP I and PP III) identified as follows:

Location	MLI Exterior	Forward Dome	Foam Interior
PP I	C7100	C7162	C7106
PP III	C7101	C7163	C7107

The applied value of the foam conductance, 0.48 BTU/hour-ft^2-°F, was based upon a conductivity of 0.02 BTU/hour-ft-°F and a thickness of 0.5 inch. The heat flux, the product of the

foam conductance and surface temperature difference across the foam (Delta T_f*), divided by the temperature difference between the MLI surfaces (Delta T_m**) yielded the MLI conductance. The comparatively low conductance of the MLI resulted in small Delta T_f's (approximately 1 to 2^oF), the accuracy of which largely determined the accuracy of the conductance evaluations. The accuracy of Delta T_f and Delta T_m was limited by instrumentation-telemetry sensitivity (one data bit represented about 0.48^oF for the foam surface, wall and interior, temperatures and nearly 1.6^oF for the exterior temperature) and by use of different multiplexers for the foam temperature measurements on PP I. With the low heat fluxes of 2 BTU/hour-ft^2 or less, the wall thermal capacity was sufficient to require that the temperature data used for MLI evaluation be taken when essentially steady state heat transfer conditions prevail. Such conditions were found at extreme values of Beta angle ($\pm$65 degrees or more) when, in the solar inertial attitude, the external thermal environment changes were small over a period of several days. Because of the relatively large change in temperature represented by one data bit, a large number of readings was required in order to determine the critical foam temperature difference with some degree of accuracy. A further limitation was the availability of suitable data resulting from the intermittent operation of Low Level Multiplexer B through which data from sensors C7101 and C7162 were transmitted.

Suitable data were obtained for nearly all of DOY 176 at the beginning of the first storage period and for several periods totalling about 72 hours from DOY 325 through 330 during SL-4. The average conductance values from these data were as follows:

Location	DOY	Average Conductance BTU/hour-ft^2-F	Average Temperature Difference T_f ^oF	Average Temperature Difference T_m ^oF
PP I	176	0.010	1.45	69.6
PP I	325-330	0.0061	0.88	69.1
PP III	176	0.0064	1.73	130
PP III	325-330	0.0077	1.75	109

* T_f = Forward Dome Temperature - Foam Interior Temperature

** T_m = MLI Exterior Temperature - Forward Dome Temperature

The conductances at PP I and PP III differed significantly, because conduction which was sensitive to local compression, nearby joints, button fasteners, and penetrations comprised over 90 percent of the MLI heat transfer. The design requirement called for a conductance of not more than 0.02 BTU/hour-ft^2-^{o}F or nearly twice the largest value above. Combining worst case values for errors in foam conductance and measured Delta T's, the MLI conductance was still less than the design maximum value.

(2) MDA Multilayer Insulation. The MDA multilayer insulation was not thermally instrumented for subsystem performance evaluation. However, the MDA internal wall temperature data indicated that the insulation limited the structural heat loss to levels which enabled thermal management with the available heater power.

(3) AM Thermal Insulation. The AM passive insulation systems were also not instrumented for subsystem performance evaluation. As in the case of the MDA, the AM thermal curtain and other insulation systems limited the heat leak such that internal wall temperatures were maintained within desired limits.

c. OWS Heat Pipes. The purpose of the OWS heat pipes was to provide energy to certain areas of the OWS tankwall to maintain them above the predicted 55^{o}F maximum dewpoint temperature. However, those areas did not approach 55^{o}F due to the meteoroid shield anomaly, and the heat pipes were not required.

There was no temperature instrumentation for heat pipe performance evaluation. However, there was a plan to estimate heat pipe performance based on wall temperature and portable sensor measurements on the heat pipes. Since the loss of the meteoroid shield significantly altered the anticipated temperature distributions, it was not possible to use these techniques due to localized uncertainties in the external environment. An evaluation procedure was proposed during the flight which involved the crew removing one heat pipe and applying known temperature gradients to evaluate its performance in "0" g. This proposed procedure was rejected due to the crew time that was required.

d. Thermal Coatings

(1) OWS

(a) S-13G Paint

1 Installation. The aft three feet of the OWS aft skirt (figure 4-63), was painted with the S-13G paint to provide passive thermal control of electrical and attitude control equipment contained in this nonpressurized region of the OWS. In selected areas of the white aft skirt, black Cat-a-lac epoxy enamel paint stripes (α/ε= 1.0) were used for further thermal control.

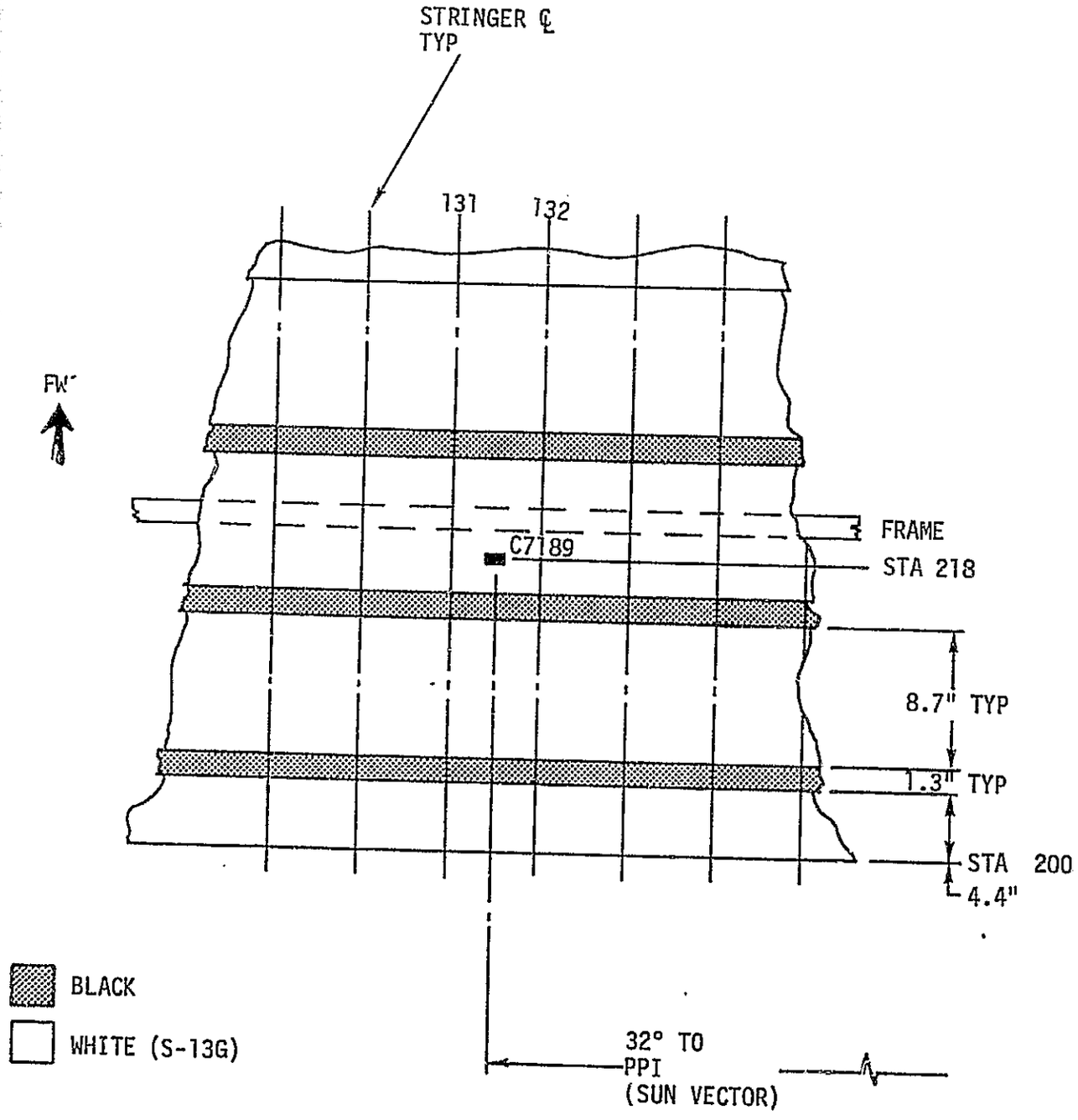

Figure 4-63. OWS Aft Skirt Transducer C7189 Location

The optical property measurement of the S-13G after application were 0.2 and 0.9 for α and ε respectively. The optical properties of the Cat-a-lac black paint were not measured at installation.

2 Prelaunch Measurements. Optical property measurements of the black and white surfaces were made prelaunch to assure proper thermal control of the associated electronic components during orbit. The following table summarizes optical property specifications and measured values.

Description	Parameter	Specification Value	KSC Measurement
S-13G White Paint	Emittance	0.85 min	0.92
	Solar Absorptance	0.22 max	0.21 to 0.25
Cat-a-lac Black Paint	Emittance	0.85 min	0.91
	Solar Absorptance	0.85 min	0.93

The range of solar absorptance values were higher than the allowable specification for the S-13G white paint. However, these conditions were determined to be acceptable since the emittance of the white paint was 0.92 which maintained approximately the same α/ε ratio, resulting in no significant change in the desired thermal control range.

3 Orbital Insertion Data. Orbital temperature data from a temperature measurement on the aft skirt located 32° from the normal solar vector was utilized to evaluate the ultraviolet and proton degradation effects on the white paint solar absorptance. A thermal model simulating the aft skirt structure in the vicinity of the transducer was set up to assess the effects of paint degradation.

The retrorocket firing to effect stage separation resulted in plume contamination of the S-13G paint on the aft skirt. The contamination, consisting of particle deposition, was visibly evident on photographs taken of the white painted surface during fly-around maneuvers prior to the docking of the first Skylab crew. The contrast between the white painted surfaces under the SAS Beam Fairing Number 1 that was protected during retrofire, and the skirt surfaces around it was clearly visible. The plume contamination primarily affected the α while the ε, being initially high, was not substantially increased.

Plume contamination effects on the white paint caused degradation that was dependent upon the plume flow impingement angle and the separation distance during staging. Assuming the aft skirt surface could be approximated locally by a flat plate surface

parallel to the plume flow, the Arnold Engineering Development Center test data of Reference 4-1 and figure 4-64 was used to predict the severity of the degradation. On this basis, the plume degradation effect on transducer (C7189) located at Station 218 resulted in an increase of α from the initial range of 0.21 to 0.25 to a value of $\alpha = 0.34$.

Orbital flight data taken within four hours after orbital inseration showed further α degradation to a value of 0.37. This condition was consistent with test data of Reference 4-2 which showed a high proportion of the UV and proton damage to S-13G white paint occurred within five hours of exposure to simulated solar sources.

4 Post Orbit Insertion Data. Orbital temperatures for surfaces viewing the Sun followed a cyclic temperature profile. As shown in figure 4-65, the aft skirt thermal model closely simulated the flight data for DOY 250, (Beta = 0^{o}). Peak cyclic temperatures for Beta = 0^{o} conditions starting at DOY 157, through DOY 343, were plotted (figure 4-66) to determine the optical property degradation and seasonal solar intensity fluctuation effects. The flight temperatures were compared with calculated temperatures for white paint with α = 0.38, 0.40, and 0.42, generated for the following seasonal variations:

	$\dot{q}_{solar}$ BTU/hour-ft^2	$\dot{q}_{IR}$ BTU/hour-ft^2
Summer Solstice	415	72.6
Autumnal Equinox	429	75.1
Winter Solstice	444	77.7

For a constant value of α the analytical seasonal temperature variation is seen in figure 4-66 to be substantially less than that of the flight data. The data clearly showed a solar absorptance degradation during this time period. Starting at summer solstice the analytical data indicate:

	α_s
Summer Solstice	0.39
Autumnal Equinox	0.41
Winter Solstice	0.42

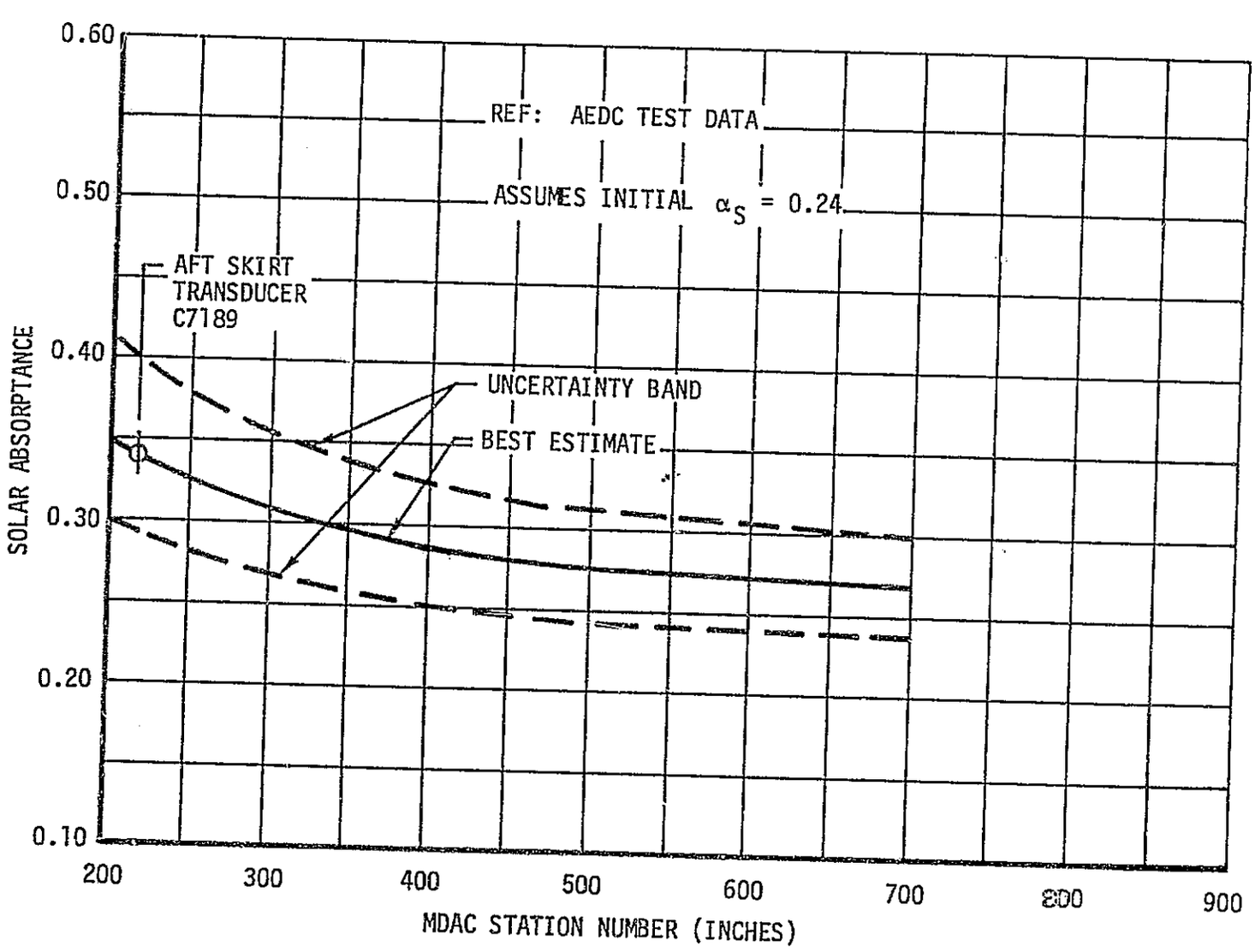

Figure 4-64. Estimated Retrorocket Plume Contamination

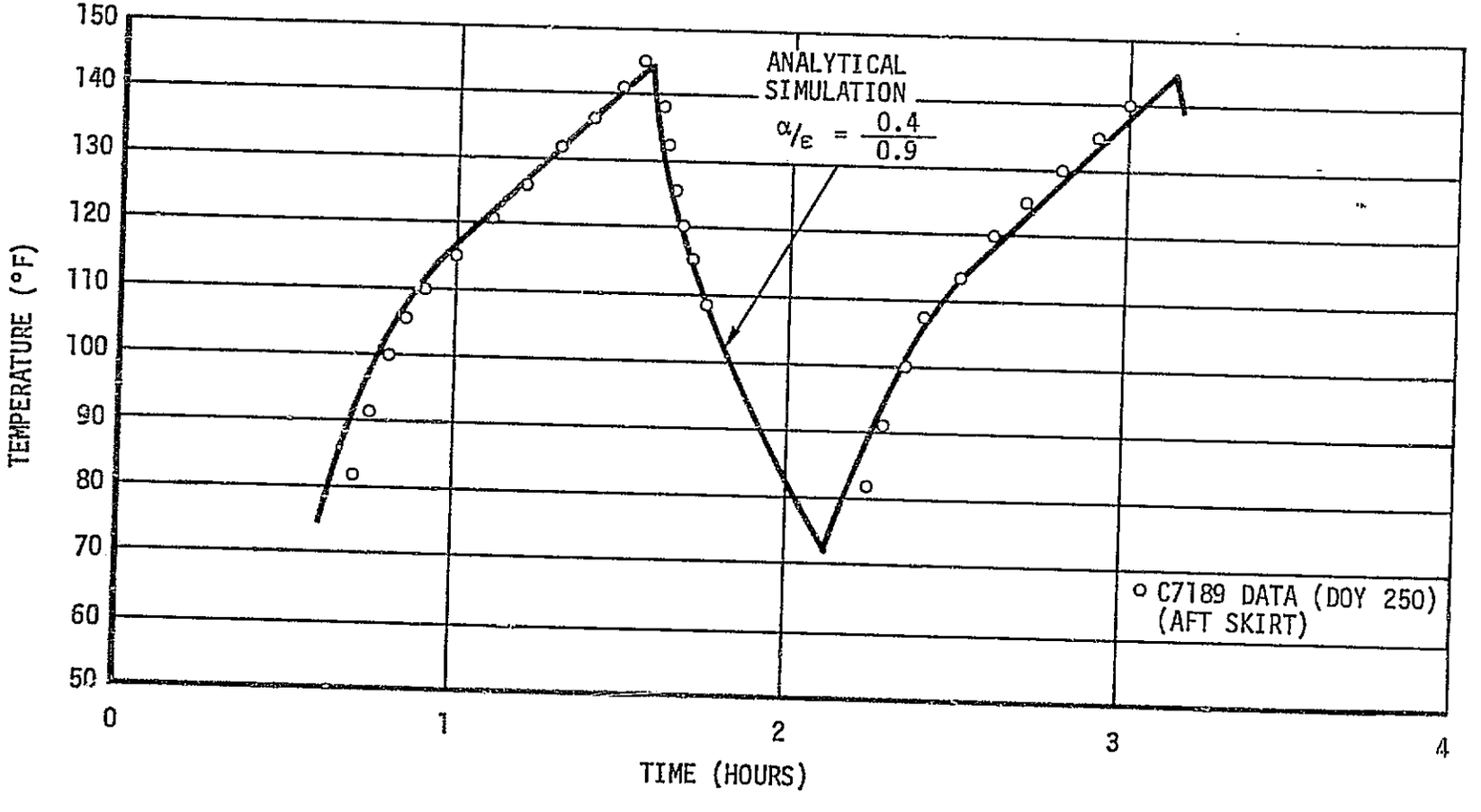

Figure 4-65. OWS Orbital Simulation of Transducer C7189, β = 0°

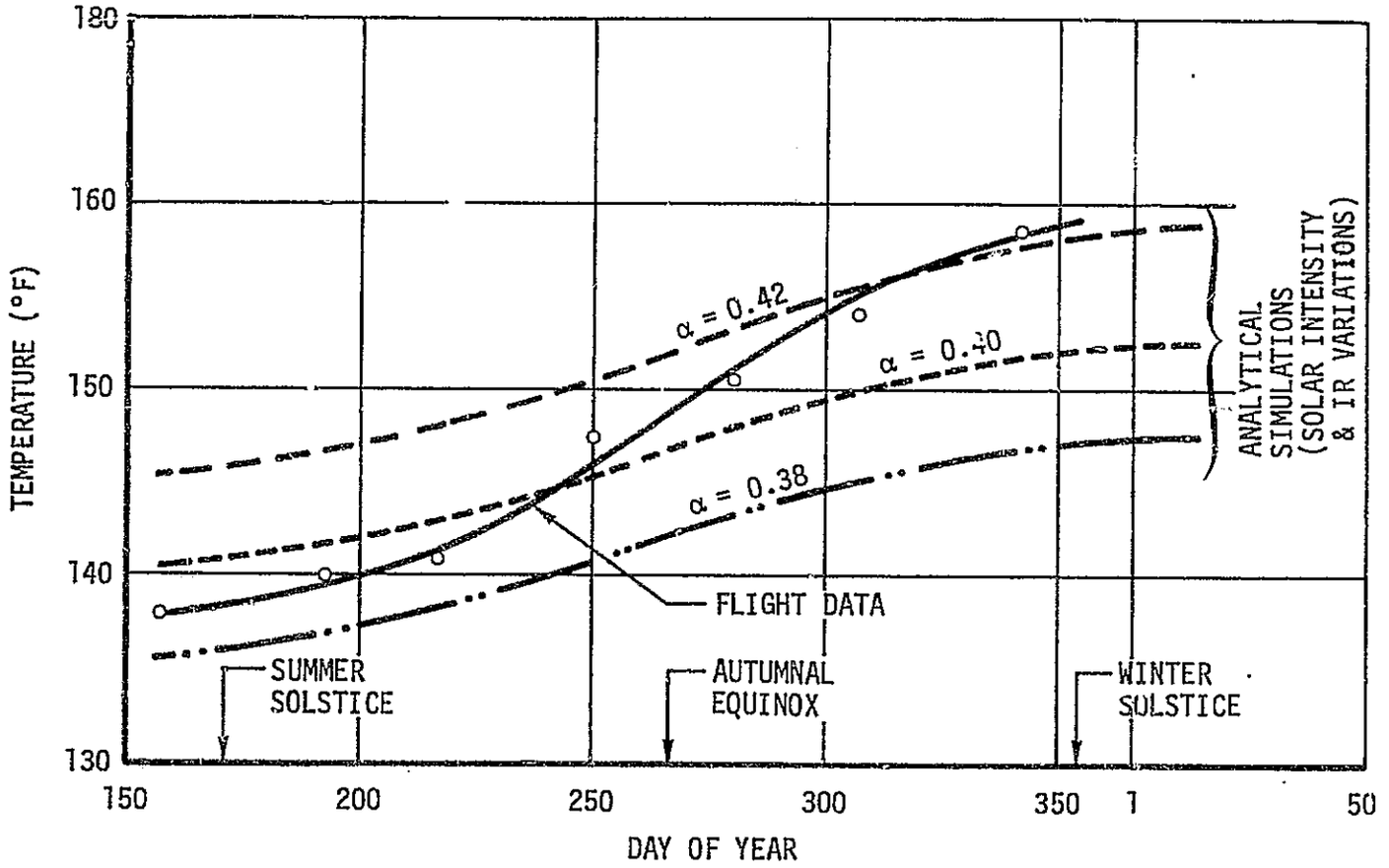

Figure 4-66. OWS Peak Orbital Temperatures of Aft Skirt Transducer C7189 Seasonal Fluctuations

Considering an initial orbital white paint absorptance value of 0.34 and reflecting the retrorocket plume contamination, the degradation effect (α/α') normalized to orbital insertion is shown in figure 4-67 in terms of solar exposure time. Compared with design test data, the flight data were seen to compare well to the test data of Reference 4-3 but were lower than the degradation rate given in Reference 4-2. It should be noted, however, that the design test data were for an S-13G surface while the flight data were for a plume contaminated S-13G surface.

(b) Z-93 Paint

1 Installation. Z-93 white paint was applied to the anti-solar side of the OWS solar array panels to reduce albedo absorption. The Z-93 was stable and had the low α (0.2) and high ε (0.9) required to keep the solar array relatively cool to maximize its electrical power generation capability. Five mils of Z-93 paint were applied to the solar panel, which consisted of two 2024-T81 aluminum face sheets on a 0.375 inch 5052-0 aluminum hex cell.

The optical properties of the Z-93 paint were monitored by a coupon, painted at the same time as the solar array panel, and packaged in the same environment. The average properties of the newly painted Z-93 surfaces were 0.18 and 0.90 for α and ε respectively.

2 Prelaunch Measurements. The Z-93 paint coupon was measured at KSC prior to the installation of the solar array on the OWS. The KSC measurement average values of 0.19 and 0.90 for α and ε respectively, indicated no significant optical property changes, as expected. The solar array was purged with dry nitrogen following OWS installation. Therefore, it was assumed that no further degradation occurred prior to launch.

3 Orbital Data. The Z-93 paint on SAS Wing 1 was enclosed by the beam/fairing during boost so that it was not exposed to boost contamination or to S-II/S-IV separation retrorocket plume contamination. Solar array temperature sensors C7147 and C7242 were selected for comparison with predicted temperatures at zero degree Beta angle conditions. As shown in figure 4-68, sensor C7242 was located on Wing Section 3 adjacent to the OWS stage and consequently recorded higher temperatures than sensor C7147 located on Wing Section 1, which was not influenced as much by the IR interchange from the stage.

Figure 4-68 presents the calculated maximum transducer temperatures accounting for the seasonal variation of solar constant. The Z-93 paint α and ε values of 0.20 and 0.93, respectively, were used in the analysis. The analysis assumed that the solar array had

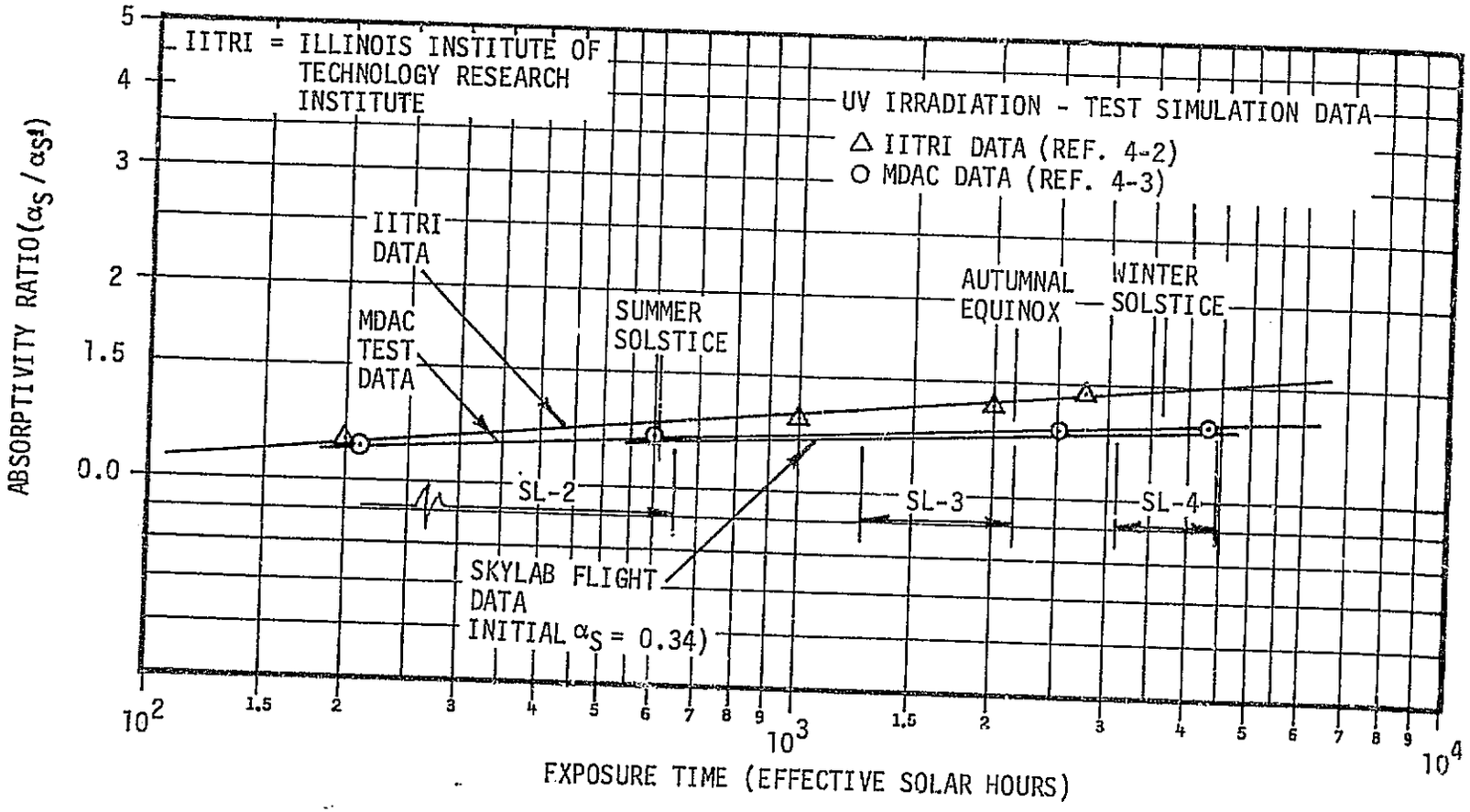

Figure 4-67. S-13G White Paint Degradation

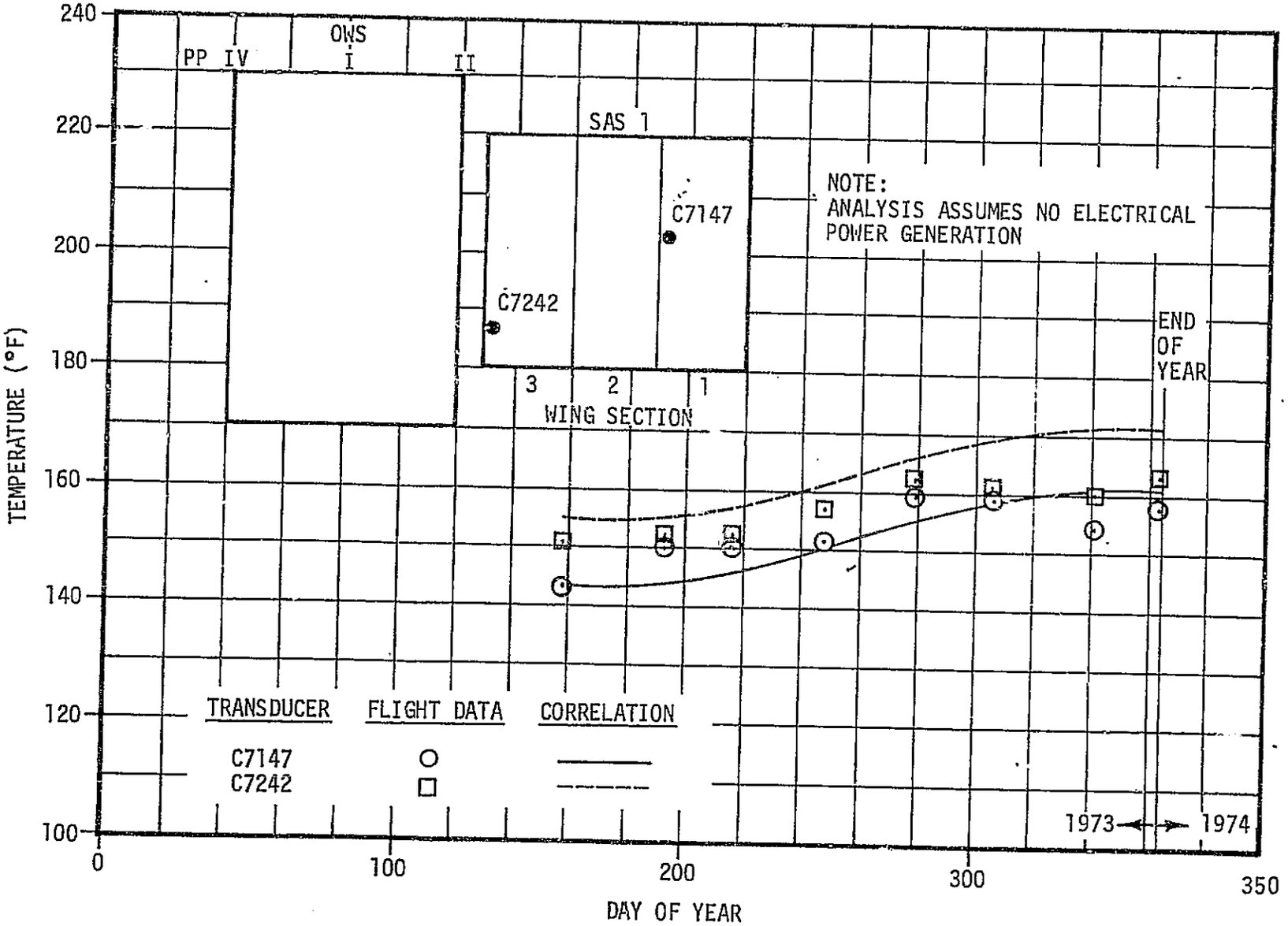

Figure 4-68. Maximum SAS 1 Transducer Temperatures, β = 0°

fully charged the AM batteries during the early part of the orbital daylight and consequently was not generating electrical power at the time of peak temperature (orbital noon). The energy normally converted to electrical power was then dissipated as heat, raising the solar array temperature.

The correlation of flight data and analysis was generally good. It is noted that the measurements were lower than the predicted temperatures during the later part of the mission e.g., DOY 342. This deviation resulted from the fact that on those days, contrary to the general analysis assumption, electrical power was being generated throughout the sunlight portion of the orbit due to increased power demands to perform the EREP maneuvers. The sensitivity of the analysis to α was also investigated. Results indicated that if α had degraded from 0.2 to 0.3 during the mission, the solar array temperatures would have increased about 5°F for a fixed solar constant. There was no progressive increase in solar array temperatures during the mission. It was apparent that no major degradation of Z-93 paint optical properties occurred.

(c) Goldized Kapton Tape

1 Installation Properties

The goldized Kapton tape was installed on the external surface of the habitation area sidewall to provide a low emittance (ϵ) surface. This surface, in combination with the black and white painted meteoroid shield originally covering it, was to have provided the desired heat balance to meet crew comfort and other thermal control requirements within the habitation area. The six-inch wide tape, Mystic 4017, consisting of 680 angstroms of gold on a one mil Kapton film backed with silicone adhesive, was installed in butted circumferential bands on the habitation area sidewalls. The tape was installed by a controlled application procedure which included air bubble removal between the tape and the sidewall surface. The gold surface of the tape was protected by a plastic film until just prior to installation of the meteoroid shield in October 1973.

Extensive measurements were made of the gold tape ϵ after installation on the habitation area sidewall. The average value from 50 measurements was 0.03.

The measurements of the installed goldized Kapton were made at KSC from March 31, 1973 to April 13, 1973. Measurements were made at four general locations and values obtained were 0.022, 0.022, 0.036 and 0.040. An average of the four measurements gave 0.030 which agreed well with data obtained from new material as well as that obtained shortly after installation. No data were taken for solar

absorptance (α) since the Kapton surface was not designed to be exposed to direct solar impingement or albedo. Measurements of α for samples of the goldized Kapton gave a value of approximately 0.15. Therefore, a reasonable estimate of the optical properties at liftoff was $\alpha/\varepsilon = 0.15/0.03$.

2 Orbital Properties Prior to Sunshade Deployment

Following orbital insertion, the main complication in evaluating the gold tape optical properties was that the temperature instrumentation on the sunside of the vehicle went off-scale high because of the higher than expected heat fluxes, resulting in ill-defined boundary temperatures for the OWS heat balance. Two evaluation methods were employed to determine optical properties for the period immediately after insertion on DOY 134. A small scale thermal model was used to analyze the large transient response of the Position Plane I internal and external temperature data before their respective maximum temperature scales of 120°F and 190°F were exceeded.

For the transient analysis of Position Plane I, temperature data taken at MDAC Stations 319, 420, and 460 approximately 75 minutes after liftoff were utilized to estimate the optical property values. The data consisted of the outboard and inboard surface temperature responses of the tank sidewall foam insulation on the Position Plane. During the time period chosen, sunlight was directly incident on the area. The thermal model was used to solve for the tank sidewall temperatures for a given set of external surface optical properties. From this postflight evaluation utilizing a solar flux of 419 BTU/hour-ft^2 and an albedo of 0.3, it was found that at MDAC Station 420 and α and ε of 0.175 and 0.035, respectively, best matched the flight data as shown in figure 4-69. Similar analyses of the temperature data at MDAC Station 460 and 319 gave α/ε values of 0.165/0.03 and 0.21/0.05, respectively. The optical property variation with the longitudinal station was indicative of a decreasing degradation effect from retrorocket plume contamination with increasing distance from the plume source. The results of the transient response analyses of Position Plane I as well as the overall heat balance analyses using the OWS thermal model were indicative of a degradation in the gold tape α and ε. Surface degradation of the tape is verified by photographs which indicated contamination from the retrorockets fired during separation of the OWS from the Saturn S-II stage, scratches from the meteoroid shield and bubbling on the Position Plane I side of the vehicle, probably resulting from the high temperature occurring before deployment of the sunshade.

3 Orbital Properties After Sunshade Deployment

The evaluation of the gold tape properties following sunshade deployment was difficult in that there were many parameters strongly influencing the habitation area heat balance which could not be individually assessed in any given period. The changes during the mission in orbital sunlight fraction, angle between the orbit plane and the solar vector (Beta), habitation area waste heat loads and cooling, shading from partial deployment of the two different sunshade configurations, deployment of SAS Wing 1, and variations in the solar and albedo flux led to a very complex set of conditions to analyze.

Based on temperature data taken on DOY 244 during an Earth Resources maneuver which resulted in large temperature transients in the Position Plane IV area, the gold tape α and ϵ at MDAC Station 389 were calculated to be 0.27 and 0.05, respectively, (see figure 4-69). For this analysis a solar flux of 426 BTU/hour-ft^2 was used. A similar analysis of temperature data taken during a maneuver to photograph a barium cloud on DOY 331, was indicative of the same calculated optical properties.

An analysis of temperature data taken at MDAC Stations 319 and 389 in the Position Plane II area during two consecutive Earth Resources passes on DOY 258, indicated gold tape optical properties at Station 319 of 0.35 and 0.10 for α and ϵ, respectively, and 0.30 and 0.06 for Station 389 as indicated by the correlation in figure 4-70. A solar flux of 428 BTU/hour-ft^2 was used in the analysis.

In late December 1973, and in January 1974, a series of Kohoutek comet viewing maneuvers and Earth Resources maneuvers were performed. These maneuvers again exposed the Position II area to direct sunlight, resulting in large temperature transients because of the high Beta angles and associated large orbital sunlight fractions. The analyses of these temperature transients at MDAC Stations 319 and 389 indicated an α of 0.35 and an ϵ of 0.10 for Station 319 and 0.30 and 0.06 respectively, for Station 389. A solar flux of 441 BTU/hour-ft^2 was assumed. The data correlation for DOY 009 (1974) is shown in figure 4-71.

4 Data Summary. The calculated optical properties cannot be considered as exact values because of the potential errors associated with the accuracy of the temperature data and vehicle attitude history during maneuvers. However, the results are valid for determining variations and establishing trends in the optical properties over a period of time. The computed optical properties are also sensitive to the orbital heat flux. The solar flux used was the nominal value

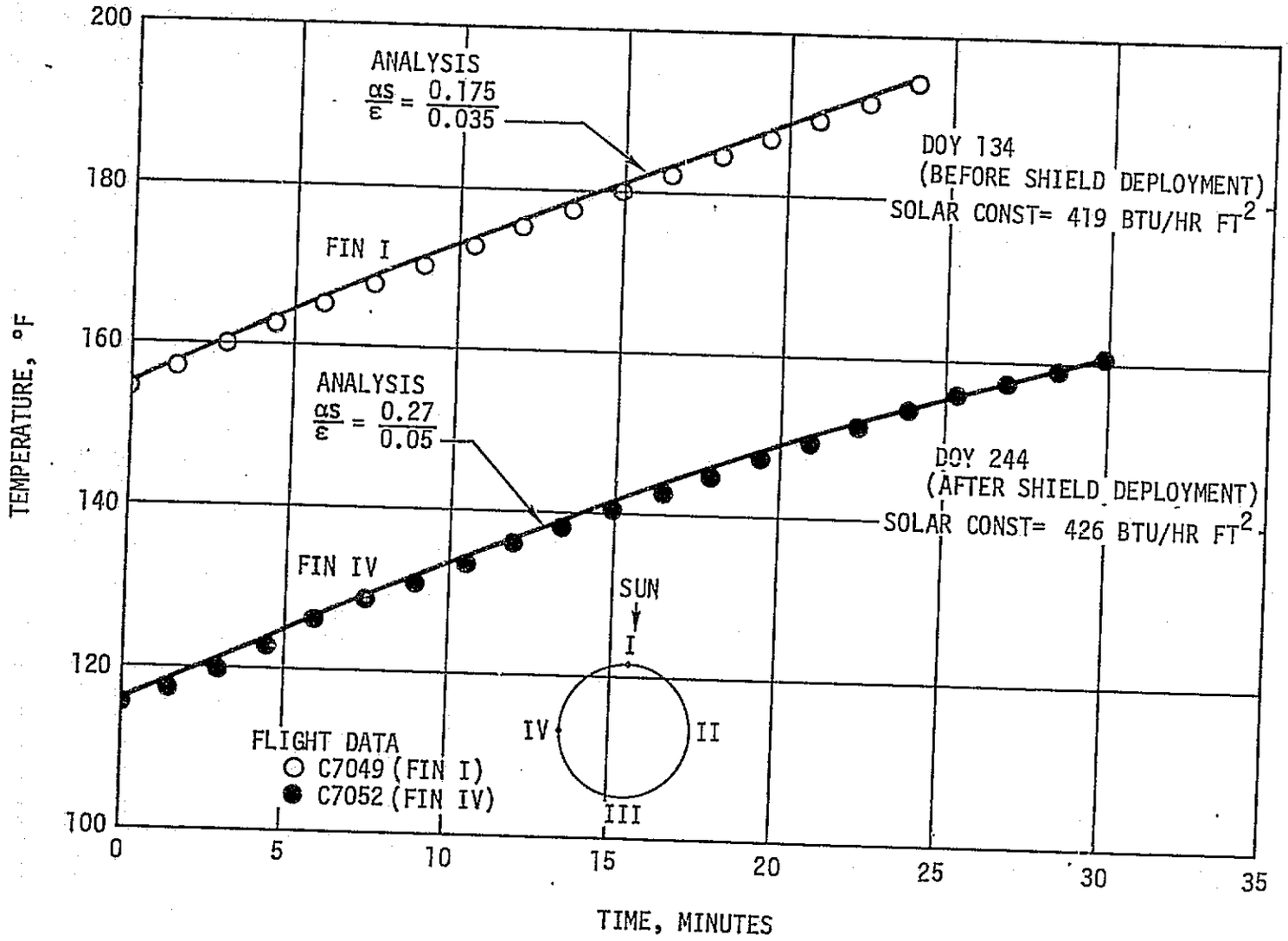

Figure 4-69. Temperature Response of Gold Taped Sidewall to Direct Solar Exposure

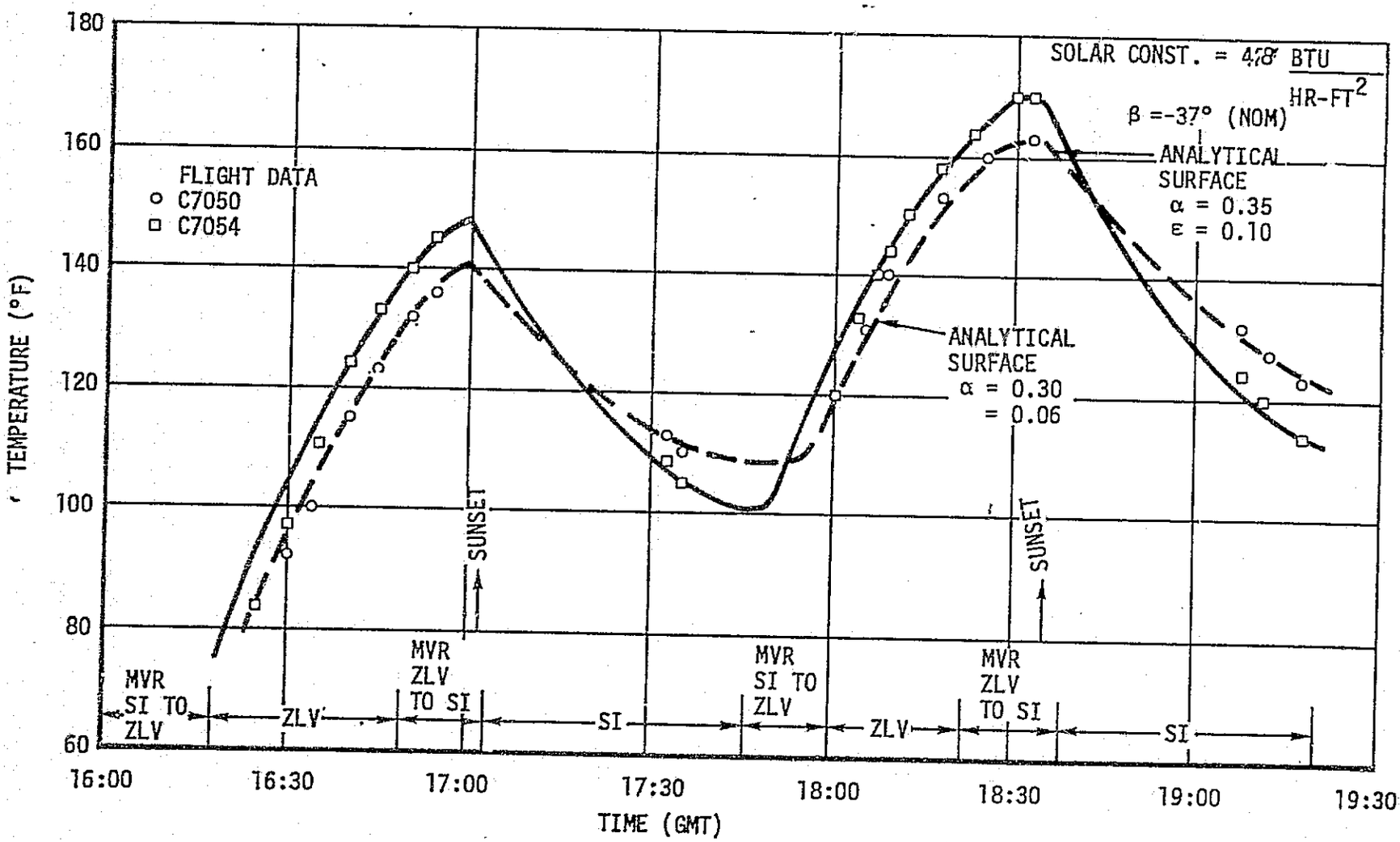

Figure 4-70. OWS External Wall Temperature Simulation for EREPs 31 & 32, DOY 258

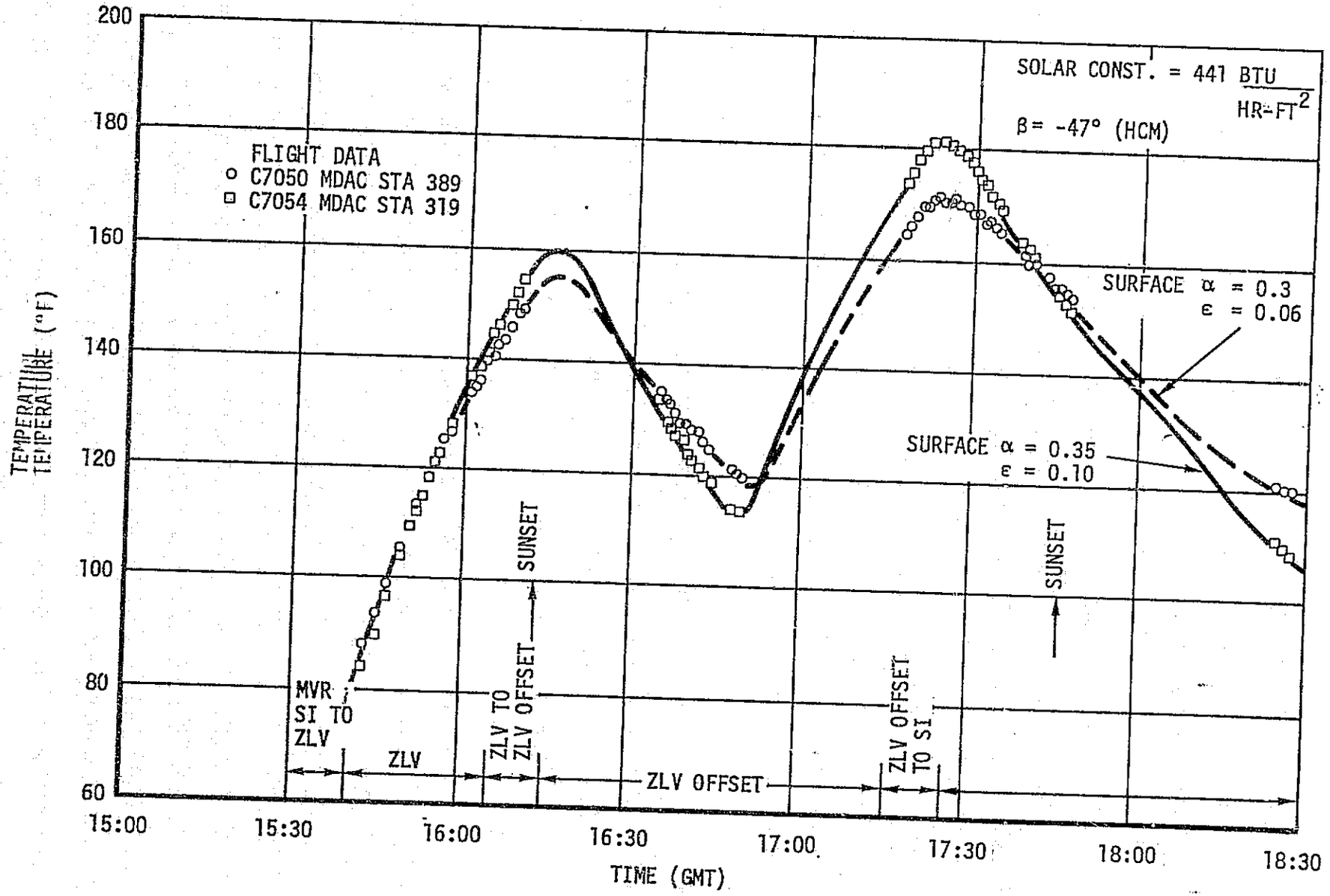

Figure 4-71. OWS External Wall Temperature Simulation for EREP 24, DOY 009

based on the distance from the Earth to the Sun for the particular season of the year being considered. The transient analyses were not sensitive to the values of albedo and Earth IR assumed.

The gold tape optical property data are summarized in figure 4-72 and Table 4.8. The results show the effect of two parameters, retrorocket plume contamination and exposure time to the orbital environment. The results presented for DOY 134 are based on temperature data read from three longitudinal stations on PP I. They show that the degradation effect of the retrorocket plume impingement decreases with increasing distance from the plume. Both α_s and ε are increased by the contamination. The results presented for DOYs 134, 244, 258 and 9 show the effect of orbit time on the optical properties. The trend indicated is an increase in α and ε for the first 100 days and essentially constant values thereafter.

(2) AM/MDA. The Z-93 coating on the AM radiator experienced discoloration as reported in the crew debriefing and in the flyaround photographs. A discussion of the radiator coating is contained in Section VII.

e. Evaluation of the OWS External Thermal Environment. During the SL-2 and SL-3 missions, analyses of the OWS thermal control system were performed to develop a thermal model which could be used to predict OWS temperatures and evaluate OWS thermal performance. Changes to the thermal model were required as follows: removal of the OWS meteoroid shield and removal of the solar arrays, addition of the nondeployed SAS Wing 1 and meteoroid shield beneath it, addition of the parasol solar shield, revision of SAS Wing 1 to the deployed configuration, revision of parasol coverage to 75 percent, and addition of the twin pole solar shield with additional coverage of 85 percent.

Two trends were noticed during SL-3 which could not be explained until later. One trend was that increasing values of Beta (going from negative to positive) seemed to effect an increase in the OWS temperature. Additionally, it was noticed that the OWS temperature was not the same for a given Beta angle later in the mission. During the manned missions variations in the heat flux caused by maneuvers, variations in the internal heat load and ECS cooling, and the thermal lag of the OWS complicated the analysis to determine the cause of the trends. The heat leaks through the common bulkhead and forward dome were investigated and found not to be the cause of the trends. However, analysis did indicate that negative Beta angles were 2 to 4°F cooler than positive Beta angles due to the locations of SAS Wing 1 and the piece of the meteoroid shield near Position II. The SAS Wing and shield provided more blockage of incident albedo on the gold foil for a negative Beta angle than for a positive one. The absorbed heat rate for the gold as a function of Beta is shown in Figure 4-73. Analytical results indicated the difference in OWS temperature to be between 2 and 4°F depending on the absolute

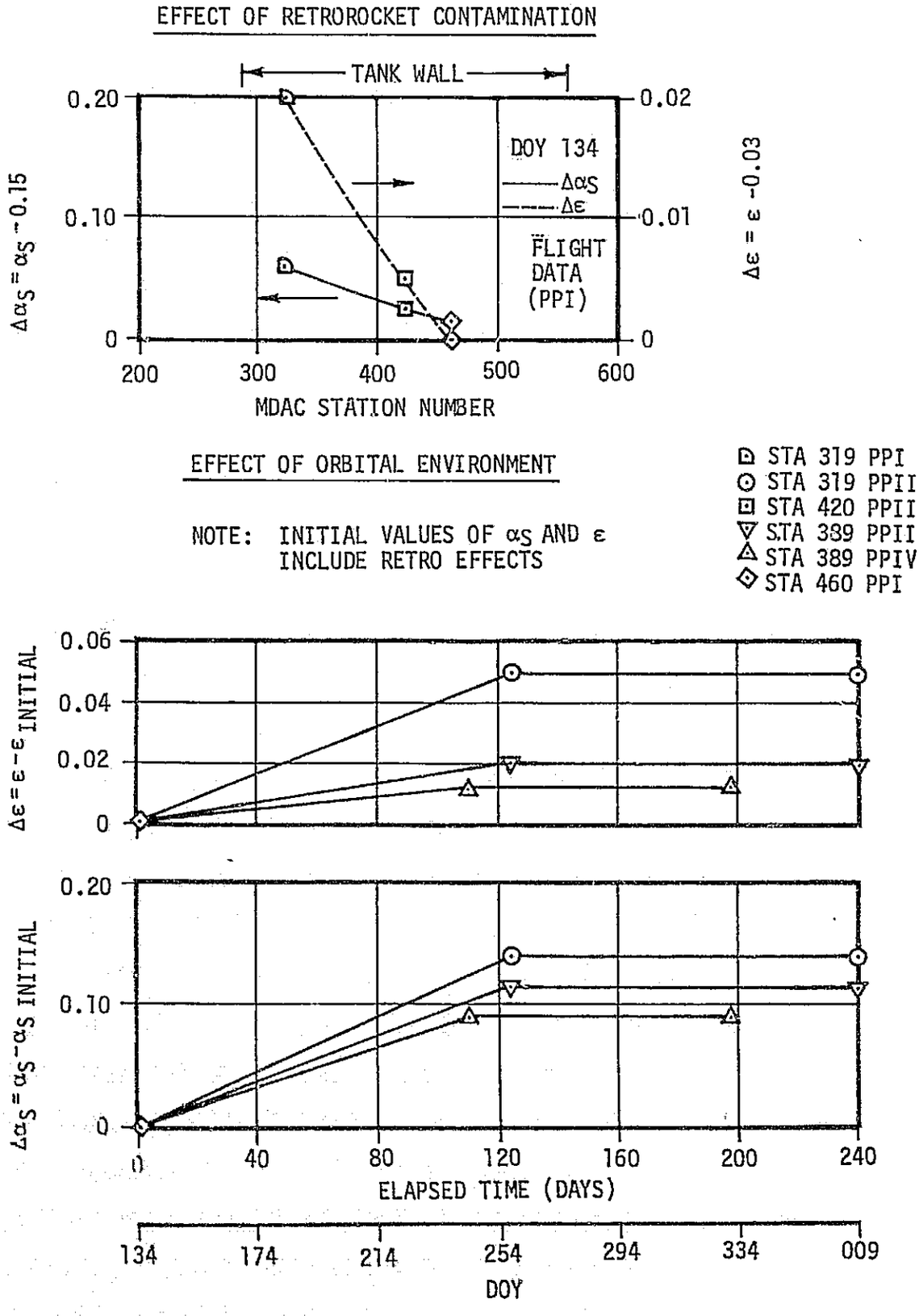

Figure 4-72. Tank Wall Optical Properties

TABLE 4.3 GOLD TAPE OPTICAL PROPERTIES

DOY	Mission Phase	Orbital Solar Flux Btu/hour-ft^2	Orbital Solar Flux (watt/m^2)	Location PP/MDAC Sta. Number	α_s	ε	α_s/ε
134(1973)	Prelaunch	N/A		Average Sidewall	0.15*	0.03**	5.0
134	Orbital Insertion	419	1324	I/460	0.165	0.03	5.5
134	Orbital Insertion	419	1324	I/420	0.175	0.035	5.0
134	Orbital Insertion	419	1324	I/319	0.21	0.05	4.3
134	Orbital Insertion	419	1324	Average Sidewall	0.20	0.04	5.0
225	On-Orbit	424	1340	Average Sidewall	0.21	0.04	5.3
234	On-Orbit	424	1340	Average Sidewall	0.21	0.04	5.3
244	On-Orbit	426	1346	IV/389	0.27	0.05	5.4
258	On-Orbit	428	1352	II/319	0.35	0.10	3.5
258	On-Orbit	428	1352	II/389	0.30	0.06	5.0
331	On-Orbit	439	1387	IV/389	0.27	0.05	5.4
9(1974)	On-Orbit	44?	1394	II/319	0.35	0.10	3.5
9(1974)	On-Orbit	441	1394	II/389	0.30	0.06	5.0

* Based on measured α_s for new material.
**Average value based on measured ε values at 4 sidewall locations.

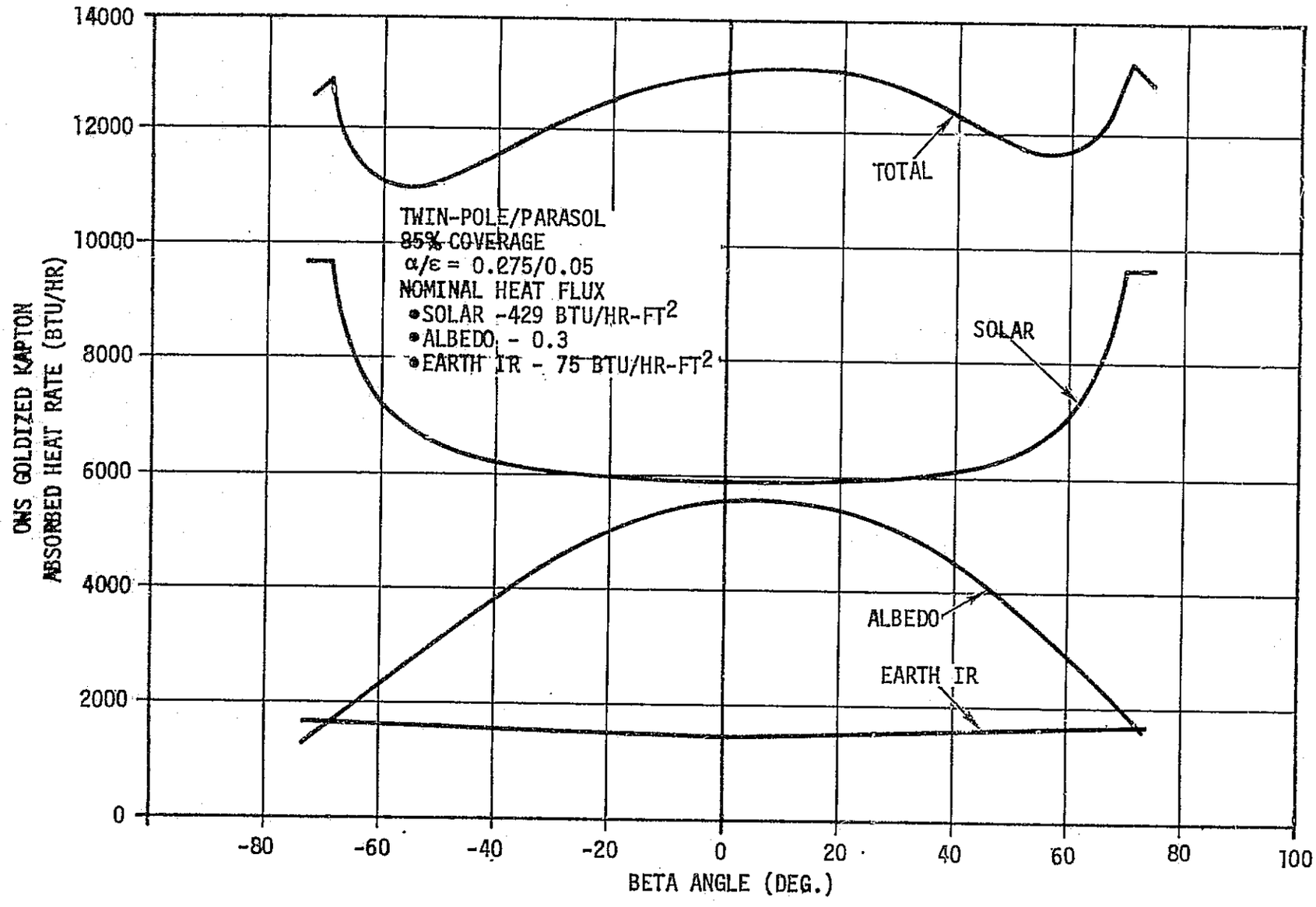

Figure 4-73. OWS Goldized Kapton External Heating

value of Beta. However, no explanation could be made initially for the higher Beta angles being hotter than Beta =0.

During the SL-3 storage period these trends continued as shown in figure 4-74. Since the internal heat loads and vehicle attitude were constant, the cause of the 9°F variation in temperature had to be changes in the external environment. Analytical predictions utilizing the nominal solar constant (429 BTU/hour-ft^2-°F), albedo (0.3), and Earth infrared radiation (75.5 BTU/hour-ft^2-°F) did not yield the trend experienced by the OWS as shown in figure 4-74. Each of these contributors to the orbital heat flux were investigated to determine their relative importance.

The solar constant was known to be increasing about 2 percent during this time period but this fact did not explain the trend of rising temperatures with increasing Beta and decreasing temperature with decreasing Beta. It was determined that a 2 percent change in the solar constant would only change the OWS temperature 1/2°F. The effect of the 1 percent uncertainty in the solar constant would change the OWS internal temperature an additional 1/4°F. Therefore, variations in the solar constant did not explain the trends. A review of the information on the variation in the Earth infrared (IR) heat flux yielded data given in figure 4-75, as a function of the latitude of the orbit and season of the year. The Skylab vehicle was in a 50 degree inclination orbit so its orbit always cycled between 50°N and 50°S latitude. Additionally, the seasonal variation during the entire year was very small (1 percent) when integrated over the region between 50°N and 50°S latitude. The Earth IR variation during the SL-3 storage period should have been less than the yearly variation. Since only approximately five percent of the Earth IR was absorbed by the gold (α = 0.05), and since IR comprized only 13 percent of the total heat flux, the known variation in IR was concluded to have a negligible effect on the OWS internal temperature.

The variation in albedo as a function of latitude and season of the year is given in figure 4-76. Using the Beta angle history and the expected albedo as a function of latitude, a history of the albedo at orbital noon was constructed (figure 4-77). The OWS thermal model was run using the variation in albedo from figure 4-77. Since the major contribution of albedo heating occurs at or near orbital noon, this value was used in the analysis. Additionally, it was not practical to run a transient analysis for such a long time, so steady state solutions were determined for several sets of Beta angles and albedo conditions.

Since the OWS internal temperature lagged the predicted steady state value for any particular day, only at those times when the OWS temperature versus time curve had a zero slope was the OWS internal

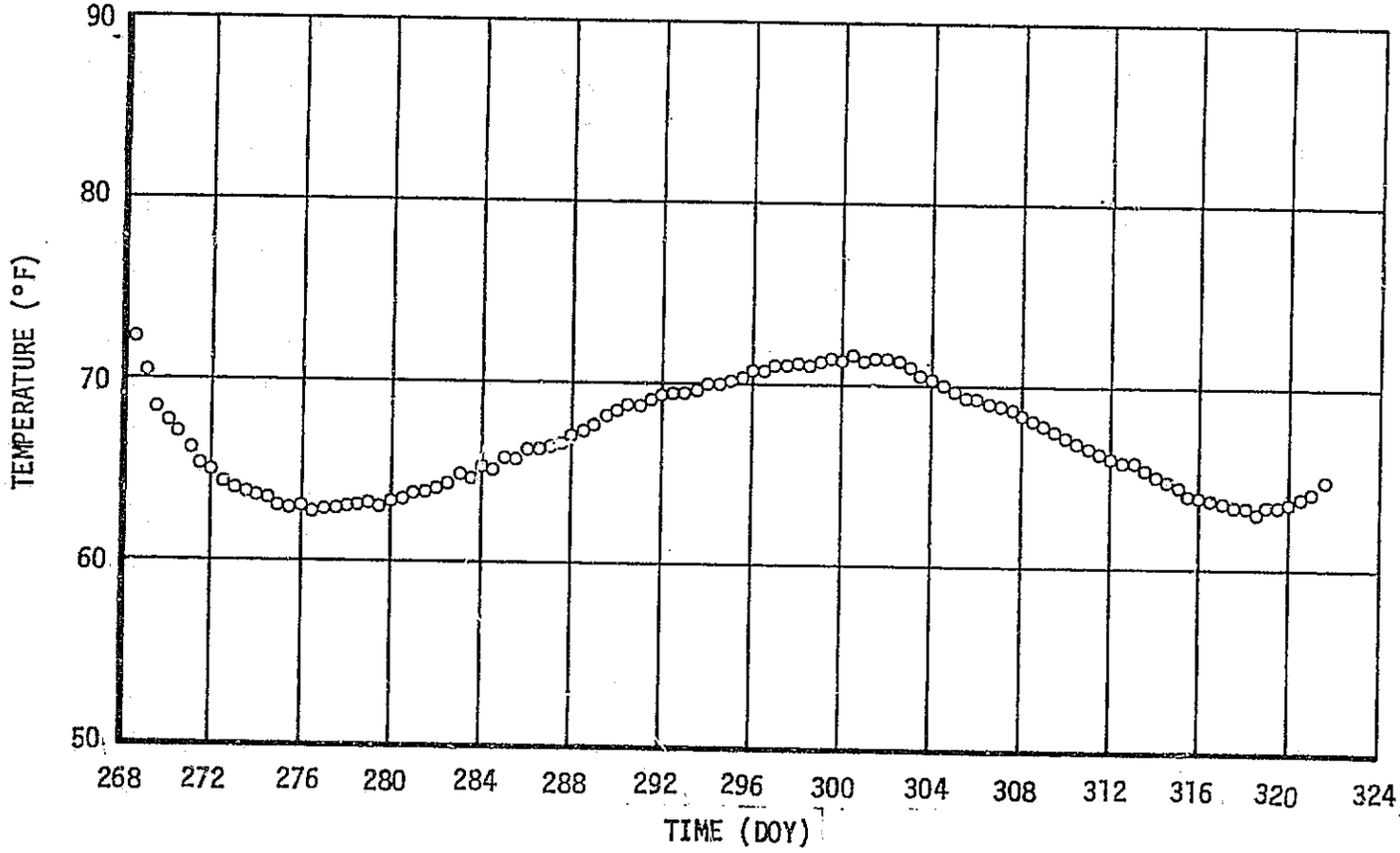

Figure 4-74. OWS Average Internal Temperature During SL-3/SL-4 Storage

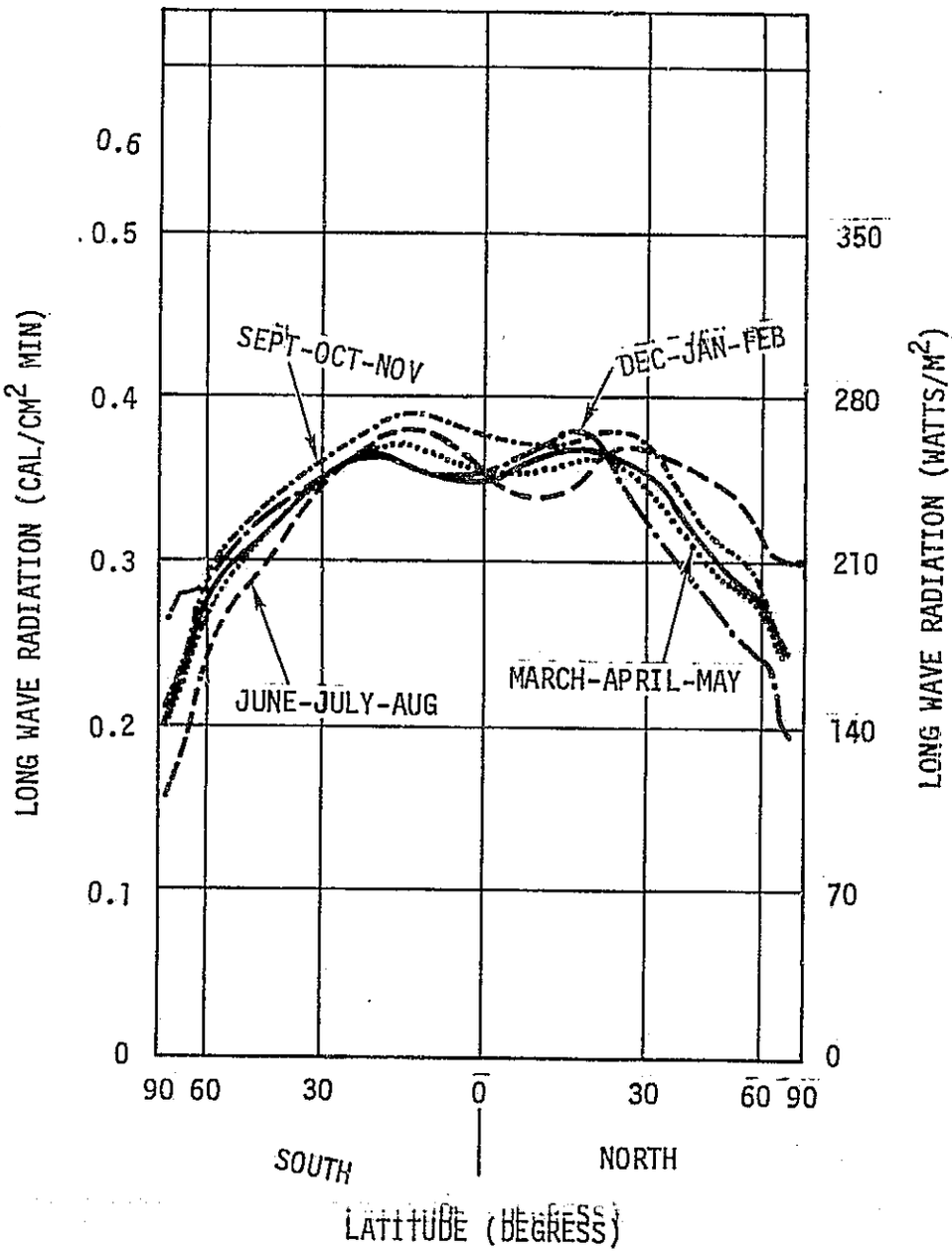

Figure 4-75. Long Wave Radiation for the Seasons and the Annual Case (Solid Line) (Ref. 4-4)

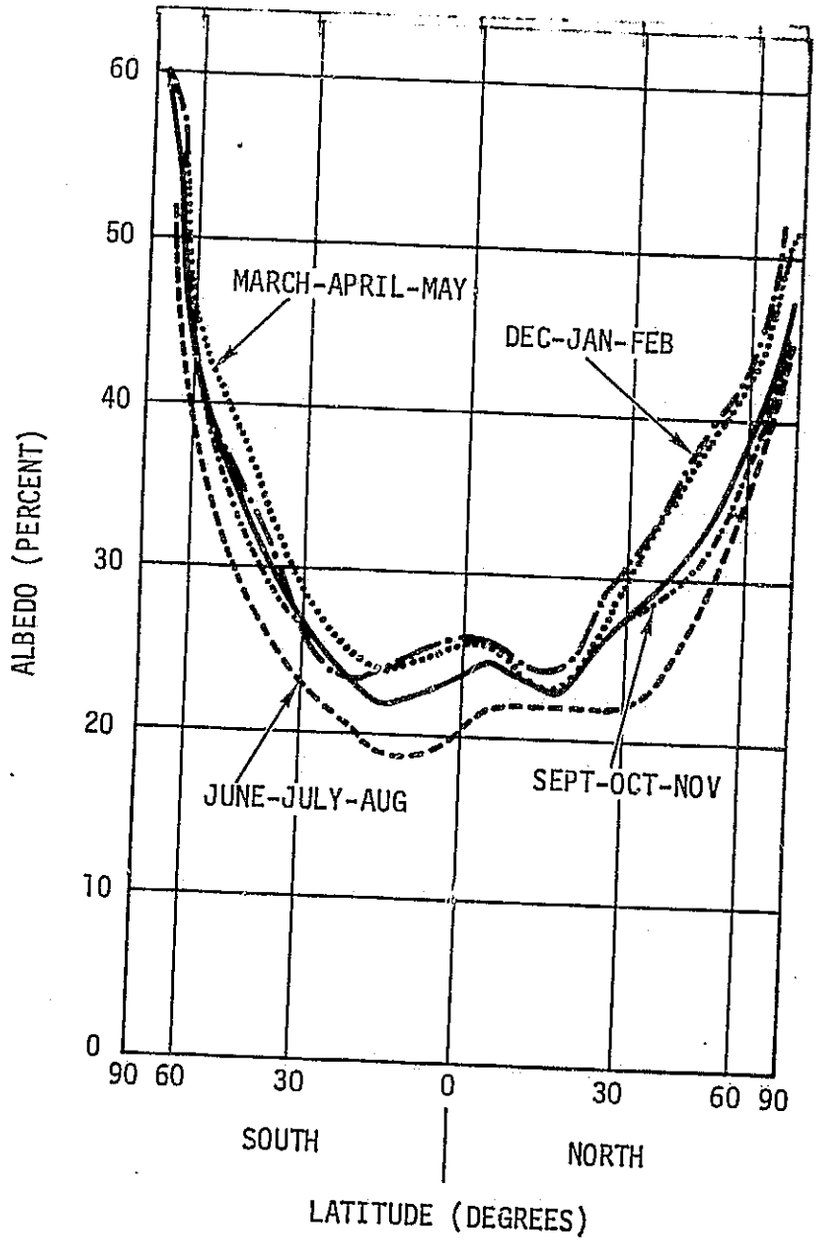

Figure 4-76. Mean Meridional Profiles of Earth Albedo for the Seasons and the Annual Case (Solid Line) (Ref. 4-4)

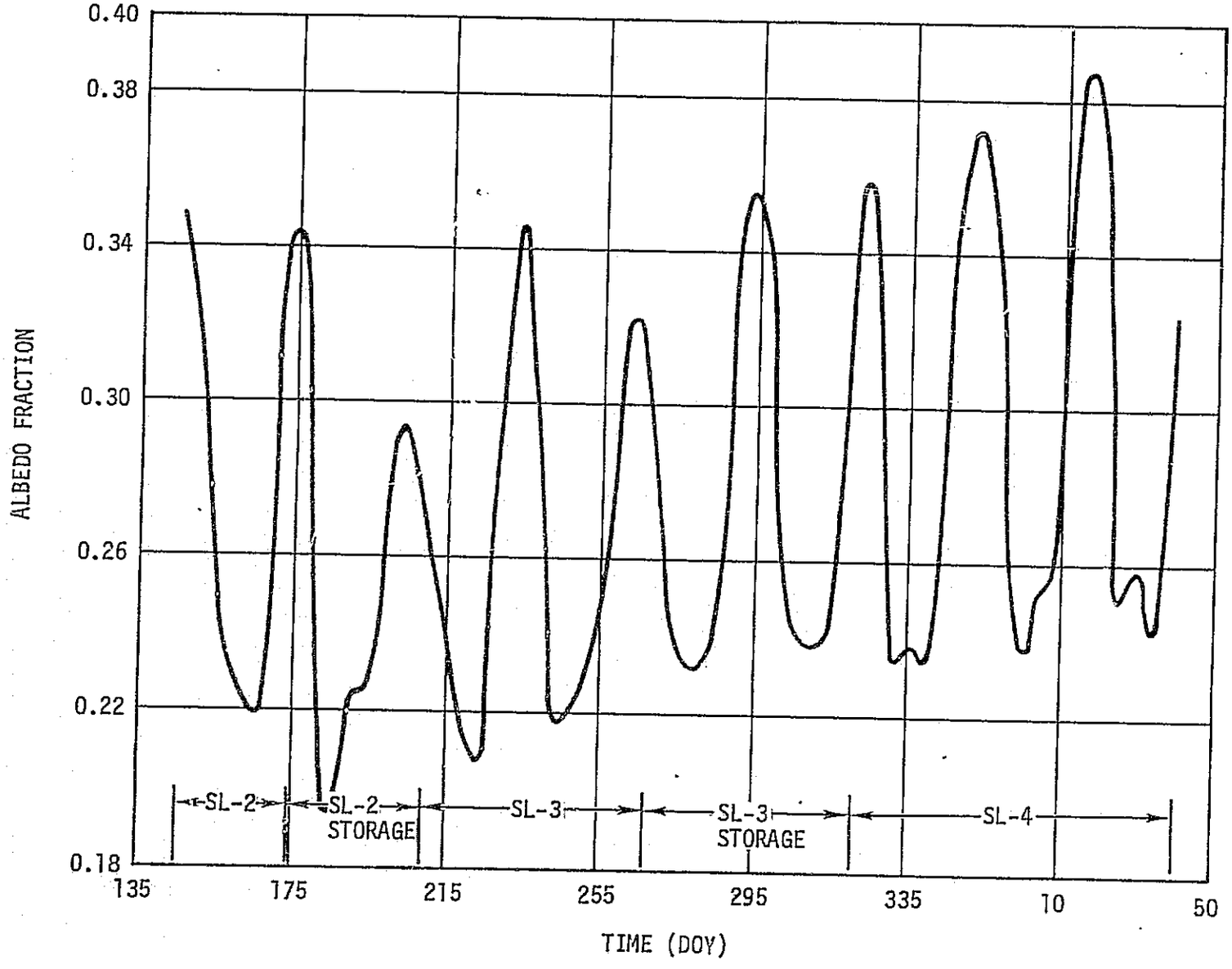

Figure 4-77. Skylab Albedo at Orbital Noon

temperature at steady state. Therefore, the steady state predictions could be checked by plotting the steady state predictions and the flight data as shown in figure 4-78. Since the flight data had a zero slope at the point the two curves crossed, the steady state predictions checked with the flight data. It was concluded therefore, that the assumed values for albedo from figure 4-76 and 4-77 were correct and this was the reason the temperature increased at the higher Beta angles.

Because of the variation of albedo with Beta angle and season, the OWS performance for a long duration mission was not a simple function of Beta angle. The increase in albedo with latitude in connection with the higher Beta angles was counteracted by the decrease in the amount of albedo incident to the vehicle with increasing Beta angle. The relative importance of these two effects determined whether the OWS temperature increased or decreased with Beta angle.

In conclusion, the only parameter (other than the physical configuration) which explained the OWS temperature trend was the albedo. Although the albedo variation was well within the $\pm 2\,\sigma$ ($.3 \pm .12$) design criteria values, the changes in albedo had a significant effect on the OWS temperatures due to the high α/ϵ ratio of the gold foil. During the SL-4 mission, the variation in albedo with latitude was therefore taken into account for flight predictions with measurable success.

f. Component Thermal Environments and Test Levels. OWS components were tested at $\pm 3\,\sigma$ predicted temperatures during the development and qualification program. These temperatures were exceeded for many components located internal to the OWS due to the meteoroid shield/high temperature anomaly. A few components located in the forward and aft skirt areas may have exceeded their maximum qualification test levels by as much as 10°F due to warmer flight environments than predicted. However, no components were determined to have failed or performed in a degraded manner due to thermal conditions. Component test temperature levels based on the $\pm 3\,\sigma$ external environments were, in retrospect, appropriate. There was no indication that the vehicle experienced these $\pm 3\,\sigma$ environment extremes, but components did experience or exceed the test temperature levels due to unforeseen events such as the meteoroid shield loss and the excessive degradation of the S-13G paint on the aft skirt. The following contains a summary of the component thermal analyses and assessments performed during the mission.

A complete thermal assessment of electrical components in OWS systems was made prior to SL-3 launch. This assessment included the effects of the high temperature anomaly experienced during the first two days after SL-1 launch, EREP maneuvers, and retrorocket plume contamination observed by photograph. The electrical systems components included in this assessment were from the following systems:

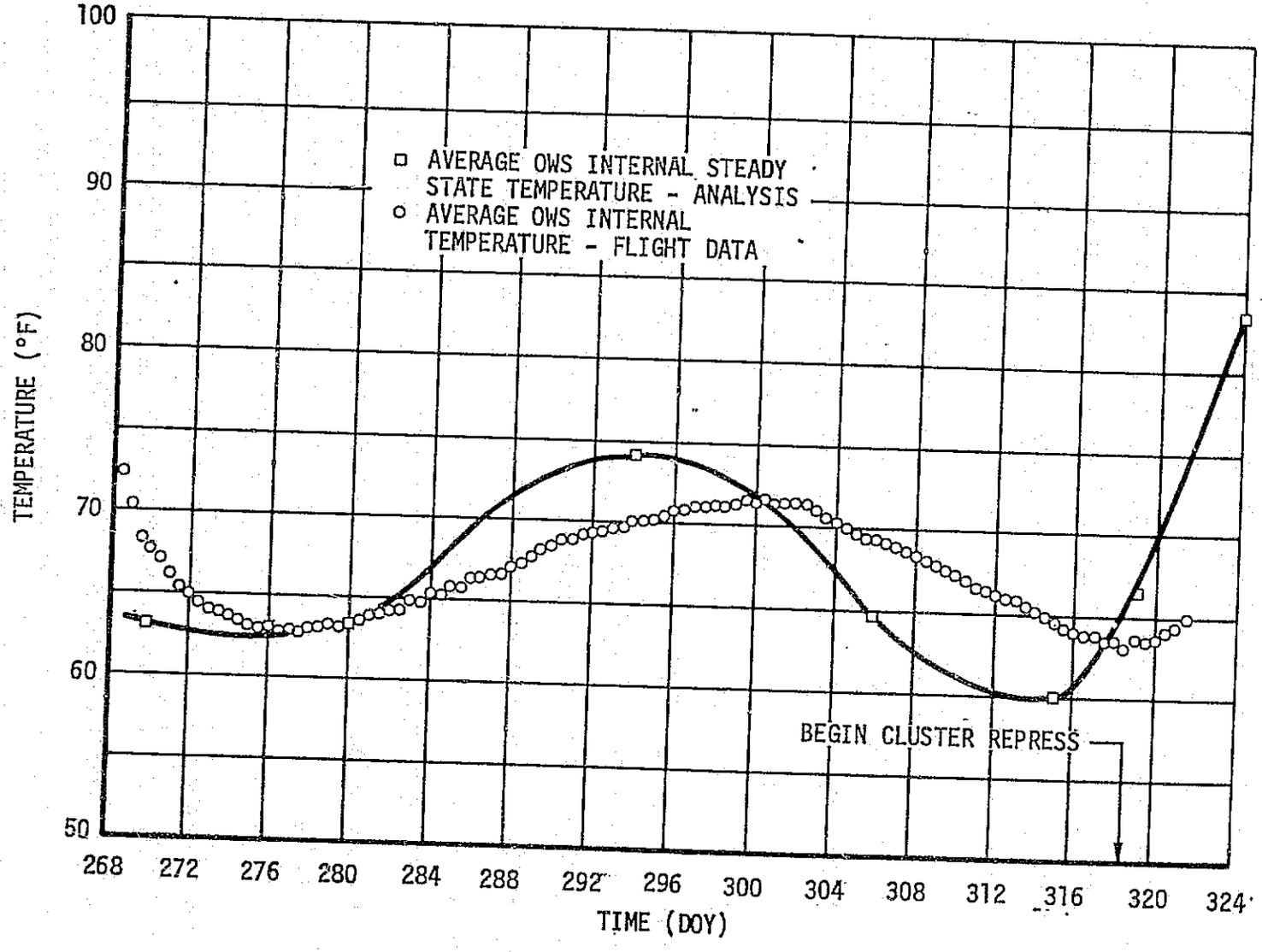

Figure 4-78. OWS Thermal Predictions for SL-3/SL-4 Storage

(1) Power Distribution

(2) Pressure Control

(3) SAS

(4) TACS

(5) Communications

(6) Experiments

(7) TCS

(8) C&W

(9) Illumination

(10) Refrigeration

(11) Electrical Command

(12) Food Management

(13) Waste Management

(14) Water Management

(15) Telemetry

(a) Pressure control, TACS, Experiment Accommodation, Refrigeration, Waste Management, Water System

(16) Ventilation Control

(17) Storage Items

In this assessment, the temperature experienced by each electrical component in each system during the time from orbit insertion until after system activation by the crew was reviewed and compared with its high operational or non-operational qualification temperature depending on whether the component was operational or non-operational during this time. No components in either the forward or aft skirt areas were determined to have exceeded their high qualification temperatures. All components interior to the OWS which were determined to have exceeded their high qualification temperatures were re-evaluated. As a result of this re-evaluation, it was determined that none of these components had reached temperatures which caused failure or malfunction of the component.

Subsequent to the SL-3 mission assessment, it was determined from studying the flight data that the temperature of the external surface of the forward dome insulation (MLI) was higher than the preflight predictions. Consequently, components in the forward skirt area could be 10°F higher during the SL-4 mission than had been originally predicted for their high operational temperatures. The effect of this possible increase in temperature was evaluated and found to be acceptable. Since there was insufficient temperature instrumentation in the forward skirt area to determine component temperatures from flight data, actual temperature of the components during SL-4 were unknown. No components located in the forward skirt area failed during SL-4.

An analysis of worst case maximum temperatures expected during SL-4 for electronic components mounted on the aft skirt was also performed, based on flight data which indicated that the S-13G thermal control coating had degraded due to retrorocket plume contamination, and further degradation could occur due to prolonged solar exposure. The review of aft skirt electronic module temperatures for SL-4 worst-case conditions revealed that the RS secondary bypass controller monitor module and instrumentation system 5 volt modules could exceed their maximum qualification temperature (210°F) by 25°F. Although all subcomponents and materials within the modules had design limits of 257°F, failure analyses of the components were performed to define system impacts. However, the aft skirt S-13G paint apparently did not continue to degrade; and the SL-4 temperatures for these components were 20°F cooler than the worst case predictions. Both modules performed satisfactorily during SL-4.

Except for excessive O_2 bottle temperatures which are discussed in Section V, examination of flight data revealed no components in the MDA or AM which exceeded thermal qualification limits.

g. OWS Temperature Instrumentation. Program considerations dictated that telemetry instrumentation be limited. Consequently the number of temperature measurements required for the Thermal Control System performance evaluation was minimized, and the temperature measurements to provide forward and aft skirt electrical component temperatures and environments were deleted. Recognizing this basis, the flight temperature instrumentation is discussed in terms of its usefulness in providing system performance and flight status.

(1) Thermal Control System. The temperature sensors installed in the OWS to evaluate the performance of the Thermal Control System produced the expected data quality. They were, for the most part, properly located for their intended purposes and were in sufficient number to provide the necessary data. For purposes of determining temperature levels, the instrumentation accuracy (Table 4.9) was adequate.

TABLE 4.9 INSTRUMENTATION ERROR SUMMARY

Transducer Measurement No.	Transducer Part No.	Location	Total System Error (%)	Temperature Range (°F)	Temperature Error (°F)
C7011 thru C7018	1B75673-517	Meteoroid Shield (Lost at L/O + 63 Sec)	± 2.16	-250 to 400	± 14.04
C7049 & All Ext. Tank XDucers	1B75673-507 (-505 Bridge)	Habitation Area Sidewall	± 2.32	-10 to 190	± 4.64
C7057 & All Int. Wall XDucers	1B75673-507 (-507 Bridge)	Interior Sidewall	± 2.35	0 to 120	± 2.82
C7100/1	1B75673-513 (-501 Bridge)	HPI Exterior	± 2.17	-110 to 290	± 8.68
C7162/3	1B75673-513 (-507 Bridge)	Forward Dome Exterior	± 2.35	0 to 120	± 2.82
C7106/7	1B75673-507	Forward Dome Interior	± 2.35	0 to 120	± 2.82
C7181 & All Int. CBH XDucers	1B75673-507	Common Bulkhead Interior Surface	± 2.35	0 to 120	± 2.82
C7179 & All Foam/ CBH XDucers	1B75673-507	Common Bulkhead/ Foam Interface	± 2.35	0 to 120	± 2.82

For purposes of determing heat flux utilizing the temperature difference (Delta T) of adjacent sensors, the instrumentation yielded errors as large as 60 percent using Delta T across the sidewall foam. Temperature sensors used as a set to calculate Delta T's were placed on the same multiplexer where possible in order to reduce the relative error for determining the temperature difference. This cut the error range approximately one-half across the foam insulation, for example.

For purposes of determing habitation area heating rates, it would have been desirable to have had a number of Delta T sensors and/or heat flux gauges to supplement the temperature sensors. This was particularly true for the habitation area sidewall and forward dome where Delta T's acrosss the foam insulation were generally less than 10°F.

The loss of the OWS meteoroid shield during launch caused high temperature conditions in orbit beyond that which could reasonably be designed into the instrumentation range. The shield loss caused items such as the film vault, ambient food storage lockers and internal insulation to exceed their design temperatures and to exceed the range of associated instrumentation. Therefore, it became necessary to approximate the temperature of these items with the temperature instrumentation which remained on-scale. It is apparent that from data requirements during this period as well as after Sun shade deployment when measurements were back on-scale it would have been highly desirable to provide temperature instrumentation directly on the film vault and the ambient food racks rather than estimating these temperatures from wall and ceiling measurements.

Installation of the Wardroom window sensor C7293 and C7294 in closer proximity to the window heater element would have allowed these sensors to be more useful in determining the operation of the window heater. Such an installation, however, was precluded by viewing considerations.

(2) Components. No instrumentation was allocated for components except on the TACS manifolds. It was apparent from mission support experience, e.g., questions related to the temperature status of components such as Mux "B", fuse modules, and other mission or reliability critical components, that additional instrumentation at key locations would have been useful for the purpose of troubleshooting. To establish the general environment of the forward skirt, one additional temperature sensor at PP I, approximately Station 650, would have been invaluable. This would have provided data which, together with the aft skirt temperature data could have been used to evaluate the thermal performance of the white (S-13G) thermal control paint with and without retrorocket plume degradation. It would also have been desirable to have selected temperature measurements on critical components located on typical mounting panels of differing passive thermal control design.

One sensor on a component on the gold shrouded signal conditioning panels, e.g., a multiplexer, and another sensor on a TACS electronics panel component, e.g., a 10 amp mag latch relay module would have provided sufficient information to assess all forward skirt mounted components. The aft skirt sensors C7189 and 7190 together with the TACS manifold sensors C7261 and C7262 provided sufficient data to adequately assess the thermal status of all aft skirt mounted components.

(3) SAS. Temperature instrumentation was strategically located on SAS panels to provide cell temperatures and cell temperature gradients in support of inflight SAS power performance analysis. The selected locations and numbers were adequate for this purpose.

The SAS deployment system design and deployment scheme were developed to account for many contingencies including backup deployment, ground station coverage, thermal deformation effect, and beam/fairing and wing actuator/damper temperature conditions. Under normal operation, no deployment-related temperature instrumentation would have been required. As it was, with the meteoroid shield failure and the delayed SAS Wing Number 1 deployment, temperature sensors on beam/fairing actuator/damper and the wing actuator/dampers would have been extremely useful in determining fluid temperature conditions for contingency deployment.

REFERENCES

4-1. Muse, W. W., "Full-Scale Simulated Altitude Investigation of the Centaur-Payload Surface and Functional Degradation Resulting from the Saturn S-IVB Retro-Rocket Exhaust Contaminants", ARO, Report No. AEDC-TR-66-57, May 1966.

4-2. Zerlaut, G. A. and Gilligan, J. E., "Study of In Situ Degradation of Thermal Control Surfaces", IIT Research Institute Report No. 11TRI-U6061-17, March 7, 1969

4-3. Steube, K. E. and Linford, R. M. F., "Long-Duration Exposure of Spacecraft Thermal Coatings to Simulated Near-Earth Orbital Conditions, "AIAA 6th Thermophysics Conference, Paper No. 71-454, April 26-28, 1971.

4-4. "Earth Albedo and Emitted Radiation", NASA SP-8067, July 1971

SECTION V. GAS SUPPLY SYSTEM

A. System Configuration

The AM Gas Supply System configuration is shown in figure 5-1. Gaseous oxygen was stored in six cylindrical metal lined fiberglass tanks located on the Fixed Airlock Shroud. Gaseous nitrogen was stored in six spherical titanium tanks located in pairs on three of the four AM trusses. A total of 6113 pounds of oxygen was loaded of which 5432 pounds were considered useable at specification limits. A total of 1630 pounds of nitrogen was loaded of which 1439 pounds were considered useable at specification limits. The oxygen tanks were pressurized prelaunch to pressures ranging between 2978 and 3013 PSIA with temperatures ranging from 67.7 to 71.6 deg. F. The nitrogen tanks were pressurized prelaunch to pressures ranging from 2904 to 2990 PSIA with temperatures ranging from 63.9 to 70.1 deg. F.

The six O_2 tanks were connected into common tubing with check valves provided downstream of each tank to prevent loss from other tanks if one tank should leak. From the tanks, the O_2 passed first through a common 10 micron absolute filter and then into two parallel latching solenoid valves. These solenoids could be operated by ground command or by the crew. They were opened by ground command for each mission pressurization and remained open until the beginning of each storage period. A bleed orifice was provided around the two latching solenoids to equalize the pressures on either side of the solenoids when closed to prevent high pressure oxygen surges when the valves were reopened.

Downstream of the two latching solenoids was another orifice which limited the flow into the cluster to 5 lb/min. maximum in the event of a rupture of an internal high pressure line. The gas then flowed into the 120 PSIG regulator assembly which contained two parallel, redundant, shutoff toggle type valves, 120 PSIG regulators, relief valves and check valves. A 10 micron filter was also included at the inlet of the assembly and was common to both parts. Each regulator was designed to provide O_2 flow rates of 22.8 lb/hour minimum at a nominal output pressure of 120±10 PSIG with supply pressures of 300 to 3,000 PSIA. The O_2 then passed through a heat exchanger on the exterior of the AM where the O_2 was controlled to a temperature of 40 deg. F to 65 deg. F depending on AM cooling system loads. The O_2 was then split into three paths. The first went into the O_2/N_2 Two-Gas Control System, described later in this section. The second went to the two parallel O_2 fill solenoid valves which were used to supply O_2 for MDA/AM pressurization, for OWS pressurization, and for O_2 partial pressure sensor calibration. The third path went to the three IVA quick disconnects located in the STS and to the four EVA quick disconnects located in the AM Lock Compartment.

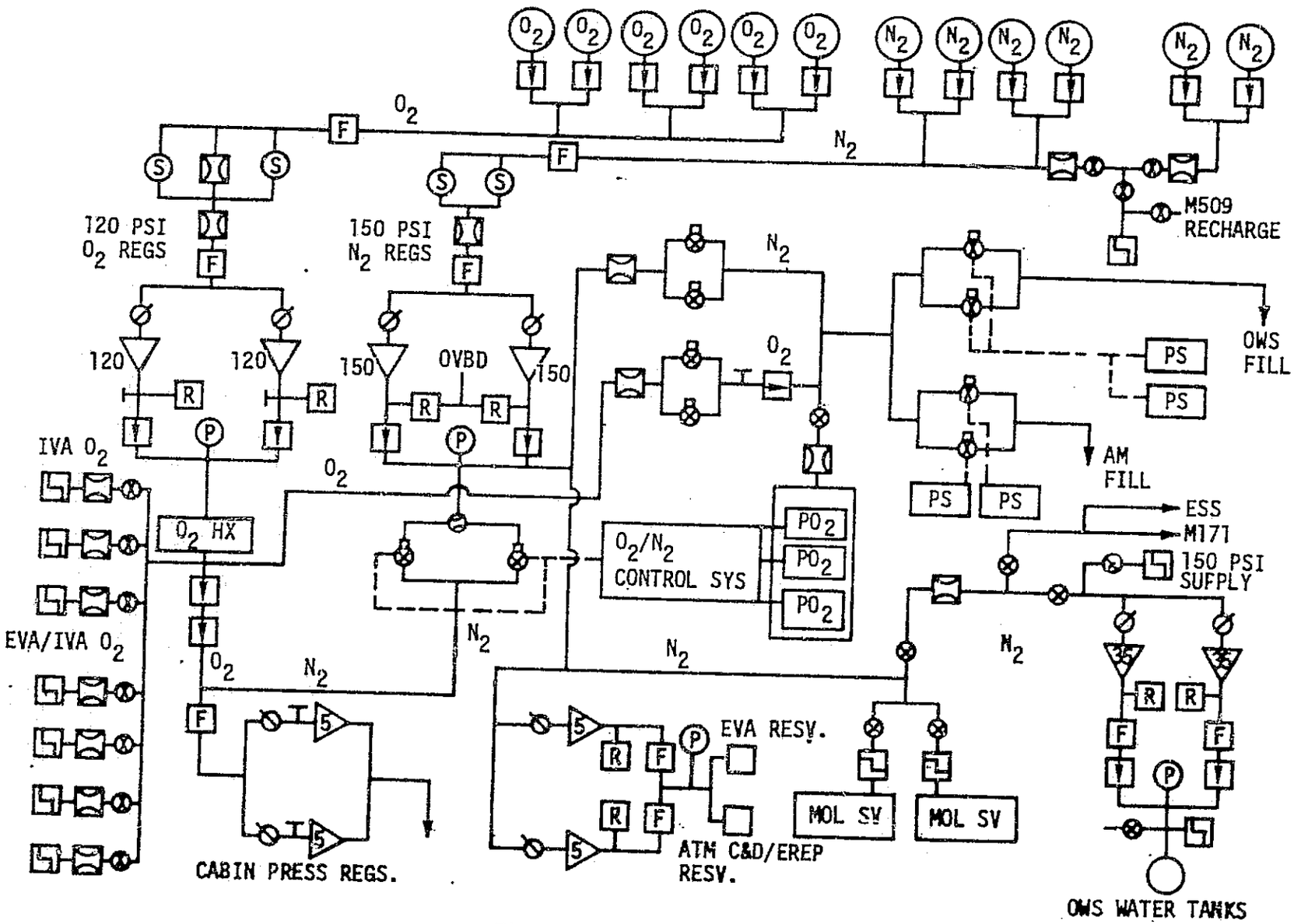

Figure 5-1. Gas Supply System

The six nitrogen tanks were separated into three modules on the AM trusses. Each tank had a check valve to prevent excessive loss of N_2 due to leakage in any one tank. Tanks 1 and 2 were manifolded together and were used for M509/T020 experiment propellant tank fill topoff to as close as possible to 3,000 PSIA. Orifices were provided in the experiment bottle pressurization system to limit the maximum flow to 5 lb/min. The remaining four tanks were manifolded together and served the N_2 cluster supply system as described below. The two tanks which were dedicated to M509/T020 topoff could be routed to the cluster supply system via manual shutoff valves if required.

Nitrogen from the supply tanks passed through a 10 micron absolute filter and then into two parallel latching solenoid valves which were opened whenever cluster pressurization was required and remained open during all manned phases of the mission. Next the N_2 passed through an orifice which limited the flow to 5 lb/min. in the event of a rupture of an internal line. The N_2 then flowed to the 150 PSIG regulator assembly, which contained the same type components as the 120 PSIG O_2 regulator assembly. However the N_2 relief valves were connected to an overboard vent line whereas the O_2 relief valves relieved into the cabin. The regulator assembly (either regulator) was designed to flow 22.8 lb/hour minimum at 150 ± 10 PSIG outlet pressure with supply pressures of 300 to 3,000 PSIA. The N_2 gas then split into five paths. The first path went to the O_2/N_2 Two-Gas Control System, which is described in the following paragraphs. The second path went to the N_2 fill valves, which provided for AM/MDA pressurization, for OWS pressurization, and for O_2 partial pressure sensor calibration. The next path provided N_2 for the Molecular Sieve pneumatics. Another path provided N_2 for the 5 psia N_2 regulator, which maintained a positive pressure on the EVA/IVA and ATM C&D/EREP Cooling System Reservoirs. The final path supplied 150 PSIG N_2 to the OWS where it was used to supply experiments M171 and M092 and also to feed a 35 PSIG regulator which supplied N_2 pressurant for the OWS water supply tanks.

Atmospheric total pressure was maintained and composition was controlled during the manned operation by the Two-Gas Control System. This system consisted of two series check valves, a pressure regulator assembly, an N_2 3-way selector valve, two solenoid valves, three O_2/N_2 controllers, three PO_2 sensors, a sensor calibration housing, an orifice, a manual shutoff valve and various lines and fittings.

Total pressure was maintained at 5.0 ± 0.2 PSIA by either of the two redundant cabin pressure regulators in the assembly. Both remained open. The regulator assembly had a flow capacity of 1.15 ± 0.15 lb/hour of O_2 through either or both circuits with an outlet pressure of 4.8 to 5.2 PSIA. Manual valves upstream of the cabin pressure regulators provided a means of shutting off the supply gas to either

one or both regulators. A warning alarm was set to trigger if the cabin pressure dropped to 4.6 ±.1 PSIA. A rapid delta P Emergency Alarm was set if the cabin pressure began dropping at a rate of 0.1 PSI/min. or greater.

Oxygen partial pressure was sensed as a basis for supplying either O_2 or N_2 to the cabin pressure regulators. Nitrogen was supplied after PO_2 reached the upper end of the control range and oxygen was supplied after PO_2 reached the lower end of the control range. Considering the maximum width of the controller band and a tolerance of ± 3% for the sensor/amplifier, the cluster PO_2 could be a minimum of 3.3 PSIA and a maximum of 3.9 PSIA when the system was in control.

Three sensor/amplifier, controller systems were provided. One could be used for control, another for monitoring, and the third held in reserve as a backup for the other two.

Three PO_2 display gages were provided on O_2/N_2 Control Panel 225. Each indicator had a range of 0 to 6 PSI. The indicator accuracy was ± 2.0 percent of full scale or ± 0.12 PSI.

A C&W alarm could be initiated from either the monitoring or controlling sensor at a nominal PO_2 of 3.05 PSIA to warn the crew of the low PO_2. Because of the system tolerances discussed above, the C&W low PO_2 alarm point could be 2.81 to 3.28 PSIA (see figure 5-2).

The PO_2 sensor used in the Two-Gas Control System was provided with an inflight calibration check capability. This capability was provided by supplying a hinged PO_2 sensor calibration shroud and a valve in the AM/MDA/OWS pressurization line to actuate either O_2 or N_2 gas flow to the PO_2 sensors. A reading equal to cabin total pressure should occur on the PO_2 meters while flowing pure O_2 and a zero scale reading should occur while flowing pure N_2. The calibration shroud was positioned during launch so that it covered the PO_2 sensors. It was moved to the open position by the crew during activation of SL-2.

The Two-Gas Control System was designed to be "fail-safe". Pure O_2 would have been supplied to maintain total pressure in case of electrical power failure, most types of solenoid valve failures, and PO_2 sensor degradation. Redundant oxygen check valves, redundant nitrogen solenoid valves, and a nitrogen selector valve provided the capability to correct failures of the valving that determined which gas flowed to the cabin pressure regulators.

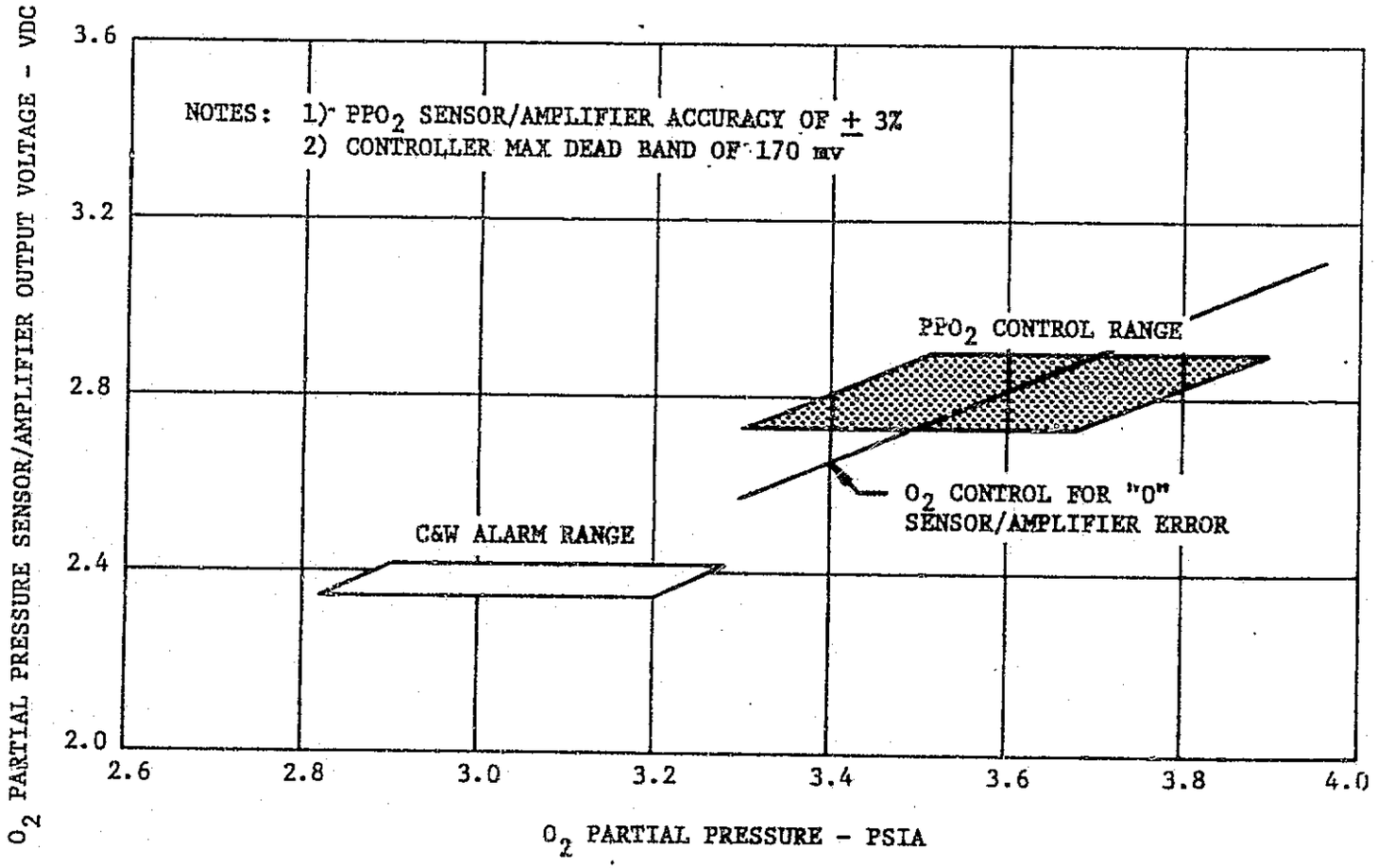

Figure 5-2. Control and Alarm Ranges for Two-Gas System

B. System Performance

The AM Gas Supply System performed within the prelaunch specified limits except for the 150 PSIG N_2 Regulator outlet pressure which drifted low and is discussed in detail in paragraph B.5 of this section. The following paragraphs describe the performance of the various elements of the system.

1. O_2/N_2 Storage System - The O_2 Tanks were filled with 6113 pounds and the N_2 Tanks to 1630 pounds. Both of these were well above the minimum launch quantities of 5,611 lbs and 1,511 lbs. respectively. No detectable leakage in the tanks, external lines or valves was detected. Some stratification in the storage tanks was seen during the mission. It was particularly noticeable prior to launch of SL-2 while the cluster was being maintained in off-nominal attitudes. During this time temperature and pressure transducers indicated that the mass in O_2 tank 4 was about 50-60 pounds greater than the mass launched, even though the first O_2 pressurization (using about 257 pounds) had been completed.

2. Gas Distribution System - The 120 ± 10 PSIG (125 ± 10 PSIA) regulator functioned within its specification limits. A plot of the 120 PSIG O_2 and the 150 PSIG N_2 regulator outlet pressures are shown in figure 5-3.

The AM & OWS Fill Valves and their pressure limiting switches functioned properly. Oxygen supply for EVA and IVA was nominal. The nitrogen supply to the Mole Sieve pneumatics, M509 recharge, and experiments operated properly throughout the mission.

3. Two-Gas Control System - The two-gas control system performed properly and operated within its design limits. When in control of the cluster pressure, the system maintained total pressure well within the required limits (5 ± .2 PSIA) and at a relatively constant pressure as can be seen from the total pressure history provided in figure 5-4. Since there were many events which influenced total pressure and they played a major role in producing the vehicle pressure history of figure 5-4, a summary of the events has been compiled and is provided in Table 5.1. As a result of these events, the automatic system was not in control during much of the Skylab missions. The majority of the pressure perturbations were caused by experiments M509 and T020 and crew or ground atmospheric management to prepare for or to recover from these experiments.

A comparison of preflight and flight cabin pressure regulator performance is provided in figure 5-5. The flow provided was well within the required range.

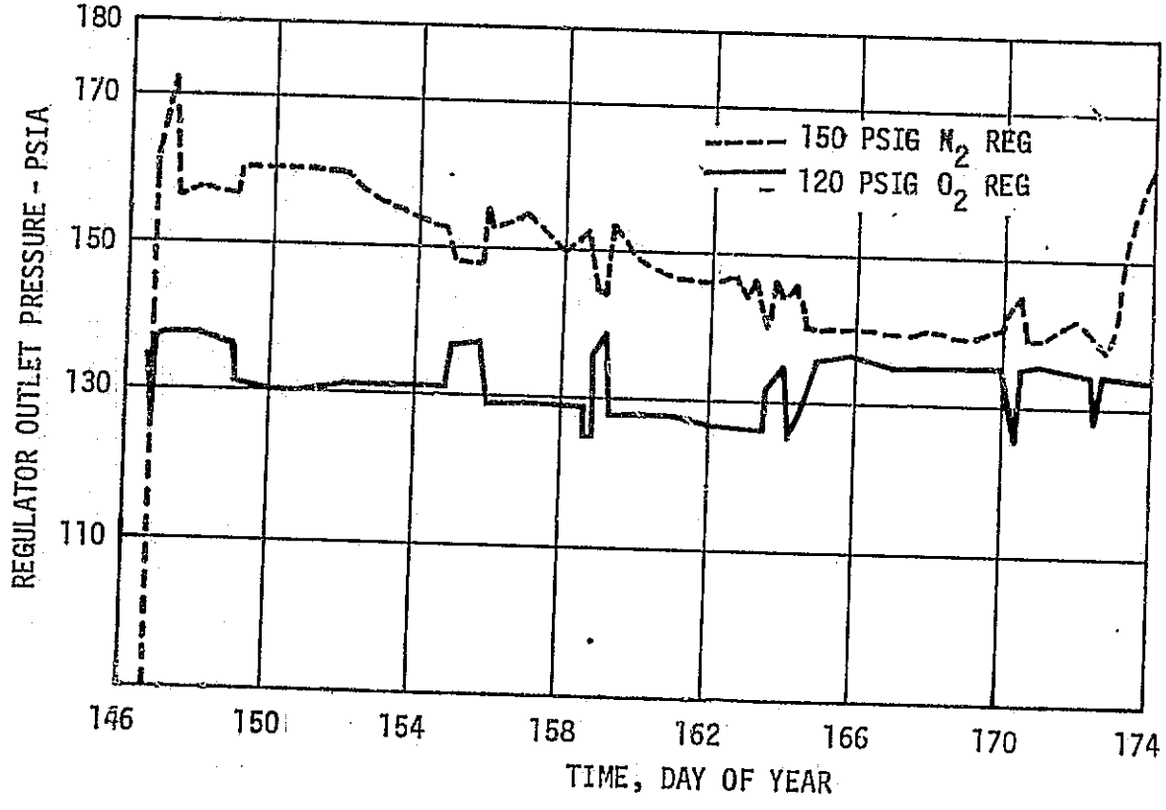

Figure 5-3a. SL-2 O_2 Reg & N_2 Reg Outlet Pressure Profile

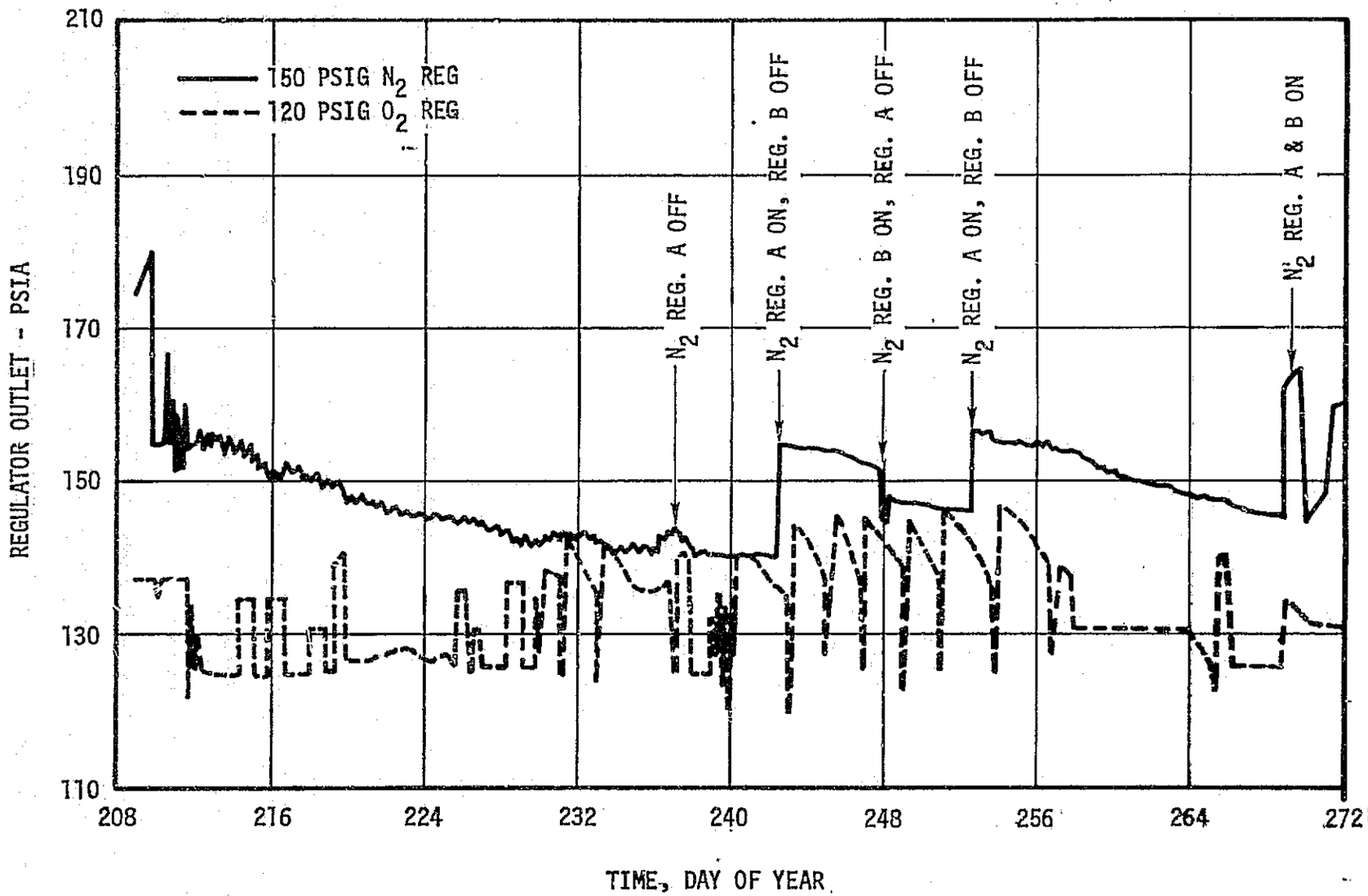

Figure 5-3b. SL-3 O_2 Reg & N_2 Reg Outlet Pressure Profile

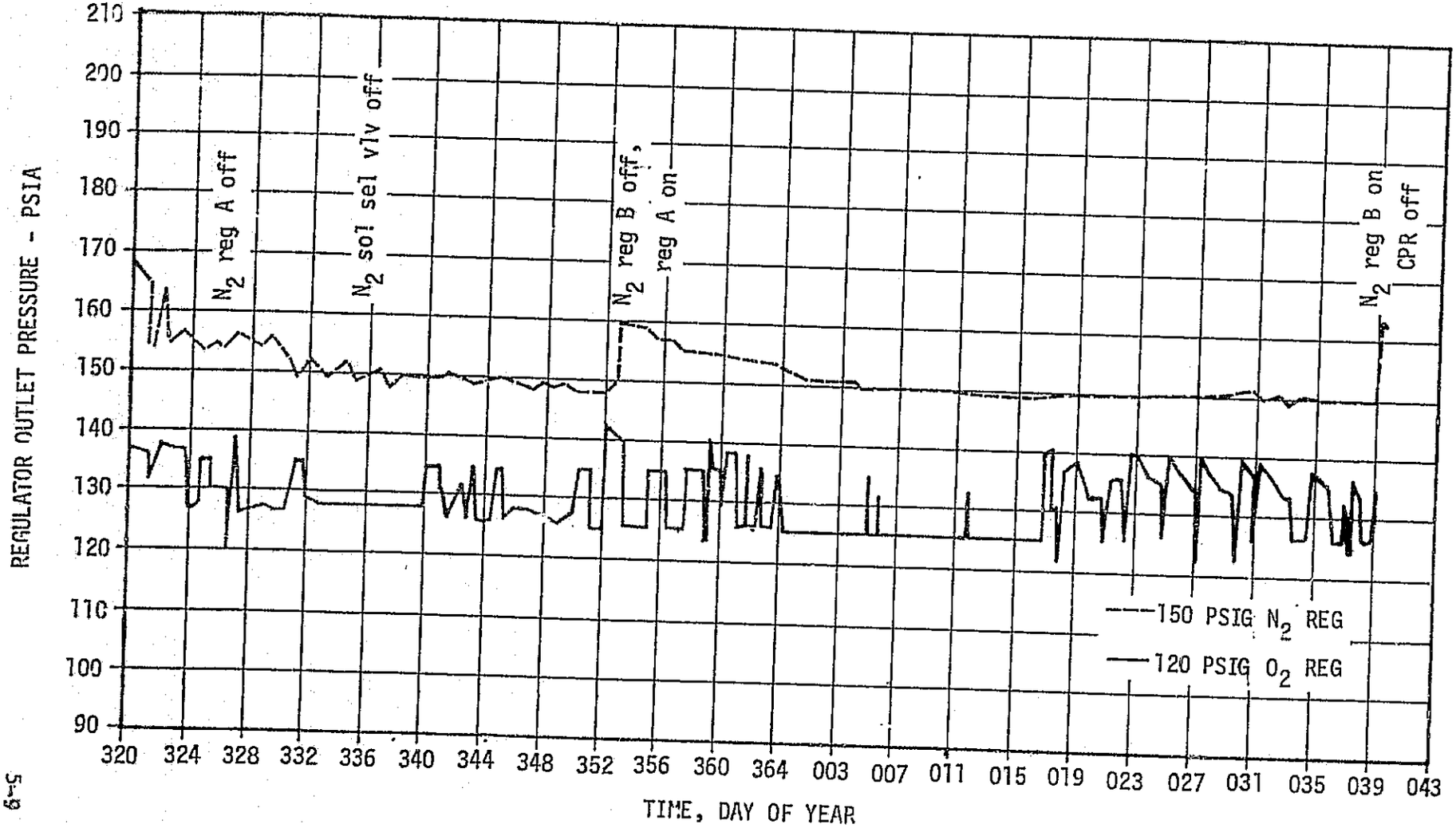

Figure 5-3c. SL-4 O_2 Reg & N_2 Reg Outlet Pressure Profile

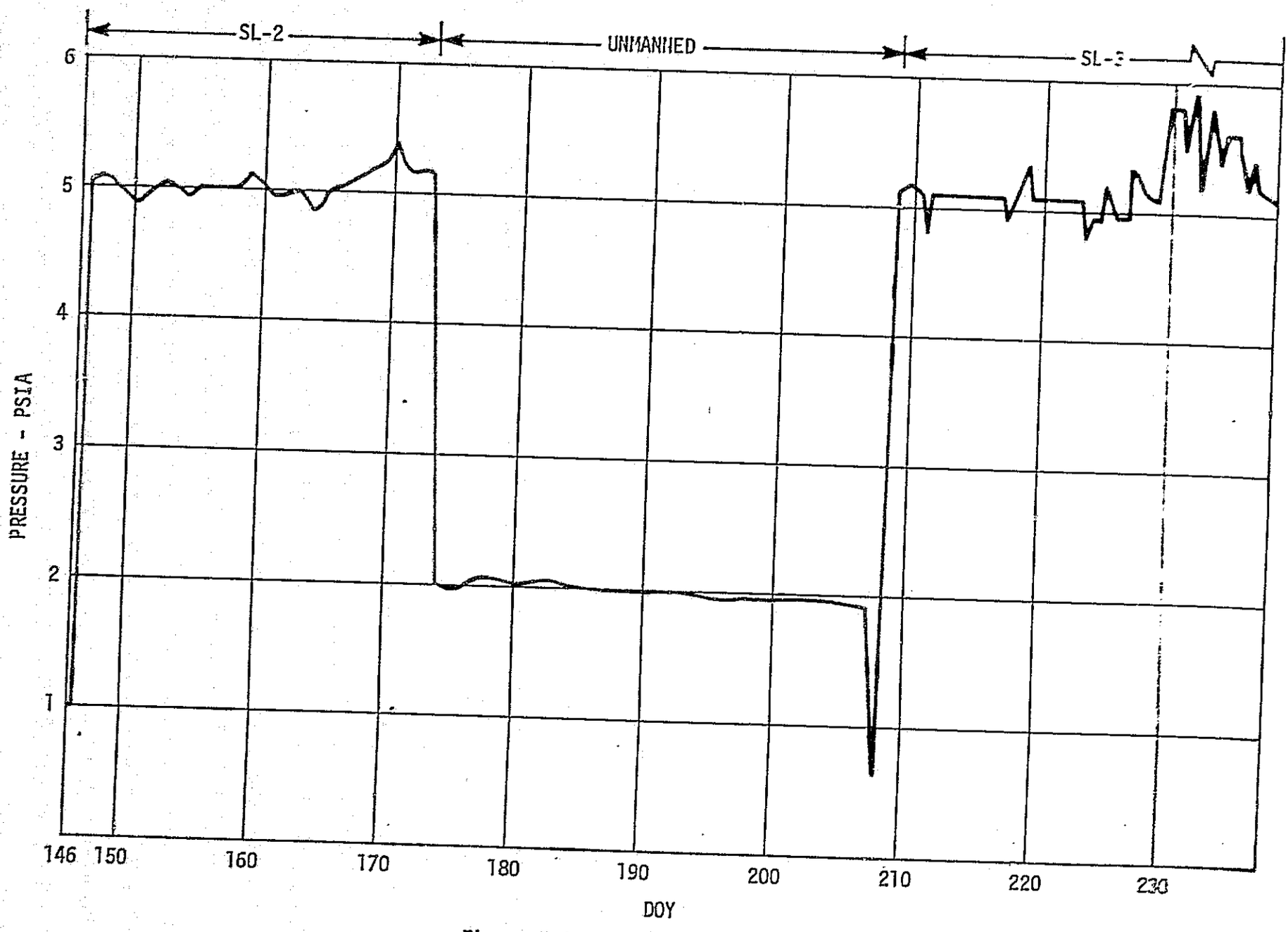

Figure 5-4. Total Pressure History

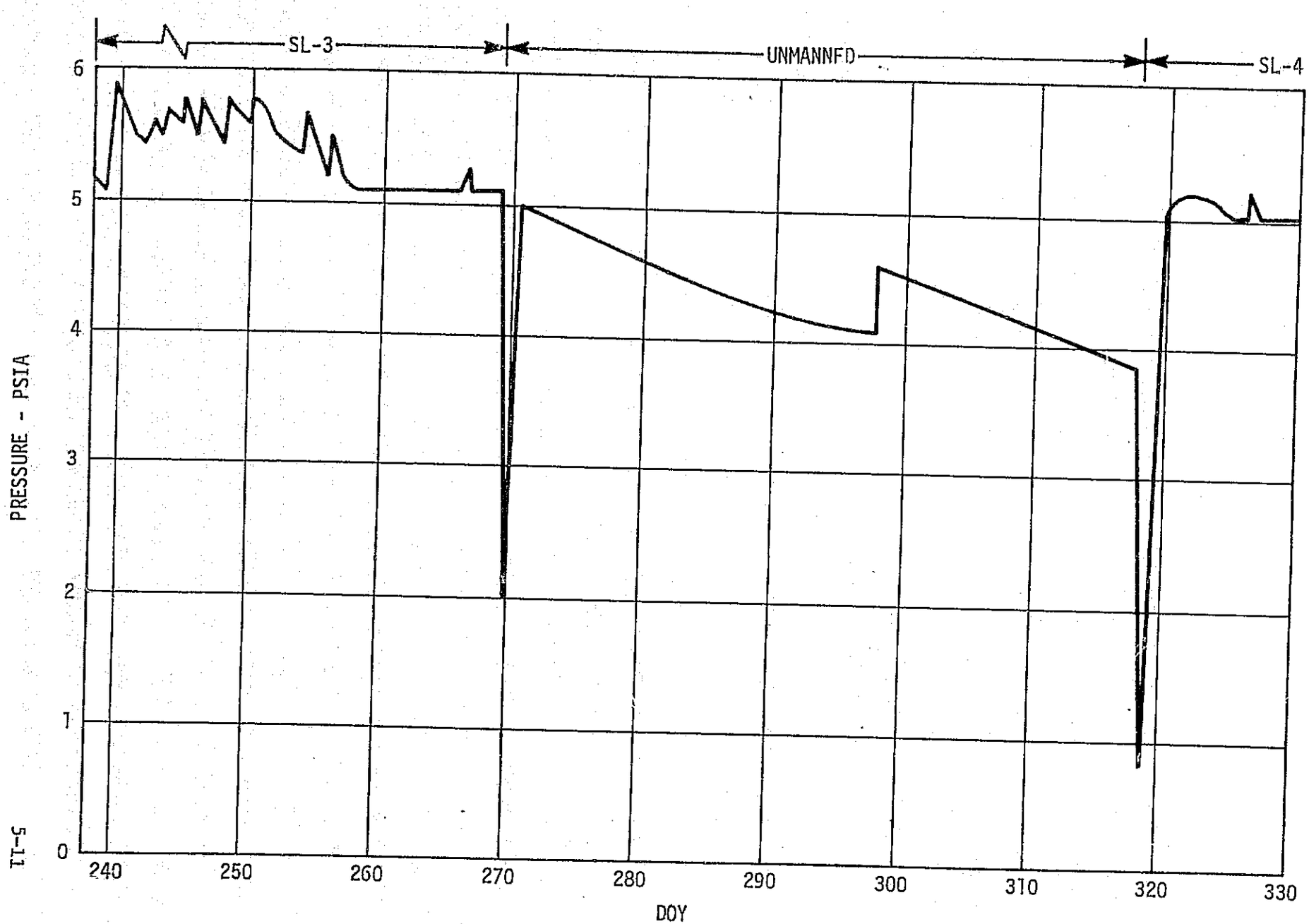

Figure 5-4. Total Pressure History (Con'd)

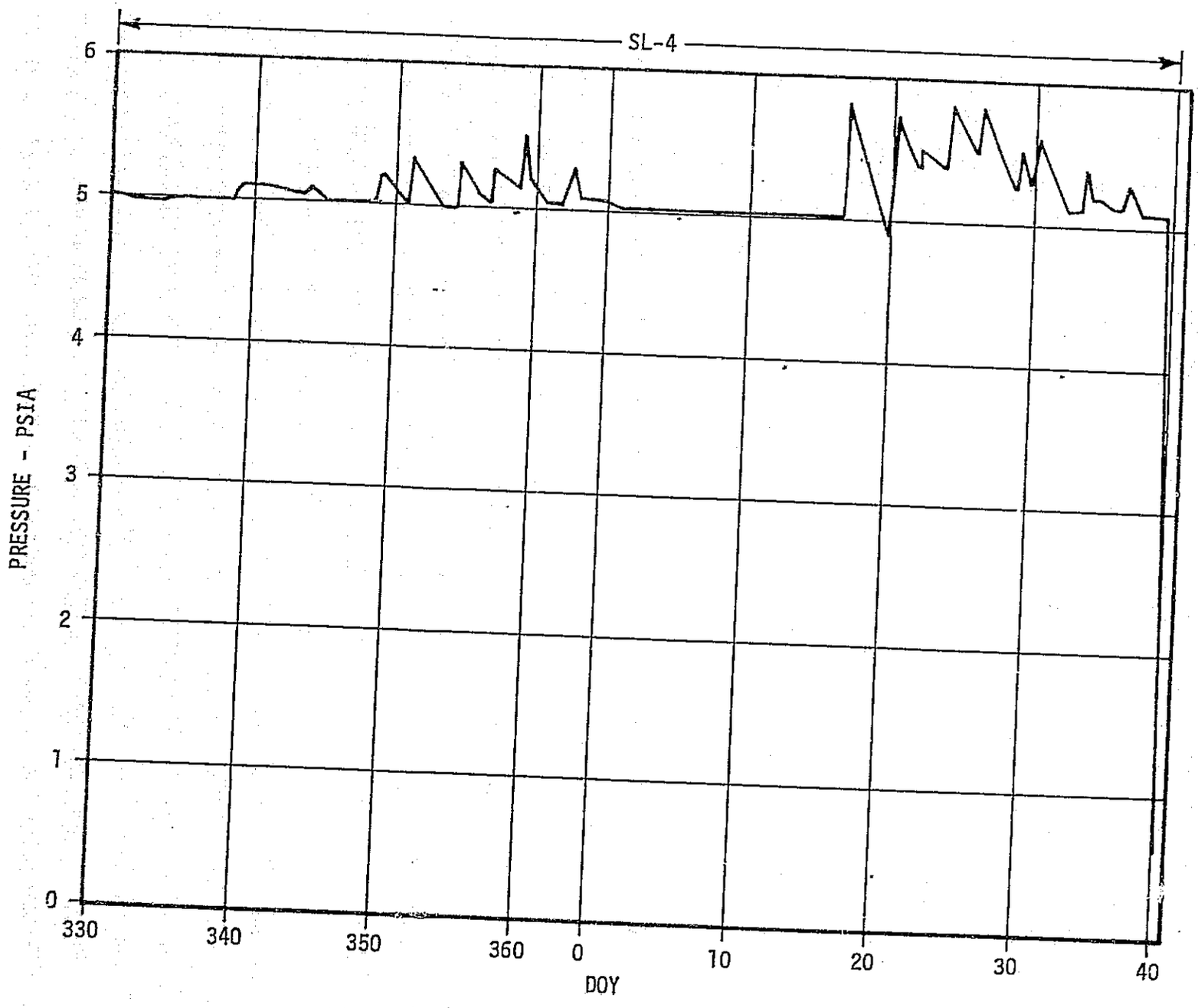

Figure 5-4. Total Pressure History (Con'd)

Table 5.1 Events Which Perturbed the Automatic O_2/N_2 Control System

EVENT	TIME(DOY:HR:MIN)	MISSION
CLUSTER LEAK (TRASH AIRLOCK)	149:19:00	SL-2
SL-2 EVA-1 (LOCK DEPRESS)	158:15:15	SL-2
CLUSTER LEAK (TRASH AIRLOCK)	163:15:00	SL-2
CSM POLYCHOKE FLOW (ORIFICE #1)	166:21:00	SL-2
CSM POLYCHOKE FLOW (ORIFICE #2)	168:19:00	SL-2
SL-2 EVA-2 (LOCK DEPRESS)	170:10:45	SL-2
CLUSTER LEAK (TRASH AIRLOCK)	211:05:39	SL-3
OPEN AM/O_2 FILL VALVES	211:09:58	SL-3
CLOSE AM/O_2 FILL VALVES	211:11:31	SL-3
CLUSTER LEAK (SAL)	217:07:00	SL-3
SL-3 EVA-1 (LOCK DEPRESS)	218:17:21	SL-3
M509 VENT #1	222:15:30	SL-3
M509 VENT #1 TERMINATED	223:15:30	SL-3
M509 VENT #2	224:18:00	SL-3
M509 VENT #2 TERMINATED	225:02:00	SL-3
SL-3 M509-1 PERFORMANCE	225:14:15	SL-3
M509 VENT #3	225:18:56	SL-3
M509 VENT #3 TERMINATED	226:11:00	SL-3
SL-3 M509-2 PERFORMANCE	227:19:56	SL-3
M509 VENT #4	228:18:00	SL-3
CSM POLYCHOKE FLOW (ORIFICE #1)	228:18:00	SL-3
M509 VENT #4 TERMINATED	229:03:06	SL-3
SL-3 M509-3 PERFORMANCE	229:15:30	SL-3
M509 VENT #5	230:14:00	SL-3
OPEN AM/O_2 FILL VALVES	231:00:48	SL-3
CLOSE AM/O_2 FILL VALVES	231:02:30	SL-3
SL-3 T020-1 PERFORMANCE	231:20:00	SL-3
M509 VENT #5 TERMINATED	232:19:30	SL-3

Table 5.1 Events Which Perturbed the Automatic O_2/N_2 Control System (Continued)

EVENT	TIME(DOY:HR:MIN)	MISSION
OPEN AM/O_2 FILL VALVES	232:21:44	SL-3
CLOSE AM/O_2 FILL VALVES	233:00:29	SL-3
M509 VENT #6	233:02:00	SL-3
SL-3 M509-4 PERFORMANCE	233:19:05	SL-3
M509 VENT #6 TERMINATED	233:23:29	SL-3
M509 Vent #7	236:00:43	SL-3
TERMINATE CSM POLYCHOKE FLOW (#1)	236:02:36	SL-3
M509 VENT #7 TERMINATED	236:14:00	SL-3
SL-3 EVA-2 (LOCK DEPRESS)	236:16:15	SL-3
M509 VENT #8	238:19:00	SL-3
COMMAND AM/O_2 FILL VALVES OPEN	238:19:00	SL-3
SL-3 M509-5 PERFORMANCE	239:21:37	SL-3
OPEN AM/O_2 FILL VALVES	240:00:04	SL-3
CLOSE AM/O_2 FILL VALVES	240:01:36	SL-3
M509 VENT #8 TERMINATED	240:14:00	SL-3
SL-3 T020-1A PERFORMANCE	241:21:35	SL-3
OPEN AM/O_2 FILL VALVES	243:01:12	SL-3
CLOSE AM/O_2 FILL VALVES	243:02:04	SL-3
SL-3 M509-4 (2ND PERFORMANCE)	243:18:00	SL-3
OPEN AM/O_2 FILL VALVES	244:23:52	SL-3
CLOSE AM/O_2 FILL VALVES	245:00:57	SL-3
OPEN AM/O_2 FILL VALVES	247:01:22	SL-3
CLOSE AM/O_2 FILL VALVES	247:02:28	SL-3
OPEN AM/O_2 FILL VALVES	249:01:10	SL-3
CLOSE AM/O_2 FILL VALVES	249:02:35	SL-3
OPEN AM/O_2 FILL VALVES	251:00:03	SL-3
CLOSE AM/O_2 FILL VALVES	251:01:10	SL-3
OPEN AM/O_2 FILL VALVES	253:23:10	SL-3
CLOSE AM/O_2 FILL VALVES	254:00:13	SL-3

Table 5.1 Events Which Perturbed the Automatic O_2/N_2 Control System (Continued)

EVENT	TIME(DOY:HR:MIN)	MISSION
SL-3 T020-2 PERFORMANCE	256:20:55	SL-3
CLUSTER LEAK (WASTE PROCESSOR)	257:03:00	SL-3
SL-3 EVA-3 (LOCK DEPRESS)	265:11:18	SL-3
CLOSE N_2 FILL VALVES	318:13:00	SL-3
SL-4 EVA-1 (LOCK DEPRESS)	326:17:37	SL-4
CLUSTER LEAK (SAL VENT & REPRESS)	329:23:00	SL-4
CSM POLYCHOKE FLOW (ORIFICE #1)	339:03:39	SL-4
TERMINATE CSM POLYCHOKE FLOW (#1)	340:02:00	SL-4
SL-4 M509-1C PERFORMANCE	349:21:36	SL-4
OPEN AM/O_2 FILL VALVES	351:21:58	SL-4
CLOSE AM/O_2 FILL VALVES	351:22:51	SL-4
SL-4 M509-2 PERFORMANCE	354:23:00	SL-4
SL-4 M509-2C PERFORMANCE	357:17:00	SL-4
OPEN AM/O_2 FILL VALVES	358:21:04	SL-4
SL-4 EVA-2 (LOCK DEPRESS)	359:16:44	SL-4
SL-4 EVA-3 (LOCK DEPRESS)	363:17:23	SL-4
SL-4 T020-1 PERFORMANCE	015:16:00	SL-4
SL-4 M509-3C PERFORMANCE	017:20:00	SL-4
M509 VENT #9	019:13:09	SL-4
CLUSTER LEAK (-Z SAL)	019:14:00	SL-4
M509 VENT #9 TERMINATED	019:23:37	SL-4
SL-4 M509-3P PERFORMANCE	020:23:00	SL-4
OPEN AM/O_2 FILL VALVES	022:12:05	SL-4
CLOSE AM/O_2 FILL VALVES	022:13:18	SL-4
SL-4 T020	024:12:00	SL-4
AM & O_2 FILL VALVES OPEN	025:00:00	SL-4
AM & O_2 FILL VALVES CLOSED	025:00:45	SL-4

Table 5.1 Events Which Perturbed the Automatic O_2/N_2 Control System (Concluded)

EVENT	TIME(DOY:HR:MIN)	MISSION
AM & O_2 FILL VALVES OPEN	027:00:27	SL-4
AM & O_2 FILL VALVES CLOSED	027:01:56	SL-4
AM & O_2 FILL VALVES OPEN	029:20:42	SL-4
AM & O_2 FILL VALVES CLOSED	029:21:40	SL-4
CLUSTER LEAK (WMC VENT)	030:10:00	SL-4
AM & O_2 FILL VALVES OPEN	031:00:13	SL-4
AM & O_2 FILL VALVES CLOSED	031:01:19	SL-4
SL-4 EVA-4 (AM DEPRESS)	034:15:13	SL-4
SL-4 M509-FSA	036:02:13	SL-4
SL-4 M509-FSB	036:03:39	SL-4
AM & O_2 FILL VALVES OPEN	037:02:15	SL-4
AM & O_2 FILL VALVES CLOSED	037:03:15	SL-4

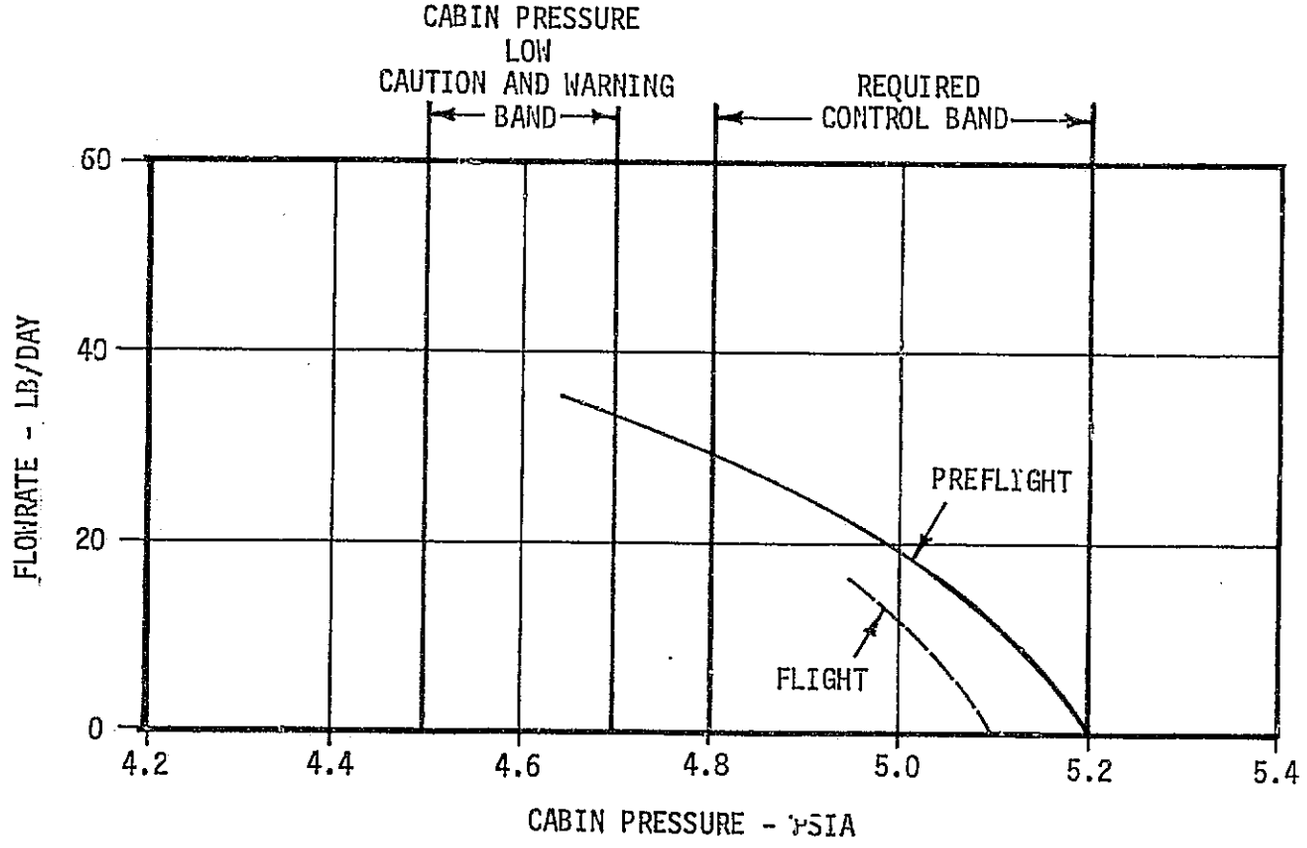

Figure 5-5. Cabin Pressure Regulator Control Characteristics

Oxygen partial pressure control within the 3.6 ±.3 PSIA limit was provided when the two-gas control system was in control of the cluster balance. The above mentioned experiments as well as O_2 additions during EVA and IVA operations caused the limits to be violated slightly on occasion. A summary of O_2 partial pressure history is provided in figure 5-6. During SL-2 the lower limit of the PO_2 control band was 3.46 PSIA and the upper limit was 3.67. During SL-3 and SL-4, M509/T020 experiments perturbated the cabin atmosphere sufficiently such that the control band could not be determined. A check on telemetry (TM) sensor O_2 partial pressure readings were provided by the experiment M171 mass spectrometer. The values compared well, and the data are provided in figure 5-7.

4. <u>O_2/N_2 Consumable Usage</u> - Figures 5-8 and 5-9 present the oxygen and nitrogen consumables usage profiles for the Skylab mission. Table 5.2 presents a summary of the individual usages for each mission, depicting how much of the O_2 and N_2 was used for each. As can be seen, O_2 and N_2 consumables were more than adequate and a considerable quantity of gas remained after SL-4.

Preflight specification requirements indicated that 5,611 pounds of O_2 would be loaded of which 681 pounds would be residual (based upon 300 PSIA and 0 deg. F in each bottle) leaving a usable load of 4,930 pounds. To conduct a nominal mission, 3,865 pounds of O_2 would be required leaving a usable margin of 1065 pounds at the end of SL-4. The pre-flight data indicated that 6113 pounds of O_2 had been loaded before liftoff. Based on the average O_2 tank temperature seen during the flight, the residual O_2 (at 300 PSIA) was 652 pounds leaving a usable onboard at lift-off of 5461 pounds. The total amount of O_2 used during the mission was 3437 pounds, leaving a usable margin of 2024 pounds at the end of SL-4.

Preflight specification requirements for the nitrogen system indicated that 1511 pounds of N_2 would be loaded of which 191 pounds would be residual (based upon 300 PSIA and 0 deg. F in each bottle) leaving a usable load of 1320 pounds. To conduct a nominal mission, 770 pounds of N_2 would be required, leaving a usable margin of 550 pounds of N_2 at the end of SL-4. The preflight data indicated that a total of 1630 pounds of N_2 had been loaded before liftoff. Based on the average N_2 tank temperatures seen during the flight, the residual N_2 (at 300 PSIA) was 177 pounds, leaving a usable onboard at liftoff of 1453 pounds. The total amount of N_2 used during the mission was 984 pounds, leaving a usable margin of 469 pounds at the end of SL-4.

At liftoff, a total of 502 pounds of O_2 and 119 pounds of N_2 more than specification was onboard. Due to the average tank temperatures in orbit the residual O_2 was reduced by 29 pounds and the

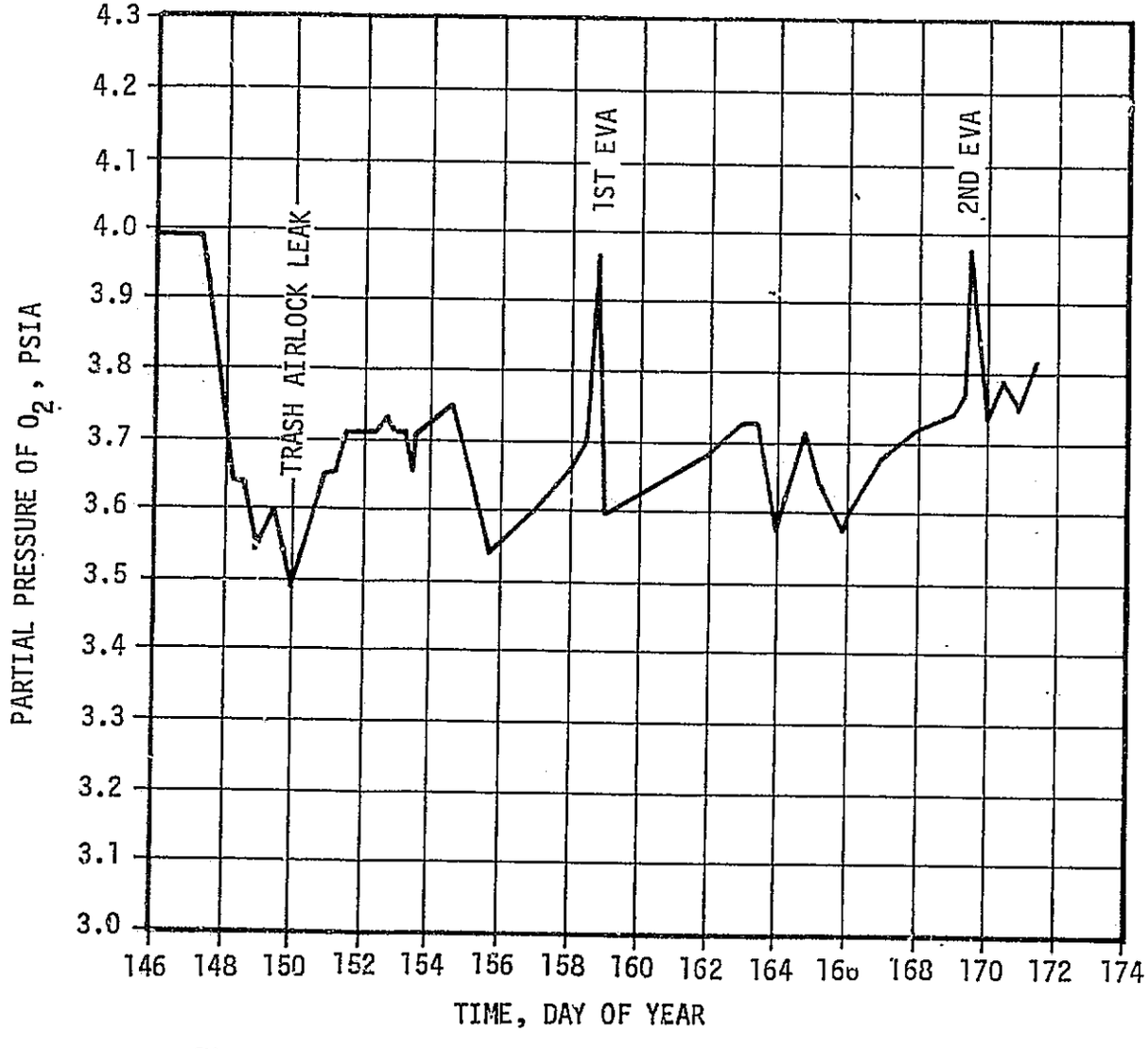

Figure 5-6a. SL-2 Partial Pressure of Oxygen Profile

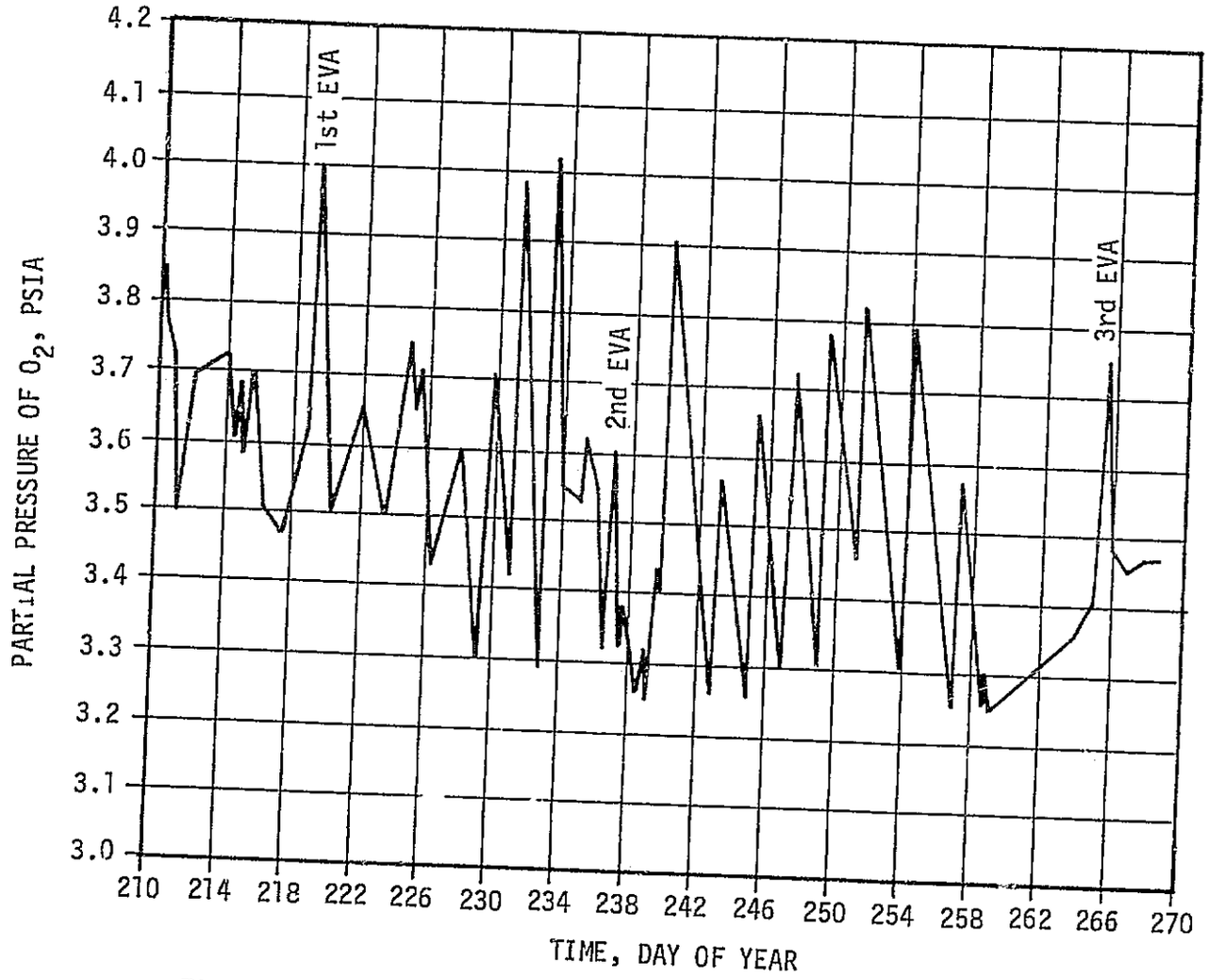

Figure 5-6b. SL-3 Partial Pressure of Oxygen Profile

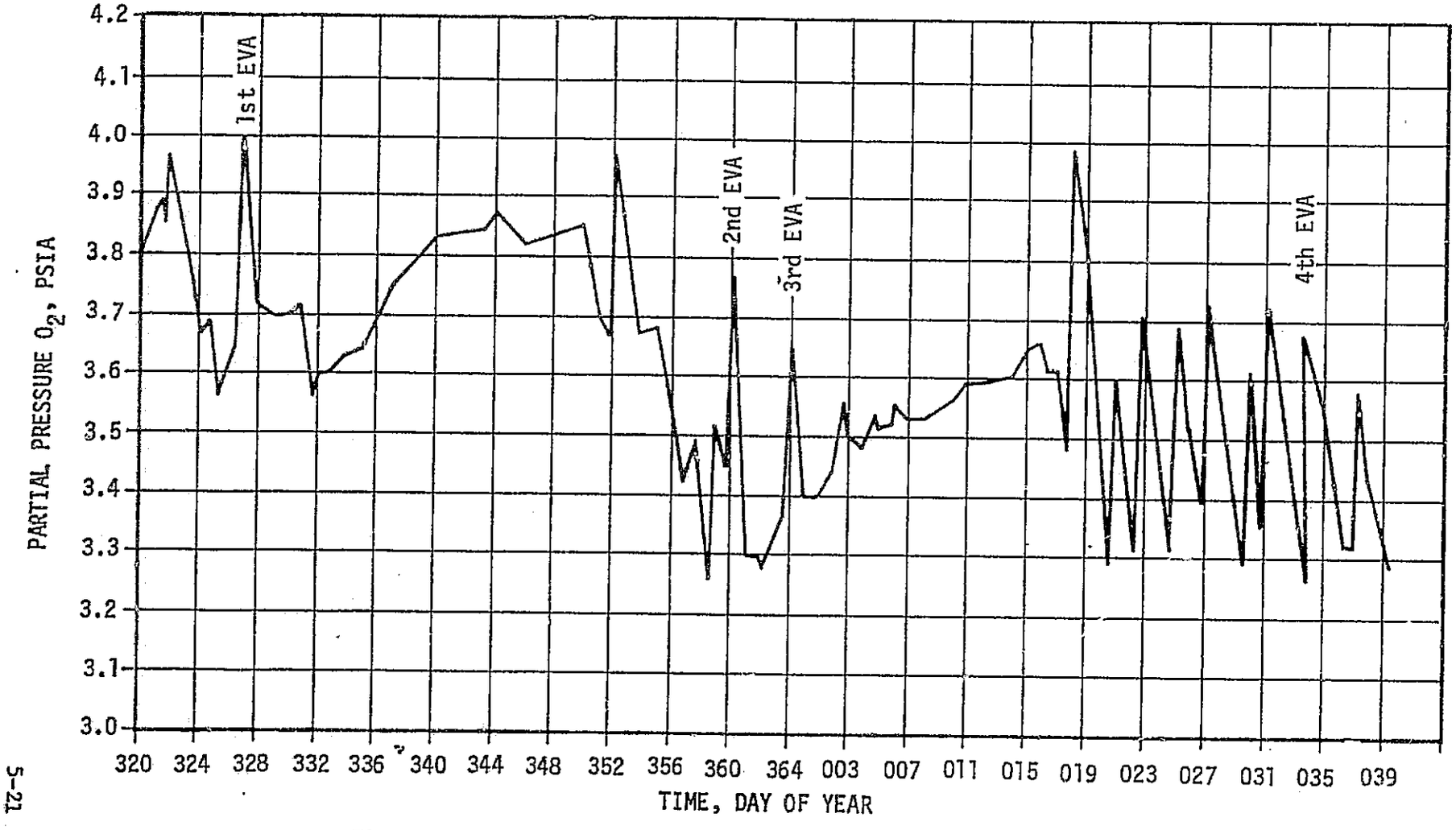

Figure 5-6c. SL-4 Partial Pressure of Oxygen Profile

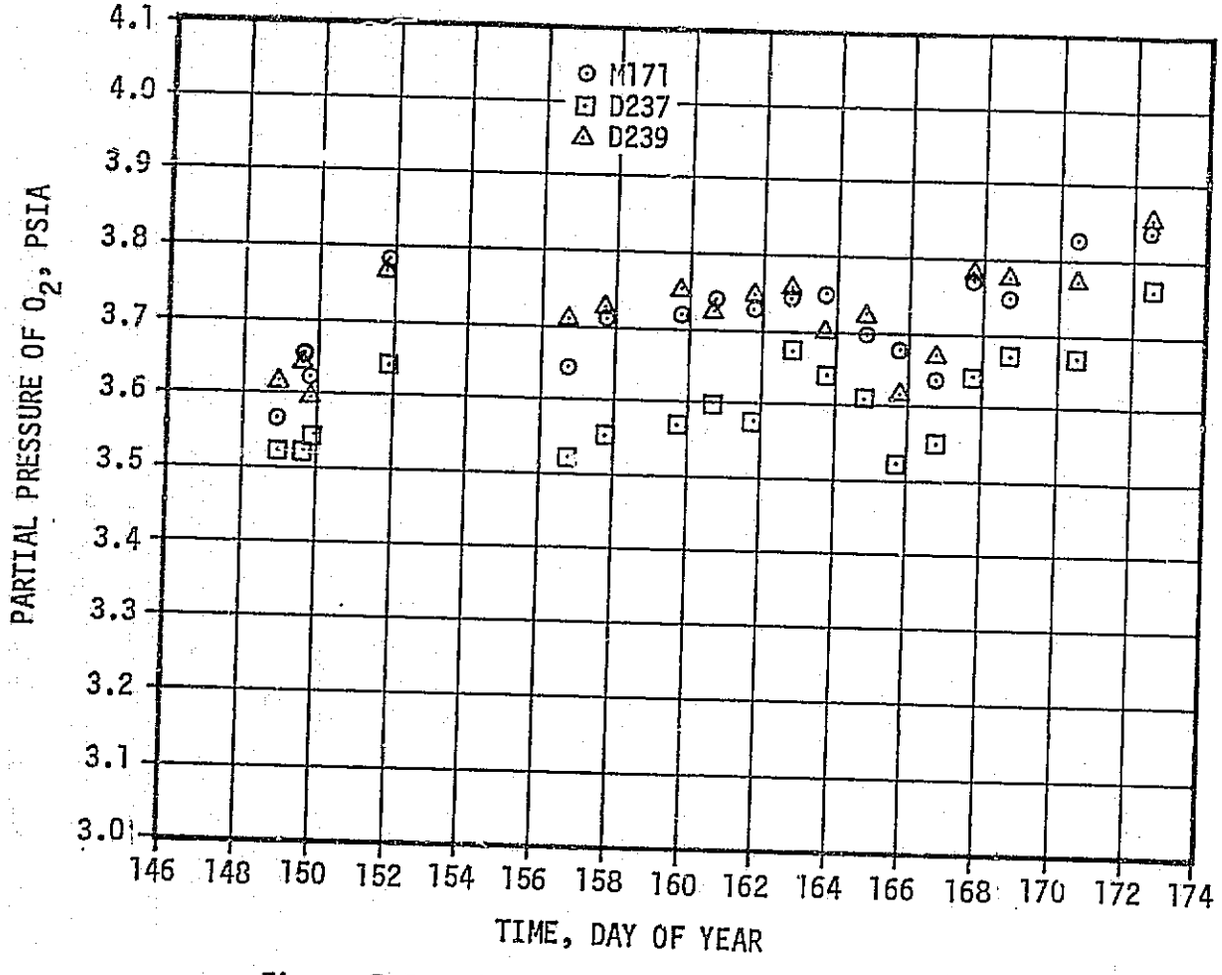

Figure 5-7a. SL-2 M171 - PO_2 Data Comparison

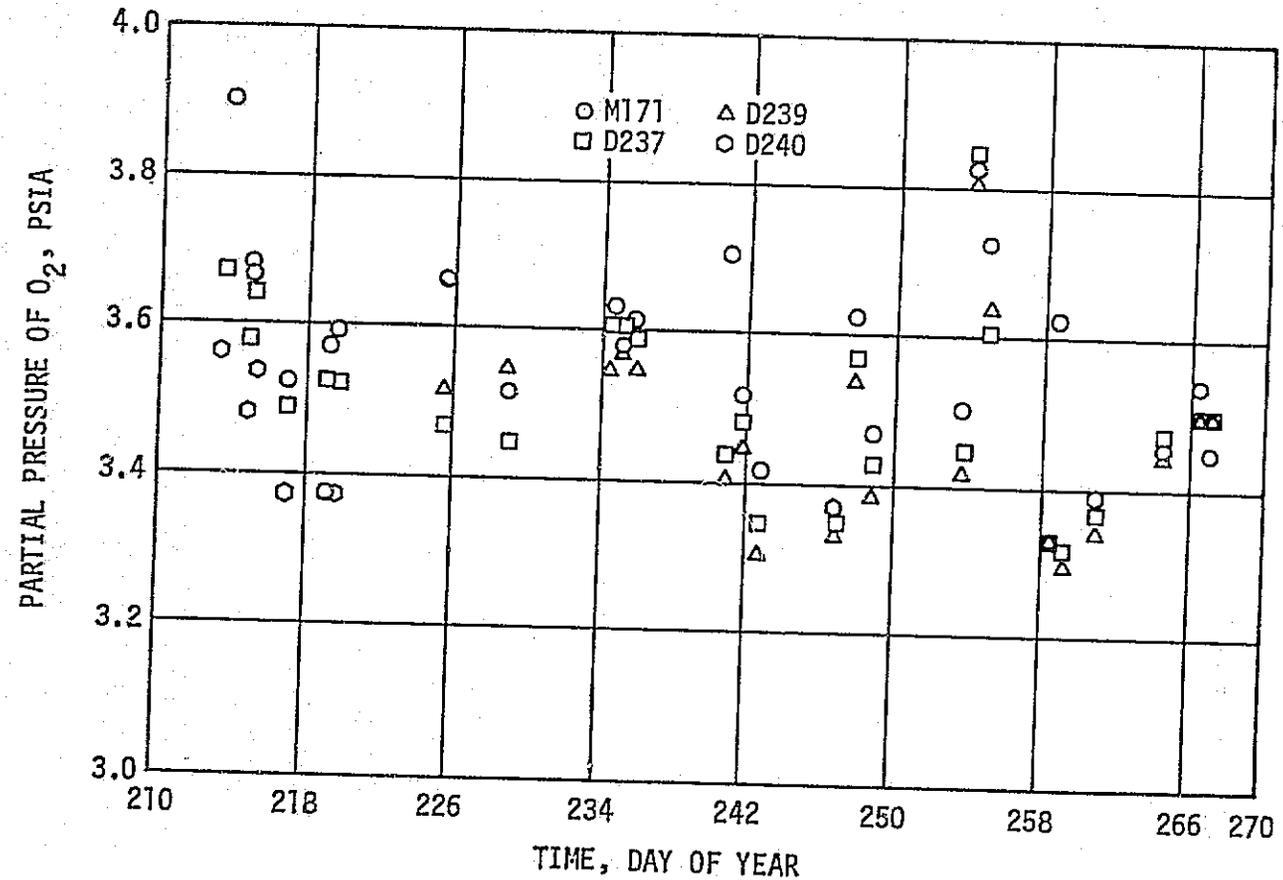

Figure 5-7b. SL-3 M171 - $\dot{W}_{O_2}$ Data Comparison

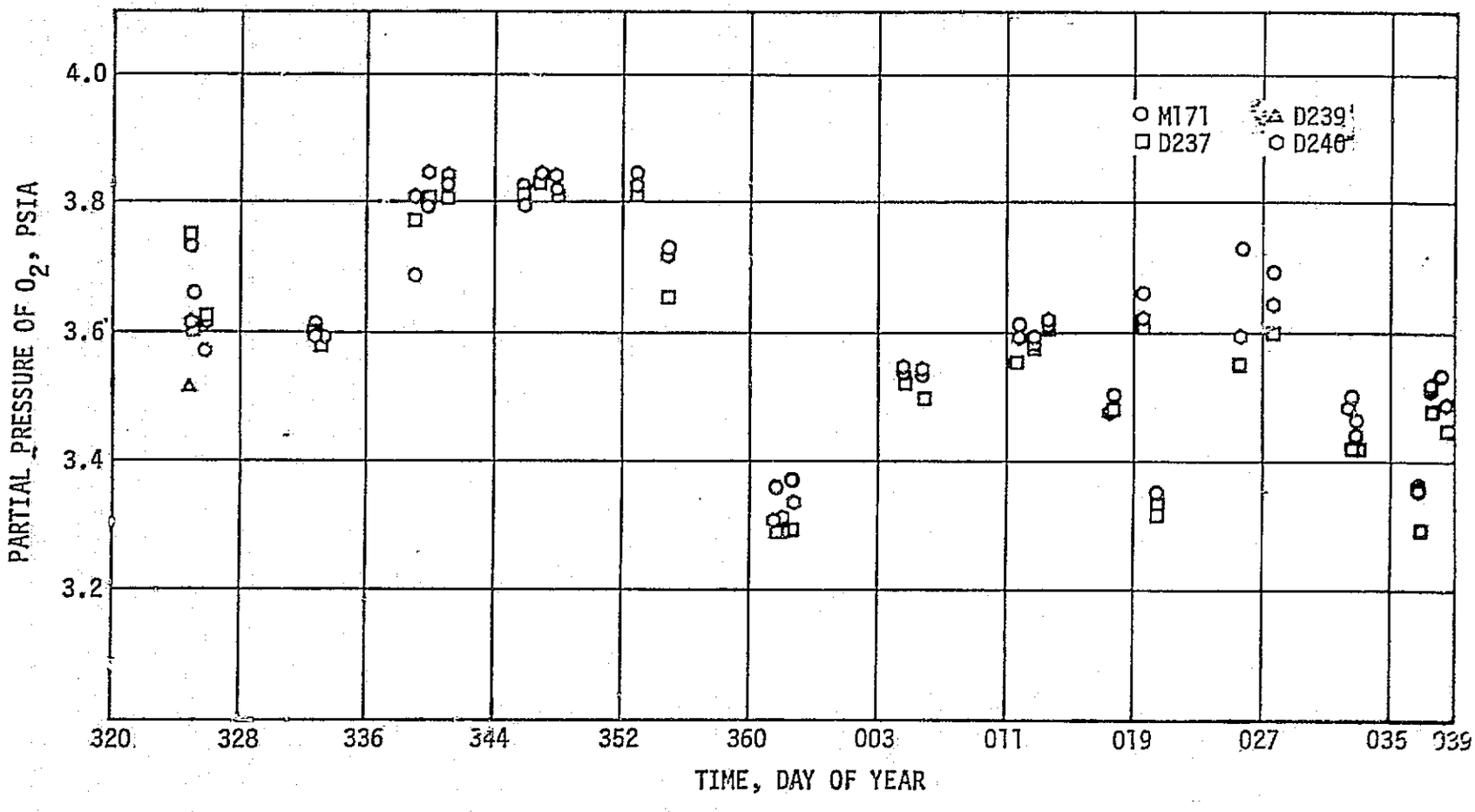

Figure 5-7c. SL-4 M171 - PO_2 Data Comparison

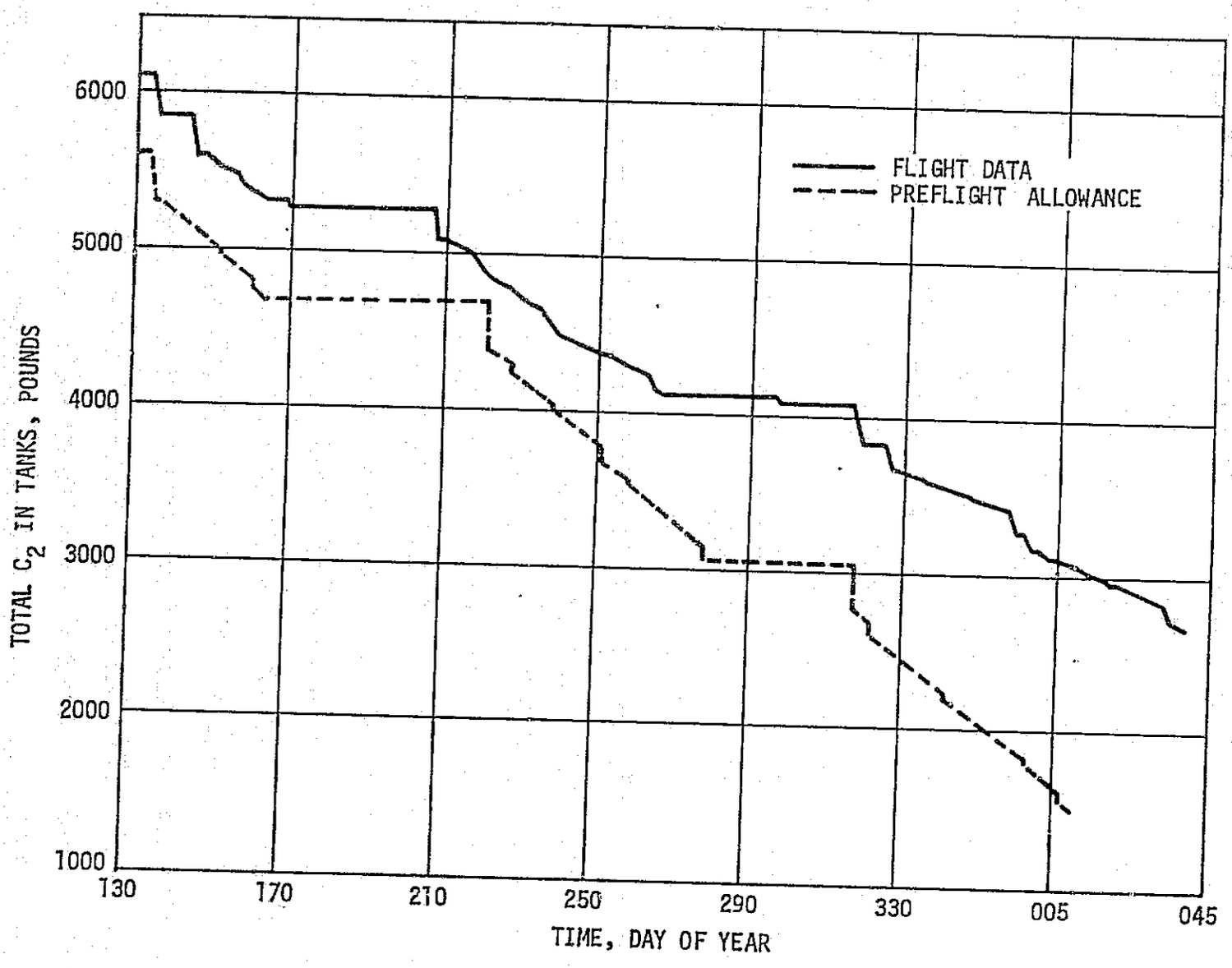

Figure 5-8. Skylab Oxygen Consumables Use Summary

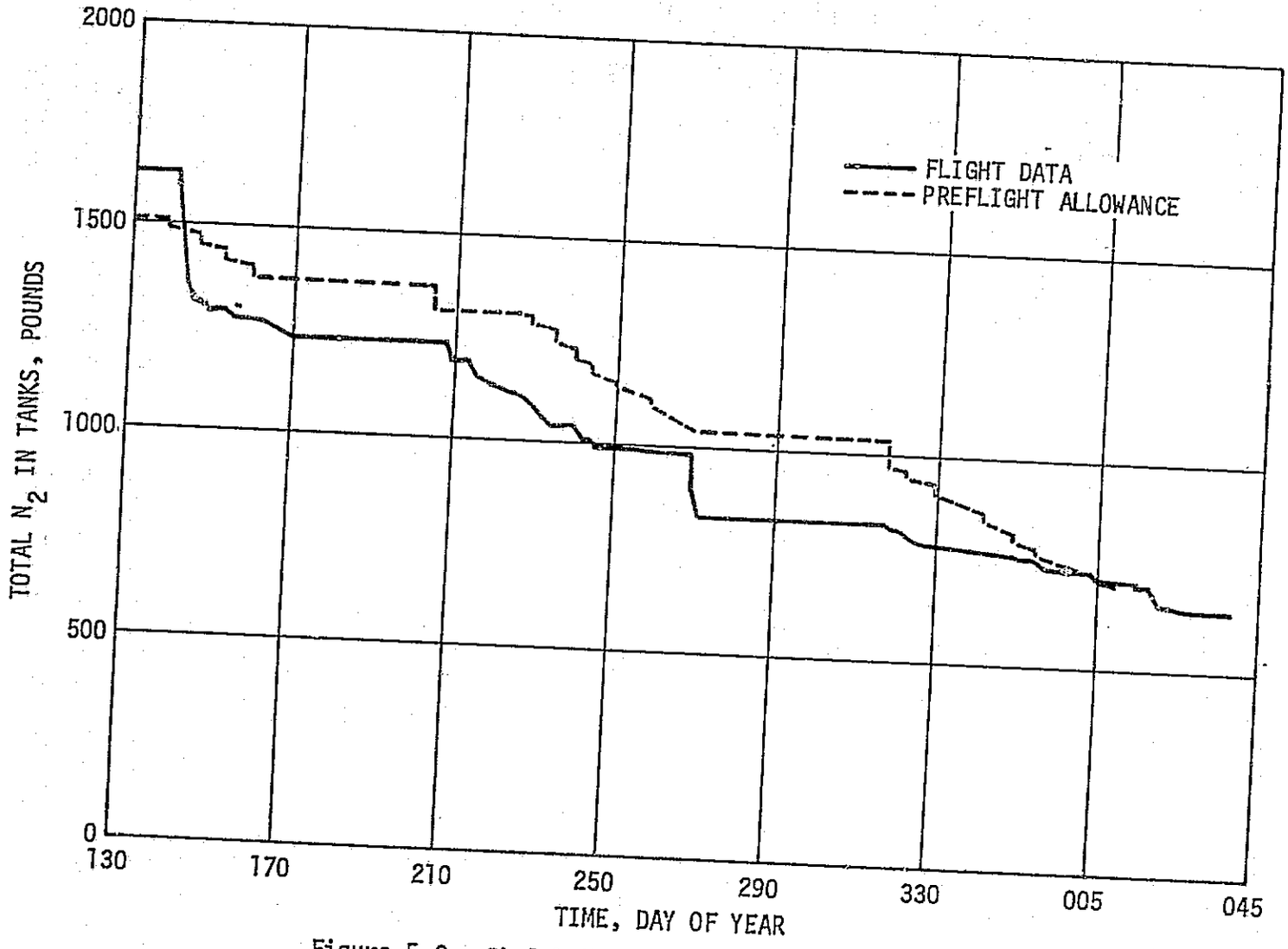

Figure 5-9. Skylab Nitrogen Consumables Use Summary

Table 5.2 O_2/N_2 Consumables Summary

	SL-2		SL-3		SL-4		TOTAL	
	O_2	N_2	O_2	N_2	O_2	N_2	O_2	N_2
PRESSURIZATION	257		222	45	246	12	725	57
SL-1 PURGES	254	329					254	329
GYRO 6-PACK PRESS.					30	159	30	159
METABOLIC	146		324		456		926	
EVA	101		284		420		805	
EVA REPRESSURIZATION	11	4	17	6	23	8	51	18
LEAKAGE (STRUCTURAL, MOLECULAR SIEVE, MISCELLANEOUS)	126	61	221	109	274	165	621	335
M509 VENTS			171	82	8	4	179	86
-CSM POLYCHOKE	-77		-68		-9		-154	
TOTAL	818	394	1171	242	1448	348	3437	984

	O_2	N_2
TOTAL GAS LOADED	6113	1630
TOTAL GAS USED	3437	984
TOTAL GAS REMAINING	2676	646
TOTAL NON-USEABLE	652	177
TOTAL USEABLE REMAINING AFTER SL-4	2024	469

residual N_2 was reduced by 14 pounds, resulting in an increase of usable O_2 of 531 pounds and an increase of usable N_2 of 133 pounds.

The flight data showed that 428 less pounds of O_2 were used than originally allowed, even though the duration of the mission was extended over a month. The data also showed that 214 more pounds of N_2 were used than originally planned. The major differences between preflight specification usage and actual flight usage were due to the extra O_2 and N_2 gas used for purging on SL-2 and the smaller flight leakage. The differences are discussed in more detail in the following paragraphs.

a. Pressurization - A total of 745 pounds of O_2 and 98 pounds of N_2 was allocated for three pressurizations of the Orbital Assembly. A total of 725 pounds of O_2 and 57 pounds of N_2 were actually used.

b. SL-1 Purges - Due to the purge requirements brought about by the high temperatures on the OWS during SL-1, an extra 254 pounds of O_2 and 329 pounds of N_2 were expended during the 10 days between SL-1 and SL-2 launches. Since this was caused by an anomaly, none of this had been allocated in the preflight requirements.

c. Gyro 6-Pack Pressurization - In order to provide cooling to the rate gyro 6-pack during the SL-3/SL-4 storage period the cluster was pressurized with N_2 to 5.0 PSIA (after first being vented to 2.0 PSIA to dry out the atmosphere). In the middle of the storage period the cluster was pressurized back up to 4.5 PSIA with O_2 after leaking down to 4.0 PSIA. This required an extra 30 pounds of O_2 and an extra 159 pounds of N_2.

d. Metabolic - A total of 828 pounds of O_2 was allocated to metabolic requirements (based on a usage rate of 2 pounds per man-day for 138 days). Preflight analyses showed that for the average Skylab metabolic rate of about 440 Btu/hour, 1.84 pounds of O_2 would be required per man-day. The manned mission (MDA hatch opening to closing) was extended to a total of about 168 days and the total metabolic oxygen used was approximately 926 pounds.

e. EVA - A total of 351 pounds of O_2 was allocated for 6 EVAs lasting a total of 19.5 hours. There were actually 9 EVAs lasting a total of about 42.5 hours and 805 pounds of O_2 were used during the EVAs.

f. Airlock Repressurization - A total of 34 pounds of O_2 and 12 pounds of N_2 was allocated to replace the atmosphere vented overboard for each EVA. Three more EVAs than planned were performed, increasing the total gas used to 51 pounds of O_2 and 18 pounds of N_2.

g. Leakage - On SL-3 and SL-4 following the M509/T020 experiments or the M509 atmospheric management when O_2 was added manually to the atmosphere, the cabin pressure regulator would be off for long periods of time. During these periods, there would be only very minor amounts of gas being added to the atmosphere and it was possible to calculate the total amount of gas leaving the cluster atmosphere. Figure 5-10 presents a typical profile showing the decline of pressure during one of the periods. There were 21 such periods during the mission and approximately 11 pounds of gas per day was the average flow rate out of the cluster seen during these periods. However, even though the cabin pressure regulator was off there were still other amounts of gas flowing into the atmosphere. Mole Sieve pneumatic and experiment N_2 were estimated to add about half a pound a day during the mission on the average, and this value must be added to the 11 pounds per day, resulting in a total gas usage rate of about 11.5 pounds per day. This total usage rate consists of gas used for metabolic purposes, gas lost by leakage, gas lost by mole sieve dumps, and gas lost by miscellaneous dumps. Metabolic O_2 use has already been estimated at 5.52 pounds per day, leaving 5.98 pounds per day for leakage, mole sieve dumps and miscellaneous losses.

During the unmanned storage periods it was possible to calculate cluster leakage. Results from the storage periods differed slightly. During the storage period between SL-2 and SL-3 a leak rate of .25 $\pm$ 0.1 lb/day at 2.0 PSIA was calculated resulting in a leak rate of about 1.56 $\pm$ .62 lb/day at nominal cluster conditions (5 PSIA). However, data were clouded during this period by the temperatures affects of the high beta angle. During the storage period between SL-3 and SL-4 a much better leakage profile was obtained and the cluster leakage was calculated to be approximately 2.68 lb/day for nominal cluster conditions (5 PSIA). The CSM leakage, the docked MDA port leakage and molecular sieve dumps were not included in this number. Based on preflight testing, molecular sieve dumps were 2.0 to 2.5 pounds per day.

The total gas used for leakage, mole sieve dumps, and miscellaneous dumps during the mission was 621 pounds of O_2 and 335 pounds of N_2.

h. M509 Vents - A total of 179 pounds of O_2 and 86 pounds of N_2 were expended due to unplanned vents of cluster atmosphere through the wardroom and WMC dump probes to aid in managing the total pressure and O_2 partial pressure. This was necessary since there was not time between M509/T020 performances to allow normal leakage and the cabin pressure regulator to maintain the cluster O_2 partial pressure and total pressure within normal limits.

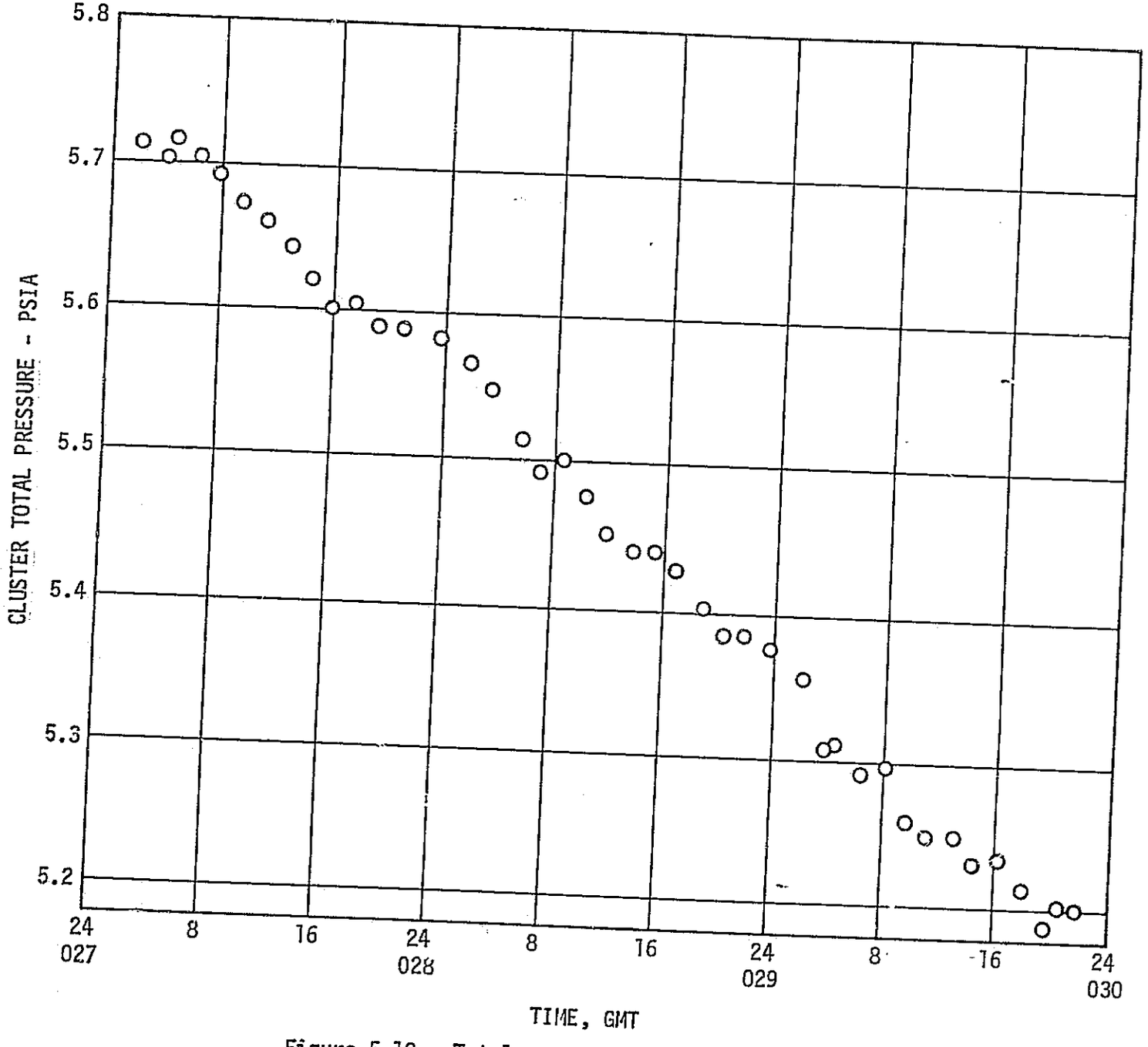

Figure 5-10. Total pressure Decay Profile with Cabin Pressure Regulator Off (MANNED)

i. CSM Polychoke O_2 - About 154 pounds of oxygen from the CSMs were used in the cluster atmosphere. None of this amount had been included in preflight allocations, even though it had been known that some O_2 from the CSMs would be available.

5. 150 PSIG N_2 Regulator Outlet Pressure Decreased - During SL-2, it was noted that the 150 PSIG regulator outlet pressure (D205) was decreasing. It had dropped from 160 PSIA on DOY 149 to 140 PSIA on DOY 165. (Reference figure 5-3). On DOY 167 the crew verified that both N_2 regulator toggle valves were open and the onboard meter was reading 140 PSIA. Telemetry also read approximately 140 PSIA. No further decrease was seen during the first manned mission. When the Mole Sieve was deactivated on DOY 173 the outlet pressure began to increase and was 175 PSIA by DOY 176 at which time lines downstream of the regulator were vented to 4 PSIA.

At SL-3 activation (DOY 209) the N_2 regulator outlet (D205) was 158 PSIA. By DOY 218 the pressure had dropped to 150 PSIA. The pressure continued to drift downward until it was 141 PSIA on DOY 236. During EVA on DOY 236 the pressure increased to 145 PSIA. The reason for this is unknown. The pressure decreased to 141 PSIA the following day.

Since terminating the N_2 regulator flow had somehow restored the outlet pressure at the end of SL-2, it was decided to close one regulator toggle valve and leave it closed for five days in an attempt to increase the outlet pressure. On DOY 237 toggle valve A was closed. Five days later on DOY 242 the regulator outlet pressure was 140 PSIA. At that time, toggle valve A was opened and toggle valve B was closed. The regulator outlet pressure immediately increased to 155.5 PSIA. By DOY 247 (5 days later) D205 had decreased to 151 PSIA. Toggle valve A was closed and valve B opened. The regulator outlet pressure fell immediately to 148 PSIA. Five days later (DOY 252) the outlet pressure had decreased to 145 PSIA. Toggle valve B was closed and toggle valve A was opened and the pressure increased to 155.5 PSIA. It was decided that rather than switch toggle valves every 5 days, they would be switched when the N_2 regulator outlet pressure approached the O_2 regulator outlet pressure. By deactivation (DOY 268) the pressure had decreased to 146 PSIA. When the Mole Sieve Supply was closed the regulator outlet pressure increased to 165 PSIA.

At SL-3 deactivation, both toggles A&B were opened per procedure. The Supply solenoids were closed and the regulator pressure slowly drifted down as the system leaked during storage. The toggle valve configuration was not changed during SL-4 activation. On DOY 326 toggle valve A was closed. By DOY 352 the pressure had drifted only from 155 PSIA to 148 PSIA. On this day the crew inadvertently closed the open toggle valve (B). When they reconfigured the system they

opened A. The pressure went up to 160 PSIA. By DOY 005 the pressure had drifted to 150 PSIA and by the end of the mission (DOY 039) the pressure was still 150 PSIA.

The above chronology describes the onboard troubleshooting. In addition, ground tests were run to try and duplicate the regulator characteristics. These included low demand and moisture tests, but the symptoms were not reproduced. The reason for the drift in outlet regulator pressure has not been established. The O_2 regulator is mechanically very similar but did not display these drift characteristics.

6. Oxygen Bottle #6 Temperature - Four times during the mission as the beta angle approached $\pm$ 60 degrees, Oxygen Bottle #6 exceeded its qualification limits of 160 deg. F. Analysis indicates that bottle #6 reached 208°F on DOY 176, 170°F on DOY 234, 214°F on DOY 324 and 225°F on DOY 017. Figure 5-11 shows bottle #6 temperatures and the beta angle-vs-time. Bottle #6 is mounted inside and onto the Fixed Airlock Shroud, 30 deg. off the vehicle +Z axis (+Z toward Sun during Solar Inertial Attitude).

Investigation indicated that no problem existed based on the following:

(a) The glass resin system is cured at 320 deg. F three times for one day durations.

(b) The manufacturer had tested tanks with the same resin systems and a similar glass at 275 deg. F, cycling 0-3000 PSIA for for 5,000 times.

(c) The maximum tank #6 pressure was 2400 PSIA, and tank was proof tested to 7500 PSIA.

(d) No pressure cycling of tank #6 occurred. (Cycling is worse case condition for tank fatigue).

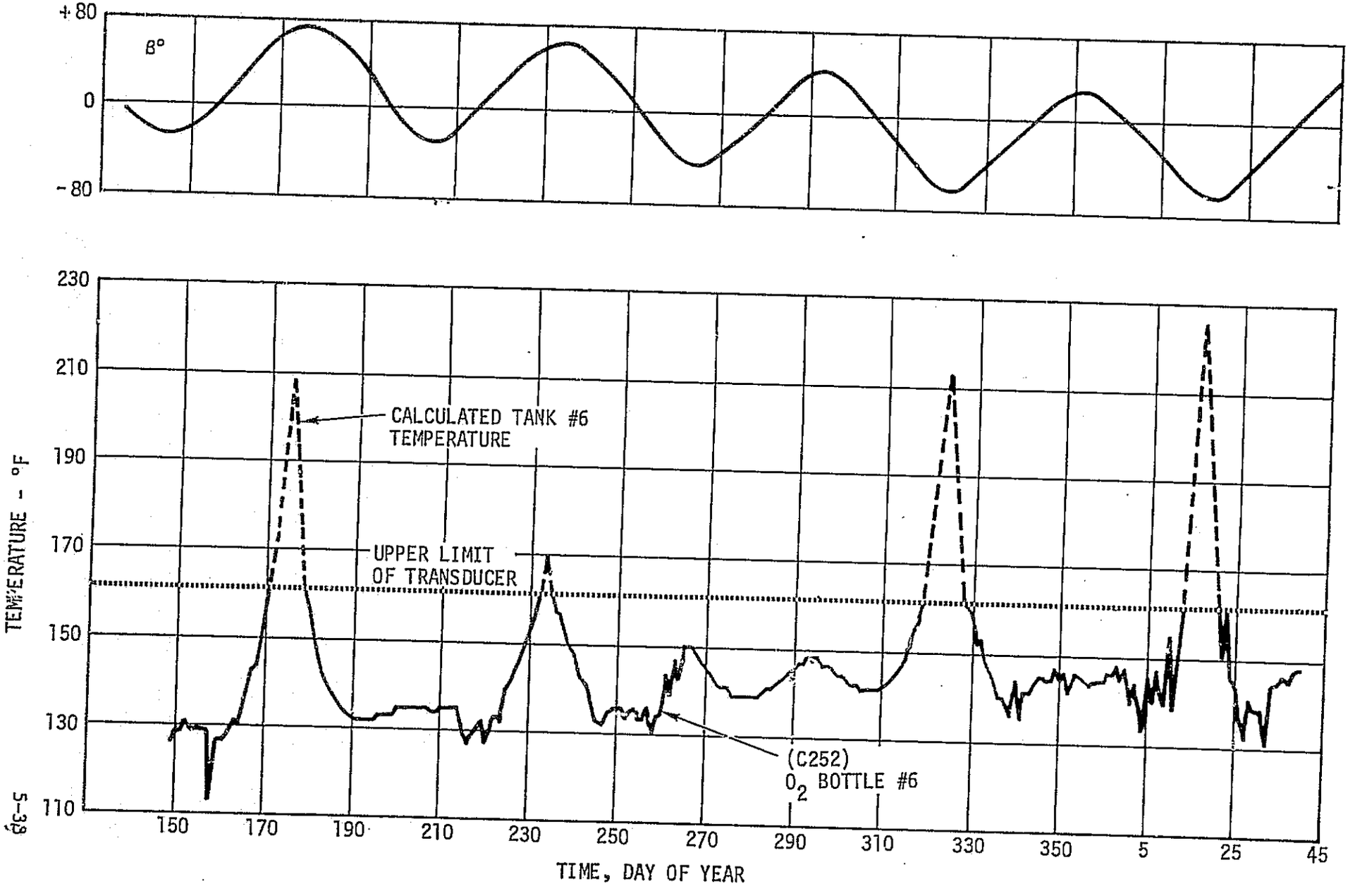

Figure 5-11. O_2 Bottle #6 Temperature

SECTION VI. SKYLAB PRESSURIZATION/DEPRESSURIZATION

A. Configuration

The major components and subsystems of the Depressurization System and their locations are shown on figure 6-1. A functional description of each is provided below. The Pressurization System is depicted in figure 5-1.

1. Waste Tank Vent System - The Waste Tank Vent System consisted of two short vent ducts, with pneumatically actuated caps, penetrating the waste tank 180 degrees apart to achieve non-propulsive venting. At the time of venting, two redundant pneumatic actuators released the caps. Activation of the actuators was performed by applying pneumatic pressure from an actuation control module and pneumatic sphere. After orbital insertion, the switch selector sent the commands to release the vent caps. The waste tank was vented to vacuum. Once opened, the waste tank vents could not be closed. Three pressure sensors in the waste tank were used to monitor performance of the vent system.

After the waste tank was vented it provided a vacuum source for (a) the OWS water system activation, deactivation, and washcloth squeezer operations; (b) waste processing; (c) lower body negative pressure (LBNP) device*; (d) the OWS condensate holding tank dumping operation; (e) the OWS backup urine dump operation; and (f) the refrigeration pump container evacuation. These systems that vented into the waste tank are shown on figures 6-2 and 6-3.

* The LBNP originally vented overboard but the SL-4 crew installed a line to the waste tank to eliminate the propulsive effects of the overboard vent.

2. Habitation Area Vent Valve System - The Habitation Area Vent Valve System consisted of a pair of parallel-redundant, normally closed, pneumatically actuated vent and relief valves used for ground operation and initial blowdown. The pneumatic valves were identical to those used on the Saturn S-IVB except for a reduced relief setting. These valves provided relief protection for the habitation area during launch and also provided for rapid blowdown of the habitation area. The vent valves passed gases into two equal-length wrap-around ducts, each of which terminated in an oritice plate at the forward skirt. The orifice plates were directed 180 degrees apart so that venting was non-propulsive.

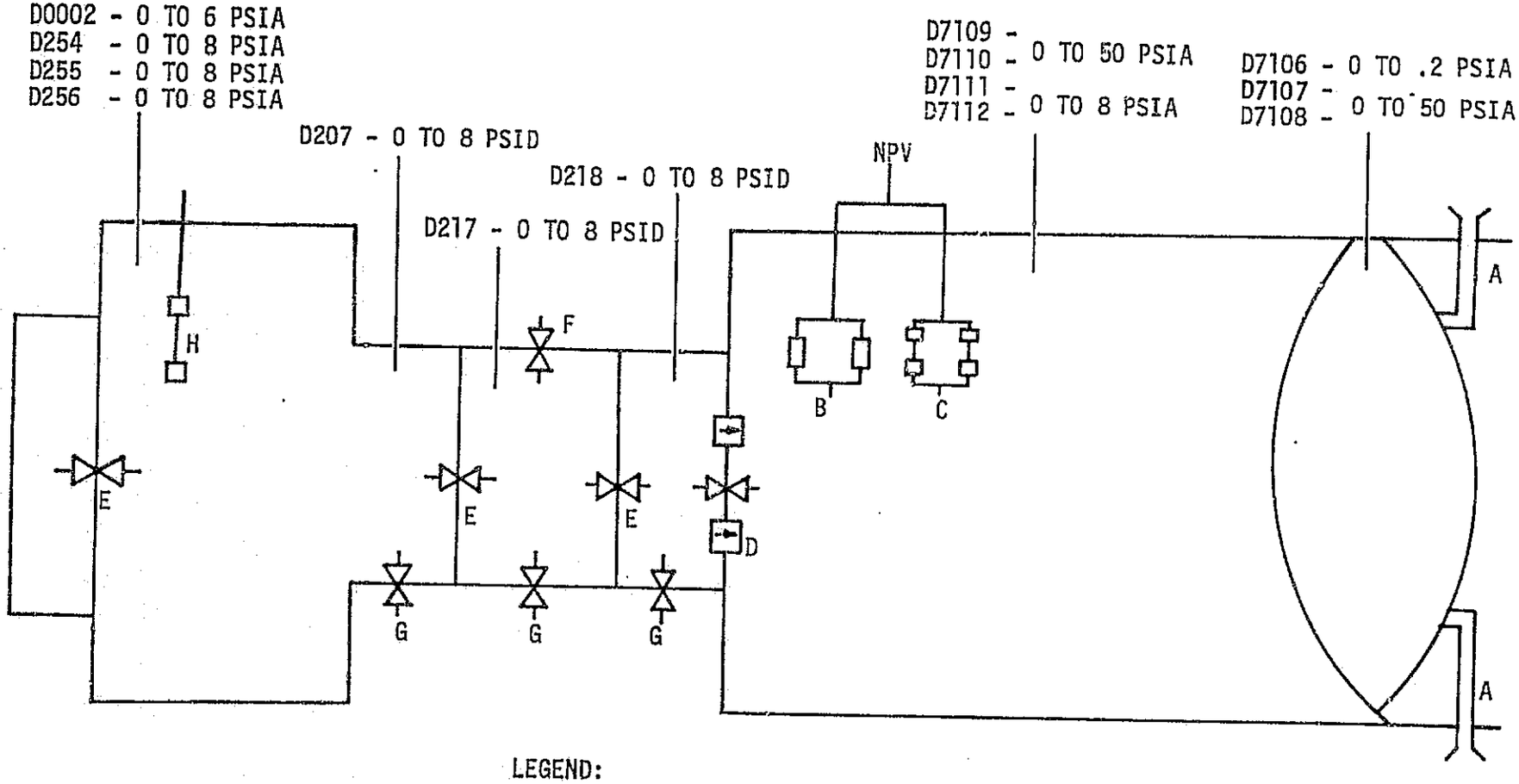

LEGEND:

A - WASTE TANK VENT

B - HABITATION AREA VENT VALVES

C - SOLENOID VENT VALVES

D - OWS CHECK & EQUALIZATION VALVES

E - EQUALIZATION VALVES

F - AM LOCK DECOMPRESSION VALVE

G - AM CABIN PRESSURE RELIEF VALVES

H - MDA VENT VALVES

Figure 6-1. Cluster Depressurization Systems

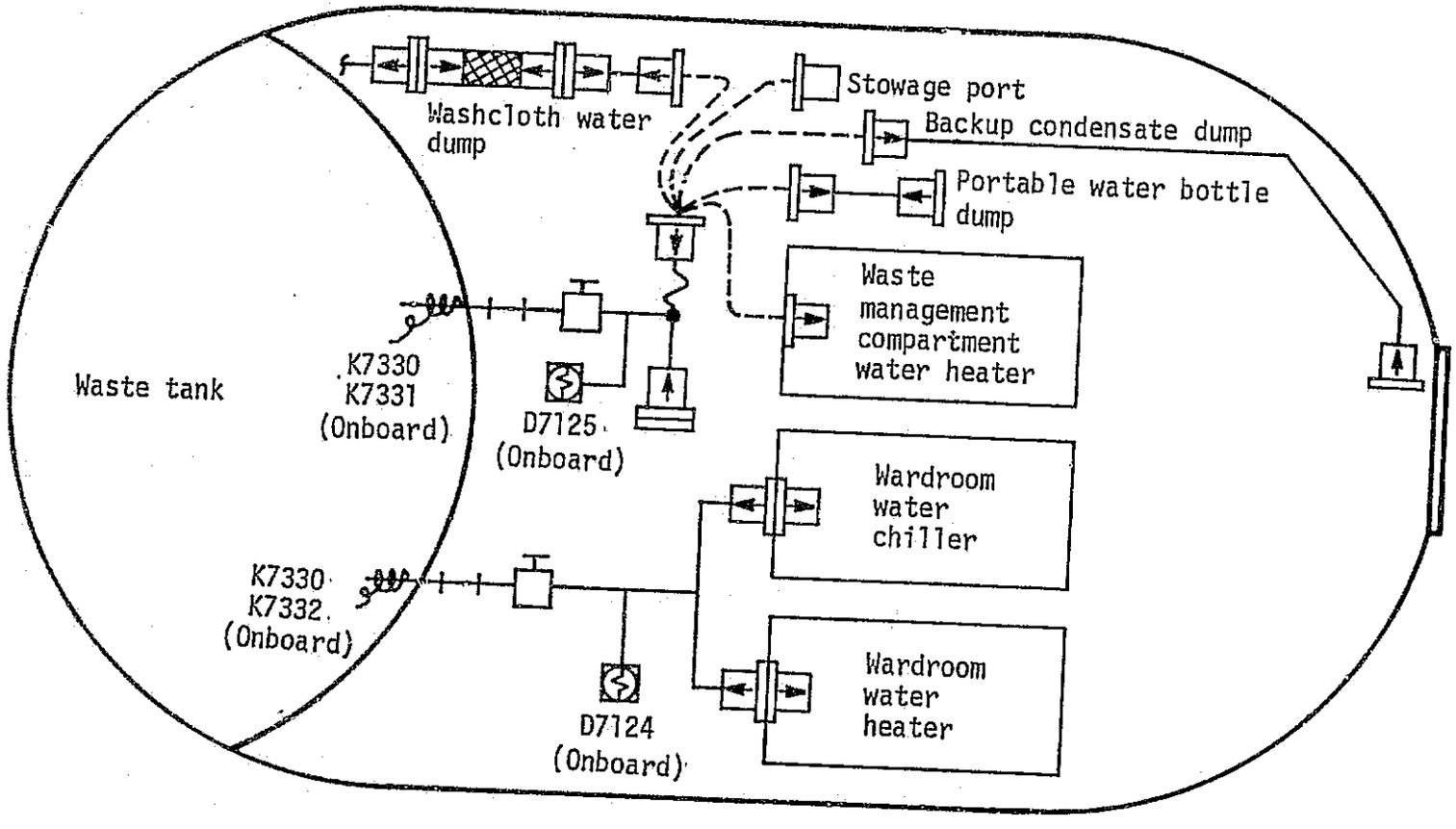

Figure 6-2. OWS Vacuum Subsystems

Note: Line from LBNP to waste tank was added by SL-4 crew.

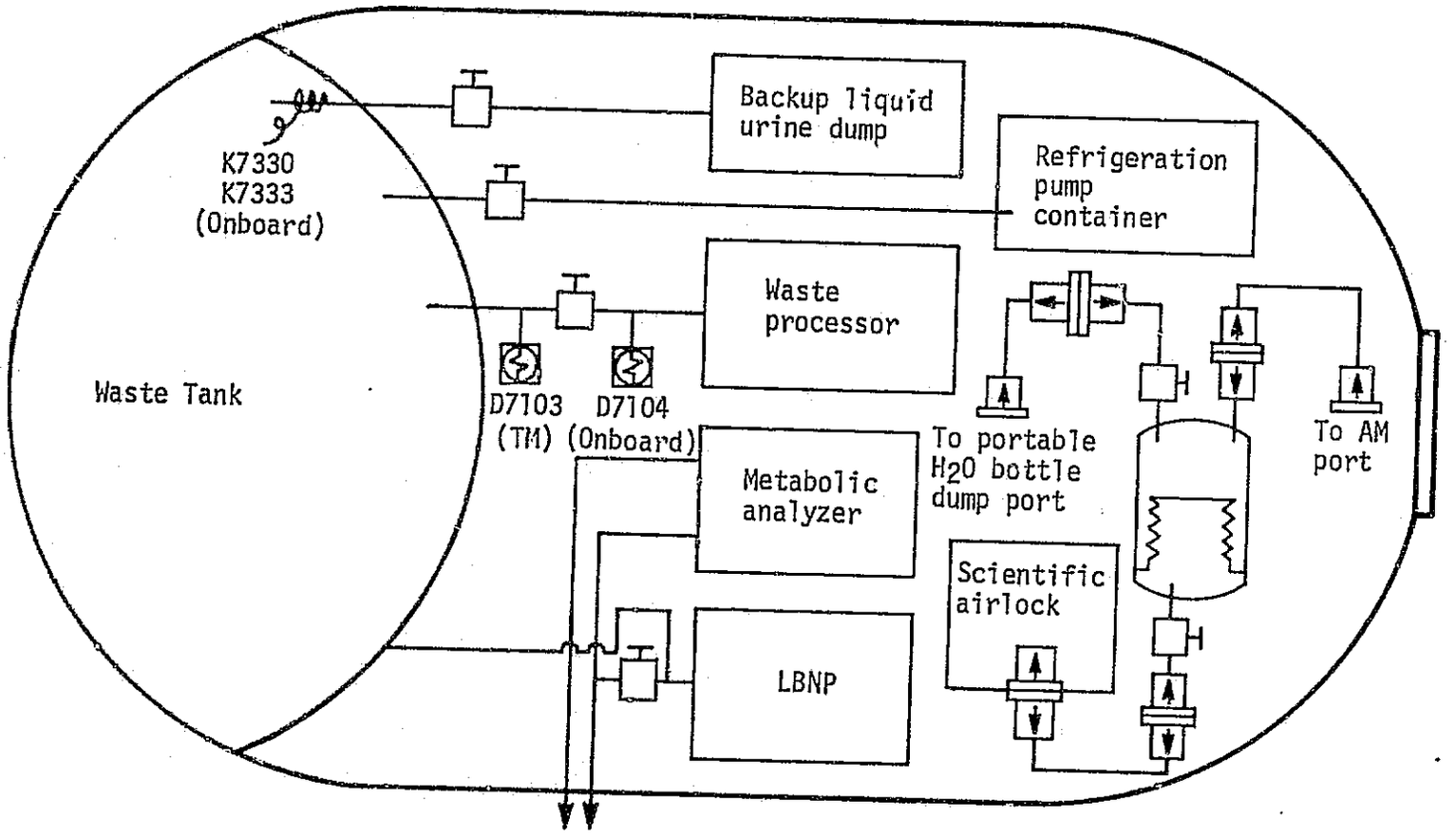

Figure 6-3. OWS Vacuum Subsystems

The command venting function of the pneumatic valves was operated by the IU command system through the OWS switch selector to the actuation control module. The OWS initial venting sequence was set up to provide at least 22 PSIA in the habitation area at max. q (maximum dynamic pressure) and to protect the habitation area/waste tank common bulkhead from the effects of a waste tank vent failure at lift off. Both habitation area vent valves were commanded open by the IU at 205 seconds after lift off. Four pressure sensors in the habitation area were used to monitor performance of the vent system. Open/close indicators were also available via telemetry to monitor valve position. A sealing device was installed in the pneumatic vent port by the SL-2 crew during cluster activation.

3. Solenoid Vent Valve System - The quad-redundant solenoid valves provided the capability for venting of the habitation area by ground action. These valves could be commanded open or closed by the AM DCS. The port for the solenoid valves could be covered with a sealing device during habitation periods. At termination of each mission, the solenoid vent valves were commanded open to vent from 5 PSIA to 2 PSIA to prevent condensation during storage.

Two pressure sensors in the habitation area were used to monitor performance of the vent system when the OWS hatch was closed. When the OWS hatch was open seven sensors in the cluster were available. Open/close indicators were available to monitor valve positions via telemetry.

4. OWS Check and Equalization Valves - Redundant check valves were located in the OWS hatch to prevent the AM aft lock compartment pressure from exceeding the OWS habitation area pressure by more than 0.3 PSID. The check valves protected the forward dome from excessive reverse pressure during pre-launch and the initial orbital pressurization sequences. An equalization valve was manually opened to equalize pressure between the AM and OWS during initial activation and for each EVA.

5. MDA/AM Hatch Equalization Valves - An equalization valve was mounted on each of the two AM internal hatches and one located on the EVA hatch. These valves provided the capability to manually evacuate the lock compartment prior to EVA and then, in conjunction with the OWS hatch equalization valve, equalize the pressure in the tunnel sections after completion of the EVA activities. The internal hatch valves equalized pressure between AM compartments during ascent and pressurization periods. Equalization valves were also provided in the MDA hatches, one of which was used to equalize MDA/CSM pressure prior to MDA hatch opening for each mission.

6. Cabin Pressure Relief Valves - Three cabin pressure relief valve assemblies were located in the AM. There was one valve assembly each in the aft, forward, and lock compartments. The purpose of these relief valves was to eliminate the possibility of cabin overpressurization. The maximum total pressure was limited by these valves to 5.65 PSIA within the limits of their flow capabilities. There was also a cabin relief valve assembly in the CM which was designed to open at approximately 6.2 PSIA. Each valve assembly contained two pressure relief valves in parallel. Manual shut off provisions were also available on both assemblies.

7. MDA Vent Valve System - The MDA vent valves consisted of two 4-inch motor operated vent valves mounted in series. The vent valves provided a means of venting the MDA atmosphere during launch, ascent, and the initial phase of the mission. The series arrangement of the valves provided a redundant capability to ensure that the valves closed before the MDA vented to hard vacuum. The valves were opened prior to launch and were closed by IU automatic sequencing during ascent at 288 seconds after lift off.

Open/close indications were available to monitor MDA vent valve position and four pressure sensors in the MDA/AM were used to monitor performance. A sealing device was installed on the MDA vent valves port during SL-2 activation.

8. Pressurization System - The pressurization system (figure 5-1) was located in the Airlock Module and consisted of four sets of solenoid valves and interconnecting flow lines. The valves could be ground controlled through the AM DCS or manually operated by the astronauts. This system allowed the MDA/AM/OWS to be pressurized as a unit or separately with O_2 or N_2 or an O_2/N_2 mixture. Pressurization was automatically terminated by pressure switches in the AM and OWS at 5 ± 0.2 PSIA if the pressurization was by ground control. Up to nine pressure sensors in the OWS and MDA/AM were used to monitor pressurization system performance.

B. System Performance

1. Waste Tank Vent System - The waste tank vent system requirements were to decrease the waste tank pressure to near vacuum conditions after orbital insertion and thereafter provide continuous venting of the waste tank to allow for waste collection. The waste tank vent operation was normal and close to predictions as shown on figure 6-4. The waste tank pressure had decreased to .02 PSIA 40 minutes after vent cap release. All dumps into the waste tank during the manned portion of the mission were successfully completed.

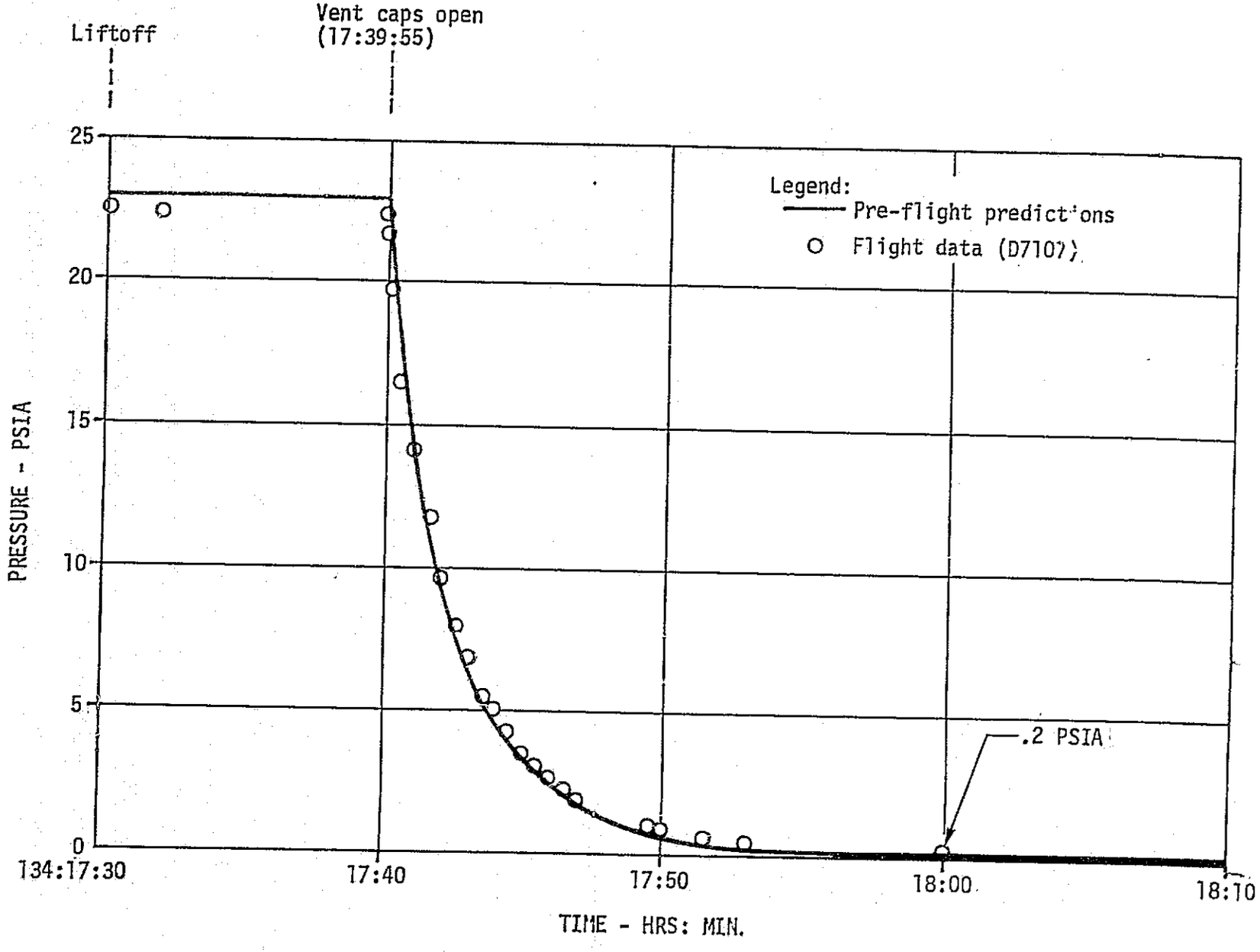

Figure 6-4. Waste Tank Vent Operation

It was desired to maintain the waste tank pressure below the triple point pressure of water in order to preclude free water from being vented overboard, forming ice crystals and thereby causing contamination of the optical environment surrounding Skylab. On three occasions waste tank pressure sensor D7106 indicated that the tank pressure had exceeded the triple point pressure. The events which produced the high pressure indications were: (1) SL-2 activation, wardroom chiller purge (figure 6-5), DOY 147:16:20; (2) SL-2 condensate holding tank dump (figure 6-6), DOY 167:15:50; and (3) SL-3, troubleshooting of waste management compartment water dump heater probe assembly (figure 6-7), DOY 242:18:35. On the three occasions in question, the waste processor exhaust pressure sensor (D7103), which also records waste tank pressure, approached but did not exceed the triple point pressure. However, this sensor was located in a line upstream of the waste tank and exhibited relatively slower response times than the waste tank sensor, D7106. Although some uncertainty exists due to sensor inaccuracy, it is probable that the pressure actually exceeded the triple point pressure. No evidence of optical contamination was observed during the specified time period.

2. Habitation Area Vent Valve System - The habitation area vent valve system operated normally and achieved all system requirements. Pressure relief protection was provided during pre-launch and launch so that the maximum pressure of 26 PSIA was not exceeded. These relief valves did not crack during pre-launch or launch. The habitation area pressure at max. q was 22.78 PSIA which was above the minimum level of 22 PSIA. The habitation area vent was nominal and close to predictions as shown on figure 6-8. The pressure at the end of the vent was 1.13 PSIA as compared to the predicted value of .93 PSIA at valve closure. It was required that the pressure control system pneumatic sphere be vented to approximately 35 PSIA after utilization of the system was complete to prevent inadvertent opening of the habitation area pneumatic vent valves and for astronaut safety. The pneumatic sphere vent was nominal as shown on figure 6-9. The habitation area vent system performance achieved all requirements and was close to pre-flight predictions.

3. Solenoid Vent Valve System - The system requirement was to provide a means to vent the cluster by ground command. It was intended that the primary use of this system would be to perform the pre-storage blowdown at the end of each mission. Loss of the meteoroid shield during boost caused high OWS temperatures with suspected offgassing of contaminants from the OWS polyurethane foam. A vent/repressurization scheme utilizing the solenoid vent valves to vent was initiated to purge the OWS habitation area of these contaminants prior to SL-2 crew entry. Five vent/repress

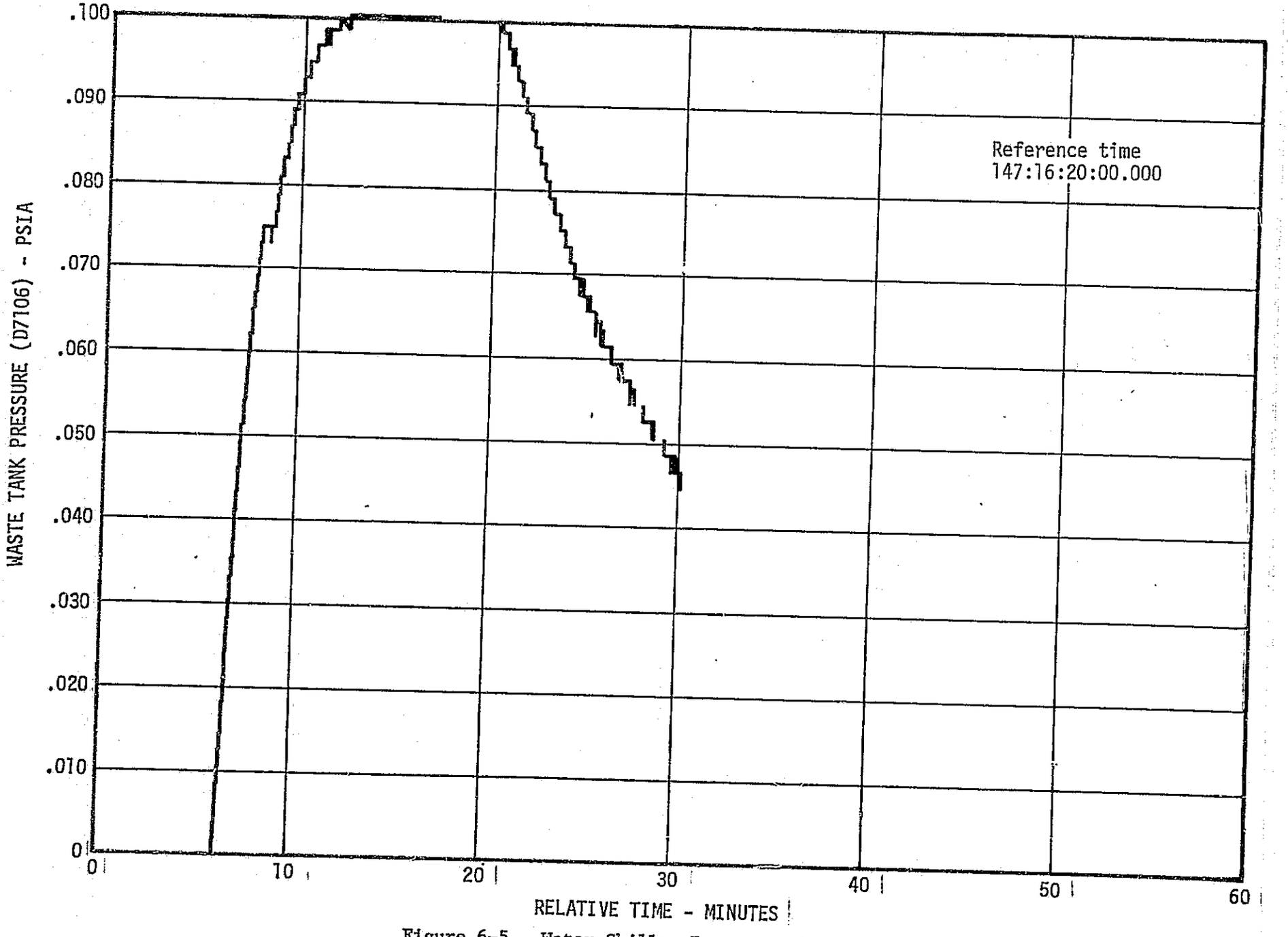

Figure 6-5. Water Chiller Purge, SL-2 Activation

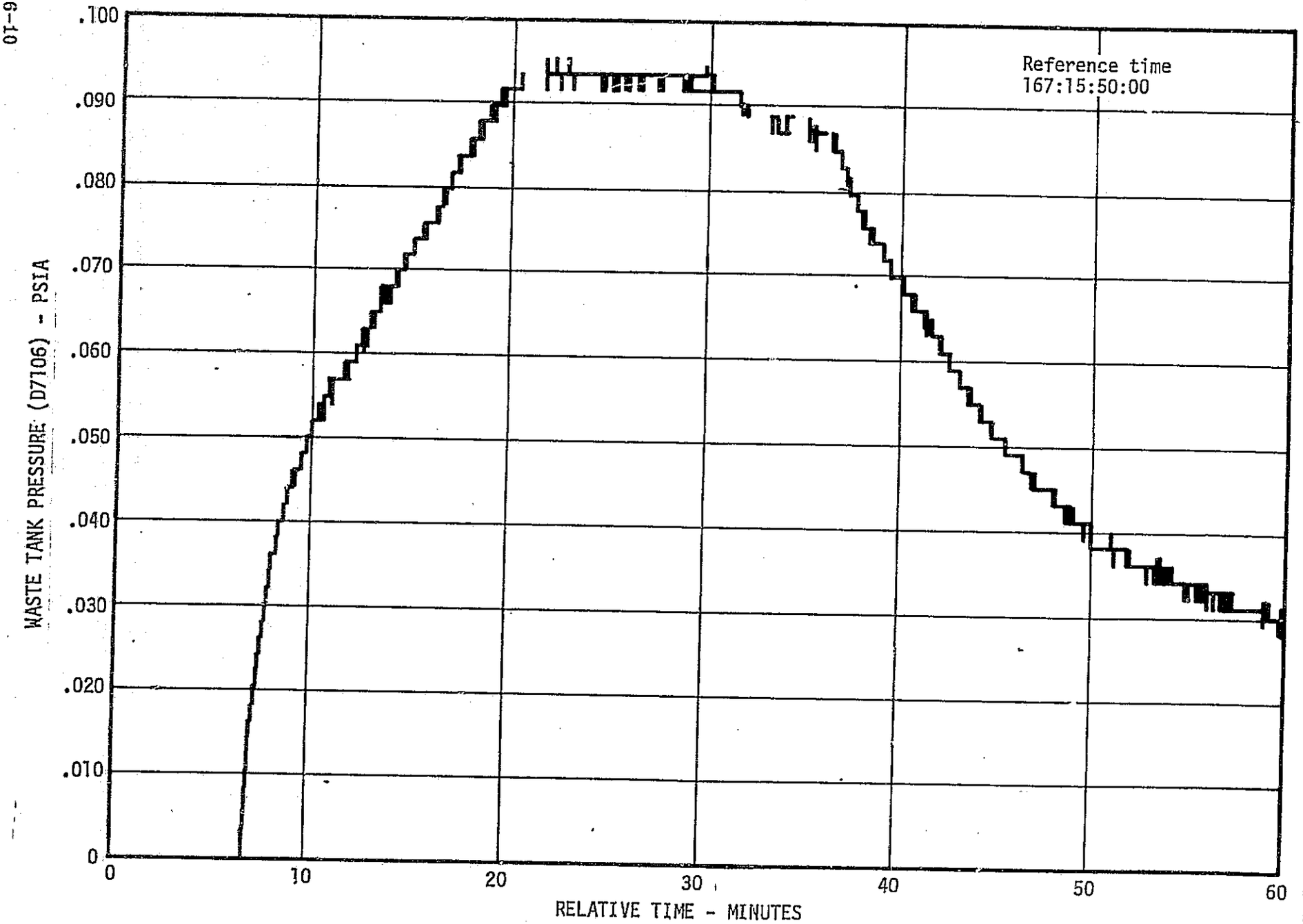

Figure 6-6. Condensate Holding Tank Dump

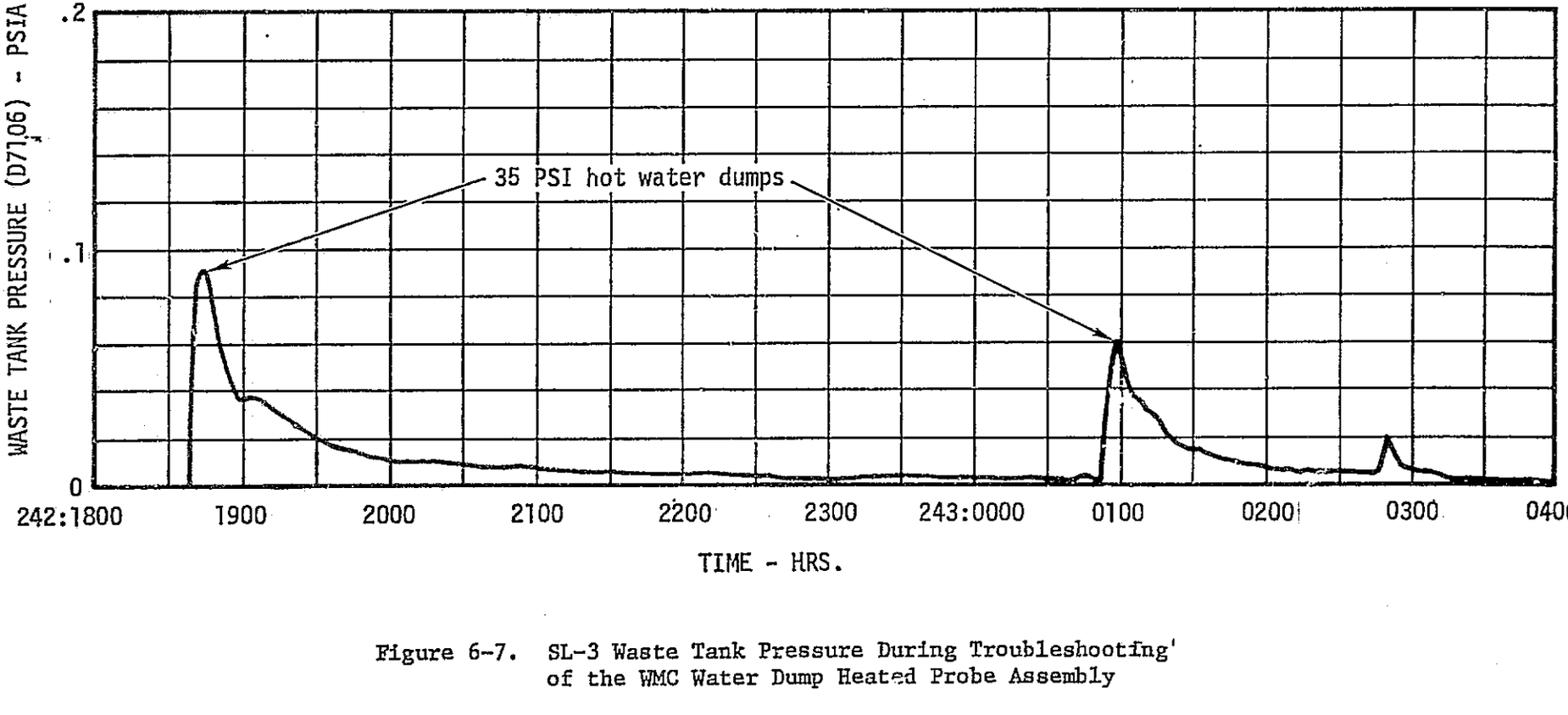

Figure 6-7. SL-3 Waste Tank Pressure During Troubleshooting of the WMC Water Dump Heated Probe Assembly

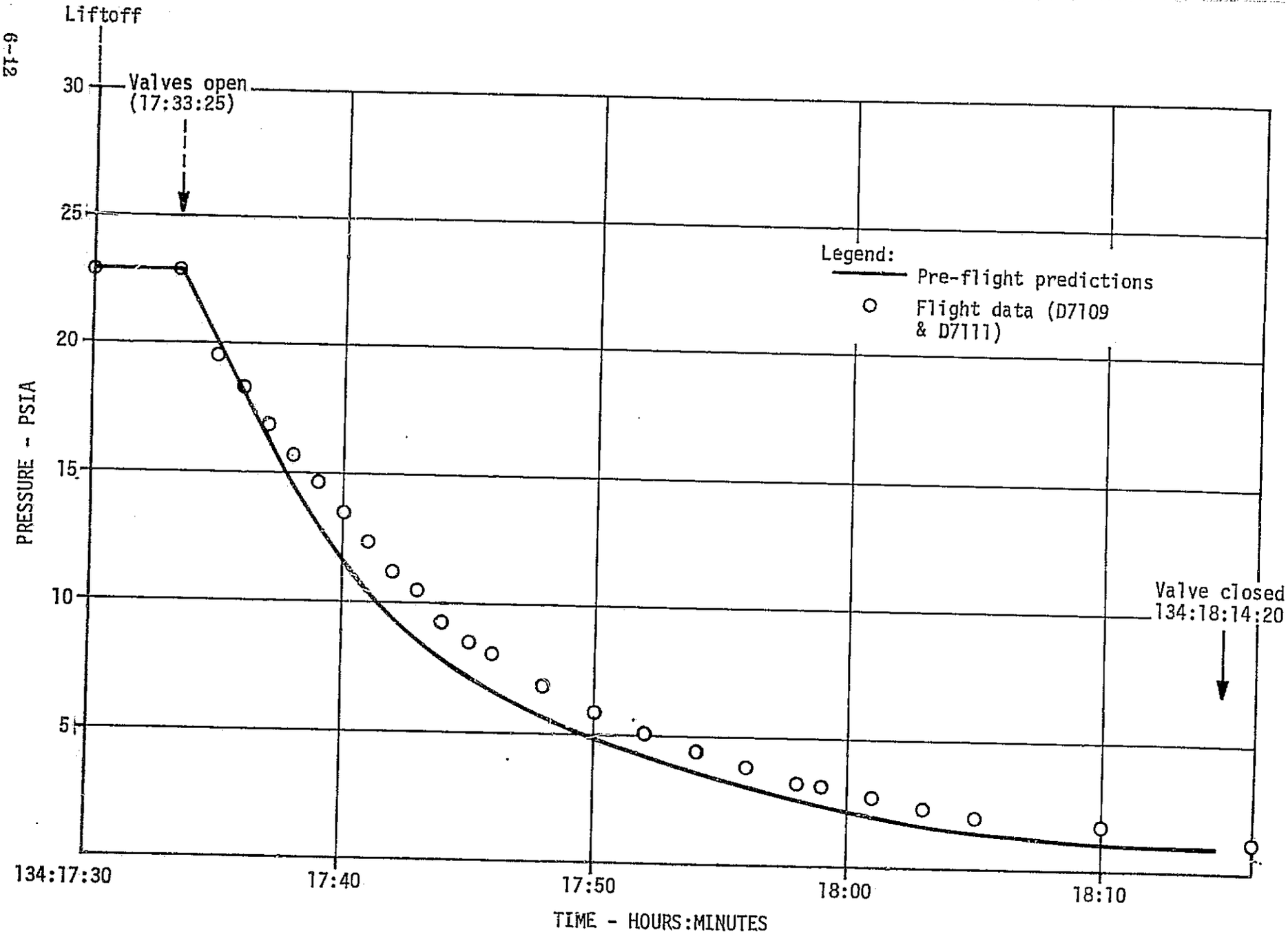

Figure 6-8. Habitation Area Vent Valve Operation

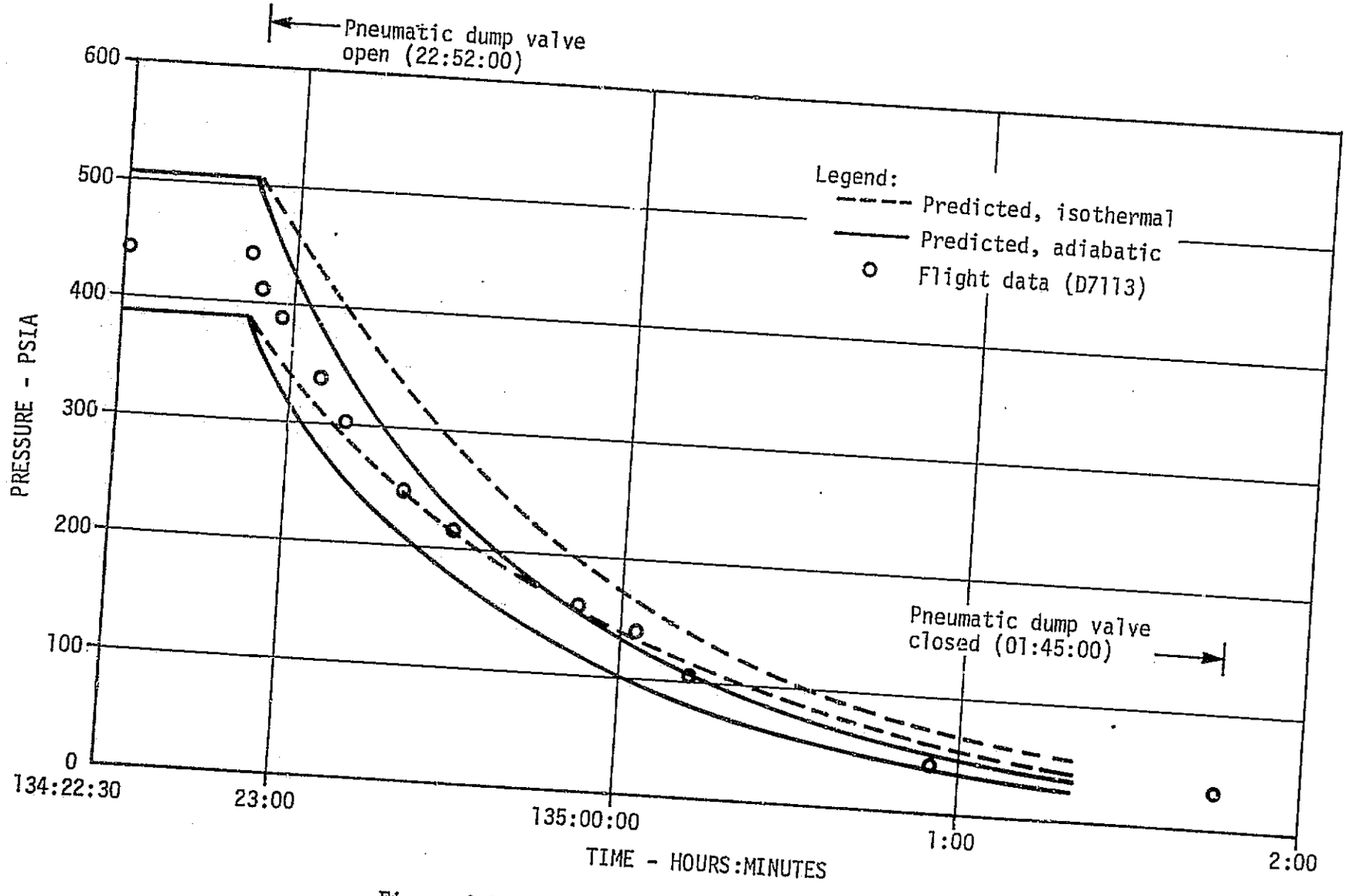

Figure 6-9. Pneumatic Sphere Operation

sequences were accomplished between DOY 138 and DOY 146 for this purpose. This vent sequence is depicted in figure 6-10.

At 138:20:58 and again at 139:07:19 solenoid valve venting was terminated (until better ground coverage was available) because it appeared that a vehicle roll condition was being caused by the propulsive effect of the vent. However, it was later concluded that the vent was not causing the vehicle roll condition. The vent system was designed to be non-propulsive.

During the depress/repress cycles preceding SL-2 launch, it was observed that the depressurization time increased with successive vents. The effective flow area of the system decreased as shown in figure 6-11. It was theorized that debris was being pulled up into the vent valve inlet screen and was obstructing flow. This was verified by both the SL-2 and SL-3 crews when they examined the vent valve screens. During both the SL-2 and SL-3 mission the crew vacuumed the inlet screen with an increase in effective vent area noted on both occasions as shown on figure 6-11. After vacuuming, the solenoid vent valve system performed close to pre-flight predictions for the pre-storage blowdowns as shown on figure 6-12.

At 146:01:47 following the final vent prior to SL-2, venting was terminated by sending solenoid vent valve close commands. A "close" indication was received for valves 2 and 4, but not for valves 1 and 3. Since valves 1 and 3 are in series with 2 and 4 and since the Skylab pressure did not show a decrease, a decision was made to delay troubleshooting until late in the SL-2 mission. Troubleshooting of valves 1 and 3 was carried out at 162:13:26 as shown below:

1. Valves 1 and 2, 3 and 4 opened - crew noted flow through the valves.

2. Valves 1 and 3 closed - No flow was noted by the crew and valve 1 and 3 discrete showed closed.

3. Valves 2 and 4 closed - No flow was noted by the crew and valve 2 and 4 discrete showed closed.

The probable failure mode was either a stuck microswitch or a mechanically failed open valve. Subsequent operation of the solenoid vent valves during SL-2/3/4 were normal and this anomaly did not occur again.

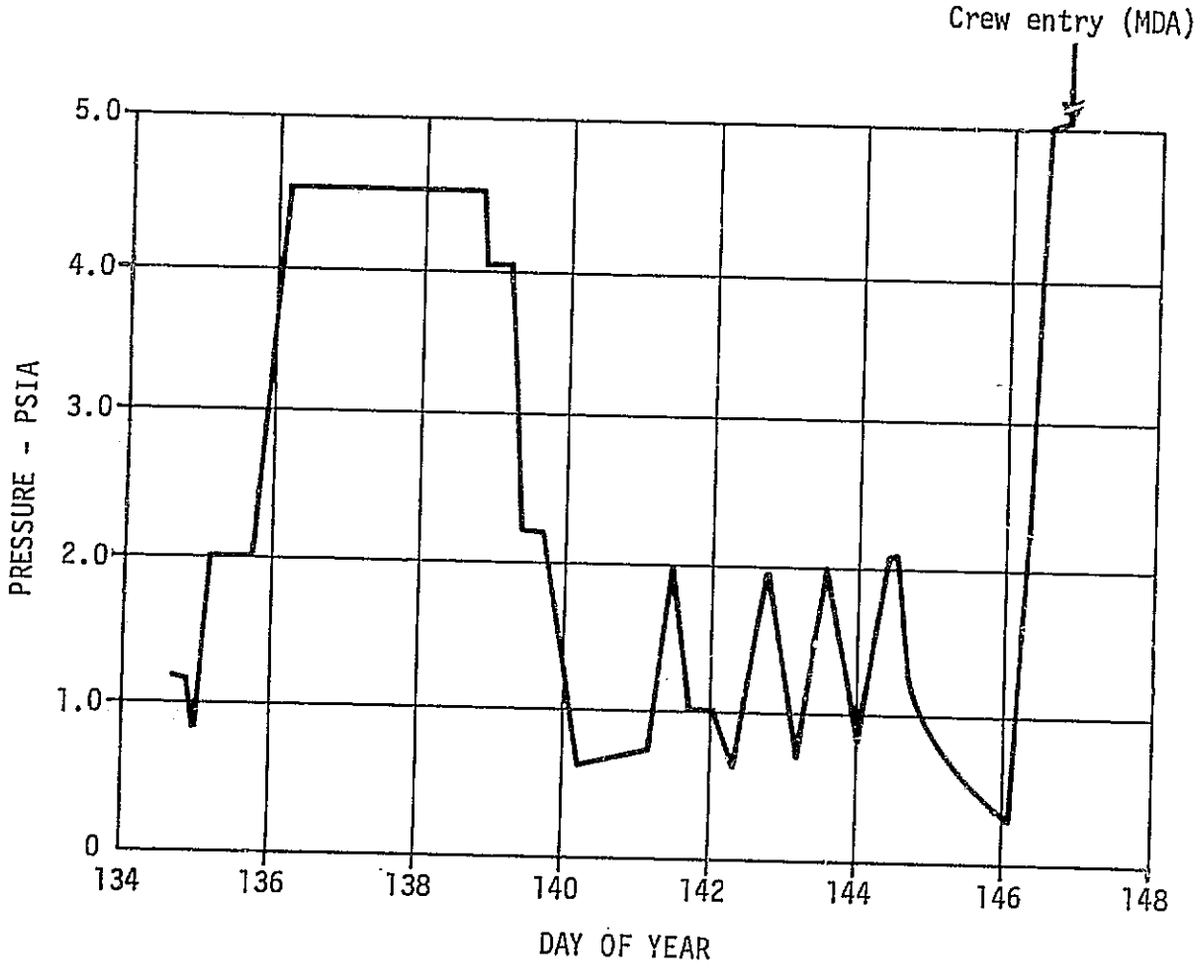

Figure 6-10. Vent/Repressurization History Prior to SL-2

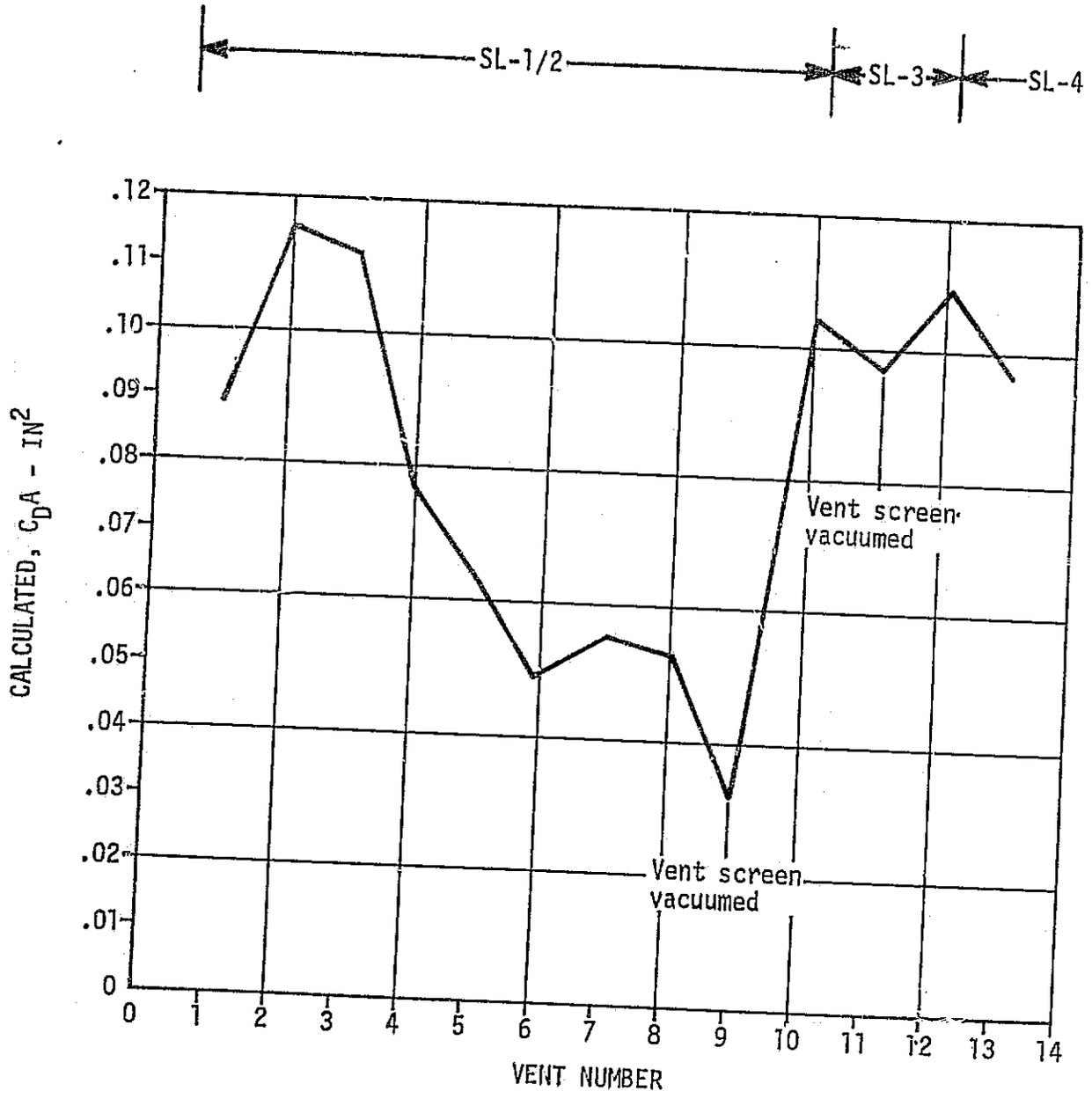

Figure 6-11. Solenoid Vent Valve Effective Flow Area

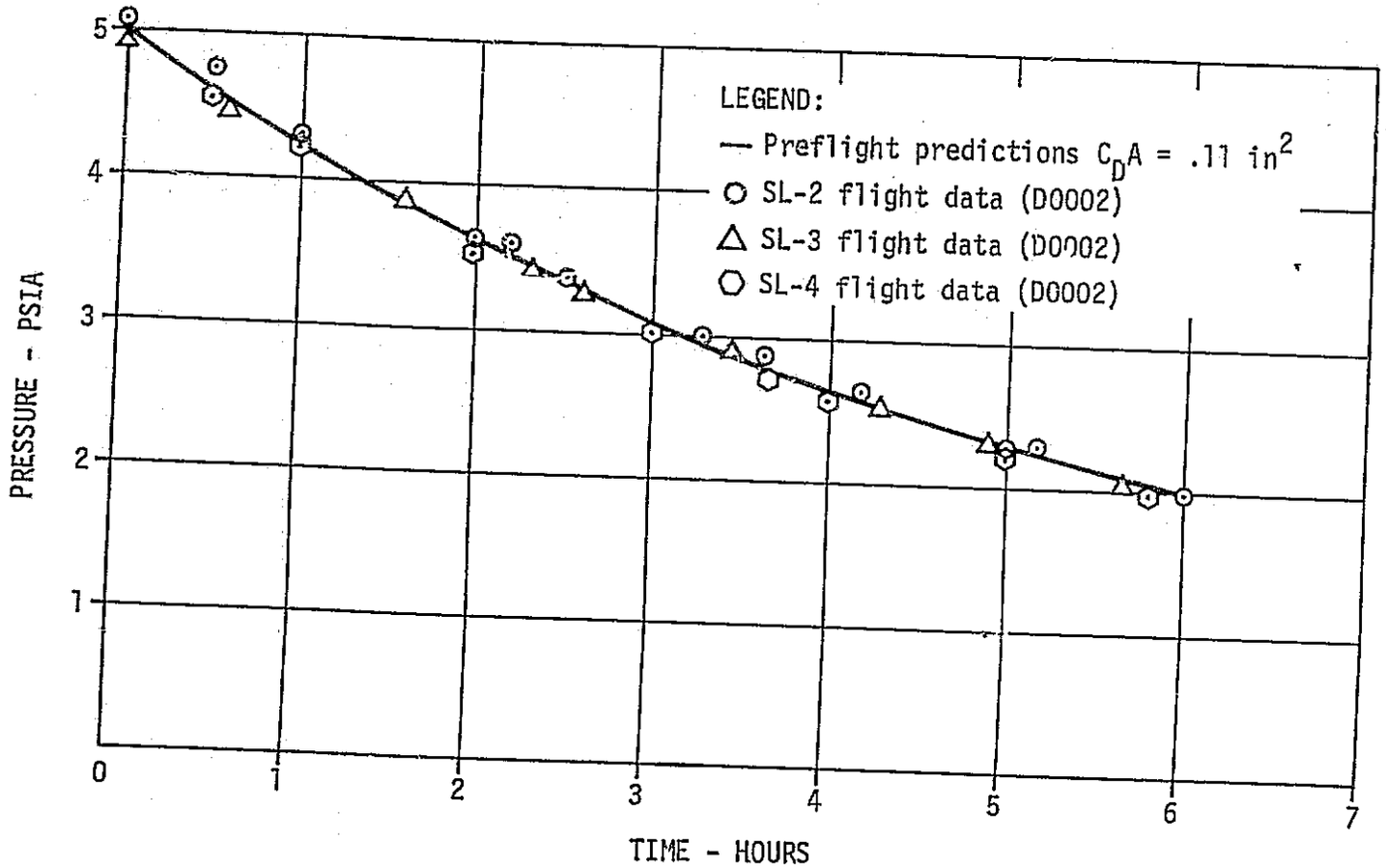

Figure 6-12. Pre-Storage Blowdown Using Solenoid Vent Valves

4. OWS Hatch Check and Equalization Valves - Equalization valve performance was satisfactory throughout all missions. A leak occurred through the hatch check valves. This leak is discussed in Section VI.C.

5. MDA/AM Hatch Equalization Valves - Performance of the pressurization valves in the MDA and AM forward internal hatch was satisfactory throughout all missions. The aft AM hatch was not used. A detailed discussion of the performance of the EVA hatch pressure equalization valve is provided in the following paragraphs.

Figure 6-13 presents a summary of all AL/AFT AM depressurizations prior to EVA for the Skylab missions. A total of nine EVA's were performed including two on SL-2, three on SL-3, and four on SL-4. The solid band presents the preflight prediction band, based on an effective vent area of 1.44 $in.^2$. Lying slightly higher than the preflight band is the profile for blowdown of EVA #2 on SL-2. (Although not enough data were received to include the blowdown for EVA #1 on SL-2, enough data were received to indicate that both vents on SL-2 were essentially the same). The apparent effective vent area for the Lock Depress Valve was about 0.9 $in.^2$ on SL-2. During both lock blowdowns, the crew indicated that icing occurred on the screen immediately over the valve. It was estimated that one-third to one-half of the screen was covered by ice near the end of the vent. It was apparent from the data that this icing resulted in blockage of the vent area.

It was suggested by the first crew that a screen be provided which could be placed in front of the first screen over the Lock Depress Valve. Ice would then form on the new screen and, at the appropriate time, the new screen and all of the ice could be removed. This would present two advantages. The additional screen would help to prevent ice from being blown into the valve and possibly damaging the seals and would also provide a simple and safe means of removing ice. (During the first two blowdowns, the crew had to rely on knocking the ice away to complete the blowdown.)

The new screen was carried up for SL-3 and all further blowdowns were accomplished using it. With two exceptions, all remaining blowdowns were accomplished with an apparent effective vent area of around 0.3 $in.^2$. The two exceptions included a slower blowdown during EVA #2 on SL-4 and a slightly faster blowdown on EVA #4 on SL-4. Both of these EVAs were the EVAs during which a water leak in the SWS loop occurred. Having additional water present in the atmosphere could have accounted for the

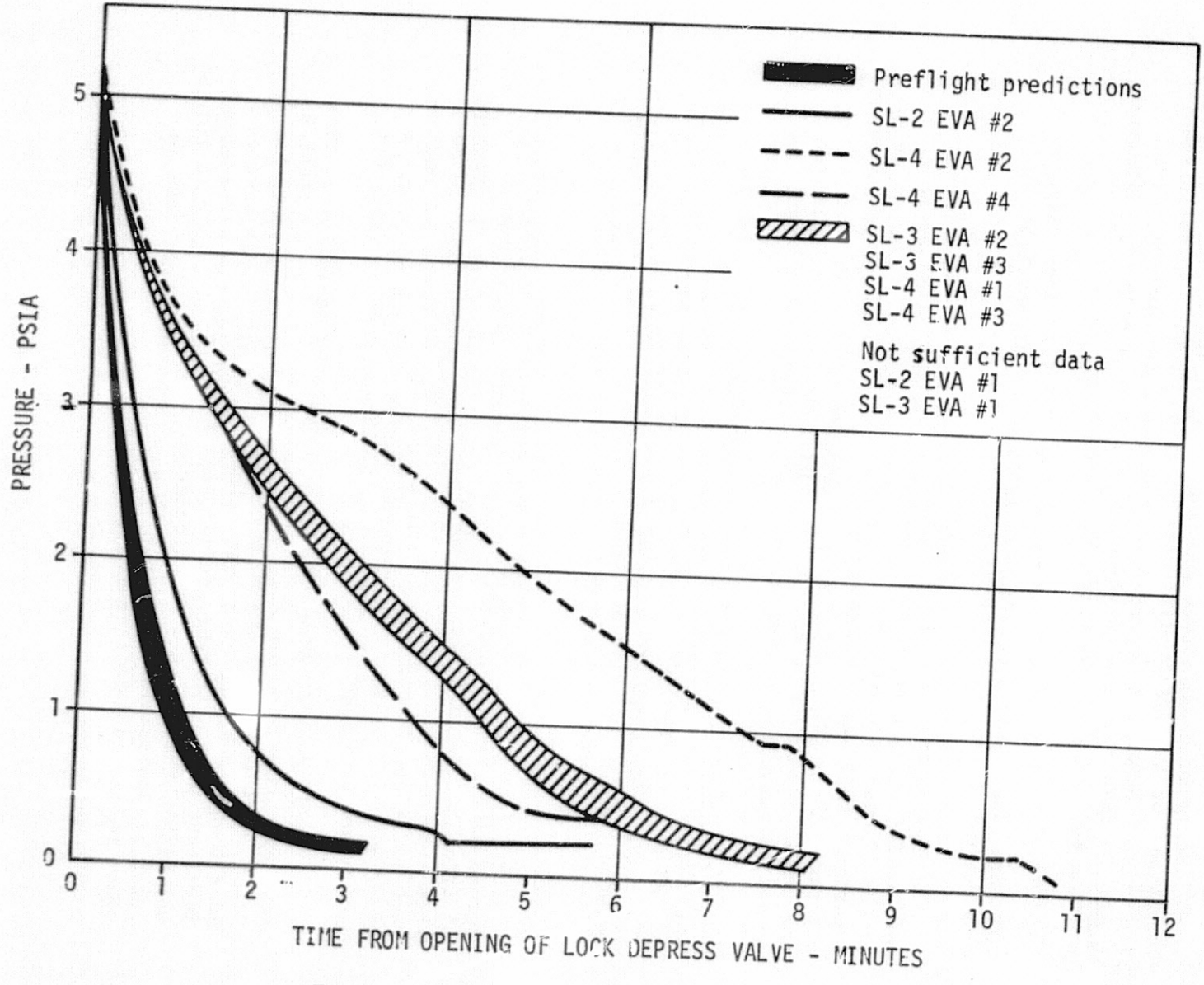

Figure 6-13. Skylab EVA Airlock Blowdown Summary

slower blowdown for EVA #2 on SL-4 due to additional icing over the screen. However, it is also possible that debris being blown into the screen, or a partially open depressurization valve could have caused the increased vent time. The faster blowdown seen on EVA #4 during SL-4 could have been due to less ice being formed on the screen, or a slightly different position of the depressurization valve. Since the depressurization valve is a manual valve, it was possible that the valve could be put in a slightly different position each time it was used.

Even though the blowdown of the AL/AFT AM took slightly more time than planned during preflight, all depressurizations were performed satisfactorily.

6. Cabin Pressure Relief Valves - The aft AM cabin pressure relief valve cracked and reseated twice during SL-4, once on DOY 17 and again on DOY 21 (at approximately 5.7 PSIA) while experiment M509 was being performed. Normal procedure was to close all three AM relief valves prior to the performance of M509 and use the CM relief valve to prevent overpressurization. The aft AM relief valve manual shutoff was inadvertently left open.

7. MDA Vent Valve System - The MDA vent valves operated satisfactorily. The valves were opened prelaunch and were closed at 288 seconds after SL-1 liftoff at an MDA pressure of 1.3 PSIA. The valves were required to maintain the differential pressure between the MDA interior and ambient below 6.2 PSID. A comparison of preflight predictions and flight performance is provided in figure 6-14.

8. Pressurization System - The pressurization system performed normally and satisfied all performance requirements. In addition to pressurizing the Skylab prior to SL-2/3/4 activation, this system was utilized for atmospheric management associated with Experiments M509 and T020 as summarized in Table 5.1 and provided required pressure adjustments during storage periods. A comparison of O_2 and N_2 flow rates is shown below in Table 6.1.

As shown by this table the calculated in-flight O_2 flow rate was slightly below pre-flight values while the in-flight N_2 values were scattered around pre-flight calculated values, but less than pre-flight check-out values. The difference between in-flight and pre-flight was not significant and the difference was within the accuracy of calculation techniques. An SL-4 calculated pressurization profile with superimposed flight data is shown on figure 6-15.

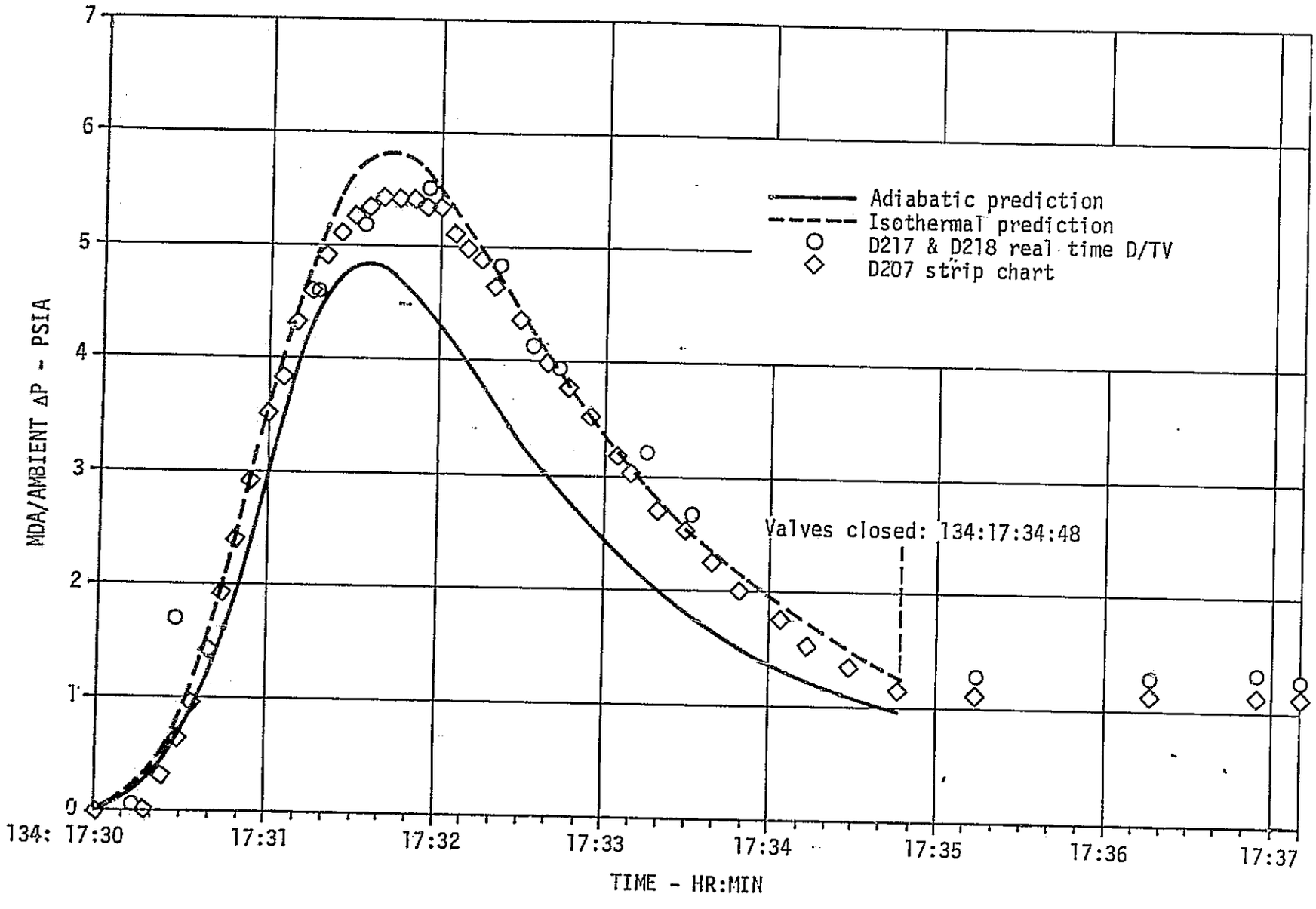

Figure 6-14. MDA Vent Valve Operation

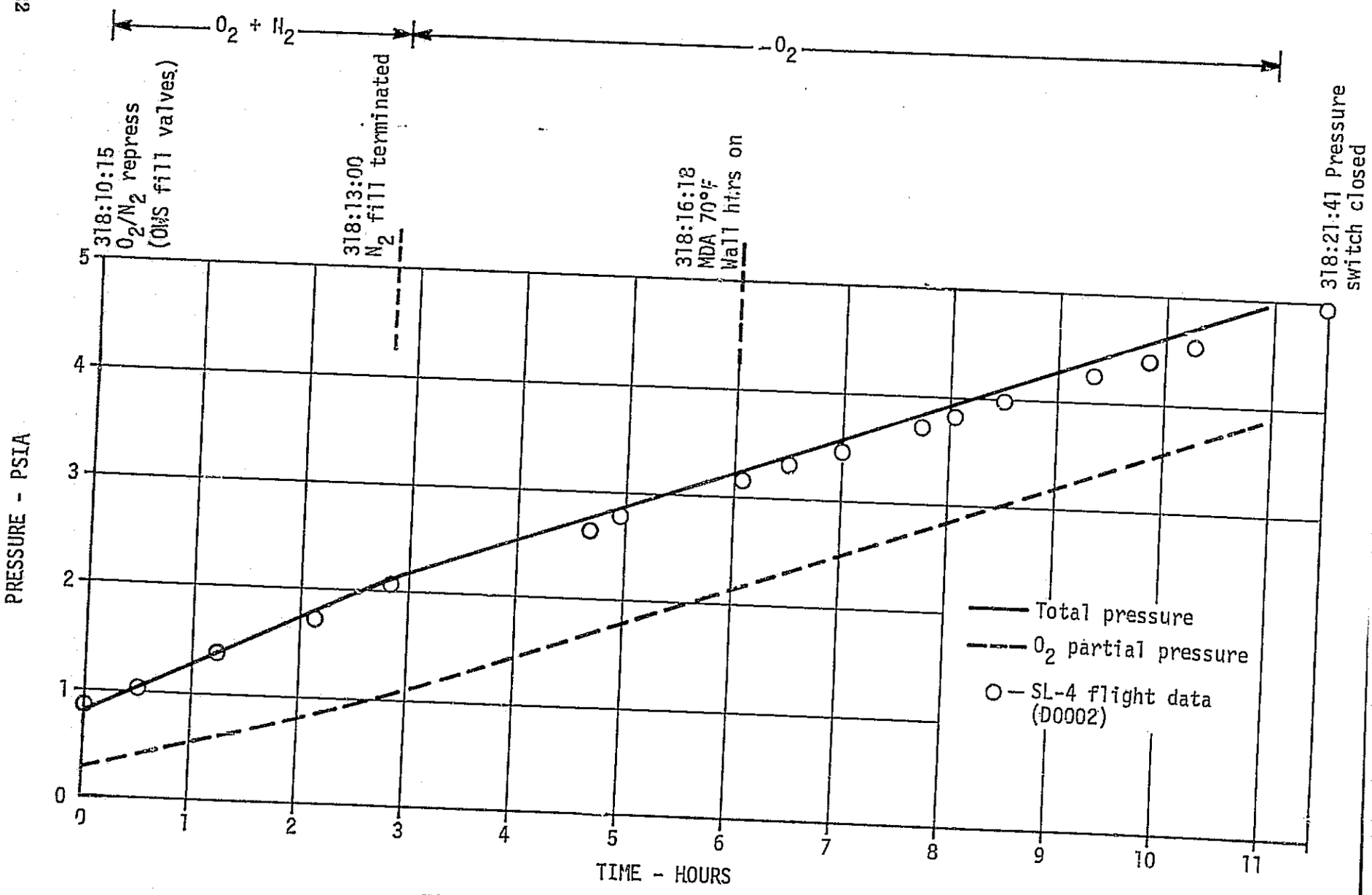

Figure 6-15. SL-4 Pressurization Profile

Table 6.1. Pressurization System Flow Rates

		O_2 Flow, lb/Hour	N_2 Flow, lb/Hour
1.	PRE-FLIGHT (CALCULATED)	22.65	6.95
2.	PRE-FLIGHT (MEASURED AT MDAC-ED CHECK-OUT)	22.24	8.10
3.	IN FLIGHT (CALCULATED)	20.5 - 21.67	5.41 - 7.65

C. Anomaly - OWS Hatch Check Valve Leakage

During OWS pressurization on DOY 135, the MDA/AM pressure increased indicating either a leak through the OWS hatch check valves or around the hatch seal. Inspection of the hatch seal by the SL-2 crew indicated no problem. Prior to the first EVA the crew taped the check valve orifices on the OWS side of the hatch and no subsequent leakage was observed. The check valves had been used on DOY 134 during trim venting of the cluster through the OWS solenoid valves and may not have reseated properly at that time.

SECTION VII. AIRLOCK MODULE COOLANT LOOP

The Airlock Module (AM) coolant loop removed waste heat from cluster waste heat sources and rejected the heat to space via a radiator located on the AM Structural Transition Section (STS) and Multiple Docking Adapter (MDA). The loop removed heat from:

a. The atmosphere (sensible and latent) by means of gas/liquid heat exchangers.

b. Cold-plated equipment.

c. The suit cooling system water loop by means of an interface heat exchanger.

d. The ATM Control and Display (C&D) Panel and Earth Resources Experiments Package (EREP) water loop by means of an interface heat exchanger.

A. Configuration

The configurations of the AM Cooling Loop, Suit Cooling Loop and the ATM C&D/EREP Loop are provided in the following paragraphs.

1. AM Coolant System - The coolant system shown in figure 7-1 provided active cooling to ECS equipment, and cold plated electrical equipment. The ECS equipment consisted of suit cooling heat exchangers, condensing heat exchangers, cabin heat exchangers for the OWS and AM/MDA, and an oxygen heat exchanger. The cold plated equipment consisted of three tape recorders, an ATM C&D Panel and EREP interface heat exchanger, two battery modules, six electronics modules, and two coolant pump inverter cold plates. Flow through the tape recorder and the battery and electronics modules was paralleled to reduce system pressure drop. Two separate (primary and secondary) coolant loops were provided for redundancy. Both active coolant loops could remove and dissipate approximately the same amount of waste heat. Each cold plate except the pump inverter cold plates contained coolant passages for both primary and secondary loops.

Operation of the system was controlled automatically by the three temperature control valves in each coolant loop. While rejecting loads below its maximum capacity, the system would operate with the 47°F temperature control valve (TCVB) at the inlet to the condensing heat exchangers always within its control band. The system was also designed so that the 40°F valve, (TCVC) at the inlet

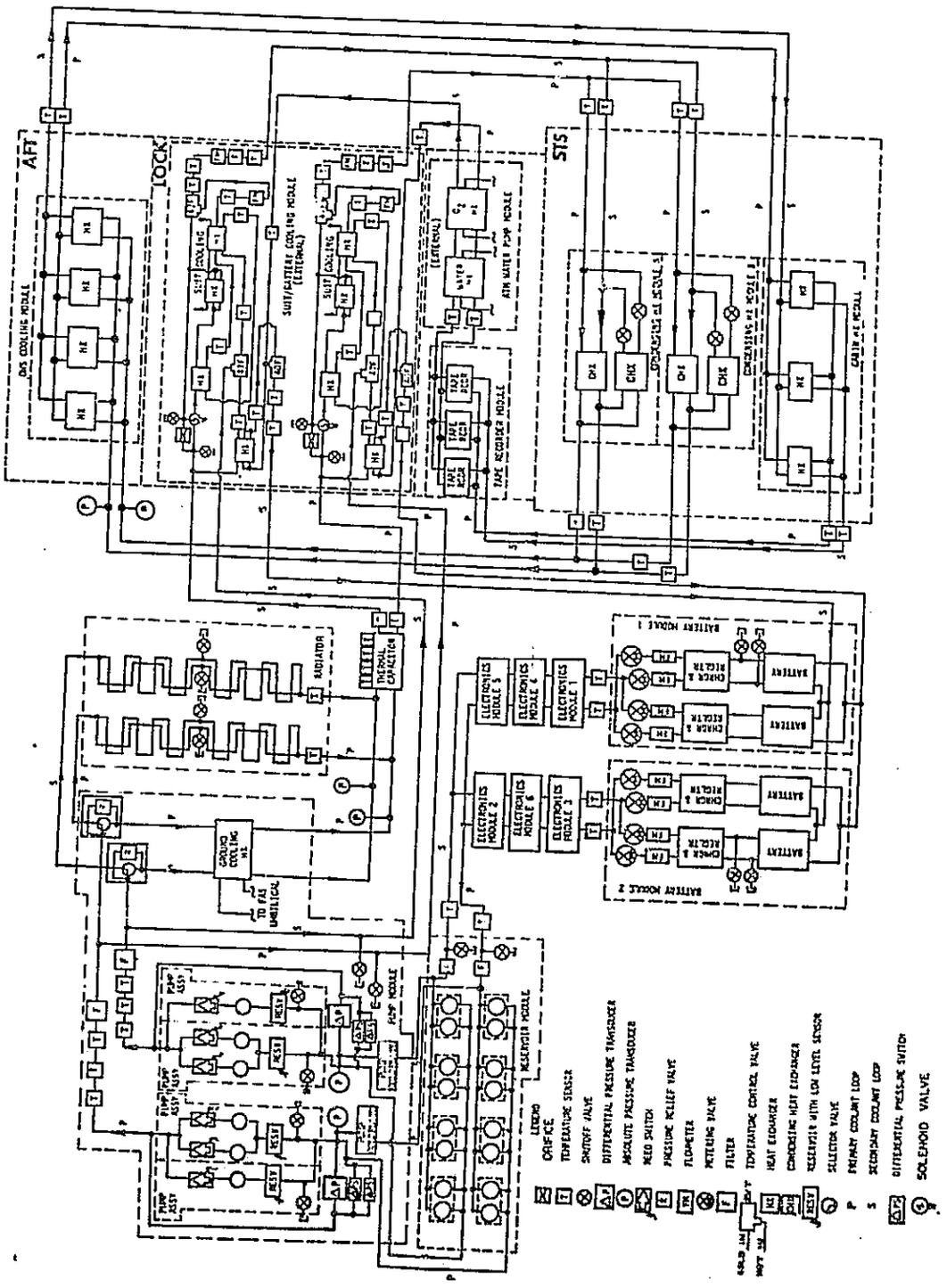

Figure 7-1. Airlock Module Coolant System

to the battery modules, and the 47°F TCVA were controlling whenever the heat loads would allow. However, the TCVB valve took precedence so the TCVC and TCVA valves would exceed their limit if required to maintain control at the TCVB valve outlet. Should the radiator/capacitor system be loaded beyond its capacity, the TCVB valve would also exceed its control band. A maximum allowable radiator inlet temperature of 120°F was established as an operating limit based upon the qualification of electronic equipment with a cold plate maximum coolant inlet temperature of 120°F.

Each loop had two pump packages containing three coolant pump/motor units. Each power supplies were provided for the three pump/motor units of each loop to convert spacecraft supplied DC power to the AC power required by the pump motors. During prelaunch and preactivation and during orbital storage, one pump was to be operated in one loop. During normal operation, one pump was to be operated in each loop, with each pump powered by a separate inverter. For a contingency mode after loss of one coolant loop, two pumps were to be operated in the remaining loop, with both pumps powered by a single inverter. Pump and inverter selection was provided by onboard switches and also by Digital Command System (DCS) command. Inverter No. 1 powered pumps A and B, inverter No. 2 powered pumps B and C, and inverter No. 3 powered pumps C and A. Reservoirs were provided to maintain pump inlet pressure and to provide an additional quantity of Coolanol 15 should coolant leakage occur.

Prior to launch, heat was dissipated to ground cooling equipment through the ground cooling heat exchanger. In orbit, heat was rejected to space by a radiator. The selector valve used to change from ground heat exchanger to radiator cooling was activated by DCS command prior to liftoff. Transient heat rejection was supplemented by two thermal capacitors (charged with tridecane wax) plumbed in series downstream of the ground cooling heat exchanger and radiator. The capacitors were cooled to a temperature below the phase change during prelaunch to accept the heat load during launch ascent and maintain the TCVB outlet temperature below 47°F. During orbital operation the capacitors were to supplement the radiator by storing heat while the vehicle was on the hot side of the orbit and rejecting the heat on the cold side.

During the active portion of the mission, the Caution and Warning (C&W) system provided monitoring to indicate condensing heat exchanger inlet temperatures below 38 ±1.75°F, equipment cold plate outlet temperatures above 120 ±2°F, and coolant pump low flow. In the event either of the temperature criteria were violated a caution signal was provided. In the event of low coolant pump flow rate, a warning signal was provided. During orbital storage- an automatic pump switching system was enabled to automatically switch pump operation from a failed active loop to the standby loop. An out-of-tolerance

condition in system pressure rise across the pump ($\Delta P < 18 \pm 2$ PSID) or the 47°F temperature control valve (TCVB) operation (temperature $\leq 38 \pm 1.75$°F) would result in the switching of power from the failed loop pump inverter to the corresponding pump inverter in the other loop.

The radiator, shown in figure 7-2, rejected waste heat to space during the orbital operations. The radiator consisted of eleven panels. Four quarter panels were mounted on the STS [Airlock Module Station (AMS) 152.75 to AMS 200], four quarter panels were mounted on the lower MDA (AMS 200 to AMS 280.57), and three panels were mounted on the upper MDA (AMS 280.57 to AMS 364.10).

Each STS panel consisted of an 0.050 inch thick magnesium skin seam welded to magnesium extrusions which formed the flow passages. The MDA panel configurations were similar except the skin was 0.032 inch thick.

Each coolant loop (primary and secondary) was divided into parallel flow paths at the inlet to the radiator and the flow was rejoined to one path at the radiator outlet. The panel skins were bolted to fiberglass stringers which were riveted to the pressure wall. Spiral turbulators (42 total) were installed in both flow passages of the primary and secondary crossover lines between all STS and MDA radiator quarter panels except for the STS quarter panel crossovers between -Z and -Y and between +Z and +Y where turbulators were installed in only one of the two flow passages.

The eleven radiator panels had a total surface area of 432 ft^2. The panels viewed other parts of the AM, externally mounted experiments, the ATM, the CSM, and the OWS.

A summary of the major parameters which could be monitored and controlled in the AM Coolant System (including the ATM C&D/EREP and EVA/IVA water loops) is provided in Table 7.1.

2. Suit Cooling System Water Loop - The Suit Cooling System, shown in figure 7-3 provided astronaut cooling during EVA and IVA by circulating temperature controlled water through umbilicals, Liquid Cooled Garments (LCG) and a LCG bypass flow diverter valve in the Pressure Control Unit (PCU). The system was part of the suit/battery cooling module and consisted of two identical subsystems (one subsystem for each AM coolant loop). Each subsystem was to be capable of delivering a minimum of 200 lb/hour of water. Astronaut cooling was regulated by adjusting the flow rate of temperature controlled water through each LCG using the flow diverter valve in the Pressure Control Unit.

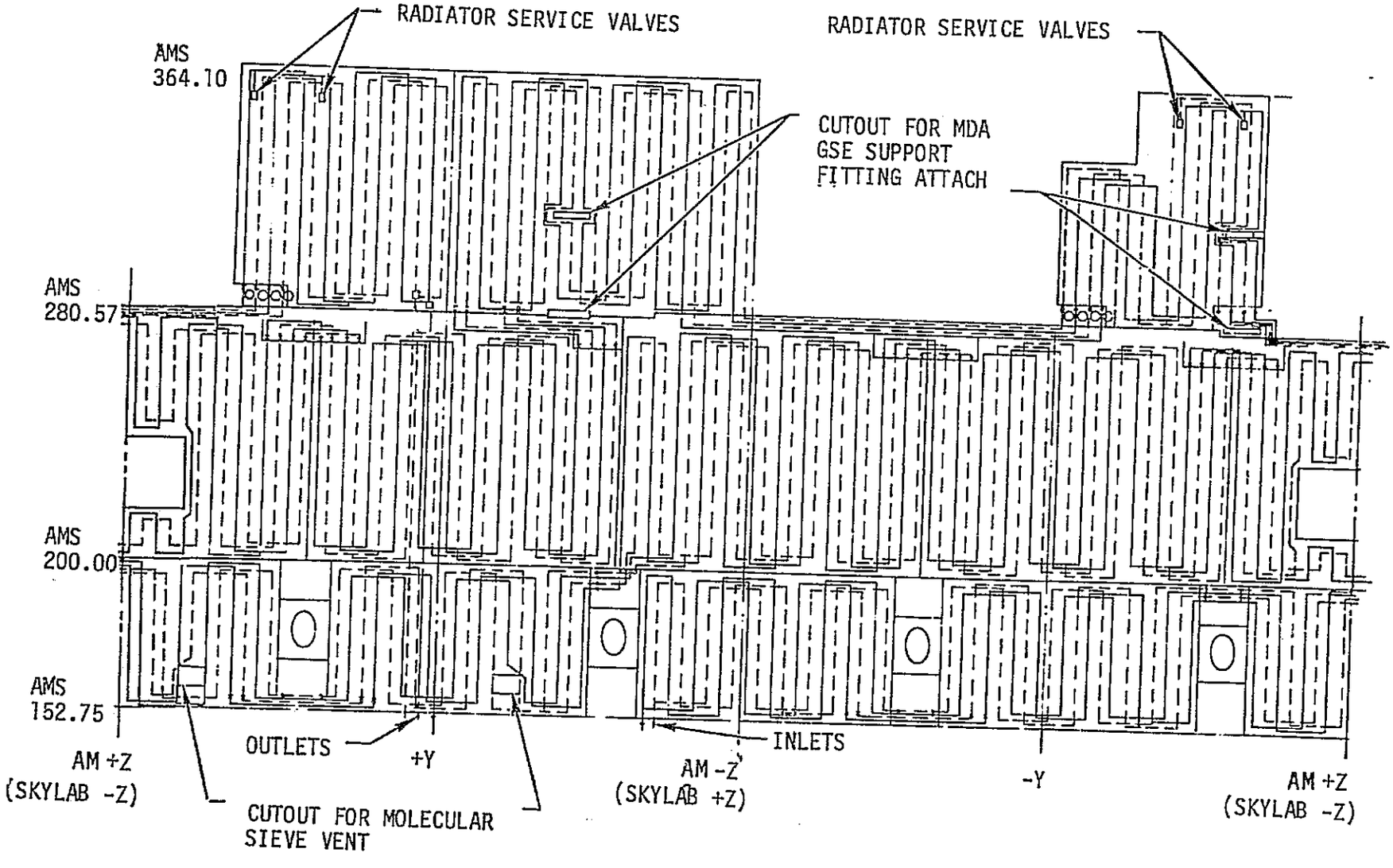

Figure 7-2. AM/MDA Radiator Stretchout Looking Outboard

Table 7.1. Coolant Systems Performance Monitoring

MAJOR MEASUREMENTS	TM	C&W	ON BOARD DISPLAY
1. AM COOLANT LOOP PERFORMANCE			
A. PRIMARY TEMP CONTROL VALVE OUTLET TEMP	X		
IF LESS THAN 40°F (C&W)		X	
B. RADIATOR INLET TEMP	X		
IF GREATER THAN 120°F (C&W)		X	
C. RADIATOR OUTLET TEMP	X		
D. PUMP FLOWRATE	X	X	
E. THERMAL CAPACITOR TEMPERATURE	X		
F. ALL COOLANT INLET AND OUTLET TEMPERATURES OF MAJOR COMPONENTS	X		
C. COOLANT RESERVOIR LOW LIMIT LIGHT	X	X	X
2. ATM C&D/EREP LOOP PERFORMANCE			
A. WATER INLET TEMP	X		
B. COOLANT OUTLET TEMP	X		
C. PUMP Δ P			LOW LIMIT LIGHT
D. FLOW RATE	X		

Table 7.1. (Cont.) Coolant Systems Performance Monitoring

MAJOR MEASUREMENTS	TM	C&W	ON BOARD DISPLAY
III. EVA/IVA LOOP PERFORMANCE			
A. WATER DELIVERY TEMPERATURE TO EVA/IVA UMBILICALS. IF LESS THAN 33.5 ± 1.5°F (C&W)	X	X	
B. WATER RETURN TEMPERATURE FROM EVA/IVA UMBILICALS	X		
C. OUTLET OF 47°F THERMAL CONTROL VALVE. IF LESS THAN 38 ± 1.75°F (C&W)	X	X	
D. WATER PUMP FLOWRATE (FLOW INDICATOR LIGHT)	X		X
E. WATER PUMP Δ P (LOW Δ P LIGHT)			X
F. EVA SUIT COOLANT RESERVOIR PRESSURE	X		

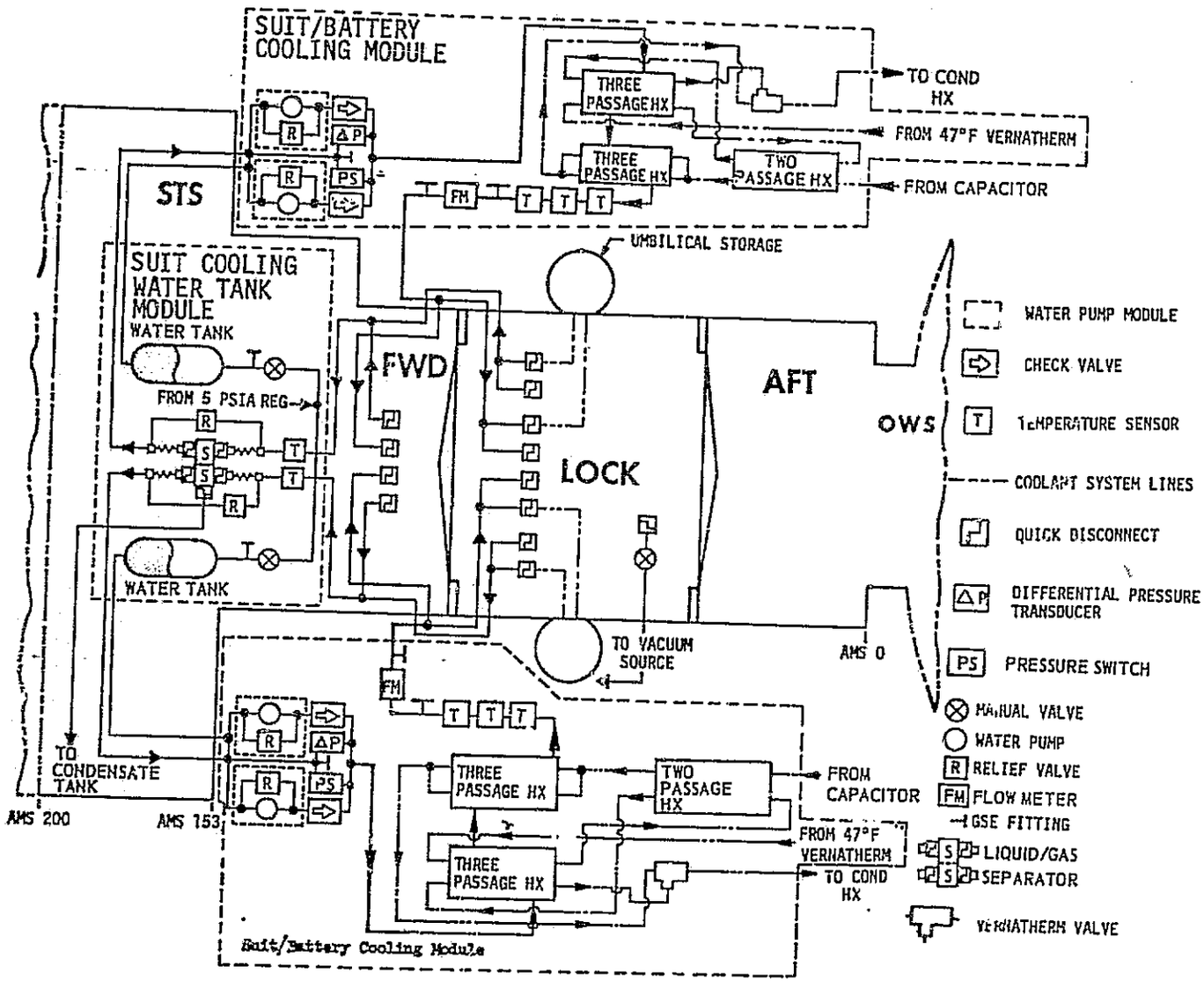

Figure 7-3. Suit Cooling System

Each subsystem contained a water reservoir and redundant water pumps. Relief valves around the pumps limited water pressure at the LCG to a maximum of 37.2 PSIA in case of a blocked line. Each subsystem had an inflight replaceable liquid/gas separator for removal of gas entrapped in the subsystem. Umbilical disconnects were provided so that the system could be used from either the lock compartment or the STS.

A removable jumper hose assembly was attached to each pair of quick disconnects in the STS, to prevent excessive pressure build-up due to thermal expansion of the water in each water loop downstream of the pump outlet check valves when the umbilicals were disconnected.

Each subsystem was equipped with extra disconnects so that three astronauts could be cooled by one of the water cooling loops in the event of a failure of one AM coolant loop. Freezing water in the lines while the system was inoperative was prevented by providing a controlled heat leak from warm coolant lines. Both coolant and water lines were isolated from their environment.

Each subsystem was launched serviced with McDonnell Material Specification MMS-606 water, containing 500 PPM sodium chromate and 10 PPM Movidyn to prevent corrosion and bacteria growth. Instrumentation was provided via telemetry to monitor water flow rate and temperature at the system inlet and outlet. Excessive positive or negative heat loads could be detected by C&W alarms, which were activated if the system outlet water temperature dropped to 33.5 $\pm$1.5°F or if the coolant temperature at the outlet of the downstream 47°F control valve dropped to 38 $\pm$1.75°F. The C&W alarms were to be off when the outlet water temperature was $\geq$36°F and the coolant temperature at the outlet of the downstream 47°F control valve (TCVB) was $\geq$45°F.

The suit cooling system could be reserviced with water inflight. The LSU's and PCU's could also be serviced or deserviced inflight.

3. ATM C&D/EREP Water Loop - The ATM C&D/EREP Water Loop, shown in figure 7-4, provided active cooling to the cold plated equipment in the MDA. Heat was removed from the equipment by cold plates and cold rails and was transferred from the water into the AM Coolant Loop by an interchange heat exchanger.

A portion of the system located in the STS consisted of the tank module containing a water tank, filter and filter bypass relief valve. The water tank contained approximately 12 pounds of water and was pressurized to 5 PSIA with nitrogen. Additives in the water consisted of two percent (by weight) dipotassium hydrogen phosphate, 0.2 percent (by weight) sodium borate and 500 PPM (by volume) Roccal. The filter in this module could be changed in flight and the loop was designed for inflight reservicing with water. The pump module

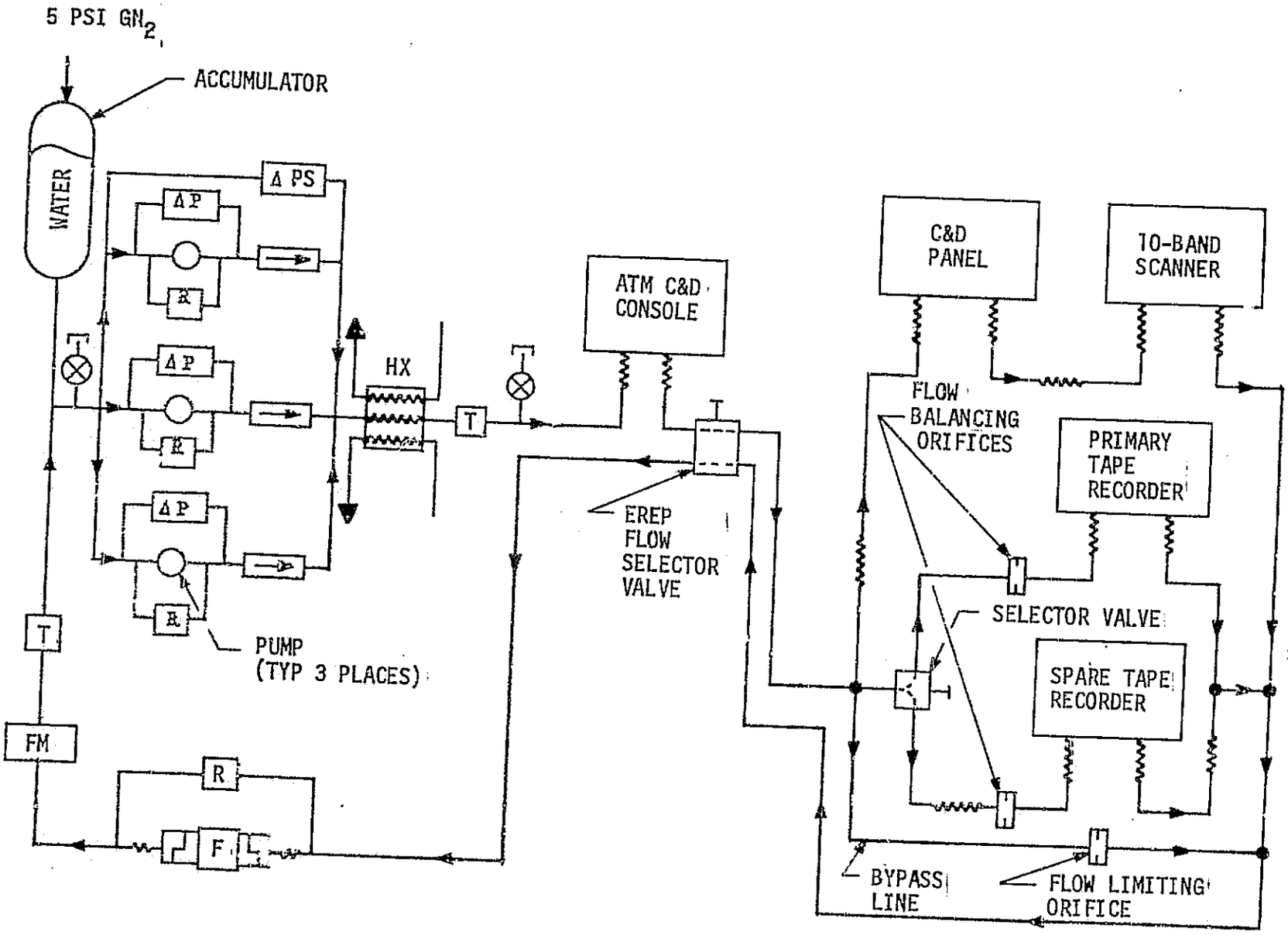

Figure 7-4. ATM C&D/EREP Water Loop

was located on the outside of the AM and contained three parallel plumbed positive displacement rotary vane pumps and the heat exchanger interfaced with the AM coolant system. Each pump had an integral bypass relief valve to limit system pressure and an outlet check valve. Single pump operation was the normal flight mode and all pumps were off during orbital storage. Telemetry sensors were provided to measure pump flow rate and the inlet and outlet temperatures to the MDA system. An onboard indication of low pump delta pressures was available.

The portion of the system located in the MDA consisted of the ATM C&D Console and its associated cooling lines. The EREP Module was also in the MDA and consisted of the EREP C&D Panel, tape recorders, multi-spectral scanner electronics and their associated cooling lines. The cooling system in this module contained four parallel plumbed branches. Branch one was a bypass containing an orifice to limit the flow to approximately 80 lb/hour. Branch two provided cooling for the EREP C&D Panel and the S192 electronics, and had a flow rate of approximately 70 lb/hour. The two components in this branch were plumbed in series. Branches three and four each contained an orifice and provided cooling for the primary and secondary tape recorders, respectively. These two branches were preceded by a common selector valve which routed the coolant to one of the tape recorders at an approximate flowrate of 70 lb/hour. All four branches in this module had a common outlet. Flow was routed from this outlet to the EREP flow selector valve and thence to the AM portion of the system. The EREP components located in the EREP Module required cooling only during predata taking checkout, data taking, and postdata taking cool down. During nonactive EREP periods, the EREP flow selector valve routed the total system flow around the EREP Module and back to the AM portion of the system. During active EREP cooling periods, the total system flow was routed to the EREP Module and then back to the AM portion of the system. Figure 7-5 shows the relative location of the various components which were cooled by the ATM C&D/EREP Water Loop in the MDA.

B. System Performance

During orbital operation, the radiator and coolant loop had to be capable of rejecting 12,000 Btu/hour during EVA and 16,000 Btu/hour during other normal operations. The system had to be designed for operation at a nominal orbital altitude of 235 nautical miles and beta angles between -73.5 and +73.5 degrees. Vehicle attitude was to be normally solar inertial except during the Earth resources pointing mode, when the Z axis was parallel to the local vertical

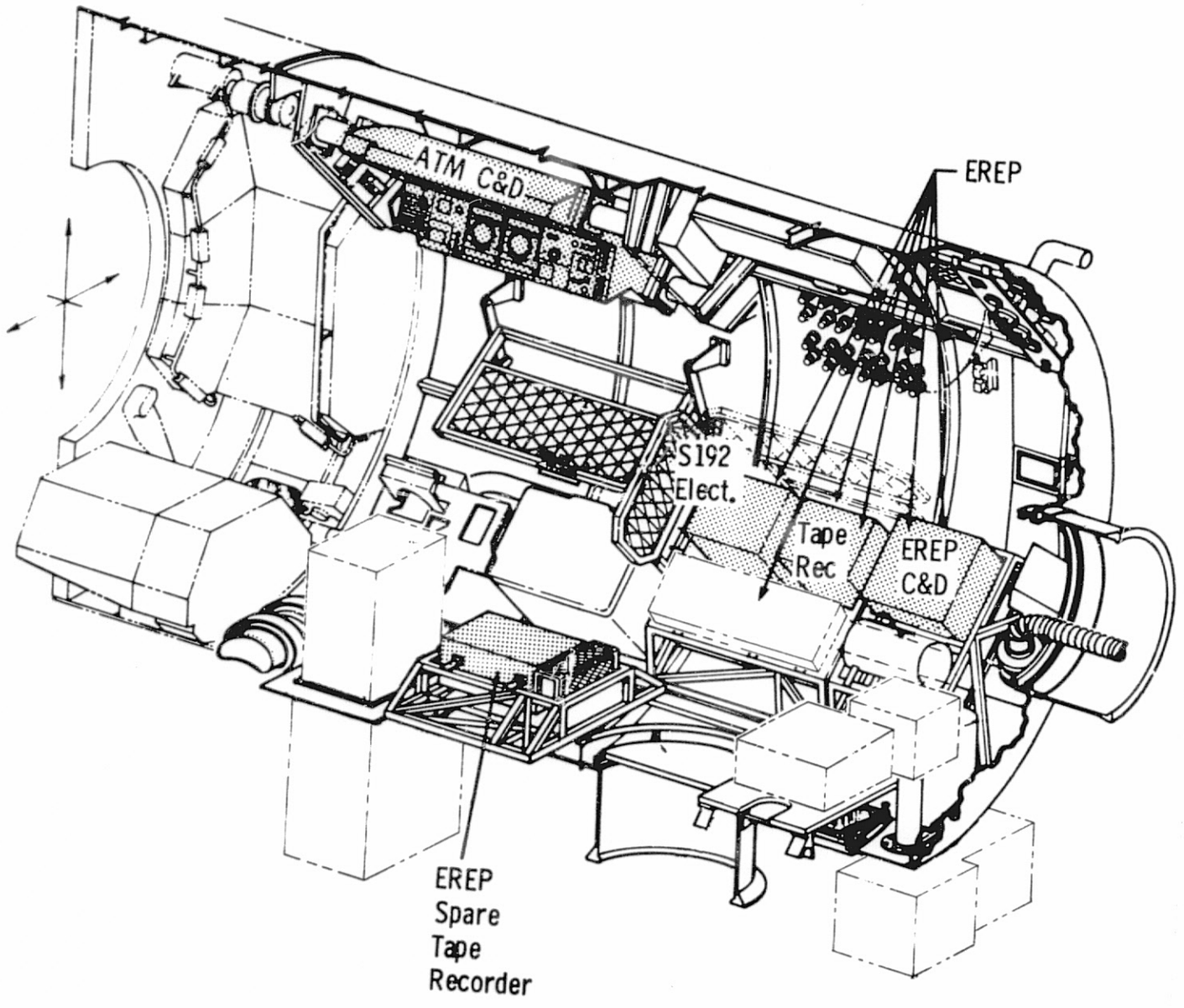

Figure 7-5. ATM C&D/EREP Internal Installation

(Z-LV with +X axis in velocity vector direction), rendezvous mode (Z-LV with -X axis in velocity vector direction), and during CMG desaturation maneuvers. Additional maneuvers were also accommodated during the mission when the Skylab was maneuvered for observations of stars, a barium cloud and the Kohoutek Comet. In these attitudes the vehicle was nearly solar inertial but the vehicle was rolled about the X axis.

In addition to the overall system requirements, the cooling loop had to provide sufficient cooling of the cluster atmosphere through the condensing and cabin heat exchangers such that this system, in conjunction with the cluster Passive Thermal Control System, could provide a comfortable environment for the crew. It had to also provide adequate cooling of cold plated equipment to maintain the equipment within acceptable temperature limits and remove sufficient heat from the suit cooling water loop and the ATM C&D/EREP Water Loop to allow those systems to provide the thermal conditioning required. A summary of the cold plate allowable temperature range and component heat dissipation is given in Table 7.2.

In general, the Airlock Module Coolant System performed well. The pump flowrates were always considerably higher than the values which were used for design purposes with the exception of the flow dropout problems in the ATM C&D/EREP loop (see paragraph C.4.). The radiator and thermal capacitor performance exceeded preflight predictions for nominal conditions and the cooling capabilities of the system exceeded the specification requirements. The major problems associated with the system were stuck thermal control valves (see paragraph C.2.) and coolant loop leakage (see paragraph C.3.).

1. System Heat Loads - The Skylab was not maintained in the solar inertial attitude prior to the SL-2 launch as planned. This fact as well as the fact that the two OWS solar arrays and AM batteries were inactive, contributed to a very low heat load on the system during the unmanned phase of SL-1. In order to illustrate the system load variations, the radiator heat loads for selected portions of the missions are provided in figure 7-6. The loads for the entire first mission are shown along with the loads during the first storage period and a portion of the final mission. The portions of the total load which were upstream and downstream of the 40°F thermal control valve C (TCVC) are also depicted and are represented by ECS and EQP respectively. A summary of the contributions to these loads from major system items is given in Table 7.3.

Table 7.4 shows the coolant loads which were estimated prior to launch and were used for design purposes. As shown, the orbital storage load was estimated to be 3096 Btu/hour, considerably more

Table 7.2. Coldplates

ITEM	ELECTRICAL COMPONENT	LOCATION	HEAT DISSIPATION BTU/HOUR	ALLOWABLE COLDPLATE TEMPERATURE RANGE MIN(°F)	MAX(°F)
1	Battery	Battery Module	170.7	40	100
2	Battery	Battery Module	170.7	40	100
3	Battery	Battery Module	170.7	40	100
4	Battery	Battery Module	170.7	40	100
5	Battery	Battery Module	170.7	40	100
6	Battery	Battery Module	170.7	40	100
7	Battery	Battery Module	170.7	40	100
8	Battery	Battery Module	170.7	40	100
9	Charger & Regulator	Battery Module	124.5/88.9	40	128
10	Charger & Regulator	Battery Module	124.5/88.9	40	128
11	Charger & Regulator	Battery Module	124.5/88.9	40	128
12	Charger & Regulator	Battery Module	124.5/88.9	40	128
13	Charger & Regulator	Battery Module	124.5/88.9	40	128
14	Charger & Regulator	Battery Module	124.5/88.9	40	128
15	Charger & Regulator	Battery Module	124.5/88.9	40	128
16	Charger & Regulator	Elect. Mod. #1	45	40	120
17	Suit Compressor Pwr Supply	Elect. Mod. #2	31	40	120
18	CRDU	Elect. Mod. #2	191	40	138
19	VHF TM 10W Transmitter		66	40	120
	Telemetry 2W Transmitter	Elect. Mod. #3	0.23	30	120
20	Hi Level Multiplexer		0.49	30	120
	Lo Level Multiplexer		19.1	36	120
	Instrument Package 2A				

Table 7.2. (Cont.) Coldplates

ITEM	ELECTRICAL COMPONENT	LOCATION	HEAT DISSIPATION BTU/HOUR	ALLOWABLE COLDPLATE TEMPERATURE RANGE MIN(°F)	MAX(°F)
	PCM Interface Box	Elect. Mod. #3	45	36	120
	Instrument Package 2A		19.1	36	120
	Programer	Elect. Mod. #3	21	40	120
	Level Multiplexer	Elect. Mod. #3	0.49	30	120
24	DC/DC Converter	Elect. Mod. #4	158	36	138
25	Instrument Package	Elect. Mod. #5	4	40	120
	Caution & Warning Unit		322	40	120
26	VHF Transceiver	Elect. Mod. #5	96	40	120
27	RTTA	Elect. Mod. #5	14	40	120
28	Instrument Package	Elect. Mod. #5	10.2	36	120
	Hi Level Audio Amp C&W		24	40	120
29	Tracking Light Elect. Pkg	Elect. Mod. #6	201	40	120
30	Coolant Pump Power Supply	Pump Module	47	40	120
31	Coolant Pump Power Supply	Pump Module	47	40	120
32	Tape Recorder	Tape Rec. Module	52	36	100
33	Tape Recorder	Tape Rec. Module	52	36	100
34	Tape Recorder	Tape Rec. Module	52	36	100

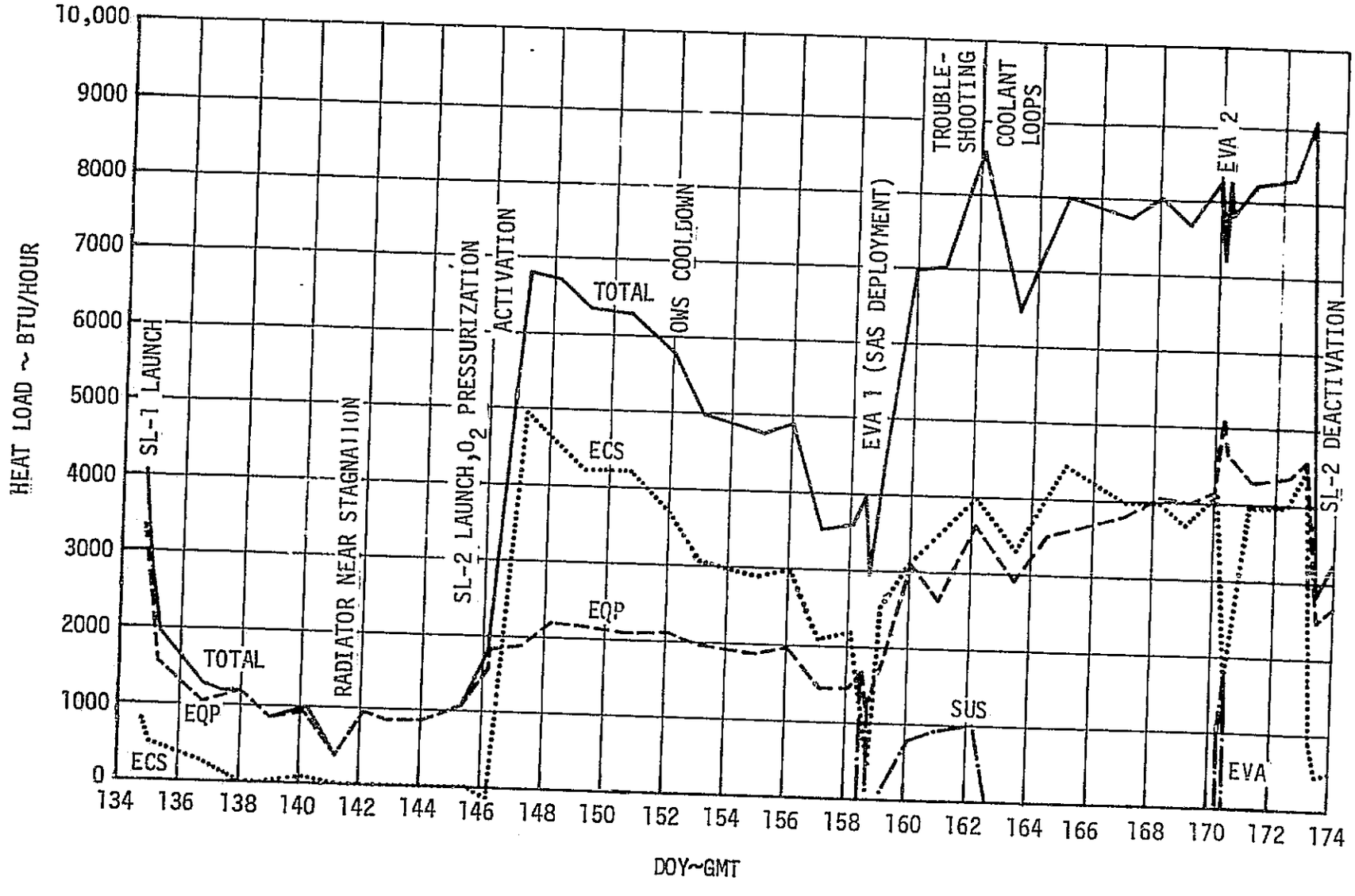

Figure 7-6a. AM Radiator Heat Load, SL-1/SL-2

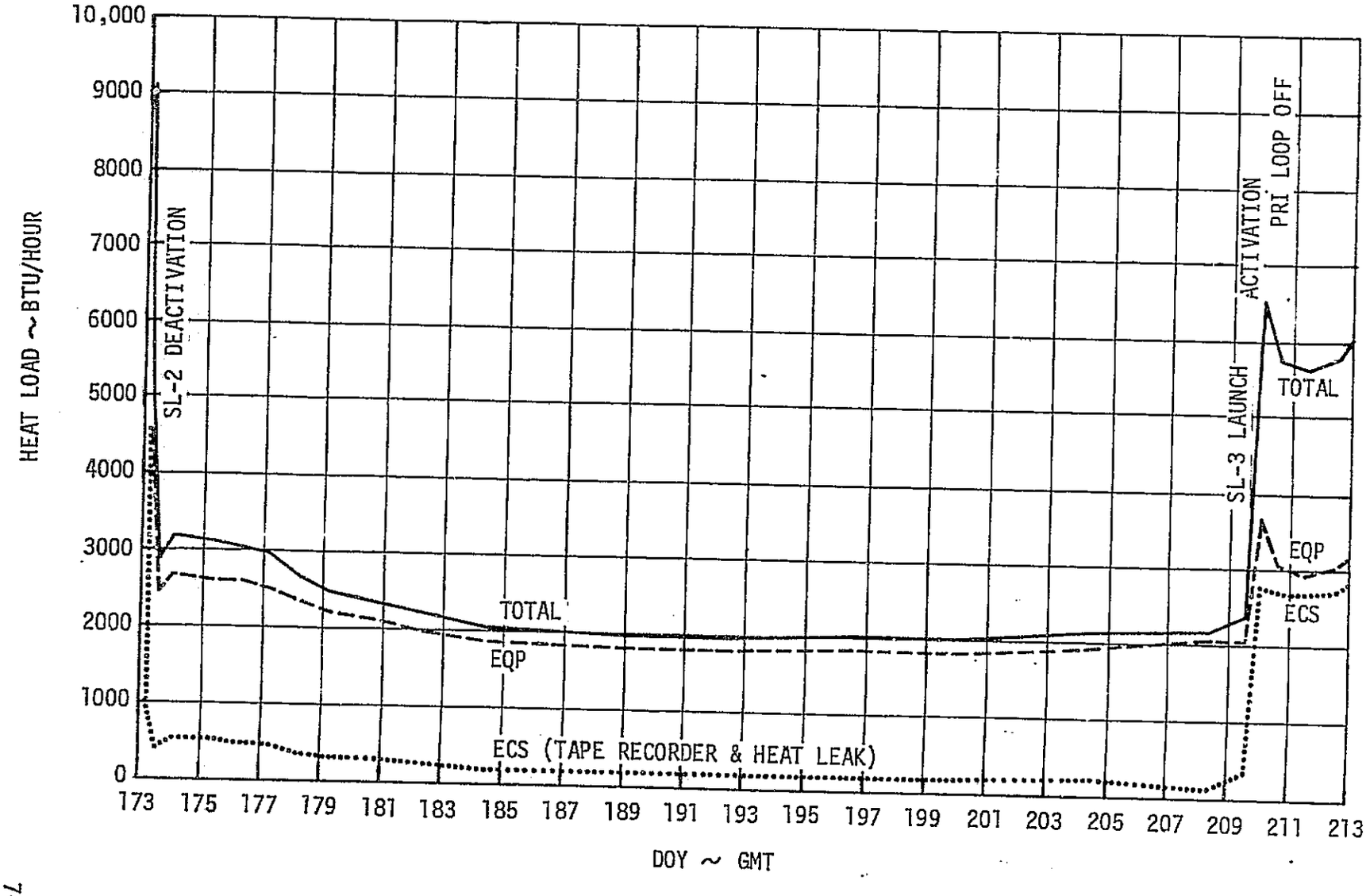

Figure 7-6b. AM Radiator Heat Load, SL-2/SL-3 Storage

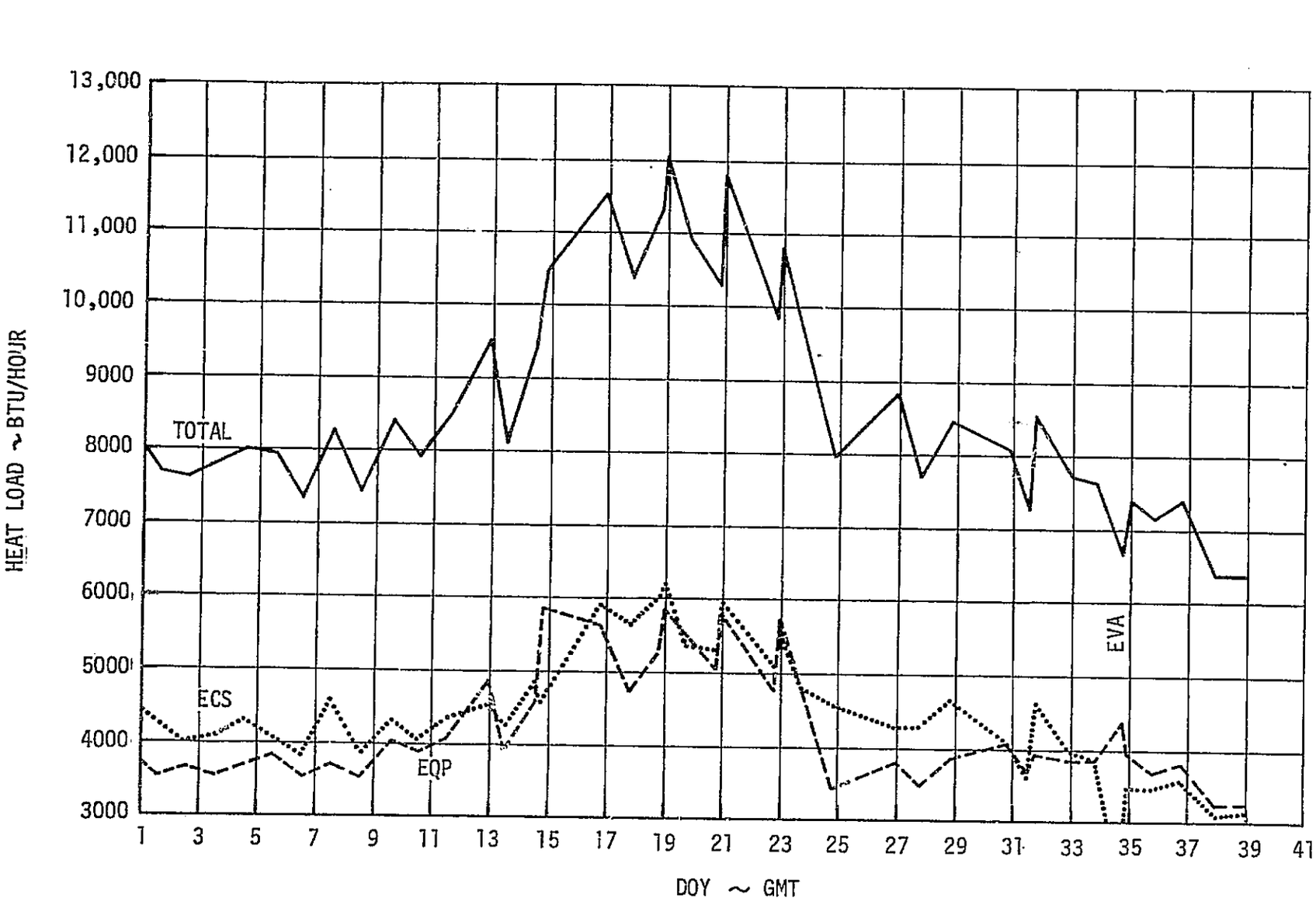

Figure 7-6c. AM Radiator Heat Load, DOY 001 - DOY 039 of SL-4

Table 7.3. AM Coolant Loads (BTU/HOUR)

ECS LOADS (UPSTREAM OF 40°F VALVE)	SL-2	SL-3	SL-4
1. Condensing Heat Exchangers	600 to 1300	600 to 1500	550 to 1600
2. OWS Heat Exchangers	1100 to 3500	100(2) to 1700	1250 to 2350
3. STS Heat Exchangers	-100 to 750	0 to 900	0 to 800
4. Tape Recorders	-150 to 200	- 50 to 250	0 to 250
5. ATM C&D & O_2 Heat Exchanger Module	-150 to 800	0 to 2014	0 to 2783
EQP LOADS (DOWNSTREAM OF 40°F VALVE)			
1. Battery Modules	-300(1) to 2300	1200 to 2100	1050 to 3800
2. Electronics Modules	950 to 1600	800 to 1500	500 to 1450
3. Pump Modules	200(3) to 900(4)	200(3) to 850(4)	250(3) to 1600(5)

NOTES

(1) Prior to OWS Solar Array Deployment
(2) All OWS Heat Exchangers Off
(3) 0 Primary Pumps + 1 Secondary Pump
(4) 1 Primary Pump + 1 Secondary Pump
(5) 2 Primary Pumps + 1 Secondary Pump

SOURCE	OPERATING MODE: HOT AM/MDA	HOT OWS	COLD AM/MDA/OWS	EVA/IVA	EREP	ORBIT STORAGE	PRE LIFT-OFF	RENDEZVOUS
1. COMPARTMENT LOADS								
MDA (2)	(1056)	(798)	(798)	(762)	(1056)	(0)	(0)	(0)
AM (TOTAL) (3)	(2003)	(1392)	(792)	(1353)	(1432)	(0)	(0)	(0)
AFT	361	276	100	100	276	0	0	0
LOCK	269	139	0	269	9	0	0	0
FWD	0	0	0	0	0	0	0	0
STS	1373	977	692	984	1147	0	0	0
OWS ATMOSPHERE COOLING	(1740)(4)	(1900)(4)	(55)	(0)	(920)(13)	(0)	(0)	(0)
METABOLIC (5)	(1245)	(530)	(0)	(0)	(1565)	(0)	(0)	(0)
SENSIBLE								
MDA	480	0	0	0	690	0	0	0
AM	235	0	0	0	345	0	0	0
LATENT	530	530	0	0	530	0	0	0
2. AM/MDA WALL HEATER LOAD	(0)	(0)	(1858)	(0)	(0)	(1200)	(0)	(1790)
3. COLDPLATES, HX'S ETC.	(5668)	(4695)	(5094)	(9659)	(6064)	(3203)	(1885)	(3782)
EVA/IVA HX'S	0	0	0	5064(6)	0	0	0	0
ATM C&D PANEL/EREP HX	1126(7)	153(9)	153(9)	153(9)	1042(10)	0	0	0
ELECTRONICS MODULES (11)	1116	1116	1116	1116	1116	315	387	944
PCG'S (EIGHT) (12)	2750	2750	3200	2650	3230	2550	1160 (16)	2500
TAPE RECORDERS	102	102	51	102	102	51	51	51
COOLANT PUMP MODULE	574	574	574	574	574	287	287	287
4. TOTAL HEAT LOADS								
GROSS SYSTEM HEAT LOAD	(11,712)	(9315)	(8597)	(11,774)	(11,037)	(4403)	(1885)	(5572)
EXTERNAL HEAT LEAK (14)	1177	715(15)	2343	574(15)	1500	1307	-5957	1672(15)
RADIATOR HEAT LOAD	10,535	8600	6254	11,200	9537	3096	7842(18)	3900

Table 7.4. Internal Design Heat Loads (BTU/HOUR)

NOTES:

(1) NOMINAL EQUIPMENT AND METABOLIC HEAT LOADS FOR SUSTAINED OPERATION AT MISSION MODE INDICATED. (4 HOUR EVA LIMIT.)
(2) MDA COMPARTMENT HEAT LOADS PER AM/MDA ENVIRONMENTAL CONTROL DATA, S&E-ASTN-PL (72-130)
(3) BASED ON AM EQUIPMENT LOADS.
(4) BASED ON 83°F OWS RETURN GAS TEMPERATURE.
(5) CREW METABOLIC SENSIBLE LOADS PER S&E-ASTN-PL(72-214), BASED ON TOTAL METABOLIC LOAD OF 500 BTU/HOUR PER CREWMAN, CLO=0.35, V(GAS)=40 FT/MIN. LATENT METABOLIC HEAT LOADS EXCLUDE 220 BTU/HOUR (MOLECULAR SIEVE VENTING).
(6) 3130 BTU/HOUR (ONE EVA/IVA LOOP) + 1730 BTU/HOUR (OTHER EVA/IVA LOOP) + 204 BTU/HOUR (PUMPS).
(7) AVERAGE LOAD OF 310 WATTS (1058 BTU/HOUR) + PUMP LOAD (68. BTU/HOUR).
(8) AVERAGE LOAD OF 90 WATTS (307 BTU/HOUR) + PUMP LOAD (68. BTU/HOUR).
(9) AVERAGE LOAD OF 25 WATTS (85 BTU/HOUR) + PUMP LOAD (68. BTU/HOUR).
(10) ORBIT AVERAGE HEAT LOAD BASED ON 25 WATT LOAD DURING STANDBY, AND EREP EQUIPMENT LOAD PROFILE ESTIMATED PREFLIGHT.
(11) BASED ON NOMINAL ELECTRONIC EQUIPMENT OPERATION; INCLUDES NON-COLDPLATED EQUIPMENT.
(12) ORBIT AVERAGE HEAT LOADS.
(13) BASED ON 70°F OWS RETURN GAS TEMPERATURE.
(14) INCLUDES LOSSES TO CSM; EXCLUDES HEAT LEAK TO RADIATOR.
(15) ESTIMATED VALUE
(16) BASED ON BATTERIES ON TRICKLE CHARGE.
(17) OWS POWERED DOWN.
(18) REPRESENTS PRELAUNCH GCHX LOAD WITH RADIATOR IN BYPASS. BASED ON GCHX HEAT LOADS MEASURED DURING U-1 SEDR D3-E75 SIMULATED FLIGHT TESTS. TOTAL LOAD AT GSE/AM INTERFACE WITH GROUND COOLANT SUPPLY PER 65ICD9542, -15°F @ 900 LB/HOUR.

than the 300 to 1000 Btu/hour on the system during the unmanned phase of SL-1 shown in figure 7-6a. Later, when the Skylab was solar inertial oriented and the one OWS solar array was deployed, the orbital storage heat loads were closer to the preflight predictions. As shown in figure 7-6b, during the high Beta portion of the SL-2/SL-3 storage period the heat load was approximately 3100 Btu/hour. The remaining storage periods had loads at approximately 2200 Btu/hour. As shown, there was a 200 to 600 Btu/hour ECS heat load during storage even though the heat exchangers were off. This was the result of heat leaks and the tape recorder heat load.

As shown in figure 7-6a for the initial portion of SL-2, the low load of 6800 Btu/hour on the system was a result of the power shortage during this period. The load decreased further with the decreasing OWS temperature until the OWS solar array was deployed on DOY 158. The AM batteries then added heat to the system and the electrical power was also no longer constrained. Loads during the remaining portion of the SL-2 ranged between 6500 and 9000 Btu/hour. During the manned portions of SL-3 and SL-4, the normal solar inertial load was approximately 8000 Btu/hour. During the full Sun portion of SL-4, the solar inertial load peaked at approximately 10,000 Btu/hour.

The heat loads during the EREP maneuvers were sometimes higher than anticipated being a maximum of 12,021 Btu/hour for EREP 31 on DOY 18 of SL-4. The heat exchanger loads were higher during this period since three pumps were in operation and the atmosphere temperatures were warmer at the high beta angles.

The radiator heat loads during the EVA operations were considerably below the 12,000 Btu/hour specification limit and also less than the 11,200 Btu/hour design value estimated prior to the flight. This was partially attributed to the fact that only one of the EVA heat exchangers was used after the problems occurred with the TCVB valves.

Because the radiator heat loads were always below the maximum specification values of 16,000 Btu/hour for non-EVA and 12,000 Btu/hour for EVA there were never any problems meeting the cold plate requirement of 120°F at the pump outlet. The maximum temperature occurred at 323:23:00 and was approximately 75°F.

2. AM Cooling System Performance During the Launch Phase - The AM coolant loop prelaunch performance is given in Section IX. As indicated in that section, only one of the two cooling loops was active until crew entry. The configuration at launch had one pump operating in the primary loop flowing through the radiator. The

secondary loop was dormant with the radiator bypass valve in the normal or radiator flow position. The system heat load, induced by convective heating from the radiator at launch, internal system heat load, and aerodynamic heating during the boost/ascent phase, was rejected to the two thermal capacitors at the radiator outlet. The capacitor cooling mode was used until payload shroud jettison at T + 15 minutes 20 seconds. Following this the radiator began to reject heat to deep space. Data indicates that of the approximately 5700 Btus of cooling capability stored in the two capacitors at launch, 2200 Btus remained when the radiator began to provide the required cooling. During this period of time the capacitors maintained all coolant loop temperatures within the required tolerances. Figure 7-7 shows the actual radiator outlet temperature history for the first 6 hours of the mission along with predicted values for a short period at mission start.

3. Radiator/Capacitor Non-EVA Performance - The heat rejection capability of the radiator/capacitor system was better than anticipated prior to the flight and at no time were there problems in having adequate capacity for the planned operations. The parametric curve shown in figure 7-8 was prepared prior to the flight and was used to monitor the relative performance of the radiator periodically throughout the mission when the vehicle was in the solar inertial attitude and the Beta angle was between 0 and $\pm$30 degrees. As shown, the outlet temperature of the radiator was equivalent to the preflight studies with a degraded coating α/ε = .25/.85 and an external environment between nominal and minimum fluxes. It was concluded therefore, that there was more than adequate capacity since preflight studies showed that even for maximum flux conditions, the radiator rejection capability was greater than the required 16,000 Btu/hour without exceeding 47°F at the valve B outlet and the flight loads were considerably below this.

4. Radiator/Capacitor Performance for Maneuvers - The impact of maneuvers on the performance of the radiator and thermal capacitor was of little significance during SL-2 and SL-3 because the capacitor outlet temperature was always below the phase change of 22.3°F for the tridecane wax. Some maneuvers which were performed during SL-4, however, occurred at Beta angles greater than the -65 degrees which was analyzed as an upper limit prior to flight. Results of the preflight studies showed that the thermal capacitors would thaw and all three control valves would exceed their control band for some maneuvers at Beta angles approaching full Sun. As anticipated, the thermal capacitors did completely thaw during the flight and all of the thermal control valves exceeded their control band during some of the maneuvers. Typical plots of the system parameters are shown in figure 7-9, for EREP 29 and 30 on DOY 14. Refer to figure 7-10

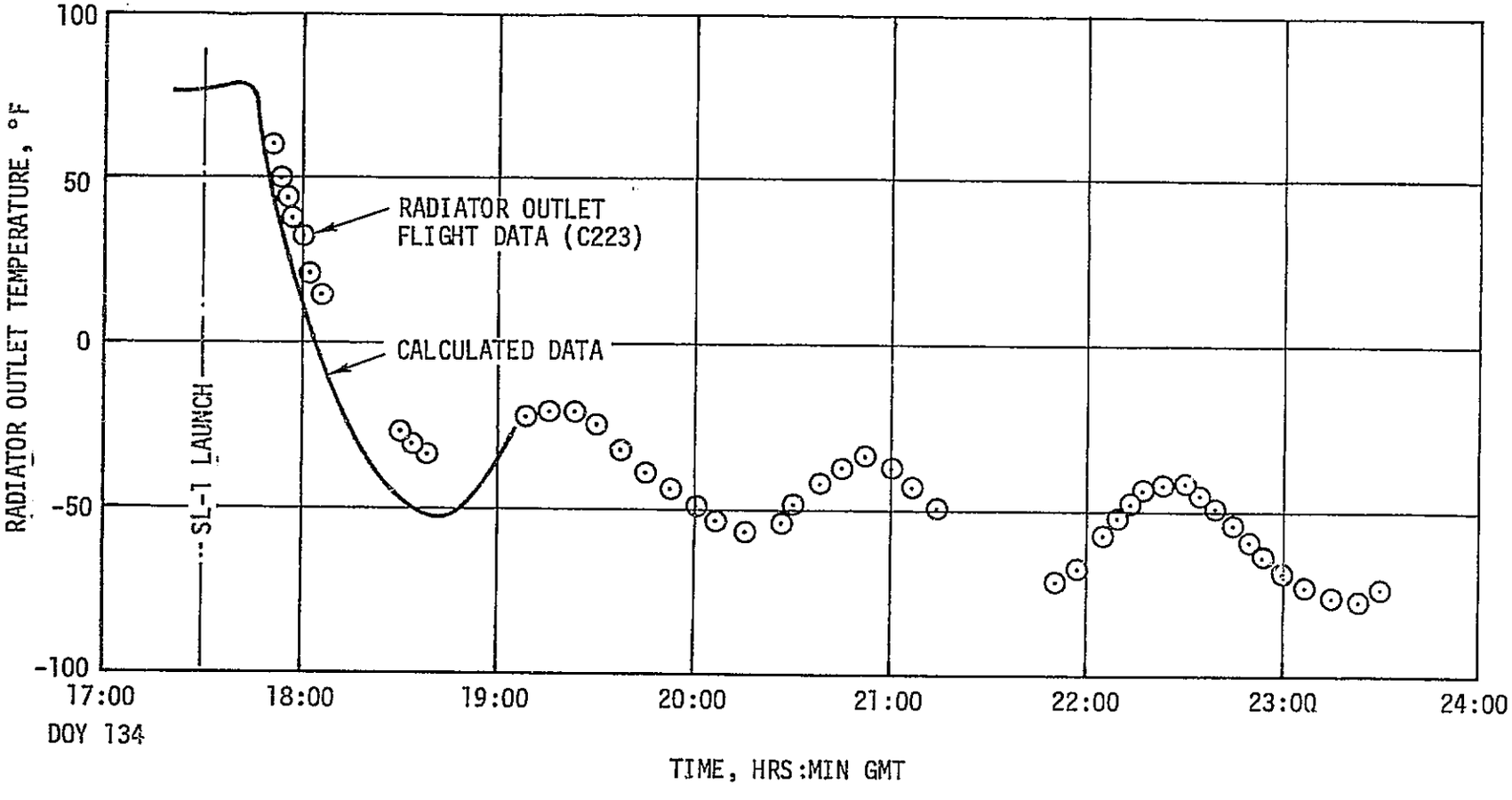

Figure 7-7. Cooldown of AM Radiator

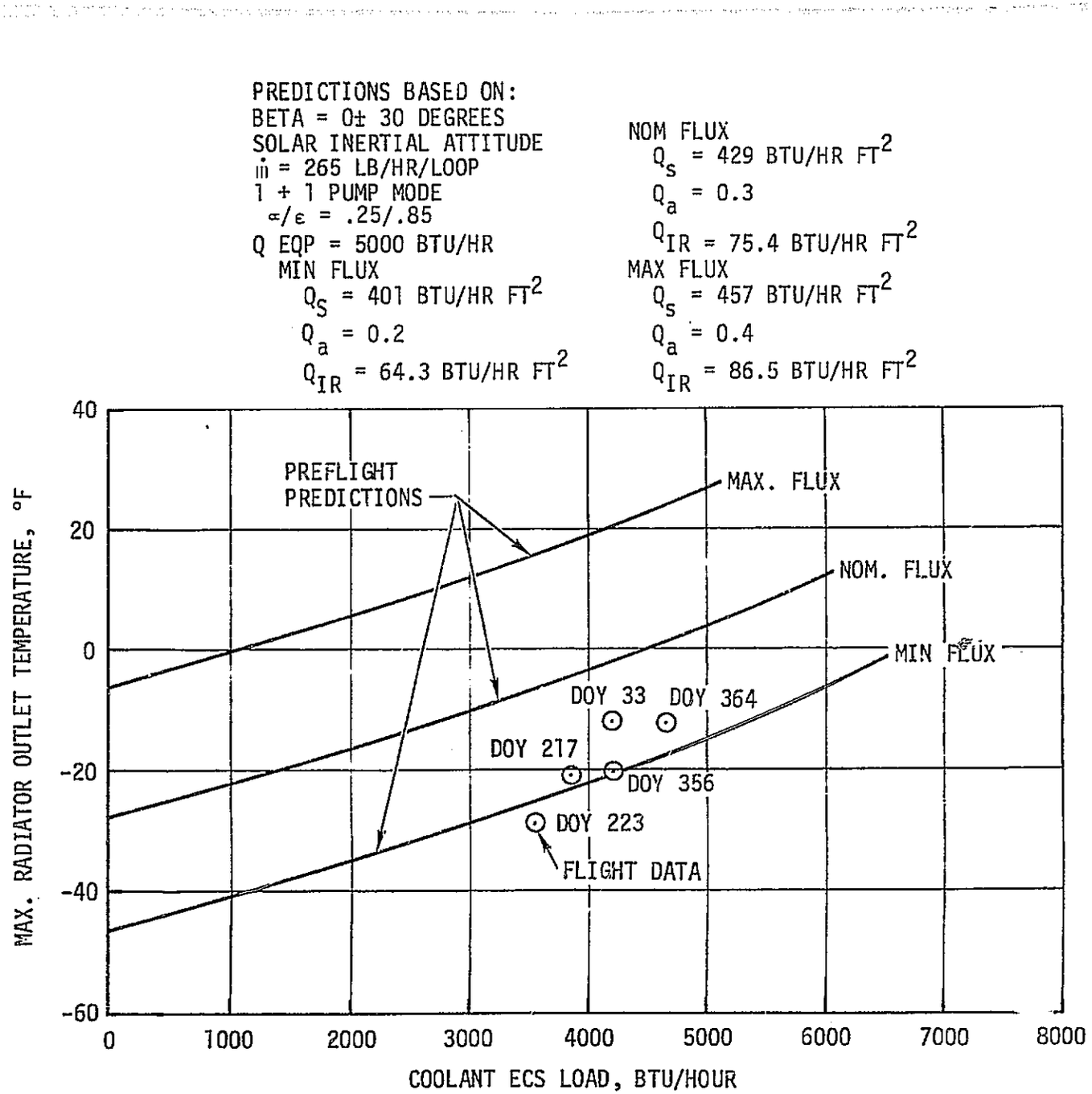

Figure 7-8. AM Radiator/Capacitor Performance

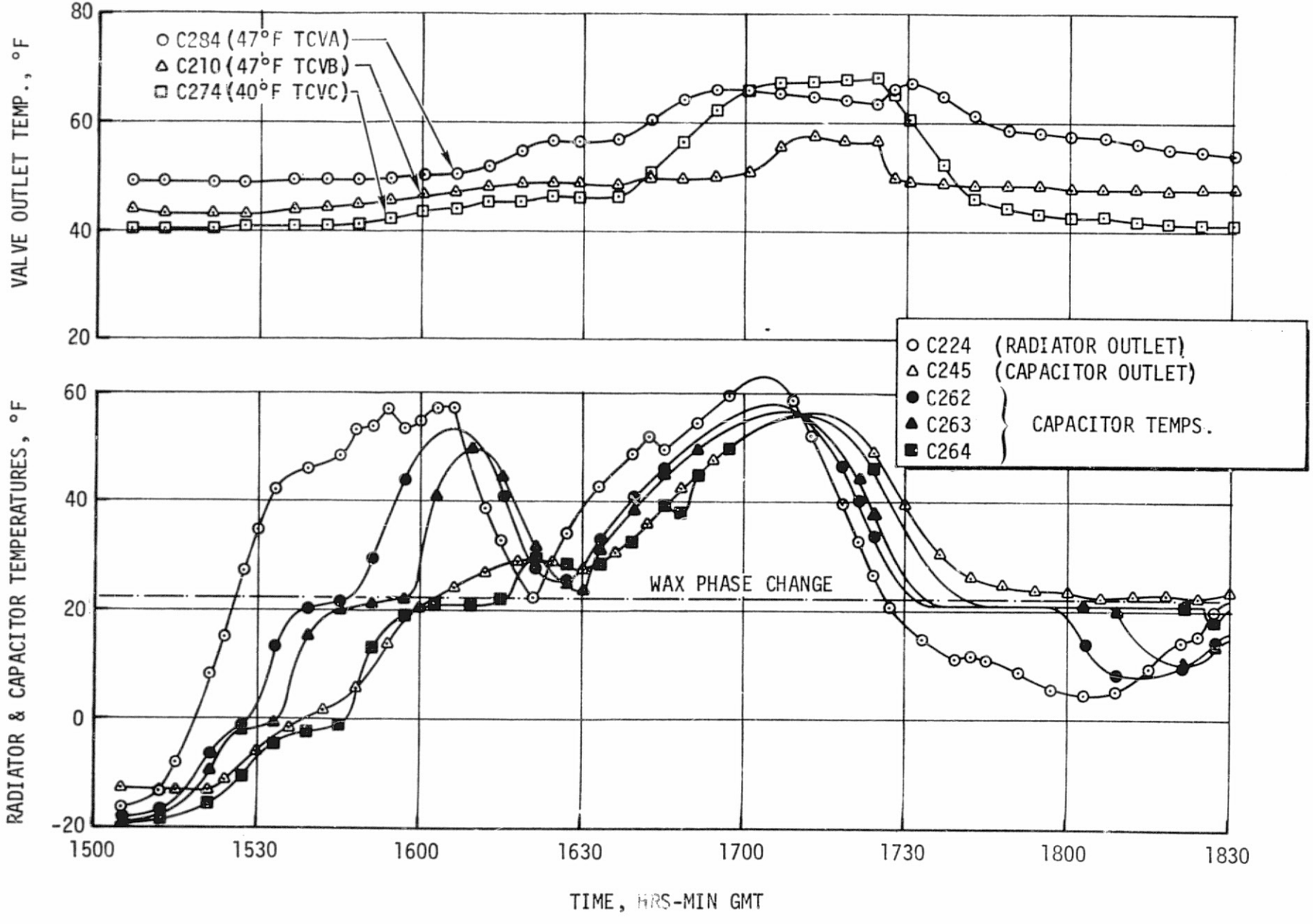

Figure 7-9. Two Consecutive Z-LV Orbits on DOY 014

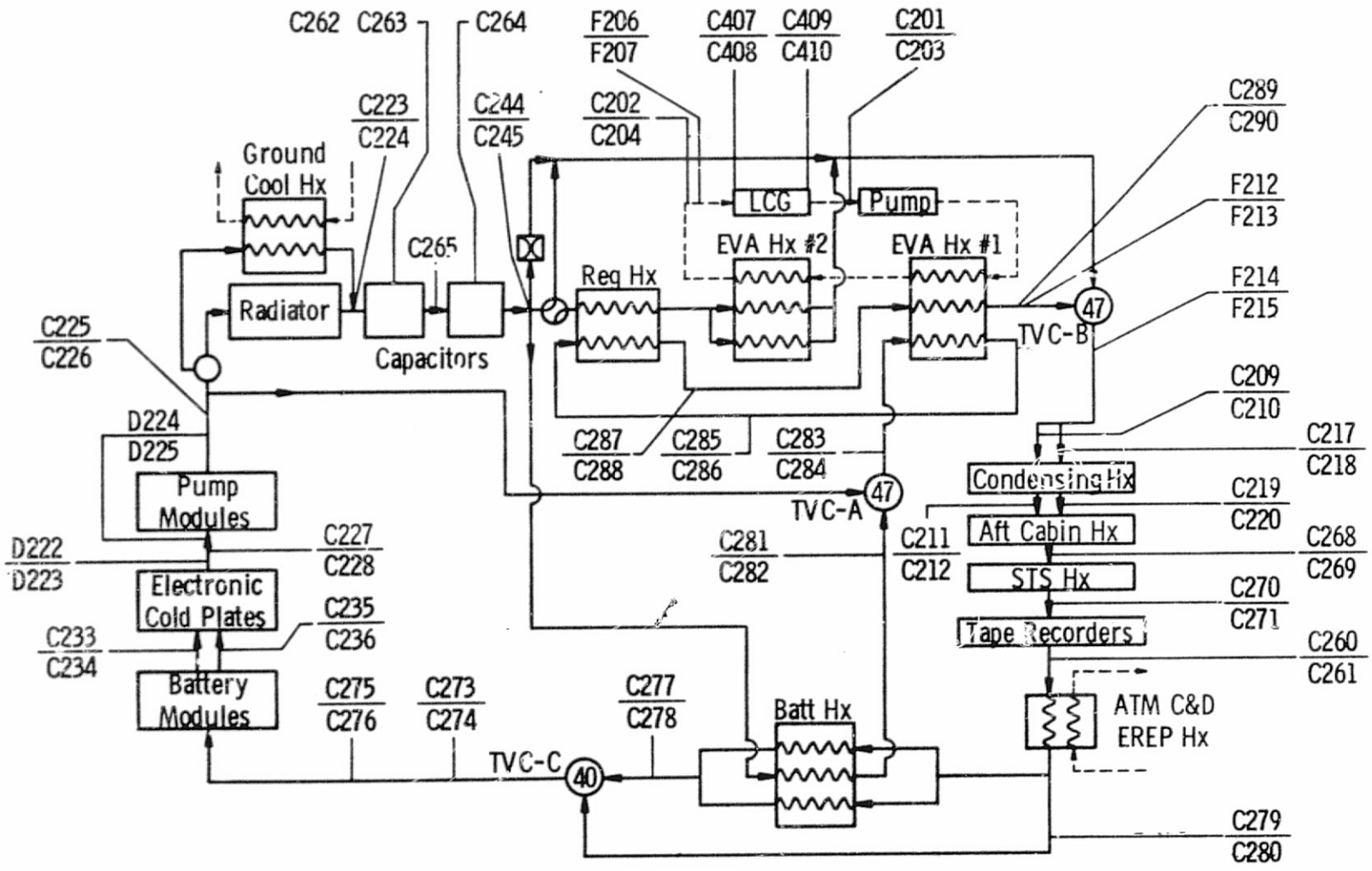

Figure 7-10. Location of Flight Measurements

for the location of the various temperature sensors. The fact that the valve outlet temperatures exceeded their control band was of no concern however, since the excursion was for a relatively short period of time and had little effect on the atmosphere conditions and cold plated equipment.

5. EVA Performance - The baseline requirement for EVA/IVA cooling system design was to remove 2000 Btu/hour for each of two men while maintaining the water supply temperature between 41°F and 49°F. A change in program groundrules required that three crewmen be suited rather than two. This change required water cooling for the third crewman with the resulting loads estimated preflight for the primary and secondary cooling loops as shown in figure 7-11. Analysis indicated that the load profile for the primary loop would result in a water supply temperature of 50.5°F, which exceeded the specified upper limit of 49°F. However, a decision was made to accept the higher water supply temperature.

The peak heat loads in the EVA water loop during the flight are summarized in Table 7.5 for each Skylab mission. As shown, the heat loads were considerably lower than the 5000 Btu/hour maximum which was estimated for the preflight studies. This could be due partially to the water supply temperature being warmer than assumed preflight since the EVA bypass valve had to be operated in the bypass mode. (See paragraph C.2.) Figures 7-12 and 7-13 show the approximate water and coolant temperatures which were provided with the EVA valve in bypass. The crew reported that the cooling was adequate and tended to position their flow diverter valve with less than 100% flow, even though the supply temperatures were higher than the 49°F specification upper limit.

The third EVA of SL-3 was accomplished with O_2 cooling since there wasn't adequate coolant in the primary coolant loop (see paragraph C.3.) and the decision was made not to use the secondary loop for EVA with the risk of the control valve sticking in a worse position. The approximate heat removal which could be provided by using the high O_2 flow is shown in figure 7-14 for similar conditions to those in flight. The crew reported that the O_2 cooling was adequate for the work loads experienced during the EVA but that tasks requiring high work loads would require water cooling.

6. Radiator Coating Degradation - The solar absorptivity of the Z-93 coating on the radiator was measured prior to launch and an average value of approximately 0.14 was established. Periodically throughout the mission, a flight support computer model was run and the inputs of solar absorptivity and emissivity were modified until the model results matched the flight data. Figure 7-15 shows a typical comparison which was made using the data for DOY 264. Using

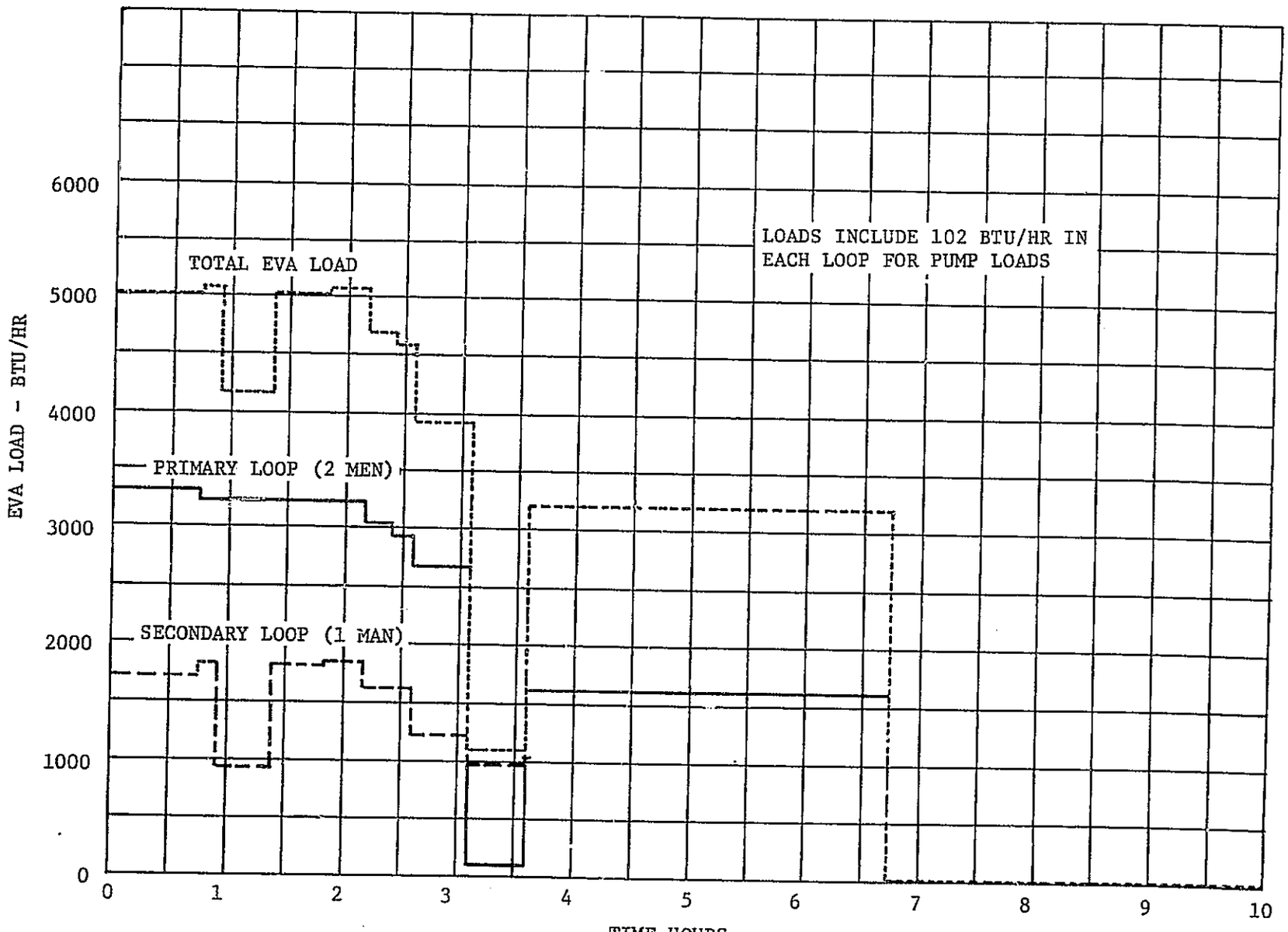

Figure 7-11. Three Man EVA Load Profile

Table 7.5. EVA Heat Loads

MISSION	EVA	TIME (DOY:HR:MIN)	SUIT COOLING SYSTEM	EVA LOOP[1] PEAK LOAD (BTU/HOUR)
SL-2	#1	158:14:30	SUS 2	1835 (Deployed OWS SAS)
	#2	170:12:21	SUS 1	1700
SL-3	#1	218:17:00	SUS 1	1770 (Deployed Twin Pole Shield)
	#2	236:15:00	SUS 2	1500
	#3			Oxygen Cooling Only
SL-4	#1	326:20:45	SUS 1	2205
	#2	359:16:30	SUS 1	1460
	#3	363:17:10	SUS 1	1515
	#4	034:18:10	SUS 1	2045

NOTES

(1) Startup Transients Were Larger

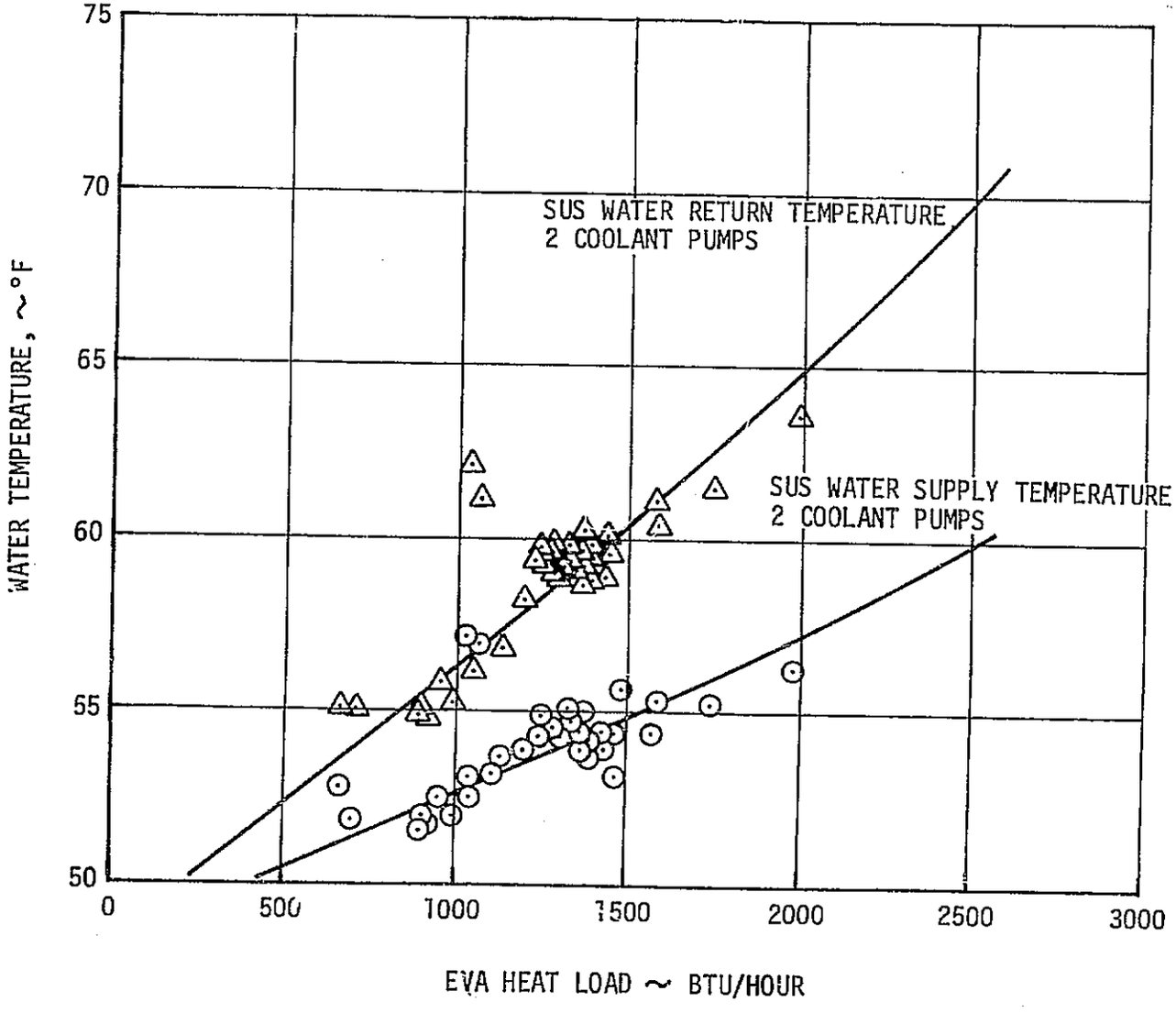

Figure 7-12. Suit Cooling Loop Water Temperatures

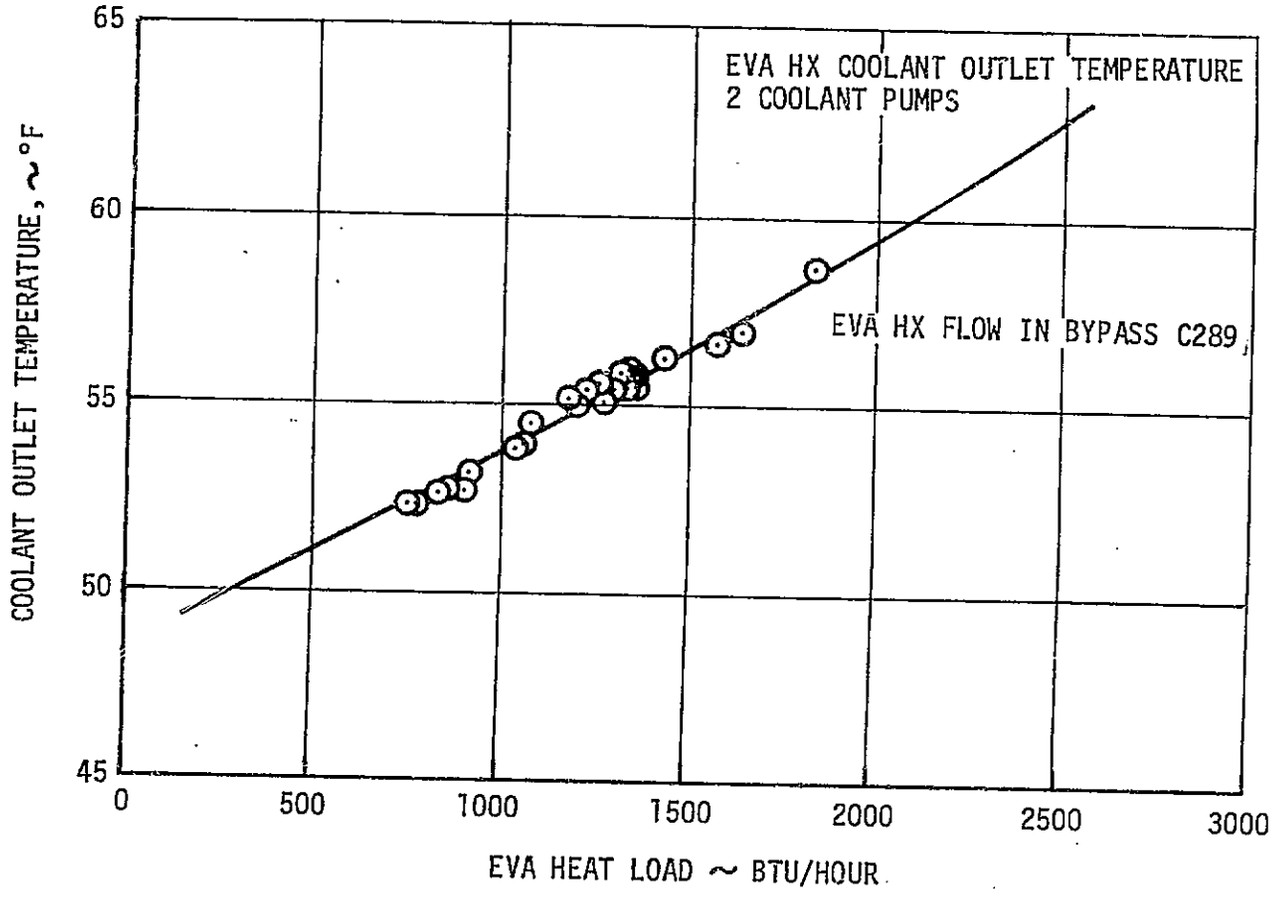

Figure 7-13. EVA Heat Exchanger Coolant Outlet Temperature

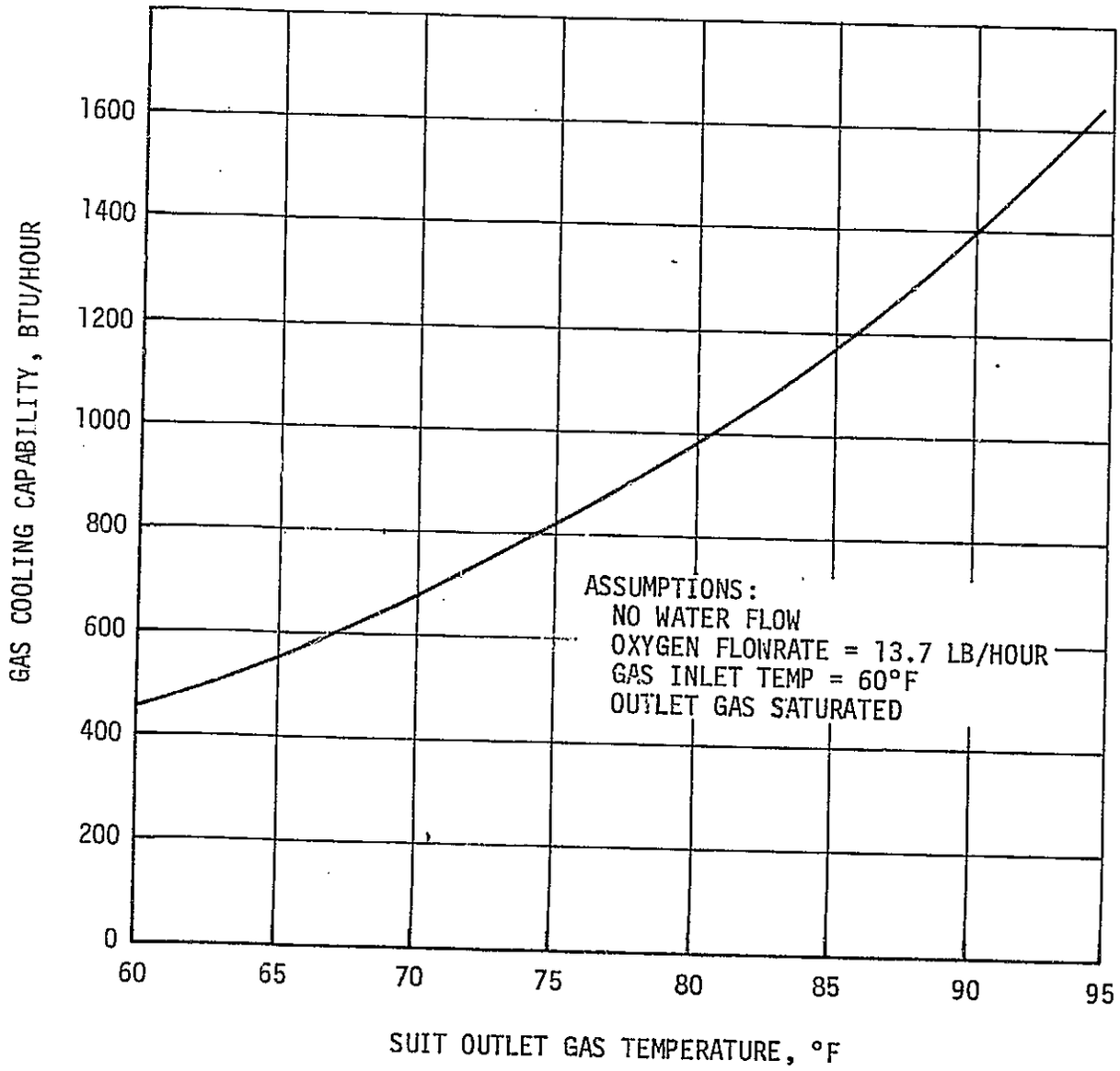

Figure 7-14. EVA Cooling with O_2 Flow

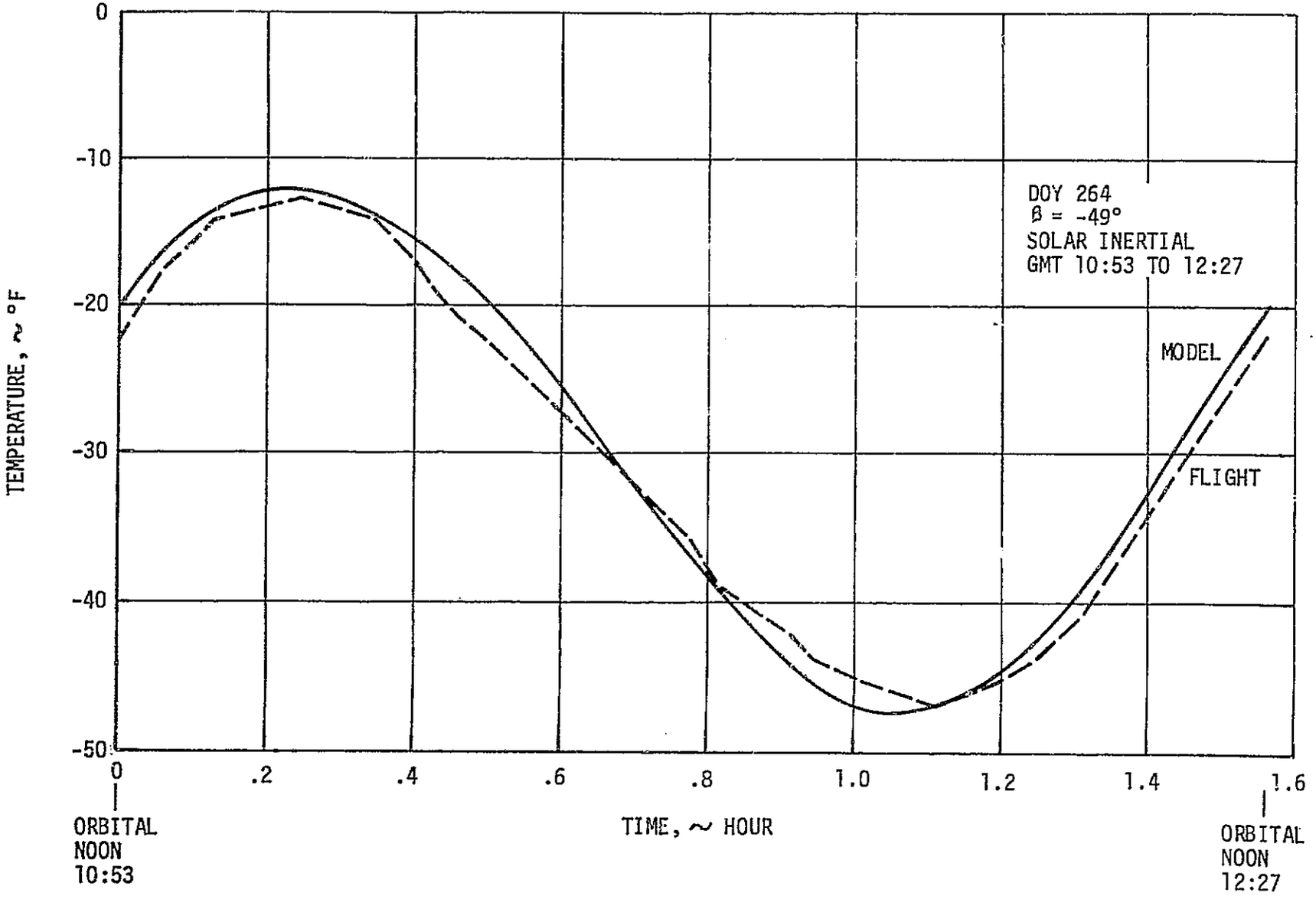

Figure 7-15. Thermal Model Comparison with Flight Data

the model and flight comparisons, the degradation in the coating could then be determined versus time. The results are plotted in figure 7-16. As shown, the solar absorptivity of the radiator at the end of the SL-4 mission was approximately 0.25. No change in the emissivity could be distinguished. The results showing the degradation of the Z-93 sample coating which was contained in the D024 experiment are also shown in figure 7-15. As shown, the trend is similar to the degradation of the coating on the radiator except that the D024 samples had degraded to a value of approximately 0.34 by the end of the mission. This was attributed to the fact that the D024 experiment was mounted on the sun side of the vehicle with no shadowing. Crew comments during the debriefings indicated that where the sun impinged on the radiator coating, they could see a pattern of definitely lighter color where it was shadowed by the ATM deployment struts or other equipment. This would lead to the conclusion that the radiator coating had probably degraded to the values corresponding to the D024 samples where it was not shadowed but had degraded considerably less where it was shadowed by the ATM or was on the backside of the vehicle. This accounts for the lower value calculated for the radiator since this would be the equivalent value if averaged over the entire radiator surface.

7. ATM C&D/EREP Loop Performance - The ATM C&D/EREP loop had to provide adequate cooling for the ATM C&D console and all cold-plated EREP equipment in the MDA and maintain their temperatures within specification limits. In addition, all local areas had to be maintained between 55°F and 105°F to meet touch temperature criteria and assure that no condensation occurred. Crew comfort criteria as specified in MSC Document BRO-BD-57-67 also had to be met while the operator was at the ATM C&D console. These criteria had to be met while satisfying the various modes of operation as specified in paragraph 2.3.3.10 of the Mission Requirements Document for operation of the ATM and EREP experiments.

There was only limited flight instrumentation for monitoring the temperature of specific components on the ATM C&D console and the EREP equipment had no flight temperature indications. However, using the flight water inlet temperatures and flowrates in a detailed analytical model which was developed for the components, it can be concluded with a reasonable degree of confidence that the temperature requirements were met throughout the entire Skylab mission. All design studies prior to the space flight showed the ATM C&D and EREP components would not exceed their maximum temperature limits if the water inlet temperature did not exceed 78°F and the average MDA temperature did not exceed 80°F. The water inlet temperature during the flight was always maintained below 78°F and was a maximum of 74.9 at 264:14:30. The maximum average MDA temperature was approximately 71.5°F, well below the assumed 80°F.

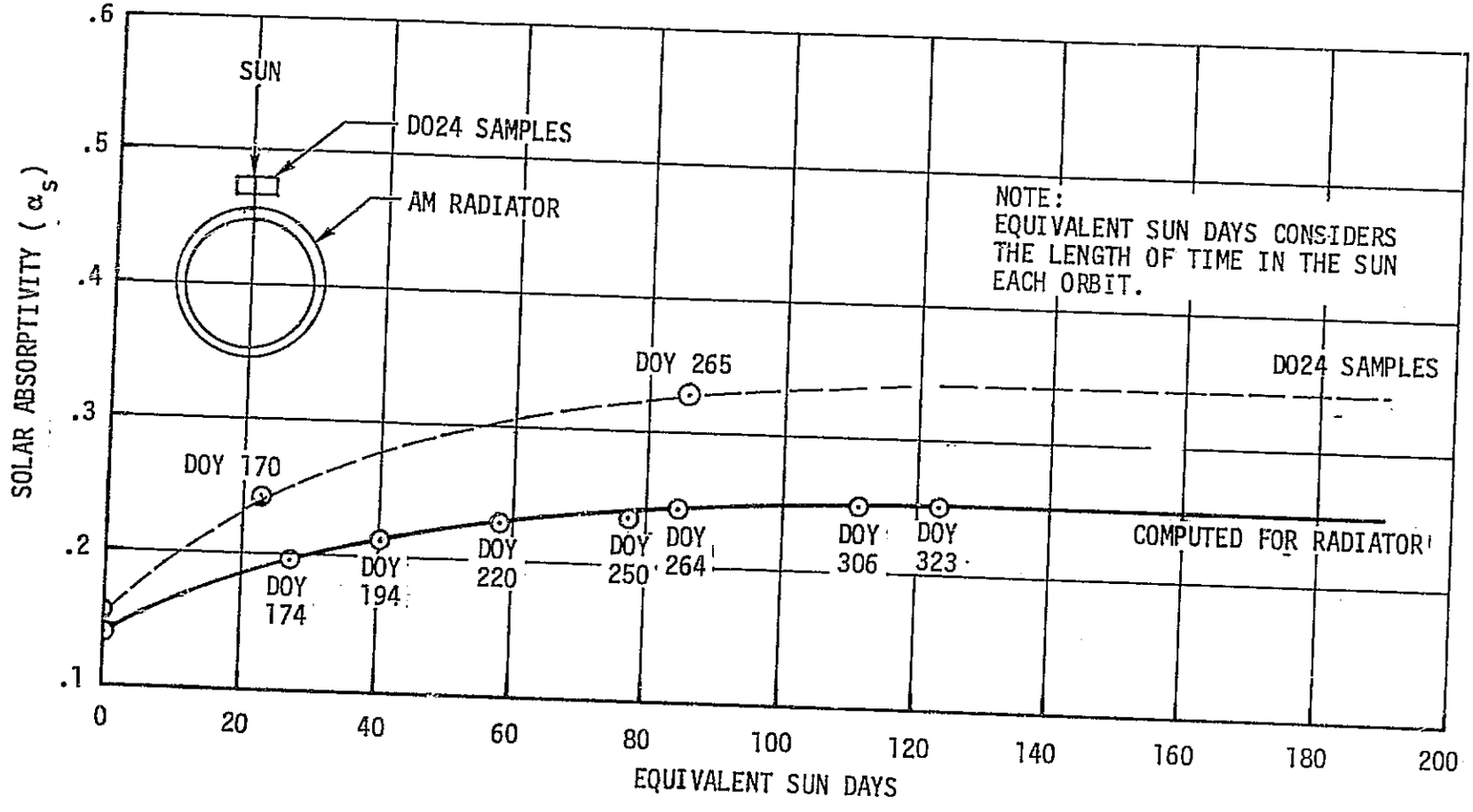

Figure 7-16. AM Radiator Solar Absorptivity

Additional studies were accomplished which showed that the heat load on the system was composed not only of the equipment load and the heat leaks into the system from the MDA, but also of an additional load from environmental heating in the portions of the system which were mounted on the outside of the Airlock Module. This load, in the solar inertial attitude, varied from approximately 180 Btu/hour at the low Beta angles to approximately 500 Btu/hour at the higher Beta angles of 50 degrees and above. The amount of heat from the environment appeared to increase during the periods that the vehicle was in the Z-LV attitude. There was also evidence that the conductances which had been assumed for design purposes were conservative. This would result in even lower component temperatures than the preflight predictions for the various heat generating components such as the EREP tape recorder motor and the ATM C&D TV monitors. However, it would also result in higher transient heat loads being imposed on the coolant loop since more heat would be transferred to the water. Figures 7-17 and 7-18 show the water outlet temperatures for typical days when ATM experiments and EREP experiments were operated, respectively. As shown, the higher outlet temperatures in flight indicate that more of the heat went into the water loop and was probably the result of the conservatively small values assumed for the conductances.

The combined effect of the larger conductance and the environmental heating in the airlock area therefore contributed to the ATM C&D/EREP loop peak heat loads being higher than those calculated preflight. The maximum load during ATM C&D operations was approximately 1450 Btu/hour while the preflight predictions were approximately 800 Btu/hour. The maximum load during EREP operations was approximately 2780 Btu/hour for the EREP pass on DOY 20 while preflight predictions were a maximum of approximately 1440 Btu/hour. Though these loads were considerably higher than preflight predictions they were of such short duration that there was no adverse effects on the performance of the ATM C&D/EREP loop or the AM coolant loop.

It was also significant to note that the temperatures which could be monitored on the ATM C&D console were well below the redline limit that had been assumed prior to the flight. Table 7.6 shows the maximum values which were observed for the sensors versus their redline values.

8. Low Temperature in Suit Cooling System #1 - The attempt to reduce OWS structural and internal temperatures during the period before launch of the SL-2 crew by pitching the cluster about the Y axis (and thereby reducing the incident solar flux) resulted in an excessively cold environment in the Airlock Module. The structural temperatures gradually decreased and approached the freezing point of water beneath the thermal curtain in the area of the suit/battery

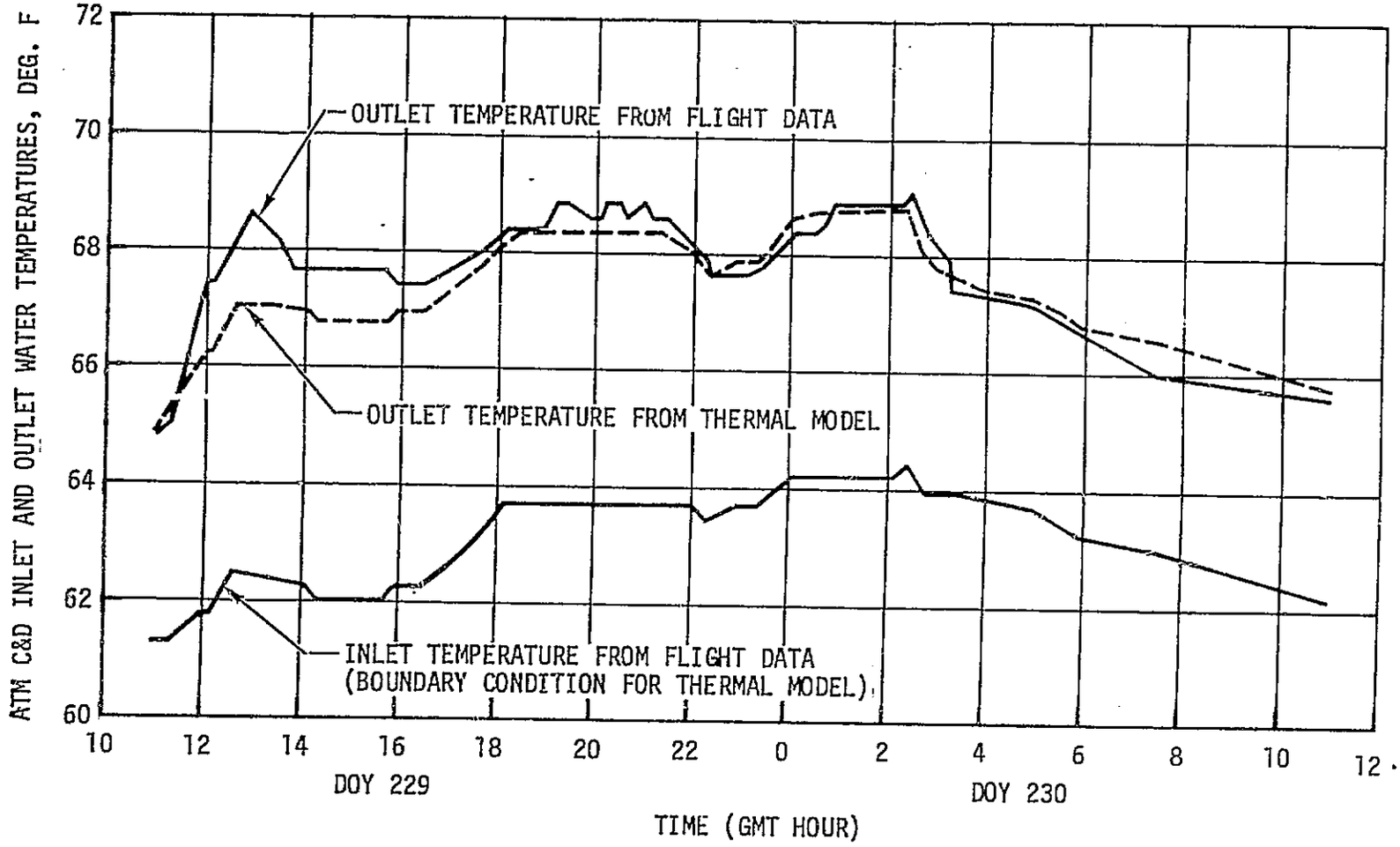

Figure 7-17. Typical ATM C&D Operations

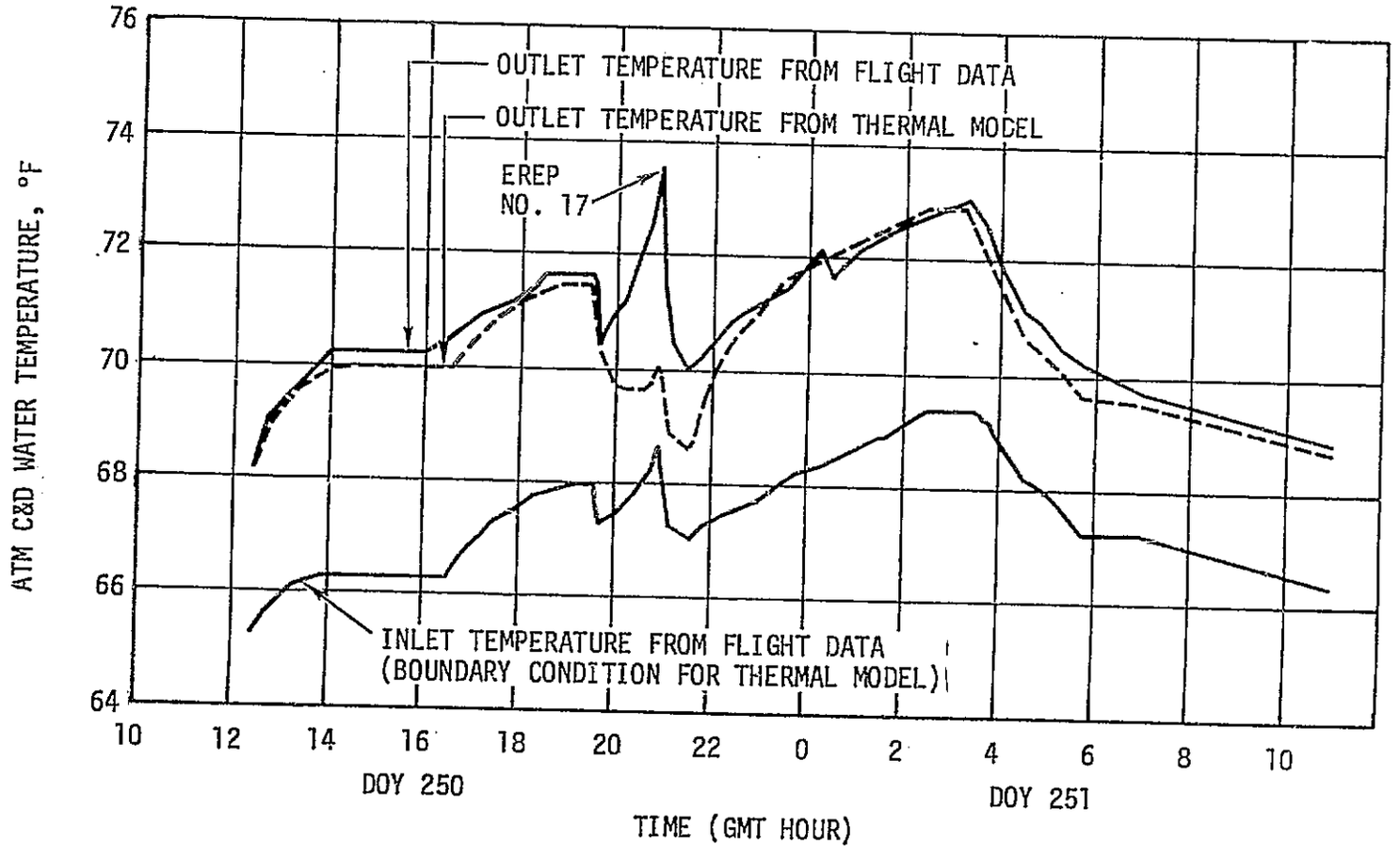

Figure 7-18. Typical EREP Experiment Operations

Table 7.6. ATM C&D Console Temperatures

SENSOR NO.	DESCRIPTION	ASSUMED REDLINE LIMIT TEMP (°F)	*MAX. FLIGHT TEMP (°F)
C154	Intensity Display Counter	140	84
C155	Exposure Display Counter	140	84
C156	CRT HV Pwr Supply	140	86
C157	Intensity Modulator	140	82
C159	C&D Low Volt Pwr Supply	140	86
C376	Video Monitor No. 1	185	102
C377	Video Monitor No. 2	185	91

*Temperatures monitored between DOY 324 and 355

cooling module (figure 7-19). If allowed to freeze, the loop could have been lost due to breaking of water lines. A more serious concern, however, was that freezing might occur within the water/coolant interface heat exchanger with a resulting potential loss of an Airlock Module cooling loop.

Several vehicle attitude changes were made in an attempt to improve the thermal environment in the suit/battery module area. At 141:12:37 the vehicle pitch was decreased from approximately -50° to -40°F while no temperature increase was observed, the rate of decrease was diminished.

In order to provide additional solar energy in the area of the thermal curtain, a -80° pitch maneuver was performed and maintained for one revolution at 142:11:09. The effect of the maneuver is illustrated in figure 7-20 which depicts the shadowing of the Airlock Module area with the vehicle in a -50° pitch attitude (which was nominally maintained throughout this period) and also shows the direct solar impingement into the area of the Airlock Module meteoroid curtain with the vehicle in a -80° pitch maneuver. The photographs in figure 7-20 were made with a Skylab model and solar lamp on DOY 142 to aid in selecting a maneuver to provide solar flux into the desired area. Extreme pitch maneuvers of this type caused low temperature problems on the ATM solar arrays solder joints and were therefore undesirable. On the revolution prior to executing the -80° pitch, the vehicle was placed in the solar inertial attitude to warm the solar arrays prior to the maneuver and to charge the batteries. This attitude also provided additional solar energy to the Airlock Module.

Other pitch maneuvers which provided some improvement in the suit/battery module environment were performed at 143:21:50 (-65° for two revolutions) and at 144:22:45 (-68° for two revolutions).

A temperature history for suit cooling system #1 pump outlet temperature is provided in figure 7-21. The warming trend which begins just before DOY 146 was apparently caused by the influence of heat transfer from the OWS dome since a review of OWS dome temperatures showed a corresponding increase in temperature at that time.

The minimum temperature observed was approximately 33.5°F. The accuracy of the measurement was approximately ±2°F. Even though the water temperature approached the freezing point, it is believed that freezing was prevented. Subsequent performance of the suit loop verified that no water leak developed as a result of the cold temperatures.

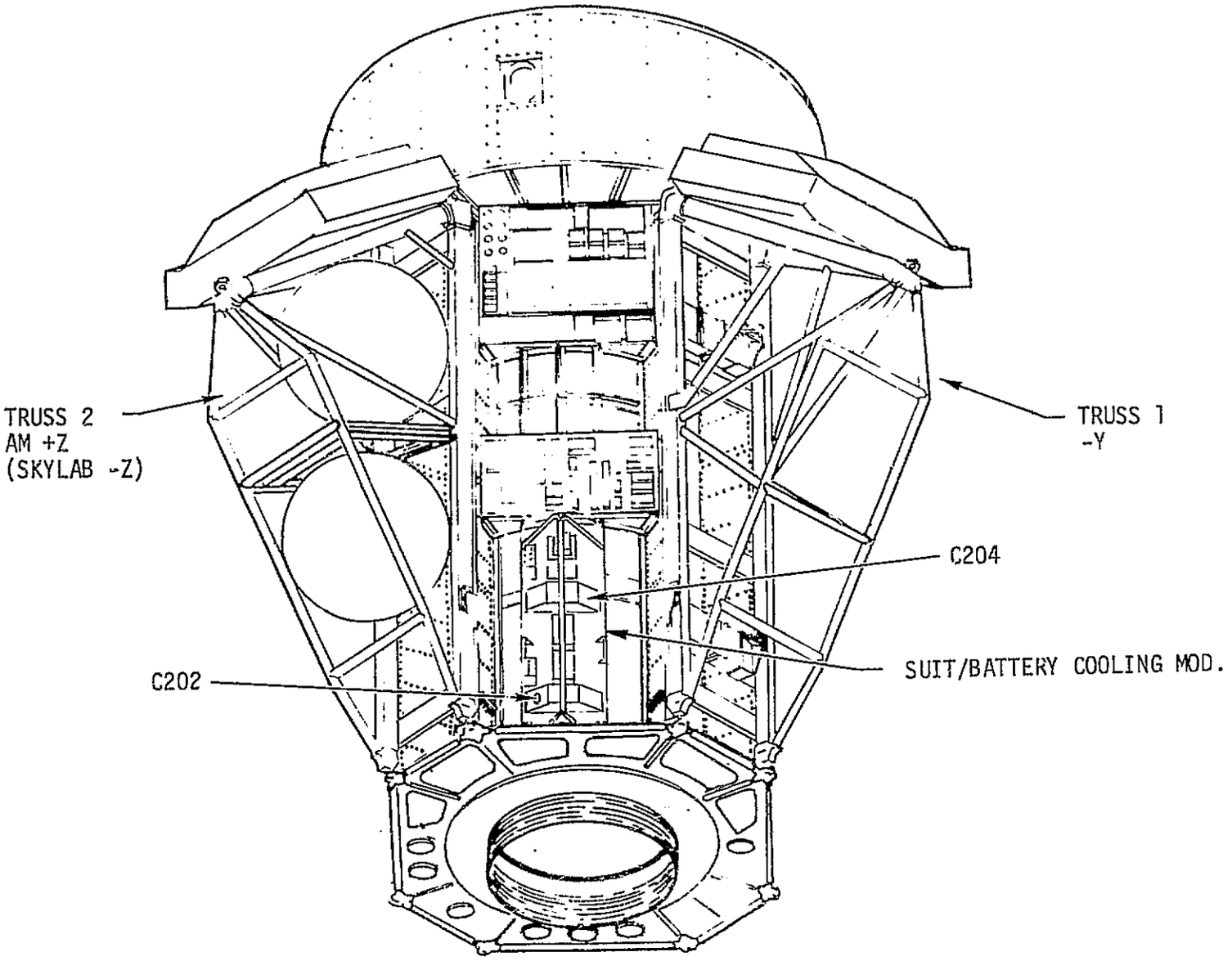

Figure 7-19. Location of Suit/Battery Module

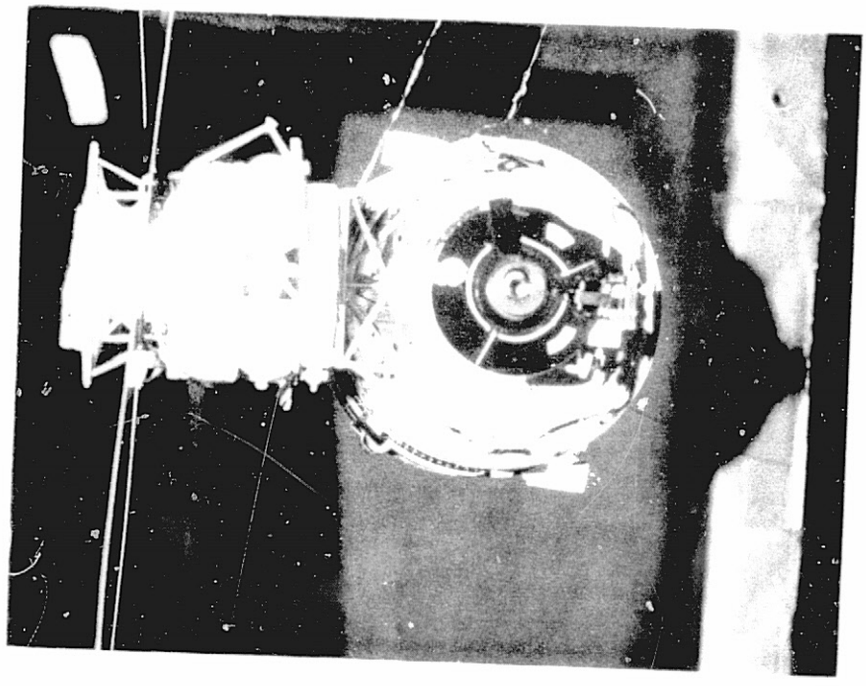

-80° PITCH

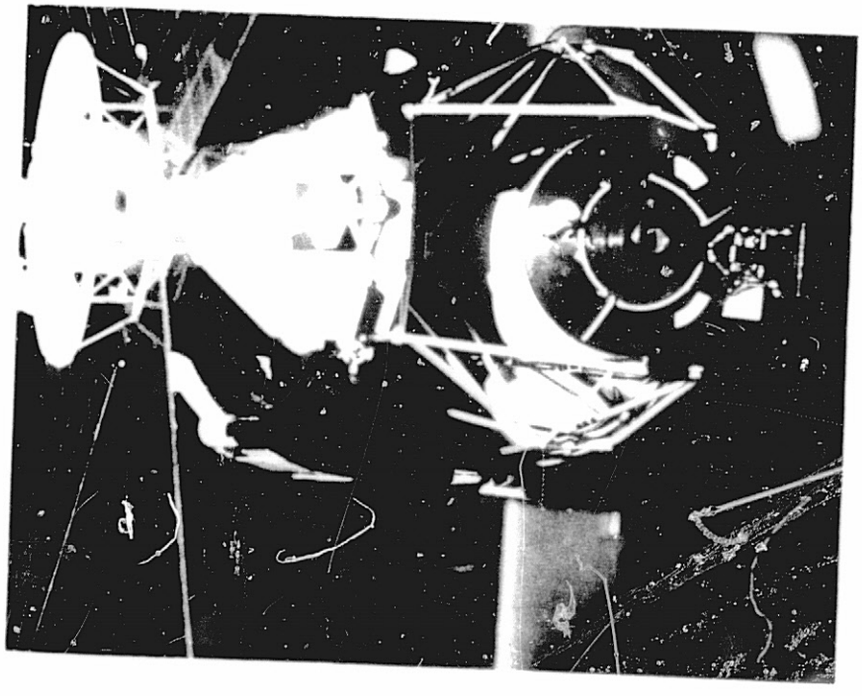

-50° PITCH

Figure 7-20. Effect of Pitch Maneuvers on Shadowing of Airlock Module

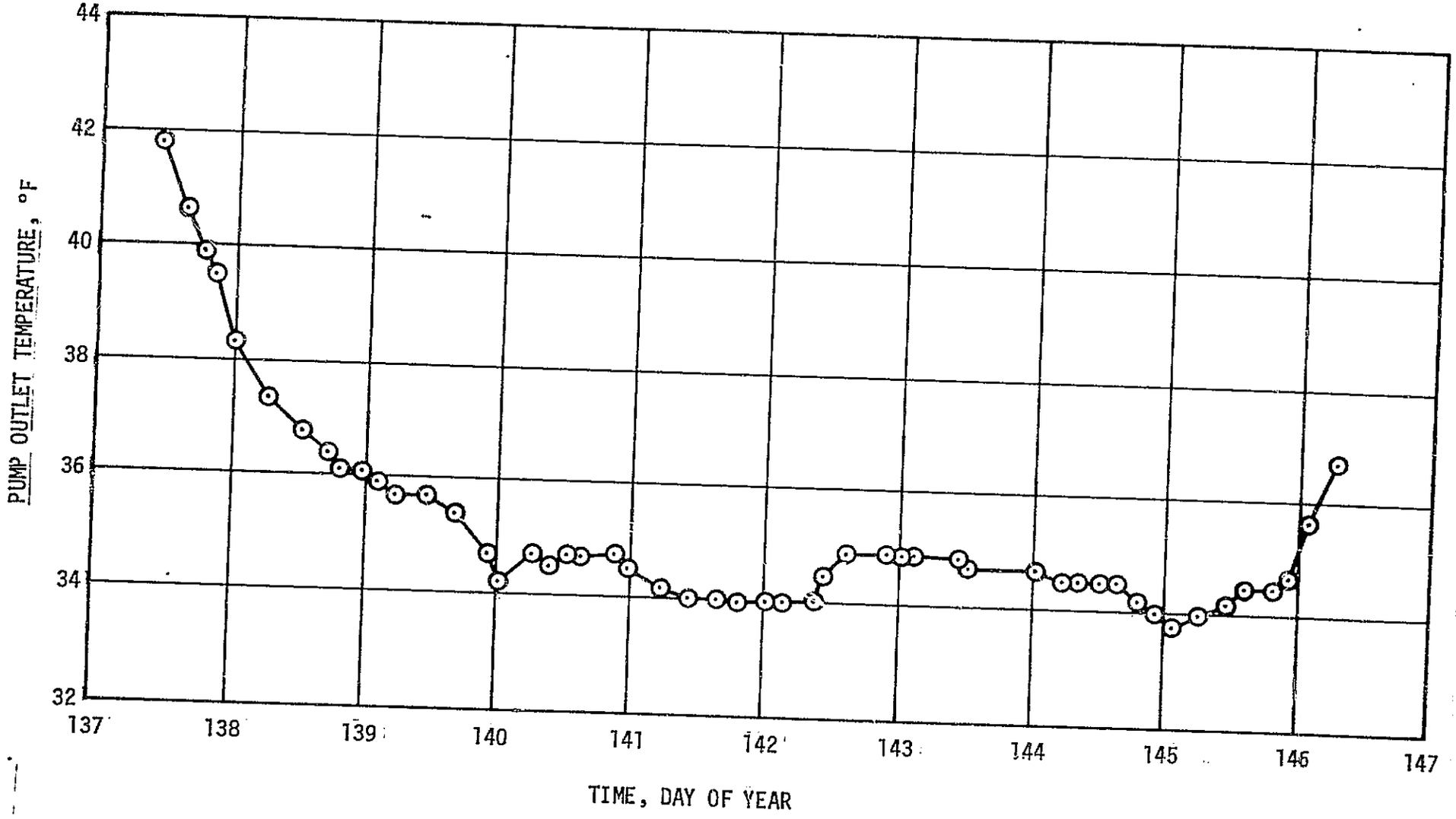

Figure 7-21. Suit Cooling System Outlet Temperature

9. Potential Freezing of AM Radiator - At approximately 137:02:01, it was determined that the outlet temperature of thermal control valve C (TCVC) was 45.7°F which was above its control point of 40 ±2°F. Since the radiator inlet temperature was only 48°F, this implied that the radiator flowrate was nearly zero and might be in the process of freezing. Although this condition in itself was not thought detrimental, the thawing required to reactivate the radiator had never been attempted and was therefore considered undesirable. The following items were therefore turned on to add more heat to the loop.

Component	Approximate Load (Btu/hour)
Tape Recorder #3 & DC/DC Converter	51
10 Watt transmitter A	165
10 Watt transmitter C	165
(2 Watt transmitter turn off)	-66
Net Heat Load Added	315 Btu/hour

This corrective action caused the TCVC outlet temperature to decrease from 45.7°F to 41.4°F and the pump delta P increased from 39 to 46 PSID indicating that the radiator flow had been reinitiated.

It was later shown by analysis that the thermal capacitance of the radiator was large enough that freezing would not occur with zero flow in the radiator. This proved to be true on DOYs 141 and 142 when the system heat loads were very low and the radiator flow actually did drop to approximately 0 lb/hour on the cold side of each orbit and there was no apparent freezing.

10. AM Coolant Pump Performance - Coolant flowrates during the flight were better than the design values and did not decrease with time of operation. The flight values for the various inverter/pump combinations utilized throughout the mission are summarized in Table 7.7. Since the system heat loads, temperatures, pressures, and other parameters were directly dependent upon the pump combinations which were utilized at any given time, Table 7.8 is provided for reference. Table 7.9 shows the total run time that was imposed on each pump. Endurance tests on the ground prior to the flight had been run on a pump for approximately 9000 hours without failure.

Prior to SL-2, the automatic switchover system switched from the primary to the secondary loop on two occasions. At 139:20:00:10, while PRI-Inv 1/Pump A was running, the AM coolant loop switched automatically from the primary to the secondary loop. Switchover measurements were at the following values prior to switchover, well above the automatic switchover limits:

Table 7.7 Coolant Flowrates

COOLANT LOOP	INVERTER	PUMP(S)	FLOWRATE (LB/HOUR)	
PRIMARY	1	A	270	
		B	1	
		AB	510	2
	2	B	270	
		C	1	
		BC	510	2
	3	C	1	
		A	1	
		AC	1	
SECONDARY	1	A	270	
		B	1	
		AB	520	
	2	B	270	
		C	1	
		BC	515	
	3	C	275	
		A	270	2
		AC	1	

NOTES: 1 Inverter/pump(s) combination not utilized
2 Estimated from TCV-B hot inlet flow measurement since TCV-B outlet flowmeter not available at time of designated operation

Table 7.8. Coolant System Pump Configuration Status

CODE: PRIMARY OR SECONDARY LOOP
INVERTER NO. 1
PUMP
STATUS * * TURNED ON OR OFF
(PUMPS NOT NOTED ARE OFF)

PRI IA ON

TIME (GMT)	STATUS	TOTAL PUMPS (PRI + SEC)
134:17:30	LAUNCH CONFIGURATION PRI. 1A	1+0
139 [illegible]:00	PRI 1A OFF SEC 1A ON (AUTO SWITCH)	0+1
140:[illegible]:16:00	PRI 1A ON SEC 1A OFF	1+0
140:01:41:00	PRI 1A OFF SEC 1A ON (AUTO SWITCH)	0+1
146:00:18:00	SEC 1A & B ON	0+2
146:13:52:00	SEC 1A SEC 1B OFF	0+1
146:16:16:00	SEC 1A & B ON	0+2
146:16:25:00	SEC 1A SEC 1B OFF	0+1
147:04:17:31	PRI 1A ON SEC 1A	1+1
148:14:17:17	PRI 1A SEC 1A OFF	1+0
149:01:44:00	PRI 1A SEC 1A ON	1+1
149:02:04:55	PRI 1A SEC 1A OFF (CIRCUIT BREAKER POPPED)	1+0
149:02:05:55	PRI 1A SEC 2B ON (CREW COMMAND)	1+1
149:03:29:00	PRI 1A SEC 2B OFF SEC 3C ON (GROUND COMMAND)	1+1
150:22:42:00	PRI 1A OFF SEC 3C	0+1
151:00:19:00	PRI 1A ON SEC 3C	1+1
151:12:09:00	PRI 1A OFF SEC 3C	0+1
152:00:40:35	PRI 1A ON SEC 3C (HIGH ΔP PRI AT START)	1+1
153:12:00:58	PRI 1A OFF SEC 3C	0+1
154:02:35:00	PRI 1A ON SEC 3C (HIGH ΔP PRI AT START)	1+1
154:12:20:00	PRI 1A OFF SEC 3C	0+1
155:00:42:00	PRI 1A ON SEC 3C (HIGH ΔP PRI AT START)	1+1
155:12:16:54	PRI 1A OFF SEC 3C	0+1
155:23:26:00	PRI 1A ON SEC 3C (HIGH ΔP PRI AT START)	1+1
156:11:23:00	PRI 1A OFF SEC 3C	0+1
158:12:59:30	PRI 1A ON SEC 3C (EVA)	1+1
158:13:42:47	PRI 1A OFF SEC 3C (SUS #1 FROZE & TCV B OFF TEMP SCALE LOW)	0+1
158:16:05:00	PRI 1A ON SEC 3C (CREW COMMAND)	1+1

Table 7.8. Coolant System Pump Configuration Status (Continued)

TIME (GMT)	STATUS	TOTAL PUMPS (PRI + SEC)
158:16:17:00	PRI 1A OFF SEC 3C (CREW COMMAND)	0+1
158:19:00	PRI 1A ON SEC 3C OFF (CREW COMMAND)	1+0
158:19:43	PRI 1A OFF SEC 2B ON (CREW COMMAND)	0+1
159:01:07:30	SEC 2B OFF (CREW COMMAND)	0+0
159:01:08:30	SEC 2B ON	0+1
159:01:58:48	SEC 2B OFF	0+0
159:02:07:30	SEC 3C ON (CREW COMMAND)	0+1
159:02:40:30	SEC 3C OFF (CREW COMMAND)	0+0
159:02:41:30	SEC 2B ON	0+1
160:02:16:34	PRI 1A ON SEC 2B	1+1
160:02:17:46	PRI 1A OFF SEC 2B ON	0+1
160:18:15:00	PRI 1A & B ON SEC 2B	2+1
160:18:23:46	PRI 1A & B OFF SEC 2B	0+1
160:18:42:41	PRI 1A ON SEC 2B	1+1
160:18:47:00	PRI 1A OFF SEC 2B	0+1
161:13:54:23	PRI 2B ON SEC 2B	1+1
162:16:49:13	PRI 2B SEC 2B & C ON	1+2
162:16:56:25	PRI 2B SEC 2B & C OFF	1+0
162:22:07:22	PRI 2B SEC 2B & C ON	1+2
162:22:08:47	PRI 2B SEC 2B & C OFF	1+0
163:14:35:00	PRI 2B SEC 2B & C ON	1+2
163:14:56:32	PRI 2B SEC 2B SEC 2C OFF	1+1
170:08:54	PRI 2B & C ON SEC 2B (EVA)	2+1
170:13:07	PRI 2B, PRI 2C OFF SEC 2B	1+1
173:09:07:50	PRI 2B OFF SEC 2B (DEACTIVATION)	0+1
207 STATUS	SEC 2B (STOWAGE)	0+1
209:20:42	PRI 2B ON SEC 2B (HIGH ΔP AT START) (ACTIVATION)	1+1
210:04:35	PRI 2B OFF SEC 2B	0+1
215:19:40	PRI 2B ON SEC 2B	1+1
218:14:26	PRI 2BC ON SEC 2B (EVA)	2+1
219:00:22	PRI 2B PRI 2C OFF SEC 2B	1+1
233:13:30:45	PRI 2B SEC 2C ON SEC 2B BUS 1 CIRCUIT BREAKER OPENED, BOTH SECONDARY PUMPS OFF. GROUND THEN COMMANDED INVERTER 2 OFF, THEN ON. NO PUMP STARTED UP. THEN PUMP C TO INVERTER 3. CREW THEN RESET BUS 1 CIRCUIT BREAKER AND SEC 2B STARTED.	1+0

Table 7.8. Coolant System Pump Configuration Status (Concluded)

TIME (GMT)	STATUS	TOTAL PUMPS (PRI + SEC)
233:13:34:30	PRI 2B SEC 2B ON	1+1
233:18:20:57	PRI 2B SEC 2B OFF	1+0
233:18:21:17	PRI 2B SEC 3C ON	1+1
233:18:22:10	PRI 2B SEC 3C OFF	1+0
233:18:22:45	PRI 2B SEC 2BC ON	1+2
233:20:26:30	PRI 2B SEC 2C OFF SEC 2B	1+1
235:18:30:50	PRI 2B OFF SEC 2B	0+1
236:12:52:00	SEC 2BC ON (EVA)	0+2
237:17:20:00	SEC 2B SEC 2C OFF	0+1
268:00:00:00	SEC 2B (DEACTIVATION)	0+1
269 STATUS	SEC 2B (STOWAGE)	0+1
324:00:33	PRI 2B ON SEC 2B (FOLLOWING COOLANOL RECHARGE OF PRI LOOP)	1+1
324:00:35	PRI 2BC ON SEC 2B	2+1
324:00:52	PRI 2C OFF PRI 2B SEC 2B	1+1
326:15:51	PRI 2B OFF SEC 2B	0+1
326:15:51:25	PRI 2BC ON SEC 2B (EVA PREP)	2+1
327:01:27:45	PRI 2C OFF PRI 2B SEC 2B	1+1
327:16:42:51	PRI 2B OFF SEC 2B	0+1
353:12:53:45	PRI 2B ON SEC 2B	1+1
359:15:08	PRI 2BC ON SEC 2B (EVA PREP)	2+1
360:00:24	PRI 2C OFF PRI 2B SEC 2B	1+1
363:14:50:39	PRI 2B OFF SEC 2B	0+1
363:14:51:03	PRI 2BC ON SEC 2B (EVA PREP)	2+1
363:21:21	PRI 2C OFF PRI 2B SEC 2B	1+1
16:16:38:24	PRI 2B OFF SEC 2B	0+1
16:16:38:32	PRI 2BC ON SEC 2B (MORE OWS COOLING)	2+1
24:11:32:15	PRI 2C OFF PRI 2B SEC 2B	1+1
34:12:28	PRI 2BC ON SEC 2B (EVA PREP)	2+1
34:21:53	PRI 2C OFF PRI 2B SEC 2B	1+1
36:19:25:16	PRI 2B OFF SEC 2B (POWER SAVINGS)	0+1
39:22:21	SEC 2B (RAN SHORT SEC IA TEST)	0+1
40:15:00	SEC 2B OFF	0+0

Table 7.9 Total Accumulated Pump Run Time

COOLANT LOOP	PUMP	TIME (HOURS) PRELAUNCH	FLIGHT	TOTAL
PRIMARY LOOP	A	1202	223	1425
	B	1110	2041	3151
	C	1199	236	1435
SECONDARY LOOP	A	1223	210	1433
	B	1136	5926	7062
	C	1096	288	1384

	Flight Value	Switchover Limit
PRI TCVB Outlet (C209)	46.6°F	38 ± 1.75°F
PRI TCVB Outlet (C217)	46.5°F	38 ± 1.75°F
PRI PUMP ΔP (D224)	40.9 PSID	18 ± 2 PSID

Primary inverter 1/pump A was again selected at 140:01:15 and both auto switchover groups were enabled. At 140:01:34, the AM coolant loop switched from the primary to the secondary loop again. The temperature and pressure drop (C209, C217, and D224) values were 44.5°F, 45.7°F, and 33.6 PSID respectively, well above the switchover limits again. Telemetry was examined and indicated that Auto Switchover Group #1 Sensor circuitry initiated the first switchover at 137:02:01 but insufficient data was available to determine which group initiated the second switchover at 140:01:34. Since the Auto Switchover Group #1 Sensing Circuitry was suspect, the PRI-Inv 1/Pump A was commanded on again at 148:14:17 with only switchover group #2 enabled and performed normally with no automatic switchover. Switchover was disabled at 149:01:44. It was concluded that the switchover group #1 was suspect in the primary loop and a decision was made that the secondary loop be operated during the storage mode with both of its sensor groups enabled and if operation of the primary loop was necessary only to enable its sensor group #2. The primary coolant loop was operated several times later in the mission with group #2 without problems.

Operation of inverters and pumps was normal except an apparent failure of Inverter 1 in the secondary loop which is discussed in paragraph C.1.

11. Leakage of Water From Suit Cooling System #1 - During the EVA on DOY 359 the gas inlet temperature dropped to 33°F on suit circuit number two but the EVA crewman reported he was comfortable. This could not be explained until after the EVA, when the commander reported ice at the LSU/PCU composite connector and also said that when he disconnected the connector he got a "ball of water in the face." It was therefore concluded that the sublimation of the water, which was leaking at the composite connector was the reason for the low gas inlet temperature indication. The SUS #1 reservoir was also empty so it was concluded that the water had leaked out through the faulty connection during the EVA. The SUS #1 loop, a dry LSU, and PCU were reserviced with water and leak checked on DOY 361. The loop was used for the EVA on DOY 363 with no incidents of leakage reported. Later, on DOY 364 during the last EVA of SL-4, one crewman reported a 1/16 inch stream of water leaking from his composite connector. When the reservoir was checked during the EVA, it was found to be 20% full, so the crew was told to do the "sneak up" procedure (defined in paragraph C.2. of this section) on SUS #2 and switch the umbilicals to SUS #2 should all of the water leak out of the SUS #1 reservoir during the remainder of the EVA. The EVA was completed, however, and the SUS #2 loop was not required.

12. Water Spillage Out of the ATM C&D/EREP Loop - During the process of changing the filter in the ATM C&D/EREP water loop at 148:22:29, the crew reported a slight spillage of water (approximately 2 to 4 ounces) from one of the water quick disconnects. The crew said during the postflight debriefing that the internal plunger of the quick disconnect (QD) did not close fully when it was disconnected. It was reconnected and disconnected again with no apparent leakage. There was no leakage when the filter was changed again on DOY 165. It is believed that the leakage was a momentary malfunction of the QD which was cleared up by the connect/disconnect procedure used by the crew.

13. Malfunction of Suit Cooling System #1 Flowmeter - During the second EVA in SL-2 the SUS #1 flowmeter TM (F206) became erratic, oscillating between 228 and 293 lb/hour and dropped to 0 lb/hour sometime after 170:12:09. It appeared to have failed for the rest of the EVA. However, during EVA #1 of SL-3 on DOY 218, it showed an indication again but was oscillating near the same range as before and ceased operating at 218:22:12. The SUS #1 system was used for the four EVAs during SL-4 as well as for the various "sneak up" procedures and the flowmeter appeared to operate properly during these periods.

14. Failure of F214 Flowmeter - During the first EVA on SL-2, the primary coolant loop TCVB outlet flowmeter (F214) failed. A further discussion of the events occurring at the time of the failure is presented in paragraph C.2.

15. Failure of F212 Flowmeter - During the first EVA of SL-4, the primary loop TCVA flowrate (F212) dropped to zero when the second pump was activated in the loop. Since no reading was recorded thereafter it was concluded that the flowmeter had failed.

C. Anomalies

1. Secondary Coolant Loop Inverter Circuit Breaker Open - At 149:01:44 the secondary Inv #1/pump A was turned on by ground command. At 149:02:05 the circuit breaker for secondary Inv. 1 opened and at 149:02:06 the crew turned on secondary Inv. #2/Pump B. To provide a different power source to the secondary loop than the primary loop, the secondary Inv. #3/Pump C was turned on by ground command. (AM Bus 2 powering SEC loop and AM Bus 1 powering PRI loop). The cause of the circuit breaker opening could not be determined due to lack of data availability. It was decided that neither pump A nor inverter 1 would be used as long as other pumps and inverters were available or until troubleshooting could establish the cause of the problem. A troubleshooting procedure was developed, but was not used during the missions since pumps B and C and inverters 2 and 3

operated satisfactorily. Troubleshooting was performed, however, during the testing period after the splashdown of SL-4. From these tests it was determined that the problem was in the electronics associated with inverter 1. Neither pumps A or B would operate when powered by inverter 1 but would operate with alternate inverters.

2. Anomalies During First EVA of SL-2/Stuck Thermal Control Valves - The following sequence of events and anomalies occurred during the first EVA: The corresponding thermal control valve B (TCVB) outlet temperatures are shown in figure 7-22.

Prior to 158:13:00	The secondary loop was running with with Inv 3/Pump C on.
158:12:59:30	The primary loop was turned on with Inv 1/Pump A in preparation for EVA.
158:13:26:00	Primary loop EVA valve switched to EVA position.
158:13:26:13	EVA water loops for SUS #1 and #2 were both turned on.
158:13:26:30	Secondary loop EVA valve switched to EVA position.
158:13:26:45	Flowmeter (F214) failed in primary loop. It is thought that this occurred as a result of contamination flowing through the flowmeter which originated in the EVA heat exchanger #1 or the regenerative heat exchanger and was released when the EVA valve was put in the EVA position.
158:13:29	The EVA heat load drove the primary and secondary TCVB valves to the full cold position initially, which is normal.
158:13:30	As the primary valve traveled back toward an interim position to maintain the 47°F outlet it stuck at 93 lb/hour hot flow. This also is thought to have occurred as a result of the contamination released in the system when the EVA valve was put in the EVA position.

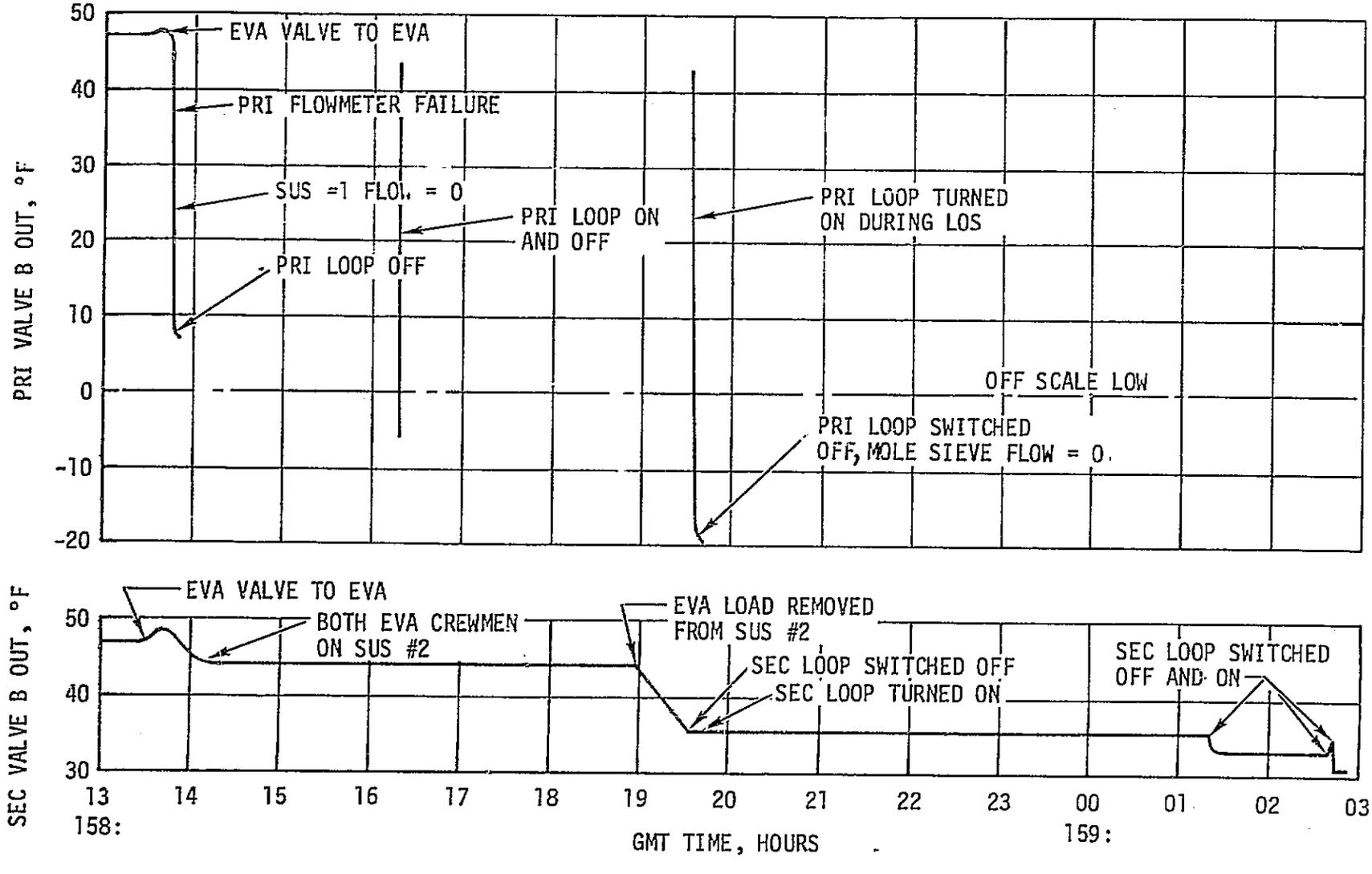

Figure 7-22. AM Coolant Loop Anomalies

158:13:39	As a result of a squealing noise and a low temperature C&W at the outlet of primary TCVB, ($T \leq 38 \pm 1.75°F$), the crew switched the primary loop EVA valve back to Bypass.
158:13:40	Crew reported when they went to Bypass the squealing noise started again and they got an EVA 1 Caution and Warning light indicating EVA water loop temperature below 33.5 $\pm 1.5°F$.
158:13:40:30	The SUS #1 flowmeter (F206) read 0 lb/hour probably as a result of water freezing in the EVA heat exchangers, since the coolant inlet to the EVA heat exchangers (C287) was reading 0°F.
158:13:41:30	The crew switched Primary EVA valve back to EVA.
158:13:42:47	The primary TCVB outlet dropped down to 7°F so the primary loop was turned off.
158:14:15:00	SUS #1 and SUS #2 water pumps were turned off.
158:14:16:00	The commander's umbilical was switched to SUS #2 and SUS #2 primary pump turned on so that both EVA crewmen were on SUS #2 and went EVA in this configuration.
158:15:52:00	The STS crewman tried both pumps in the SUS #1 water loop but got no flow.
158:16:05:00	The STS crewman turned on the primary loop Inv 1/pump A with the EVA valve in bypass.
158:16:10:00	The primary TCVB outlet went off scale low at 0°F.

158:16:17:00	Primary loop turned off by STS crewman.
158:19:00:42	When the SUS #2 water loop was turned off during LOS, the secondary TCVB valve tried to move back to an interim position to maintain a 47°F outlet but stuck at 225 lb/hour hot flow causing the valve outlet to drop to 35°F. The crew got a caution and warning (SEC COOL TEMP LOW, $T \leq 38 \pm 2.9$°F), so the secondary loop was turned off and the primary loop, was turned back on. At this time the Mole Sieve fan was reported to be making a noise and there was a Caution and Warning for a low gas flow in Mole Sieve A.
158:19:43:00	The Mole Sieve A fan flowrate was reading 0 CFM probably as a result of freezing the condensate in the condensing heat exchangers. The primary coolant loop was turned off, and the secondary loop Inv 2/Pump B was turned on. The Mole Sieve A fan was then turned off, on, and off but there was no flow.
158:19:46:00	The Caution and Warning was triggered again indicating a low temperature at the secondary TCVB outlet.
158:21:51:00	The Mole Sieve A fan was turned on again and there was flow. (The condensate had apparently thawed during the 2 hours that the primary loop was off).
159:01:08:22	The crew switched the secondary loop Inv 2/Pump B to off then command. The ground commanded the Inv 2/Pump B on. As a result, the TCVB hot flow shifted from 225 to 217 lb/hour and the TCVB outlet shifted from 35.4 to 33.0°F.

159:01:58:48	Secondary loop Inv 2/Pump B commanded off and on again, but would not restart.
159:02:07:30	The crew restarted the secondary loop by turning on Inv 3/Pump C. The TCVB hot flow shifted from 219 lb/hour to 230 lb/hour and valve outlet shifted from 33.0 to 34.6°F.
159:02:40:30	The crew switched the secondary Inv 3/Pump C off and then to command.
159:02:41:30	The ground commanded Inv 2/Pump B on. The TCVB hot flow shifted to 210 lb/hour and the valve outlet shifted to 30.7°F.

Remedial actions (see figure 7-23).

159:03:03:16	The AM and MDA heaters were commanded on to add more heat into the secondary coolant loop.
150:03:06:53	The ATM C&D was powered up to approximately 170 W to add more heat.
159:04:43:00	The crew was requested to install two liquid cooled garments near the warmest OWS water tank and turn on SUS loop #2. This procedure added enough heat to the hot inlet of the secondary loop TCVB that the outlet temperature was increased to 40°F and stabilized at that value.

The TCVB valve was designed such that a warming of the sensor cartridge caused it to expand and provided a positive movement, while a cooling of the sensor caused it to contract and the opposite movement was provided by a spring. By turning off the loop to warm up the sensor, the valve would be subjected to a large force from the expansion of the sensor cartridge and would likely unstick the valve. This procedure was used on both primary and secondary coolant loops and was successful in unsticking both valves as follows:

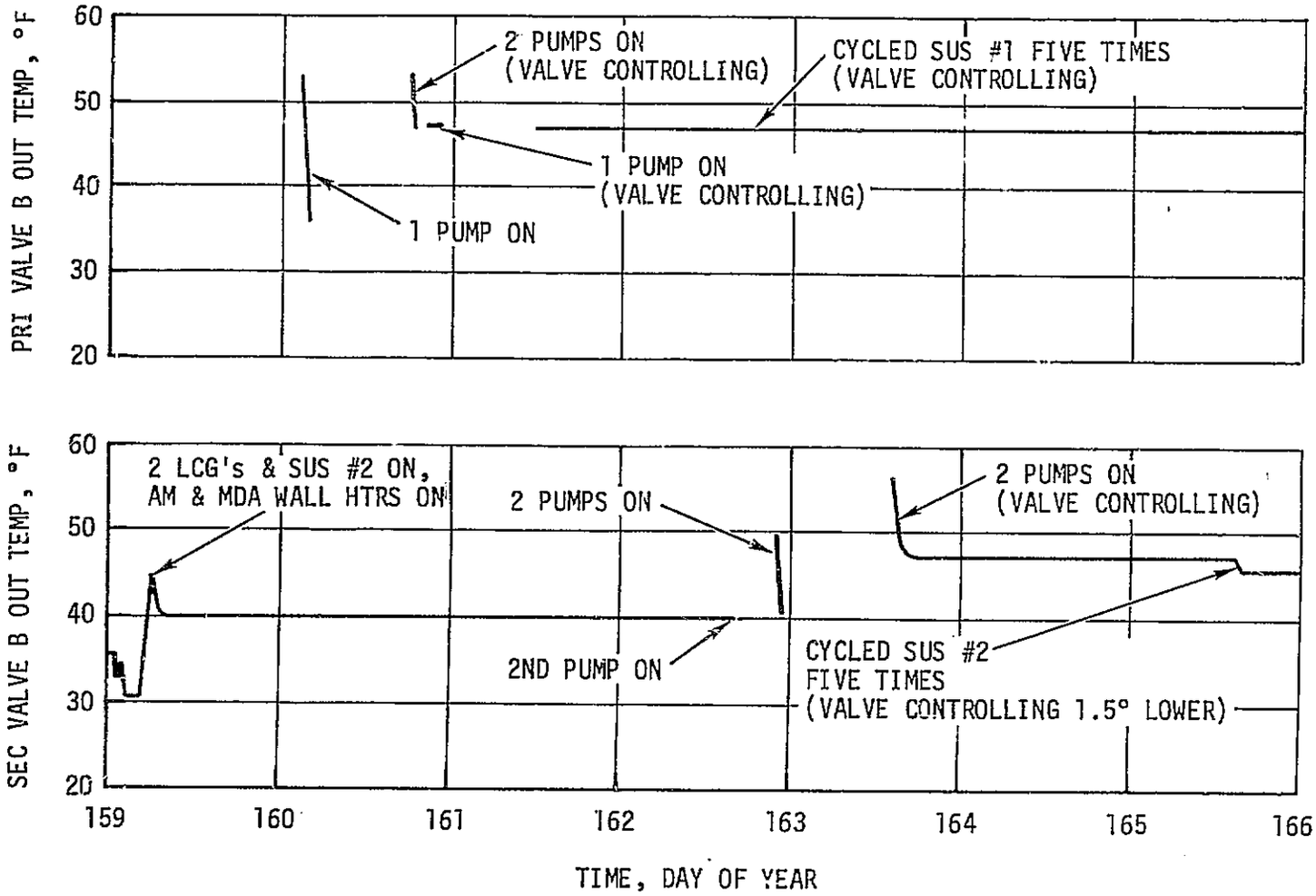

Figure 7-23. Remedial Actions for AM Coolant Loops

160:02:16:34	The primary loop was turned on (Inv 1/Pump A) but the hot inlet flow was still stuck at 87 lb/hour.
160:02:17:46	The primary loop was turned off when the valve outlet dropped to 36°F.
160:02:23:23	The crew turned on SUS #1 to check out the EVA water loop. The flow was then 248 lb/hour indicating that the water had thawed in the EVA heat exchangers.
160:02:23:58	The SUS #1 loop was turned off.
160:18:15:00	Two pumps (Inv 1/Pumps A & B) were turned on in the Primary loop. The outlet of the TCVB returned to 47°F indicating that it was unstuck.
160:18:23:46	The primary loop was turned off.
160:18:42:41	One pump was turned on in the primary loop (Inv 1/Pump A) to determine if the valve would modulate with one pump on. The valve outlet was 48°F.
160:18:47:30	The primary loop was turned off.

To assure that the primary loop TCVB valve would modulate to control the outlet temperature within limits during an EVA the following "sneak up" procedure was recommended:

> Connect LSU & PCU to panel 217 with the diverter valve in position 1.
>
> Turn SUS Pump on for 15 seconds and off for 1 minute, on for 30 seconds and off for 1 minute, on for 1 minute and off for 1 minute, on for 2 minutes and off for 1 minute, on for 15 minutes.

The intent was to add heat to the loop gradually so the TCVB would not travel to the full cold position and risk it sticking in this position. Also, the EVA valve remained in Bypass for this procedure and it was recommended that it never be placed in the EVA position again since the contamination which caused the EVA #1

anomalies was postulated to have originated in heat exchangers which were activated when the valve was placed in the EVA position.

The "sneak up" procedure was used as follows:

161:13:54:23	Primary loop Inv 2/Pump B turned on with TCVB outlet = 47°F and modulating.
161:13:37:00	Five SUS #1 on/off cycles were run according to the "sneak up" procedure and the valve controlled at 47°F.

The secondary loop TCVB valve was then unstuck and checked out as follows:

162:16:49:13	Pump C was turned on in secondary loop so that both pumps B&C were running. The TCVB valve was still stuck and the outlet temperature was 40°F. Pumps B&C were turned off.
162:22:07:22	Secondary loop Inv 2/Pumps B&C were turned on.
162:22:08:47	Secondary loop was turned off as valve was still stuck and outlet was 40°F.
163:14:35:00	Secondary loop was turned on (Inv 2/ Pump B&C). Outlet temperature was 47°F and modulating the flow properly.
163:14:56:32	Secondary loop Pump C turned off (valve still controlling).
165:14:20:00	Five SUS #2 on/off cycles were run according to the "sneak up" procedure and the valve outlet temperature shifted to 45.5°F.

As a result of the sticking of the TCVB valve in both coolant loops, a heater was built and taken on SL-3 to provide the capability to add heat to the SUS loop and thereby add heat at the hot inlet to the TCVB valve without using the liquid cooled garments as required during SL-2. A heater controller was also provided which would

regulate heat in steps for a total of 250, 500, and 1000 watts by DCS command. Figure 7-24 shows the heater power required to maintain the valve outlet temperature above 40°F. Use of the heater was never required.

After both the primary and secondary coolant loop thermal control valves were unstuck, both maintained temperatures within the control band of 47 ±2°F. Reviewing performance data, however, indicated that the secondary loop valve was somewhat sluggish. As a result, EVA's were conducted with all crewmen on Suit Cooling System #1 with the primary coolant loop until loss of the primary loop due to leakage on SL-3. At that time, a decision was made to risk use of the secondary loop rather than perform the second EVA of SL-3 with only O_2 cooling.

The SUS loop was turned on at 236:13:32 and the secondary TCVB appeared to be modulating normally until the SUS loop was turned off at 236:21:08:30. At this time, the valve traveled from a hot flow of 448 lb/hour to 454 lb/hour (two coolant pumps on) and stuck at that point. As a result, the valve outlet temperature dropped from 47.3 to 41.7°F as shown in figure 7-25 and stayed at approximately this temperature for the remainder of the SL-3 manned mission. The temperature dropped to approximately 40°F during the storage period when the loads on the system were very low. No attempt was made to free the valve as in SL-2 since the valve was stuck in an acceptable position and it was found that one time when the loop was cycled off and on to attempt to unstick the valve in SL-2, the valve outlet actually moved to a colder position than before. The secondary loop was operated continuously with the TCVB stuck in this position until the SL-4 EREP pass on DOY 12. At this time the higher radiator outlet temperature during the Z-LV attitude increased the valve inlet temperature and the valve came unstuck. The hot leg flow was decreased to 144 lb/hour during the pass, but returned to the original position following the pass. During the EREP pass on DOY 14 the valve decreased the hot flow to 0 lb/hour, but again returned to the original position. Later during the EREP pass on DOY 18 the valve came unstuck again but began to modulate following the pass and continued to modulate until the end of the SL-4 mission.

The third EVA of SL-3 was accomplished with O_2 cooling since the primary loop did not have sufficient coolant and there was the possibility that the TCVB valve in the secondary loop might stick in a less desirable position if it were used again during an EVA. After

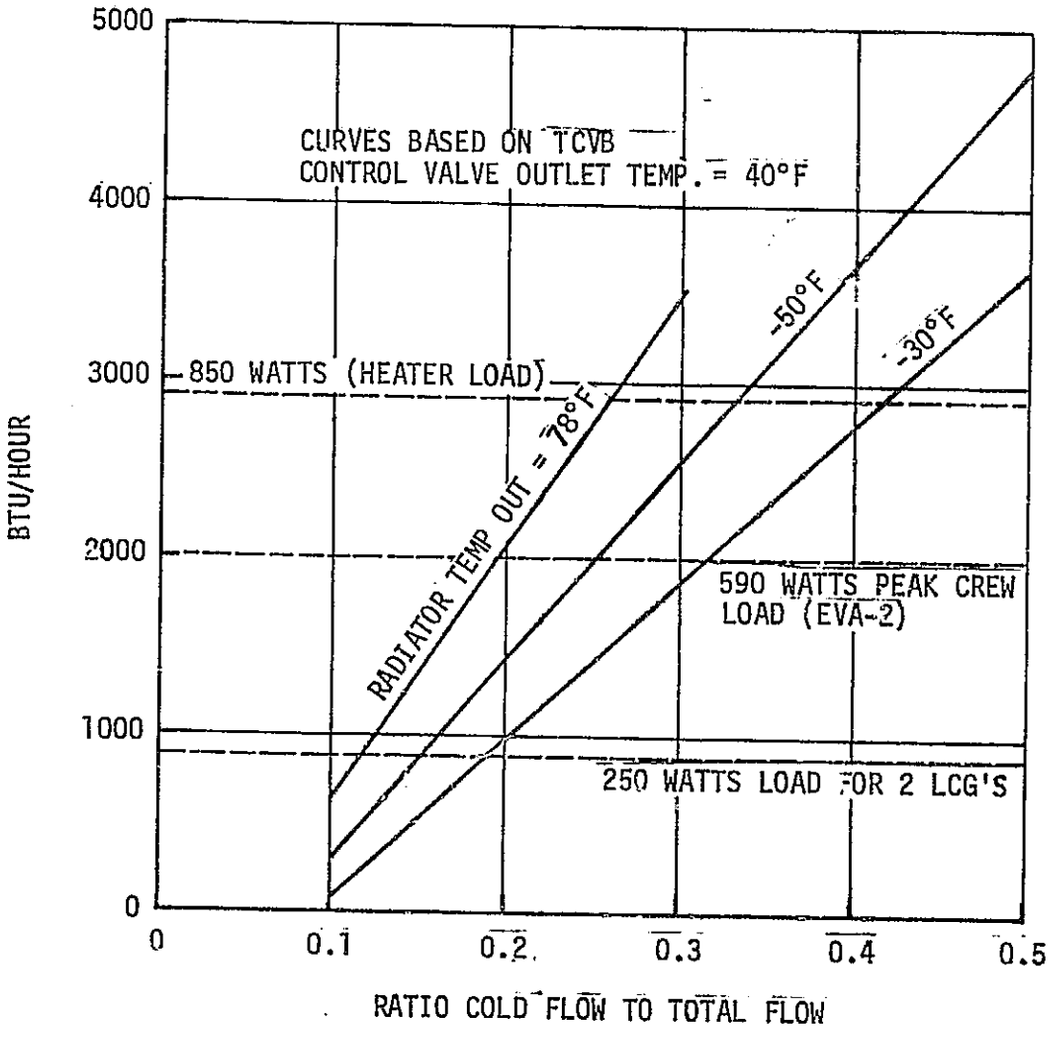

Figure 7-24. SUS Loop Heater Performance

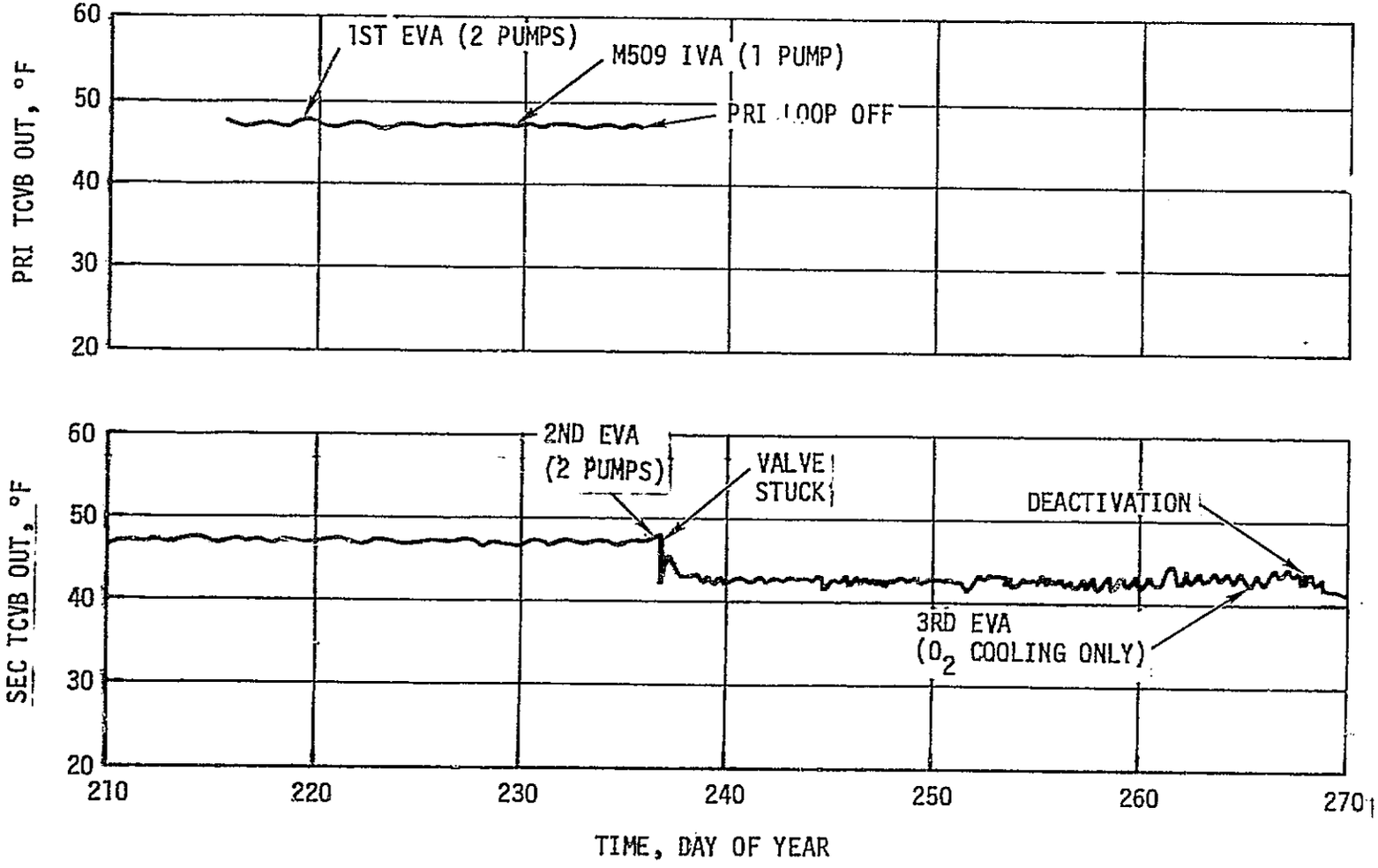

Figure 7-25. Secondary TCVB Anomaly During SL-3

reservicing of the primary coolant loop, all EVAs were accomplished during SL-4 using the primary coolant loop and suit cooling system #1.

3. Airlock Module Coolant Loop Leakage - At 217:07:10 an accumulator low limit indication occurred in the primary coolant loop. Data analysis indicated slow leaks in both the primary and secondary coolant loops. A compressed history of coolant pump inlet pressures for both coolant loops is provided in figure 7-26 and a history of calculated coolant loop mass for each loop is provided in figure 7-27. As can be seen, the primary loop pressure continued to decrease after the reservoir low level light indication and the loop was turned off at 235:18:31 to prevent pump cavitation. (Tests had shown that the pump would cavitate at inlet pressures less than 3 PSIA). The secondary coolant loop provided the required cooling throughout the remainder of SL-3.

During the SL-3 mission, the crew thoroughly inspected the interior of the vehicle, but no evidence of coolanol leakage was identified. However, post SL-3 analysis of the CO_2 filter cartridges utilized during SL-3 indicated a trace of coolanol in the cartridge material. The primary pump inlet pressure dropped to approximately 2.6 to 3.0 PSIA when the cabin was depressurized to 2.0 PSIA at the beginning of the SL-3/SL-4 storage period. Following cabin repressurization to 4.96 PSIA, the pump inlet pressure slowly increased until the end of the storage period. This indicated that the pump inlet pressure was sensitive to the cabin pressure and that a leak was probably inside the cabin. However, the fact that the pressure was less than the cabin suggested that there might also have been an additional leak on the outside. The location of the leaks therefore, could not be determined with any degree of certainty since there were two loops involved and each loop may have had more than one leak. To provide a method of recharging the coolant loop should it be required in SL-3, procedures were developed and ground testing was performed to provide a method of extracting coolanol from the secondary refrigeration loop in the OWS and introducing the fluid into the AM coolant loop. The method appeared to be possible. However, it was not required.

In order to insure that adequate coolanol would be available to complete the planned SL-4 mission without using the coolanol in the Refrigeration System (RS), a reservicing kit was designed, manufactured and carried to Skylab by the SL-4 crew. The kit provided the capability of servicing either or both of the coolant loops. A saddle valve was provided to penetrate the coolant line and coolanol was to be forced into the system from a tank containing approximately 42 pounds of the fluid. The 35 PSIG OWS N_2 regulator was used as a

1. FLIGHT DATA, NOT CORRECTED FOR GAGE HYSTERESIS
2. PRIMARY LOOP SENSOR AT D222
3. SECONDARY LOOP SENSOR AT D223

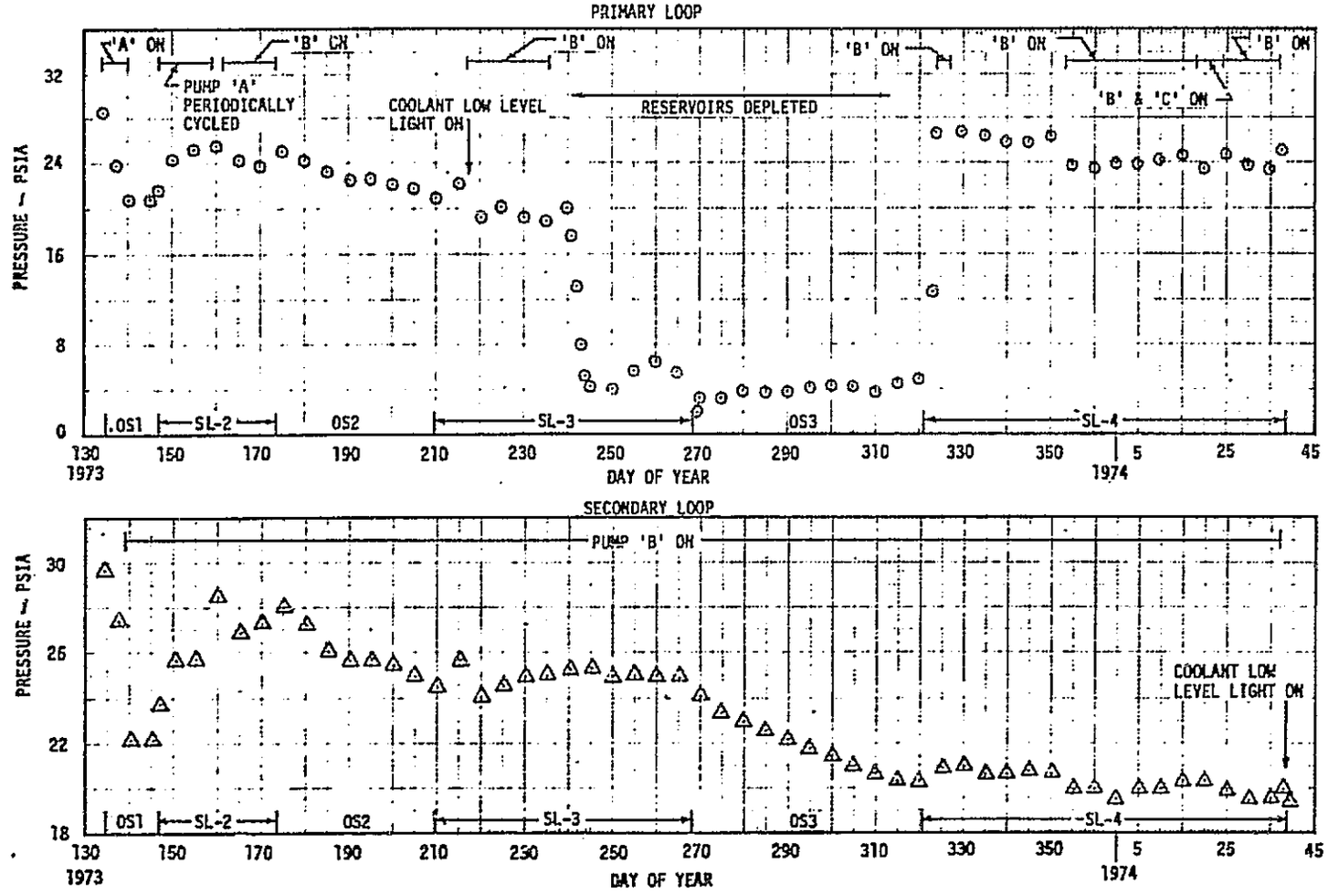

Figure 7-26. Coolant System Pump Inlet Pressures

1. CALCULATED FROM FLIGHT DATA USING THE "DAILY MASS MONITOR"
2. MASS AT LAUNCH ESTIMATED USING PREFLIGHT GSE DATA

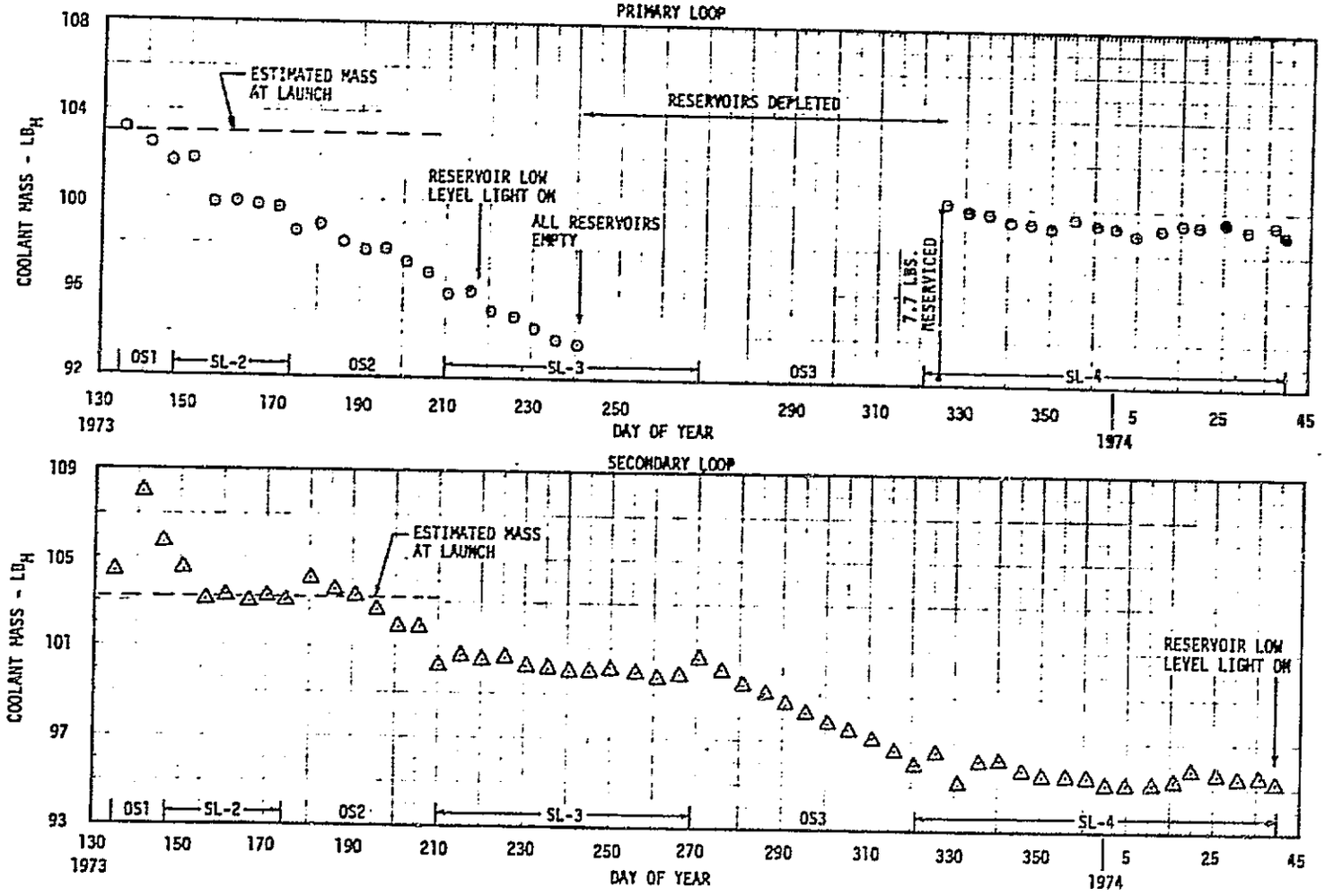

Figure 7-27. Coolant System Coolanol Mass

pressure source. A schematic of the reservicing equipment is shown in figure 7-28. Additional details of the design can be found in TMX-64824, "MSFC Skylab Structures and Mechanical Systems Mission Evaluation Report."

Reservicing of the primary coolant loop was initiated at 323:22:17. Insulation was removed from a coolant line in the STS cabin heat exchanger module and the saddle valve was installed on the line. After the valves were opened to pressurize the assembly between the 35 PSIG N_2 source and the saddle valve it was found that the pressure decayed at approximately 0.1 PSI/min. indicating that there was a potential leak between the saddle valve and the line. However, when the QD was disconnected from the saddle valve and the assembly was again pressurized, it was found that the pressure decayed at approximately the same rate. It was therefore, concluded that the gas leakage was not between the saddle valve and the line. Since a leakage on the gas side of the assembly was of no concern, the charging procedure was continued. The QD was reconnected and the line then pierced with the saddle valve. Weighing of the coolant tank before and after the servicing procedure indicated that 7.7 pounds of coolanol had been added to the loop. The primary loop was then restarted and checked for coolant leakage with both one and two pumps in operation. No leaks were observed. The primary loop continued to operate successfully throughout SL-4. The loop leakage rate appeared to be less during SL-4 than was seen during SL-3 and no additional recharging was required. The secondary loop pump inlet pressure decreased slowly during the SL-4 mission but the loop did not require recharging. The secondary reservoir low limit discrete did occur, however, at DOY 39:07:19 following deactivation of the manned SL-4 mission.

4. ATM C&D/EREP Water Loop Flow Anomaly - Pump A was initially turned on at 148:22:25 during SL-2 activation, and the flowrate oscillated from 240 to 305 lb/hour. The pump was turned off at approximately 148:22:36 to change the filter and was restarted at approximately 149:13:24. At that time, the flowrate was stable at 244 lb/hour. This flowrate was considerably lower than the approximately 300 lb/hour which was obtained in ground tests but there was no immediate concern since the flowrate was greater than the 220 lb/hour minimum specification flow.

During SL-3, at 265:14:39, the crew mentioned they had heard a gurgling sound and heard it periodically several times thereafter. It was reported to sound like high pressure air being squirted underwater or a relief valve relieving. Based on crew description, the noise appeared to be located in the area of the ATM C&D/EREP coolant pumps. When the crew reported the noise again, telemetry data indicated that the ATM C&D coolant flow fluctuated down to 74 lb/hour

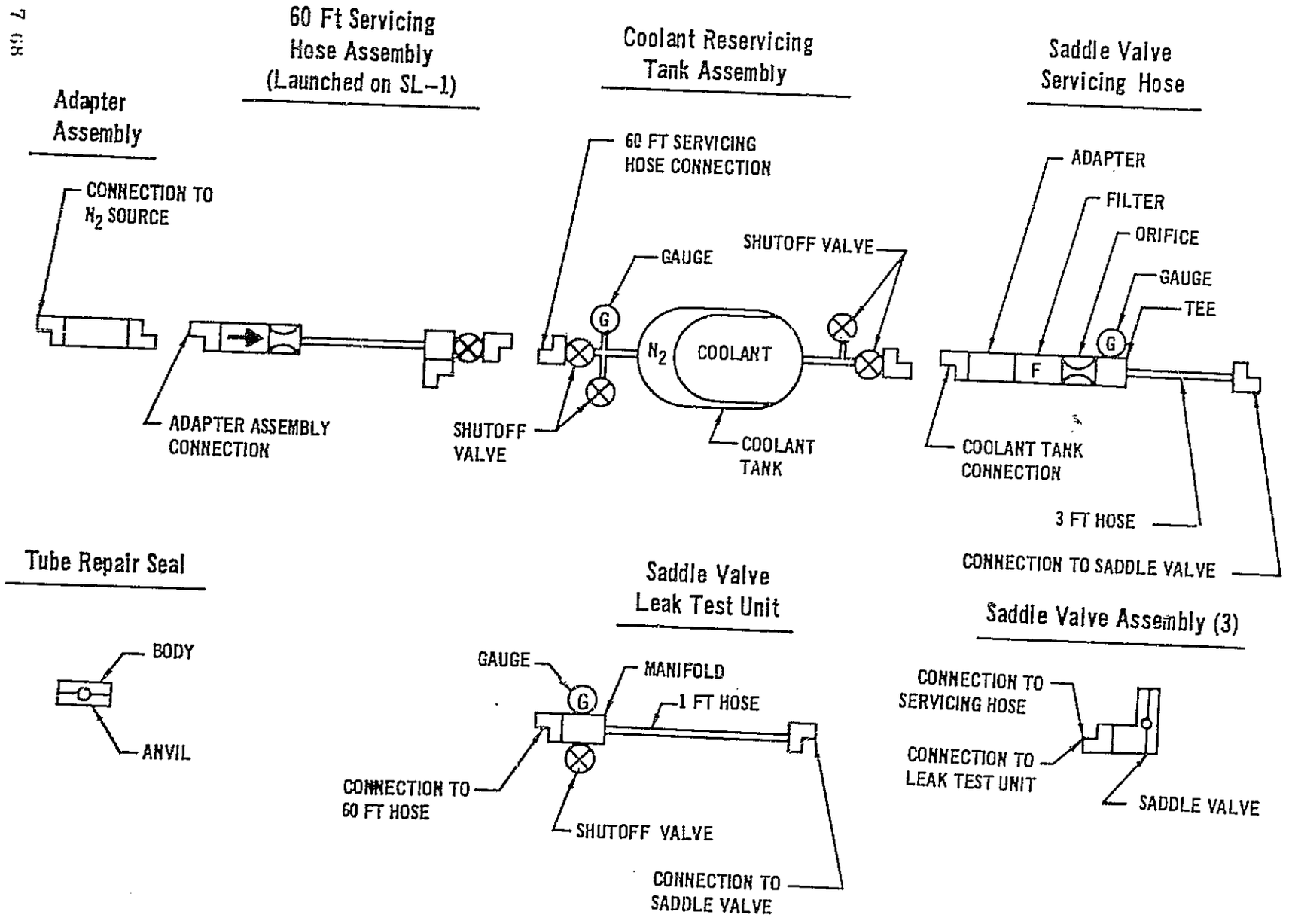

Figure 7-28 SL-4 Coolant Reservicing

(see figure 7-29). It was therefore thought that the pump was failing which might cause contamination in the loop from the deterioration of the pump bearings. Therefore, at 266:16:33 pump A was turned off and a new filter was installed. At 266:19:48, pump B was turned on and appeared to be operating properly with a stable flowrate of 231 to 234 lb/hour. Later at 267:14:45 pump C was also checked out and its flowrate appeared to be stable as well, however, the flowrate was somewhat lower at 225 to 228 lb/hour. No further use of pump A was planned. Since a bearing failure was suspected in pump A, the water filter was returned for analysis at the end of SL-3. Results showed residue to be 0.2688 grams. This was not significantly different from the residue found in the two filters returned following SL-2 which had 0.4502 and 0.1557 grams of residue each. The major elements of the residue following both missions was nearly the same at 8.9% Aluminum, 16.2% Potassium, and 43.7% Phosphate as PO_4.

During activation of SL-4, at 321:23:10, pump B was turned on and the flowrate oscillated between 216 to 269 lb/hour before becoming stable at approximately 241 lb/hour. Later, at 323:13:50, a flow dropout from 245 to 165 lb/hour occurred. Since pump B appeared to be experiencing the same problem as pump A did during SL-3, it was thought that there was a problem common to both pumps such as a flow sensor problem, gas in the system, contamination in the loop, or possibly the system pressure drop had increased enough to cause the pump relief valve to open and bypass the flow. An instrumentation calibration shift or other sensor failure modes could explain a continuously lower flow, however, it did not appear to explain why the flow was cyclic in nature. Since all three pumps had flowrates above 280 lb/hour prior to launch, the possibility existed that there was more resistance in the system. Also, ground tests accomplished during SL-3/SL-4 storage were able to duplicate similar noises to the pump A noise by increasing the system delta P to 25.8 PSID, opening the relief valve. One of the components which was suspected of restricting the flow was the EREP flow selector valve should it have failed in an intermediate position. The loop was therefore turned off at 324:22:18 while ground tests were run to determine the flow characteristics of the EREP flow selector valve in various intermediate positions so that its flow characteristics could be compared with the flight valve's characteristics. Pump B was turned back on at 329:14:02 and the EREP flow diverter valve was cycled through various intermediate positions. Flight results were similar to the ground tests so it was concluded that the valve was not causing the problem. The loop was left on since the flow was more than adequate for cooling and did not appear to be deteriorating except for the momentary dropouts in flow similar to that shown in figure 7-30. Later at 336:00:19, pump C was turned on to determine if its lower flowrate characteristics might be less likely to cause the pump pressure relief valve to open

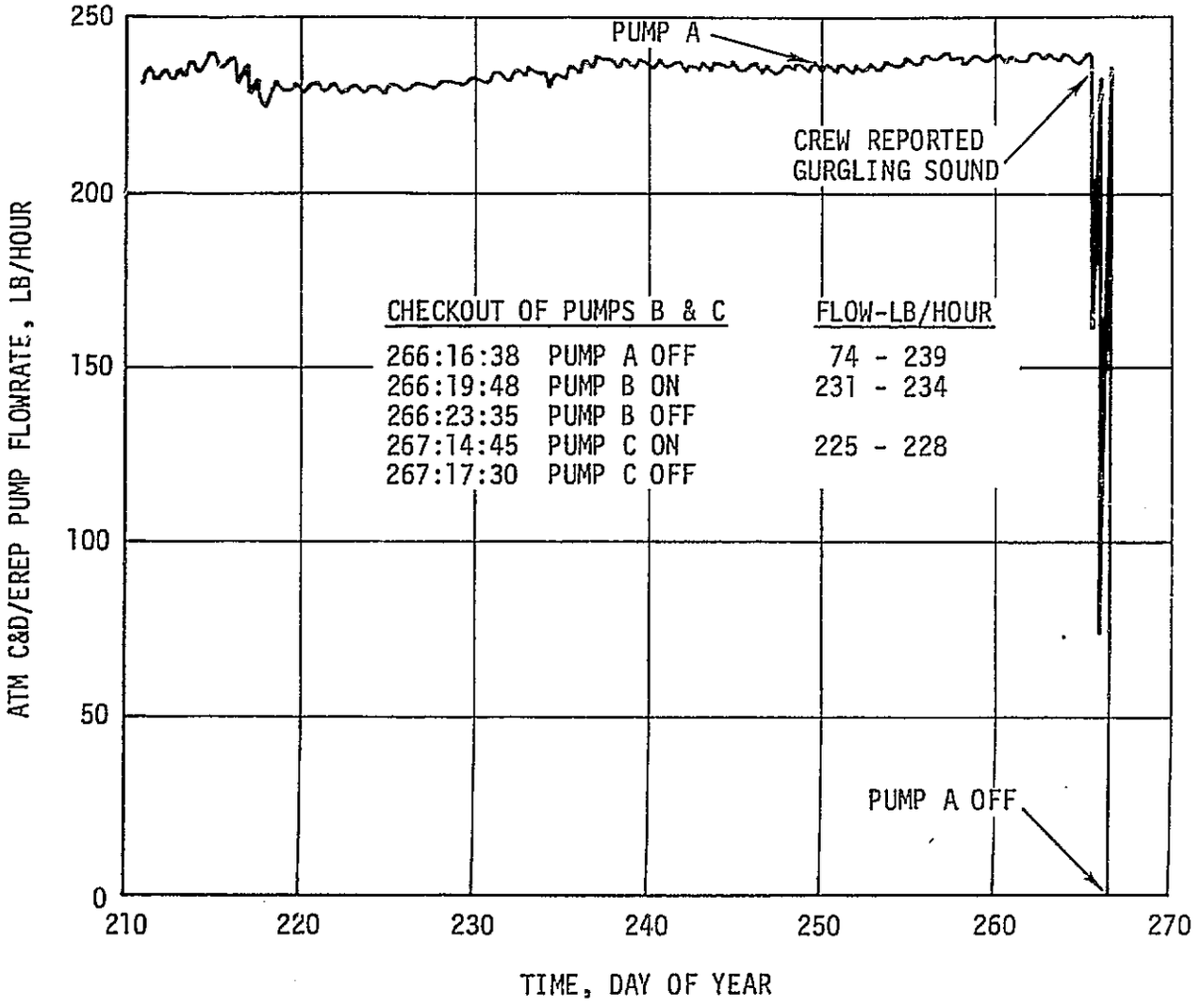

Figure 7-29. ATM C&D/EREP Loop Flow Anomaly

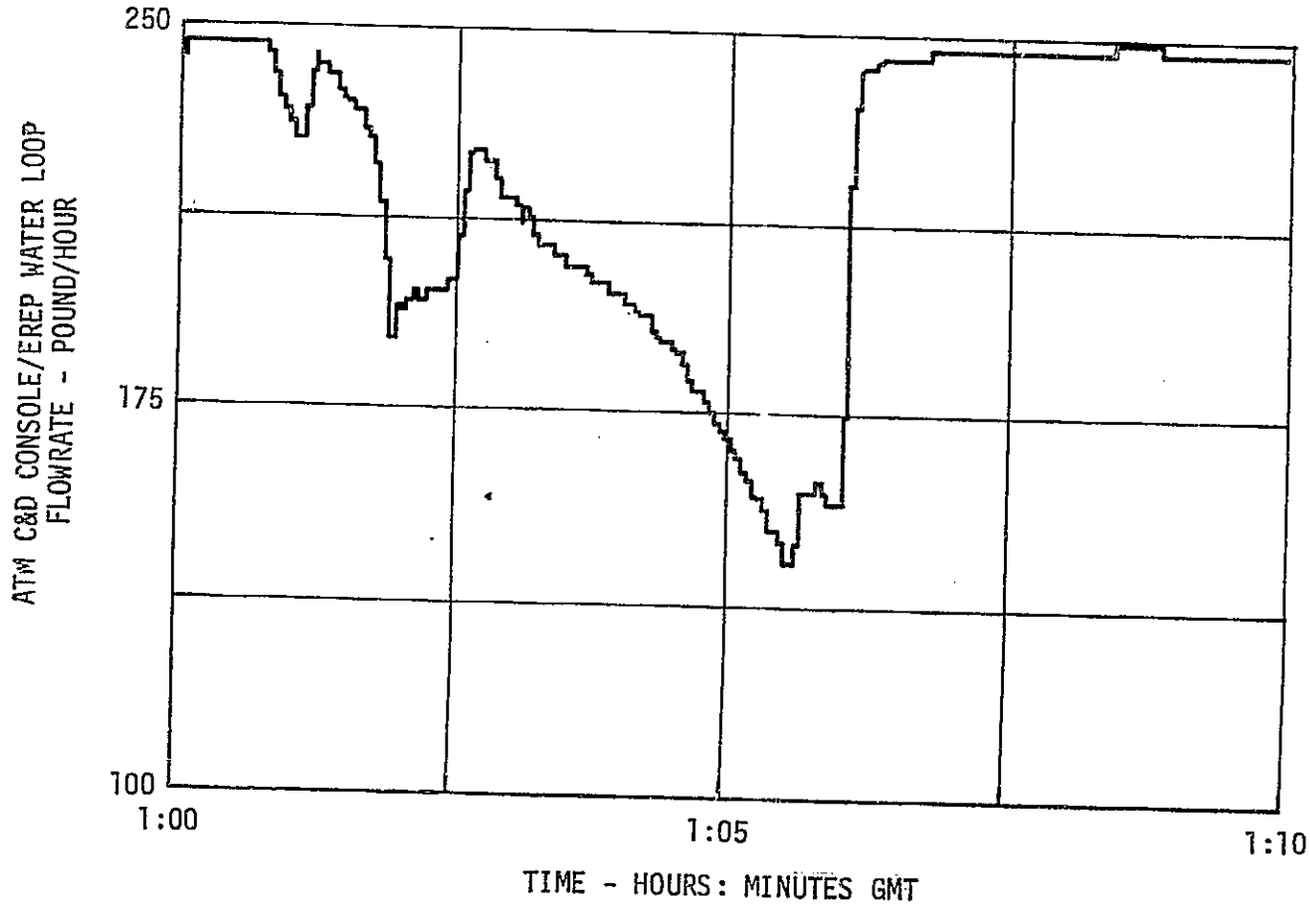

Figure 7-30. Typical Flow Dropout, Pump B, DOY 335

should this be the problem. However, the system continued to experience flow dropouts periodically with pump C operating. At 347:13:32 the crew reported that the low delta pressure light came on at the same time that the flow dropout was observed on the ground and that there was a definite decrease in the pump noise during this period. This suggested that the problem probably was not a high system pressure drop but either gas in the system or contamination which was binding the pump. Ground tests were then accomplished which showed that if the pump motor should become locked, the pump should not be operated longer than 30 minutes to preclude possible damage to the pump. To assure that this would not happen during the crew sleep period, an operational procedure was initiated at 348:03:05 turning off the loop during each sleep period. Ground tests were then run with a liquid/gas separator installed in the backup ATM C&D/EREP loop and showed that gas could be removed from the water should it be present in the system. As a result, it was recommended that the flight spare liquid/gas separator be installed in place of the filter to remove any gas or contamination. The loop was turned off at 352:12:35 so that the filter could be removed and disassembled for inspection. No microbial growth or solid particles were observed, but some debris, 1 to 2 mm in size, was found in the filter which looked like pieces of human skin and when rubbed between the fingers turned to a dry white powder. There also appeared to be a considerable amount of gas in the liquid, at the quick disconnects, in the barrel of the filter, and in the folds of the filter cartridge. The liquid/gas separator was installed at approximately 352:17:57 and after running pump C for 15 minutes, the flowrate increased to a stable flow of 287 lb/hour. Pump B was also run with the gas separator in the loop and its flow increased to a stable flow of 299 lb/hour at 352:20:30. It was concluded therefore that the gas in the system and possibly some of the contamination had caused the flow problems in the loop.

The system operated normally for approximately 15 days with only occasional flow oscillations and a gradual decrease in the continuous flow. It then started having significant flow dropouts again on DOY 002 which continued periodically until the liquid/gas separator was installed again at approximately 004:13:15. The flowrates increased to similar values which were obtained when the separator was installed before and the flow dropouts also stopped. Flow dropouts were observed again prior to the end of SL-4. However, the frequency did not warrant reinstallation of the separator.

Pump A was turned on at 036:01:17 to determine if it had actually failed mechanically or whether the gas in the system had caused its flow to drop. The flow appeared to be normal with no dropouts so it was concluded that the pump had not failed mechanically.

In summary, the flow dropouts were not of long enough duration to compromise the cooling capability of the system and all scheduled operations of ATM and EREP experiments were accomplished. However, the flow dropouts were of concern since they may have eventually been detrimental to the pumps if the liquid/gas separator had not been installed.

SECTION VIII. REFRIGERATION SYSTEM

A. Configuration

1. Thermal Requirements. The Orbital Workshop (OWS) Refrigeration System (RS) thermal performance requirements were:

a. The 24-hour urine pool shall be maintained at a temperature below $59^{\circ}F$. The pool shall not exceed $59^{\circ}F$ for more than 3 hours during the 24-hour period.

b. The urine freezer shall be capable of reducing the temperature of urine samples to below $30^{\circ}F$ within 90 minutes and below $-2.5^{\circ}F$ within 8 hours after placement in the freezer.

c. The urine return container shall maintain the samples below $17^{\circ}F$ for 22 hours.

d. The food freezer compartment temperature must be maintained at $-10 \pm 10^{\circ}F$.

e. Frost buildup shall not impair food removal.

f. The refrigerator and water chiller compartment temperature must be maintained at $45 \begin{smallmatrix} +10 \\ -12 \end{smallmatrix}^{\circ}F$.

The OWS was equipped with five food freezer compartments, a food and water chiller, and a urine chiller and freezer which were an integral part of an active cooling system (figure 8-1). A simplified system schematic is shown in figure 8-2. Although only one loop is shown, the entire cooling circuit was redundant for reliability. The circuits were identical and independent of each other, except for common utilization of the radiator, ground cooling heat exchanger (GCHX), and thermal capacitor units (these units had separate coolant paths for each of the two loops). The RS utilized a single-phase liquid coolant, Coolanol-15, which was circulated through the various components to absorb heat. This heat was then rejected by either the externally mounted radiator or the GCHX (used only prior to launch as a heat rejection component). In general, the system was composed of the heat rejection loop segment and the internal loop segment.

2. Heat Rejection Loop Segment. The heat rejection loop consisted of the radiator, thermal capacitor, and GCH cold plate. The radiator (the only heat removal apparatus after launch) utilized a S-13G thermal coating (low α_s/ε) to obtain the necessary heat rejection capability. This 84-ft^2 radiator was located on the thrust structure and was mounted 5° from the perpendicular to the stage centerline to avoid the incidence of direct sunlight during solar inertial attitude. The radiator was octagonally shaped (figure 8-1),

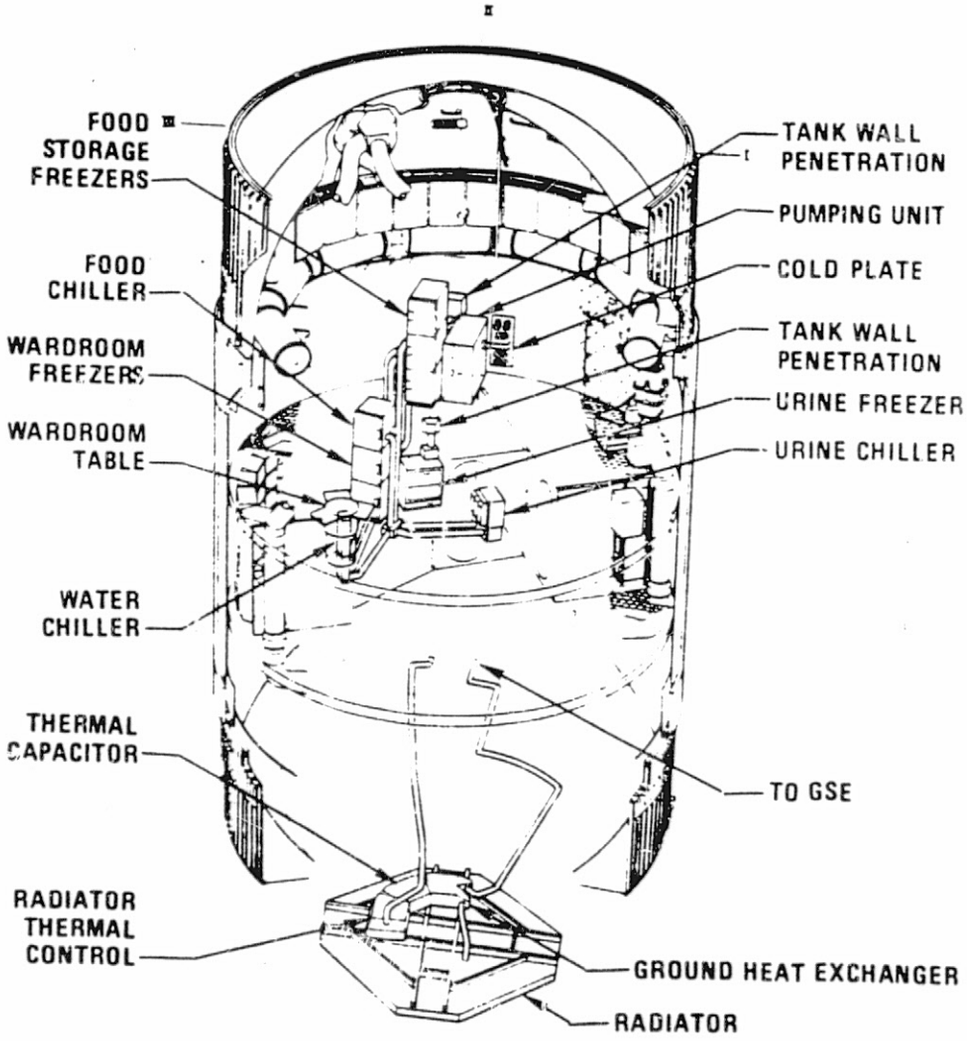

Figure 8-1. OWS Refrigeration System Component Location

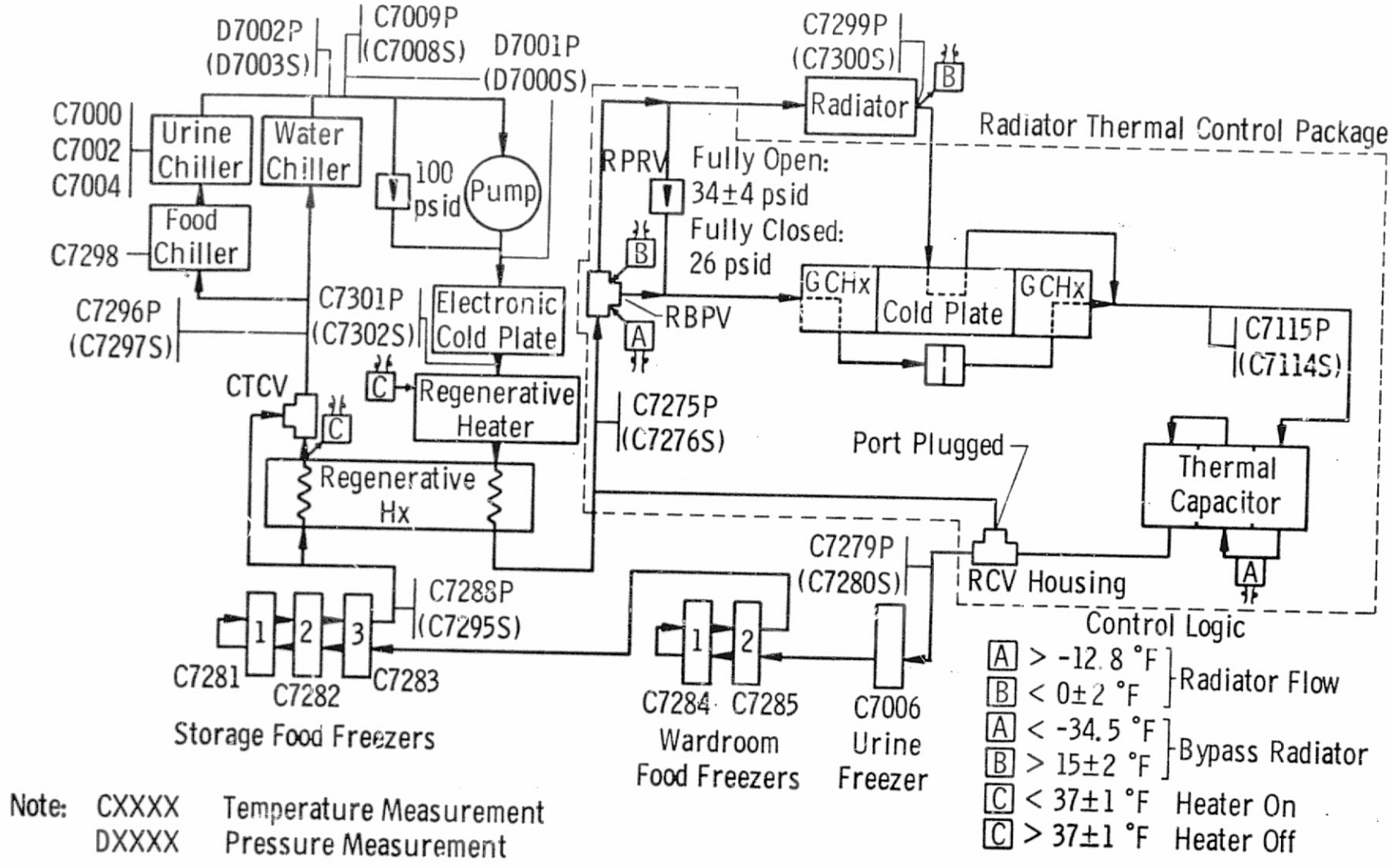

Figure 8-2. OWS Schematic and Temperature/Pressure Flight Instrumentation Locations

to provide a maximum surface area while maintaining clearance between the radiator edge and the S-II/S-IVB interstage during staging when assuming a single engine out clearance profile. The radiator coating was protected from the S-II stage retrorocket impingement by a "plume impingement shield" which was ejected at orbital insertion. Coolant flowed out of the radiator through a cold plate mounted between the two portions of the GCHX before going to the thermal capacitor. The cold plate served to dampen fluid temperature change rates into the capacitor units. Prior to launch, the coolant bypassed the radiator and was routed through the GCHX which maintained the thermal capacitor as well as the urine sample trays and food in a frozen state.

The thermal capacitor, which consisted of three in-series phase changing wax compound heat sinks (Undecane, $C_{11}H_{24}$), absorbed RS heat following launch (before radiator activiation) and when the surface temperature of the space radiator exceeded system operating temperature and could not be used for heat rejection. If the radiator surface temperature reached $15 \pm 2^{o}F$, a control circuit driven by a temperature transducer on the radiator surface actuated the radiator bypass valve (RBPV) to the bypass position (termed "hot" radiator bypass). The coolant flow was directed past the radiator and through the GCHX to the thermal capacitor where heat was transferred from the coolant to the thermal capacitor at essentially a constant temperature of $-14.5^{o}F$ (the phase change temperature of the Undecane). When the radiator surface temperature dropped to $0 \pm 2^{o}F$, the radiator temperature transducer caused the RBPV to open to the radiator position, allowing full flow of coolant through the radiator. Coolant from the radiator outlet passed through the thermal capacitor, refreezing the phase change wax. During the thawing or freezing of the thermal capacitor, a constant temperature of $-14.5^{o}F$ was maintained at the thermal capacitor outlet. If the radiator outlet temperature continued to drop until the temperature of the coolant between the first and second thermal capacitor segments reached $-34.5^{o}F$, the RBPV was actuated to cause the coolant to flow directly to the thermal capacitor units (through the GCHX) and bypass the radiator (termed "cold" radiator bypass). This mode of operation continued until the temperature of the coolant between the first and second thermal capacitor units reached $-12.8^{o}F$ (first thermal capacitor unit melted) and the RBPV valve was actuated to direct the coolant back through the radiator.

A 34 PSID radiator pressure relief valve (RPRV) was located in such a manner as to limit the maximum pressure differential across the radiator, in the event of coolant blockage or near blockage, which could occur when the coolant in the radiator was at an extremely low temperature. This occasion could exist when the radiator was reactivated, following a "cold" bypass period.

3. Internal Loop Segment. From the outlet of the last thermal capacitor unit, the coolant flowed in series through the urine freezer, the wardroom food freezer, and the food storage freezer. The coolant was then controlled to 39 $\pm$ 3°F (to prevent freezing in the chillers) by means of a 75-watt heater, three regenerative heat exchanger units, and the chiller temperature control valve (CTCV). The 39 $\pm$ 3°F fluid temperature at the outlet of the CTCV was achieved by proportional flow mixing of the regenerative heat exchanger outlet, warmed by counterflowing coolant from the regenerative heater. The coolant was routed in parallel paths with one path through the water chiller and one path through the chilled food compartment and urine chiller. The paths then combined and a single path was routed to the pump assembly.

The pump assembly consisted of a double two-pump package plumbed in parallel for each of the two loops (primary and secondary). A single two-pump package consisted of: two parallel pumps with discharge check valve, a 53 in^3 accumulator, and a 100 PSID bypass relief valve. Two pump packages (four pumps) were in each loop. The requirement for four pumps was based on a 2250 hour qualification lifetime. The pump assembly outlet fluid was routed through a 15-μ filter, through the inverter and heater control cold plate, and to the regenerative heater. The regenerative heater was provided to ensure the CTCV outlet temperature. A transducer, located between the CTCV inlet and the regenerative heat exchanger cold side outlet would cause the regenerative heater to energize and deenergize as the temperature reached 37 $\pm$ 1°F. From the regenerative heater, the flow passed through the three regenerative heat exchanger units and then to either the radiator or thermal capacitor, depending on the operational mode of the RBPV.

4. Control Logic Unit. The RS contained a control logic unit that continuously monitored and automatically provided system switching to rectify the following malfunctions:

a. Low differential pressure across the pump package. If the pump differential pressure dropped below 25 PSID, the logic unit automatically switched off the active pump and activated a second pump in the same loop. The sequence was primary pump numbers 1,2,3, and 4 and the secondary pump numbers 1,2,3, and 4. If the secondary pump number 4 was operating and a low differential pressure signal was received, the logic unit would recycle back through pump numbers 1,2, 3, and 4 of the primary loop. A 30-second delay in pressure logic was provided to allow for pressure buildup after a pump had been switched on.

b. Low pump accumulator liquid level. When any one of the primary pumps was operating and both primary loop accumulator liquid levels dropped below 5 in^3, the logic unit would automatically switch from the primary loop to the secondary loop (pump number 1). When any one of the secondary pumps was operating and both secondary accumulators

were sensed low, the logic unit would automatically cycle back to the primary loop (pump number 1). If loop switching occurred, there would be up to a 2 minute delay before the accumulator low-liquid-level monitor was enabled.

c. High freezer inlet temperature. The logic unit switched to the secondary loop (pump number 1) when a primary pump was operating and a temperature of 1 $\pm$ 1°F was sensed at the wardroom food freezer inlet.

d. Low chiller inlet temperature. The logic unit switched to the secondary loop (pump number 1) when a primary pump was operating and a temperature of 13.5 $\pm$ 1°F was sensed at the chiller temperature control valve outlet. When a secondary pump was operating and a low CTCV outlet temperature was sensed, the logic unit switched back to the primary loop (pump number 1).

e. Out-of-tolerance logic power supply voltage. The logic unit switched to the secondary loop (pump number 1) when the primary loop logic power supply voltage was not within the tolerance band of 5.0 $\pm$ 0.45 volts. If the secondary loop was operating and an out-of-tolerance condition existed, the logic would transfer to pump number 1 of the primary loop.

The RS logic unit allowed only a single pump to be operating at a given time; therefore, if a pump other than the active pump was switched on, the logic switched off the previously active pump. The RS logic unit also provided signals to the following OWS control and display (C&D) console panel 616 malfunction indicator lights for both the primary and secondary loops:

a. Pump low pressure

b. Accumulator low

c. Inlet temperature freezer high

d. Inlet temperature chiller low.

5. Activation. Temperature control of the RS was initiated a short time before the mission food supply was placed in the OWS, while the OWS was in the Vertical Assembly Building. A coolant pump was activated, and the RBPV was actuated to the bypass position. Heat from the RS was transferred through the GCHX to a ground cooling cart by way of umbilicals. Just prior to lift-off, the coolant (ethylene glycol and water) was purged from the ground loop and power to the RS primary and secondary logic systems was disabled, causing the operating pump to be deactivated.

Following S-II stage separation, the RS radiator shield was jettisoned as the RS primary and secondary logic systems were enabled, causing pump number 1 in the primary loop to be turned on. The predicted radiator temperature decrease was used to verify the shield jettison and the need for a backup jettison signal. System heat loads were absorbed by the thermal capacitor until the RS radiator surface temperature had dropped to $0 \pm 2^{\circ}F$, activating the R3PV to flow coolant through the radiator.

Normal operation and control of the RS during habitation was accomplished automatically by the RS controller logic, which had the capability to select loops and pumps in the event of anomalies. Visual displays along with RS pump switches on panel 616 of the OWS C&D console provided crew monitoring and backup control capabilities.

It was planned to operate the pumps in a specific sequence during the entire mission to avoid exceeding 2250 operating hours on any one pump. Pump number 1 in the primary loop was manually turned on first, prior to loading frozen food into the freezers. The rest of the plan was: pump number 1 to be manually turned off, and pump number 2 automatically turned on 15 days into SL-2. Pump number 2 was to be manually turned off, and pump number 3 automatically turned on at the beginning of SL-3. Pump number 3 was to be manually turned off, and pump number 4 automatically turned on at the end of SL-3 and remain in operation until the end of SL-4. This plan was altered as discussed in paragraph B.5 of this section.

B. System Performance

1. Plume Shield Ejection. The frozen food was stored in the freezers on April 20, 1973 (DOY 110), 24 days prior to the launch of SL-1 on May 14 (DOY 134). As mentioned earlier, the preflight prediction of the RS radiator surface temperature decrease was used to determine the need for a backup jettison signal. The predicted temperature for the $\pm$ 3 sigma conditions is shown in figure 8-3 for both jettison and non-jettison cases. The flight data is also shown on the curve. The initial shield jettison signal occurred at 10 minutes after liftoff, as planned. The radiator surface temperature was greater than the +3 sigma shield jettison curve at the Carnarvon (CRO) and Honeysuckle Creek (HSK) ground stations, therefore, the backup signal was sent over Goldstone (GDS) at approximately 94 minutes after liftoff.

Even though the backup signal was commanded, the comparison of the flight data and prediction in figure 8-3 indicated that the shield ejection occurred at the initial command since no discernable change in the response of the radiator surface temperature occurred at the time the backup signal was commanded.

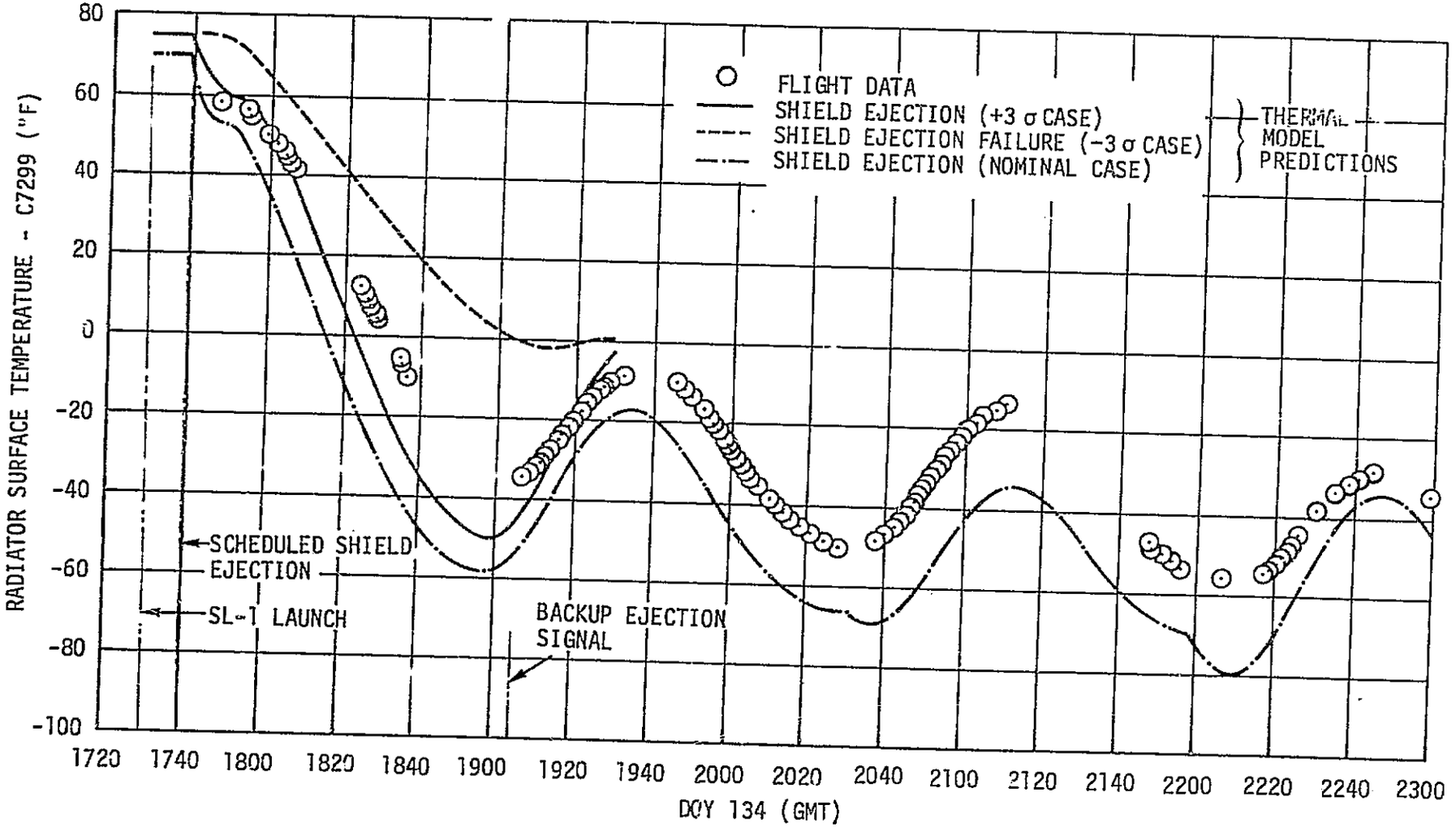

Figure 8-3. Radiator Surface Temperature During Shield Ejection

The more gradual decrease in the radiator surface temperature (figure 8-4) could have been caused by the plume impingement shield or other material trailing the radiator, and partially blocking the radiator's view to space. However, the exact cause of the difference has not been identified at this time. It should be noted that due to the difference between the flight data and the preflight predictions for the first few hours of the flight, the backup ejection signal was needlessly commanded. Since there was concern (prior to launch) about sending the backup signal if not needed, it appears that a positive ejection signal device should have been incorporated.

2. System Operation. The radiator was activated approximately 1 hour after lift-off (15 minutes later than analytically predicted) and was performing as expected within 10 hours after the launch (figure 8-4). The thermal capacitor performed as expected after the launch, by absorbing the total system heat load without depleting its latent heat storage capabilities for the 1-hour period the radiator was deactivated as indicated by the capacitor outlet temperature (C7279) not exceeding -14.5°F in figure 8-5. The warmest food compartment temperature was maintained less than -2°F during this time. The thermal capacitor was fully recharged (frozen) 3 hours after launch. The first radiator "cold" bypass occurred in the third revolution (approximately 4 hours, 35 minutes after lift-off). Figures 8-4 and 8-5 also show radiator and thermal capacitor preflight predicted analytical performance. This predicted performance was made using nominal radiator heat flux for the β angle at time of launch (-8.5°) and radiator surface coating properties (α/ε equal to 0.25/0.887). Figures 4-33 through 4-40 shows the variation in β angle over the duration of the three Skylab missions.

During boost of SL-1, the micrometeoroid/thermal shield was torn away. The loss of the meteoroid shield exposed the goldized kapton on the cylindrical walls of the Skylab to the space environment. The optical properties of the kapton are such that more heat was absorbed, resulting in high internal OWS temperatures (figure 4-33); the heat load on the RS climbed to almost 2000 Btu/hour before the deployment of the first thermal shield (parasol). The normal storage mode heat load would have been approximately 1200 Btu/hour for an OWS environment temperature of 64°F. Although the OWS environment temperature exceeded 120°F, the radiator was capable of removing the system's absorbed heat and maintaining the warmest frozen food compartment below 0°F (-1.0 to -3.0°F). The radiator was able to reject the increased heat load since it was designed for 3 sigma hot external environmental conditions and the actual conditions were nominal. "Cold" radiator bypass continued to occur each orbit until DOY 136, 2 days after SL-1 launch. However, the OWS environment temperature had increased such that, on DOY 136, the high heat load allowed only one "cold" radiator bypass for every two orbits. Following SL-2 crew arrival, the increased heat load as a result of the activiation of the OWS ventilation fans

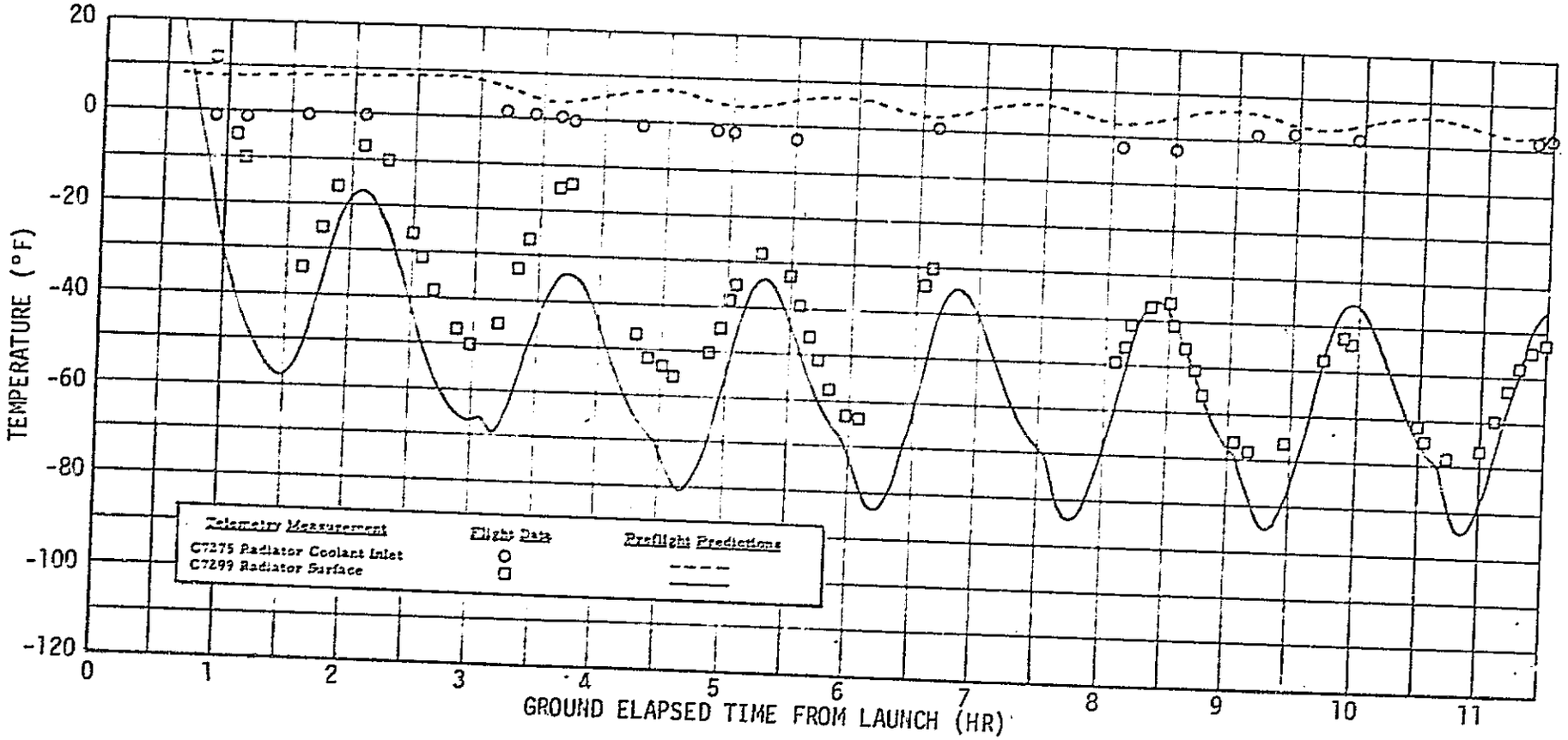

Figure 8-4. RS Radiator Flight and Preflight Predicted Performance Following SL-1 Launch

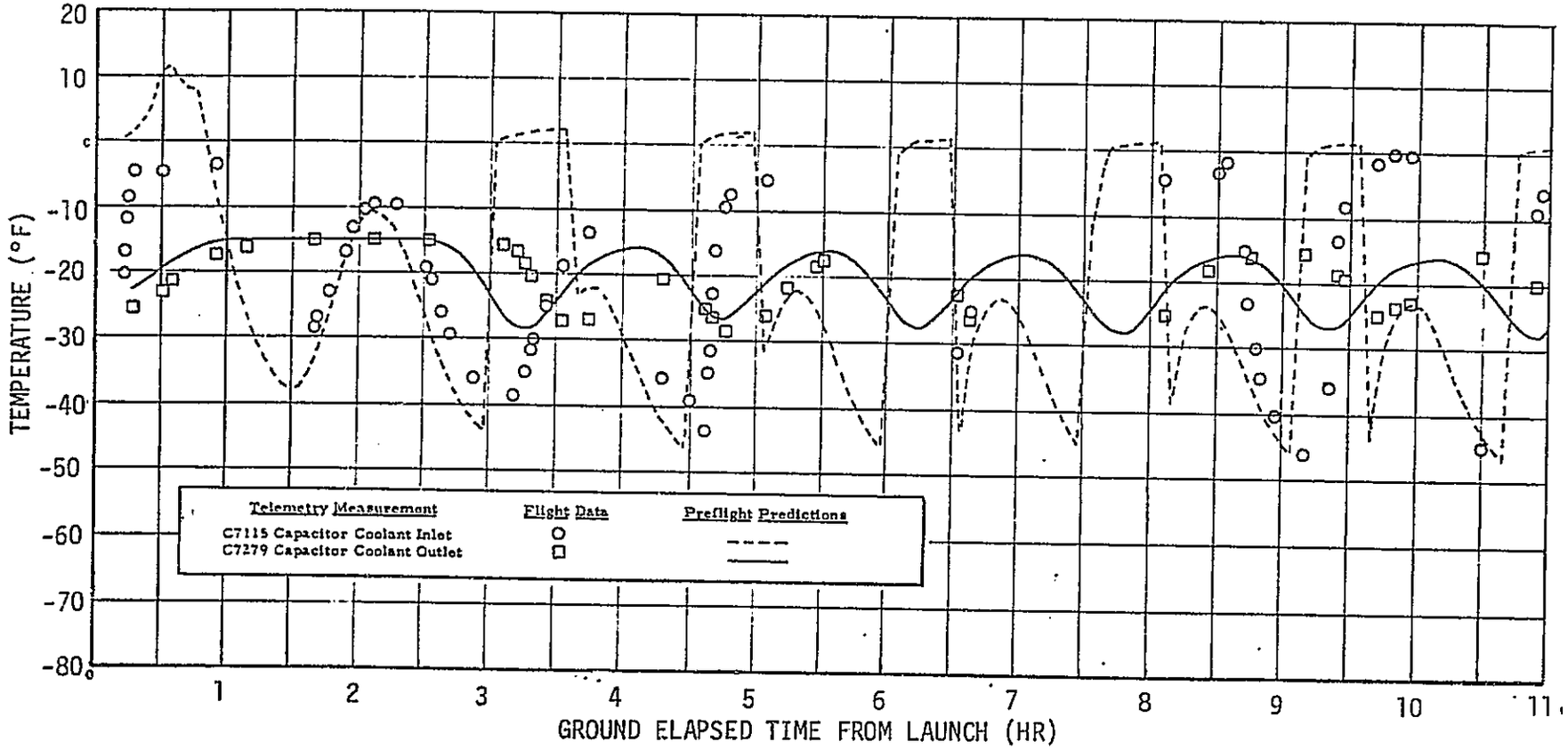

Figure 8-5. RS Thermal Capacitor Flight and Preflight Predicted Performance Following SL-1 Launch

and normal habitational operation of the RS was such that the warmest frozen food compartment temperature reached 0.5°F prior to the deployment of the parasol shield. On DOY 148, following the deployment of the parasol, the OWS internal temperature had dropped (lowering the heat load on the RS) enough to allow "cold" radiator bypasses to once again occur every orbit. By DOY 156, the orbital average temperature of the warmest food freezer compartment had dropped to -5.0°F where it remained until the anomaly of DOY 173 (see paragraph C. this section). The 11 EREP maneuvers performed by the SL-2 crew during the period from DOY 150 through 165 had a negligible effect on the frozen food compartment temperatures. Although such maneuvers served to decrease the radiator's thermal performance, none were severe enough to initiate a "hot" bypass. The comparison between the calculated and flight data for the relationship between radiator inlet and outlet temperature given in figure 8-6 indicated that the radiator's heat rejection capabilities were as predicted. Radiator performance data from different test conditions (radiator inlet temperature, flux levels, etc.) as well as flight data are compared to the calculated radiator outlet temperature for the same conditions in figure 8-7.

The telemetry data of DOY 156 were used to compare actual RS flight performance with that anticipated before lift-off. At this point in the mission, the OWS internal environment temperature (77°F) was very near its stabilization temperature following parasol deployment and the OWS ventilation fans were operating, which resulted in normal habitated heat loads. The vehicle was in a solar inertial orientation, and the β angle was very near 0°. The comparison, shown in figures 8-8, 8-9, and 8-10, revealed that the RS thermal performance was as anticipated as a result of earlier computer analysis. The difference between the maximum and minimum radiator surface temperature and the flight data in figure 8-8 was due to the difference between the surface temperature at the radiator outlet (analytical model node) and the sensor temperature located behind the surface on the radiator tube fin.

3. Performance Following Anomaly. At approximately 173:02:02:00 GMT an anomaly occurred in the RS. For reasons to be discussed in paragraph VIII.C.1 the anomaly was suspected (from DOY 173 until SL-4 deactivation) and later confirmed (following the end of mission testing) to be the result of a malfunctioning radiator bypass valve (RBPV). Following the anomaly, an automatic switch to the secondary loop revealed the secondary loop to have a similar anomaly. The RBPVs had failed in such a manner as to allow only about 20 percent (orbital average) of the total coolant flow rate through the radiator.

By enabling and disabling the loop, the primary loop radiator coolant flow rate was improved to about 40 percent (orbital average) which gave an acceptable heat rejection capability. The freezer compartment temperatures were more sensitive to OWS environment temperature changes after the RBPV anomaly due to 60 percent of the flow

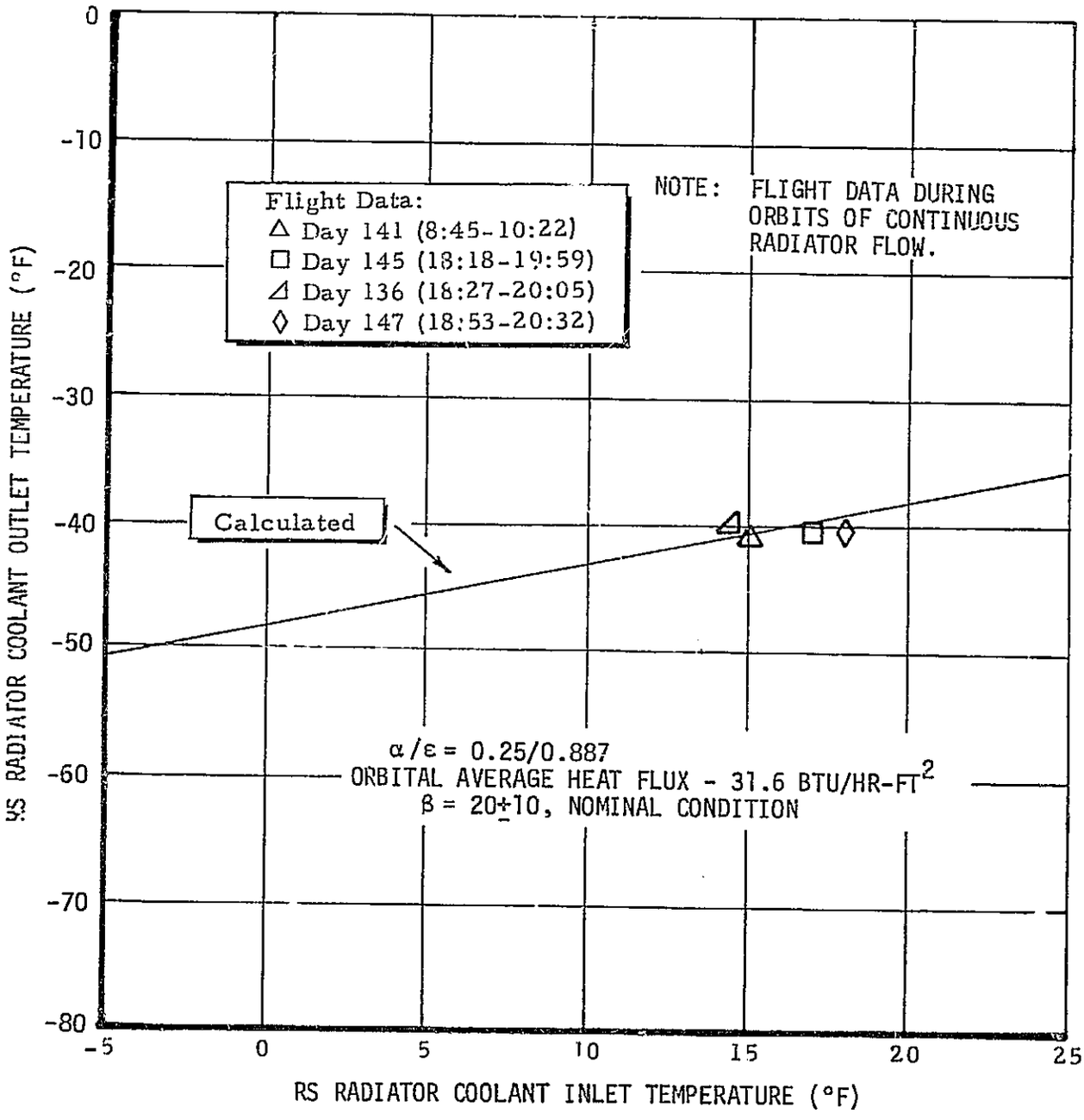

Figure 8-6. RS Radiator Slight Data and Thermal Model Comparison

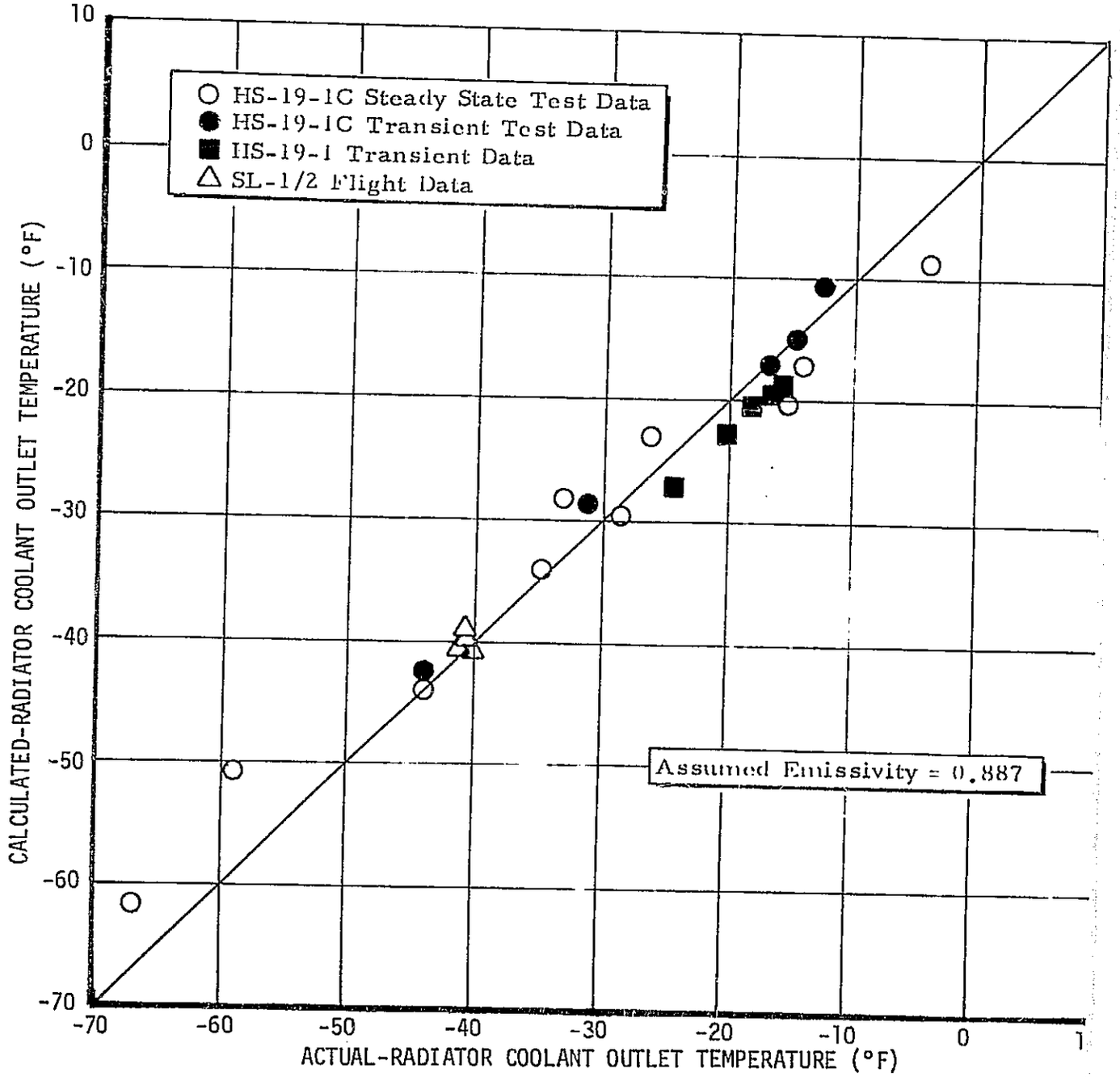

Figure 8-7. RS Radiator Flight and Test Performance Compared to Thermal Model

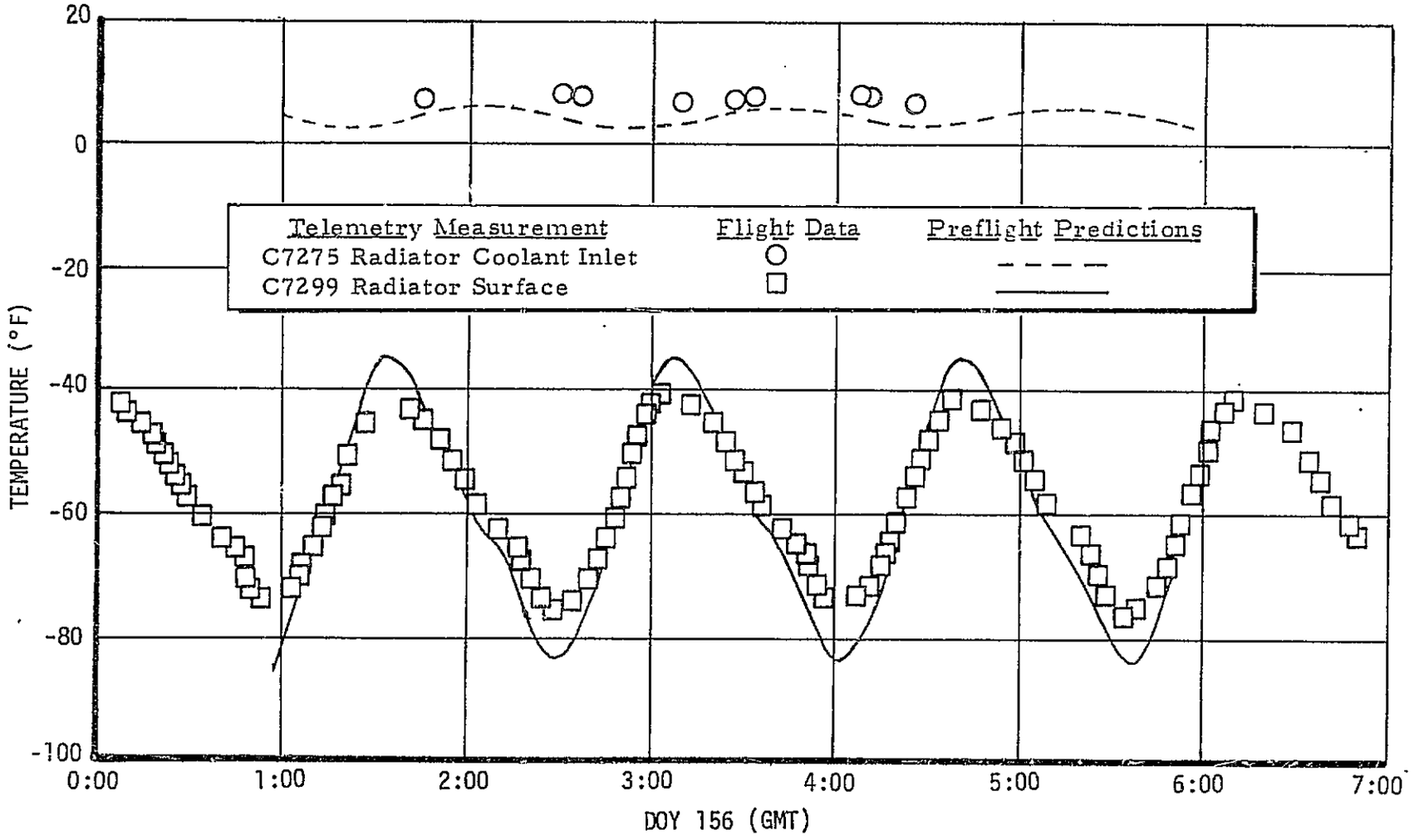

Figure 8-8. RS Radiator Flight Data and Preflight Thermal Model

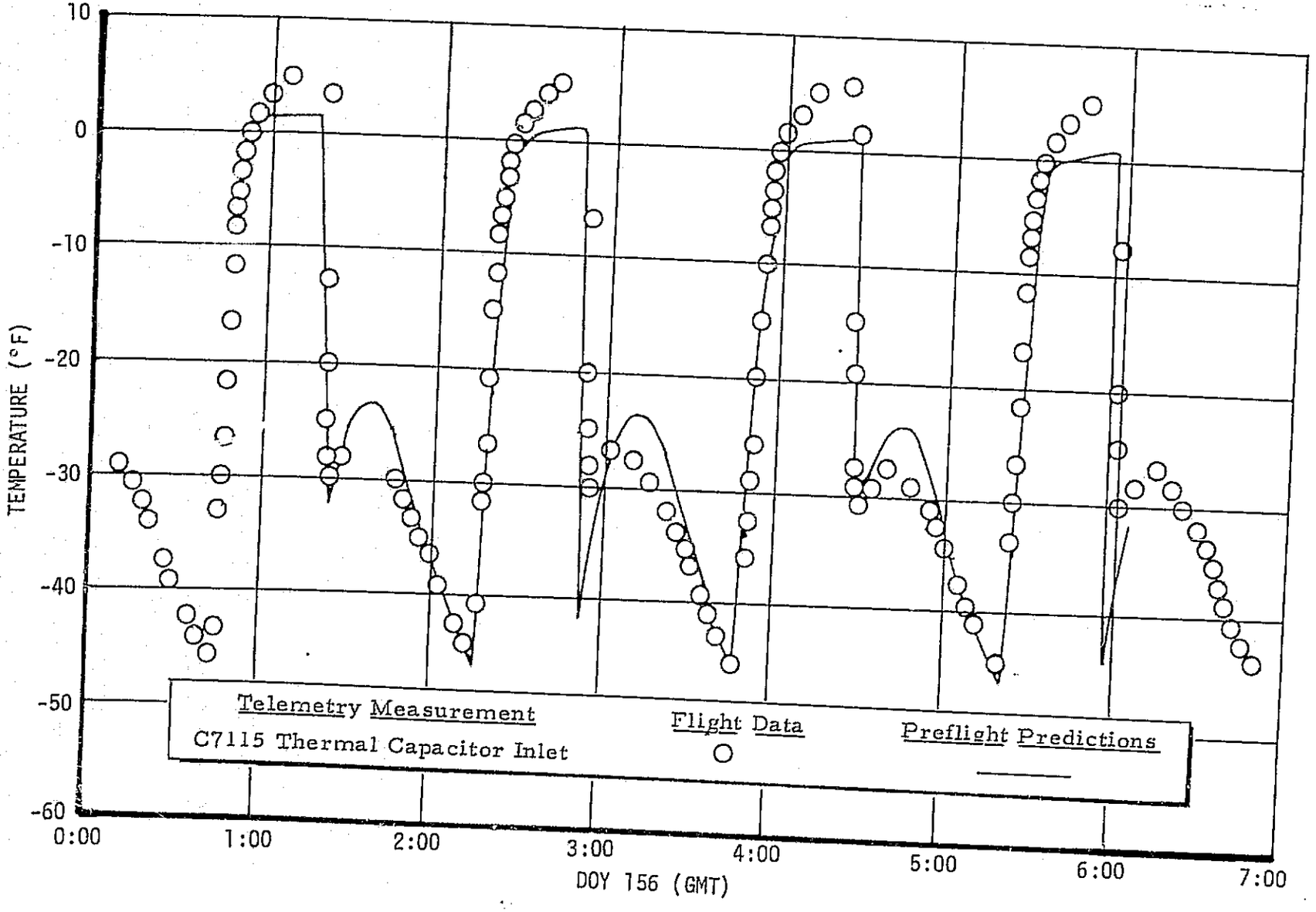

Figure 8-9. RS Thermal Capacitor Inlet Temperature Flight Data and Thermal Model Predictions

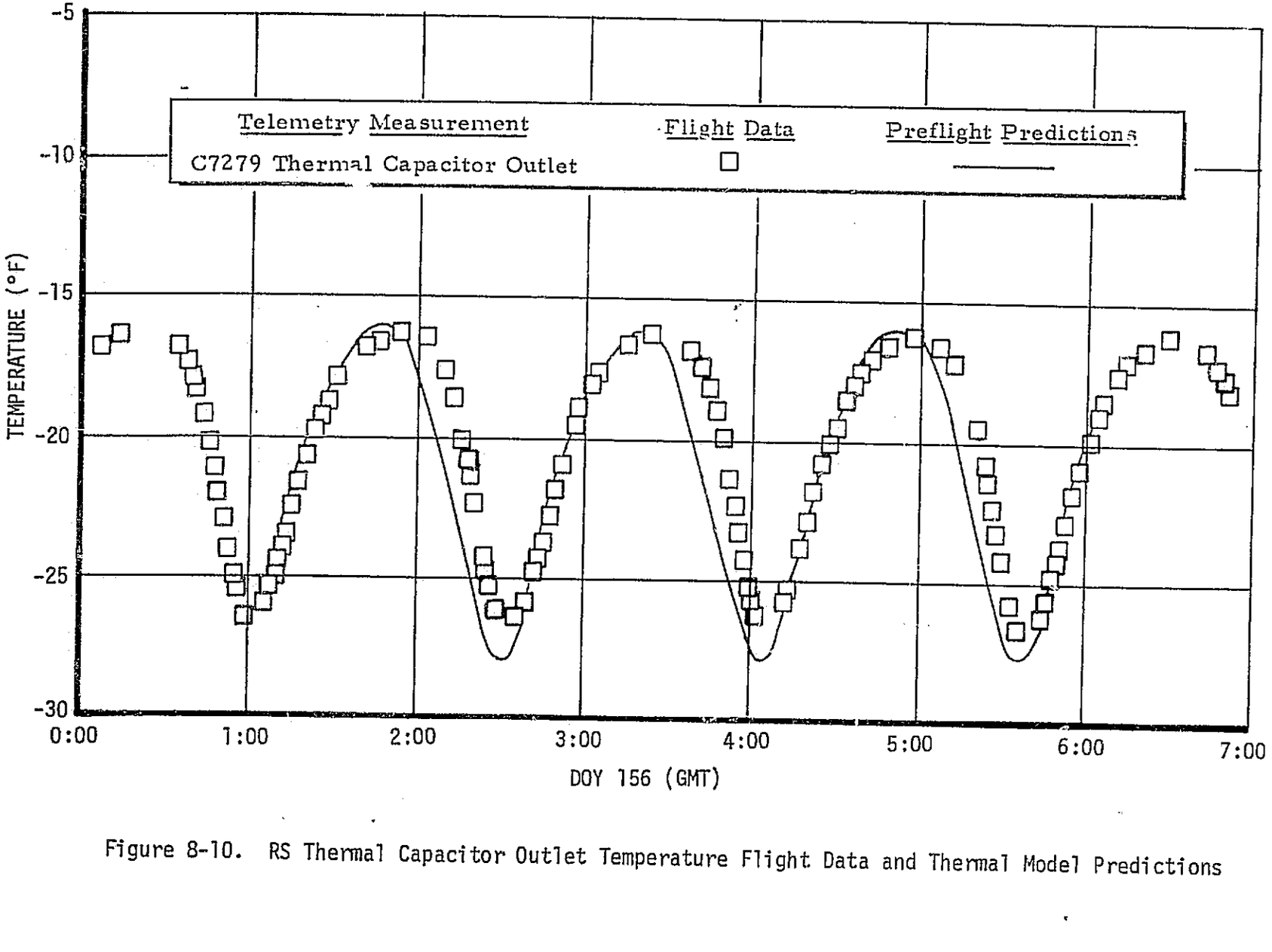

Figure 8-10. RS Thermal Capacitor Outlet Temperature Flight Data and Thermal Model Predictions

recirculating in the internal portion of the loop. The relationship between the freezer inlet temperature and OWS internal temperature is shown in figure 8-11 for habitation and storage. The system heat load as a function of internal temperature is shown in figure 8-12. The data of figure 8-12 illustrates the difference in the relationship between the RS internal loop components and the average OWS internal temperature after the DOY 173 anomaly.

4. Freezer and Chiller Performance. A history of the freezer compartment temperatures of the RS during its entire period of activation is shown in figures 8-13 and 8-14. These temperatures, which were good indicators of overall system performance, were shown to be more sensitive to vehicle attitude changes after the anomaly in the RBPV than with the normally functioning valve. The system was seen to be capable of maintaining the freezer compartments below their specified upper temperature limits during all normal operational modes (even though some EREP's near the end of SL-4 maintained an approximate Z-Local Vertical (Z-LV) attitude for a full orbit).

The upper temperature limit of $0^{\circ}F$ for the frozen food allowed a maximum storage period of 360 days, as shown in figure 8-15. Storage times at various temperatures are also indicated on figure 8-15. The percent allowable remaining food stowage time as a function of the time of year is shown in figure 8-16. The specified limit (360 days at $0^{\circ}F$) is shown along with the actual percent time remaining curve if the RBPV failure had not occurred. As shown by figure 8-16, the actual remaining stowage time began to decrease after the RBPV failure. However, since the food temperatures recovered to a lower temperature than before the RBPV failure, then the allowable food stowage time increased.

The chillers were unaffected by the RBPV anomaly as a result of the chiller thermal control valve (CTCV) continuing to maintain an essentially constant temperature coolant to the chillers. The CTCV coolant outlet temperature was seen to show slight dependence on the OWS environment temperature and operational mode as illustrated in figure 8-17.

Crew complaints concerned: (a) the ice buildup on the surface between the freezer compartment doors which impaired the latching of the freezer doors to such an extent that the ice had to be removed periodically (possibly due to door seal damage in SL-2), (b) the inconvenience of the inner doors on the food freezers and chiller (figure 8-18) and (c) the absence of a canister restraint assembly in the food chiller.

5. Pump Performance. The planned pump operation sequence was given in paragraph VIII.A.5. Due to the delay in the SL-2 launch, the switch to the second pump was made on DOY 160 instead of DOY 149. Pump 2 ran until the anomaly on DOY 173. The system was switched back to the primary loop pump number 1 on DOY 173 and remained on that pump throughout the mission. The pumps were not switched as planned after the anomaly due to the possibility of further radiator flow degradation.

Figure 8-11. Internal Temperature on Freezer Temperature

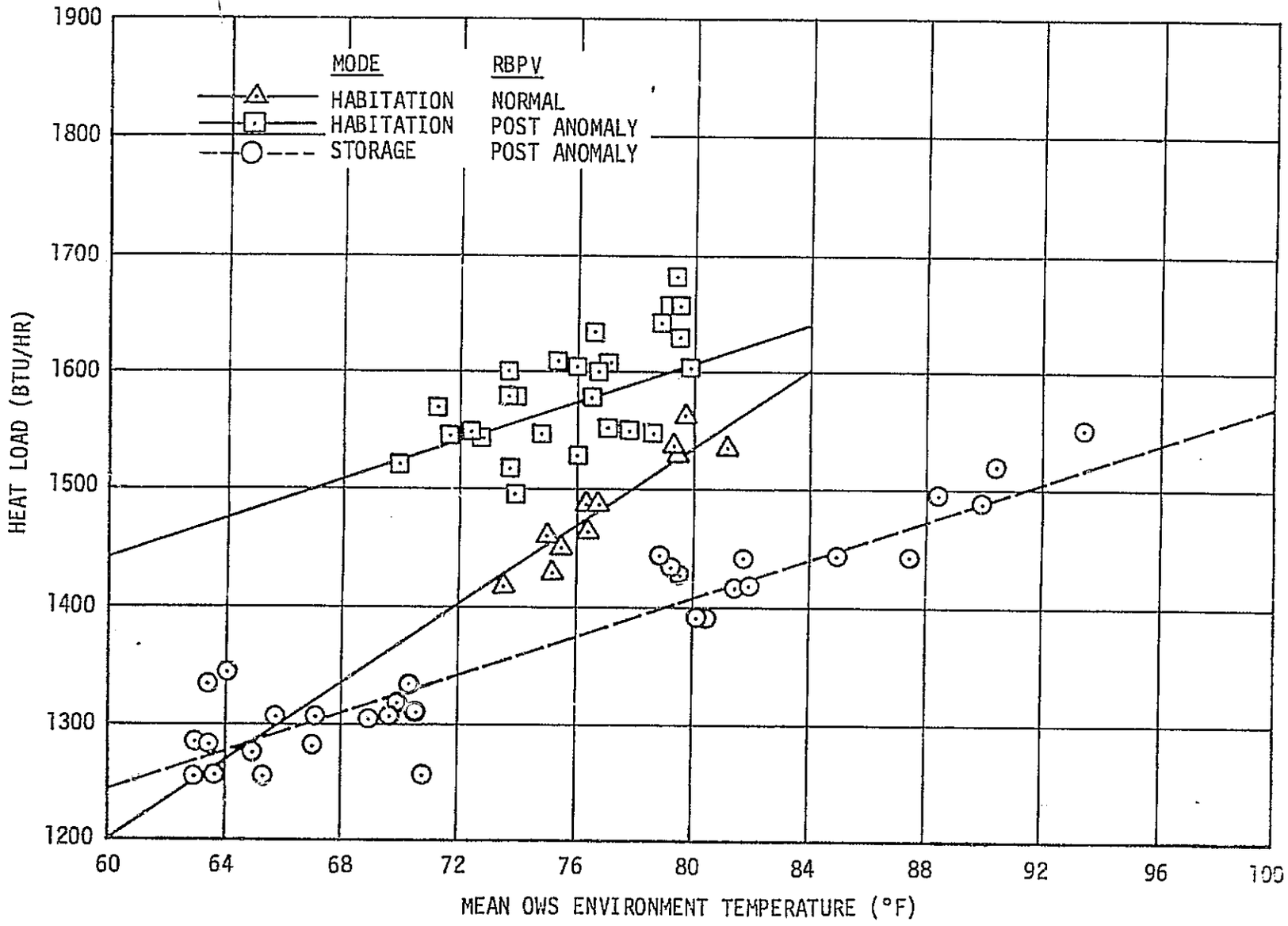

Figure 8-12. Total RS Heat Loading

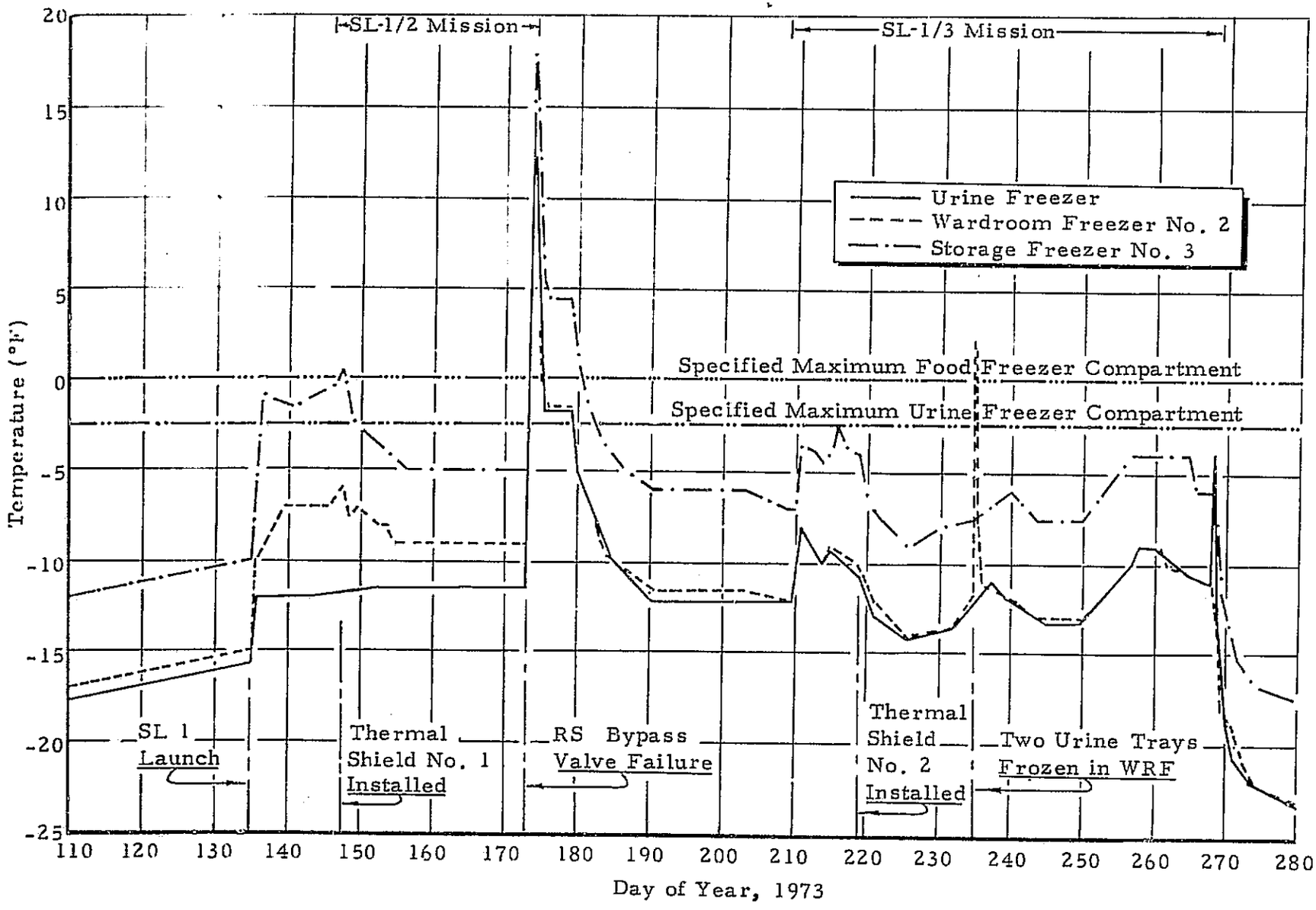

Figure 8-13. RS Freezer Compartments Temperature History for SL-1, SL-2 & SL-3

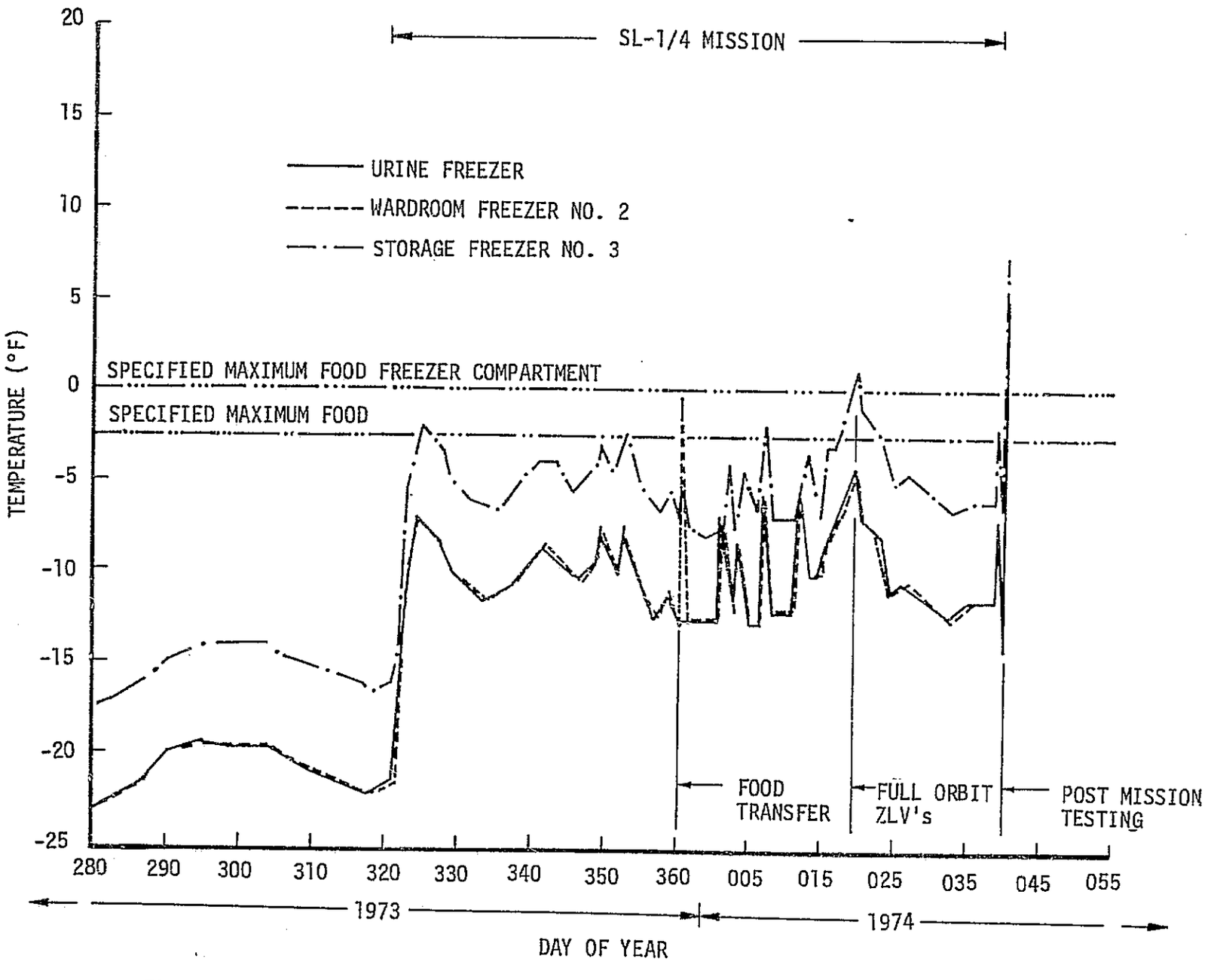

Figure 8-14. RS Freezer Compartments Temperature History for SL-4

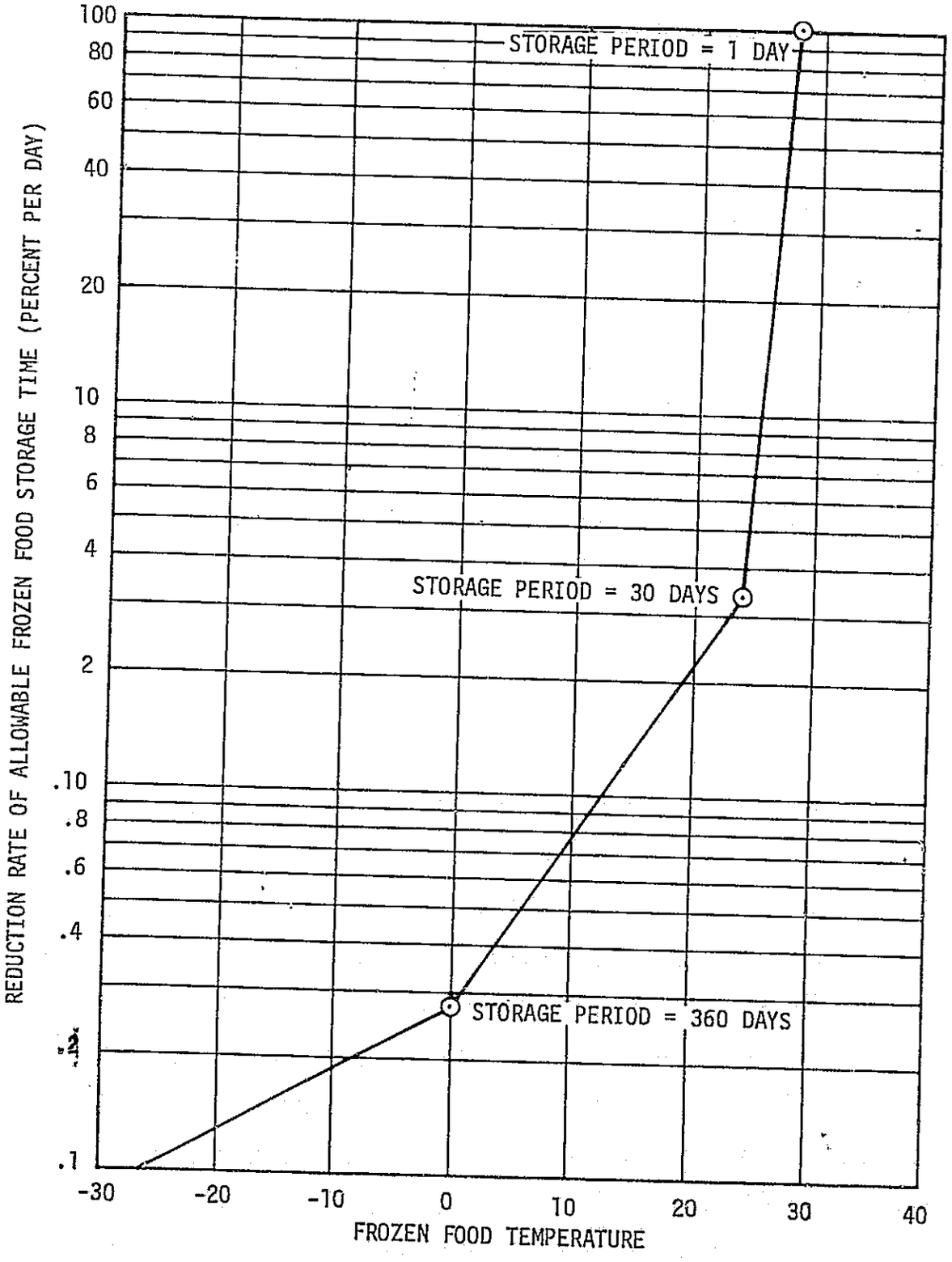

Figure 8-15. RS Frozen Food Spoilage Rate

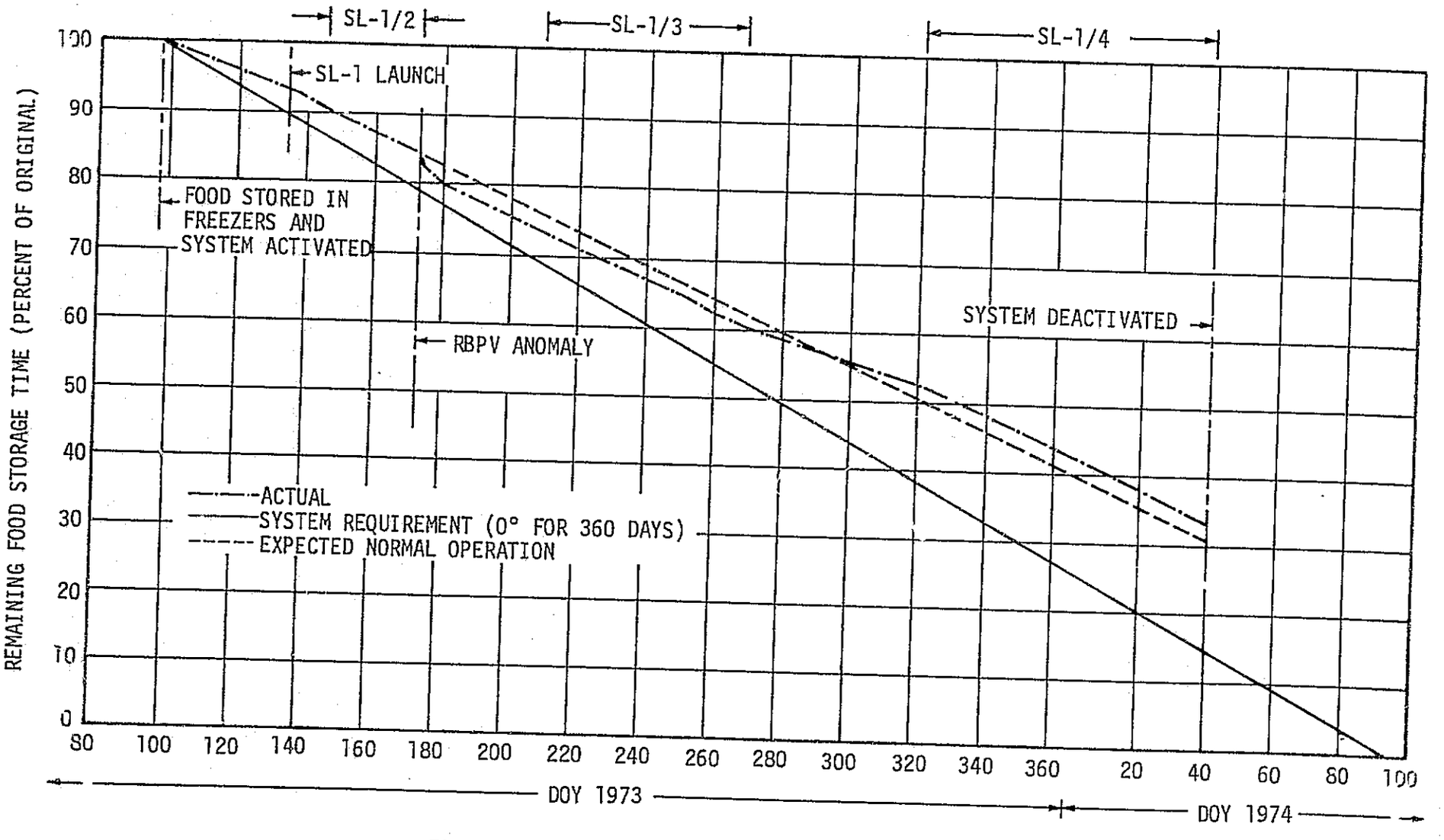

Figure 8-16. Frozen Food Allowable Storage Time

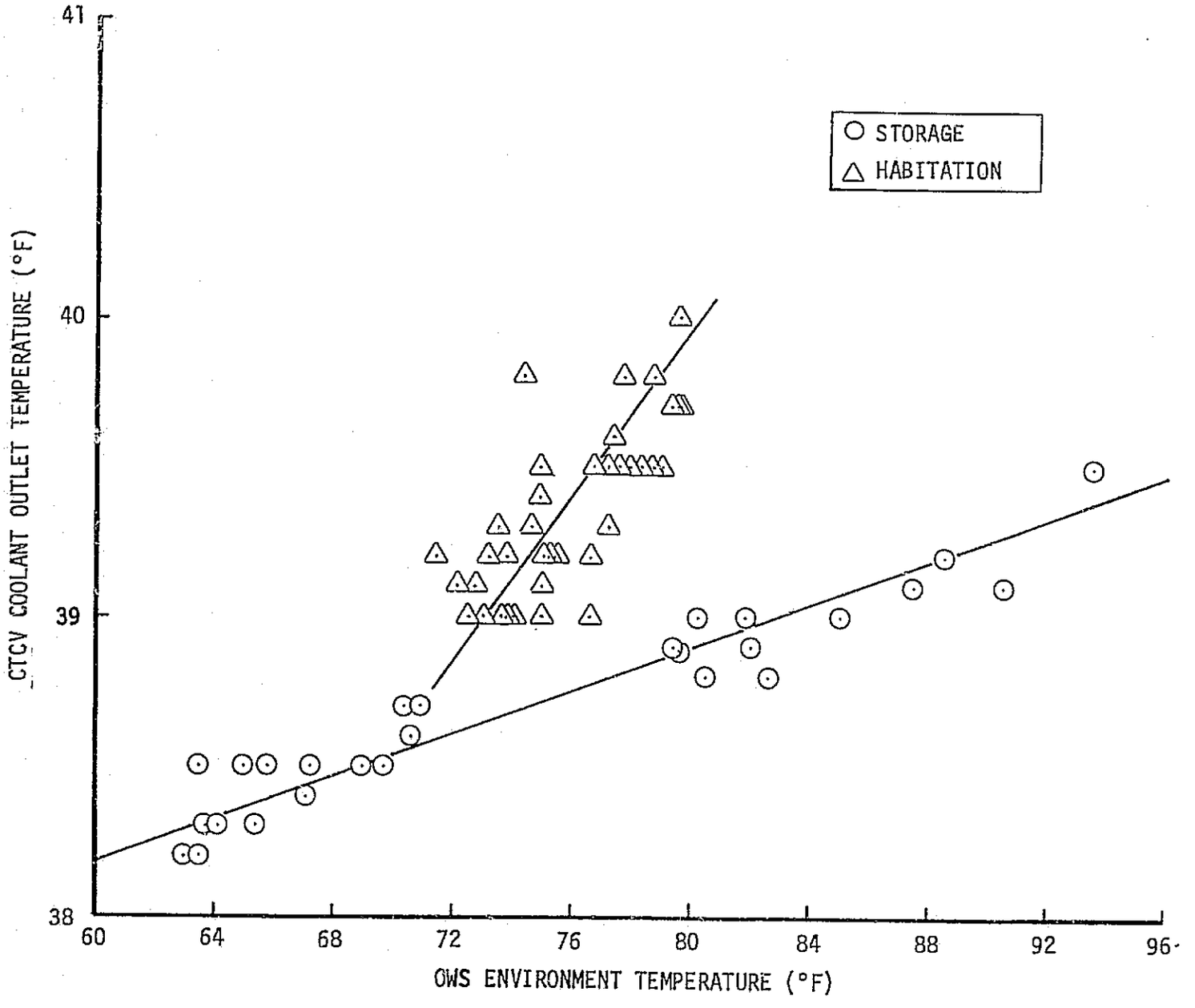

Figure 8-17. RS CTCV Coolant Outlet Temperature Dependence on the OWS Environment Temperature

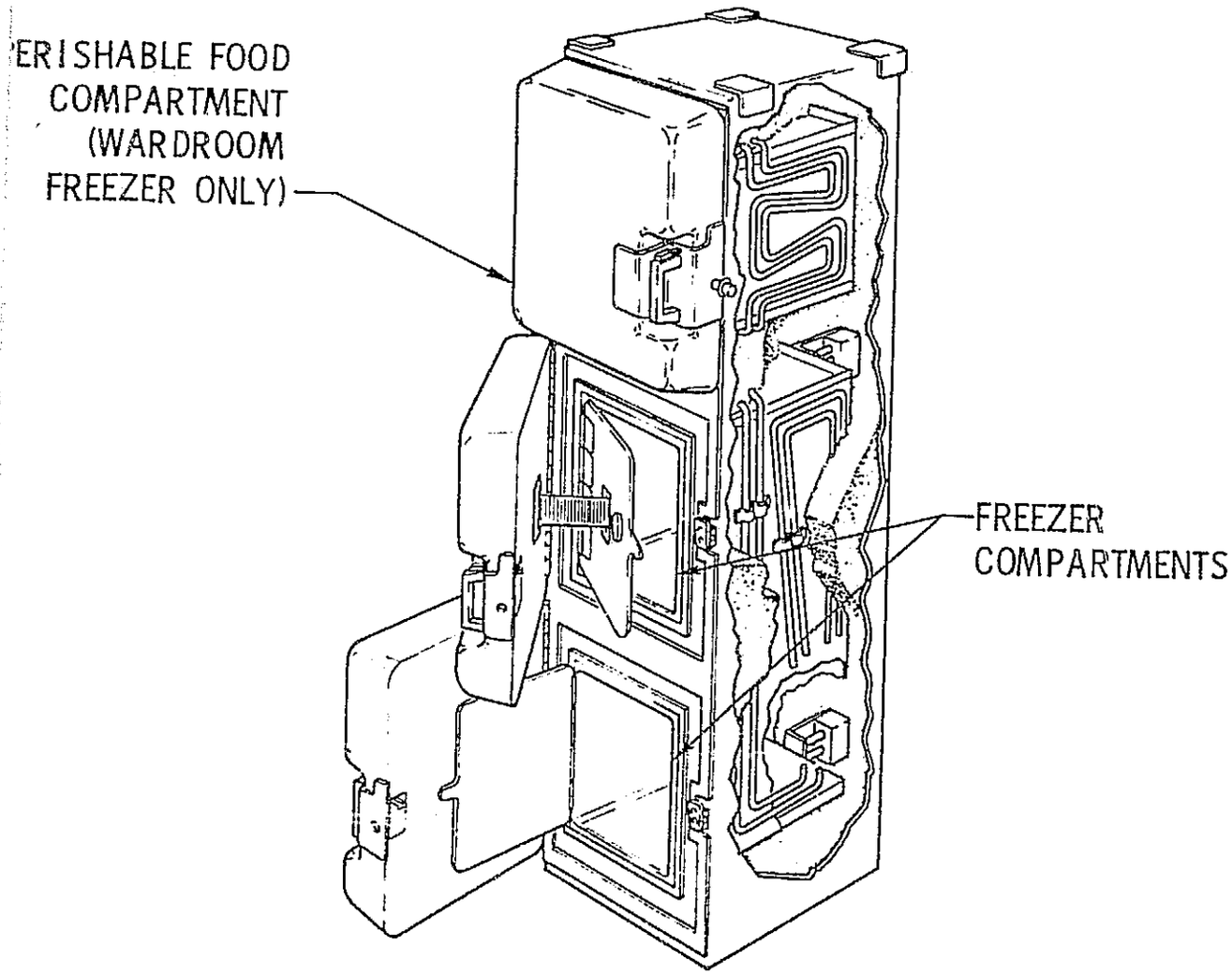

Figure 8-18. RS Food Freezer

Primary loop pump number 1 accumulated 7270 hours running time which exceeded the qualification life of 2250 hours. Review of the pump differential pressure, indicated no performance degradation. During SL-2, primary loop, pump number 2 was operated for a total of 300 hours with no degradation in performance. Secondary loop, pump number 1 operated 367 hours preflight and 2 hours during SL-2.

Evaluation of the RS pressure and temperature data through the SL-4 mission indicated that there was no detectable Coolanol 15 leakage from either the primary or secondary coolant loops. Figures 8-19 and 8-20 are plots of 10-day average leakage tracking data for both RS loops. As shown, both loops have essentially constant "measurement error" and are well within the band of measurement tolerance. The RS leakage rate was considerably less than the allowable 12 in^3/year and, in fact, no leakage could be detected from the data.

The method of predicting RS leakage was:

a. The loop pump inlet pressure was calculated based on a weighted average loop temperature distribution from flight data, and the known accumulator performance.

b. This calculated pump inlet pressure was compared to the flight recorded pressure. The average difference, based on sampled data for DOYs 176 to 219, was found to be 2.967 PSI lower than flight pressure for the primary loop, and 2.25 PSI lower for the secondary.

c. The "lower band of measurement tolerance" shown in figures 8-19 and 8-20 included the pressure transducer least bit error and a 0.3 PSI pressure transducer repeatibility. Data above this "lower band of measurement tolerance line" indicated no detectable coolant leakage.

6. Inflight System Modifications. The possibility existed after the anomaly that the system could improve to a point such that the cold bypass would again be triggered. Since the original failure occurred when the system switched back to the radiator mode from the bypass mode, the possibility of a repeated failure existed. To avoid this it was proposed to open the RBPV controller circuit breaker (C/B) on SL-3 activation. A complete analysis was made to determine the coldest operation of the system with continuous full radiator flow (in the event that RBPV bypass poppet completely closed). The results of the analysis indicated that the food freezer could reach -30°F, producing some condensation on the freezer external surfaces. Based on these studies and to avoid the reoccurrence of the failure, the SL-3 crew opened the primary loop RBPV controller C/B on panel 611 on DOY 209.

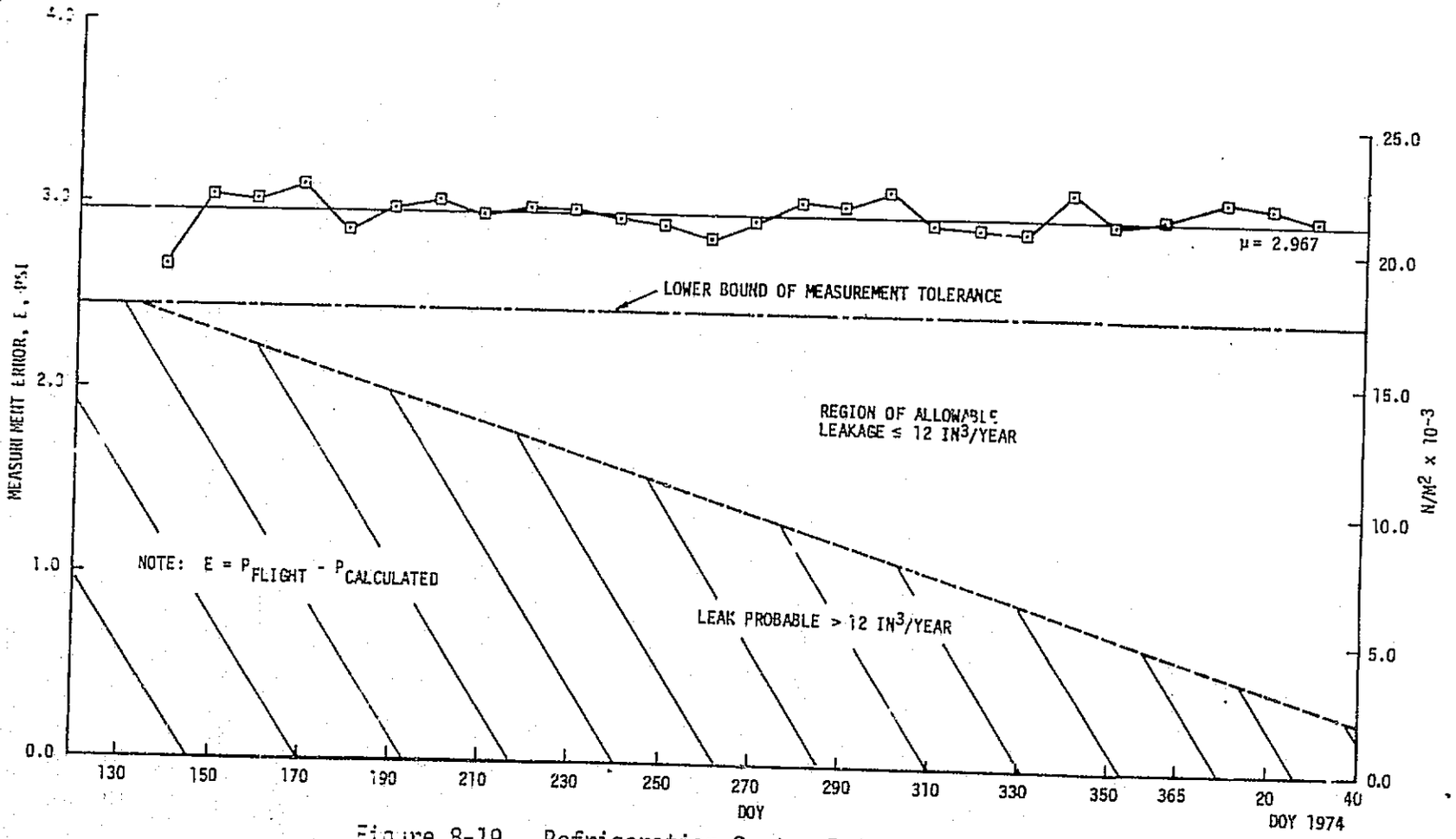

Figure 8-19. Refrigeration System Primary Loop Leakage Tracking 10 Day Measurement Error (E) Averages

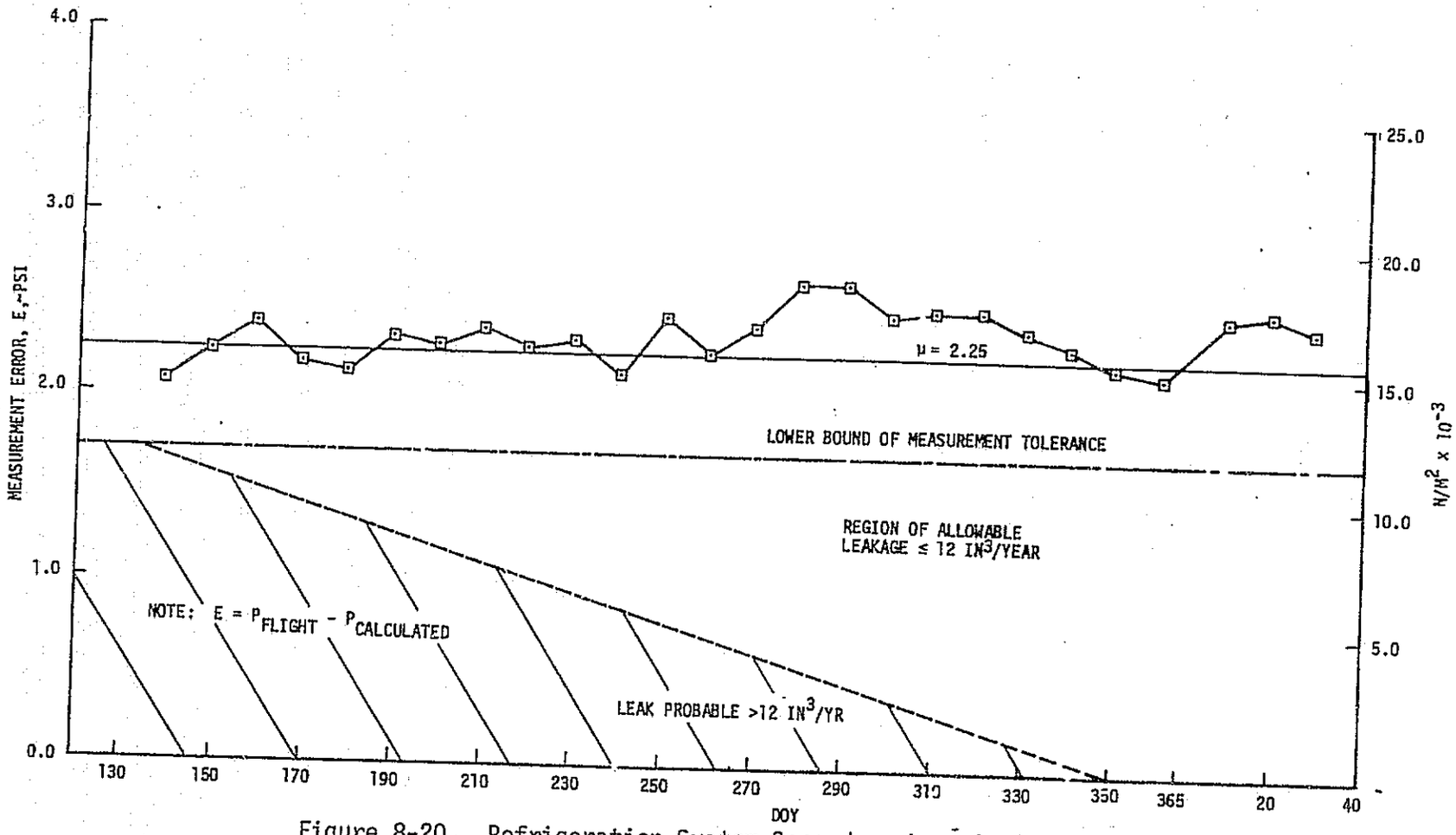

Figure 8-20. Refrigeration System Secondary Loop Leakage Tracking
10 Day Measurement Error (E) Averages

To provide further system flexibility (particularly relative to trouble shooting the secondary RS loop), a modification to provide dual loop operation was suggested. Computer analysis had shown that the warmest freezer could be decreased 2 to 3°F with dual loop operations and further that if both loops were operating with their RBPVs in their original failed configuration, the warmest freezer could be maintained at -2°F. Therefore, on DOY 266 just prior to SL-3 deactivation, the crew removed the electrical cable which provided the inter-loop logic. This modification not only allowed dual loop operation but also removed all automatic loop switching logic. No system performance changes were observed as a result of the cable disconnect operation.

7. End of Mission Testing. At the end of the SL-4 mission, ground controlled tests of the RS were performed. The test objectives were to (a) assess the failure in the secondary loop and (b) improve the performance of both loops by troubleshooting techniques. To meet these objectives, the following test sequence was used:

a. Operate both loops simultaneously

b. Secondary loop only operation

c. Cycle primary loop

d. Cycle secondary loop

e. Primary loop bypass flush

f. Secondary loop bypass flush

g. Operate primary loop in radiator mode

h. Operate secondary loop in radiator mode

In preparation for the tests, the crew closed the primary loop RBPV control logic circuit breaker. The crew also cycled (open/close) the secondary loop RBPV control logic circuit breaker. In the event that a "cold" bypass signal had been sensed during the storage period prior to SL-4 activation, this action would clear the logic memory and prevent the secondary loop RBPV from initially starting in the bypass mode. When the crew performed these functions at 039:03:52 GMT, the primary loop differential pressure dropped by approximately 4 PSID as shown on figure 8-21, and the thermal capacitor began to melt as seen in figure 8-22. These changes were indicative of reduced radiator coolant flow rate attributed to movement in the RBPV. The flow change could have been due to the interaction of the particular RBPV controller monitor and the temperature sensing bridges in the controller,

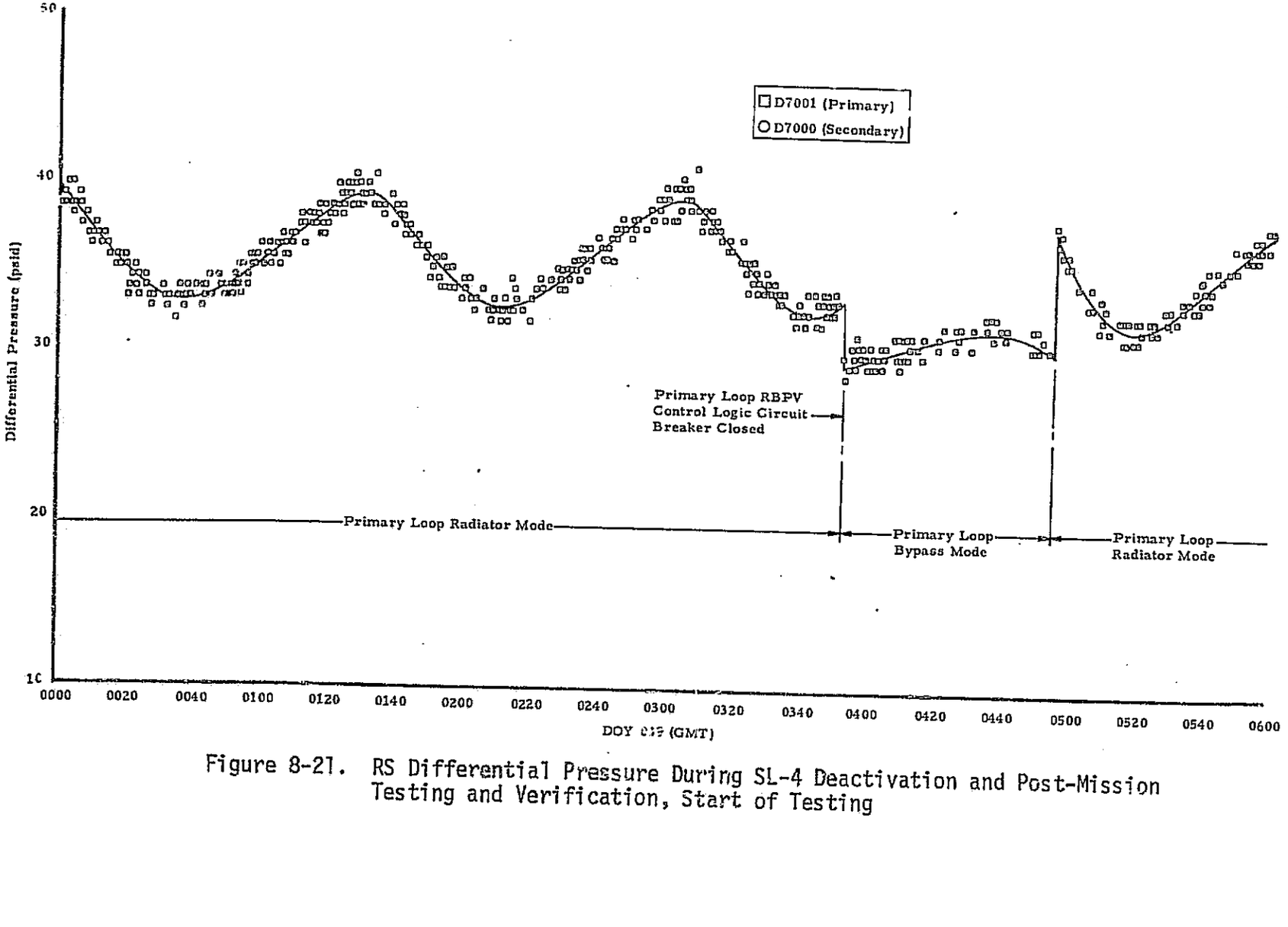

Figure 8-21. RS Differential Pressure During SL-4 Deactivation and Post-Mission Testing and Verification, Start of Testing

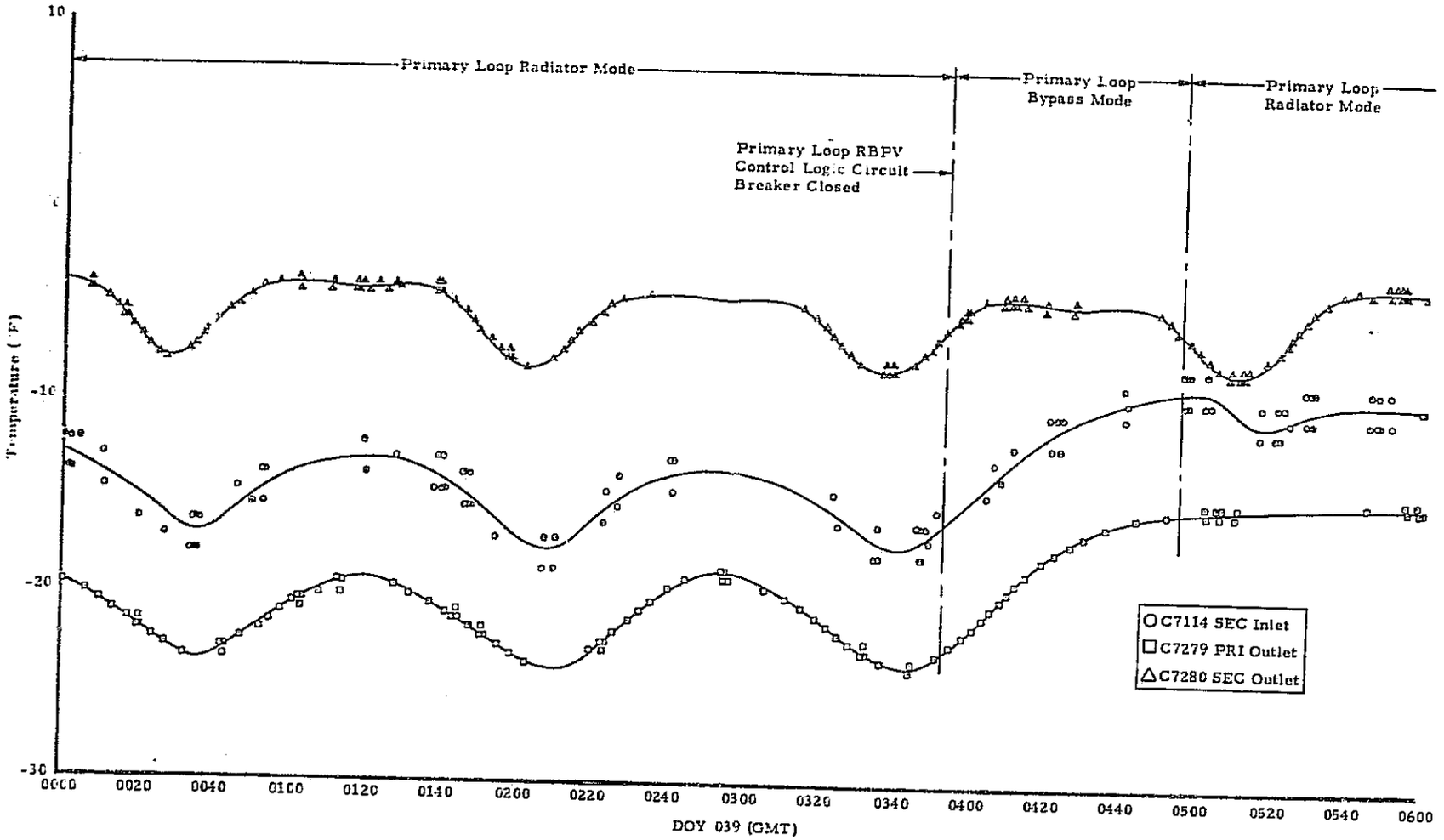

Figure 8-22. RS Thermal Capacitor Temperatures During SL-4 Deactivation and Post-Mission Testing and Verification, Start of Testing

initiating a bypass signal causing the RBPV to attempt to configure itself to the bypass position. Approximately one hour following the closing of the circuit breaker (039:04:56 GMT), the radiator coolant flow abruptly increased as shown from the rise in the differential pressure (figure 8-21) and the decline in the thermal capacitor coolant outlet temperature as shown in figure 8-23. This increase in radiator coolant flow to its previous magnitude was the result of the RBPV attempting to configure itself to the radiator position (radiator poppet unseated and bypass poppet seated, figure 8-24) as a result of the logic sensing a temperature greater than -12.8°F at the outlet of the first thermal capacitor segment.

The actual post-mission tests began at approximately 039:17:13:30 GMT with the enabling of the secondary loop. The results of the end of mission tests are given in the following paragraphs.

The secondary loop was operated simultaneously with the primary loop until approximately 039:19:59:00 GMT. The test results indicated that the secondary loop RBPV bypass poppet was effectively full open. The warmest food freezer temperature decreased from -8.0 to -11.0°F after secondary loop activation. This compared favorably with the 2.5° F temperature decrease predicted by computer analysis assuming the bypass poppet was fully opened.

At approximately 039:19:59:00 GMT, the primary coolant loop was deactivated and the secondary loop was allowed to continue in operation for approximately 3 hours and 50 minutes. The test results again indicated that the secondary loop RBPV was in the same configuration as the primary loop RBPV at the time of failure (bypass poppet effectively full open).

The primary and secondary RBPVs were cycled (radiator mode -- 10 second/cycle; bypass mode -- 10 seconds/cycle), and then each loop was operated in the bypass mode to flush the bypass poppets. The results of these tests indicated no improvements in performance. Furthermore, it was not possible to obtain full bypass flow in either loop, since the required differential pressure of 37.5 PSID was not observed (figure 8-25).

The system differential pressures during the "bypass" operation did not follow the same trend in each loop (figure 8-25 and 8-26). The primary loop system differential pressure was lower during the "bypass" mode than during the "radiator" mode. In the secondary loop, the system differential pressure was higher during the "bypass" mode than during the "radiator" mode. In explaining the above situation it is useful to keep in mind the following conclusions from the earlier discussion of the end of mission testing:

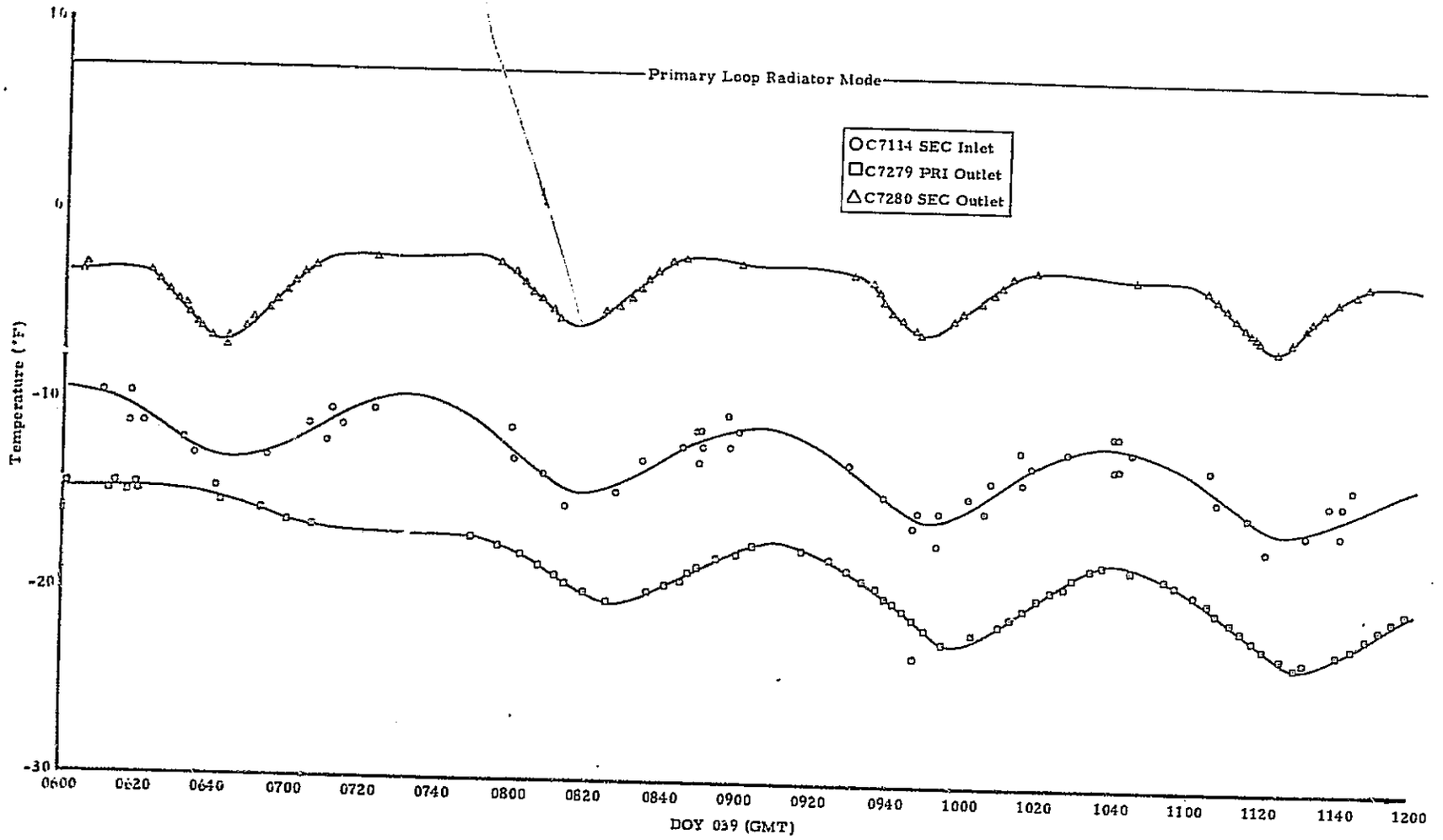

Figure 8-23. RS Thermal Capacitor Temperatures During SL-4 Deactivation and Post-Mission Testing and Verification, End of Testing

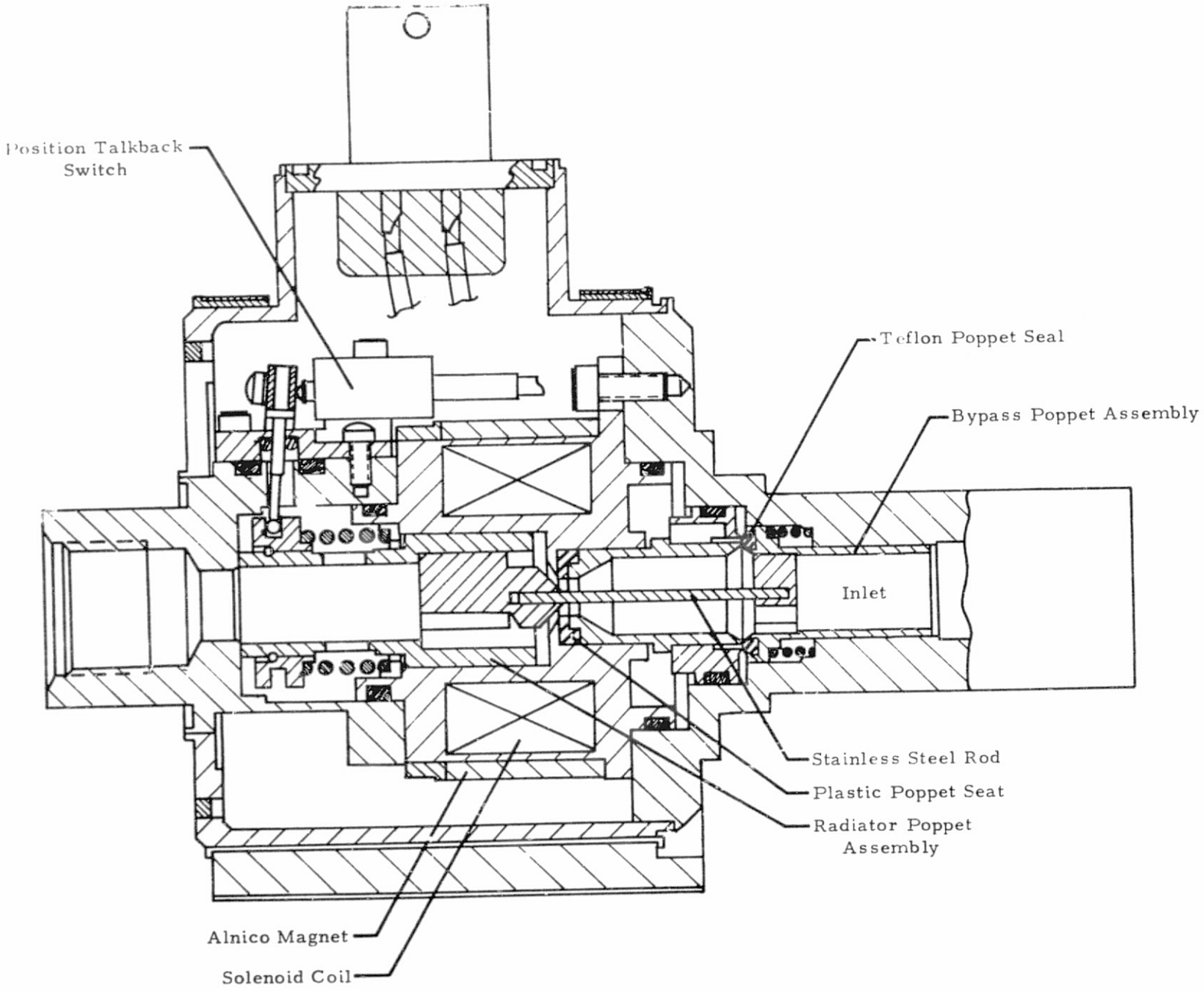

Figure 8-24. Radiator Bypass Valve Schematic (Radiator Mode)

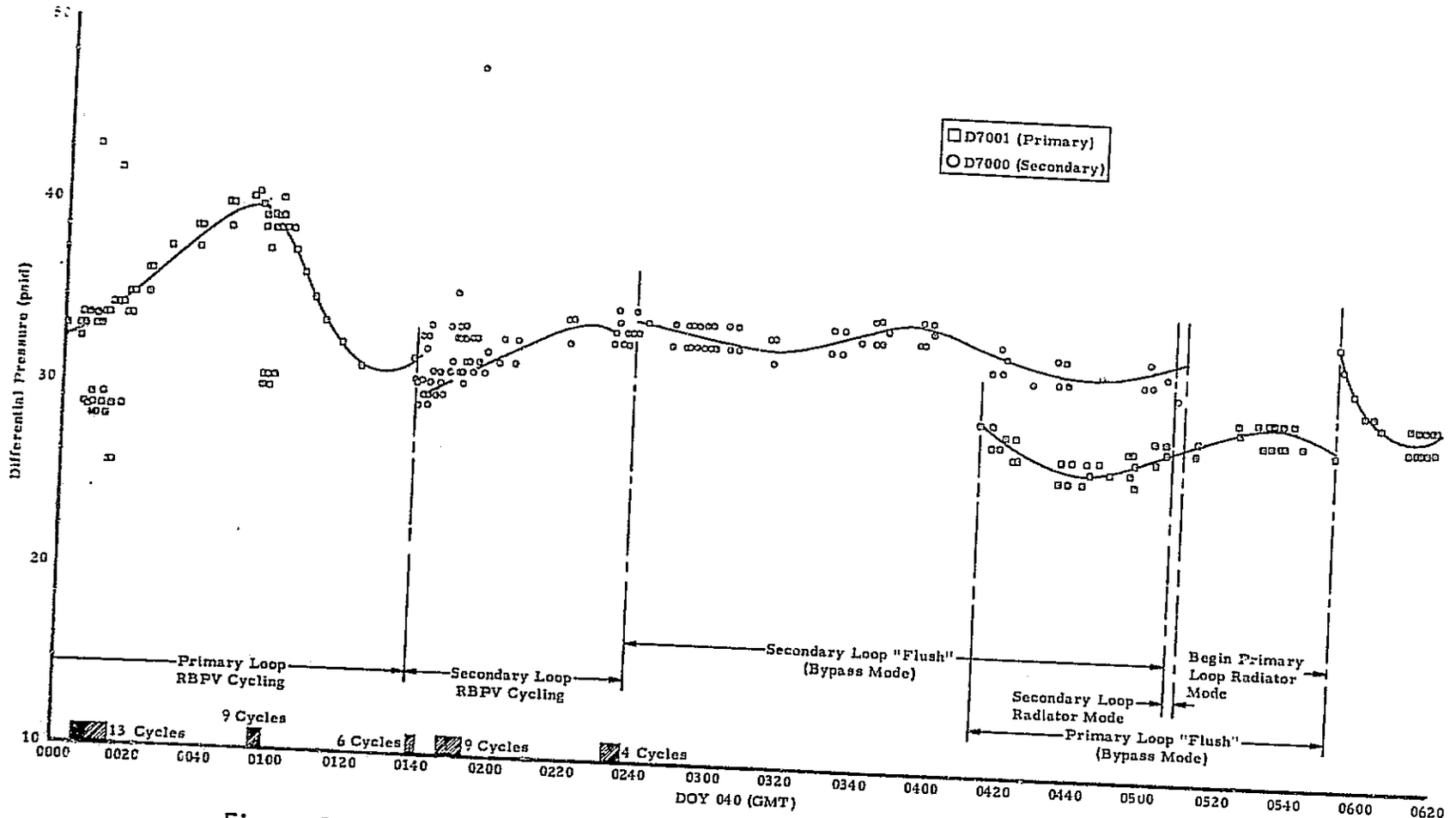

Figure 8-25. RS Differential Pressure During SL-4 Deactivation and Post-Mission Testing and Verification, End of Testing

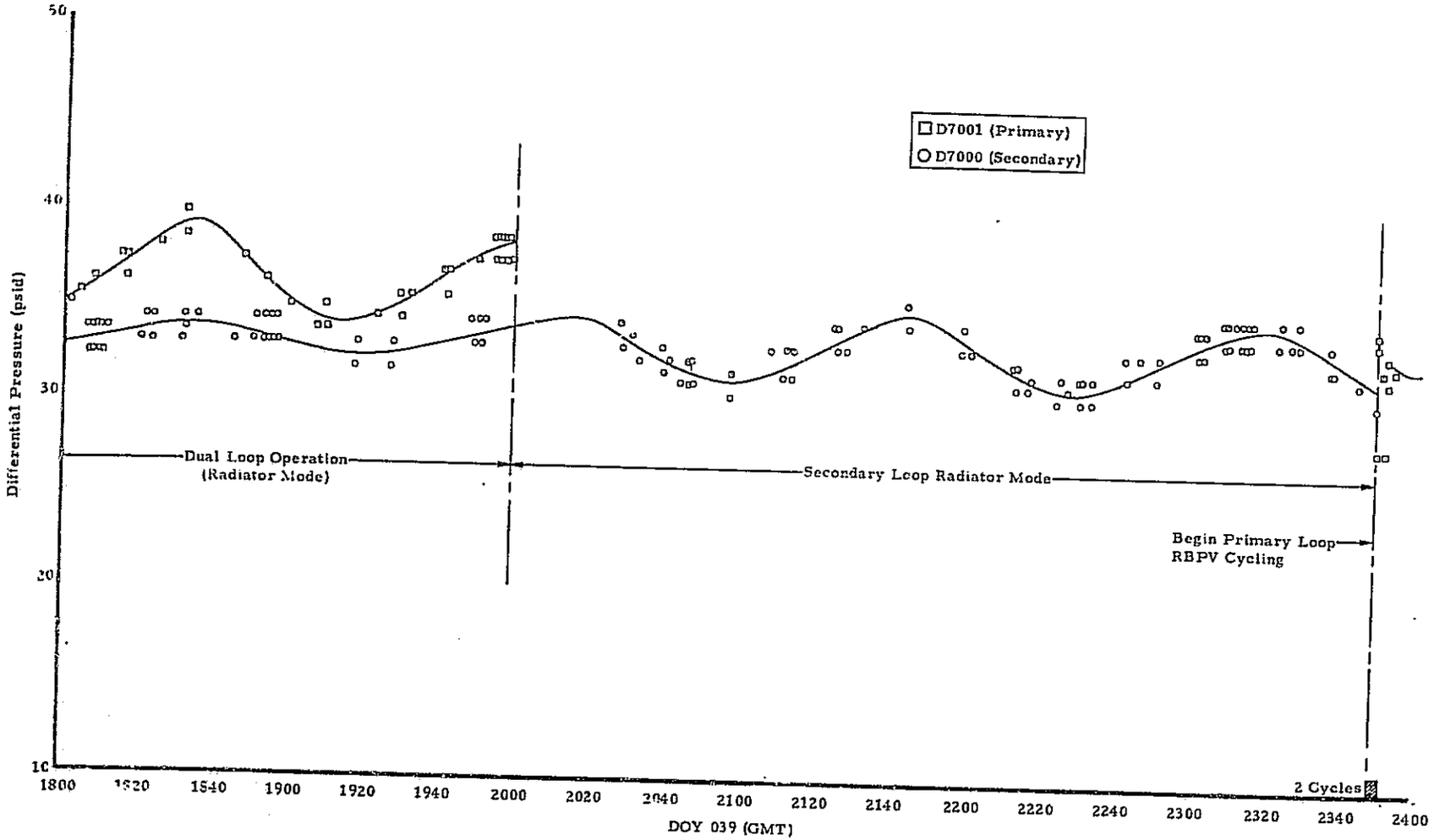

Figure 8-26. RS Differential Pressure During SL-4 Deactivation and Post-Mission Testing and Verification

a. The radiator poppet in each loop fully opened in the radiator mode since the radiator event light was triggered.

b. Full bypass flow was not attained for either loop because the bypass pressure difference was less than 37.5 PSID.

c. The bypass poppet in each loop did not close in the radiator mode because the flow through the radiator was less than 100 percent.

Items a. through c. may be summarized by the following: The radiator poppets in each loop fully opened and neither poppet in either loop fully closed. It could have been that the bypass poppet in the secondary loop was "frozen or stuck" with little motion in either direction. This was indicated by the increase in the system differential pressure in the bypass mode position (the flow area through the bypass flow passage remained constant, the coolant flowrate increased). Since the system differential pressure decreased in the primary loop in the bypass mode, it may be that movement of the radiator poppet forced the bypass poppet further away from its seat (but not far enough to allow the radiator poppet to seat). Following the completion of the tests the secondary coolant loop was disabled for the final time at 040:05:09:12 GMT; primary loop, 040:06:22:47 GMT.

C. Anomalies

The only anomaly of the RS involved the radiator bypass valve and occurred during the deactivation of SL-2 at approximately 173:02:02:00 GMT. The effect of this anomaly on the thermal performance of the system is illustrated in figure 8-27. Note from figure 8-27 that the anomaly occurred at the time of radiator reactivation following a "cold" radiator bypass period. The pump differential pressure dropped abruptly by approximately 5 PSID. The radiator surface temperature near the coolant outlet port was greatly reduced in the orbits that followed. Since this sensor was an indication of the temperature of the coolant at the radiator outlet, reduced radiator coolant flow was evident (maintaining all other parameters constant, decreasing the radiator coolant flow rate decreased the coolant temperature at the outlet of the radiator). Reduced coolant flow through the radiator eventually resulted in the depletion of the thermal capacitor (figure 8-28). The depletion is indicated by the increase above -14.5°F of the capacitor outlet temperature (C7279). A rapid rise in the freezer compartment temperatures followed. The magnitude of both the thermal capacitor coolant inlet temperature and the system differential pressure after the anomaly indicated that split flow existed (coolant flow through the radiator and GCHX simultaneously). Malfunction of one of two components only could have resulted in split flow--the radiator pressure relief valves (RPRV) or the radiator bypass valve (RBPV). A review

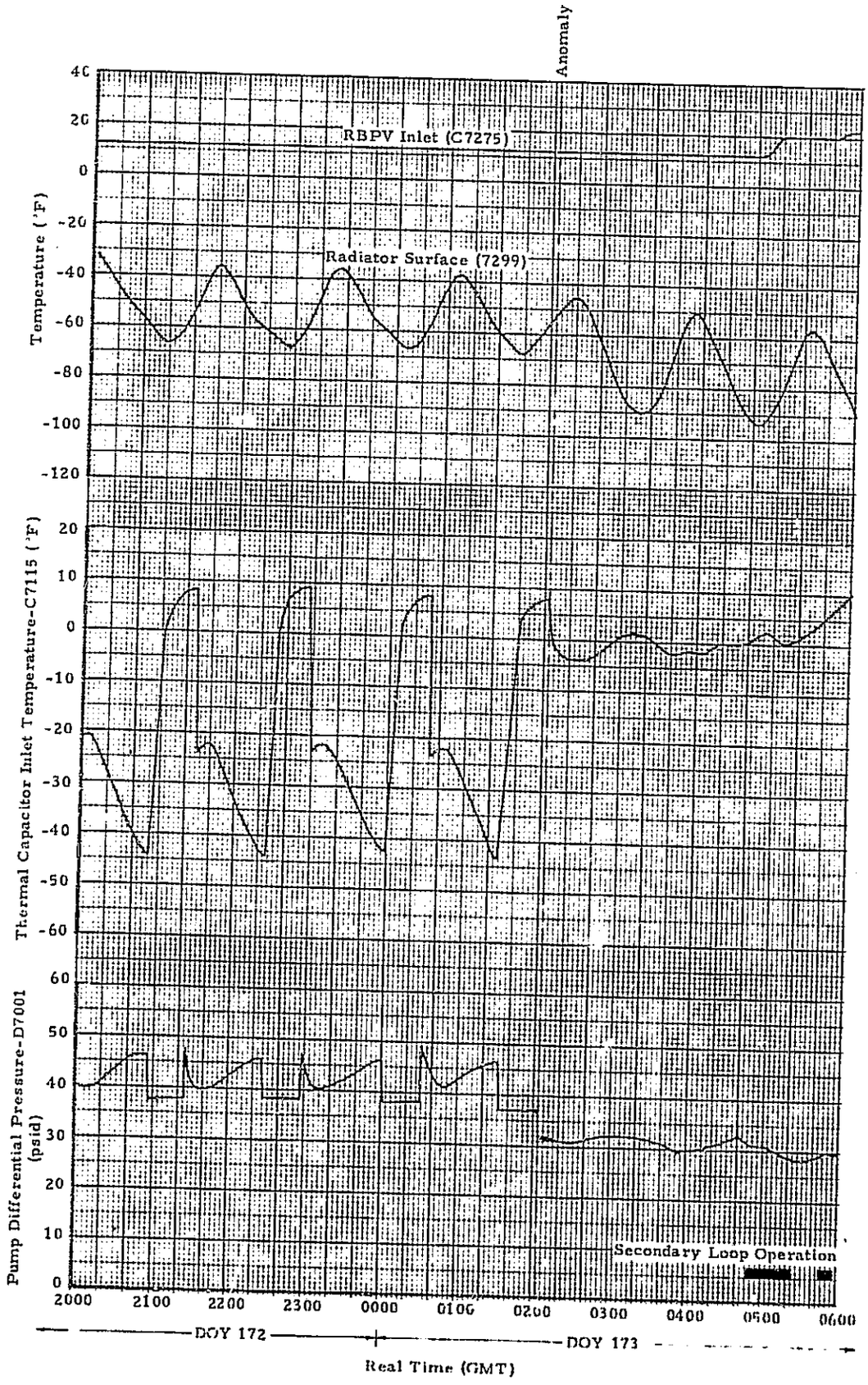

Figure 8-27. RS Anomaly Effects

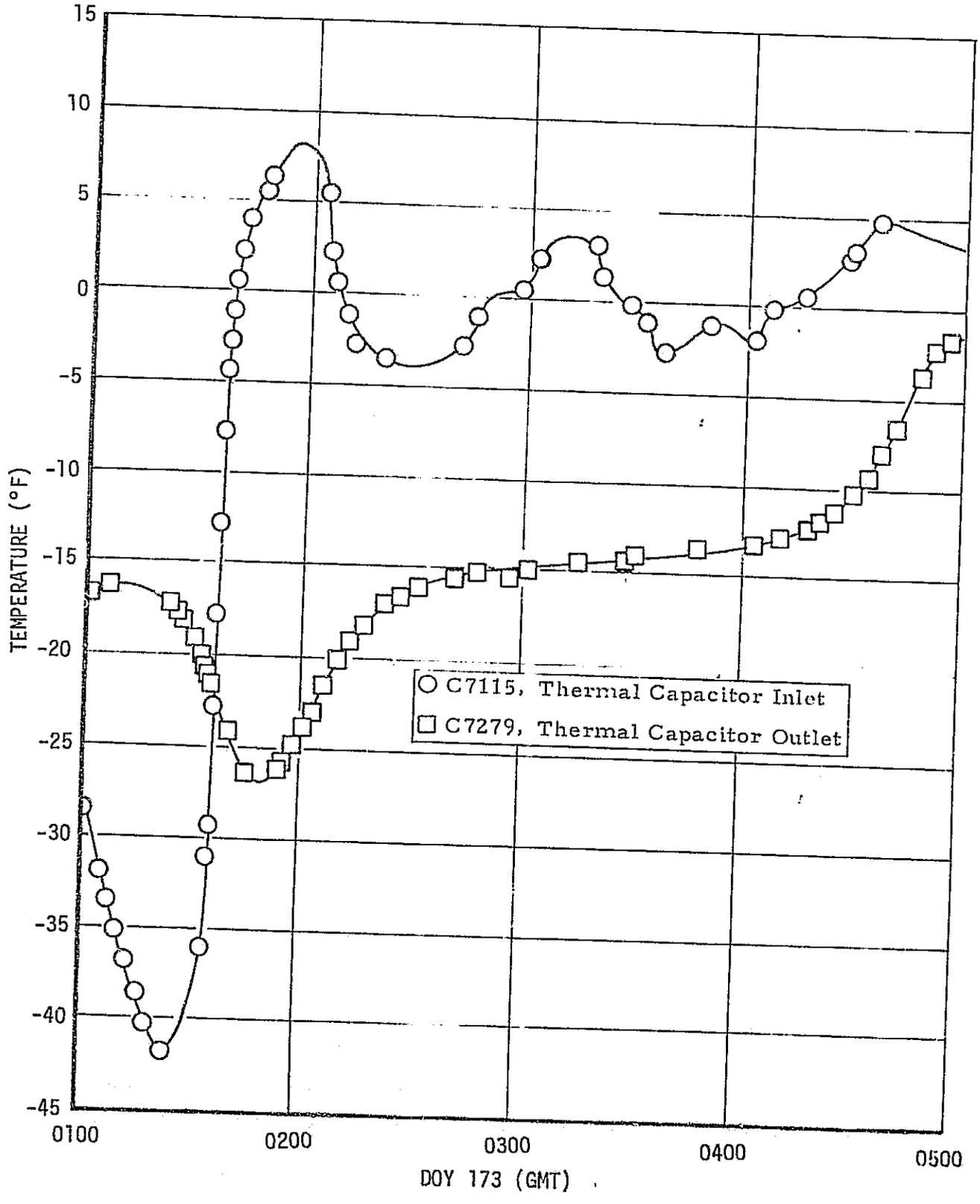

Figure 8-28. Depletion of RS Thermal Capacitor Following Anomaly of DOY 173

of the system differential pressure (figure 8-27) indicated that the pressure difference was not great enough to open the relief valve (≈ 65 PSID). However, the possibility existed, although very slight, that the instance peak pressure was missed due to data sampling rates. However, the end of mission test results verified that the pressure differences were consistant with a failed radiator bypass valve not a failed radiator pressure relief valve. Less than 3 hours after the occurrence of the anomaly, the automatic loop switching logic sensed a high freezer coolant inlet temperature and disabled the primary loop and enabled the secondary loop at 173:04:50:00 GMT. The secondary loop ran until 173:05:25:00. After finding the secondary loop to have a similar anomaly as the primary (based on the decreased system differential pressure), it was manually disabled and the primary loop was enabled. The secondary loop was enabled again from 173:05:47:39 to 173:05:57:56 for a further system differential pressure check.

Two actions were taken after the anomaly in an attempt to regain the thermal performance of the RS. The first was to pitch the vehicle +45° about the Y-axis so the radiator would receive direct solar flux. The radiator surface temperature is shown on figure 8-29. The purpose of this maneuver was to increase the radiator temperature in the event that partial blockage due to coolant freezing had occurred. After the radiator surface temperature increased to -20°F, normal vehicle attitude was restored. The impact of the pitch maneuver on the secondary loop was checked from 173:07:39:42 to 173:07:43:23. No improvements were observed at that time. However, more detailed data analysis indicated an improvement in the primary loop occurred when the primary loop was disabled and enabled during the secondary loop check at 173:07:39:42. The second action taken to restore the RS performance was to cycle the bypass poppet of the RBPV by enabling and disabling the loops in rapid succession. When the loop was disabled, the control logic would activate the loop's RBPV to the bypass position. Thus pump cycling would serve to cycle the bypass poppet of the RBPV, aiding in trash removal from the bypass poppet seal or in trash particle compaction in the bypass poppet seal (either would allow the poppet to move closer to its seated position).

The system differential pressure and the thermal capacitor inlet temperature during this time is shown in figures 8-30 and 8-31. Also indicated in figures 8-30 and 8-31 are the periods of primary and secondary loop operation and cycling. The system differential pressure and, to a lesser extent, the capacitor inlet temperature were used as indications of performance improvements. An increase in system differential pressure and a decrease in capacitor inlet temperature would have indicated increased radiator flow. The primary loop cycling began at 173:18:27:49 and ended at 174:10:50:20 after 105 cycles. The secondary loop was operated five times during the period from 173:20:00:18 to 173:21:05:02. However, secondary loop cycling begain at 174:01:45:05 and ended at 174:09:14:40 after 28 cycles.

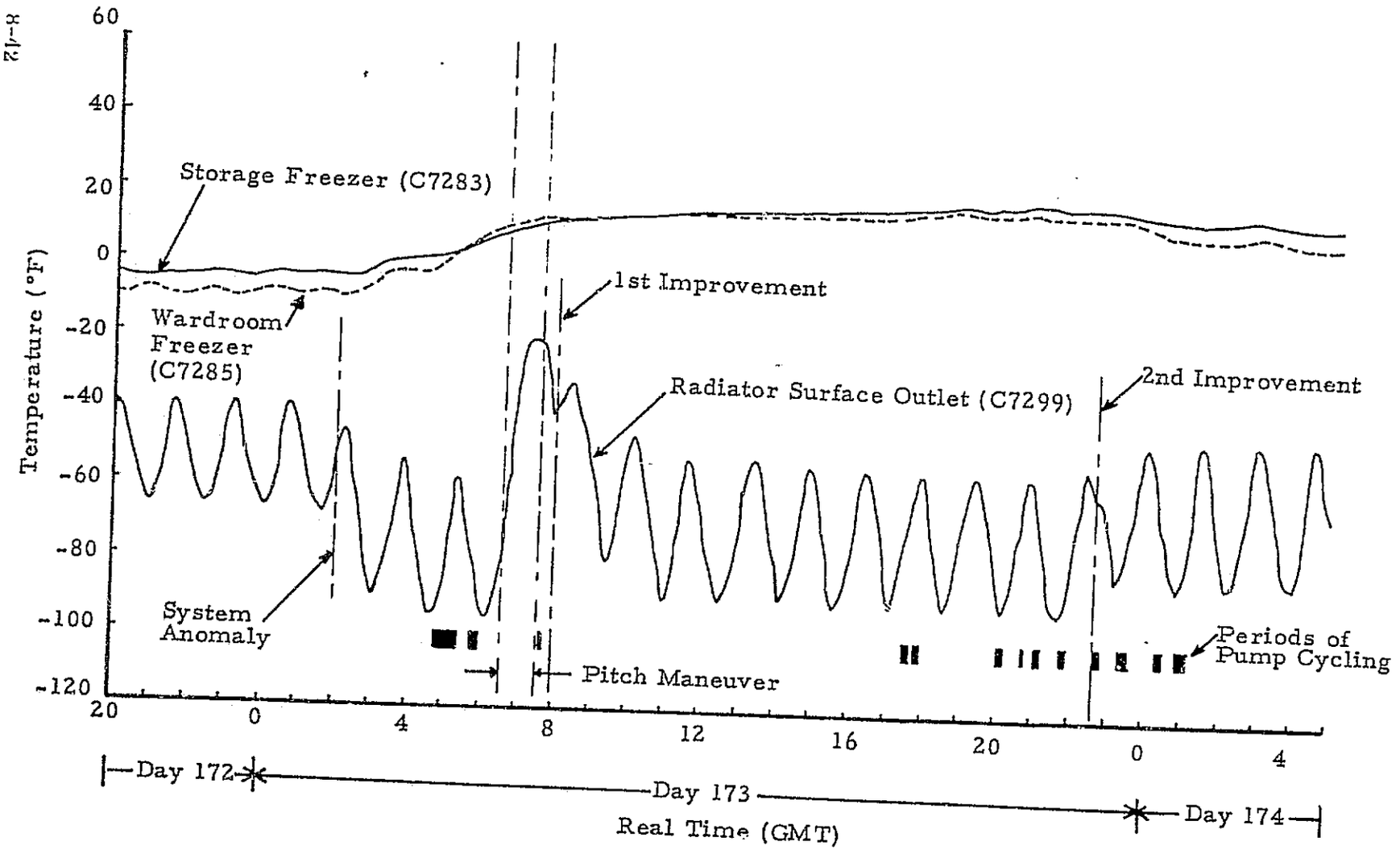

Figure 8-29. RS Parameters Showing Improvements in Primary Loop Radiator Coolant Flowrate Following System Anomaly

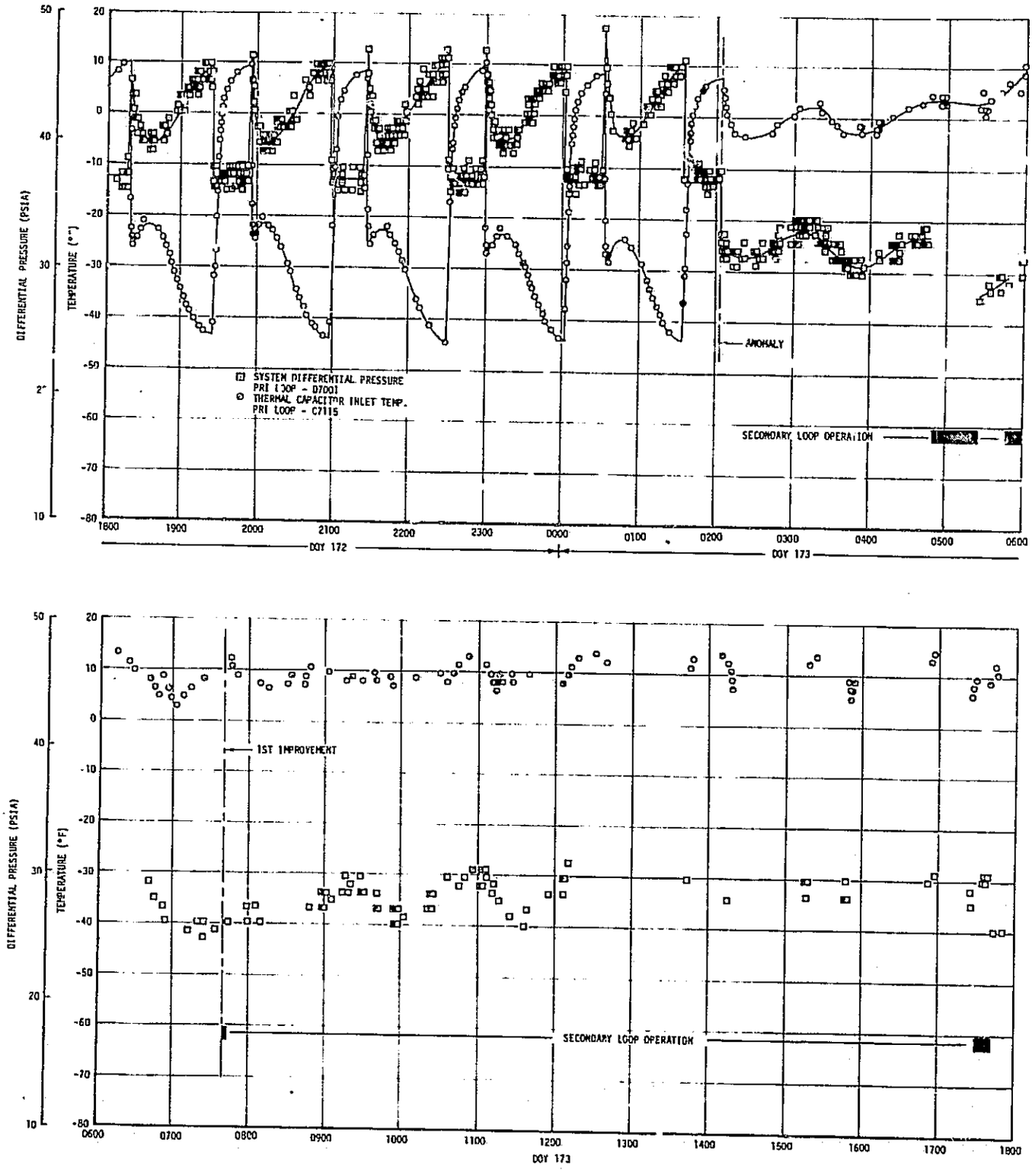

Figure 8-30. RS Performance During DOY 172 and DOY 173

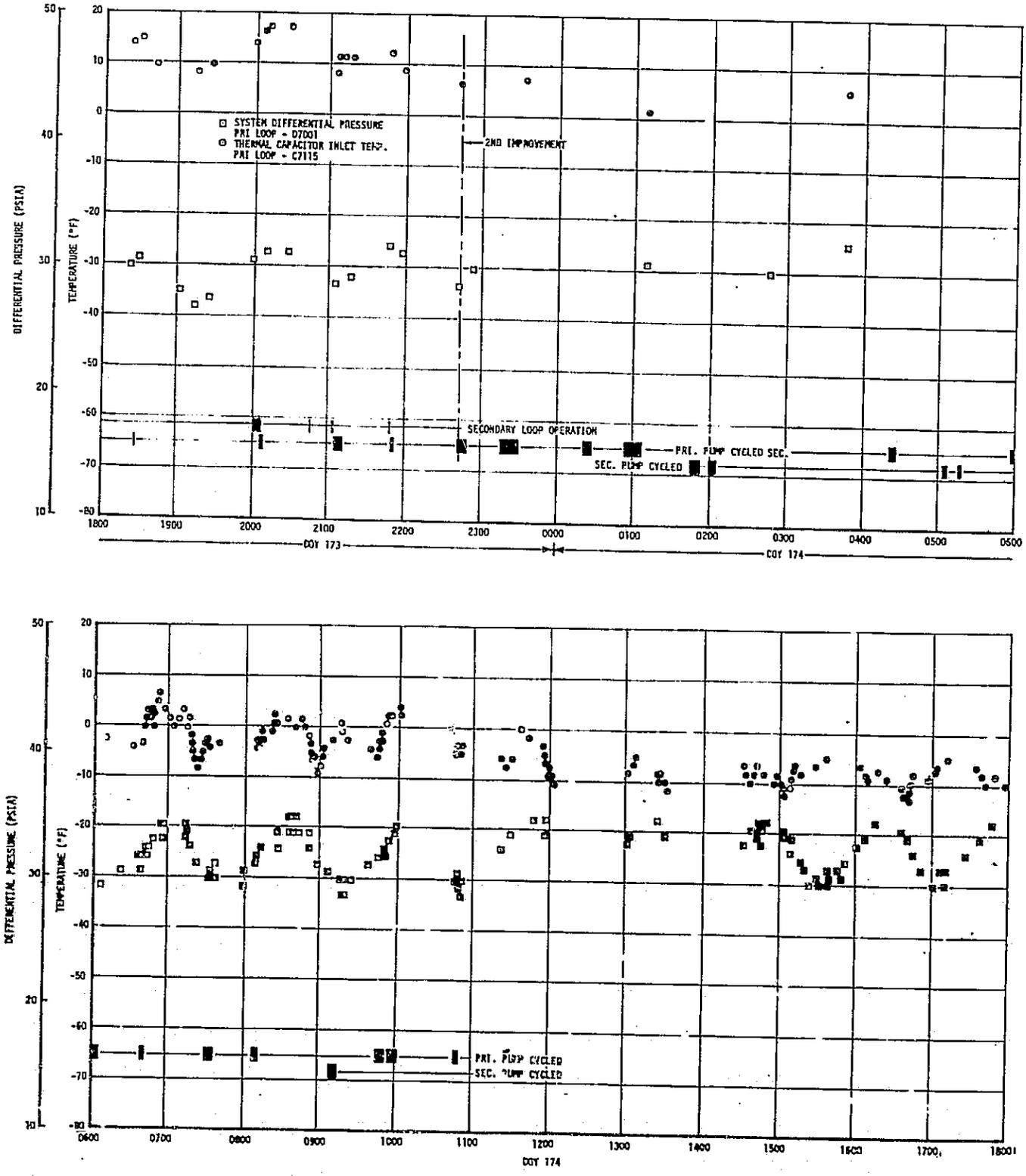

8-44

Figure 8-31. RS Performance During DOY 173 and DOY 174

A second improvement in the primary loop occurred at approximately 173:22:45:00 as a result of loop cycling. No improvement in the secondary loop was observed.

Cycling was discontinued at 174:10:50:20 because of the improvement in differential pressure and the frozen food temperature had begun to decrease as a result of the second improvement (figure 8-32). Computer analyses indicated that the frozen food compartments would have reached a temperature of approximately 30°F if these improvements had not occurred. A further decrease in the temperature of the freezers (below 0°F) occurred after the second improvement in the radiator coolant flow rate. However, as shown by figure 8-33, this decrease in the system temperature was the result of the decrease in the OWS environment temperature which resulted in a decreased heat load on the RS.

Computer analysis revealed that the malfunction could be simulated by an effectively fully open bypass poppet in the RBPV (earlier tests had shown that the bypass poppet of the valve may be only one quarter of the way open and yet bypass as much coolant as when fully open) with the radiator poppet in the radiator flow position. The radiator surface temperature and the capacitor outlet temperature simulation results are shown in figures 8-34 and 8-35, respectively. With the bypass poppet in this position, only about 20 percent (orbital average) of the total coolant flow rate (assuming a total flow of 130 lb/hour was allowed through the radiator. The radiator coolant flow after the anomaly varied over an orbit period due to the variation in heat flux on the radiator's surface over an orbit.

An extensive test program was initiated after the anomaly using the RS qualification test (HS-19) unit. The purpose of the tests were three-fold. (a) To try and duplicate the failure using the flight data and the SL-2 deactivation timeline, (b) to determine the system capabilities with the split flow, and (c) to determine the cause of the malfunction within the valve. The HS-19 system tests were not able to duplicate the failure. However, a RBPV did "stick" in a component bench test (due to contamination) and was freed after approximately 16 cycles. The tests to determine the decreased system performance indicated that the RS could maintain the upper food temperature limit of 0°F.

A third improvement (although small) in the primary loop radiator coolant flow rate was evident from a comparison of flight data taken before SL-3 activation (but after the second RS improvement) and after SL-3 activation. Figure 8-36 shows the thermal capacitor coolant outlet temperature plotted as a function of the RBPV coolant inlet temperature for these two periods. Note from the figure that the improvement apparently occurred at the time of SL-3 activation (DOY 209).

C 5

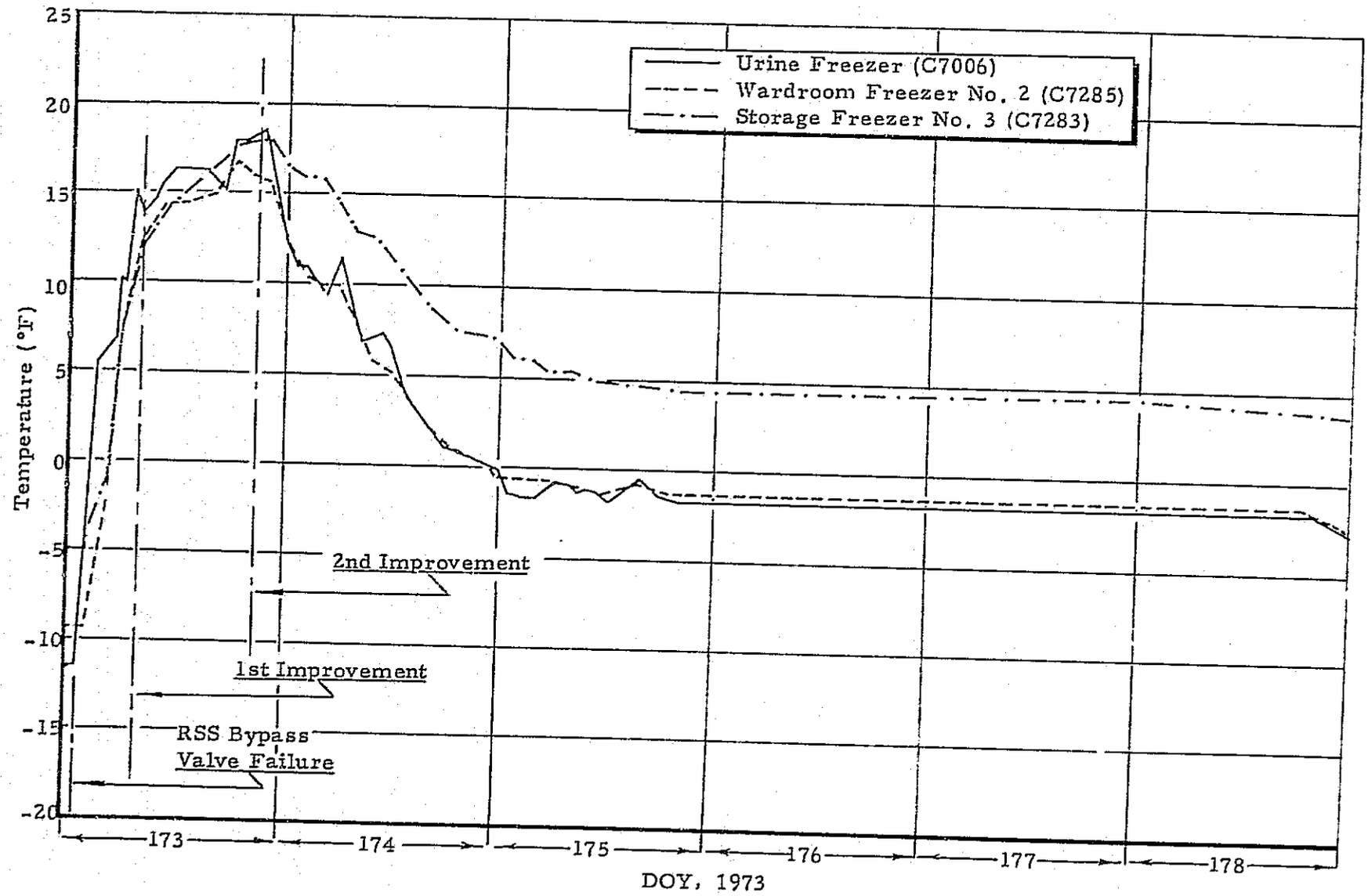

Figure 8-32. RS Freezer Temperatures Following RBPV Failure

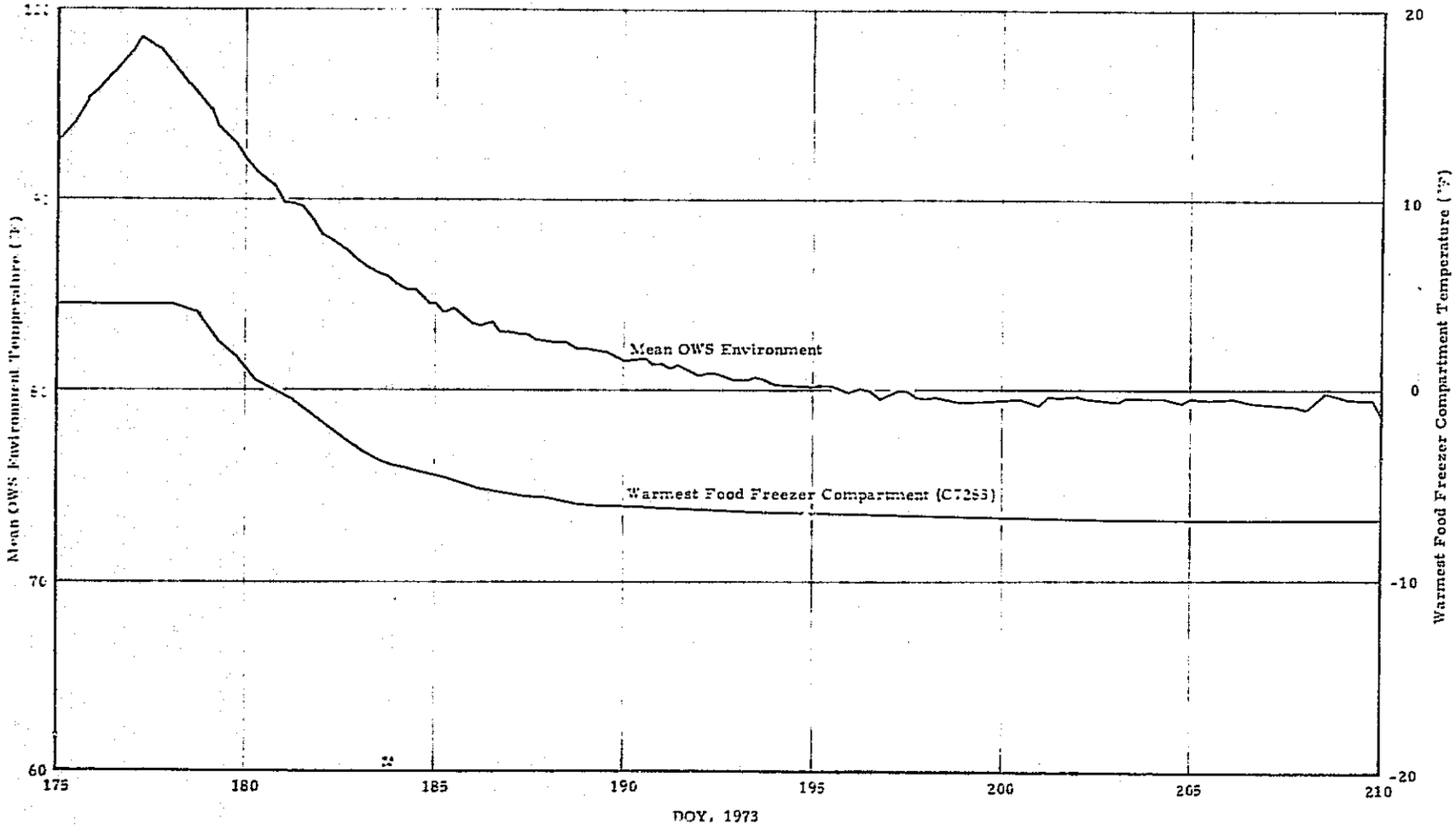

Figure 8-33. RS Warmest Freezer Compartment Temperature Decrease as a Result of a Decrease in the OWS Environment Temperatures

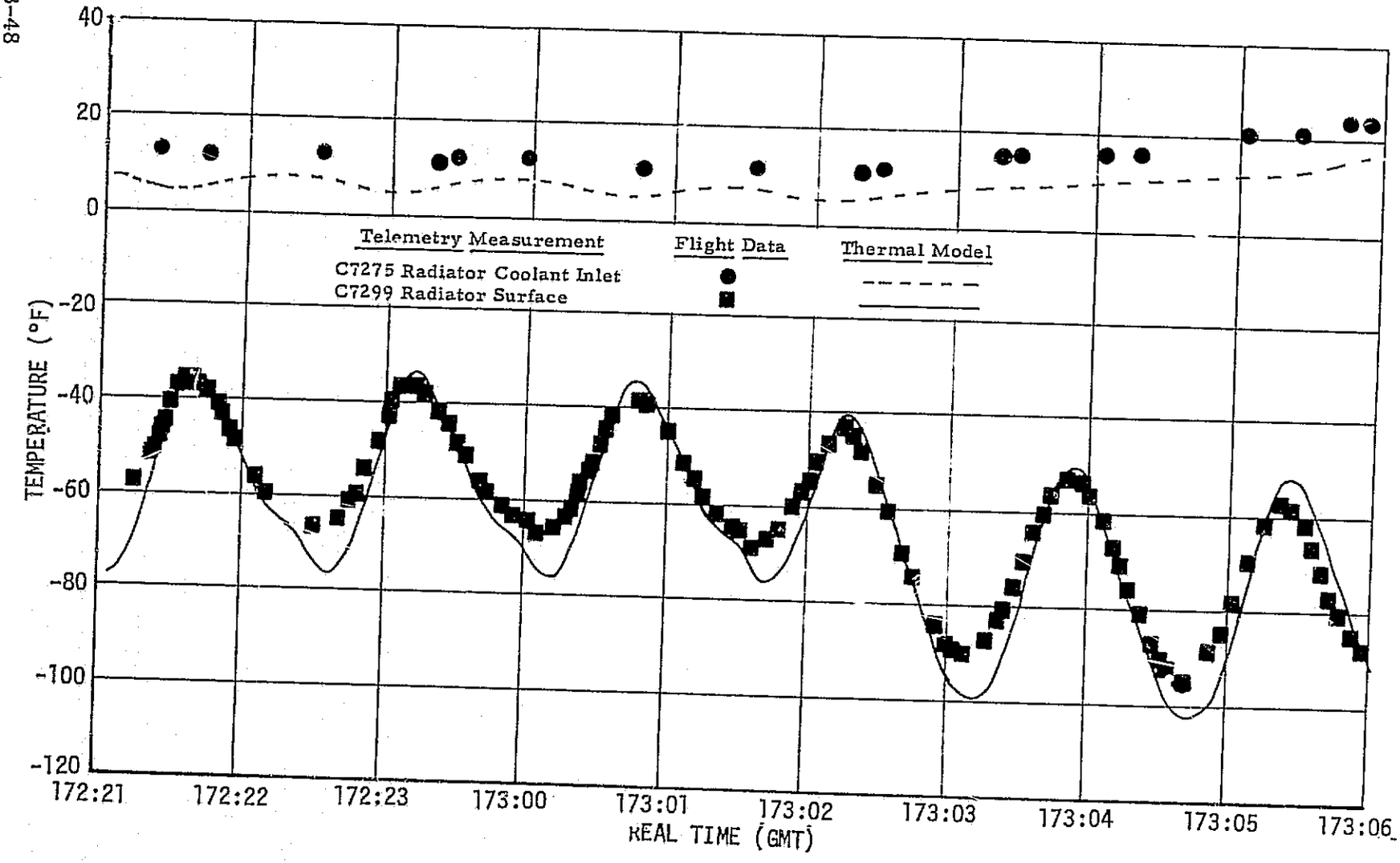

Figure 8-34. RS Anomaly Simulation Comparison with Flight Data, Radiator Temperatures

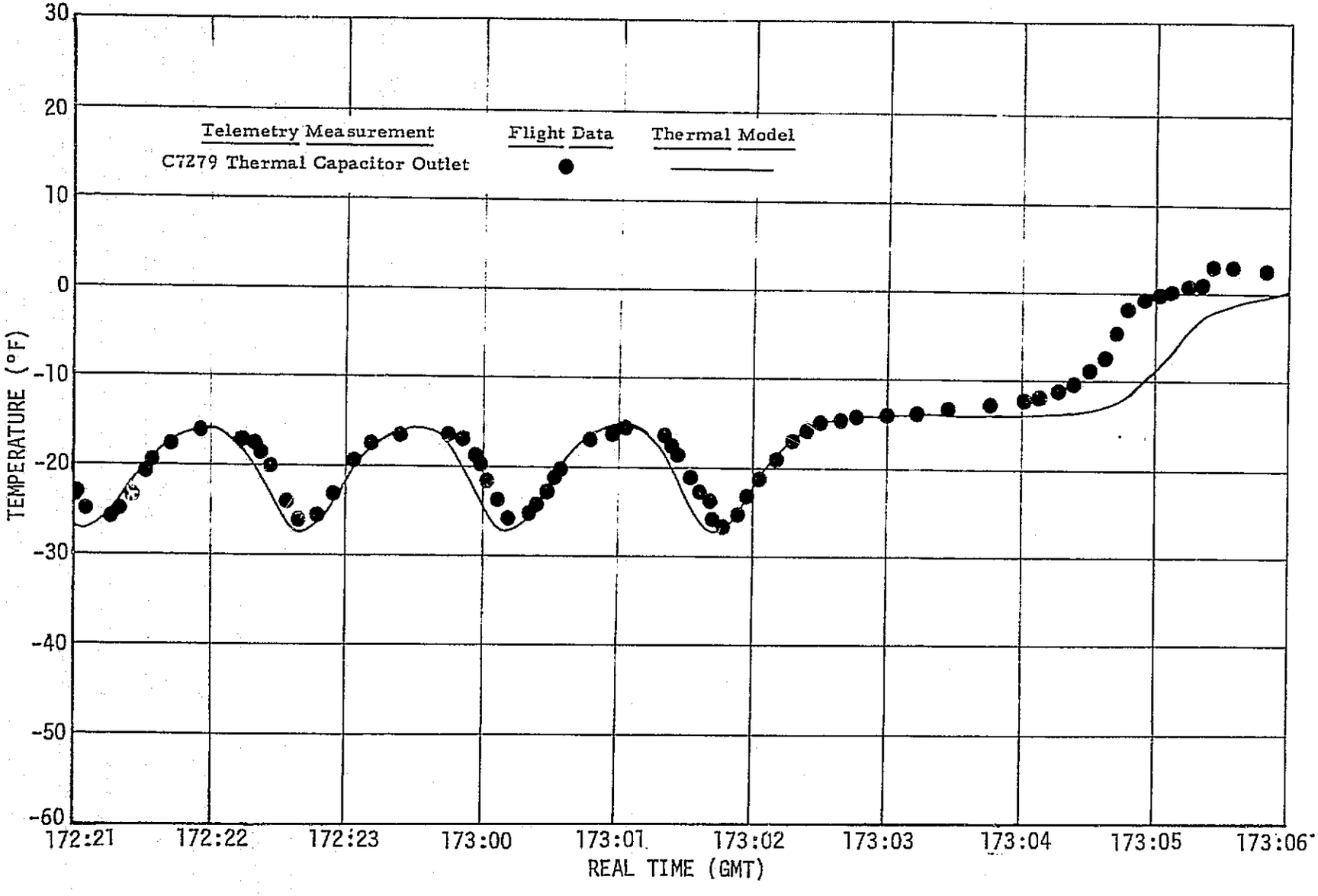

Figure 8-35. RS Anomaly Simulation Comparison with Flight Data, Thermal Capacitor Coolant Outlet Temperature

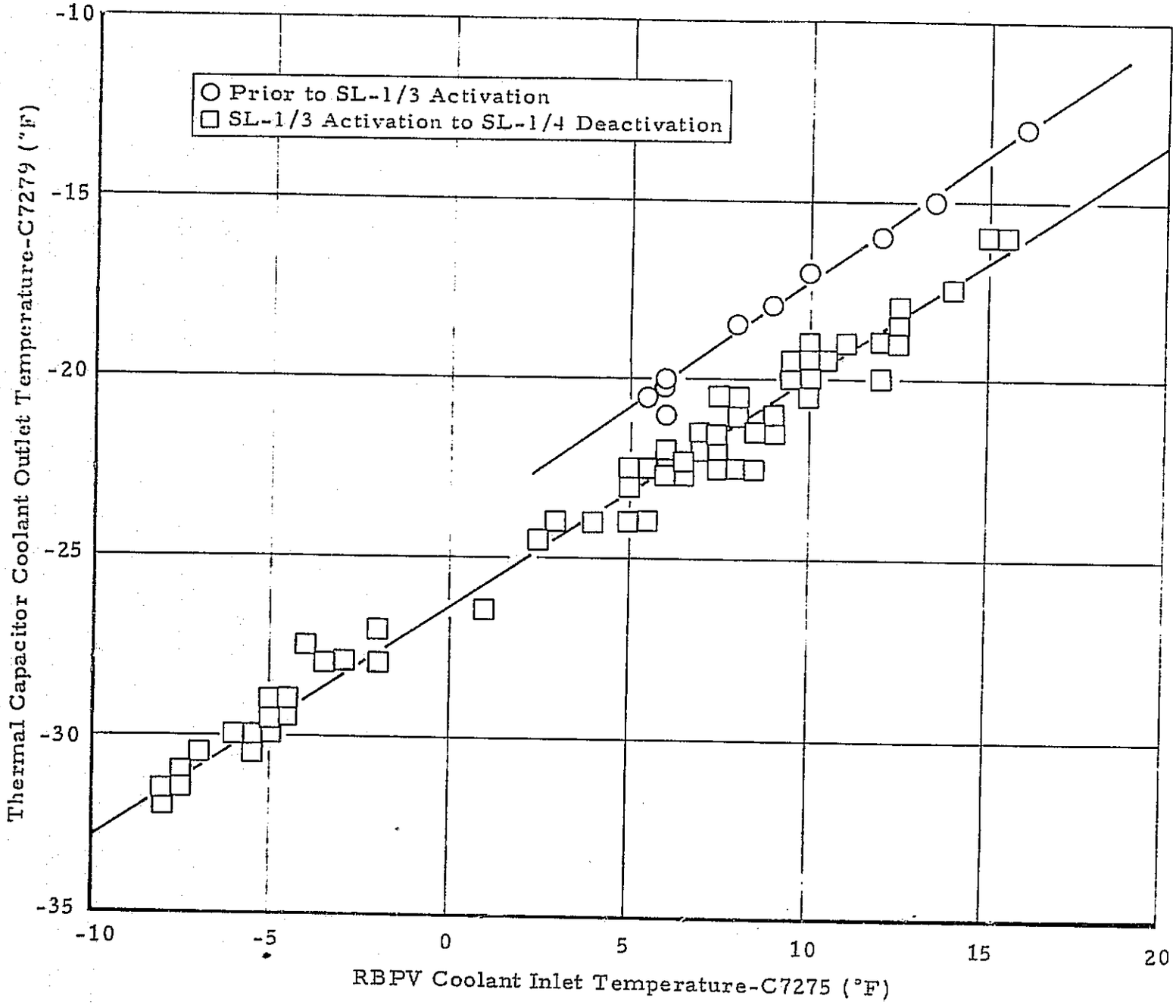

Figure 8-36. Flight Data Revealing Change in RS Primary Loop RBPV Bypass Poppet Position

The β angle effects on the absorbed radiator heat flux were ignored in plotting figure 8-36 since it had been determined that the RS radiator was relatively insensitive to a change in the β angle. Using the data plotted in figure 8-36, the heat rejection capability of the RS was plotted as a function of RBPV coolant inlet temperature (figure 8-37). Figure 8-37 clearly shows the improved heat rejection capability after SL-3 activation. It is not known what caused the improved RS performance after SL-3 activation. However, the SL-3 crew did open the primary loop RBPV control logic circuit breaker on panel 611 of the OWS C&D console during activation. It is interesting to note that after the closing of this breaker during SL-4 deactivation (before post-mission testing and verification), the performance of the RS did decrease slightly (radiator mode) but not to the level just prior to SL-3 activation (figure 8-37).

Following the RBPV anaomaly of DOY 173, the secondary coolant loop was activated for the first time. The secondary loop pump differential pressure (figure 8-38) and radiator surface temperature (figure 8-39) show the secondary loop to be operating essentially identical to the failed primary loop. Re-evaluation of the preflight tests performed on the RS at KSC revealed that those tests performed would not have detected a malfunctioning RBPV. Therefore, launch with a failed secondary loop RBPV was a possiblity.

Following the improvements in the primary loop, it was assumed that the secondary loop had remained in its original failed operation. This assumption was verified from the flight data on DOY 222. On this day at 14:31 GMT, the primary loop was deactivated and the secondary loop was activated with the intention of cycling the bypass poppet of the RBPV in an attempt to improve the secondary loop's performance, as had been done with the primary loop. However, in this instance a method of operating the bypass poppet of the RBPV in both positions with coolant flow had been devised (when the bypass poppet of the primary loop RBPV was cycled by pump deactivation/activation, there was no coolant flow when the bypass poppet was in the bypass position). This method involved enabling and disabling the loop with time as a critical factor in a manner so as to preclude the normal operation of the RBPV control logic. (when a loop is disabled, the control logic activates the loop's RBPV to the bypass position). Only at the beginning of the proposed cycling period was there any indication of the RBPV being in the radiator flow mode. At the time, it was thought that the secondary loop RBPV "talkback" switch had malfunctioned. It was not until the post-mission testing and verification that it was realized that the data of the secondary loop operation on DOY 222 was valid for the "bypass" position of the RBPV (on DOY 222, it was not known that due to the anomaly a flow split would also exist with the RBPV configured to its bypass position). As it turned out, post-mission testing revealed that the system differential pressure was

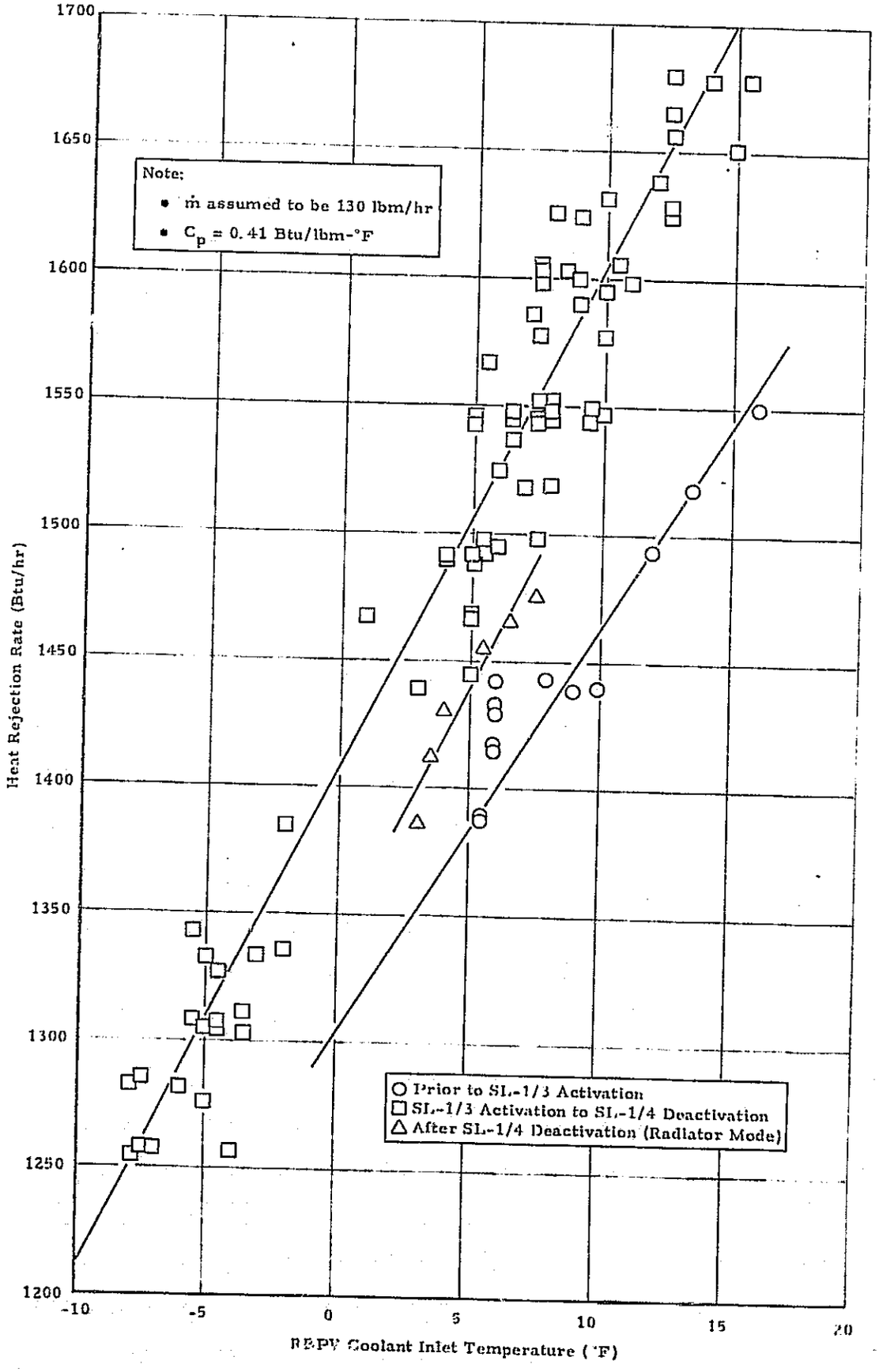

Figure 8-37. Changes in RS Primary Loop Heat Rejection Capability

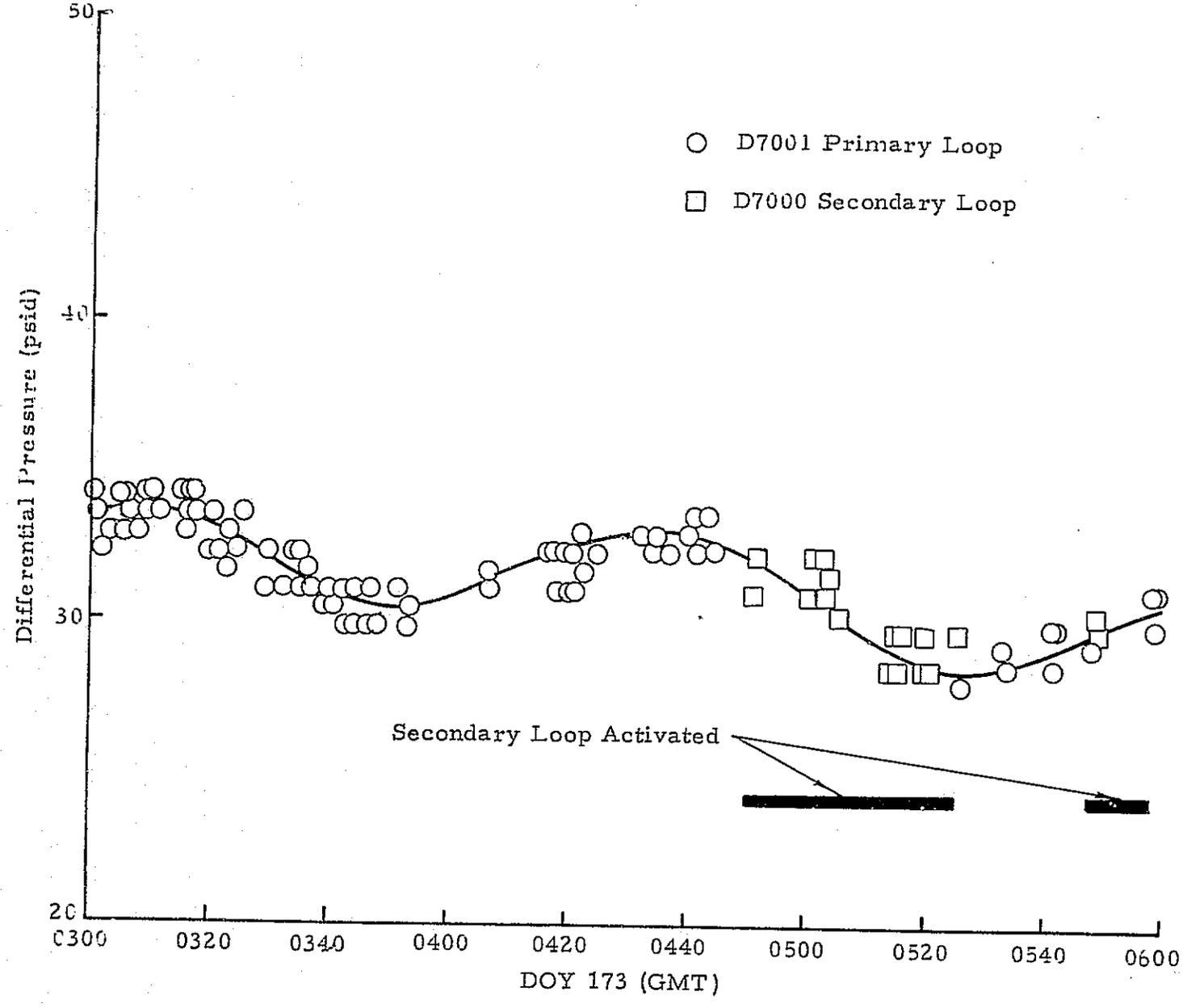

Figure 8-38. RS Pump Differential Pressure Following Valve Anomaly

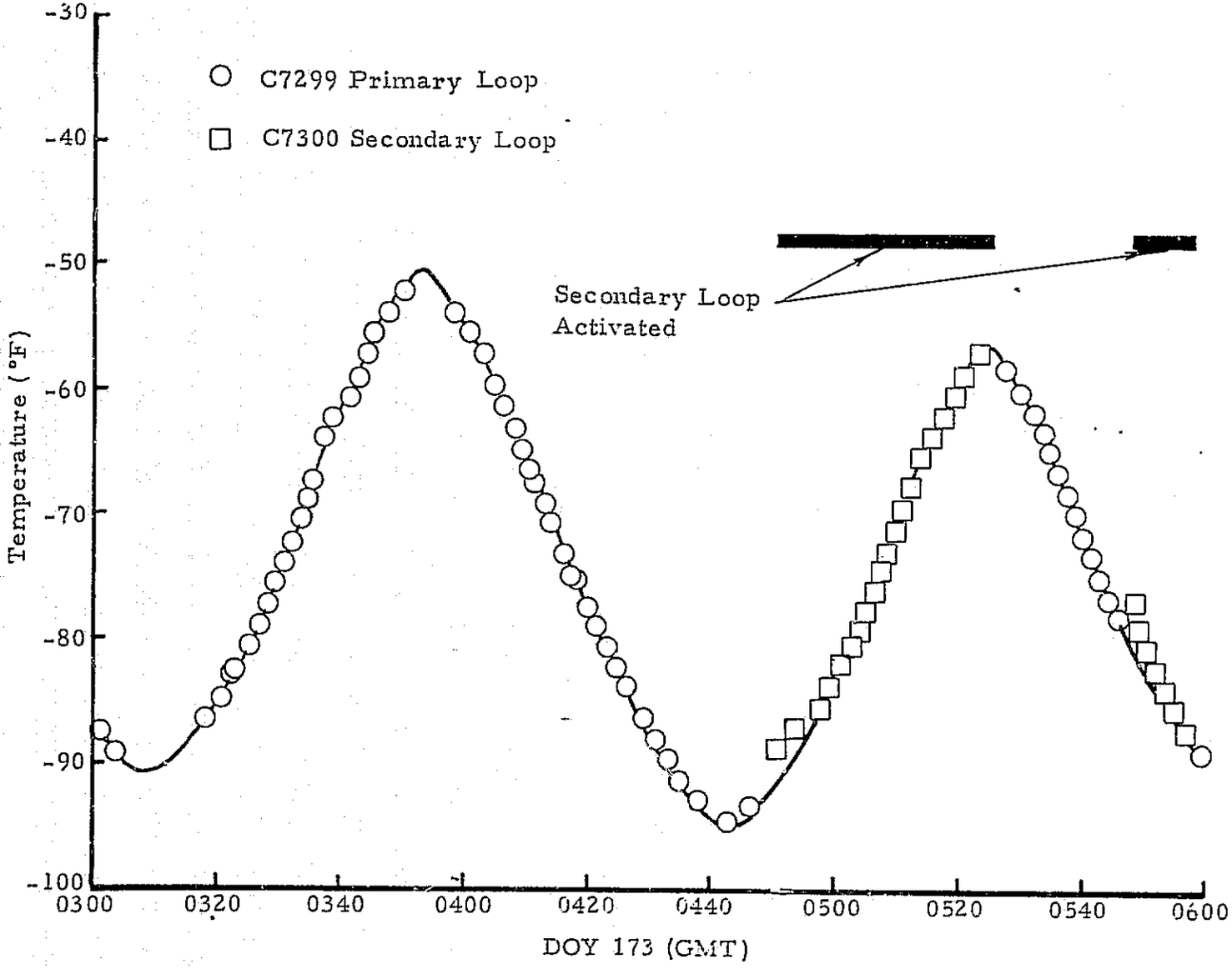

Figure 8-39. RS Radiator Surface Temperature Following Valve Anomaly

approximately equal for both flow configurations of the secondary loop RBPV (the bypass mode being only slightly higher). Thus, the conclusion (that the secondary loop was operating as the primary loop had immediately following the anomaly of DOY 173) was confirmed during the post-mission testing and verification session following SL-4 deactivation.

SECTION IX. GROUND THERMAL AND FLUID CONDITIONING SYSTEM

The Ground Thermal and Fluid Conditioning System consists of the purges and active coolant loops used to maintain required thermal conditions for equipment and vehicle compartments prior to launch.

Pre-launch purging was provided for the AM/MDA habitation area, Payload Shroud (PS), ATM Canister, MDA High Performance Insulation (HPI) blanket, OWS forward dome HPI, OWS Solar Array System, OWS forward skirt, and OWS aft skirt. The purges controlled the temperature, pressure, humidity, and composition of gases in the compartments that they serviced during launch preparation. The AM Active Coolant Loop interfaced with a ground cooling loop to provide heat removal from AM coldplated equipment during ground checkout. The OWS Ground Thermal Conditioning System (GTCS) utilized a combination of purging and active loop cooling to maintain desired thermal conditions in the OWS habitation area.

The habitation area and the waste tank of the OWS were pressurized during prelaunch by an external Ground Support Equipment (GSE) system to provide pressure integrity verification prior to launch and structural integrity during boost. The Refrigeration System (RS) required a ground thermal conditioning unit (TCU) to maintain frozen food thermal requirements from food loading in the Vertical Assembly Building (VAB) to liftoff.

A. Configuration

1. AM/MDA Habitation Area Purge and Prelaunch Pressurization. The AM/MDA pressurized compartments were purged with ambient air in the VAB to provide a habitable atmosphere for the ground crews. Prior to final leak check on the pad, the AM/MDA was purged with dry N_2 for a sufficient length of time to reduce the final O_2 concentration to an acceptable level. The compartment was then pressurized to 19.7 PSIA for final leak check at approximately 15.5 hours before liftoff. At five hours before liftoff, the MDA vent valves were commanded open and the compartment was allowed to equalize with the ambient pressure.

Purging gases were introduced at the aft compartment purge fitting (GSE 413) at a flow rate of 7.5 lb/min. The purge was flowed through the AM/MDA compartment and exhausted through the MDA vent valves. The OWS was pressurized with gaseous N_2 and maintained at a level equal to or greater than the AM/MDA pressure level during the purge operations.

2. MDA High Performance Insulation Purge. The MDA insulation purge system was used for purging the MDA insulation blankets and the

exterior surface of the S190 window with dry gaseous nitrogen prior to launch and at other times when the MDA was not in a conditioned environment. The purpose of the purge was to prevent moisture condensation on the insulation blanket and window and thermally condition the MDA film vaults. The times when the purge was specifically required to be operated at KSC were:

a. For the period of 30 minutes just before rollout from the Operations and Checkout (O&C) building. After purge, the payload shroud was sealed.

b. For a period of 30 minutes prior to cryogenic loading until launch.

c. Continuously on pad except for brief periods when a personnel breathing hazard existed.

The purge was conducted with dry GN_2 at a total flow rate of 5 ± 2 lb/min. The purge was supplied via a GSE purge console. Gas temperature supplied by the console was regulated by the ATM canister purge temperature sensor. As a result the MDA insulation purge gas supply temperature closely followed the ATM purge temperature.

Purge gas was introduced from the ground facility through one inch diameter lines that were routed from the Fixed Airlock Shroud (FAS) umbilical disconnect plate around the FAS to the AM truss #4 at the -Z axis. The line was then routed up the truss fitting at Airlock Module Station (AMS) 285.58 where the interface connection was made with the MDA. Connections across the major structure interfaces (FAS to AM truss and AM truss to STS) were made with flexible metal hoses. The exterior of the MDA pressure shell was encircled with a network of 1/2 and 3/8 inch diameter perforated tubing to provide gas distribution to the insulation and the S190 window. Figure 9-1 depicts the purge system.

3. Payload Shroud (PS) Purge. The PS purge gas was introduced at the FAS umbilical disconnect plate and was routed up the PS to the nose cone diffuser plate as shown in figure 9-2. Purge flow rate was 40 lb/min. while in the VAB and 50 ± 5 lb/min. to 65 ± 5 lb/min. after the vehicle left the VAB. The PS was purged with air until 30 minutes prior to the propellant loading when the purge was switched to GN_2. Purging with air was necessary to simultaneously provide temperature and humidity control in the PS compartment and habitable atmosphere for ground crews working inside the PS.

The GSE supply temperature was capable of control between 40°F and 80°F in the VAB and in transit to the pad and between 50°F and 135°F while on the pad. The inlet temperature controller was set at 63 ± 3°F to achieve an inlet gas temperature of 63 ± 5°F. The temperature of the purge gas supply depended on whether heating or cooling was required.

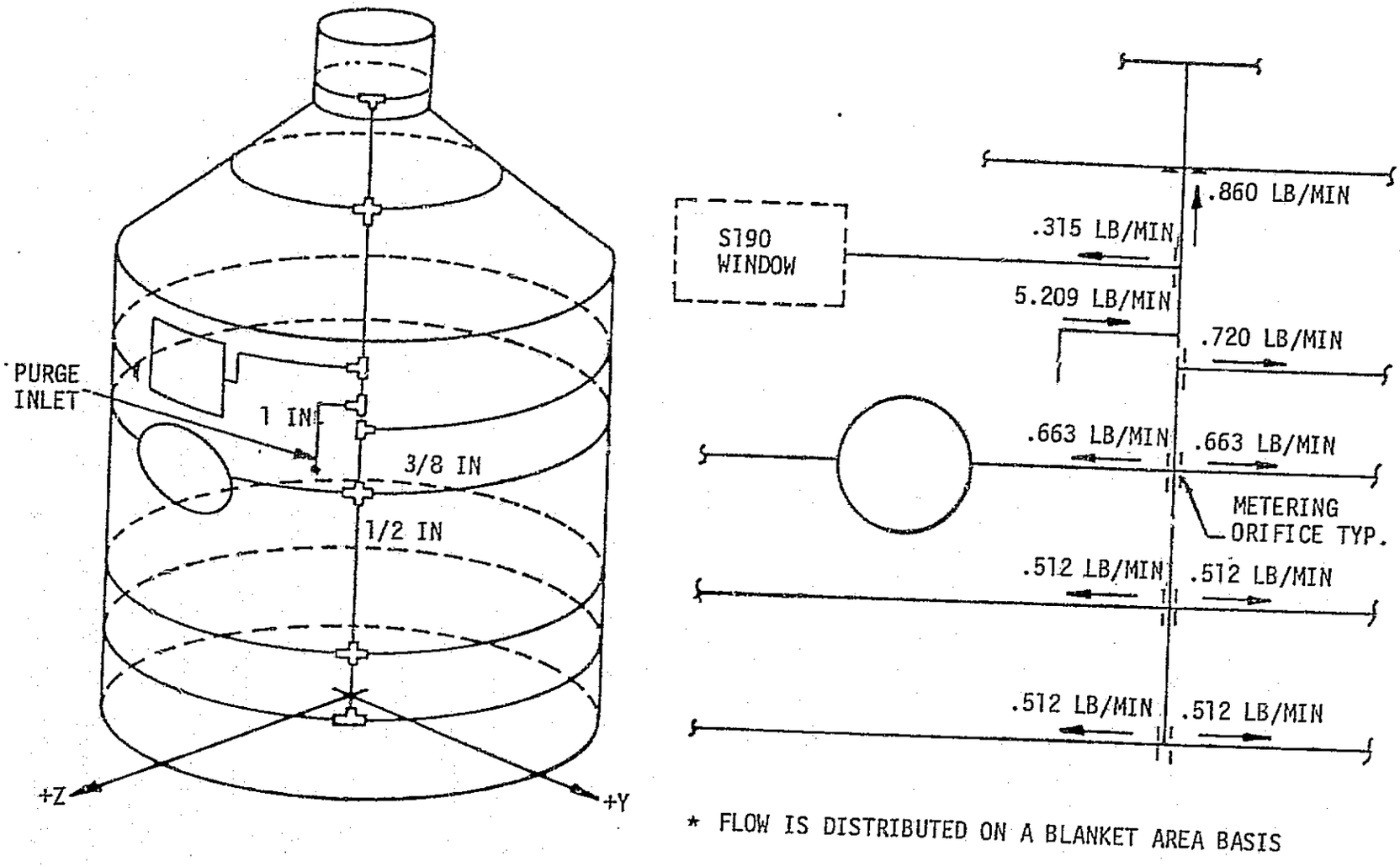

Figure 9-1. MDA High Performance Insulation and S190 Window Purge

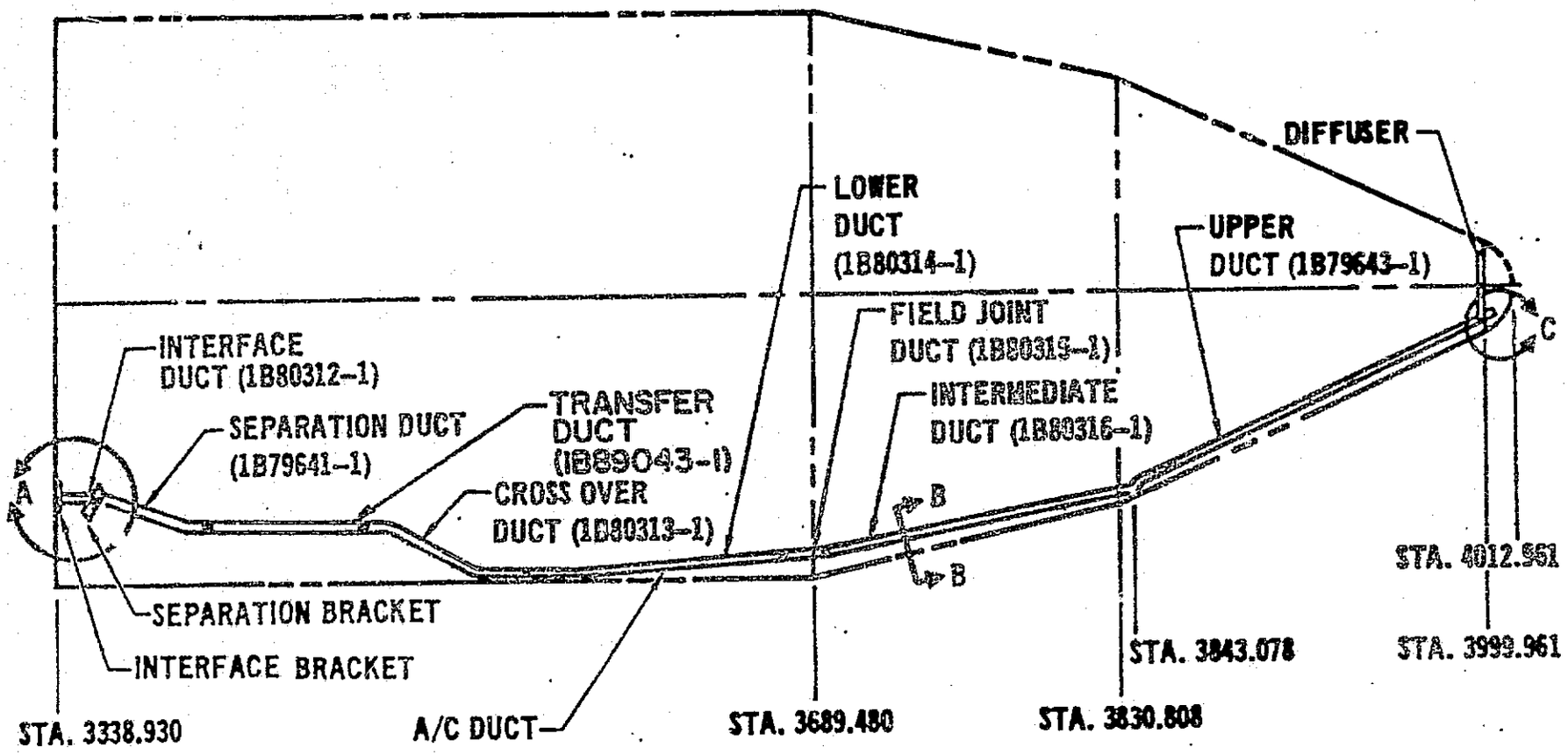

Figure 9-2. Payload Shroud Air Conditioning Duct Routing

4. AM Coolant Loop Operations. Prior to launch, heat was removed from the AM Coolant Loop (described in detail in Section VIII) by the ground cooling heat exchanger which interfaced with the Ground Cooling System. The ground cooling loop consisted of the interface heat exchanger, redundant accumulators to prevent pressure buildup from thermal expansion of trapped MMS-602 fluid, a ground cooling cart, and associated lines and fittings from the FAS umbilical disconnect plate to the coolant pump module on the STS aft bulkhead.

The Ground Cooling System was required to provide an MMS-602 flow rate of 900 lb/hour with a heat removal capacity of 16,000 Btu/Hour at a -15°F coolant inlet temperature to the GSE/Airlock interface.

The selector valve used to change from ground heat exchanger to radiator cooling was activated by DCS command from the ground. Transient heat rejection was supplemented by two thermal capacitors (charged with Tridecane wax) located downstream of the ground cooling heat exchanger and radiator. The capacitors were charged during pre-launch for accepting launch ascent heat loads prior to switching to the radiator for cooling. The maximum capacitor temperature at launch was specified at 18°F.

5. ATM Canister Purge. The ATM canister was purged for temperature, humidity, and cleanliness control. The purge was introduced through one inch diameter lines which entered the vehicle at the FAS umbilical disconnect plate and were routed around the FAS to the deployment assembly vertical tubular structural member at the +Y axis. From this point the lines followed the deployment assembly (DA) tubular structural members up to the ATM. The connections across the DA rotating joints, between the FAS and the DA and between the DA and the ATM were made with flexible metal hoses. The purge was conducted with gaseous nitrogen at a nominal flow rate of 5 $\pm$ 1 lb/min. The purge gas temperature controller was set at 53 $\pm$ 3°F to assure an inlet temperature control of 53 $\pm$ 5°F. During the 24 hours before liftoff, the temperature was increased to 70 $\pm$ 5°F to thermally condition the ATM for initial orbits without internal power.

6. OWS High Performance Insulation Purge. A dry nitrogen gas purge was provided to prevent moist air from entering the layers of HPI and subsequently degrading the insulating properties of the HPI during prelaunch operations. The normal flow rate of 5 lb/min. was reduced to 1 lb/min. by installing a smaller orifice on the ground side of the disconnect when personnel were required to work in the forward dome area. The purge inlet was located on the forward umbilical plate and was plumbed down to the forward skirt hat frame as shown in figure 9-3. The purge gas exited from holes at the bottom of the frame, filtered up through the HPI panels, and vented through the Airlock Module curtain.

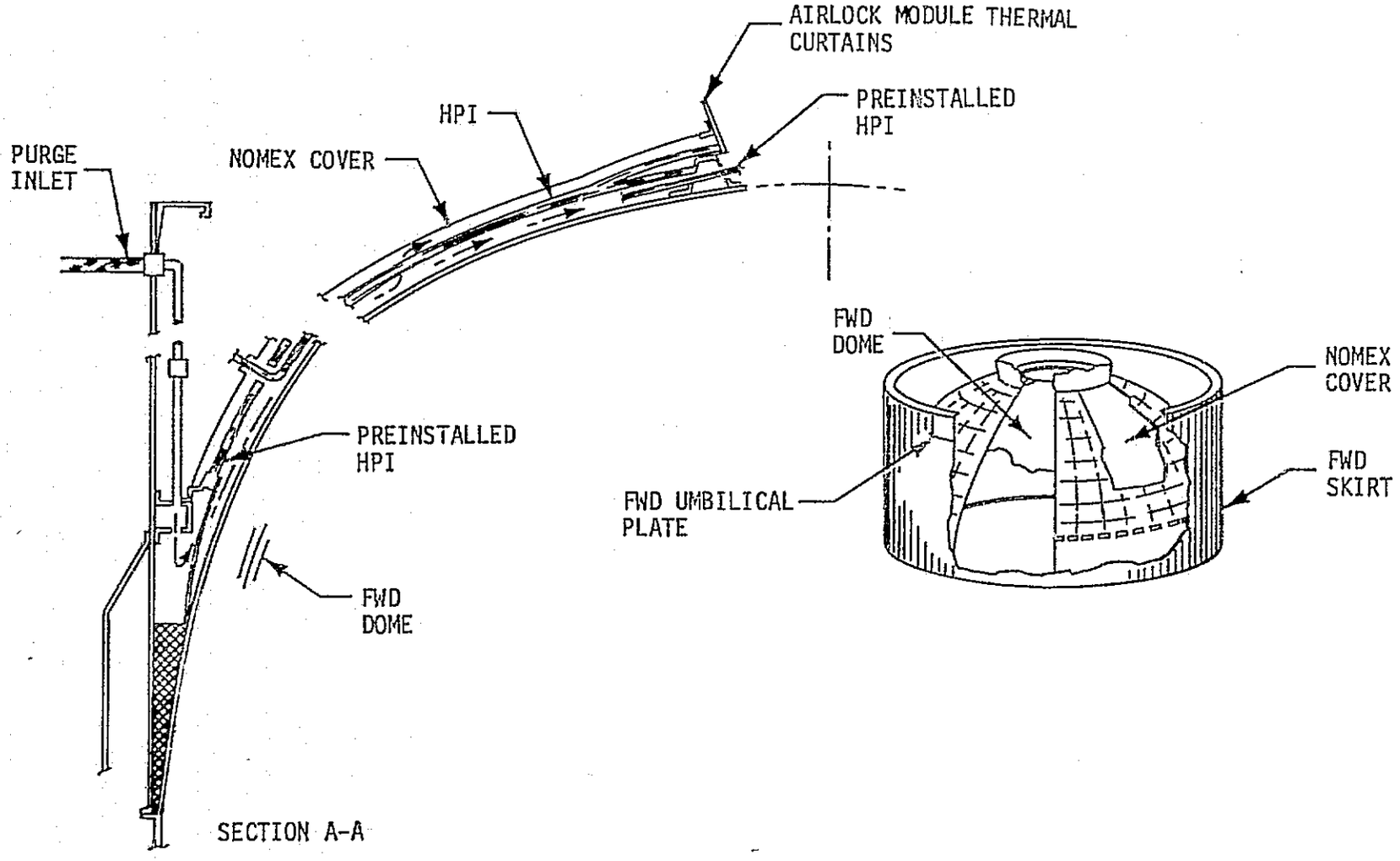

Figure 9-3. Orbital Workshop High Performance Insulation Purge System

7. OWS Solar Array System (SAS) Purge. The SAS N_2 purge was to provide a positive pressure in the SAS beam fairings to prevent moist salt air from entering the fairings and condensing on the solar cells. As an additional benefit, it maintained the fairing at moderate temperature and humidity.

The SAS Purge System consisted of a GSE/vehicle quick disconnect, four metering orifices in parallel, a purge distribution manifold in each SAS beam fairing, a Government Furnished Equipment (GFE) purge console, and associated plumbing (figure 9-4). An auxiliary purge inlet fitting was provided for use at times when the Quick Disconnect (QD) could not be used.

Leakage from the purged cavity of each beam/fairing was not to exceed 0.5 lb/min. (i.e., 2 lb/min. total to the SAS) when pressurized to 0.09 PSIG (2.5 in. H_2O). Redundant pressure relief valves were provided for each compartment of the beam/fairing. Each of these valves was capable of flowing 1.0 lb/min. of GN_2 at a pressure of 0.4 PSIG. Minimum reset pressure of the relief valves was 0.09 PSIG.

8. OWS Aft Skirt Purge. The aft skirt area was purged by the same system used for the Saturn Program aft skirt purge. Conditioned air having a moisture content of 0 to 43 grains/lb was used for purging up to 20 minutes prior to propellant loading. The air was supplied at a flow rate of 267 to 300 lb/min. at an allowable temperature range of 65°F to 140°F. Beginning 20 minutes prior to propellant loading and continuing until liftoff, the interstage compartment was purged with dry nitrogen having a moisture content of 0 to 1 grain/lb. Nitrogen was supplied at the same flow rate as air, but the temperature range was limited between 55°F and 75°F.

9. OWS Forward Skirt Purge. The forward skirt area purge (supplied from the Instrument Unit [IU]) also utilized the same system that was used on the Saturn program. Purging was accomplished using conditioned air at a flow rate of 150 $\pm$ 15 lb/min. up to 20 minutes prior to propellant loading. Temperature of the air purge was 45°F to 130°F. Beginning at 20 minutes before propellant loading, the purge media was switched to dry GN_2 supplied at a flow rate of 200 $\pm$ 20 lb/min. and a temperature of 55°F to 130°F.

10. OWS Internal Purge and Pressurization. A nitrogen purge utilizing the existing GSE GN_2 source of the Launch Umbilical Tower (LUT) and existing OWS pressurization system plumbing was used to preclude condensation of atmospheric moisture on the heat exchanger coils. The purge system was required to establish and maintain a dew point below 30°F. Purge gas entered through the habitation area ground pressurization line at a rate of 8.7 lb/min. and exited through the purge gas

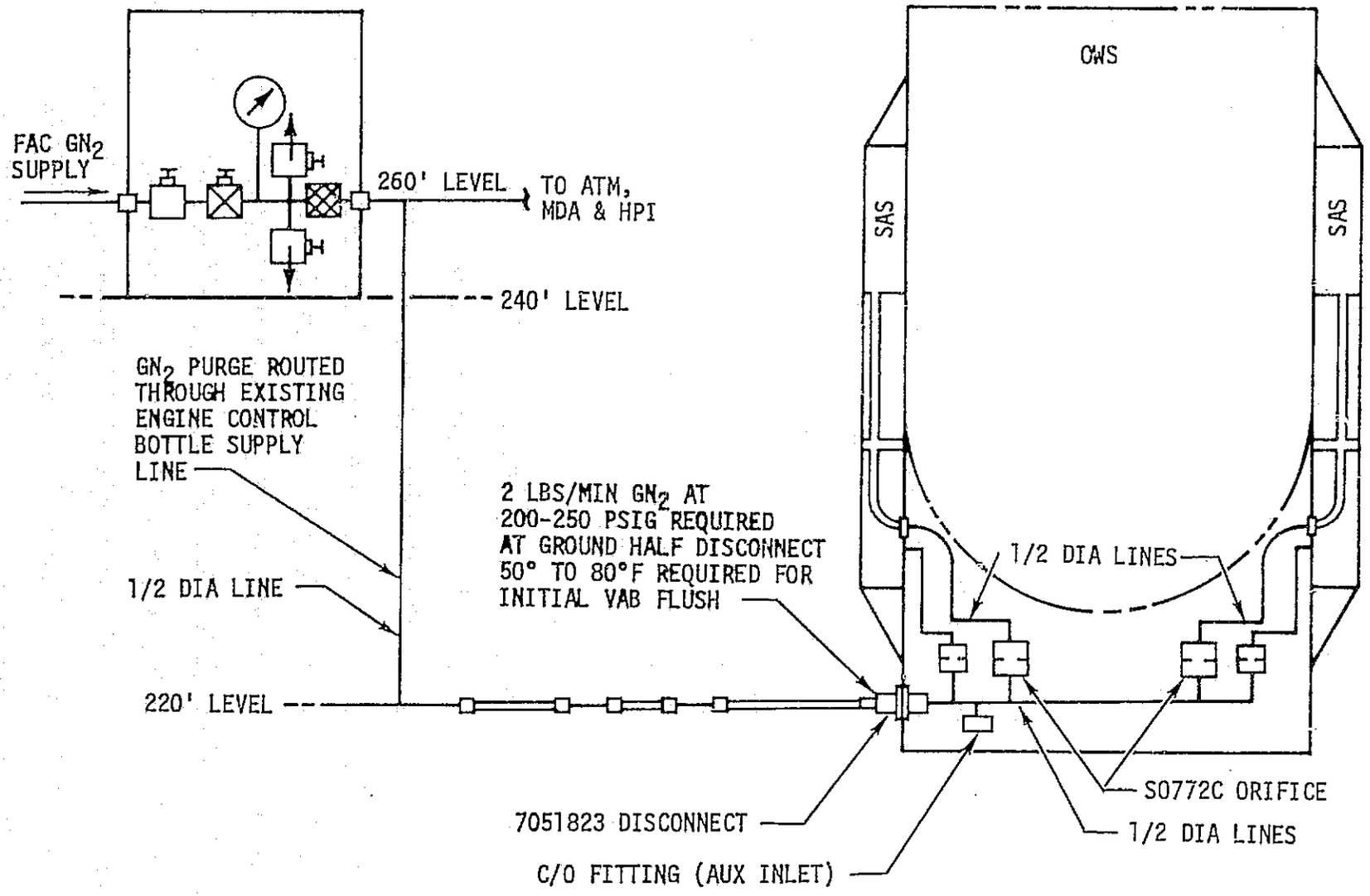

Figure 9-4. Orbital Workshop GN_2 Purge Schematic

outlet port. After the purge gas outlet port was sealed, this system was also used for pre-liftoff pressurization. Figure 9-5 illustrates the resultant atmosphere circulation pattern inside the OWS habitation area.

11. OWS Habitation Area Ground Thermal Conditioning System. The Ground Thermal Conditioning System was a closed-loop system consisting of GSE, located on the Launch Umbilical Tower, and heat exchanger equipment installed onboard the vehicle in the OWS. The GSE was joined to the SL-1 vehicle plumbing by QD couplings. The GTCS equipment installed in the OWS consisted of two heat exchangers in series and two fans in parallel. One fan heat exchanger assembly was used at the primary system with the other unit as backup. The fans induced Habitation Area atmosphere flow across the heat exchangers and then directed it across temperature sensitive equipment (film vault and food lockers) to maintain their temperature in the required range. The required temperature range for the film vault was 40°F to 50°F, with allowable excursions to 65°F. The ambient food locker temperature requirement was 40°F to 85°F. Figure 9-6 illustrates the GTCS.

The GSE on the LUT controlled the temperature and flow rate of the thermal conditioning fluid (water/glycol) that circulated through the heat exchangers in the OWS. These heat exchangers maintained the habitation area atmosphere in the required temperature range from button-up until approximately 11 minutes before launch.

In order to support Kennedy Spacecraft Center (KSC) contingency planning, analyses were performed to determine how long the GTCS could be failed without impacting the SL-1 launch. Due to the daily variation in the solar heat load and the ambient air temperature, the time of day of the failure and the time of day of the launch were the significant parameters. The results of the analysis, shown in figure 9-7, indicated that the GTCS could fail 20 minutes prior to launch without exceeding the food and film temperature limits. The results of further analyses shown in figure 9-8, provided the time it took for the GTCS to recover assuming various failure times. For future ground thermal conditioning system design, it is recommended that consideration be given to allow for loss of conditioning caused by GSE malfunctions.

12. Refrigeration System Prelaunch Conditioning. The RS thermal conditioning system is shown in figure 9-9. The ground support for refrigeration system consisted of one operating thermal conditioning unit, one redundant TCU, a valve panel and a coolant control unit (CCU), all located on the LUT. This GSE system supplied water/glycol coolant at controlled temperature and flow rate to a ground cooling heat exchanger which was an integral part of the flight RS. The ground conditioning loop was disconnected by quick disconnect couplings on the aft skirt

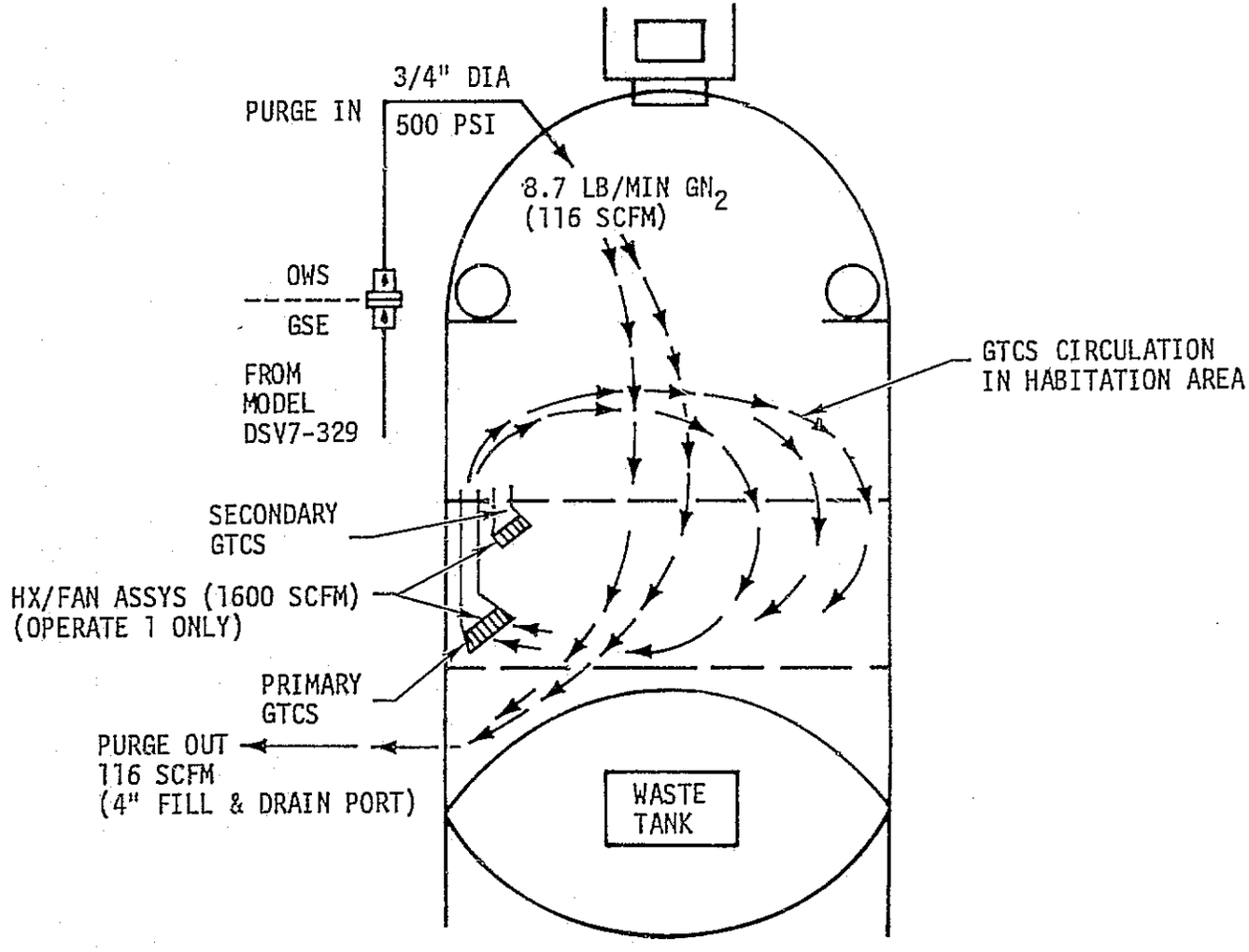

Figure 9-5. Orbital Workshop Purge Flow Schematic with GTCS Fan Operating

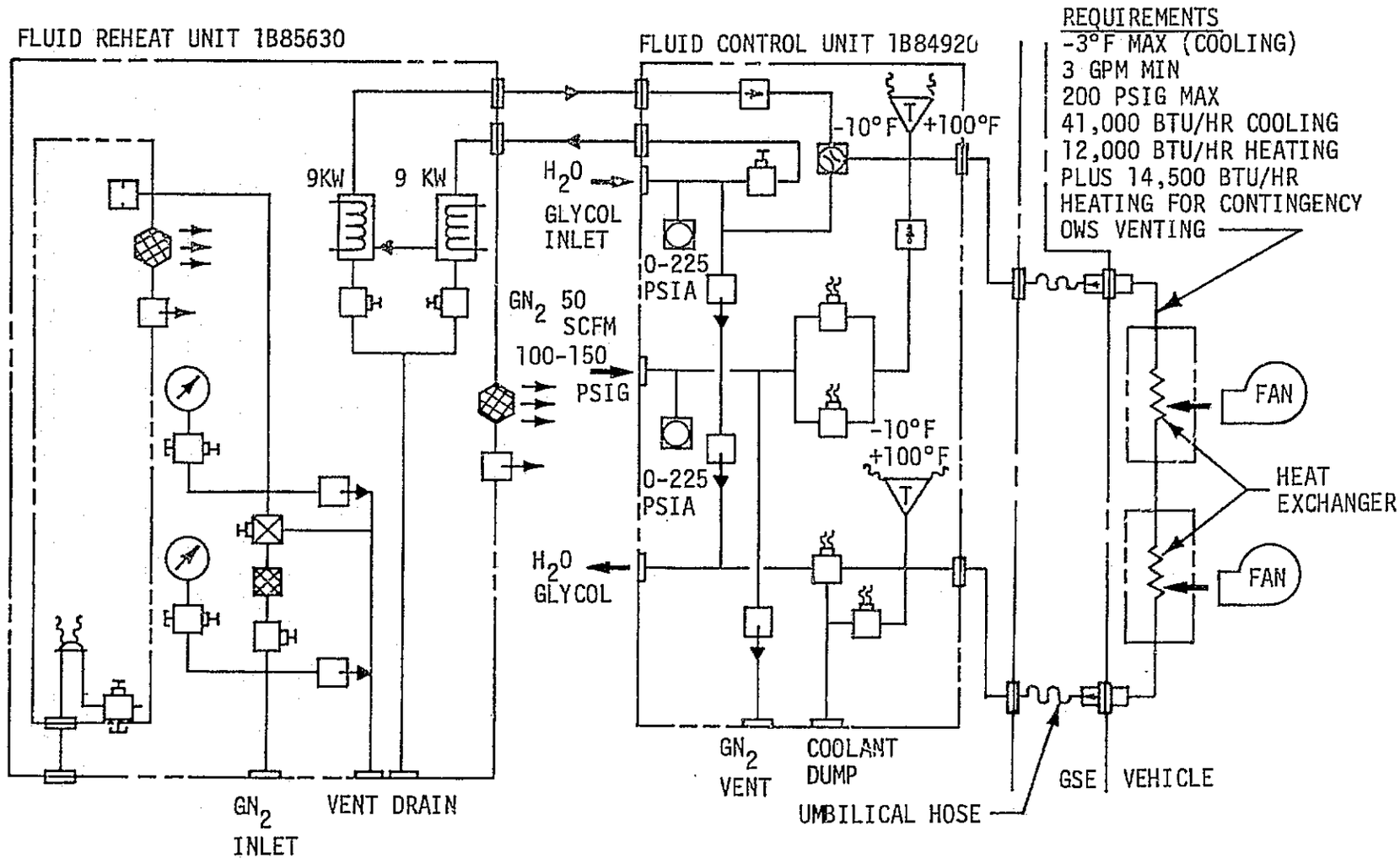

Figure 9-6. Orbital Workshop Ground Thermal Conditioning System

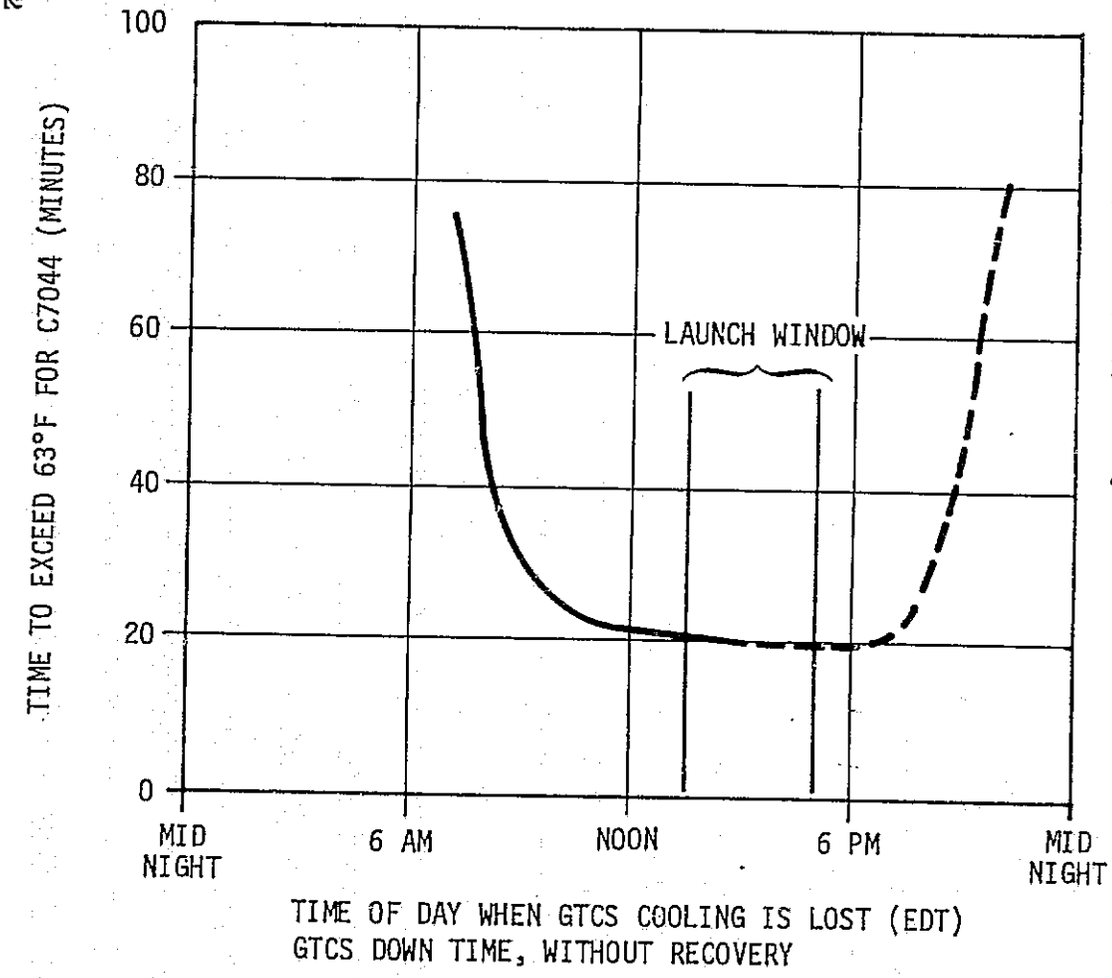

NOTES

1. ASSUMES C7044 AT 58°F WHEN COOLANT LOSS OCCURRED
2. APPLICABLE FOR HOT MAY DAY
3. ASSUMES GTCS FAN IS TURNED OFF WHEN COOLANT LOSS OCCURRED
4. 15°F HEAT EXCHANGER FLUID SUPPLY TEMPERATURE

Figure 9-7. GTCS Down Time, Without Recovery

NOTES

1. ASSUMES C7044 AT 58°F WHEN COOLANT LOSS OCCURRED
2. APPLICABLE FOR HOT MAY DAY
3. ASSUMES GTCS FAN IS TURNED OFF WHEN COOLANT LOSS OCCURRED
4. 15°F HEAT EXCHANGER FLUID SUPPLY TEMPERATURE

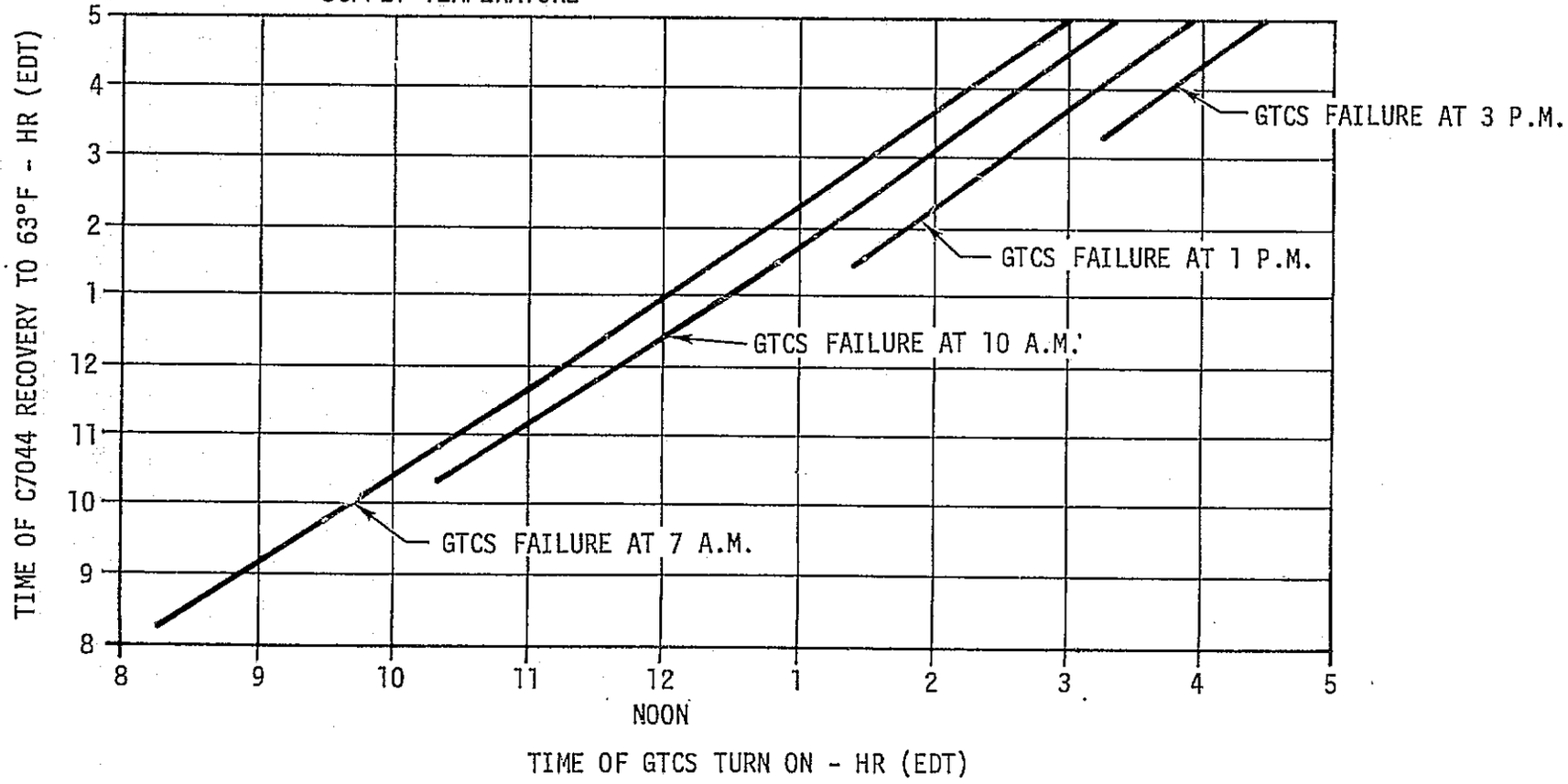

Figure 9-8. GTCS Recovery Time

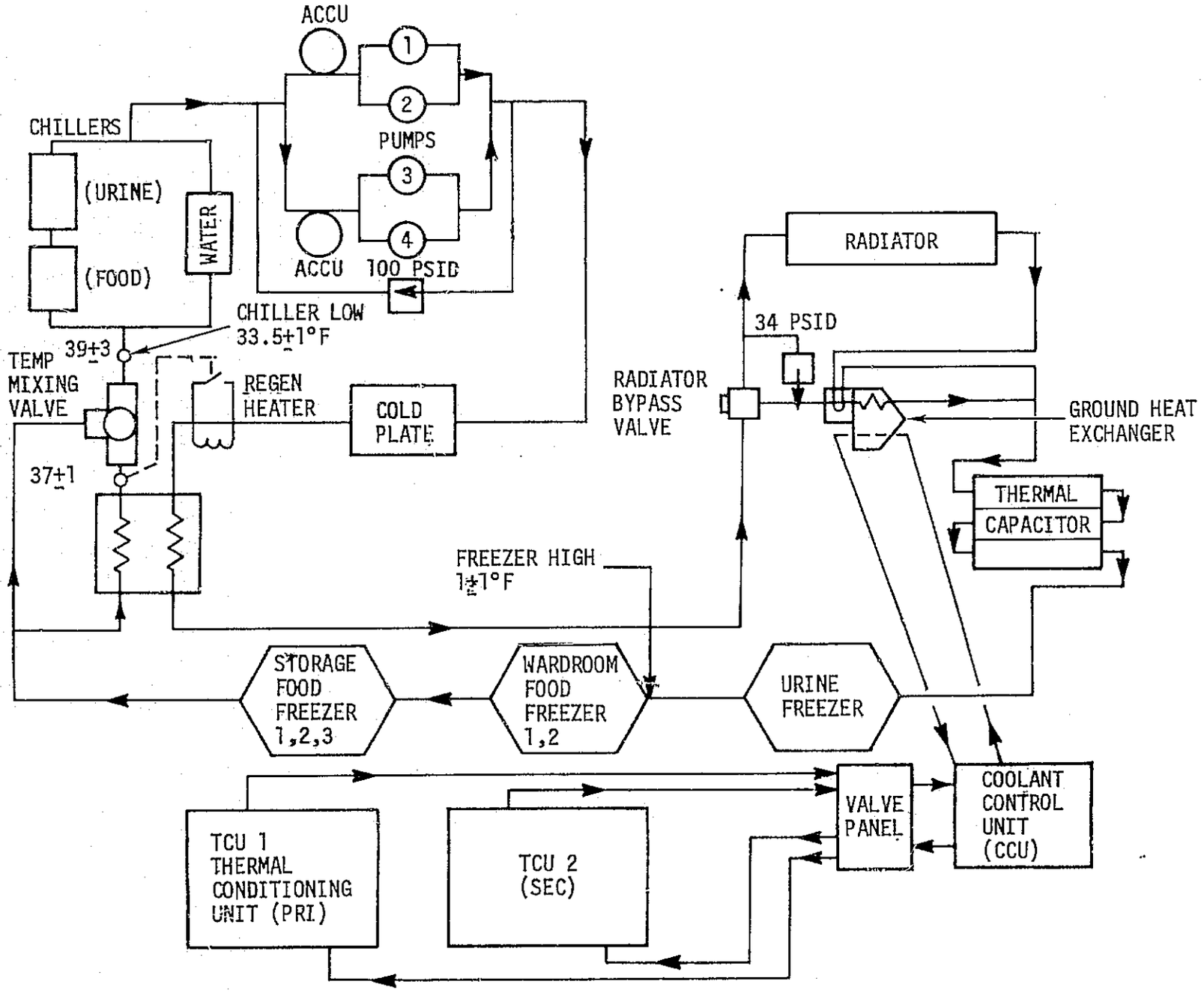

Figure 9-9. RS Ground Conditioning System

umbilical panel. At approximately T-3 minutes, the GSE coolant was stopped and the OWS water/glycol lines were purged with N_2 gas to minimize vehicle contamination during boost.

Although no significant problem was attributed to an RS GSE failure during SL-1 prelaunch, there was much concern about the capability of the GSE system to supply the temperature control required. The TCU's (DSV-7-301) had been modified for temperature capability lower than the original qualification value but this modification was not intended to provide performance in the range that was ultimately required. The specified redline values are shown in Table 9.1. The redline values were the result of much deliberation with GSE personnel and a re-examination of RS performance data to provide as much relief as possible to the TCU requirements.

The hold time information given in figures 9-10, 9-11, and 9-12, was provided in addition to the redlines to use as guidelines and planning in the event of a failure of both TCU's or an unexpected launch hold subsequent to activation of ground purge for the water/glycol lines.

The primary reason for delayed concern about the TCU low temperature capability was the late definition of RS requirements as a result of RS system thermal qualification testing (HS-19). The refrigeration system was behind schedule because of thermal capacitor and radiator control valve problems. As a result, no analysis or test for system thermal performance were available until late 1972. A secondary reason was the lack of data on the fluid temperature rise between the TCU outlet and the RS ground heat exchanger inlet.

13. Oxygen and Nitrogen Consumables. A description of the oxygen and nitrogen gas storage systems is given in Section V. Appropriate pressure and temperature prelaunch redlines for each gas bottle are given in Table 9.1. Figures 9-13 and 9-14 define the prelaunch loading requirements.

B. Performance

All thermal conditioning and pressurized systems performed satisfactorily during prelaunch and launch. The ECS/TCS mission support group provided realtime monitoring of all active systems from T-8.5 hours (corresponding to 10 hours before SL-1 launch because of a 1.5 hour built-in hold). The Launch Mission Rules Document details those parameters, along with their applicable limits, which were required to be monitored during the prelaunch phase of the mission. A list of these parameters, their limits and the actual values which occurred after T-8.5 hours is provided in Table 9.1.

TABLE 9.1 PRELAUNCH PARAMETERS MONITORED

MEASUREMENT NUMBER	MEASUREMENT DESCRIPTION	PRELAUNCH REDLINES	RANGE OF VALUES FROM T-8 1/2 HRS TO LAUNCH
C209	AM PRIMARY CHX INLET TEMP	43°F TO 51°F	LOOP INACTIVE TO T-5 1/2 HRS, 47.4°F AFTER T-5 1/2 HRS
C210	AM SEC CHX INLET 1 TEMP	43°F TO 51°F	49.0°F TO T-5 HRS, LOOP DE-ACTIVATED AT T-5 HRS
C244	AM PRIM THM CAPACITOR OUT TEMP	(TO T-30 MIN 40°F) (AFTER -30 MIN 48°F)	LOOP INACTIVE TO T-5 1/2 HRS, -40.7°F AFTER T-5 1/2 HRS
C262	AM THM CAPACITOR NO. 1, SKIN 1 TEMP	(TO T-30 MIN 40°F) (AFTER T-30 MIN 18°F)	BELOW SCALE AT -20°F
C263	AM THM CAPACITOR NO. 1, SKIN 2 TEMP	(TO T-30 MIN 40°F) (AFTER T-30 MIN 18°F)	BELOW SCALE AT -20°F
C264	AM THM CAPACITOR NO. 2, SKIN TEMP	(TO T-30 MIN 40°F) (AFTER T-30 MIN 18°F)	BELOW SCALE AT -20°F
C265	AM THM CAP 2 PRIM INLET TEMP	(TO T-30 MIN 40°F) (AFTER T-30 MIN 48°F)	LOOP INACTIVE TO T-5 1/2 HRS, -40.7°F AFTER T-5 1/2 HRS
C273	AM PRIMARY VLV C OUT 1 TEMP	34°F TO 70°F (AFTER T-30 MIN 34°F-44°F)	LOOP INACTIVE TO T-5 1/2 HRS, 38.6°F AFTER T-5 1/2 HRS

TABLE 9.1 PRELAUNCH PARAMETERS MONITORED (CONTINUED)

MEASUREMENT NUMBER	MEASUREMENT DESCRIPTION	PRELAUNCH REDLINES	RANGE OF VALUES FROM T-8 1/2 HRS TO LAUNCH
C274	AM SEC VLV C OUT 1 TEMP	34°F TO 70°F (AFTER T-30 MIN 34°F-44°F)	40.5°F TO T-5 HRS, NOT FLOWING AFTER T-5 HRS SEC LOOP DEACTIVATION
C283	AM PRIMARY VLV A OUT 1 TEMP	43°F TO 51°F AFTER T-30 MIN	LOOP INACTIVE TO T-5 1/2 HRS, 48.6°F AFTER T-5 1/2 HRS
C284	AM SEC VLV A OUT 1 TEMP	43°F TO 51°F AFTER T-30 MIN	48.1°F TO T-5 HRS, LOOP DEACTIVATED AT T-5 HRS
C247	ALT O_2 SUPPLY BOTTLE 1 TEMP	SEE FIGURE 9-13	69.3 - 70.1°F
C248	ALT O_2 SUPPLY BOTTLE 2 TEMP	SEE FIGURE 9-13	69.5 - 67.8°F
C249	ALT O_2 SUPPLY BOTTLE 3 TEMP	SEE FIGURE 9-13	71.2 - 72.0°F
C250	ALT O_2 SUPPLY BOTTLE 4 TEMP	SEE FIGURE 9-13	67.7 - 69.4°F
C251	ALT O_2 SUPPLY BOTTLE 5 TEMP	SEE FIGURE 9-13	68.9 - 69.7°F
C252	ALT O_2 SUPPLY BOTTLE 6 TEMP	SEE FIGURE 9-13	71.6 - 72.4°F
C253	ALT N_2 SUPPLY BOTTLE 1 TEMP	SEE FIGURE 9-14	66.9°F
C254	ALT N_2 SUPPLY BOTTLE 2 TEMP	SEE FIGURE 9-14	70.1°F
C255	ALT N_2 SUPPLY BOTTLE 3 TEMP	SEE FIGURE 9-14	64.0 - 64.7°F
C256	ALT N_2 SUPPLY BOTTLE 4 TEMP	SEE FIGURE 9-14	63.9 - 65.3°F

TABLE 9.1 PRELAUNCH PARAMETERS MONITORED (CONTINUED)

MEASUREMENT NUMBER	MEASUREMENT DESCRIPTION	PRELAUNCH REDLINES	RANGE OF VALUES FROM T-8 1/2 HRS TO LAUNCH
C257	ALT N_2 SUPPLY BOTTLE 5 TEMP	SEE FIGURE 9-14	66.8°F
C272	ALT N_2 SUPPLY BOTTLE 6 TEMP	SEE FIGURE 9-14	67.0 - 67.7°F
D222	AM PRIMARY CLNT PUMP INLET PRESS	25 PSIA	29.4 PSIA TO T-5 1/2 HRS, 28.2 AFTER T-5 1/2 HRS
D223	AM SEC LOOP PUMP INL. PR	25 PSIA	28.9 PSIA TO T-5 HRS, 31.6 AFTER T-5 HRS TO SEC LOOP ACTIVATION
D224	AM PRIMARY CLNT PUMP ΔP	20 PSID TO 70 PSID	0 TO T-5 1/2 HRS, 49.1 PSID AFTER T-5 1/2 HRS
D225	AM SEC LOOP PUMP ΔP	20 PSID TO 70 PSID	39.3 PSID TO T-5 HRS - 0 AFTER T-5 HRS TO SEC LOOP ACTIVATION
D226	AM O_2 SUPPLY BOTTLE 1 PRESS	SEE FIGURE 9-13	2980 TO 2995 PSIA
D227	AM O_2 SUPPLY BOTTLE 2 PRESS	SEE FIGURE 9-13	3000 PSIA
D228	AM O_2 SUPPLY BOTTLE 3 PRESS	SEE FIGURE 9-13	3013 - 3029 PSIA
D229	AM O_2 SUPPLY BOTTLE 4 PRESS	SEE FIGURE 9-13	2996 - 3012 PSIA
D230	AM O_2 SUPPLY BOTTLE 5 PRESS	SEE FIGURE 9-13	3011 PSIA
D231	AM O_2 SUPPLY BOTTLE 6 PRESS	SEE FIGURE 9-13	3013 - 3046 PSIA

TABLE 9.1 PRELAUNCH PARAMETERS MONITORED

MEASUREMENT NUMBER	MEASUREMENT DESCRIPTION	PRELAUNCH REDLINES	RANGE OF VALUES FROM T-8 1/2 HRS TO LAUNCH
D241	ALT O_2 SUPPLY BOTTLE 1 PRESS	SEE FIGURE 9-12	2974 - 2990 PSIA
D242	ALT O_2 SUPPLY BOTTLE 2 PRESS	SEE FIGURE 9-13	3005 - 3021 PSIA
D243	ALT O_2 SUPPLY BOTTLE 3 PRESS	SEE FIGURE 9-13	3017 - 3030 PSIA
D244	ALT O_2 SUPPLY BOTTLE 4 PRESS	SEE FIGURE 9-13	2986 - 3002 PSIA
D245	ALT O_2 SUPPLY BOTTLE 5 PRESS	SEE FIGURE 9-13	3006 - 3026 PSIA
D246	ALT O_2 SUPPLY BOTTLE 6 PRESS	SEE FIGURE 9-13	3025 - 3040 PSIA
D232	ALT N_2 SUPPLY BOTTLE 1 PRESS	SEE FIGURE 9-14	2965 - 2982 PSIA
D233	ALT N2 SUPPLY BOTTLE 2 PRESS	SEE FIGURE 9-14	2990 - 3007 PSIA
D234	ALT N_2 SUPPLY BOTTLE 3 PRESS	SEE FIGURE 9-14	2904 PSIA
D235	ALT N_2 SUPPLY BOTTLE 4 PRESS	SEE FIGURE 9-14	2949 - 2965 PSIA
D236	ALT N_2 SUPPLY BOTTLE 5 PRESS	SEE FIGURE 9-14	2953 - 2969 PSIA
D257	ALT N_2 SUPPLY BOTTLE 6 PPESS	SEE FIGURE 9-14	2925 PSIA
D247	ALT N_2 SUPPLY BOTTLE 1 PRESS	SEE FIGURE 9-14	2998 PSIA
D248	ALT N_2 SUPPLY BOTTLE 2 PRESS	SEE FIGURE 9-14	2982 PSIA
D249	ALT N_2 SUPPLY BOTTLE 3 PRESS	SEE FIGURE 9-14	2936 - 2952 PSIA

TABLE 9.1 PRELAUNCH PARAMETERS MONITORED (CONTINUED)

MEASUREMENT NUMBER	MEASUREMENT DESCRIPTION	PRELAUNCH REDLINES	RANGE OF VALUES FROM T-8 1/2 HRS TO LAUNCH
D250	ALT N_2 SUPPLY BOTTLE 4 PRESS	SEE FIGURE 9-14	2953 PSIA
D251	ALT N_2 SUPPLY BOTTLE 5 PRESS	SEE FIGURE 9-14	2980 - 2981 PSIA
D258	ALT N_2 SUPPLY BOTTLE 6 PRESS	SEE FIGURE 9-14	2961 - 2978 PSIA
F214	AM PRI VLV B OUT FLOW RATE	238 LB/MIN	0 TO T-5 1/2 HRS 276 TO 278 LB/HR AFTER T-5 1/2 HRS
F215	AM SEC VLV B OUT FLOW RATE	238 LB/MIN	276 TO 278 LB/HR TO T-5 HRS, 0 TO SEC LOOP ACTIVATION
K209	AM PRI RAD BYPASS MONITOR	BYPASS (UNTIL T-10 MIN) NORM AT T-10 MIN	NORM TO T-5 1/2 HRS - BYPASS TO T-10 MIN - RAD AFTER
K210	AM SEC RAD BYPASS MONITOR	(BYPASS TO T-5 HRS) (NORM T-5 HRS ON)	BYPASS TO T-5 HRS, NORM AT T-5 HRS
C0002	MDA INT FWD DOME 1 TEMP	60°F TO 80°F	71.0°F TO 68.4°F
C0004	MDA INT FWD CYL 1 TEMP	60°F TO 80°F	70.0°F TO 67.5°F
C0031	MDA INT AFT CYL 5 TEMP	60°F TO 80°F	70.0°F TO 67.8°F
C0032	MDA INT AFT CYL 6 TEMP	60°F TO 80°F	70°F
C0039	MDA INT FWD CYL 6 TEMP	60°F TO 80°F	69.5°F TO 68.1°F

TABLE 9.1 PRELAUNCH PARAMETERS MONITORED (CONTINUED)

MEASUREMENT NUMBER	MEASUREMENT DESCRIPTION	PRELAUNCH REDLINES	RANGE OF VALUES FROM T-8 1/2 HRS TO LAUNCH
C0041	MDA INT FWD CYL 7 TEMP	60°F TO 80°F	72°F
C7115	OWS PRIMARY THM CPR CLNT INL TEMP	-42°F TO -24°F	-26.6°F TO 29.1°F
C7044	OWS FWD CMP NO. 6 TEMP	42°F TO 63°F FROM T-12 HRS 55°F TO 63°F FROM T-12 HRS	57°F TO 59°F
C7279	OWS PRIMARY FRZ TCV CLNT OUT TEMP	-40°F TO -20°F	-26.9°F TO -25.7°F
C7296	OWS PRIMARY LOOP CCV CLNT OUT TEMP	35.3°F TO 42.8°F	37.7°F TO 39.0°F
D7001	OWS PRIMARY LOOP PUMP ΔP	32 PSID TO 55 PSID	41 PSID
D7002	OWS PRIMARY LOOP PUMP IN PR	30 PSIA MINIMUM	37.0 TO 37.2 PSIA
D7003	OWS SECONDARY RS LOOP PUMP INLET PRESSURE	30 PSIA MINIMUM	37.5 TO 37.8 PSIA
D7107	OWS WASTE TANK PRESSURE SENSOR 1	22 PSIA TO 26 PSIA	22.6 TO 22.9 PSIA
D7109	OWS H/A PRESSURE SENSOR 1	22 PSIA TO 26 PSIA	22.8 TO 23.2 PSIA
D7109	OWS H/A PRESSURE LOSS	MAX ΔP AFTER FILL FILL .6 PSI	0.4 PSI MAX
D7113	OWS PNEU SPHERE PRESSURE SENSOR 1	390 PSIA TO 510 PSIA	441 TO 445 PSIA

TABLE 9.1 PRELAUNCH PARAMETERS MONITORED (CONTINUED)

MEASUREMENT NUMBER	MEASUREMENT DESCRIPTION	PRELAUNCH REDLINES	RANGE OF VALUES FROM T-8 1/2 HRS TO LAUNCH
K001	MDA VENT	ON	ON
K003	MDA VENT	ON	ON
K7161	OWS RS PRIMARY PUMP 1 ON	ON	ON
M7010	OWS PRI RS LOGIC PWS OUTPUT	4.70 TO 5.30 VDC	4.98
M7011	OWS SEC RS LOGIC PWS OUTPUT	4.70 TO 5.30 VDC	4.95
K7037	OWS SOL VENT VALVE	CLOSED	CLOSED
K7036	OWS SOL VENT VALVE	CLOSED	CLOSED
K7222	OWS PNEU HAB VENT VALVE	CLOSED	CLOSED
K7224	OWS PNEU HAB VENT VALVE	CLOSED	CLOSED

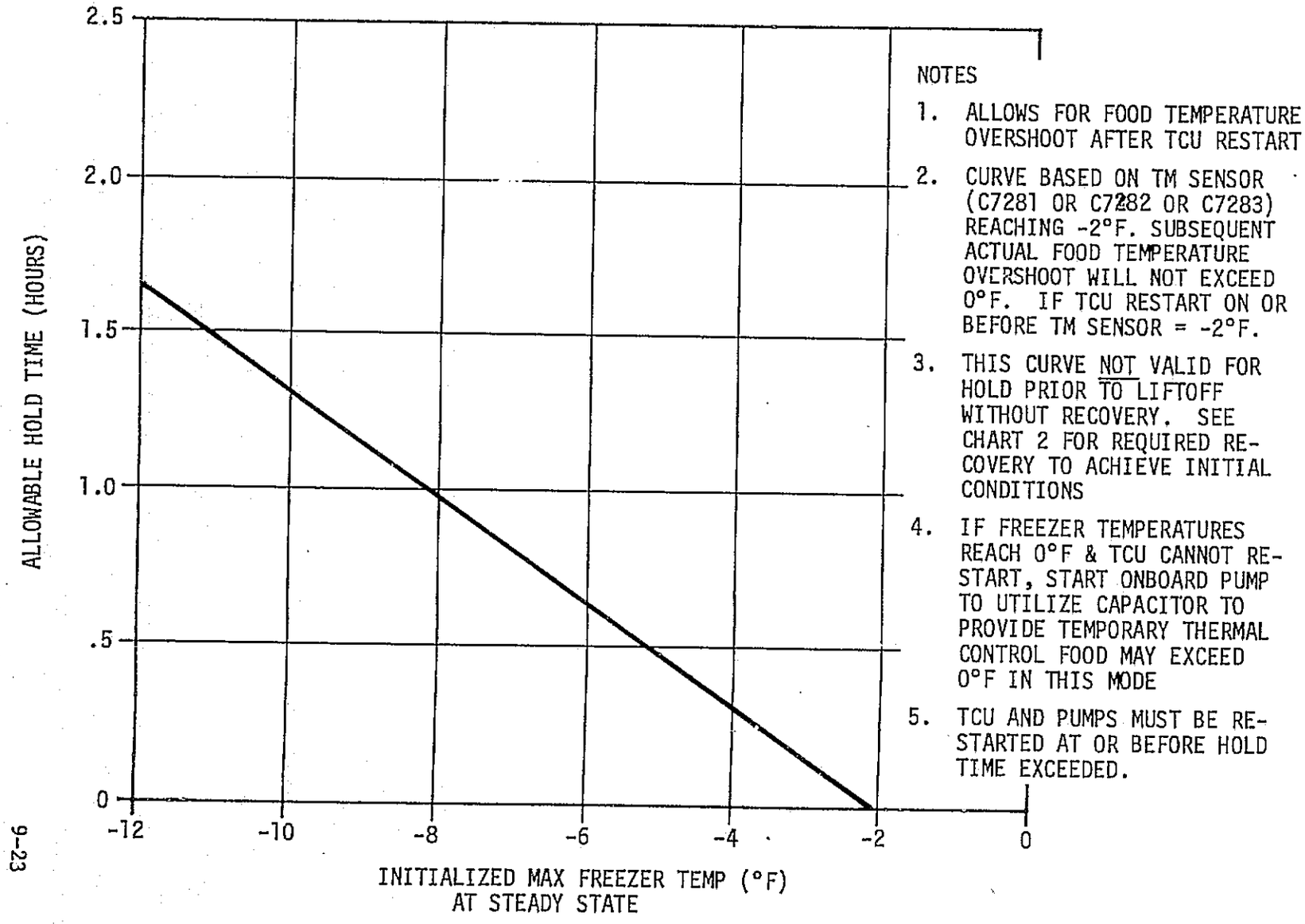

Figure 9-10. Allowable HoTd Time (Loss of TCU) as a Function of Max Freezer Temperature to Prevent Food Temperature Exceeding 0°F (On-Board Pump off During Hold) With Recovery Required.

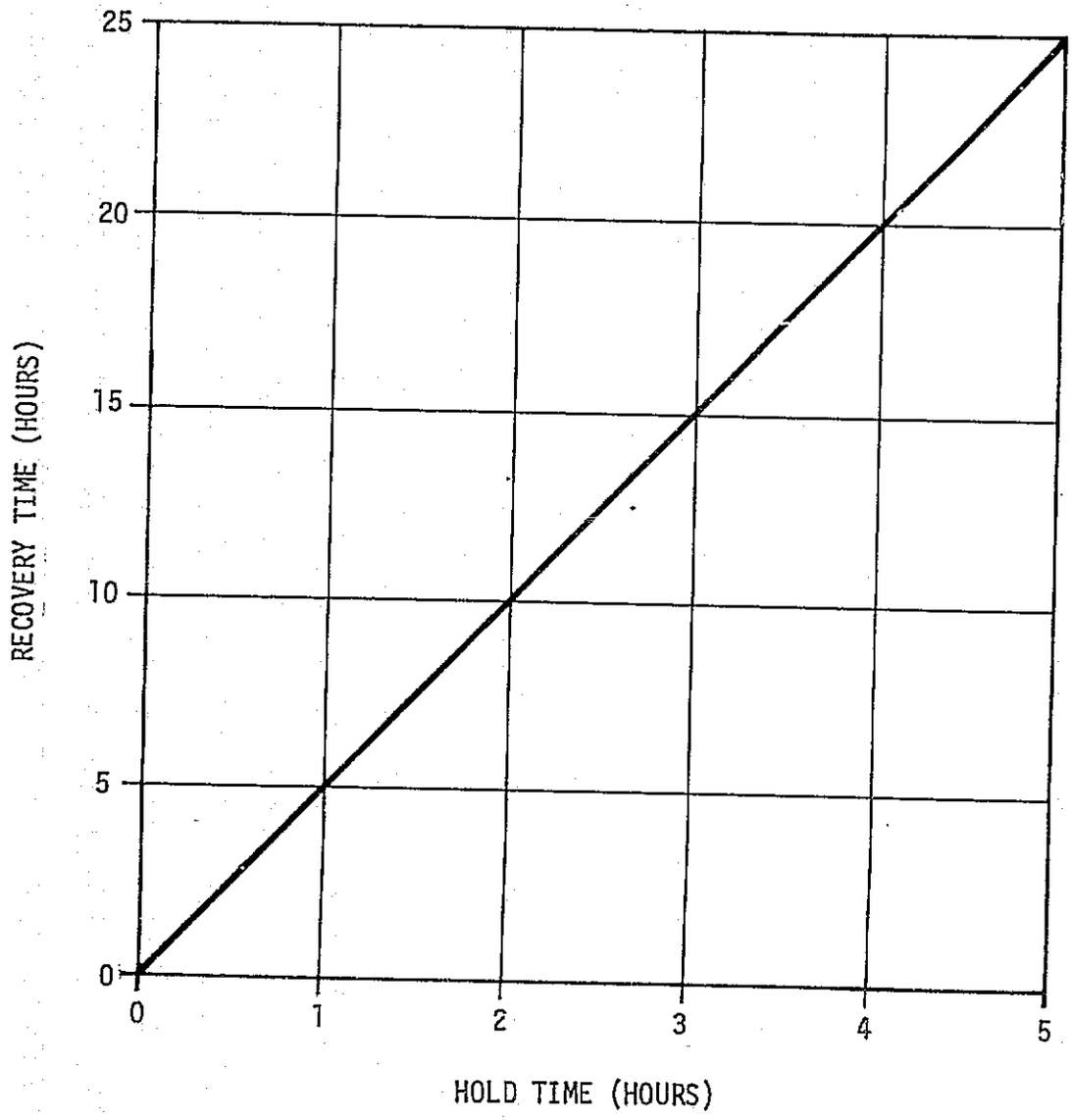

NOTES

1. TCU PERFORMANCE (TEMP & FLOW RATE) EQUAL BEFORE AND AFTER HOLD
2. FLIGHT SENSORS IN FREEZERS WILL RECOVER TWICE AS FAST AS THE ACTUAL FOOD
3. SEE CHART 1 FOR ALLOWANCE HOLD TIMES

Figure 9-11. Required Recovery Time vs Hold Time to Achieve Food Temperature Recovery to Initial Steady State Conditions

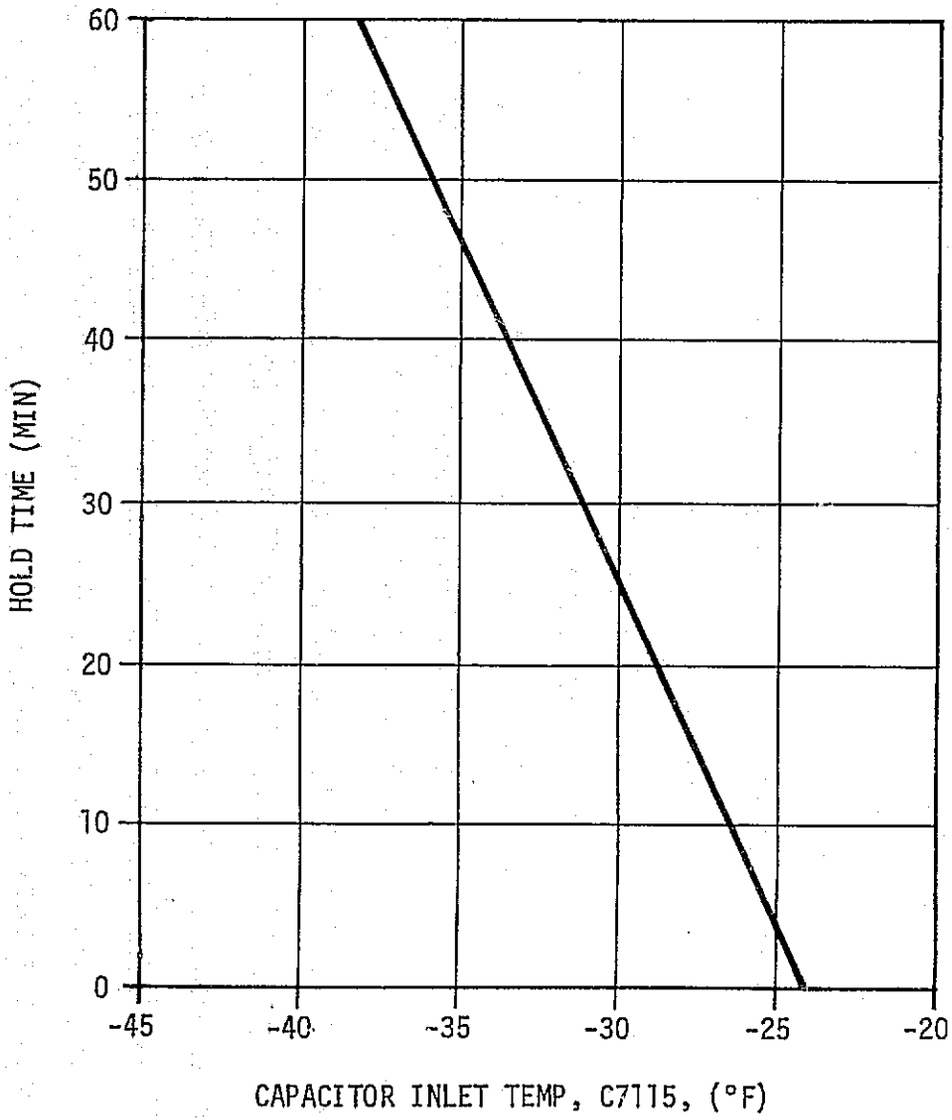

NOTE:

1. INSTRUMENTATION TOLERANCE INCL.
2. PUMPS OFF (ON BOARD) DURING HOLD
3. ALL SYSTEM TEMPS AT STEADY STATE PRIOR TO HOLD
4. ALLOWS FOR FOOD TEMPERATURE RISE DURING INSERTION.

Figure 9-12. Maximum RS/TCU Hold Times for Prelaunch with No Recovery Required Prior to Liftoff

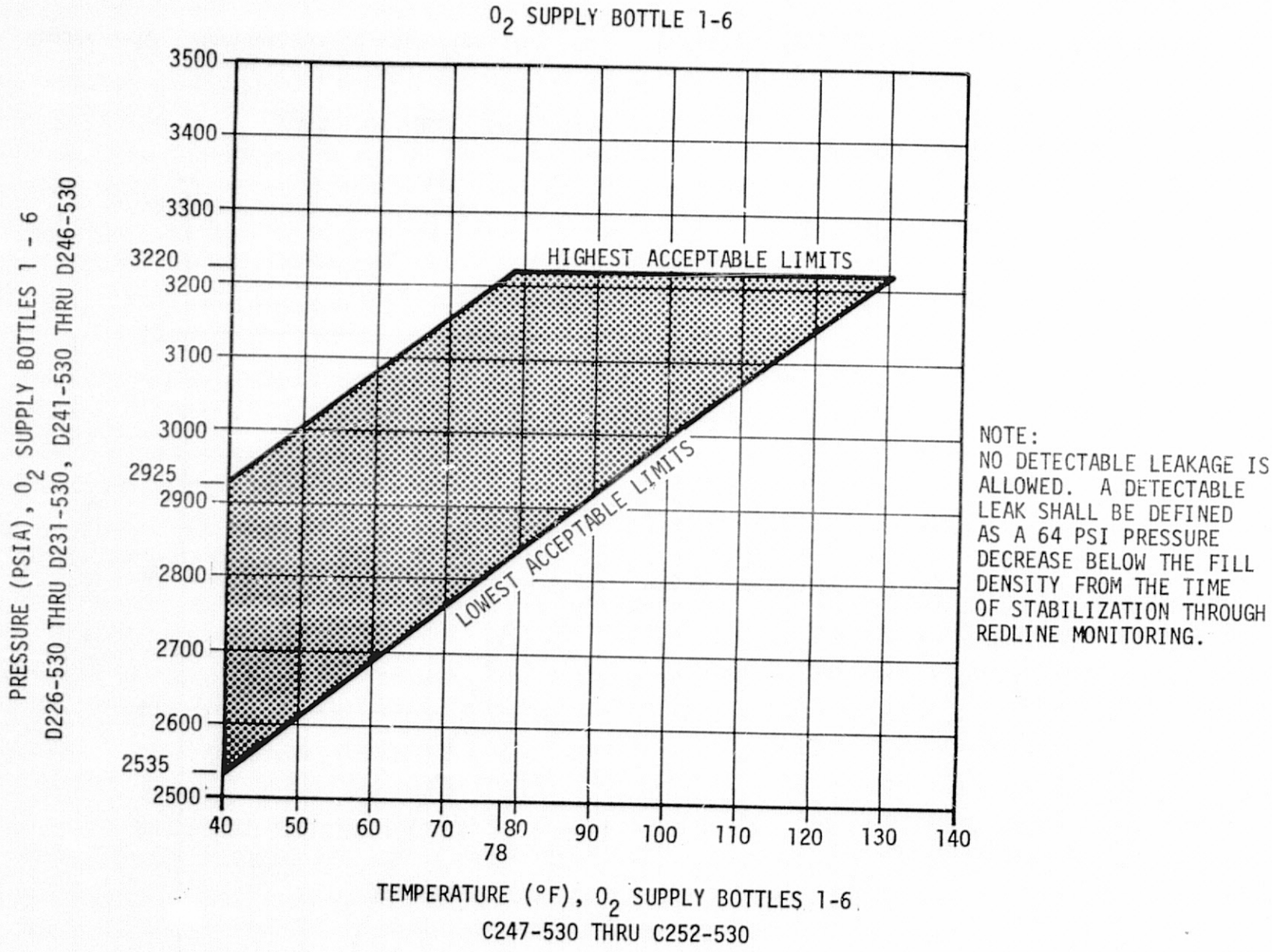

Figure 9-13. Oxygen Consumables Loading Requirements

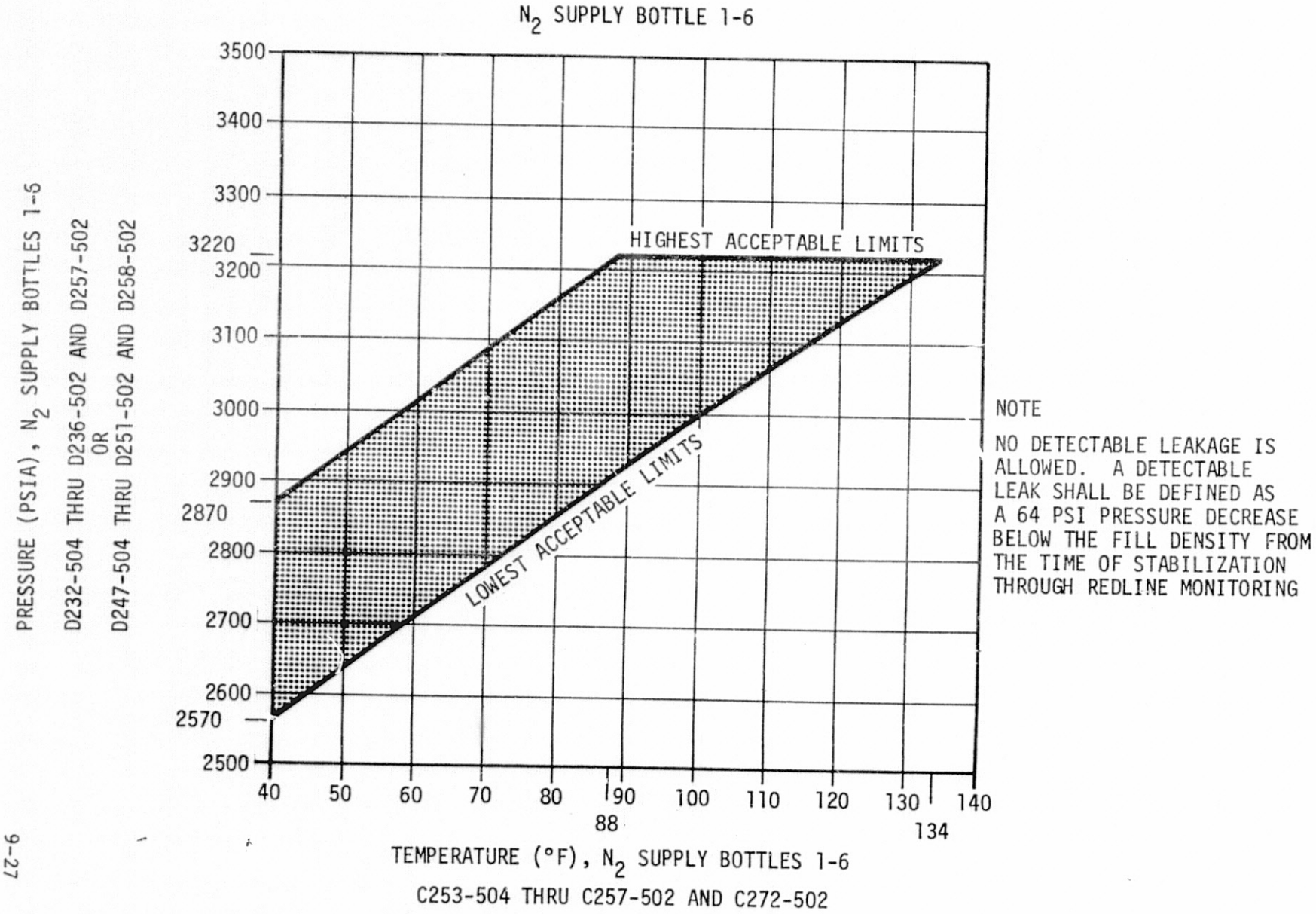

Figure 9-14. Nitrogen Consumables Loading Requirements

1. AM/MDA Habitation Area Purge and Pressurization. The AM/MDA purge system performed as expected and no problems were encountered.

2. MDA High Performance Insulation Purge. The MDA insulation purge performed nominally during prelaunch activities.

3. Payload Shroud Purge. The payload shroud purge performed satisfactorily the 27 days of prelaunch and operations of SL-1, requiring only minor adjustments to the purge requirements. The original purge requirement was 50 lb/min. flow to maintain the compartment temperature control setting at 63 $\pm$ 3°F. As the ambient environment (i.e., sunload and air temperature) increased in late April, compartment temperature response indicated temperatures exceeding the 66°F upper limit could occur at the 50 lb/min. flow rate. This indication was strengthened by data showing the umbilical interface purge gas temperature increased with increasing ambient temperature. The interface temperature could, however, be decreased by increasing the purge flow rate. Accordingly, compartment temperature limits were revised to 68 +5/-8°F. Additionally, the flow rate was increased from 50 lb/min. to a nominal value of 65 lb/min. As experience was gained, GSE operators noted that peaks and valleys in the daily PS temperatures could be attenuated by leading the ambient environment cycle (e.g., the purge gas cooling was reduced in late afternoon rather than waiting until sunset when compartment temperatures began a steep decline).

In late April, during pad operations, a significant amount of water leaked into the PS. During the day this leak occurred, approximately 0.4 inches of rain fell with wind velocities up to 37 knots. Approximately three cups of water were found in the vicinity of the ATM/AM. Subsequently the PS joints were sealed with silastic compound (RTV 140). No further leaks were reported.

4. Airlock Coolant Loop. During prelaunch activities the performance of the primary and secondary coolant loops were evaluated. At T-5½ hours a single pump was activated in the primary loop. The secondary loop, which provided onboard cooling prior to primary loop activation, was deactivated 30 minutes later, simultaneously cycling the radiator bypass valve from bypass to normal flow through the radiator. At T-10 minutes flow through the primary coolant loop was diverted from the ground cooling bypass to the onboard radiator by diverting the radiator bypass valve to normal. The operations left both radiator bypass valves in the radiator flow position precluding requirement for DCS commanding after liftoff.

Monitoring of the thermal capacitor skin and coolant outlet temperature was particularly important since, in order to insure adequate cooling capability prior to effective radiator operation, a finite ground hold time could be allowed after termination of ground cooling at T-10

minutes. The allowable hold times are shown in figure 9-15. If the hold times had been exceeded, reinitiation of ground cooling would have been required to assure the required cooling capability from the capacitors. The ground cooling system provided capacitor temperatures of approximately -40°F and there were no holds after T-10 minutes.

Outlet temperature values for the two 47°F valves and the 40°F valve in the active loops were continuously recorded to verify proper valve operation. Both loop pump inlet pressures were compared to preestablished minimum levels. All coolant loop parameters performed acceptably during the prelaunch phase.

5. ATM Canister Purge. During the 24 hour warmup period just prior to liftoff the purge temperature requirement of 75 ± 5°F taxed the CSE purge console capability because of increased flow to the SAS fairing (see paragraph 7 below). The requirement was revised to 70 ± 5°F and the flow rate was increased to 10 lb/min. The canister purge performed satisfactorily during all prelaunch activities.

6. OWS High Performance Insulation Purge. The OWS High Performance Insulation (HPI) Purge performed satisfactorily during prelaunch operations. The purge was terminated at T-8 hour 45 min. which was shortly before the OWS forward skirt GN_2 purge was initiated.

7. OWS Solar Array System Purge. The OWS Solar Array Purge System requirements were revised at KSC after the beam/fairings leakage was found to be greater than expected. After leakage was minimized, the maximum flow of 6.8 lb/min. (choked in the quick-disconnect) provided cavity pressures of 1.82 in. H_2O and 1.98 in. H_2O for Wings 1 and 2, respectively. The positive pressure requirement was changed from 2.5 to 1.80 in. H_2O (0.065 PSIG) which effected an infiltration risk of less than ten percent. The probability of wind-blown rain entering a beam/fairing was less than ten percent. The purge was terminated at liftoff when the kick-off plate was retracted.

8. OWS Forward and Aft Skirt Purges. The forward and aft skirt purges, which were the same as the Saturn Program purges, functioned nominally.

9. OWS Internal Purge and Pressurization. Prior to launch a redline was introduced to verify the OWS integrity. This was done to assure that the pressure was a minimum of 22 PSIA at maximum Q for structural integrity and to verify a large gas leak had not developed during pad operations. The OWS was loaded with gaseous nitrogen to 23 PSIA, after an equilibrium condition was reached a reference pressure was recorded. A maximum equivalent pressure loss of 0.60 PSI below the reference pressure was redlined. The OWS forward compartment gas temperatures (near

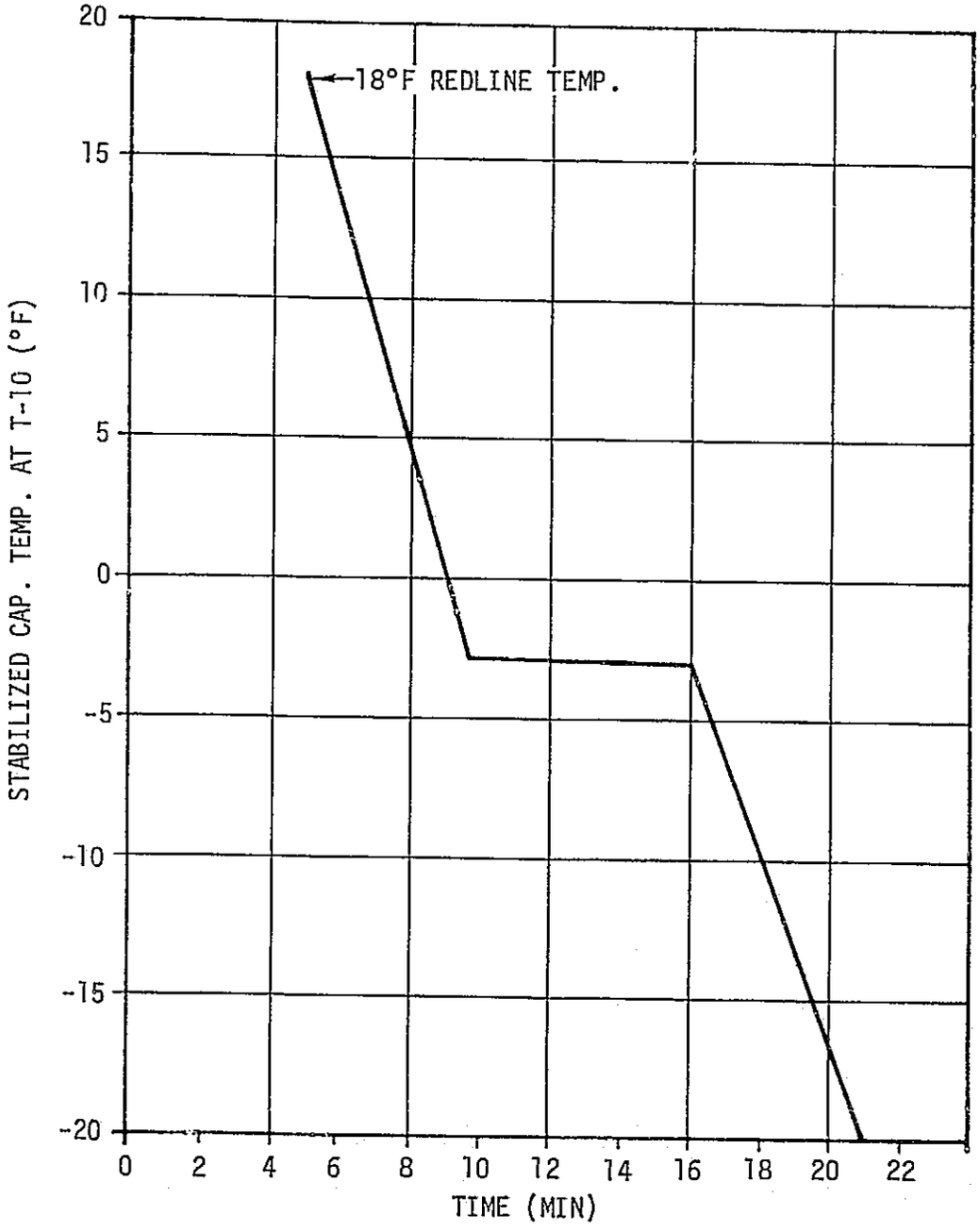

Figure 9-15. Allowable Hold Times for the AM Coolant Loop after T-10 Minutes Versus Stabilized Capacitor Temperatures at T-10 Minutes

the GTCS supply line), C7409 and C7410, were used to correct the OWS habitation area pressures, D7109 and D7110, to assess the equivalent pressure loss. From initial loading the previous day to liftoff the equivalent pressure loss was 0.4 PSI.

Pressurization of the OWS was completed approximately 15.5 hours prior to liftoff. The OWS was initially pressurized to 23.5 PSIA which was within the 23 to 26 PSIA requirement.

10. Ground Thermal Conditioning System (GTCS). The OWS GN_2 purge was completed on April 20, 1973, after final closeout. The requirement to establish and maintain a dew point below 30°F was met. Data taken in the VAB and on the launch pad indicated that the dew point ranged between -23°F and +7°F. Dry nitrogen pressurization and vent cycles occurred during this period. The last dew point measurement taken on April 28, 1973, was +4°F.

The requirements for the GTCS were to maintain the OWS food storage containers and film vault between 40°F and 65°F from rollout of the VAB until T-12 hours. At T-12 hours temperatures were to be controlled between 55°F and 65°F to precondition the EREP tapes to 55°F minimum at liftoff. No difficulty in maintaining temperatures within the required limits was encountered.

The OWS temperatures prior to liftoff are tabulated in Table 9.1. At liftoff the film vault temperature (C7408) was 51°F and the food temperature (C7411) was 50°F. The average OWS internal temperature was maintained within the required limits at approximately 58°F.

Measurement C7044 was located on the OWS interior wall opposite the film vault back face. For the preliftoff period this measurement oscillated between 57°F and 59°F. C7044 was used to control the internal temperature because of its proximity to the EREP tapes. The GTCS heat supply temperature was controlled to provide almost constant internal temperatures. The GTCS variation during pad operations ranged between 15°F and 68°F.

A comparison between the measured and maximum predicted forward compartment mean internal wall temperatures prior to liftoff are shown in figure 9-16. The predicted maximum temperatures were based on a hot May day (i.e., maximum solar heat input and external air temperature expected during the month of May). Less severe environmental conditions were actually experienced prior to liftoff. A maximum GTCS heat exchanger load of 29,000 Btu/hour was calculated for the countdown period. Most of the calculated heat loads were substantially lower than the maximum design heat exchanger load of over 40,000 Btu/hour.

The internal wall temperatures (figure 9-16) show a maximum temperature differential between the coldest and hottest walls of 5°F. This indicates that the air circulation was adequate, considering that the meteoroid shield temperature varied over 20°F due to the white and black external paint pattern and the variable direct solar heat input.

11. Refrigeration System Prelaunch Conditioning. As stated earlier, a major concern was the inability to consistently operate the TCS at temperatures appreciably below the original design requirement. The original design requirement for flow and temperature at the OWS RS ground heat exchanger interface were 3.2 gallon per minute (GPM) of water glycol at -21°F maximum. To provide this temperature, calculations showed the TCU had to supply approximately -29°F maximum. It's rated maximum supply temperature as received was -5°F.

After the TCU was modified for lower temperature operation it became evident that reaching the lower temperature was no problem but the flow dropped off considerably due to change of viscosity. The coldest temperature at which the TCU was operated was -35°F. At this condition the flow rate was 1.3 GPM and the calculated heat exchanger interface temperature was approximately -27°F. This was not a serious development since the reduced flow rate was sufficient for the OWS ground heat exchanger performance while the colder temperature achieved was highly desirable.

During actual vehicle tests the TCU was called upon to operate appreciably below the -29°F maximum supply temperature requirement; and although the TCU was only tested to temperatures as low as -35°F, it consistently and satisfactorily supported the OWS RS by delivering temperatures colder than -40°F.

The system performance was as expected, well within the redline values as indicated by Table 9.1. As mentioned earlier, the main concerns were lack of qualification testing and the possibility of a TCU failure.

12. Oxygen and Nitrogen Consumables. Initial masses of the oxygen and nitrogen systems are given in Section V. No prelaunch discrepancies occurred in these systems.

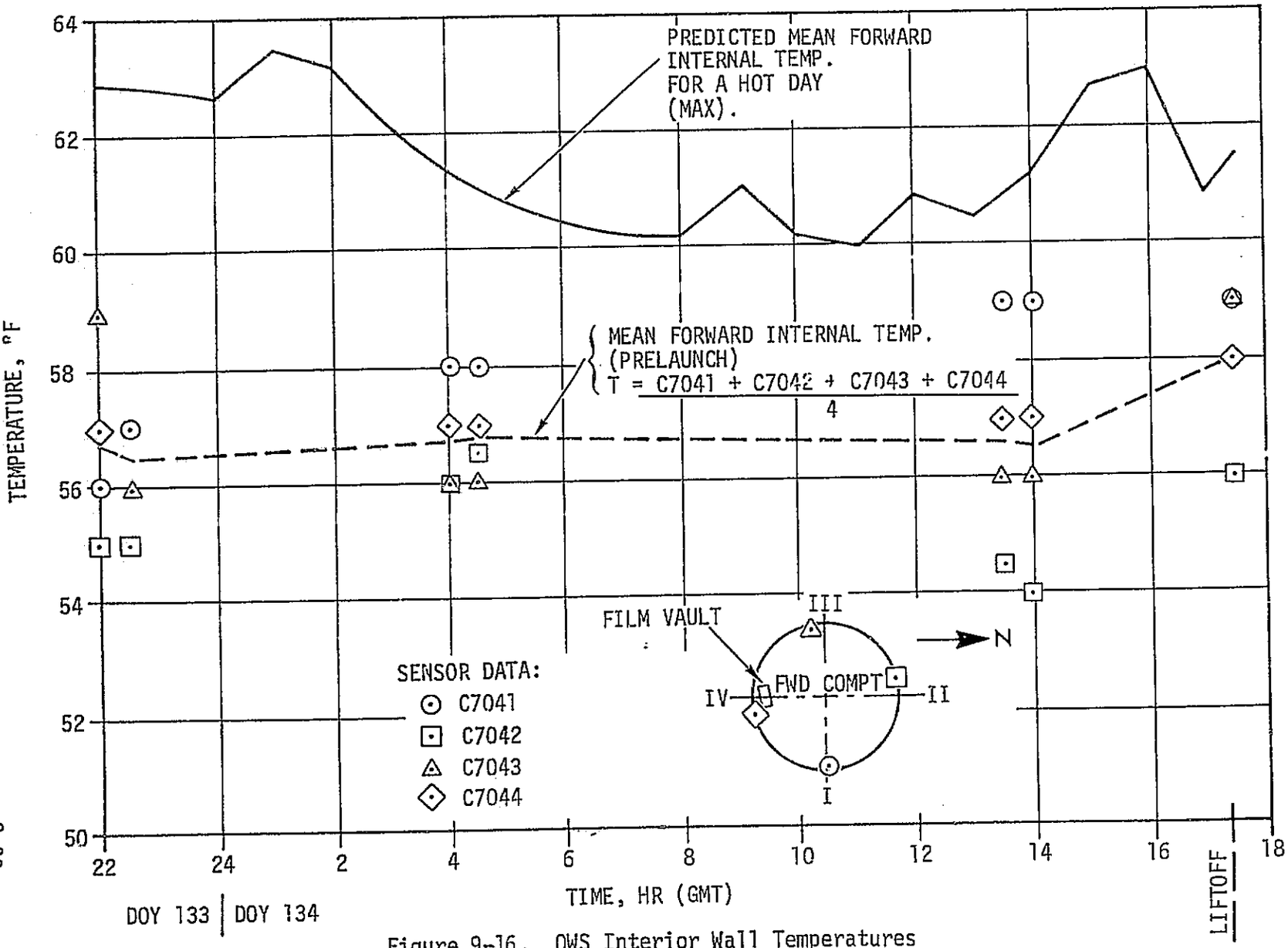

Figure 9-16. OWS Interior Wall Temperatures

SECTION X. CONCLUSIONS AND RECOMMENDATIONS

The Skylab Environmental and Thermal Control Systems provided an acceptable environment for both crews and experiments. The loss of the meteoroid shield resulted in an imbalance of the passive thermal control system for the OWS which was resolved by deploying improvised solar shields. Other anomalies occurred which required coordinated crew and ground support activities in their resolution. The major anomalies, other than loss of the meteoroid shield, were the sticking of temperature control valves in the Airlock Module cooling loop, leakage of coolant in both of the Airlock Module cooling loops and failure of the refrigeration system radiator bypass valves.

The following paragraphs provide some conclusions and recommendations for future designs. The comments are grouped by subsystem. A section is also included which contains general comments and observations.

A. Atmosphere Control System

The Atmospheric Control System includes carbon dioxide removal, humidity control, odor removal, and contamination removal. In general this system performed very well. The crews were basically comfortable and healthy. System discrepancies during the mission were corrected by designed-in system redundancies or by real-time workaround procedures. Comments and observations relative to future use of similar systems are provided in the following paragraphs.

The condensing heat exchangers using fritted glass water separator plates are an effective, durable and low maintenance means to remove atmospheric moisture.

The performance of the molecular sieve system was outstanding. The system performed CO_2, odor, and moisture removal functions effectively with no system hardware anomalies. In fact, the system performed satisfactorily throughout the 84-day SL-4 mission without a bed bakeout being required (design was 28 days). This system demonstrated that it should be considered for future manned programs, especially those of one month or more duration.

The vacuum side of the condensate system had a tendency for random leaks throughout the mission. The condensate system included many quick disconnects and it was generally agreed that quick disconnect leakage was the problem. The use of quick disconnects should be minimized on future missions in all systems, and especially in vacuum systems. Also braze-type joints are more desirable in vacuum systems than mechanical type joints.

The metabolic guidelines which appear to match the flight data are:

Approximate daily average rate = 440 BTU/hour/man

Metabolic O_2 usage = 1.84 lb/man day

Water production = 2.6 - 4.1 lb/man day

CO_2 production = 2.15 lb/man day

The odor control system performed very well. The crews reported a general absence of odor.

B. Cluster Ventilation System

The Cluster Ventilation System performed well throughout the mission. The crew were comfortable, the gas velocities were acceptable and the equipment used was reliable.

The fans used (modified Apollo PLV types) were adequate. No complaints by the crew of high fan noise levels were made. However, these fans produced a very low head and any restrictions in the systems caused flow degradation. It is suggested that future missions utilize fans with higher heads so that filter or heat exchanger contamination with lint or moisture will not so seriously effect the cabin gas flow.

Lint is added to the atmosphere on long duration flights in quantities sufficient to collect on cabin heat exchangers and cause a reduced gas flow. The susceptibility of fan/heat exchanger units contamination should be an important consideration in the choice of equipment for future ventilation systems. Future use of these type components should include finer mesh protective screens, and increased accessibility for periodic replacement and cleaning.

Much improvement in the design and installation of cabin gas flow meters is needed. The heat pulse type flow meters used in the AM systems consistantly fluctuated through 15-20 percent of the full scale flow. Single data points were of little meaning and long term averaging afforded the only means of determining the flow rate. The vane type flow meters in the OWS ducts were not satisfactory either since two of the three units failed.

C. OWS/MDA/AM Thermal Control System

The OWS/MDA/AM Thermal Control System, outside of the loss of the meteoroid shield, performed within the specified limits. As shown in Section IV, the cluster temperatures stayed within the comfort box

except prior to parasol deployment and during high Beta angle periods. A one-to-one comparison of flight-versus-design is not possible due to the loss of the meteoroid shield, but enough data are available to show that the design was adequate.

A considerable number of telemetry sensors had been installed in the OWS for TCS system evaluation. These proved to be very valuable and even more would have been useful in predicting the maximum temperatures when the meteoroid shield anomaly occurred.

When the OWS was hot and the MDA was cold, it would have been desirable to have had the capability to provide more flow from one compartment to the other. This would require very little storage volume or weight and would add a considerable amount of flexibility should a similar anomaly occur in future programs.

The crew comfort criteria appears to be a good criteria as the crew tended to turn the thermostat up or down when approaching the upper and lower limits of the comfort box. Radiation heat from hot walls was very noticeable. Jackets and gloves were worn on initial entry into the OWS to help sheild against the heat from the walls.

D. Gas Supply System

The Cluster Gas Supply System performed well and demonstrated that the design concept as well as most of the components should be considered for future flights. With the exception of the 150 PSIG N_2 regulator pressure, which drifted low, (but still within useful range), the gas system was problem free.

The two-gas control system was especially effective in providing cabin pressures and oxygen partial pressures well within the allowable range. A two-gas system most probably will be used on all future, long-term manned space flights and this type of control is suggested as a candidate.

Cluster O_2 and N_2 gas usage rates were well below design levels; significant quantities of both gases were available at the end of the mission even though unplanned purge cycles were accomplished and cabin pressures were maintained at near manned level during the orbital storage period following SL-3. The total vehicle pressure integrity design was therefore very effective and should be considered in the future.

Even though no damage resulted, the fact that the oxygen bottle number 6 went above design/qualification limits four different times during the mission demonstrates the need for thermovacuum test to backup analyses. A thermovacuum test would probably have revealed this analysis error.

To help evaluate system performance and metabolic rates and determine cluster leakage rates, flow rate measurements on gas flow during pressurization, EVA/IVA and normal cabin pressure regulator flow would have been useful.

E. Pressurization/Depressurization Systems

The Pressurization and Depressurization Systems performed nearly as predicted. All valves were adequately sized for the volumes to be depressurized.

The ice buildup on the AM depressurization valve screen during depressurization indicates that attention should be given to this problem in the future. By having a removable outer screen, such as the one used for SL-3 and SL-4, the hazard of allowing chips of ice to possibly damage the valve seat is eliminated, but the vent procedure is slightly larger and more complicated. Heaters should be considered in future designs.

An accessible screen was added to the inlet of the solenoid vent port as a result of a preflight design review. The crew was required to clean the screen on several occasions and had the screen not been present, the vent valve could have been blocked. Screens should be provided for similar future designs.

Cluster structural leakage was approximately 20 percent of maximum allowable specification leakage.

F. Airlock Module Coolant Loop

The Airlock Module coolant loops, from a performance standpoint were well designed. The electronics were properly cooled, the crew was maintained comfortable during EVA, and in general the heat rejection capabilities were more than adequate. However, these systems experienced some mechanical failures which, although they were resolved or worked around, demonstrated a need for better quality control.

The radiator/thermal capacitor performance was good.

When one of the AM coolant loop temperature control valves stuck, the other, completely separate, loop experienced the same failure at the same time. This has been attributed to contamination originating in heat exchangers which were identified and processed alike, jamming valves which were alike and processed alike. Similar failures occurred in the OWS refrigeration system, where two completely separate and redundant systems experienced solenoid valve failures from contamination at the same time. Also although the locations are not known, both AM coolant loops leaked and neither OWS refrigeration system leaked.

These failures indicate that systems containing the same generic components do not provide the degree of redundancy obtainable in systems with different generic parts. Although the latter case is obviously more expensive it definitely has merit, especially where mission or life critical systems are concerned.

Also, systems should be designed to allow inflight reservicing with ease and extra fluids should be stowed whenever possible. If Skylab had been one long continuous flight, the AM coolant systems would have been lost, terminating the mission early. The number of mechanical fasteners in fluids systems should be minimized.

Consideration should be given to ultrasonic cleaning of heat exchangers and other components in systems with contamination sensitive elements.

The EVA/IVA system performed well enough to include some lengthy and strenuous workshop repair tasks, resulting in expansion of original mission objectives. All mission objectives were accomplished and at no time was crew safety compromised. It is recommended that the Airlock EVA/IVA system - design concept, verification procedure, and operational hardware - be considered on future missions with an EVA requirement.

Some design requirements were inconsistent with Skylab EVA experience.

1. Waste heat load range requirement of -800 to +2000 BTU/hour man was too severe. Maximum heat load for all three crewmen was approximately 2200 BTU/hour and a negative heat load was not experienced.

2. The maximum allowable water delivery temperature of 50°F was too severe. Temperatures of 58°F provided adequate cooling.

3. Total duration of EVA exceeded seven hours, with cooling water flow exceeding eight hours - system requirements were three and four hours, respectively.

4. The system was designed to support two EVA crewmen on one loop with the other crewman (STS) on second loop. During the mission, a single loop effectively supported all three crewmen.

Oxygen flow and suit cooling system support was provided as required for 12 EVA/IVA operations including, on DOY 359, a record EVA hatch open time exceeding seven hours.

Loss of SUS #1 cooling fluid occurred due to leakage of LCG/PCU during an EVA. Reservice, as planned and provided for, was accomplished. Provisions to allow inflight reservicing of fluid systems should be included in all future missions.

Differential pressure instrumentation was deactivated prior to launch due to a potential of shorting out the 5 volt bus and eliminating all instrumentation connected to that bus. Loss of Delta P information complicated the determination of loop performance and the isolation of flow problems.

The ATM C&D/EREP cooling system flow became erratic late in the SL-3 mission. Successful deaeration of the loop, using the liquid gas separator, temporarily corrected the flow oscillations. Deaeration devices should be included in future systems where any point in the system operates at pressures below cabin or ambient pressures.

G. Refrigeration System

The Refrigeration System (RS) was used to thermally control the frozen food and urine samples, the refrigerator and water chiller and the chilled urine sample pool. The RS performed very well during the mission with the exception of the anomaly which occurred on DOY 173.

In fact, the system was able to maintain the specified requirements even during the abnormally hot internal conditions before the parasol Sun shield was deployed.

The only serious anomaly to occur in the RS was the failure of both the primary and secondary RBPVs on DOY 173. The failure was attributed to contamination, which prevented the bypass poppet assembly of both valves from fully seating or opening, although the radiator port poppets in each valve were only prevented from seating. The primary RBPV performance was improved by cycling the valve from the ground by enabling and disabling the loop. The improvement was such that the system was able to essentially maintain its requirements for the rest of the mission. As mentioned in the Airlock Module Coolant Loop section (paragraph F.), the same generic components in dual loops did not give the required degree of redundancy. Further, cleaning and filtration requirements must be closely scrutinized relative to the particulate contamination size which causes valve or component failure.

After the initial low performance of the RS radiator following orbital insertion, the radiator performed as predicted throughout the remaining missions. The absorbed heat flux on the radiator was nominal and there was no apparent degradation of the radiator paint (most of the white paint on other external areas of Skylab showed significant degradation as a result of solar exposure and/or retrorocket plume contamination).

Thermal capacitor performance following umbilical disconnect at SL-1 launch until radiator activation was as anticipated. Comparison of thermal capacitor data at various times throughout the mission revealed no degradation in performance.

Flight data revealed no evidence of either pump degradation or coolant leakage in either of the two RS coolant loops.

All RS internal loop segment components performed as expected including the CTCV and regenerative Hx. At no time did flight data indicate the regenerative heater in either of the two coolant loops to have been activated to aid in the regenerative capability of the regenerative Hx.

Crews' complaints with the RS consisted of:

1. Inconvenience of the inner door on the freezer compartments.

2. Poor space utilization in the freezers.

3. Lack of canister restraint in the food chiller.

4. Ice buildup on the surface between the freezer compartment doors impaired the latching of the freezer doors to such an extent that periodic cleaning became necessary.

H. Ground Thermal and Fluid Conditioning Systems

The Ground Cooling Systems provided sufficient cooling to freeze the airlock thermal capacitors (≈ 10°F). This method of using a heat exchanger to transfer waste heat to a ground system prior to liftoff and a phase change material to supply heat removal en-route to orbit seems to be a sound method and should be considered in the future.

Both the refrigeration ground conditioning system and the OWS ground thermal control system performed as anticipated. No anomalies occurred in either of these two systems.

I. General Comments

Both the AM coolant loop and the OWS refrigeration system demonstrated that when the control valves were stuck in a near optimum position, the outlet temperature would be acceptable without automatic control. This would suggest that for a reliable long life system with the man available, a backup hand valve may be desirable in parallel to the automatic system should it be required.

The nominal solar constant given in NASA SP-8005 of $429.2^{+14.6}_{-14.0}$ BTU/hour-ft^2 which allows for seasonal variation appears to match the Skylab flight data. The Earth albedo and emitted radiation values versus latitude and the seasons given in NASA SP-8067 also appear to match the Skylab flight data. In retrospect, the $\pm 3\sigma$ and $\pm 2\sigma$ environmental flux values which were used for design purposes were probably conservative but should still be used in future programs to offset degradation in coatings, actual conductances, actual heat loads, active system performance variations, and anomalies.

The Z-93 radiator coating when continuously exposed to the Sun as it was in the D024 experiment, can degrade from the as launched value of $\alpha/\varepsilon = .14/.91$ to approximately .33/.91 in 123 equivalent Sun days. If only one side of a cylinder is exposed as on the AM radiator, the degradation averaged around the cylinder would be approximately .25/.91.

All critical systems in a manned vehicle should have adequate TM, DCS command capabilities, and manual overrides as used in Skylab. This combination was invaluable in troubleshooting the problems and in providing system workarounds.

Some circuit breakers were tripped by accidentlly bumping into them. Future designs should better shield against this.

Consideration should be given to have facilities to use each others fluids in all systems with compatible fluids (i.e., O_2/N_2 could have been used for TACS, AM coolant could have been refilled by OWS Refrigeration System.)

Critical components should be accessable, and adjustable. (i.e., AM coolant control valves, OWS refrigeration control valves, etc.) All automatic controls should have manual overrides whenever possible.

Detailed review/test of tolerances, filters, and cleaning should be performed. Performance tolerance should be as loose as possible to allow increased physical tolerances in components.

Simple inflight calibration of sensors is desirable.

When real-time system anlaysis is required, sensors should be provided for as many measureable parameters as possible. Although it is classically hard to support a need for these sensors preflight, the Skylab flight demonstrated the value of adequate system instrumentation.

The crew is an important part of the machine. They were invaluable on Skylab for sensing problems, interpreting them and, most of all for fixing them.

APPENDIX A. SYSTEM EVOLUTION AND DEVELOPMENT

The system design configurations presented in this report evolved over a period of several years. The most significant changes occurred with the change from the Saturn I "wet" workshop to the Saturn V "dry" workshop configuration and corresponding changes to program philosophies. The OWS TCS originally was to provide a habitable environment for the Habitability/Crew Quarters Experiment (M487). The OWS was also to have been an operational S-IV B upper stage fully loaded with liquid oxygen and hydrogen, which were burned at orbital insertion. After the residual propellents were vented and the compartments were pressurized, the crew was to carry in and install fans and other system components in the OWS that were not compatible with liquid hydrogen. As a result, the initial OWS system had to be simple and require a minimum effort for activation. The OWS thermal design was therefore primarily passively controlled with suitable insulation and coatings and also had fans with cloth ducts on the sidewalls for additional temperature control. To meet the early launch date, all of the vehicles (including a LM vehicle) that composed the cluster had to use essentially off-the-shelf TCS and ECS hardware and each vehicle was expected to provide its own thermal control.

As the launch date was rescheduled, the entire concept was changed to the Saturn V "dry" workshop configuration (without a LM vehicle). The workshop was launched without propellents, and all hardware was preinstalled inside before launch. All the Skylab TCS/ECS systems were allowed to become more sophisticated at this time because the launch date was extended long enough to qualify new hardware. Also, the philosophy of each vehicle providing its own thermal control was dropped and the Skylab TCS/ECS systems were integrated into one overall system with central control in the AM. The following briefly describes the evolution of the systems resulting from changes to the original program requirements and development problems.

A. Atmosphere Control System

1. Carbon Dioxide (CO_2) Control and Odor Removal - Cluster CO_2 and odor removal was originally supplied by Gemini Lithium Hydroxide (LiOH) canisters which had a 14-day capacity for two men and were to be replaced in flight. A molecular sieve was to be carried in the cluster as an experiment. The status of the sieve changed with time. The sieve served as a backup for the LiOH system and then as a prime system with the LiOH as the backup system for missions longer than 28 days. The LiOH system was eventually dropped and a second molecular sieve was added with both sieves to be installed in the Airlock Module. These changes took place prior to the establishment of the Saturn V "dry" workshop configuration and the CO_2 partial pressure requirement was 7.6 mmHg. After the dry workshop concept was baselined, the CO_2 partial pressure requirement was reduced to a value of 5.5 mmHg. In order to accommodate the new requirement, the flowrate through the sorbent canisters was increased from 10 lb/hour to 15 5 lb/hour.

A concern over possible contamination of external optical surfaces by exhaust gases from the molecular sieves during bed desorption resulted in a directive to relocate the molecular sieve overboard exhaust ducts. As a result, both molecular sieve overboard ducts were combined and relocated to exhaust from a single outlet from the side opposite the optics.

2. Humidity Control- The capability to maintain the cluster dewpoint above the minimum 46°F allowable was marginal with a 40°F control valve system (see paragraph F. of this appendix) and the problem was aggravated by the required molecular sieve flow increase since more atmospheric moisture was adsorbed and dumped overboard by the molecular sieve. However, this problem was ultimately solved by increasing the coolant temperature entering the condensing heat exchangers from 40°F to 47°F, thus raising the atmosphere dewpoint by reducing the amount of moisture condensed in the heat exchangers. The original Gemini 40°F temperature control valves were replaced by off-the-shelf valves of a different design, but modified to control coolant temperature to 47°F. This change was accomplished simultaneously with that required to reduce collant temperatures delivered to the battery modules. (See paragraph F. of this Appendix.)

Concern that dumping condensate overboard might interfere with experiments which involved external sightings caused condensate system design requirement changes. Some of these changes are listed below:

a. Relocated the AM condensate overboard dump ports to the opposite side of the spacecraft from the affected optical surfaces.

b. Provided the capability to dump condensate from the AM storage tank to the OWS waste tank, which also was modified to preclude release of water or ice particles of sufficient size to contaminate the optics.

c. Modified the AM dump ports to include restricted outlets which would cause a more predictable exhaust plume profile.

d. Provided capability to transfer condensate directly from the AM condensing heat exchangers to an evacuated condensate holding tank (a modified OWS waste tank) located in the OWS. The condensate was to be stored in the holding tank and subsequently dumped to the OWS waste tank. This change resulted from water freezing at the OWS waste tank dump probe. Freezing was encountered during tests simulating condensate transfer from the AM storage tank to the OWS waste tank. The OWS dump prove was also modified to permit dumping from the AM condensate tank to the OWS waste tank. However, transfer to the OWS holding tank was retained as the primary method because the larger volume of the holding tank allowed a longer period of time between dump operations.

A design requirement change was made relatively late in the program to provide a positive means for in-flight servicing of the condensing heat exchanger water separator plates. This change was prompted by the concern that the plates might dry out during low water generation rate periods of the mission and by uncertainties associated with the previously baselined self-wetting method. The new method had the advantage of being a step-by-step process which assured positive plate wetting. Although, the self-wetting approach had been proven satisfactory during development testing, and required fewer operational steps, its success in-flight would have been strongly dependent on cluster dewpoint and proper crew attention. The self-wetting technique was sensitive to both free water carryover to the molecular sieves and gas carryover to the condensate collection system.

B. Ventilation System

The AM ventilation system originally utilized Gemini cabin fans which were later replaced by GFE Apollo Post Landing Ventilation (PLV) fans. Advantages of the PLV fans were: (1) needed no AC/DC power inverter, (2) required less power, and (3) standardized fans throughout the cluster since PLV fans were also used in the MDA and OWS. However, the PLV fans had undesirable flow/delta P characteristics for use in conjunction with the cabin heat exchangers. The lack of pressure head from the PLV fan necessitated the use of low pressure drop screens and ducting. The inclusion of sound suppression equipment in the fan module designs to satisfy cluster noise level specifications resulted in additional system resistances, which also contributed to the marginal fan characteristics. Alternate fan designs which would provide more desirable flow/delta P characteristics were pursued but a decision was made to retain the PLV fan. The fan performed well during the Skylab missions. However, problems were encountered during flight with dust and other particles passing through the coarse (low pressure drop) screens at the inlet to the OWS heat exchangers.

The OWS ventilation system was modified with the change from the Saturn I (wet) to Saturn V (dry) workshop. The diffusers in the wet workshop configuration were mounted on the ceiling and the equipment was on the floor. In the dry workshop configuration, the diffusers were mounted on the floor along with various pieces of Skylab equipment. Additional flow was required to maintain an average atmosphere velocity of approximately 40 ft/min. since the reversal of the floor and ceiling placed equipment in the vicinity of the diffusers which disrupted their flow pattern.

C. OWS/MDA/AM Thermal Control System

1. Airlock Module - The only significant change made to the atmosphere cooling system was installation of the four OWS heat exchangers and associated fans to provide more sensible cooling to the OWS. This change was made just prior to conversion to the Saturn V

workshop configuration and the heat exchanger fan assemblies were located in the space previously alloted to the LiOH system in the aft Airlock Module compartment. The change in orbit inclination angle from 30° to 50° increased the mission beta angle extremes from ±53.5° to ±73.5°. Combined with the change to the basic solar inertial attitude, this resulted in a more severe hot case external environment design condition. These factors resulted in a change from a multiple layer "superinsulation" concept to the thermal curtain insulation design for the Airlock Module.

2. Orbital Workshop - The Environmental/Thermal Control System as defined for the Saturn I (wet) workshop provided control by fan circulated gas in eight evenly-spaced ducts. These ducts were formed by a series of thermal curtains and rails around the periphery of the habitation area. This system gave gas temperatures in the range of approximately 55°F to 105°F. The design was based on a gravity gradient vehicle orientation at a 28.5 degree orbital inclination. A meteoroid shield with a black painted external surface ($\alpha/\varepsilon = 0.9/0.9$) was assumed with a moderate resistance to heat transfer (no gold) between the meteoroid shield internal surface and the tank wall. The minimum temperature for safe astronaut entry after tank passivation was defined as -150°F and no active heaters were provided for warmup.

During the latter part of 1967 and in 1968, studies delineated the advantages of controlling heat leaks in the tank sidewall, tank joint regions, the forward dome and the plenum region including the common bulkhead. These studies led to the gold tape on the tank external surface, the forward dome high performance insulation system, the thermal shields on the external joint areas, and foam insulation in the plenum region. (The addition of foam insulation was not implemented, however, until after the change from a wet to dry workshop). By mid-1969, the system concept and design had undergone many changes. Crew comfort was no longer in the category of an experiment but more stringent requirements were defined as follows:

Atmospheric Temperature	65 to 75°F
Mean Radiant Wall Temperature	65 to 75°F
Humidity	0.018 Specific (minimum) and 95% Relative (maximum)
Touch Temperature	55 to 105°F
Atmospheric Velocity	15 to 100 ft/min.

The temperatures were to be controlled automatically or manually utilizing cooling delivered from the Airlock Module and 750 watts of the 1000 watts of heater power available (500 watt capability in each of two ducts with fan clusters). All major surfaces were to be between 60°F and 80°F, but localized surfaces accessible to the crew could be as cold as 55°F or as hot as 105°F. Radiant heaters providing a maximum of 1000 watts were to be utilized for warmup to provide a 0°F mean

internal temperature at pressurization initiation and a 40°F minimum internal temperature by the time tank seal and lighting installation was completed.

The wet workshop requirements were reassessed with the change to a dry workshop configuration in September 1969, with the mission being flown in a solar inertial attitude at an orbital inclination of 35 degrees. Before completion of this assessment, change to a 50 degree orbital inclination was made in early 1970. This meant the design had to consider the increased heat loads associated with orbits in 100 percent sunlight whereas the maximum previously had been 73 percent sunlight. Performance requirements were changed to include an expanded comfort box (which was the final specification comfort box). A minimum waste heat (housekeeping) load of 250 watts and a maximum metabolic (sensible) load of 1000 Btu/hour (293 watts) were defined. Maximum heater power usage for cold conditions was redefined as 825 and 1170 watts for nominal and two sigma conditions, respectively. The minimum electrical waste heat removal was specified as between 600 and 1350 watts, being dependent on beta angle as well as consideration of nominal and two sigma conditions.

The major design changes resulting from the preceding requirements were the addition of white paint on the solar-facing side of the meteoroid shield, the addition of 500 watts of manually controlled heater power in the third duct, and foam insulation added in the plenum region to alleviate potential condensation problems and to minimize the heat leak.

In 1971, heat pipes were installed in the workshop to alleviate potential condensation problems in the regions near the floor and ceiling supports, the wall behind the water bottles, the balsa wood forward joint and the back of the storage freezer in the forward compartment. Also, in this period the Airlock Module cooling delivered to the workshop was redefined with a resultant 50 watt decrease in the specified minimum electrical waste heat removal equipment and an increase in the housekeeping load to 400 watts. The Airlock Module cooling was again redefined early in 1972 and the minimum housekeeping waste heat load was increased from 400 watts to 525 watts which became the final design value. Based on these changes, the white paint pattern on the meteoroid shield external surfaces was finalized in February 1972. No significant design changes were made between this time and SL-1 launch.

D. Gas Supply System

The initial requirements were to store and supply O_2 at sufficient quantities and flowrates for initial pressurization, for replenishment of atmospheric leakage, and for metabolic consumption for three crewmen for a 30-day mission and to provide O_2 and H_2 for the CSM fuel cell. The cluster atmosphere was to be 5 PSIA O_2. To store the required O_2 and H_2, modified Gemini O_2 and H_2 cryogenic tanks were mounted on AM trusses. Thermostatically controlled calrod heaters, installed on the lines downstream of the cryogenic tanks, warmed the gases supplied to the distribution system. Two 120 PSIG Gemini pressure regulators provided O_2 supply and pressure control.

As the wet workshop design was firmed up, the cryogenic tanks were removed from the AM. O_2 and N_2 were then supplied from the CSM for a two-gas atmosphere. O_2 flowrates available from the CSM, however, were insufficient for meeting EVA/IVA and M509/T020 experiments support requirements. To meet the higher flowrate requirements, two high pressure gaseous O_2 tanks (LM descent tanks) and two 240 PSIG O_2 pressure regulators were added to the AM in addition to the two 120 PSIG regulators for normal flow already there. The gaseous O_2 tanks were to be launched pressurized to 2250 PSIA, and then, after depletion to below 1000 PSIA by usage, were to serve as accumulators. The accumulators were to be kept recharged with O_2 delivered from the CSM to the AM. Gas in the accumulators was to be used to supplement O_2 flowrates from the CSM. The O_2 and N_2 required for S-IVB initial pressurization were to be supplied from the CSM through an umbilical to the MDA and to the AM system. The O_2 and N_2 required for maintenance of atmospheric pressure and O_2/N_2 composition control were introduced into the CSM.

Changeover to the dry workshop with the Saturn V booster permitted a larger allowable launch weight. Consequently direction was given to store all O_2 and N_2 supplies required for the Skylab mission onboard the AM. Storage of the O_2 and N_2 as high pressure gases was selected over cryogenic storage because of lower cost, lower development risks, ease of servicing, and more operational flexibility for the multi-mission Skylab program. Additional changes in design requirements which reflected on the system design during this time are listed below:

1. Requirement for both Digital Command System (DCS) ground command capability and onboard control of O_2 and N_2 flow.

2. Removal of all N_2 systems from the CSM, including removal of the automatic two-gas control system. Removal of the provisions to transfer O_2/N_2 gas via an umbilical and QD from the CSM to the MDA.

3. Addition of the automatic two-gas atmosphere control system to the AM including the addition of two 5 PSIA cabin pressure regulators.

4. Addition of two 150 PSIG N_2 regulators in the AM to regulate N_2 coming into the cluster.

5. Requirement for 10 OWS water tanks containing a total of 6000 pounds of useable water due to the decision to supply all power for the cluster from solar cells, not from the CSM fuel cells. Along with this requirement came the requirement for two 35 PSIG N_2 regulators in the OWS (supplied from the AM) to pressurize the bellows in the water tanks.

6. Requirement for supplying N_2 to the OWS for biomedical experiments.

7. Requirement to supply N_2 instead of O_2 to the mole sieve pneumatic valves.

8. Requirement to supply two 5 PSIA N_2 regulators to pressurize reservoirs in the SUS cooling loop and the ATM C&D cooling loop systems.

9. Conversion of the M509 propulsion gas from O_2 to N_2. Addition of 3 high pressure (3000 PSIA) N_2 tanks (containing 10 pounds each) to the cluster for the M509 experiment. Addition of an N_2 recharge station in the AM for inflight servicing of the M509 N_2 tanks.

Changes were later required in the controlling range of the two-gas control system. The O_2 partial pressure control range requirement of the two-gas control system was initially 3.7 $\pm$0.2 PSIA. It was determined by system analyses that this range could not be consistently achieved, based on the assumption of stacking maximum specification tolerances of the PO_2 sensor/amplifier assembly and the maximum specification deadband tolerances of the O_2/N_2 controller. In addition, there was the potential for overlap of the PO_2 control band and the C&W alarm band, again based on maximum tolerance stackup. The sensor/amplifier specification tolerances were based on extreme ranges of temperature (40°F to 90°F) and O_2 partial pressure (0 to 6.4 PSIA) in addition to further allowances for test instrumentation errors and long term drift effects. Subsequent analyses using test data applicable to a more realistic temperature range (60°F to 90°F) and O_2 partial pressure range (2.8 PSIA to 3.9 PSIA) still showed a potential problem of consistently meeting the 3.7 $\pm$0.2 PSIA requirement.

A re-evaluation of cluster O_2 partial pressure limits during this time, resulted in a system PO_2 requirement change to 3.6 $\pm$0.3 PSIA. It was determined that this new requirement could be met by limiting the sensor/amplifier full-scale inaccuracy to $\pm$3 percent and by re-adjustment of the O_2/N_2 controller trip points. Accordingly, steps were taken to improve sensor temperature compensation so that worst case sensor/amplifier inaccuracy was 3 percent or less within the PO_2 range of 2.8 to 3.9 PSIA and temperature range of 60°F to 90°F. Also, the controllers were changed by adjusting the lower trip point to minimize control band width and adjusting the upper trip point to center the band width around a nominal 3.6 PSIA O_2 partial pressure.

E. Depressurization System

1. Waste Tank Vent - The waste tank concept originated in the days of the wet workshop. The original plan was to dispose of urine by dumping it overboard through a fitting installed by the crew in the side of the fuel tank. When tests revealed that this would be detrimental to the solar arrays, it was decided to have the crew punch a hole in the common bulkhead and install a heated dump probe so that urine could be dumped into the Liquid Oxygen (LOX) tank. The LOX tank was to be vented through the existing non-propulsive vent system and a second latching vent valve was added for redundancy.

In the studies preceding the conversion to the dry workshop concept, the LOX tank (now called the waste tank) was found to be a desirable place to dump numerous types of waste materials. The trash airlock was installed in the common bulkhead and two additional heated dump probes were added for flushing and draining various water systems. Also added were fittings for venting waste processor exhaust gases and refrigeration pump coolant leakage into the waste tank. Since propellants were no longer being carried, it was possible to pre-install all of this hardware.

In the original OWS LOX tank non-propulsive vent system, flow passed through one port in the tank, two parallel valves and two 20-foot long wraparound ducts to nozzles on opposite sides of the tank. Analytical studies showed that one of the two wraparound ducts would be subjected to temperatures well below the freezing point of water so that the duct was likely to become partially or completely blocked, leading to unbalanced thrust. Since this would have placed a large load on the Skylab control system, it was decided to redesign the vent system to its present configuration. The power cost for heating the present one-foot-long duct to prevent freezing was an order of magnitude less that what would have been required for the original wrap-around ducts. The original waste tank vent system had a small filter

screen covering the vent port. Because of concern that this screen would become completely blocked with trash bags, it was replaced by large area screens which separated the waste tank into compartments. The largest compartment received trash bags from the trash airlock. Each vent outlet was in a separate screened-off compartment and these two compartments were connected by a duct made of screen material to assure balanced venting. The liquid dump outlets were separated by screens from the trash area to prevent trash bags from freezing to the dump probes and possibly blocking them.

The original large screens were coarse (16 mesh) since their objective was to control migration of the trash bags. It was later decided to use the screens to prevent overboard venting of any solid waste that might interfere with optical experiments and the 16-mesh screens were replaced with Dutch twill woven screens having 2 micron filtering capability. Extensive developmental tests verified the filtering capability of the new screens but indicated that they could become blocked when urine was dumped on them. A baffle was then added to prevent direct impingement of the dumped urine on the screens.

2. Waste Tank Heated Liquid Dump Probe - The original heated probe was 3.5 inches long and extended only 0.5 inch beyond the waste tank bulkhead. A Kapton heater blanket was wrapped around the 0.25 inch diameter silver tube and held in position with a coil spring. Front and back heaters were sized at 7.5 watts each.

During qualification testing, the heater blanket overheated and failed due to poor thermal contact between the blanket and silver tube. Two attempts to improve the thermal contact (using Eccobond to bond the blanket to the outside diameter of the silver tube and using Nomex yarn woven over the heater blanket to hold the blanket against the silver tube) were unsuccessful.

A decision was made to redesign. The basic objective was to keep the water from freezing. The approach was to double the heater power and to increase the heat flux to the probe tip. The length of the probe was increased to extend 6 inches beyond the bulkhead to reduce ice bridging potential. Redundant heater circuits were maintained and each circuit was positioned lengthwise over the entire length with a watt density of 3 watts/inch at the probe tip and a watt density of 1 watt/inch at the upper end of the probe. The orifice at the tip was angled and located radially to expel liquid parallel to the waste tank baffle, thereby preventing ice buildup.

3. Habitation Area Vent Valve System - Prior to SL-1 launch, testing indicated the possibility that an excessive delta P across the OWS common bulkhead would occur with the Saturn S-IVB wraparound duct orifice and a vent sequence which allowed the OWS habitation

area and waste tank to vent simultaneously at orbital insertion. The initial vent sequence was revised so that the OWS habitation area would be vented at 205 seconds after liftoff rather than at orbital insertion and the orfice diameter decreased from 1.78 inches to 1.49 inches. These two changes decreased the common bulkhead delta P to acceptable levels.

The OWS pneumatic system for the waste tank and habitation area vent valves was essentially the same as that used on S-IVB except that the regulator was removed. This simplficiation was the result of a shorter required operational life (1 hour versus 7 hours on S-IVB) and confidence in the system's low leakage capability built up during the S-IVB program which permitted lowering the supply pressure to a level within the operational range of the actuators.

4. Solenoid Vent Valve System - The habitation area vent system on the wet workshop consisted of the S-IVB pneumatic vent valves and a crew operated valve for venting the residual hydrogen vapor. At the time of wet-to-dry conversion, it was decided to add capability to vent by ground command at any time in the mission. Since it was felt to be impractical to maintain a pneumatic supply throughout the mission, it was decided to replace the manual valve with a set of four solenoid operated vent valves. As a result of system design review activities during the Skylab Operations Compatibility Assessment Review during 1972, a decision was made to add a vent screen over the entrance to the four solenoid valves to prevent debris from being blown into the valves. (Even with the screen, some blockage of the solenoid vent valves occurred during the flight [see Section VI.B.3]. Without the screen, the effectivity of the solenoid vent valve system would have been severely limited.)

5. MDA Vent Valve System - The initial MDA vent valve design consisted of two four-inch vent valves in parallel. These valves were later installed in series to provide redundancy for the failure mode condition of one valve not closing when commanded by the Instrument Unit (IU). The originally planned ground command capability for the valves was also deleted since the command capability would be needed only in remote contingency situations.

6. Aft AM Vent-to-Vacuum - This vent was used in the wet workshop to vent the aft section of the AM to a vacuum during boost, thereby preventing any chance of having a higher pressure in the aft AM than in the OWS while the OWS was being vented to vacuum to remove all the LH_2. The vent could be manually closed by a crewman in the airlock and the aft AM could then be pressurized. When the dry workshop concept was selected, the aft compartment could be vented to the lock compartment, so the valve was removed. Two check valves were placed in the OWS hatch to prevent any higher pressure on the aft AM side of the OWS dome.

F. Airlock Module (AM) Cooling Loop

Several design changes were made during the program due to revised system requirements and a few development problems which were encountered. The original concept of the Airlock Module cooling loop included a single 40°F thermal control valve downstream of the radiator. The requirement for this configuration was to provide a minimum dewpoint of 40°F and a 55°F water inlet temperature to the Life Support Umbilical interface while absorbing heatloads of 2000 Btu/hour from each of two astronauts. However, a requirement for 45°F water inlet temperatures resulted in moving one of the heat exchangers interfacing the water suit cooling loop with the AM cooling loop upstream of the 40°F control valve. A thermal capacitor was added downstream of the radiator in order to accommodate the system loads and maintain adequate temperature control throughout the orbital period. A requirement to provide cooling to the ATM console and various EREP components resulted in the addition of the ATM/EREP water cooling loop to interface with the AM coolant loop. The resulting system is shown schematically in figure A-1. A major perturbation to this design was produced by a combination of concerns over the life of the AM batteries with a resulting requirement to provide lower battery temperatures and a requirement to provide a 46°F minimum dewpoint. The 40°F control valve at the inlet to the condensing heat exchanger was replaced with a 47°F valve to resolve the dewpoint problem (paragraph A-2 of this Appendix) and the 40°F control valve was relocated upstream of the battery module to provide lower temperatures. A second 47°F control valve was added along with one additional heat exchanger (in each cooling loop) and the system flow paths were rerouted to provide the desired automatic control system. The resulting system is depicted in figure A-2. However, tests conducted to prove the stability of the system showed that the system was unstable.

Because of the short time available to develop a design which would provide control stability, a test approach was taken. The tests led to rearrangement of the lines interconnecting the suit cooling heat exchangers, the addition of a heat exchanger bypass line with bleed orifice, and the addition of the EVA flow selector valve. The final system configuration is depicted in figure A-3. The purpose of the above changes was to thermally isolate the hot and cold inlets to the downstream temperature control valve (TCVB). In the baseline design, the hot and cold inlets were thermally coupled through the heat exchangers upstream of the valve to such an extent that a small temperature differential existed for normal operating conditions and the thermal inertia of the system produced excessive valve movement (and instability)when valve movement was required due to load or temperature changes. Several configurations which

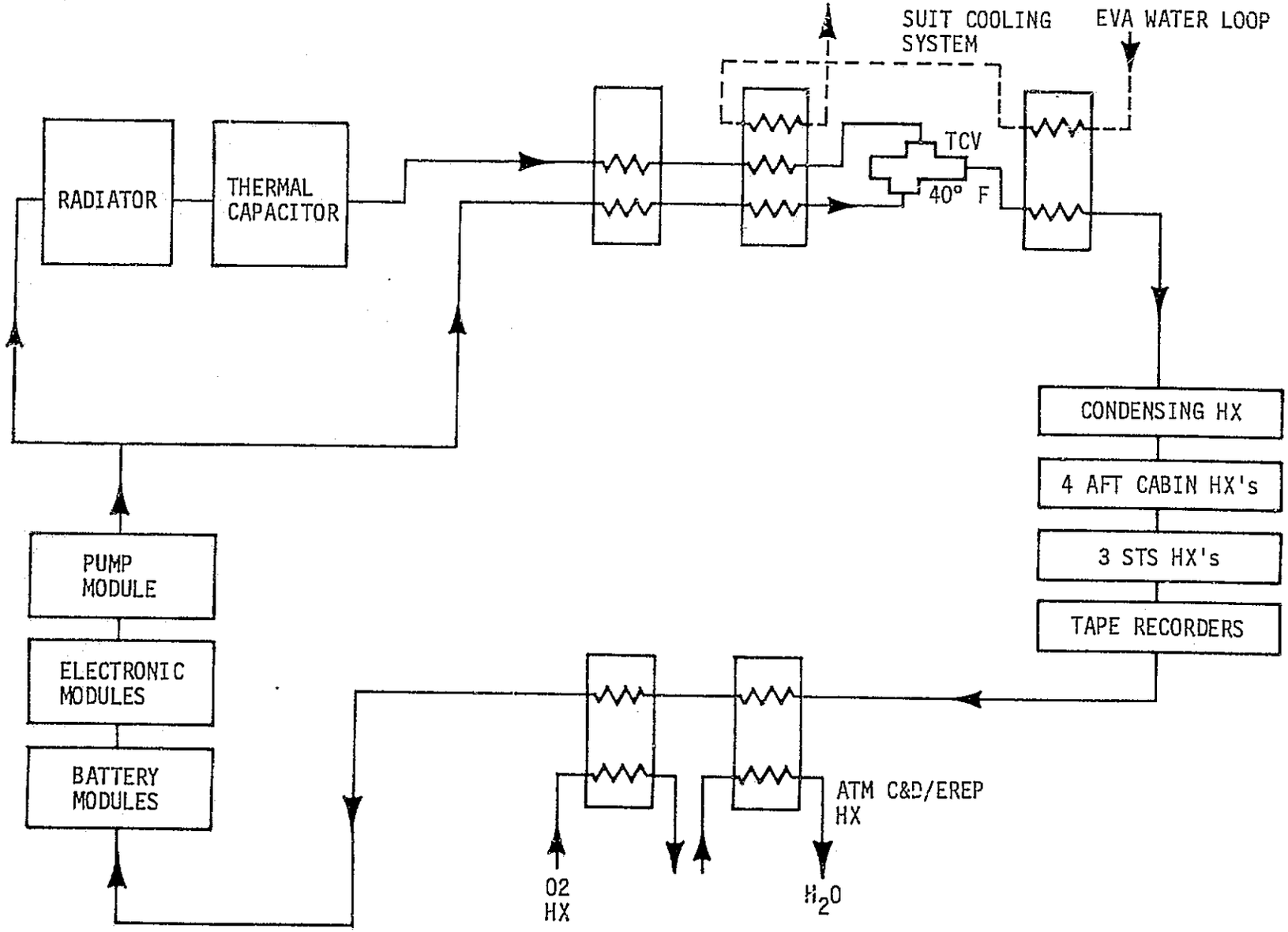

Figure A-1. AM Cooling Loop (40°F System)

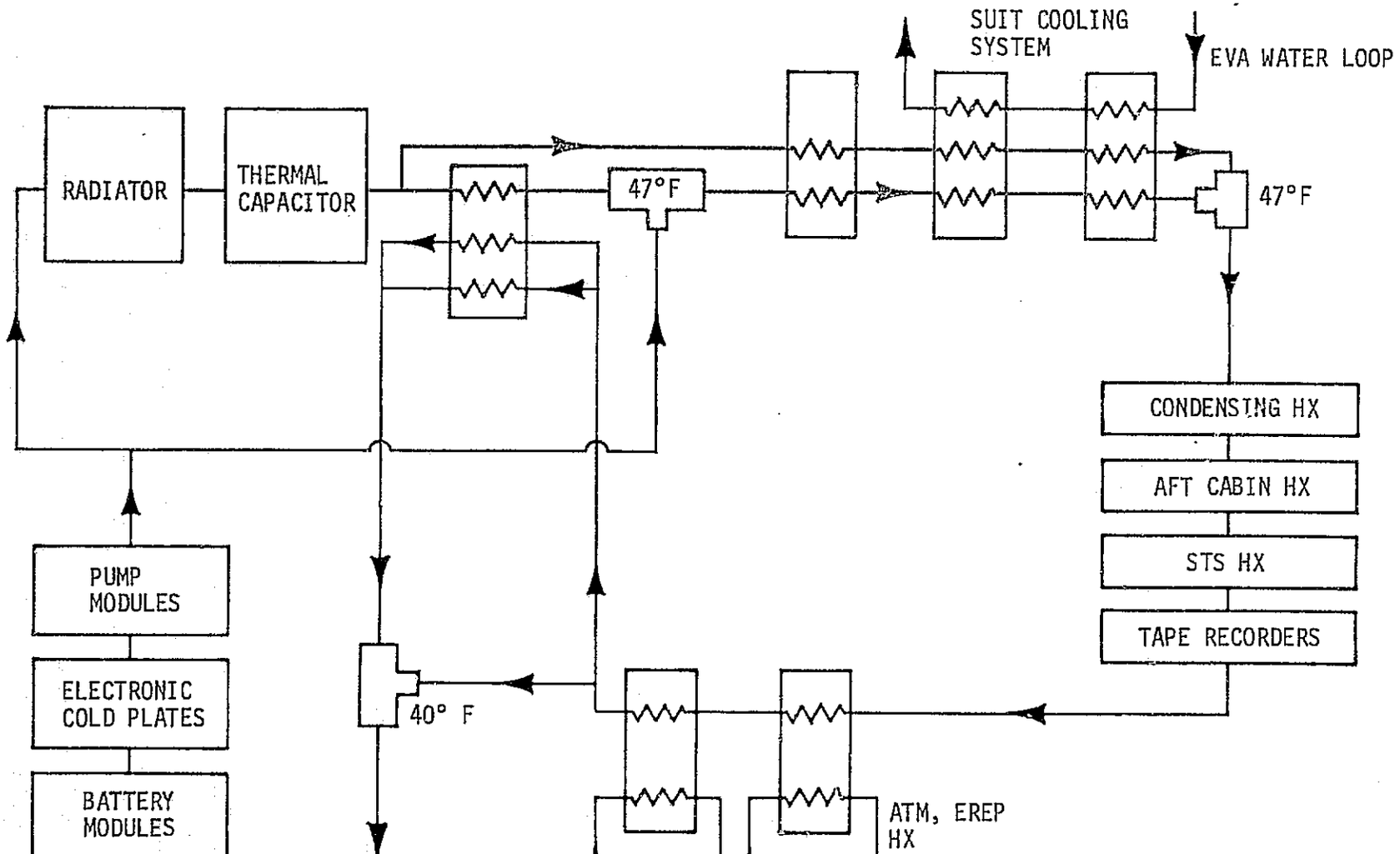

Figure A-2. AM Cooling Loop (47°F Unstable)

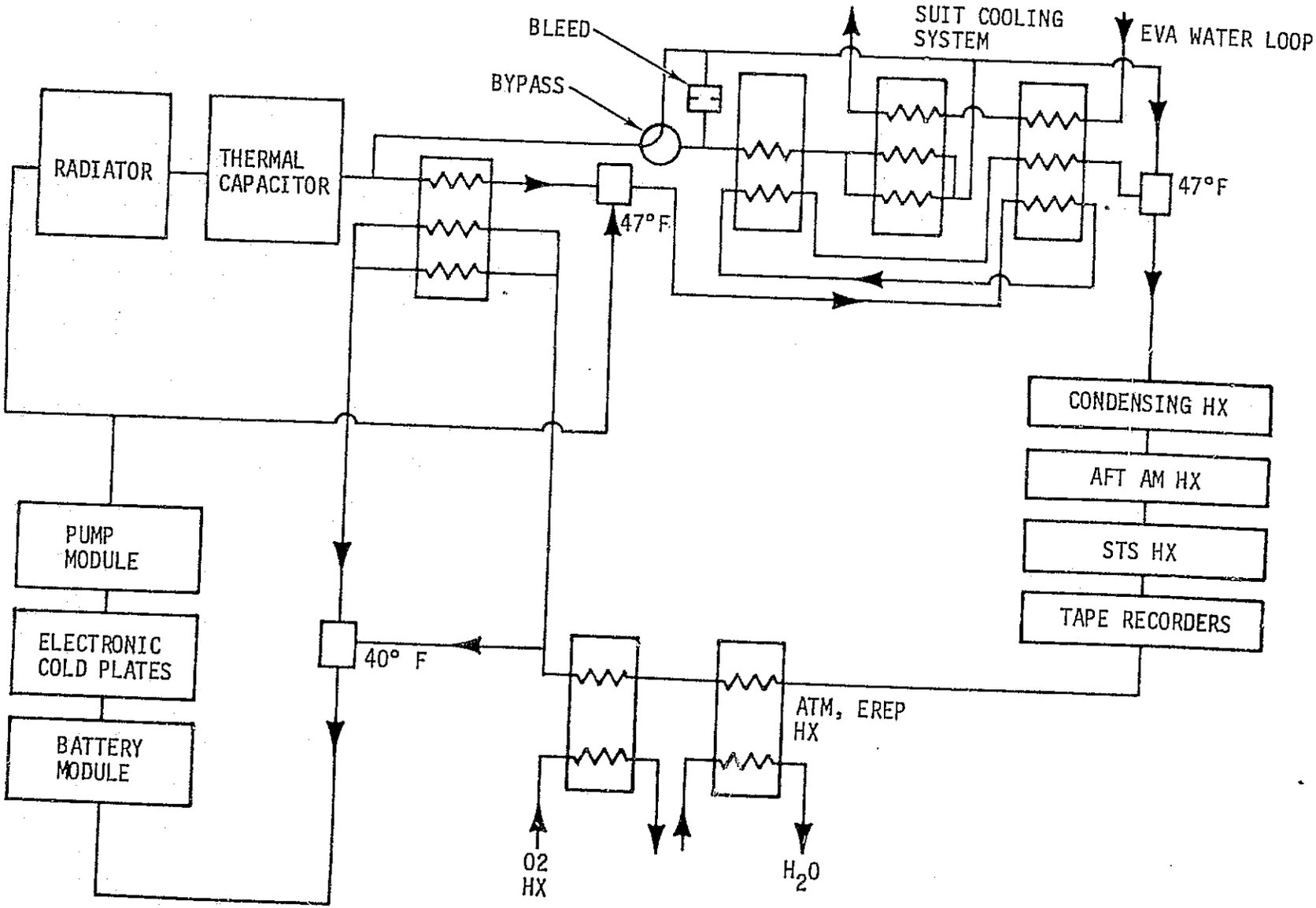

Figure A-3. AM Cooling Loop (Final)

incorporated only the rearrangement of lines interconnecting the heat exchangers were tested. Some improvement was seen, but, in order to attain stability over the required range of heat load and temperature conditions, other changes were necessary. A bypass valve was incorporated for use during non-EVA which completely bypassed the suit cooling system and regenerative heat exchanger. A bleed of approximately 30 lb/hour of cold flow was incorporated which, coupled with the rerouting of lines through the heat exchangers, resulted in stability for EVA conditions.

A design change was required for the thermal capacitor after the OWS Refrigeration System (RS) capacitor failed during qualification testing. (The only difference between the AM and RS capacitors was the use of Undecane wax in the RS design rather than Tridecane was.) The container ruptured as a result of forces produced by the volume change during melting. An ullage was available, but the design allowed the ullage to be far removed from the phase change location. In the original design, the cells within the capacitor were interconnected and the ullage could be located anywhere within the capacitor. The final design incorporated a honeycomb cell structure with ullage in each of the cells. Since requirements associated with the Z-LV orientation for expanded EREP operations had significantly reduced the radiator capability for some maneuvers, a second twenty pound capacitor was added as part of the redesign to provide additional capability.

The original design of the suit umbilical system water loop did not incorporate a liquid/gas separator. The separator was added due to concern that free gas might be introduced into the loop by frequent making and breaking of QD's for configuration changes. In retrospect, a similar separator should have been added to the ATM C&D/EREP water loop since free gas problems were encountered in flight. However, the Roccal additive in that loop was not compatible with the separator and the approach taken was to minimize the free gas present in the loop. The additives were changed in the SUS loop and the change resulted in additional problems as discussed in the following paragraphs.

The early design of the SUS loop utilized untreated MMS-606 (deionized) water as the circulating medium. Vendor pump tests using this fluid disclosed starting problems, caused by corrosion on the pump internal parts. These problems forced a change of the pump vanes, rotor, and liner materials from the more wear resistant tungsten carbide to a more corrosion resistant carboloy alloy. The materials changes combined with the addition of additives to the water for corrosion and bacterial control resulted in satisfactory pump performance. These additives were 2% by weight of dipotassium hydrogen phosphate and 0.2% by weight of sodium borate for corrosion control and 500 PPM Roccal for bacteria control. This fluid composition and pump design was also used in the ATM C&D/EREP coolant system.

After installation of the liquid/gas separator in the SUS loops, testing indicated that the Roccal additive was incompatible with the separator performance, causing water carry-over through the gas discharge port. A concern was also expressed about the presence of the Roccal reducing the strength properties of the tygon tubing in the LCGs. The Roccal was therefore replaced by 20 PPM movidyn, another biocide consisting of a colloidal silver solution. Subsequent SUS loop operation with this new fluid resulted again in problems with pump starting. Failure analysis determined that the pump locked up after dormancy due to deposits formed by interaction of the dipotassium hydrogen phosphate and silver in the movidyn with nickel from the fins of the SUS loop heat exchangers. These deposits formed between the pump vanes and rotor interfaces, preventing one or more of the vanes from moving freely in the rotor slots.

At that point in the program, the flight vehicle was undergoing final tests in preparation for shipment to KSC, so a crash effort was undertaken to determine a solution to the problem. The basic approach was to find a suitable replacement for the water solution. Simultaneously, additional design analyses and tests were conducted on alternate pumps and heat exchangers in the event of failure to find a suitable replacement fluid. An alternate pump module, utilizing a modified CSM coolant pump, powered by a transformer and compressor inverter, was designed and tested as a backup to the existing pump module. Also, a design feasibility study was initiated to modify the SUS loop heat exchangers to an all stainless steel configuration.

Neither of the above design changes was required. The final solution was arrived at by beaker-type materials testing and end-to-end systems testing on a variety of candidate fluid compositions. These tests established SUS loop compatibility with a fluid consisting of MMS-606 water containing additives of 20 PPM movidyn and 500 PPM sodium chromate. The SUS pumps were also modified by increasing the vane/rotor clearance to further minimize start up problems.

The flight vehicle SUS loops were drained, cleaned, and re-serviced at KSC with the new fluid. The modified increased clearance pumps were also installed. The final system configuration proved to be satisfactory as evidenced by the fact that no problems with SUS pumps were experienced at any time during the mission.

G. Refrigeration System

The original Refrigeration System (RS) design included a low temperature proportional mixing thermal control valve similar to the Airlock Module cooling loop thermal control valves. This valve controlled the flow through the PM radiator such that the mixed temperature was -17 ±3°F. The original system is depicted in figure A-4.

Three development problems were encountered with the thermal control valve during development:

1. A side displacement (squiring) of an internal metal bellows resulted in drift in the control temperature.

2. Outlet temperature instability due to high gain at extremes of sleeve position.

3. Poor quality control of bellows welds which resulted in failures during tests.

As a result of the above problems, the valve was deleted from the design. In order to provide low temperature control of the system, the existing radiator bypass valve control logic was modified. The temperature sense points for valve actuation were moved from the capacitor third segment outlet to the capacitor first segment outlet, and the temperature trip points were adjusted from -20°F and -40°F to -13°F and -34°F. When -34°F was achieved, the bypass valve was commanded to full radiator bypass. When the sense point warmed to -13°F, the valve returned to full radiator flow. The final system configurations is depicted in figure A-5.

The RS thermal capacitor was redesigned along with the Airlock Module cooling loop capacitor as discussed in paragraph F. of this appendix.

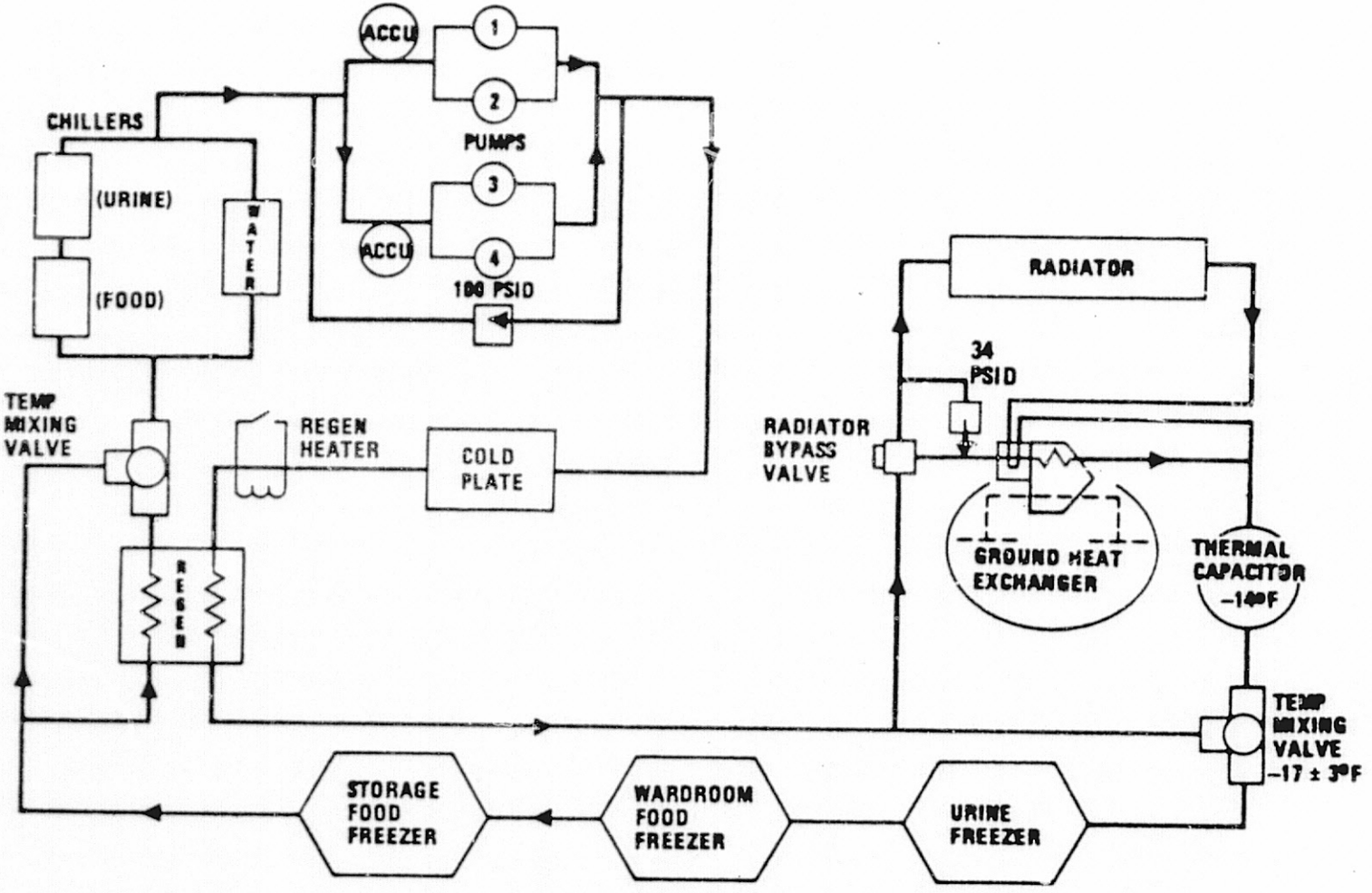

Figure A-4. Original RS Design

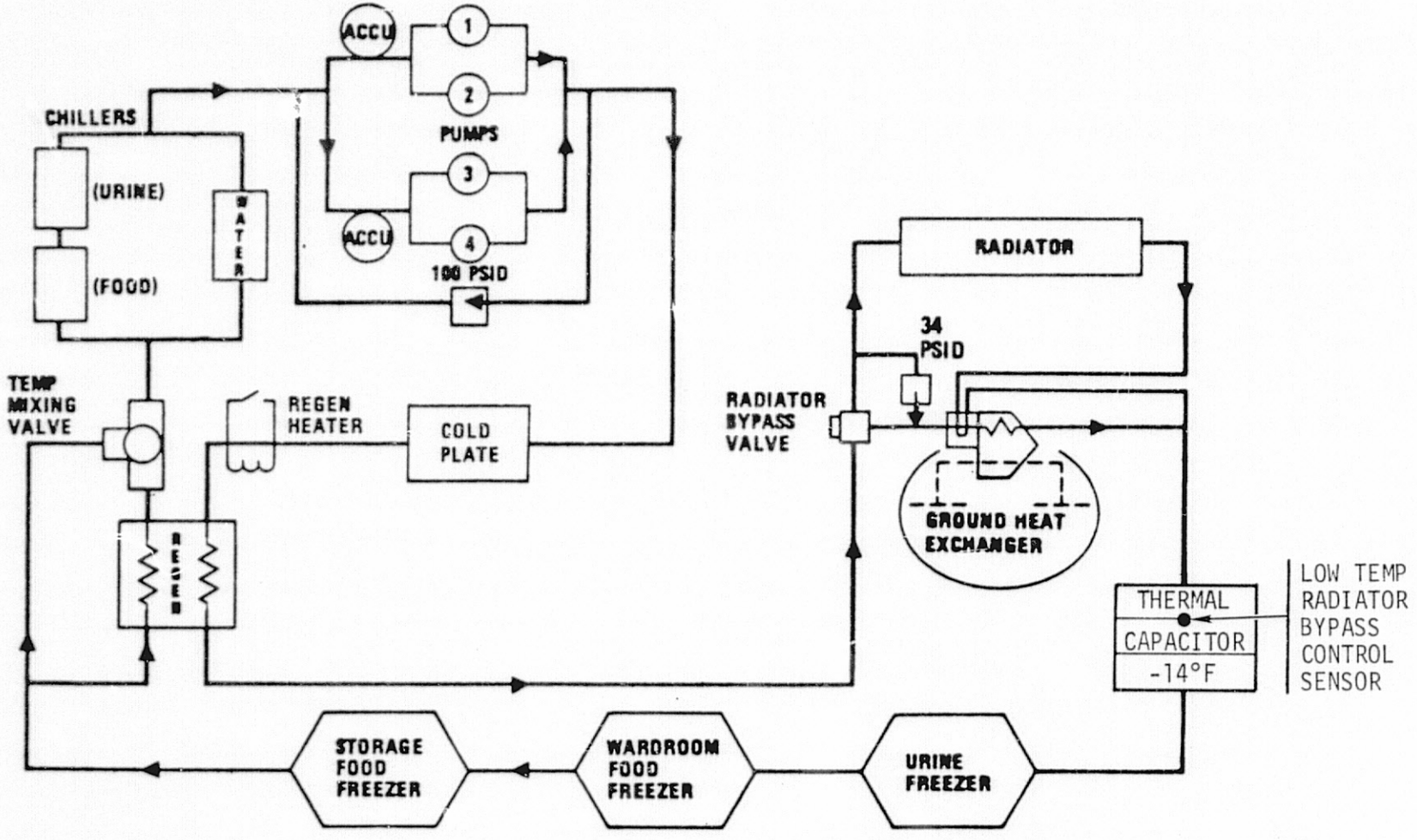

Figure A-5. Final RS Design

APPENDIX B. OWS SOLAR ARRAY SYSTEM

A. OWS Solar Array System (SAS) Deployment Description

The OWS solar array panels were stowed within two fairings approximately 180° apart on the sides of the stage. Deployment was to be accomplished in two parts. First, the beam fairings containing the panels were to be released from the OWS tank sidewall and rotated approximately 90°, extending from the OWS forward skirt. Second, the panels were to be released from the beam fairings and unfolded to the deployed position. Release of the beam fairings and the panels were to be accomplished by firing ordnance within expandable tubes which would sever the tiedown links, allowing deployment to commence. Deployment rates of the beam fairings and panels were controlled by actuator/dampers (A/D) shown in figures B-1, B-2 and B-3. The spring provided the energy source for deployment and the damping fluid served to control the deployment rate. Once deployment was completed, the panels were locked in a position such that their active surface was normal to the sun when the vehicle was in the solar inertial orientation.

B. OWS Solar Array System (SAS) Deployment Thermal Evaluation

At approximately 63 seconds into the Skylab I flight, the vehicle experienced structural failure of the OWS meteoroid shield. This failure unlatched and partially deployed SAS Wing 2 beam/fairing which was subsequently torn off by the SII retro-rocket plume impingement at 593 seconds. A bent piece of meteoroid shield splice joint held the OWS SAS Wing 1 beam/fairing (B/F) such that the three wing sections were only partially deployed as shown in figure B-4. On DOY 158 when the crew performed an EVA to deploy the SAS, the temperature of the B/F actuator/damper (A/D), located in the forward fairing, was estimated to be -60°F. The B/F and wing section A/D's were designed and tested to minimum temperatures of -7°F and -25°F, respectively. These temperatures were consistent with the SL-1 timeline which provided for nominal deployment at liftoff. Post liftoff testing results indicated that the B/F A/D would fail to move at temperatures below -40°F, due to the increase in the fluid viscosity. A sketch of the A/D is shown in figure B-5 and its fluid viscosity is given in Table B.1. The damping fluid for both wing and beam fairing A/D's was Dow Corning Silicone 200. However, different fluid viscosities were selected for the B/F and wing section A/D's based on their individual thermal and dynamic requirements. For the B/F A/D the viscosity of the fluid increases as its temperature decreases such that the spring force could not overcome the fluid damping force at -40°F.

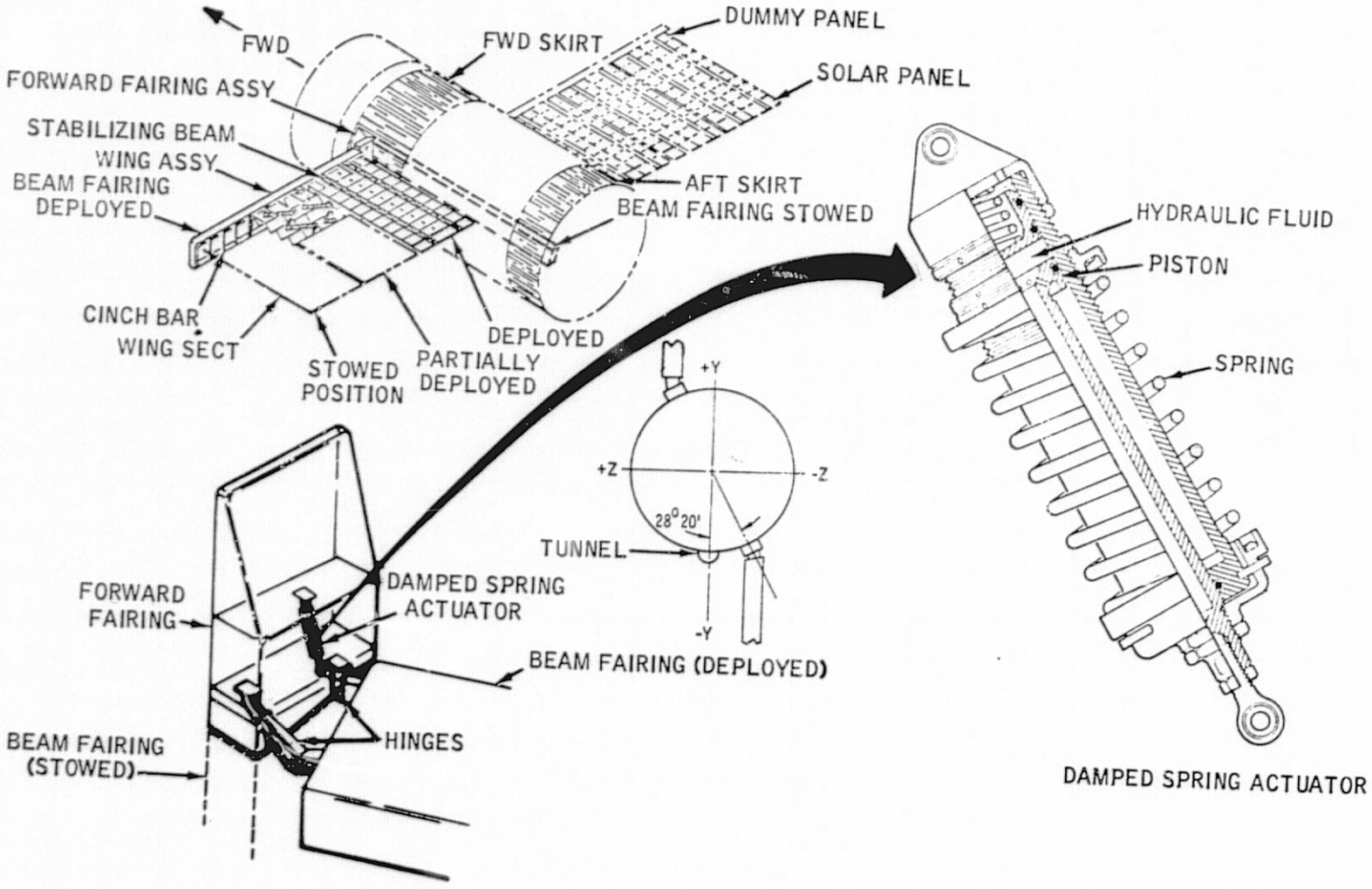

Figure B-1. SAS Deployment Mechanism

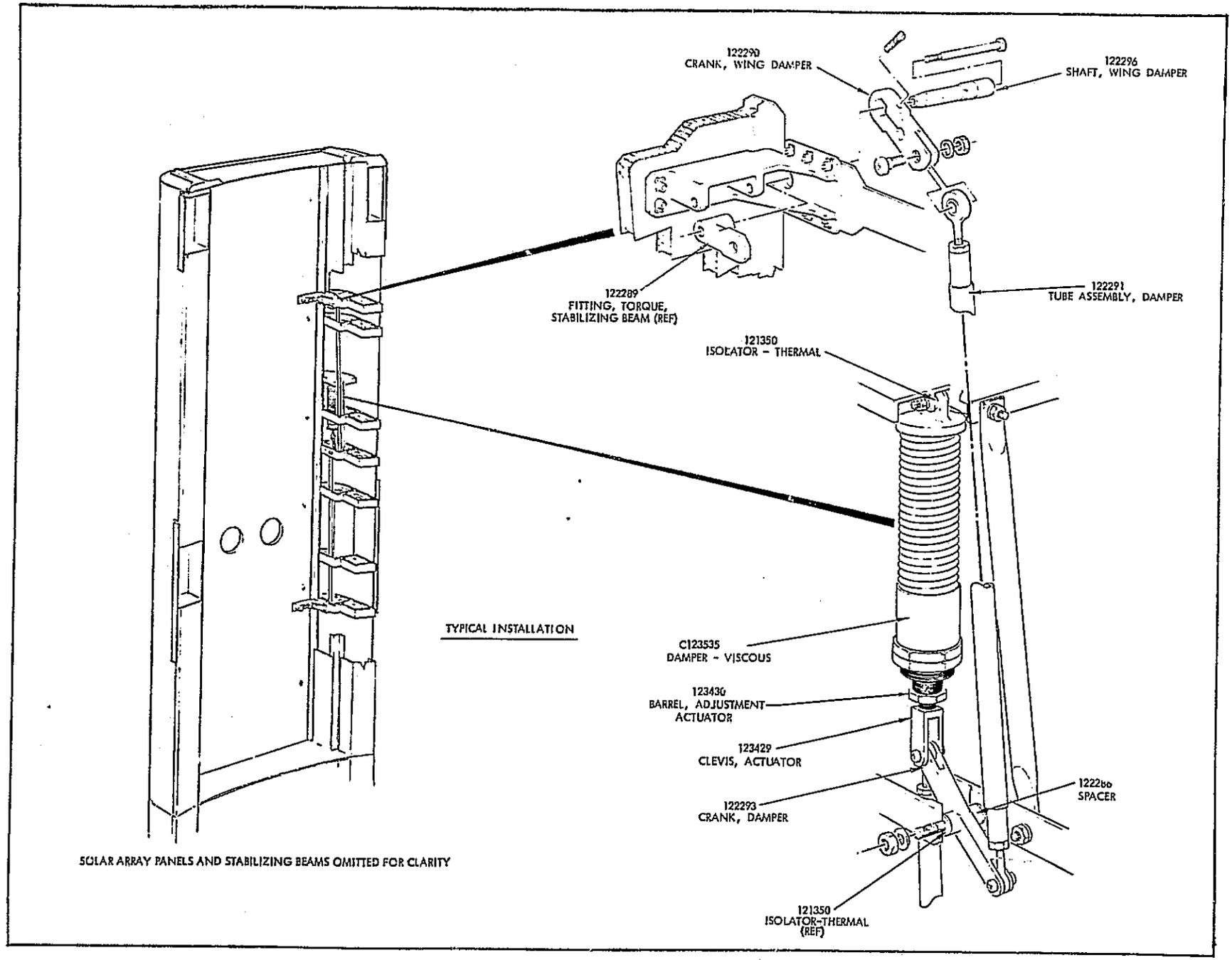

Figure B-2. Wing Section Actuator/Damper

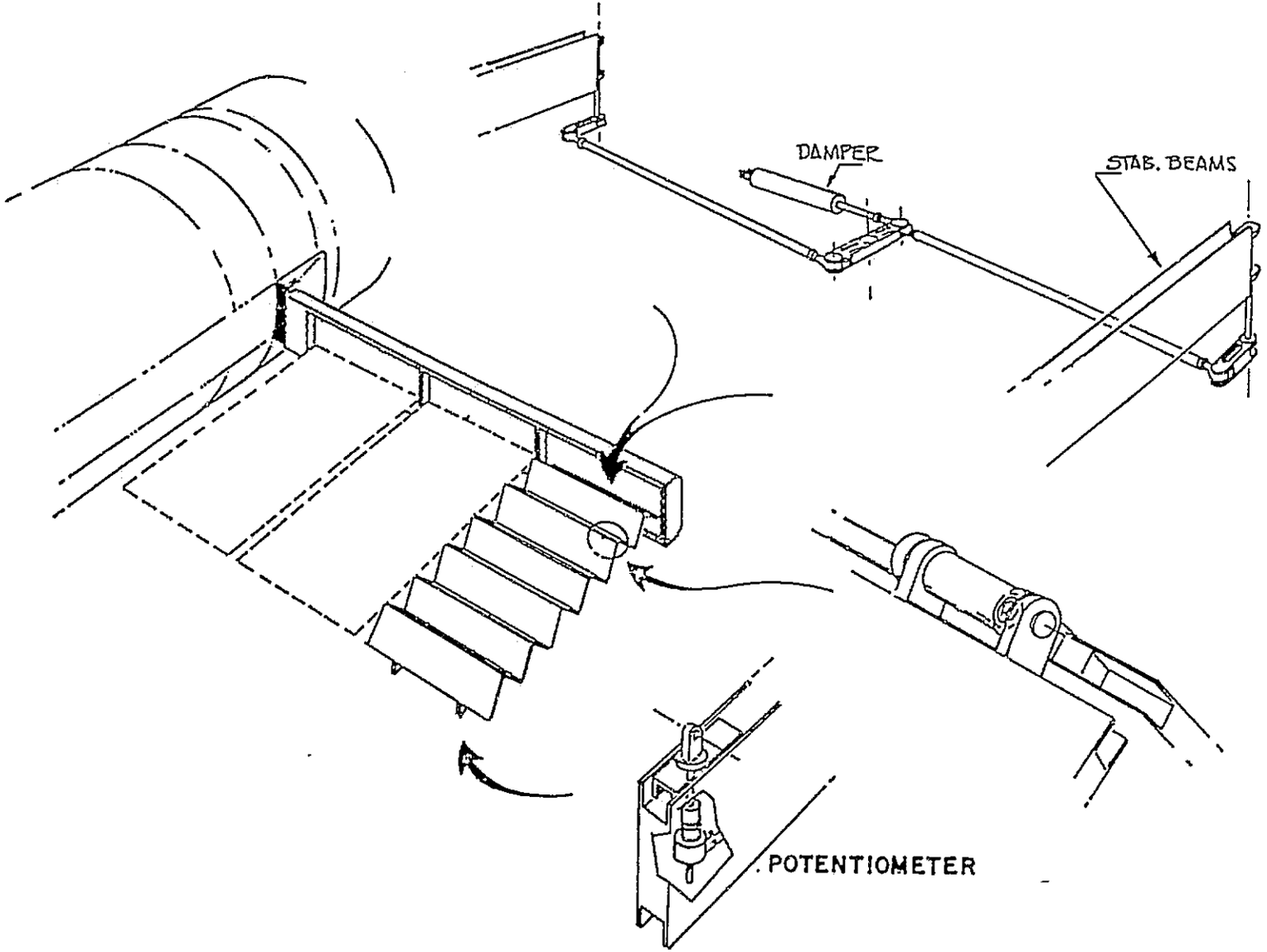

Figure B-3. Wing Sections Partially Deployed

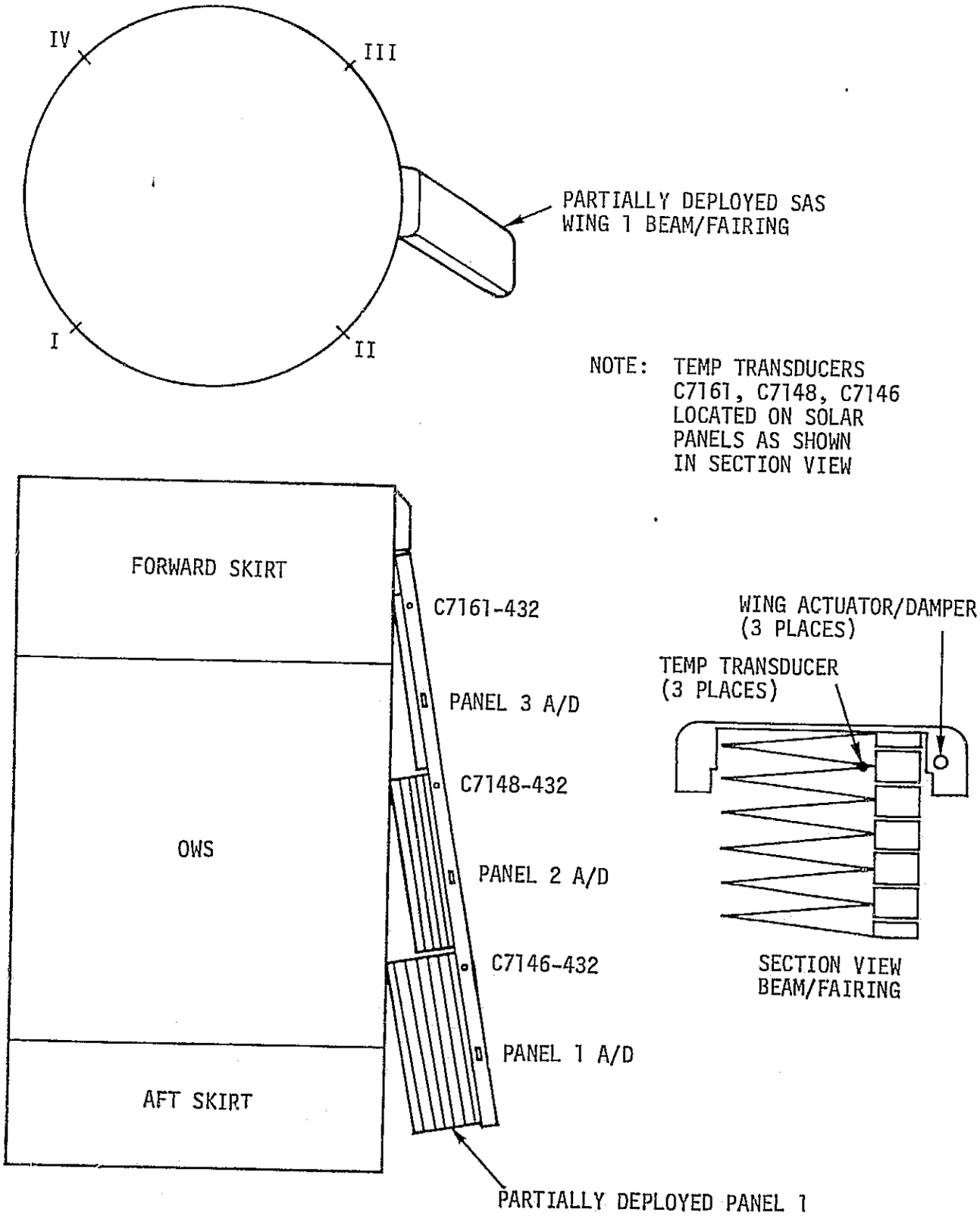

Figure B-4. Partially Deployed SAS Wing 1

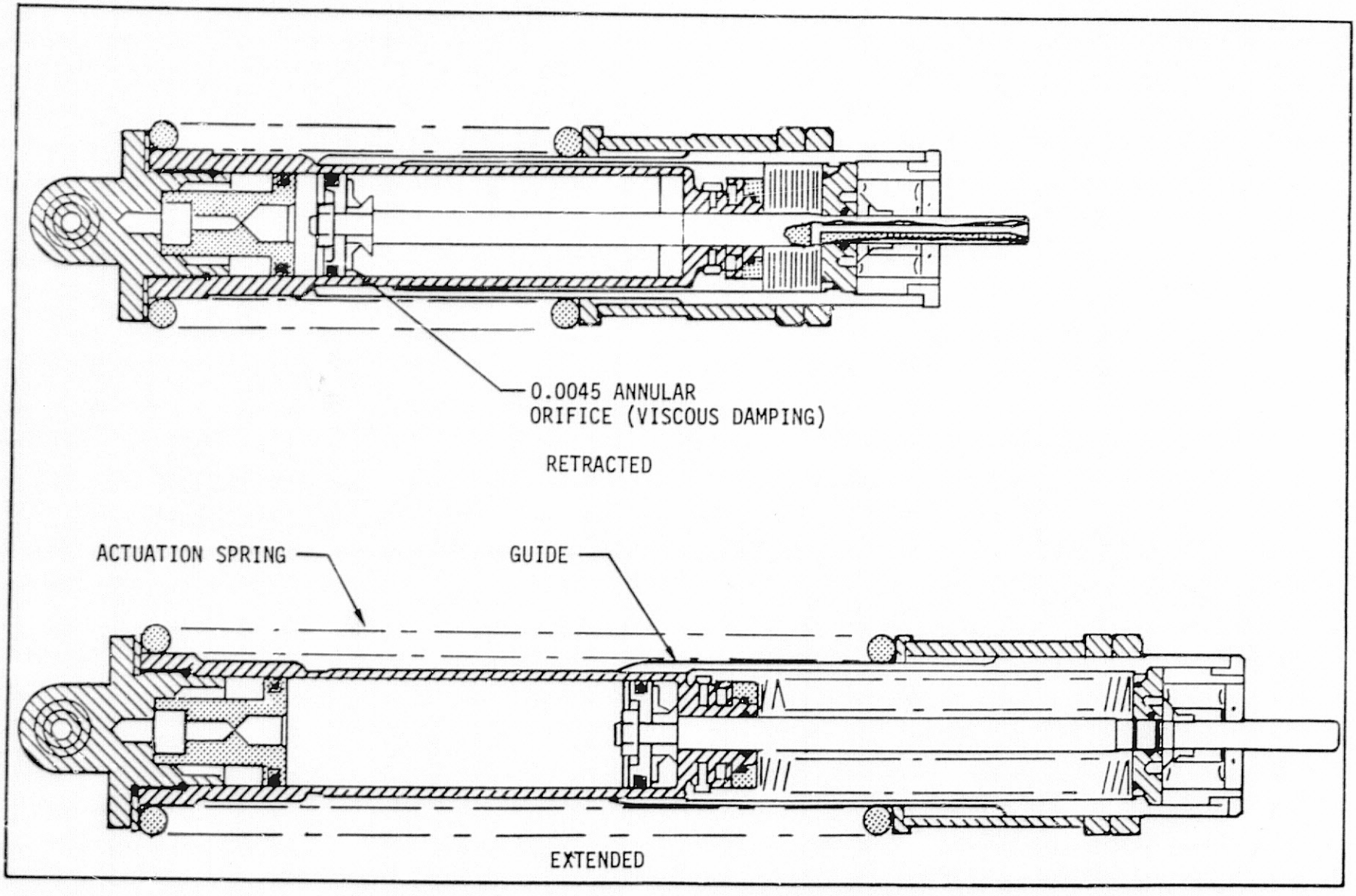

Figure B-5. SAS Beam Fairing Antuator/Damper

Table B.1 SAS Beam/Fairing and Wing Section
Actuator/Damper Fluid Viscosity
(Dow Corning Silicone 200)

TEMPERATURE (F°)	VISCOSITY (CENTISTOKES) BEAM FAIRING	WING SECTION A/D
-60	87,000	63,000
-40	62,000	45,000
-20	45,000	34,000
0	33,000	25,000
40	19,500	15,000
80	13,000	9,500
120	8,400	7,000
160	5,900	4,700

A maneuver was defined to warm-up the B/F A/D such that the B/F would deploy after the meteoroid shield debris was removed but was not implemented due to the consequent reduction in electrical power availability. Rather, the crew, after cutting loose the meteoroid shield debris, broke a clevis which provided a link between the A/D and the forward fairing. This allowed the B/F to deploy fully with the A/D still frozen. After B/F deployment, the wing sections did not immediately fully deploy because the wing section A/D's were also frozen. These A/D's were identical to the B/F A/D's except that their fluid viscosity was somewhat less as shown in Table B.1.

After B/F deployment, the wing section A/D's cooled down, since the SAS was no longer adjacent to the warm OWS stage. Figure B-6 represents the predicted cooling characteristics of the wing A/D with the B/F deployed. Subsequently, a planned -45 degree pitch maneuver was made to direct solar heating on the B/F top surface to warm the frozen wing section A/D's and allow wing section deployment. Figure B-7 shows the predicted warm-up rate of the wing A/D assuming a pitch attitude of -50 degrees, which would produce a slightly greater warm-up rate than a pitch of 45 degrees.

SAS sensor C7161-432 (figure B-4) was monitored real-time to estimate the temperature of the wing section A/D's prior to deployment. Analyses indicated that the coldest wing section A/D (Panel 3) was about 10°F colder than the sensor indication. The analysis further indicated that the outboard wing A/D (Panel 1) was about 15°F warmer than the cold

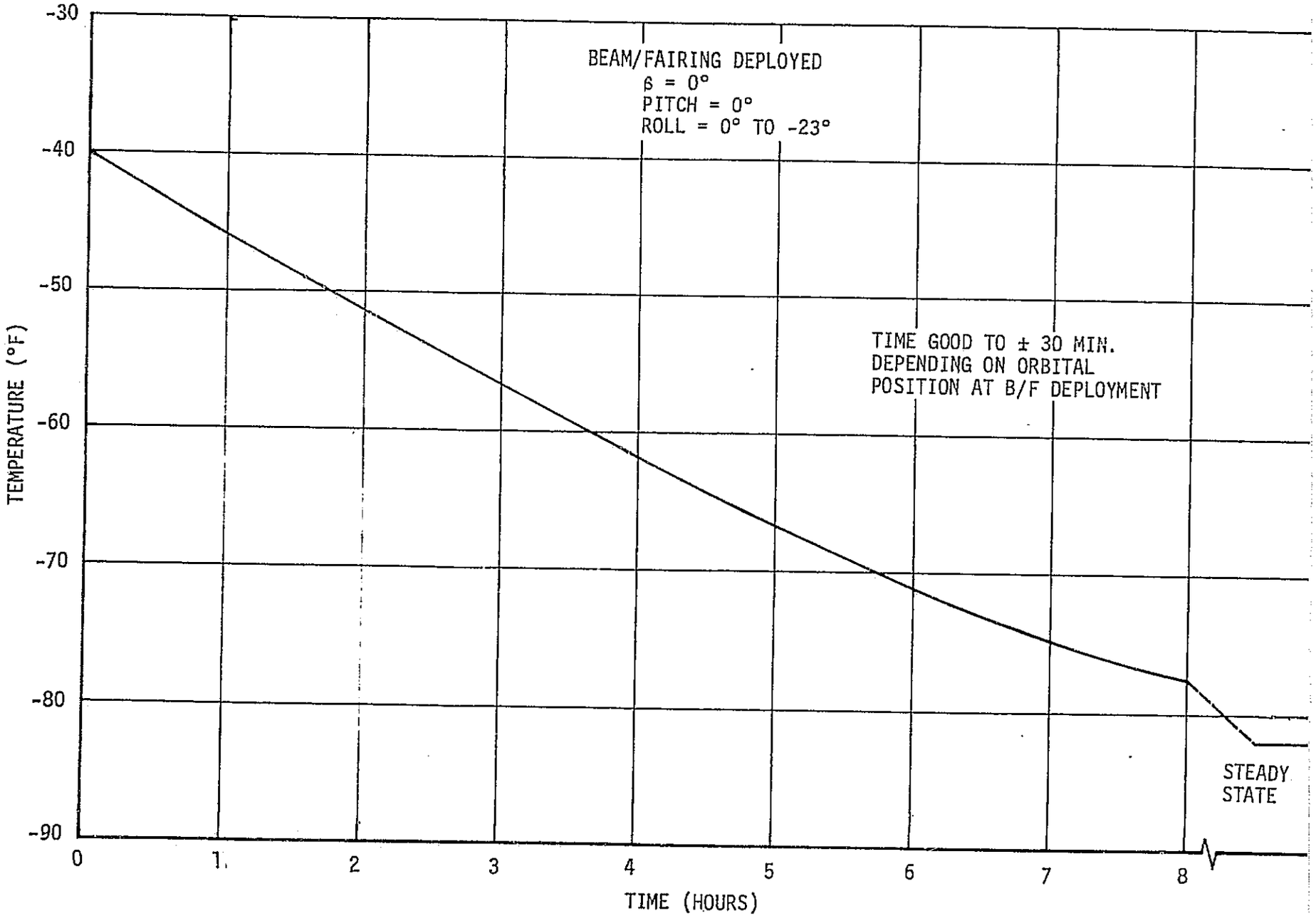

Figure B-6. Wing Actuator/Damper Cool-Down

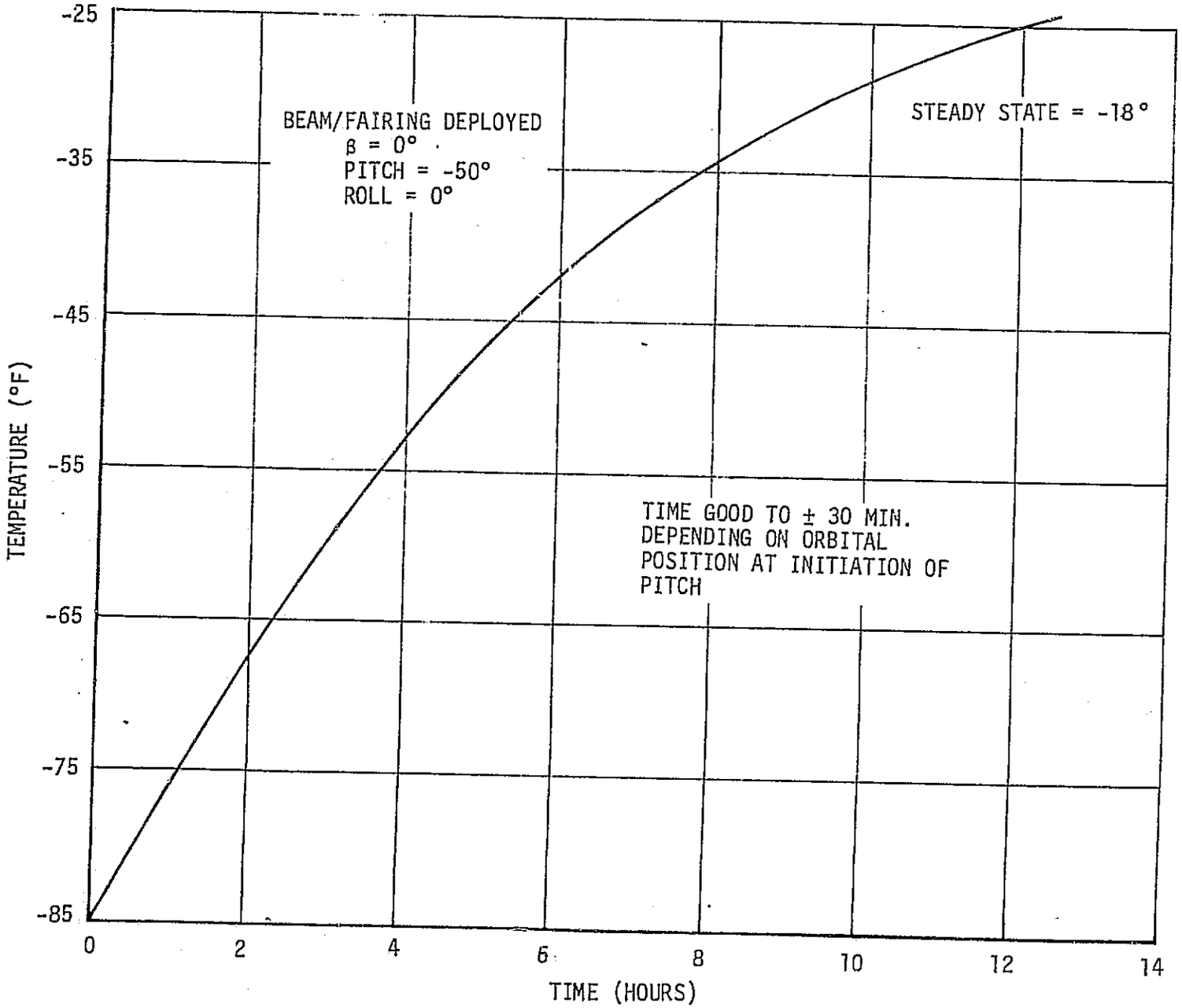

Figure B-7. Wing Actuator/Damper Warm-Up

A/D's. Locations of the A/D's and temperature sensors are shown in figure B-4. Figure B-8 shows the recorded history of C7161-432 to the time of B/F deployment, at which time, the indicated temperature was -45°F. The A/D to sensor temperature difference relationship established by analysis would indicate that the coldest and warmest A/D's were -55°F and -40°F, respectively, at the time of B/F deployment. However, the deployment test data given in figure B-9 indicate that Wing Panel 1 would have deployed within 10 minutes following B/F deployment if the Panel 1 A/D was at a temperature of -40°F. Test results also showed that below -50°F the damper fluid viscosity was too great to permit actuator extension. Since Panel 1 did not deploy shortly after B/F deployment, the Panel 1 A/D must have been initially at or below -50°F, and the A/D's on Panels 2 and 3 must have been approximately -65°F, as substantiated by the following discussion.

The SAS Panel 1 A/D temperature history was generated assuming its temperature was at -50°F at the time of B/F deployment, and compared with the deployment percent and vehicle attitude timelines in figure B-10. The analysis showed that following B/F deployment, the Panel 1 A/D cooled from -50°F to -60°F, at which time (1944 GMT) the vehicle was pitched -45 degrees, and the wing A/D began to warm up. At about 2130 GMT the Panel 1 A/D had increased to approximately -50°F, and within 40 minutes, Panel 1 was 100 percent deployed. The temperature of the cold A/D's (Panels 2 and 3) was assumed to be -65°F (15°F colder than the Panel 1 A/D) at B/F deployment. Following the cooldown and warmup, Panels 2 and 3 A/D's had reached -50°F shortly after 2300 GMT, at which time these panels started to deploy, and 100 percent deployment was noted at 0030 GMT on DOY 159. The vehicle was returned to the solar inertial attitude at 2340 GMT. The times of deployment were somewhat longer than the temperature-deployment time relationship established by the test.

C. OWS Solar Array Thermal Evaluation

Due to the changes in vehicle configuration, the pre-flight thermal models of the OWS SAS had to be verified. The OWS meteoroid shield was removed and the parasol/twin pole sun shield was added to the thermal model. The model was then used to predict temperatures of the solar cells and the SAS temperature transducers located on the edge channel of the panels. The location of the transducers is shown in figure B-11.

Comparison of flight with predicted temperature profiles showed good correlation. However, two differences did exist. Figures B-12, B-13, B-14, and B-15 show the flight and predicted temperature profiles for the transducer C7147 at β angles of 0°, 30°, 65.5° and 75.5°, respectively. As shown in figures, the temperatures compare well during the sunlit period of the orbit. However, it is seen that near orbital noon, the flight data reached and sustained peak temperatures

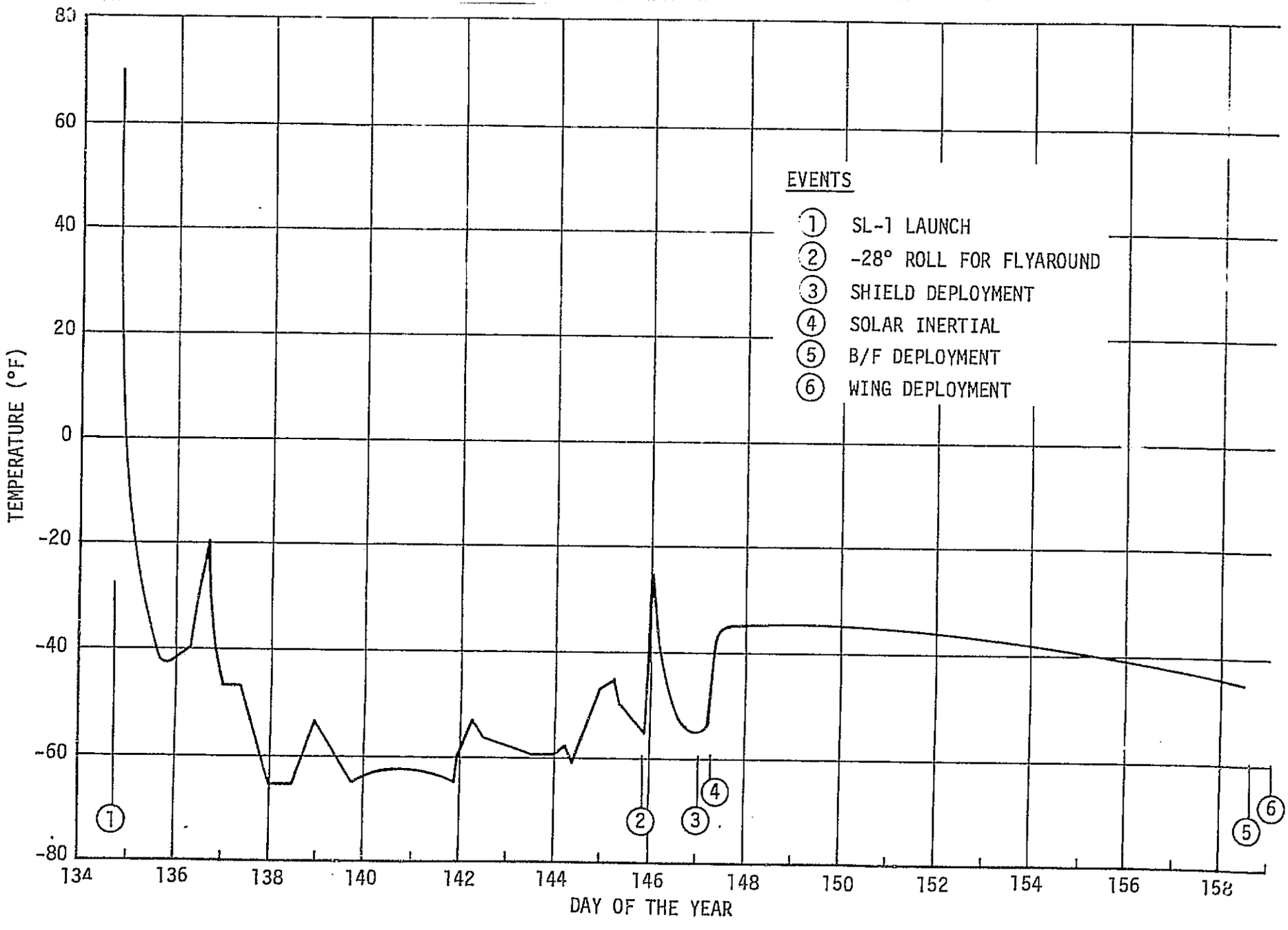

Figure B-8. SAS Wing 1 Sec 3 Panel 3
Sensor C7161-432
Temperature History

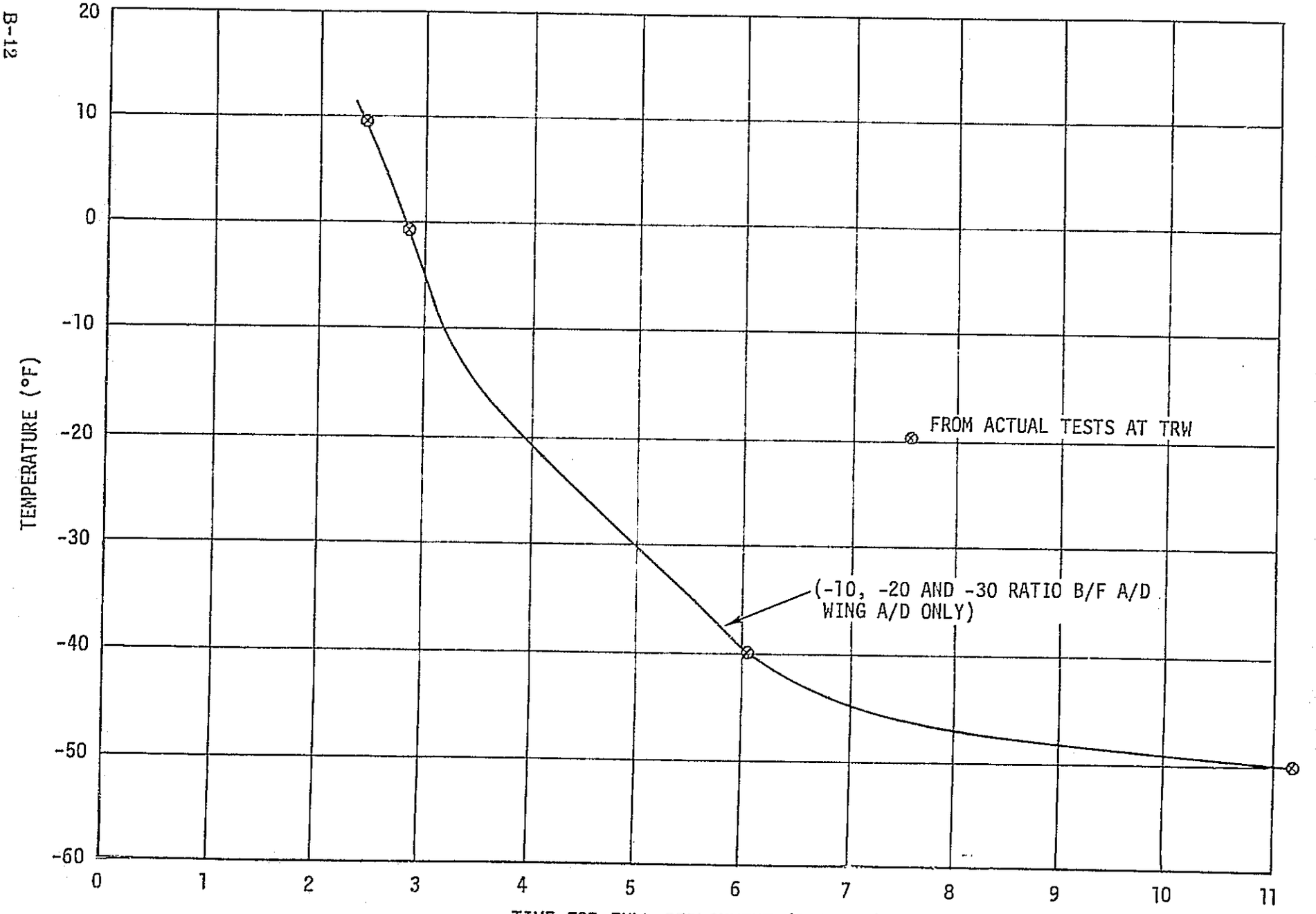

Figure B-9. SAS A/D Cold Deployment Tests and Analysis

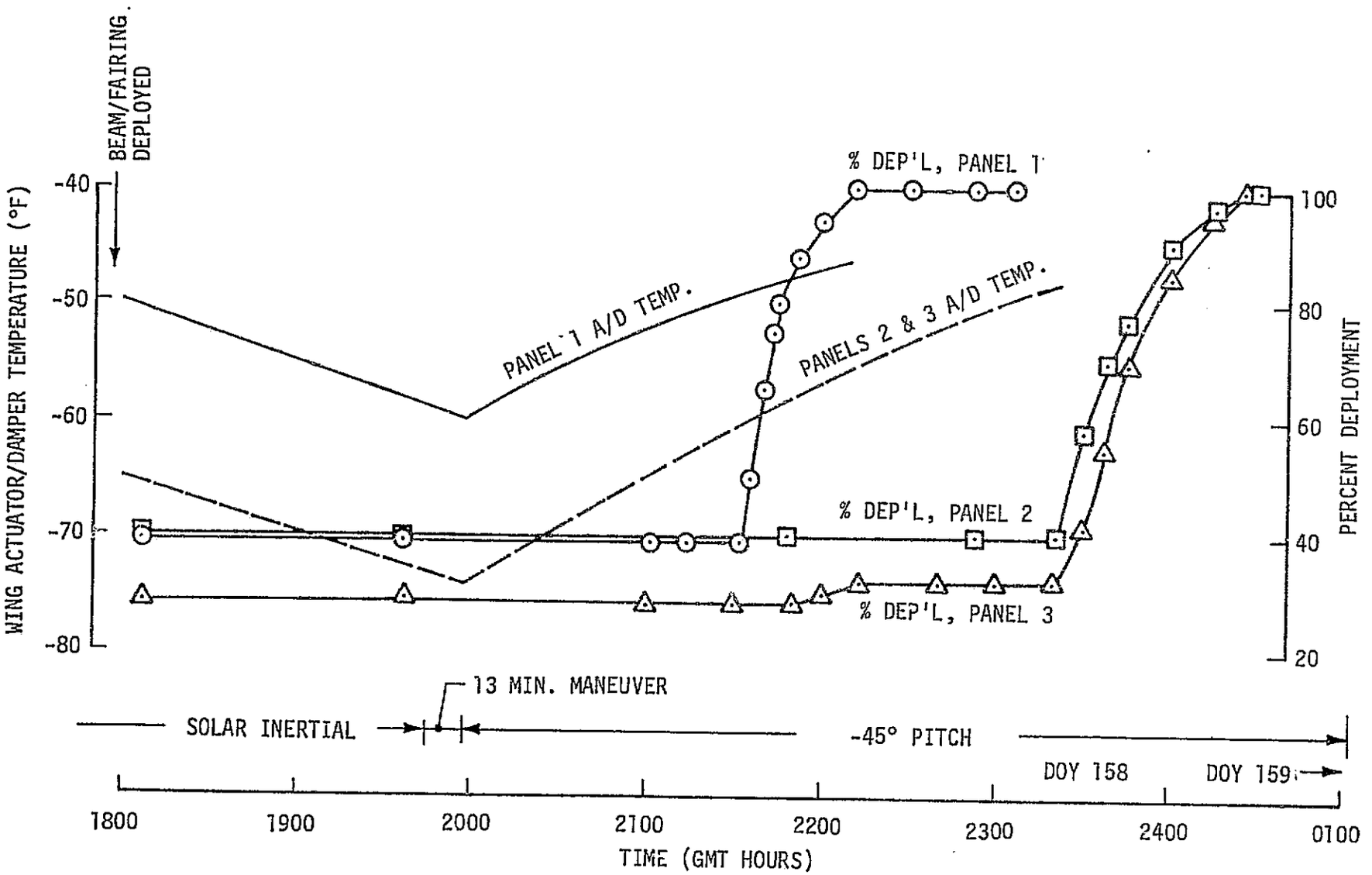

Figure B-10. OWS SAS
Wing A/D Temperature and Deployment Histories

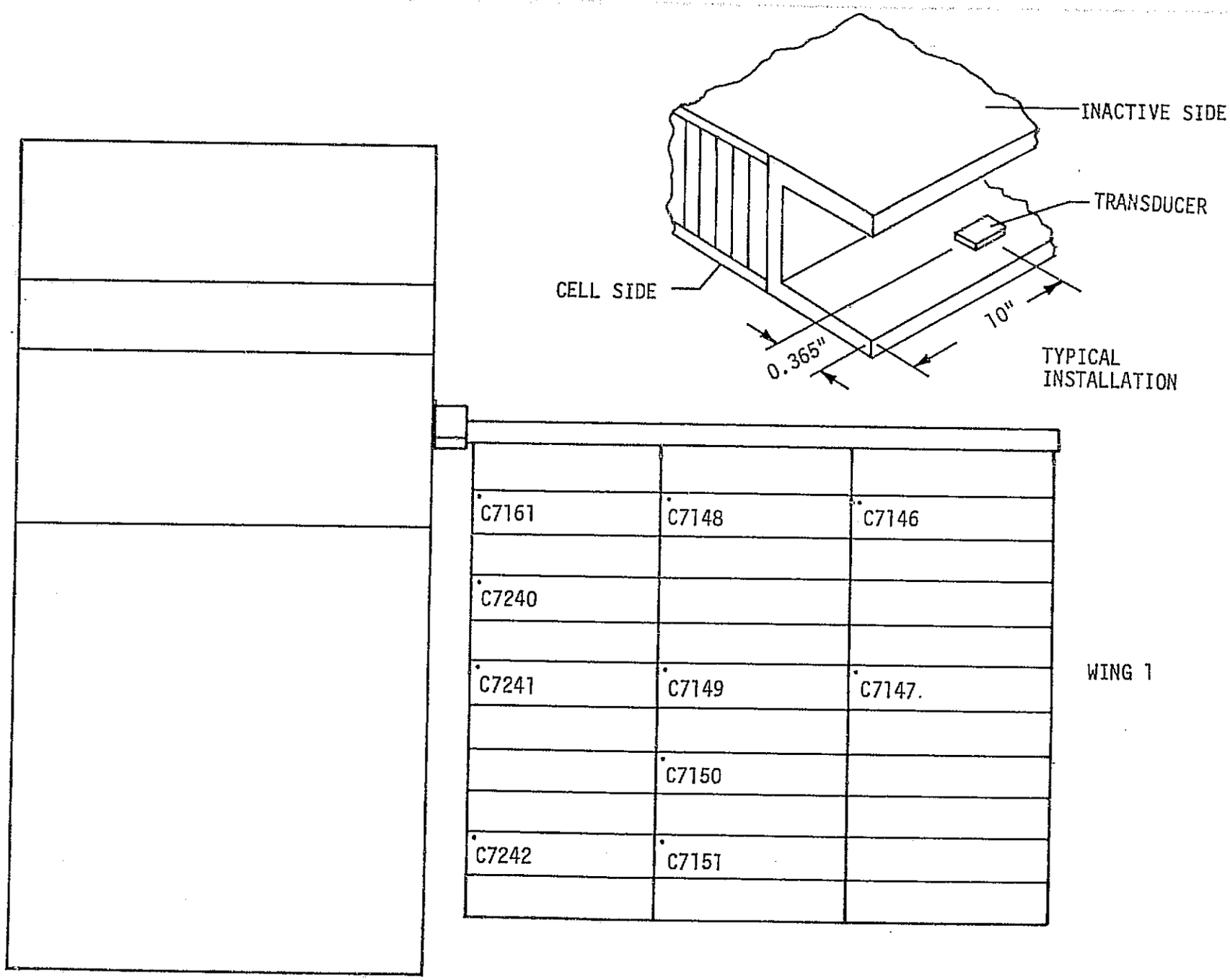

Figure B-11. Solar Array System Temperature Transducer Location

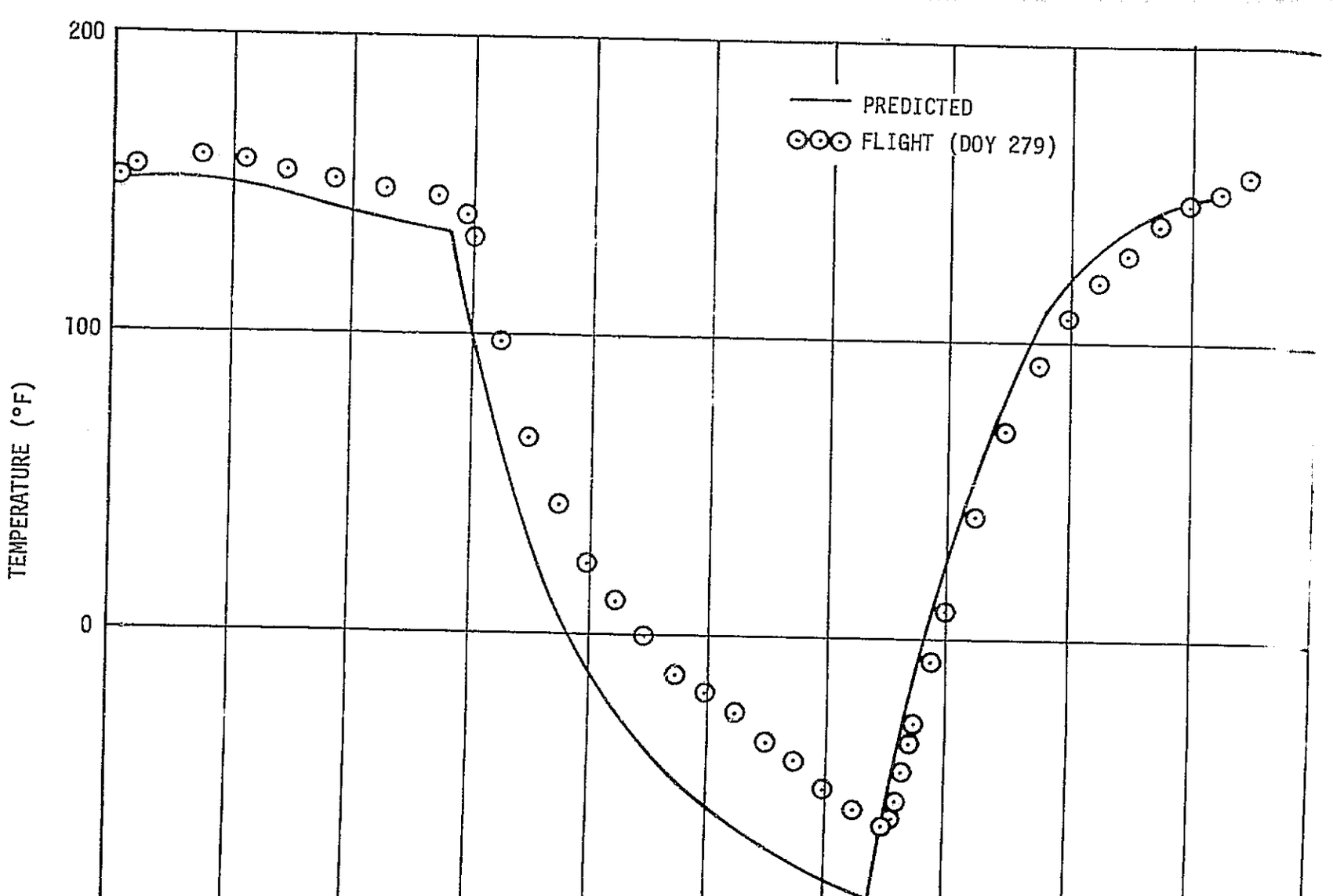

Figure B-12. Comparison of Flight and Predicted Data for Transducer C7147-432 at $\beta = 0°$

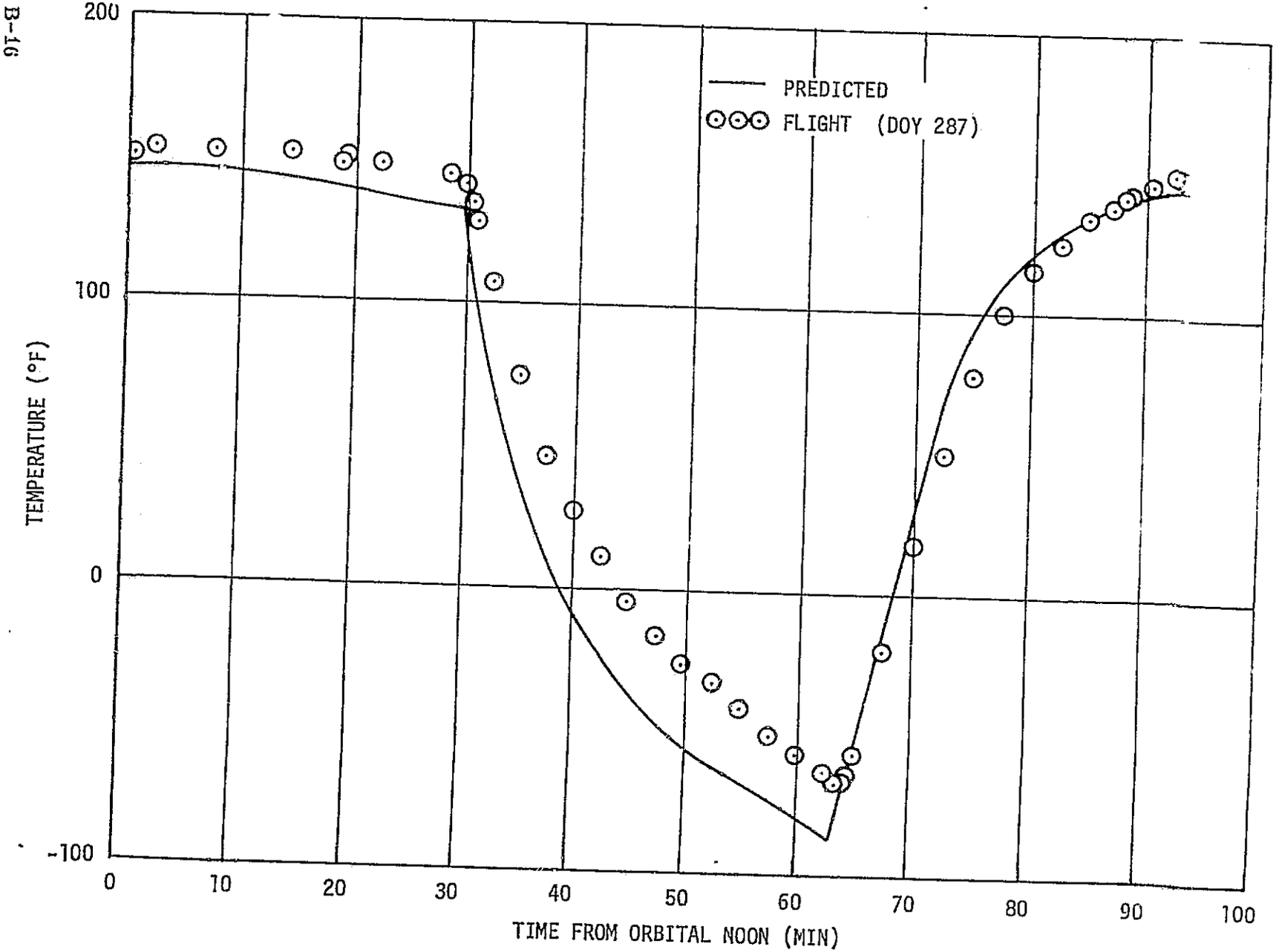

Figure B-13. Comparison of Flight and Predicted Data for Transducer C7147-432 at $\beta = 30°$

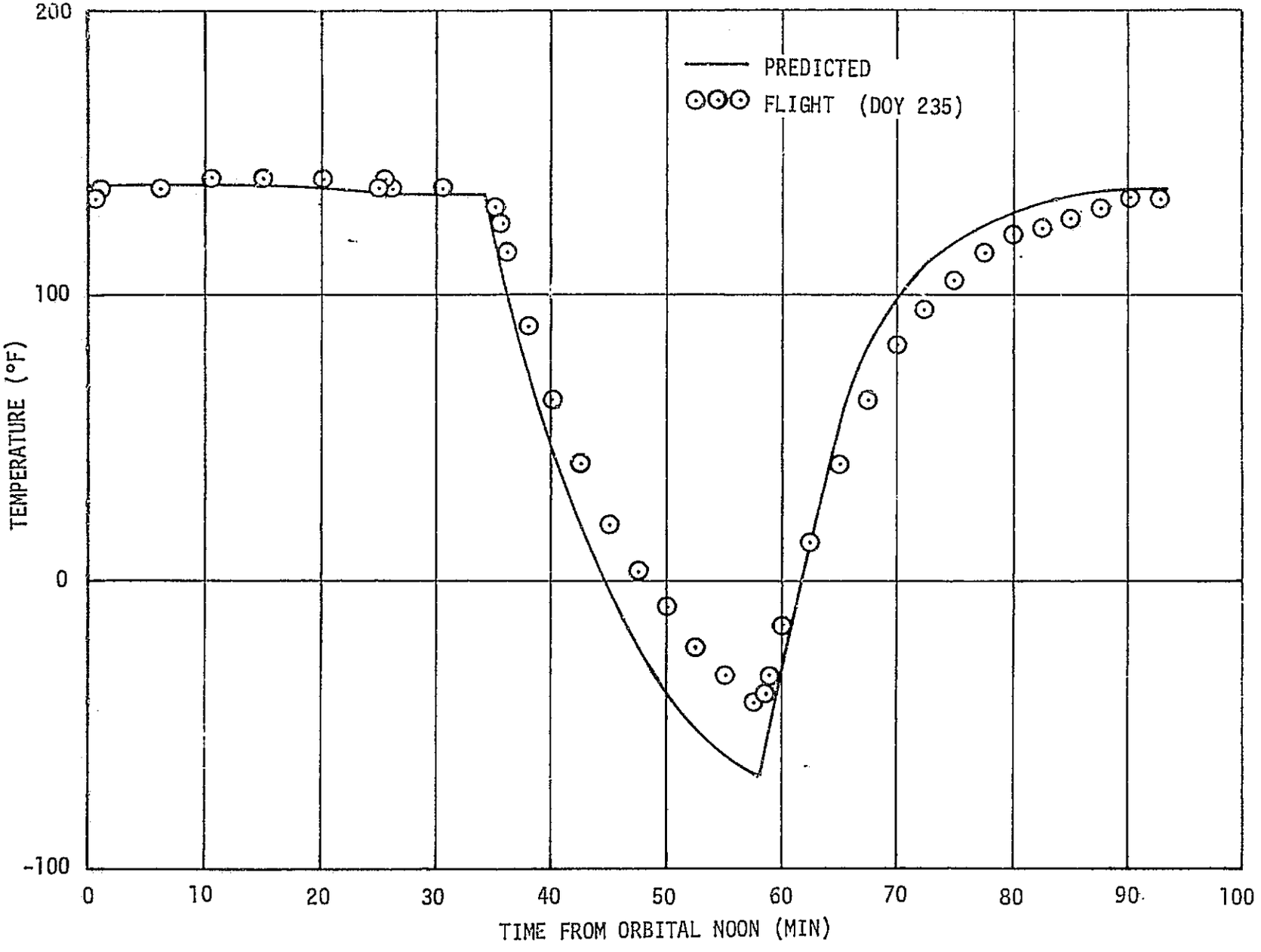

Figure B-14. Comparison of Flight and Predicted Data for Transducer C7147-432 at β = 60.5°

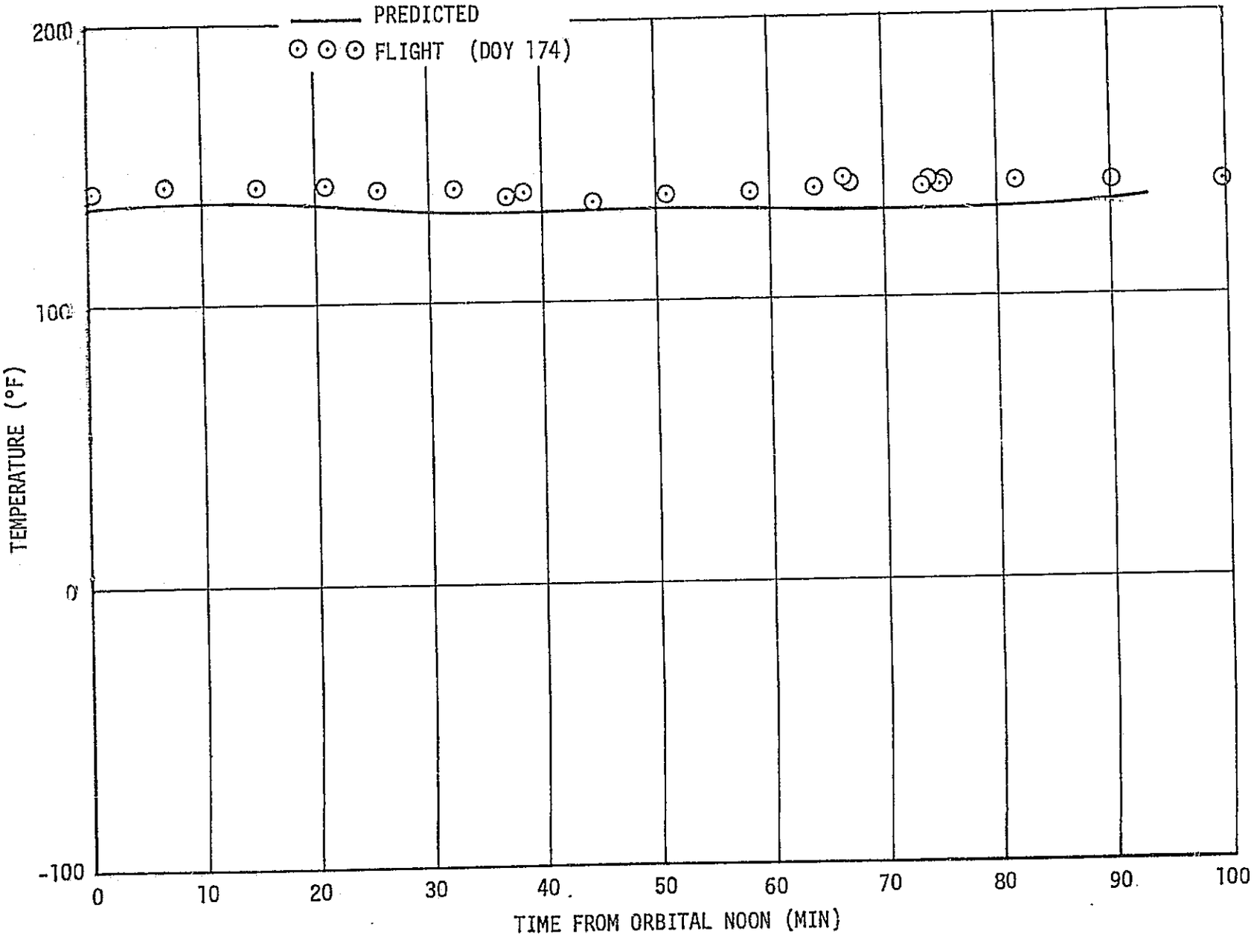

Figure B-15. Comparison of Flight and Predicted Data for Transducer C7147-432 at $\beta = 73.5°$

higher than were predicted. The predicted temperatures were based on the assumption that the SAS would be operating at peak power continuously in sunlight. In reality, the SAS was typically only operating at peak power during the first 20 minutes of sunlight in a solar inertial orbit. When it operated below peak power, the array efficiency dropped resulting in additional thermal energy to be dissipated. This additional energy caused the array temperature to increase until it could be dissipated by radiation.

The other difference is that the flight temperatures did not decrease as much as predicted during the orbital night periods (shown in figures B-12, B-13 and B-14). This difference could be caused by one or more of the following:

1. Actual solar panel thermal capacitance greater than predicted.

2. Actual localized thermal capacitance at the sensor location was greater than predicted.

3. Actual Earth infrared heat flux greater than predicted.

No justification could be found for changing any of these parameters; however, arbitrary changes were analyzed to show the effect of each parameter.

Figure B-16 presents a comparison between flight data and analytical predictions based on a 30 percent increase in panel capacitance. With this revision to the analytical model, the temperature difference that existed during the dark portion of the orbit is much improved. Also presented in figure B-16, are analytical predictions based on a maximum (rather than normal) Earth IR heat flux component. This arbitrary change also increased the temperature during the dark portion of the orbit; however, its correlation with flight data is not as good as an increased capacitance. Figure B-17 presents a comparison of flight data and analytical predictions based on an increased mass on the structural channel to which the transducer is attached. As can be seen in this figure, additional masses of 19 and 38 percent were analyzed and the results agree relatively well with flight data. The results of the analyses previously discussed indicate that the most probable cause of the difference between the predicted and flight data is the thermal simulation near the temperature sensor on the structural support channels.

Daily maximum temperatures of C7146 and C7147 are shown in figure B-18 for the entire mission. These data show several trends of interest. One trend is a general increasing of temperatures as the mission progressed. This trend was attributed to the seasonal increase in the solar constant and agrees well with analytical predictions.

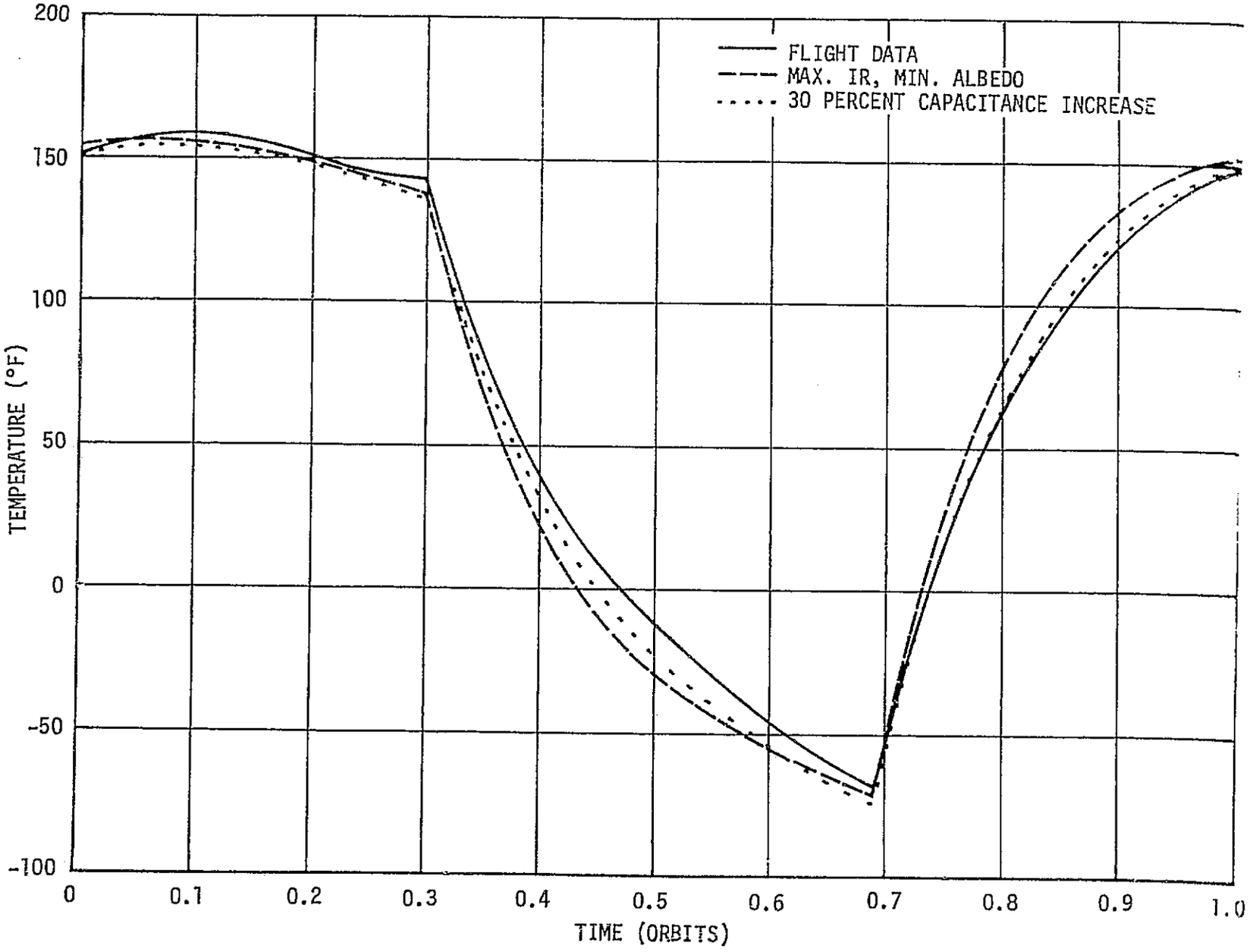

Figure B-16. Effect of Capacitance and Heat Flux Increases

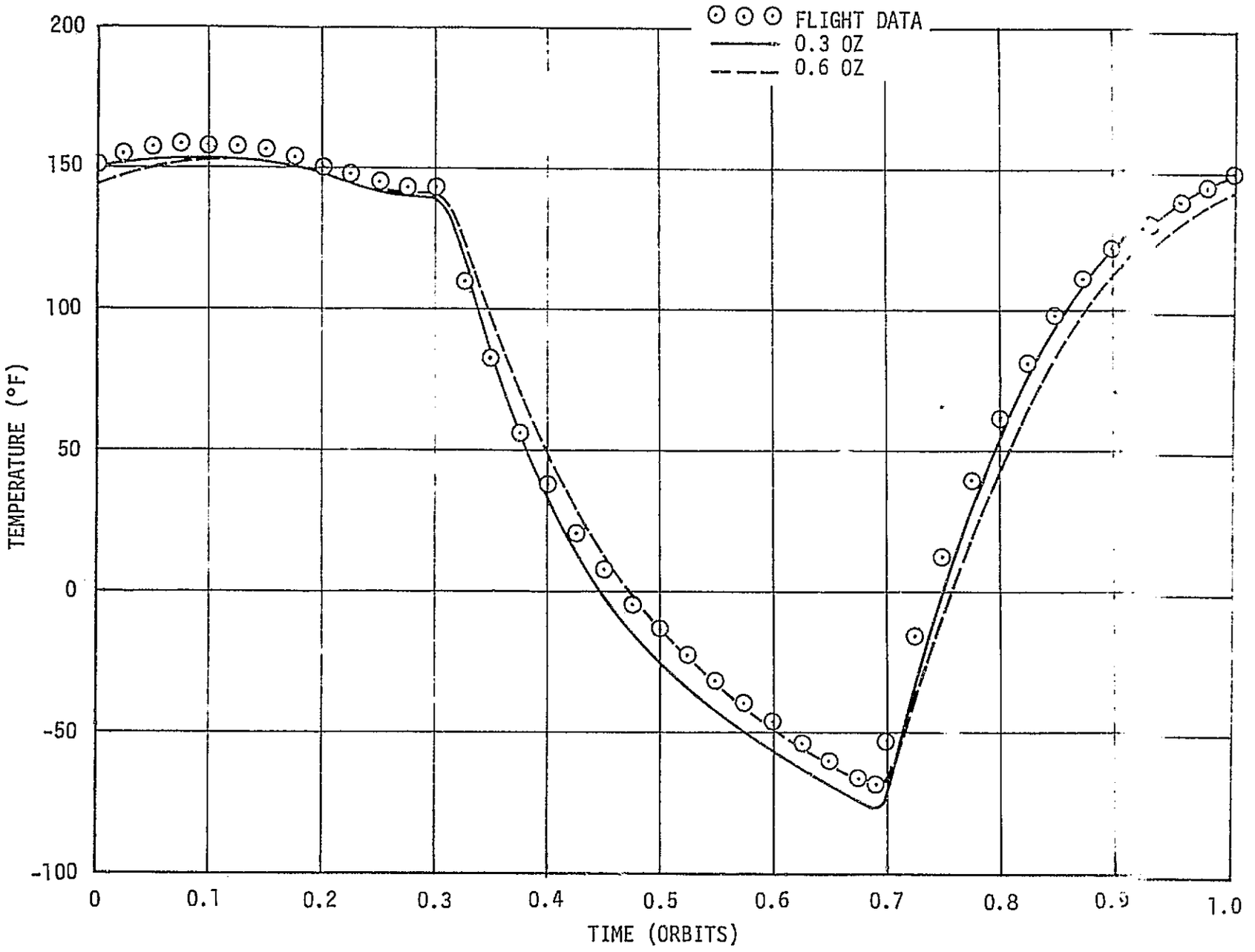

Figure B-17. Effect of Additional Channel Capacitance

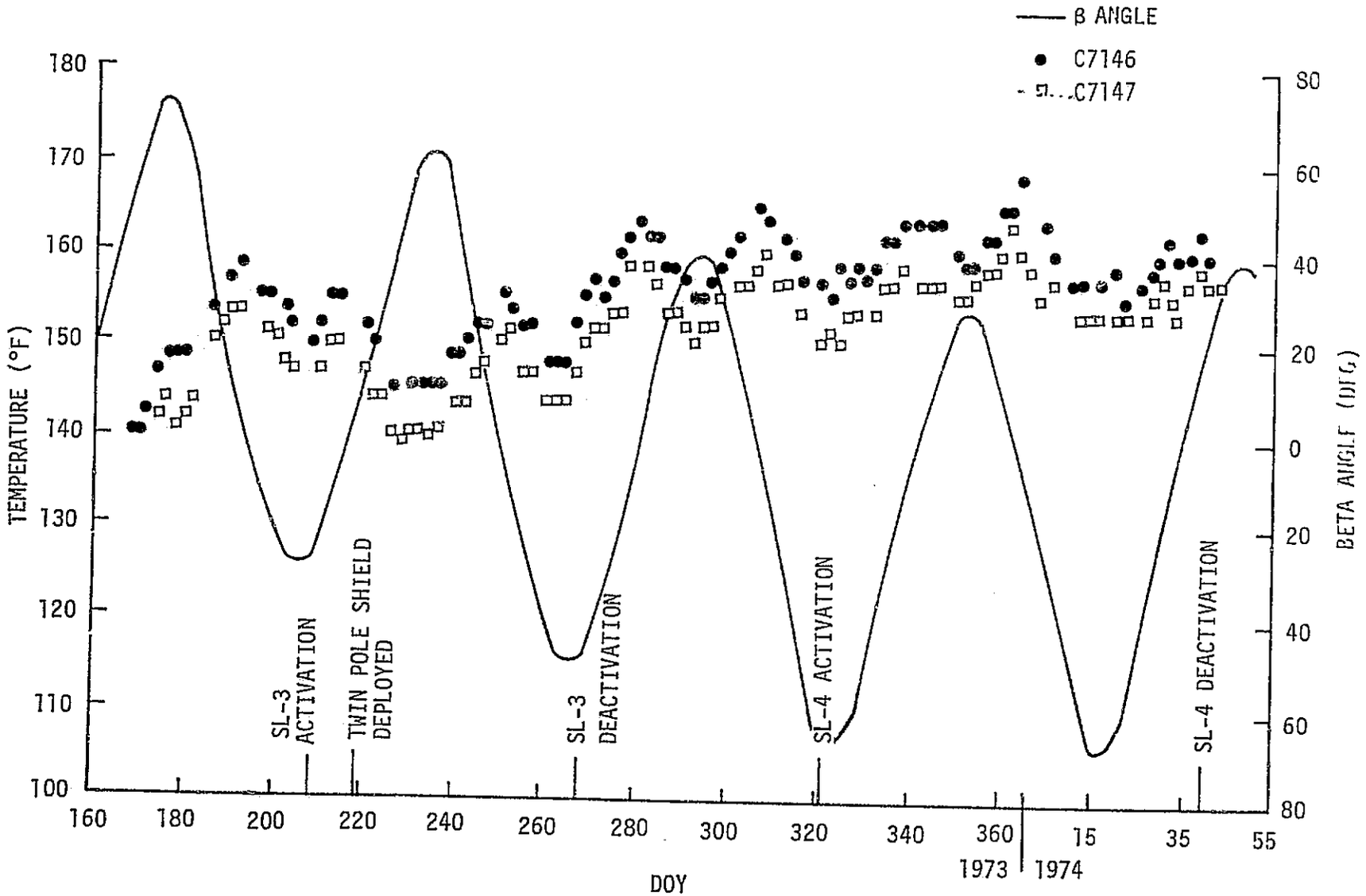

Figure B-18. Daily Maximum Temperature of Transducers C7146 and C7147

Analytical results and a discussion concerning possible degradation in the Z-93 thermal control coating used on the inactive side of the SAS panels can be found in Section IV of this report.

Another trend indicated by the data in figure B-18 is that higher absolute values of β cause cooler maximum SAS temperatures than lower values of β. This trend, which was predicted preflight, is caused by the increased albedo and Earth infrared heat fluxes on the back side of the panels at low β angles. Additionally, the data indicate that deployment of the twin pole shield on DOY 219 caused a cooler environment for the panels. Photographs indicate that the twin-pole shield provided additional solar shading of the highly reflective gold foil on the OWS tankwall near Position II. It is believed that a reduction in the reflected solar energy impinging on the cell side of SAS after this shield was deployed caused the SAS temperatures to decrease.

For future space applications of a similar nature it is recommended that the temperature transducer be located so as to measure the temperature of interest (solar cell temperature) or that thermal tests be performed to determine the correlation between the temperature of interest and the temperature measured by the transducer.

APPROVAL

MSFC SKYLAB THERMAL AND ENVIRONMENTAL CONTROL SYSTEM MISSION EVALUATION REPORT

By

G. D. Hopson
J. W. Littles
W. C. Patterson

The information in this report has been reviewed for security classification. Review of any information concerning Department of Defense or Atomic Energy Commission programs has been made by the MSFC Security Classification Officer. This report, in its entirety, has been determined to be unclassified.

This document has also been reviewed and approved for technical accuracy.

G. D. Hopson, Chief
Engineering Analysis Division

A. A. McCool, Director
Structures and Propulsion Laboratory

R. Ise, Manager
Skylab Program Office

JUN 2 1974